A National Assessment of Potential Climate Change Impacts on the Hydrological Yield of Different Hydro-Climatic Zones of South Africa

Report 1
Methodology and Results

Report to the
Water Research Commission

by

S Schütte, RE Schulze and DJ Clark (Editors)

with further contributions by
RP Kunz, P Wolski, T Lumsden, JC Smithers, SI Stuart-Hill, KR Gwena, SLC Thornton-Dibb, MJC Horan, ML Toucher and Z Jele

March 2023

This report forms part of a series of three reports. The other reports are

A National Assessment of Potential Climate Change Impacts on the Hydrological Yield of Different Hydro-Climatic Zones of South Africa. Report 2: *Perspectives on Adaptation to Climate Change in the South African Water Sector* (WRC Report No. 2833/2/22).

A National Assessment of Potential Climate Change Impacts on the Hydrological Yield of Different Hydro-Climatic Zones of South Africa. Report 3: South African and International Verification Studies of the ACRU Daily Time-Step Model across a Range of Processes, Applications and Spatial Scales (WRC Report No. 2833/3/22).

EXECUTIVE SUMMARY

Background Motivation and Aims

This study is based on a solicited call from the Water Research Commission (WRC). The terms of reference highlighted the highly variable hydrological system of South Africa (SA), which is characterised by a high-risk hydro-climatic environment. Climate change is likely to severely exacerbate risks and impacts on the hydrological system, the socio-economic system, the ecosystem and livelihoods. In light of these issues, a study was proposed that entails the assessment of potential climate change impacts on the hydrological yield. This assessment was to include climate change scenarios for the short-, medium- and long term, their impacts on the hydrological yield and on hydrological responses (e.g. resultant changes in local runoff, accumulated streamflows and recharge), as well as adaptation strategies. To transfer the gained knowledge to key decision-makers, a capacity building programme for DWS staff was to be developed.

Motivation

The hydrological system of SA, even under natural conditions, is highly variable and characterised by a variety of high-risk hydro-climatic zones. Climate change is evident through rising temperatures and altering precipitation, albeit with some uncertainties, as well as a change in the frequency and intensity of climate extremes. The adverse impacts of climate change will negatively affect progress towards development in a number of key economic sectors in SA, including those of water resources, climate-climate-related disaster risk management and natural resource management.

Given that (i) the annual average rainfall for South Africa is well below the world average; (ii) the overall water availability is unevenly distributed across the country; (iii) evaporation rates greatly exceed precipitation, and (iv) water may not always be deemed fit for use in some areas, it may be observed that the aforementioned factors translate to water scarcity now already without even taking climate change into account. Despite the remaining uncertainties regarding the exact nature, magnitudes and patterns of future rainfall changes in South Africa, it appears that water resources, which are already under pressure as a result of growing water consumption and demand, will be under even greater pressure in the future. This is a result of both climatic and non-climatic factors that include the projected changes in rainfall patterns and intensity, increased evaporation resulting from higher temperatures, and the amplifying effects of especially changes in rainfall attributes on hydrological responses such as runoff and extreme events, as well as land use change, and a change in vegetative water use through CO_2 physiological forcing. At the same time, water is vital for on-going socio-economic development and environmental sustainability in SA. Thus, a detailed national assessment on potential climate change impacts on the hydrological yield of different hydro-climatic zones of SA is essential. Identifying emerging risk patterns informing adaptation trends, and strategies will be crucial in order to ensure water availability for all.

Aims and Objectives

The aims and objectives of this study are to establish appropriate climate scenario projections for the short-, medium- and long term, to assess impacts of climate change on the hydrological yield within hydro-climatic zones based on these climate projections and to take into consideration the attribution of non-climatic factors. Furthermore, to assessments are to be made on the hydrological responses to those climate impacts (e.g. resultant projected changes in runoff, accumulated streamflow and recharge to groundwater), and additionally, to recommend appropriate short-, medium- and long-term adaptation strategies to address projected climate change impacts. Lastly, the Project is to transfer knowledge gained to capacitate Department of Water and Sanitation (DWS) staff on climate and hydrological models.

Outline of the Reporting

The final reporting for this study takes the form of four reports. Report 1 (this Report) contains background, methods, results and a discussion of the bio-physical projections of climate variables, hydrological responses and hydrological yield. Report 2 contains adaptation options and strategies while Report 3 contains verification studies of the *ACRU* hydrological model, which was used in this research. Finally a Report of Appendices contains tables related to *ACRU* model land cover inputs and configurations, reporting on a software utility to be used to interrogate results from this study further, a training program to transfer knowledge, and finally monthly streamflow input that can be used as input into other models, e.g. the Water Resources Yield Model (WRYM).

Report 1: Methods

Selection of Appropriate Climate Scenario Projections

After a review of available climate projections, an ensemble of very high-resolution climate model simulations of present-day climate as well as projections of future climate changes over SA was selected, these having been previously produced by the CSIR using the CCAM regional climate model. The selection of six GCMs from the CMIP5 archive was based on their ability to provide a reasonable representation of the El Nino-Southern Oscillation (ENSO) phenomenon for the region. The GCM simulations were first downscaled to a 50 km spatial resolution globally, followed by a strategy to obtain 8 km resolution downscalings. The simulations span the period 1961-2100. Projections for both RCP4.5 and RCP8.5 mitigation scenarios were originally considered for this study, with RCP4.5 being a high mitigation scenario, whilst RCP8.5 is a low mitigation scenario. The RCP scenarios only diverge significantly in their projections after approximately 2050. During the study, it was found that the dataset supplied under RCP4.5 was not compatible with the supplied RCP8.5 dataset, due to a likely difference in the underlying modelling assumptions. The appropriate RCP 4.5 dataset that would have enabled fair comparisons with the RCP8.5 dataset could not be located at the CSIR and may have been accidentally deleted during a clean-up of storage space. As it was not possible to re-generate the appropriate dataset within the scope of this project, CCAM RCP 4.5 projections were not considered further in the study.

Reference Database of Observed Climate

The recently revised Quinary Catchments Database (QnCDB) consists of 50 years of observed rainfall and temperature (maximum and minimum) data, as well as derived reference evaporation, which were adjusted to better represent each Quinary Catchment. For this study, the QnCDB was used to determine baseline hydrological conditions against which potential impacts of climate change were assessed and to bias correct the GCM derived projected climate data.

Bias Correction of Daily Rainfall and Temperature Projections

Daily rainfall and minimum as well as maximum air temperature projections were bias corrected to the resolution of the QnCDB with the methods described in the text, giving 5 838 datasets covering South Africa, Eswatini and Lesotho. These datasets were used as climate input into the *ACRU* model, to determine climate change impacts on hydrological responses and hydrological yield.

Land Cover Inputs for Assumed Natural Vegetation and Actual Land Cover

In addition to climate impacts, there are other, non-climatic factors that can impact upon hydrological responses, compared to baseline conditions. These non-climatic factors include land cover changes compared to previous natural land cover. For this study, both a new natural vegetation baseline as well as actual present-day (2018) land cover was used in the modelling scenarios. Land cover inputs for the configuration of the *ACRU* model were developed. Configuring a hydrological model with actual land cover/use for the whole of South Africa has been a significant undertaking. This is the first time that the

ACRU model has been configured with actual land cover/use at Quinary Catchment level for the whole of SA, Lesotho and Eswatini. This is an important step forward for *ACRU* and SA hydrology.

Report 1: Results and Discussion

Statistics of projected changes from the present (1961-1990) to the near future (2015-2044) and from the present to the distant future (2070-2099) for rainfall, means of daily minimum and maximum air temperatures as well as potential evaporation are shown and discussed for southern Africa for the selected climate projections. This is followed by results from the hydrological modelling which give changes in hydrological responses and finally, the results for climate change impacts on the hydrological yield. A summary is provided for each of South Africa's six hydro-climatic zones.

Projected Changes of Rainfall

Projected changes in mean annual rainfall show mixed results. A reduction in rainfall in the west and north is projected, especially into the distant future. Along the east coast the changes are mixed. In the eastern interior and Drakensberg area, more rainfall than at present is projected for the near future and even more for the distant future. Changes become more severe into the distant future. Comparing individual GCMs, broad overall similarities can be seen, with reduced rainfall in the west, especially towards the distant future, and increases in the Drakensberg and more central parts of South Africa. Differences in the severity of increases and reductions can be seen, with the magnitudes of decreases and increases depending on the GCM.

Spring rains generally show reductions over nearly all of southern Africa. Summer rainfall generally show increases in the interior and decreases in the south and mixed changes along the east coast. The north-east seems to experience a decrease in spring rain, but an increase in rainfall in summer, thus a shift in the onset of rain is projected to later towards summer. Autumn rainfall generally shows small to medium decreases in the west and north and small increases in the east. Winter rainfalls generally show small decreases in the north and the interior, with small increases along the east.

Design rainfall events show projected increases over most of southern Africa from the present to the near future. The increases in terms of ratio changes from present to near future in general are larger for the rainfall events for 1-day 50-year return period, compared to those of the 1-day 10-year return period.

Projected Changes of Temperatures

Projections of annual means of daily temperature show increases throughout southern Africa of between 1°C along the coast and 3°C in the north-west from the present to the near future, both for maximum and minimum daily temperatures. From the present to the distant future, projected changes are between 3° at the coast to more than 6°C in the north-west for daily maximum temperatures, while the minimum temperatures are also projected to increase by between 3° at the coast and to up to 6°C in the north-west.

Projected Changes of Potential Evaporation

Projections for potential evaporation show increases throughout and larger increases towards the distant future, especially in the north-west, the north and the interior. The east coast in general shows a smaller increase in potential evaporation.

Projected Changes of Actual

The spatial distribution of evapotranspiration is much higher in the wetter east and lower in the drier west of the country. Projected changes in evapotranspiration into the future show milder changes for the near future and more extreme changes for the distant future. The west and north of the country

have a projected reduction in evapotranspiration, the interior shows essentially no changes, but the Drakensberg area shows increases in evapotranspiration.

Projected Changes of Individual Catchment Runoff

The spatial distribution of catchment runoff is much higher in the wetter east and lower in the drier north-west of the country. Projected changes furthermore increase from the near to the distant future. For the west, a reduction in runoff is projected. The area around Cape Town shows sizeable reductions in runoff. The interior and to a lesser extent the north-east are projected to produce more runoff. The east coast generally shows little to no changes, although there are a few local patches with changes in either direction.

Projected Changes in Accumulated Streamflow

The spatial distribution shows more streamflow in the east, as well as in the south around Cape Town, but very little streamflow in the dry west, except for the areas that contain the large rivers flowing westwards. Projected changes into the near future show mixed results. There is a general reduction in the west, a lesser reduction in the far north, an increase in the interior and little change around the eastern coast. The changes are more extreme towards the distant future.

Seasonal changes in median streamflow (mm) for spring (September to November) show small absolute changes, with small increases in the interior and small decreases along the coast and bigger decreases around the western parts of the Western Cape. Changes for summer (December to February) show small absolute increases in the interior, more so towards the distant future. Small decreases can be seen in patches in the west, with the patches increasing into the distant future. Projected changes in median streamflows for autumn (March to May) show small increases in the interior, more so towards the distant future for the Orange catchment, and decreases along the coast and north-west. Projected changes in median winter (June to August) streamflows show small increases in the interior and small decreases along the coast and the north-west, with larger decreases in the western part of the Western Cape. This winter rainfall area stands out with projected reductions in winter streamflow, and the same can also be seen to a lesser degree for spring streamflow.

Projected Changes in Design Streamflow Events

Design streamflow events from the present to the near future show an increase over most of the country, of between 1.1 to 1.6 times. Generally, the 1 day 50-year return events shows bigger increases compared to the 1 day 10-year return event. A more localised analysis is required for more detailed results.

Projected Changes into the Soil Water Drainage into the Groundwater Zone

The spatial distribution shows higher magnitudes of drainage in the wetter parts of the region. Projected absolute changes are small for most of the region, but especially into the distant future a reduction can be seen in areas of the Western Cape and along some eastern regions, with some increases along the Drakensberg. In relative terms, a general reduction can generally be seen, especially towards the distant future in the west as well as along the east coast but increases in the eastern interior and the far north.

Projected Changes in Baseflow

The spatial distribution shows higher magnitudes of baseflow in the wetter parts of the region. Projected absolute changes are small for most of the region, but especially into the distant future a reduction can be seen in areas of the Western Cape and along some eastern regions and some increases along the Drakensberg. In relative terms, a reduction can generally be seen, especially towards the distant future in the west as well as along the east coast but increases in the eastern interior and the far north.

Confidence in the Results

It is not possible to verify the model results and projected climate at this point in time. This will only be possible in the future, when looking back at the past. However, the projected hydrological responses using the various GCMs can be compared for similarities and differences (convergence). A method of doing this is to calculate the ratio of the results of the relevant time periods for each GCM, for example, the results of the near future to the present. Then the coefficient of variation (CV in %), among the ratios from all GCMs is calculated to give a confidence index (CI). A comparison of the CI of various variables shows in general that the confidence in the results are highest for potential evaporation, followed by actual evapotranspiration and rainfall, then accumulated streamflow, thereafter runoff, with soil water drainage to groundwater zone displaying the lowest confidence.

Projected Changes in Hydrological Yield

The results for both naturalised flows as well as flows under actual land cover conditions (as at 2018), indicate that the western areas, especially around the Western Cape, show a decrease in yield for the near future, and further decreases in the more distant future. A decrease in yield is also projected for some areas in the east, especially the north-east. This needs to be considered in future water resources planning. Conversely, areas where the rivers originate from the Drakensberg areas are projected to have an increase in yield.

One needs to be aware that this is the first attempt to model land use impacts on a national scale and it is very useful to be able to obtain a broad picture of the whole region. However, anthropogenically modified land cover had to be simplified for national scale modelling and the approach to representing actual land cover at national scale may need to be refined. For example, currently no deep rooting of forest trees is currently modelled, while this is often the case in reality, and which is likely to result in an under-simulation of the modelled water use of forest plantations. It would be interesting to see whether climate change or land use has a larger impact on yield, and whether the impact differs at a large scale compared to a local scale. Even though a simplified yield model has been used to determine the hydrological yield, it is expected that the relative changes in yield would be similar to relative changes determined using a more detailed, stochastic yield model (e.g. WRYM). The results simulated to date have analysed the impacts of climate change on yield under assumed natural vegetation, as well as the impacts of climate change on yield for actual cover and the climate change impacts have been found to be similar for both land cover scenarios. Climate change impact might be magnified locally or be muted because of anthropogenically altered land cover; however a detailed assessment of land cover/use impacts was beyond this study.

Report 1: Limitations and Assumptions

This complex study has some limitations, some of which are outlined in more detail.

Climate projections and their input into hydrological models

Results of climate change impacts into the future on climate related variables must be interpreted on the understanding that no GCM provides "perfect" future climate scenarios, but that the projections from the suite of the six bias-corrected GCMs used in this study (where the bias correction involved matching the GCM output with observations for an overlapping historical period) fall within the spectrum of outputs from the 30 CMIP6 GCMs used in the latest IPCC Reports. Additionally, given the many factors beyond just daily rainfall that affect hydrological responses, without even considering projected climate change (e.g. rainfall intensity, soils characteristics, as well as land use, its seasonal changes and management), and the fact that errors and variability in hydrology are amplified as we move from potential evaporation to rainfall to runoff and then to groundwater recharge. Hence, uncertainty analyses have been undertaken to assess the extent to which the hydrological outputs resulting from the 6 GCMs vary among one another. Note that the projected changes in the maps are in places at variance in the

direction and magnitude of changes from GCMs used in previous studies in South Africa, and that the next generation of GCMs is likely to give results that are different again to the ones found here.

ACRU model configuration

The complex *ACRU* configuration used for this study, by its very nature, requires some compromises and many assumptions to be made. It also needs to be remembered that, for the purposes of this study, actual water use, especially engineered water use, dams and urban return flows were not modelled. These limitations need to be considered when applying the simulated runoff values produced through the use of this configuration of the *ACRU* model. The simulated runoff values are thus better suited to comparative analyses, such as (i) comparing runoff produced by actual land cover/use with runoff produced under naturalised land cover, (ii) comparing runoff produced using different GCMs, (iii) comparing runoff produced using different RCPs, and (iv) comparing runoff produced in different time periods.

Land cover/use projections

Dynamic land cover/use change and projections into the future also did not form part of this study.

Report 1: Recommendations

Climate change mitigation

There is a need for climate change mitigation. Projected temperature changes alone are showing a bleak picture for the future climate in southern Africa, while yield and hydrological responses show mixed responses. Greenhouse gas emissions globally need to be reduced, to ensure this is not the future that we leave behind for generations to come. Climate change mitigation thus needs to be given high priority, globally as well as in South Africa.

Climate change adaptation

There is a need for climate change adaptation. Climate change impacts are already being experienced and will become more severe into the future. There is, therefore, a need to understand potential impacts to be resilient and to be able to adapt to them. More on adaptation is given in Report 2.

Recommendations for future research

(i) This project produced a wealth of model outputs and statistics. These includes separate scenarios of climate change impacts under land cover of natural vegetation and under actual land cover. A comparison of results under natural vegetation and those under actual land cover does require a more detailed spatial analysis, as the impacts are likely to be localised.

(ii) Further improvements can be made in the *ACRU* model configurations. In this project, water abstractions, irrigation, dams, inter-basin transfers and urban return flows were not taken into account in the configuration of the *ACRU* hydrological model. To be able to model streamflows more realistically, these should be taken into account in a future project, where information is available.

(iii) It would be beneficial to determine changes in seasonal streamflow volume rather than only mm equivalents, as that might be more important to the water management and planning sector.

(iv) With the significant differences occurring in some regions of the country, it is recommended that future analyses should include more detail at a local level, for example, to examine hydrological yields from individual Primary Catchments and/or Water Management Areas.

(v) The climate science is evolving and this study should be repeated as and when new climate projections become available. Also the confidence in the projections can be improved if a longer time period of observed climate variables can be compared with GCM derived climate variables.

ACKNOWLEDGEMENTS

TABLE OF CONTENTS

LIST OF FIGURES

LIST OF TABLES

1   BACKGROUND AND INTRODUCTION
S. Schütte and S.I. Stuart-Hill

1.1   Background

This project is based on a solicited call from the WRC published in the year 2016. The terms of reference highlighted the highly variable hydrological system of South Africa, which is characterized by a high-risk hydro-climatic environment. The climate is undoubtedly changing as evidenced by among other, increased frequency in climate and weather extremes (such as droughts, floods and unprecedented incidence of wild fire breaks in the Western Cape). Climate change obviously will exacerbate this and impact severely on the hydrological system, the socio-economy, the ecosystem and livelihoods. Severity of impacts and needs for adaptation will vary according to sensitivities and vulnerabilities of the impacted system. Lack of adequate capacity as well as paucity of relevant and requisite skills to address water related challenges and adaptation is a commonly encountered hindrance to uptake and implementation of research outcomes. In light of these issues, a study was proposed that entails assessment of potential climate change impacts on the hydrological yield. This assessment has to reflect and include climate change scenarios for short-, medium- and long term, climate change impacts on the hydrological yield, hydrological response, e.g. resultant changes in runoff, streamflow, water levels and recharge, and adaptation strategies. Last but not least, to operationalise the gained knowledge it needs capacity building of key decision-makers, which is why a capacity building programme for DWS staff has to accompany the research.

1.2   Motivation

The hydrological system of South Africa, under natural conditions, is highly variable and characterised by a variety of high-risk hydro-climatic zones. Climate change is evident through rising temperatures and altering precipitation, albeit with some uncertainties, as well as a change in the frequency and intensity of climate extremes. The adverse impacts of climate change will negatively affect progress towards development in a number of key economic areas in South Africa, including those of water resources, climate-related disaster risk management and natural resource management. Given that (i) the annual average rainfall for South Africa is well below the world average; (ii) the overall water availability is unevenly distributed across the country; (iii) evaporation rates greatly exceed precipitation, and (iv) water may not always be deemed fit for use in some areas, it can be observed that the aforementioned translates to water scarcity already without even taking climate change into account. Despite the remaining uncertainties regarding the exact nature, magnitude and pattern of future rainfall changes in South Africa, it appears that water resources, which are already under pressure as a result of growing water consumption and demand (DWS, 2016), will be under even greater pressure in the future. This is a result of climatic and non-climatic factors that include, but are not limited to, the projected changes in rainfall patterns and intensity, increased evaporation resulting from higher temperatures, and the amplifying effects of especially changes in rainfall attributes on hydrological responses such as runoff and extreme events, as well as land use change, and a change in vegetative water use through CO_2 physiological forcing. At the same time, water is vital for on-going socio-economic development and environmental sustainability in South Africa. Thus, developing a methodology to produce a detailed national assessment on potential climate change impacts on the hydrological yield of different hydro-climatic zones of South Africa is essential. Furthermore, aspects of downscaling, bias correcting and scale issues and issues of complex uncertainty need to be reflected in more detail and understood by decision-makers. Identifying emerging risk patterns that inform adaptation trends, and strategies will be crucial in order to ensure water availability for all and economic growth at the same time.

1.3 Aims and Objectives

The aims and objectives are outlined in this section. The project had the following five aims:

(i)   Aim 1 is to establish appropriate climate scenario projections for short-, medium- and long term.
(ii) Aim 2 is to assess impacts of climate change on the hydrological yield within hydro-climatic zones based on medium to short, medium to long term climate projections and taking into consideration the attribution of non-climatic factors.
(iii) Aim 3 is to assess the hydrological response to those climate impacts (e.g. resultant projected changes in runoff, accumulated streamflow, water levels, and recharge to groundwater).
(iv) Aim 4 is to recommend appropriate short-, medium- and long-term adaptation strategies to address projected climate change impacts.
(v)   Aim 5 is to develop a training programme to capacitate the Department of Water and Sanitation (DWS) climate change and other selected staff on climate and hydrological models.

The objectives related to Aim 1 are to obtain daily climate data of six regional downscaled General Circulation Models (GCMs) from the CMIP5 ensemble under two emission scenarios (RCP8.5 and RCP4.5) for the period 1961-2099 from the CSIR. A further objective is to undertake bias correction of daily rainfall and temperature data to match local observed data for the overlapping period 1961-1990. The CSIR projections are to be compared to those of CSAG projections. Statistics are to be generated for rainfall and temperature for historical observed and GCM derived present (both 1961-1990), intermediate (2015-2044) and future (2070-2099) periods.

Aim 2 relates to assessing the impacts of climate change on hydrological yield while Aim 3 relates to assessing the impacts of climate change on the hydrological responses of catchments. To achieve these aims a hydrological modelling approach is used, where projected climate output, at a daily time step, are used as input to the *ACRU* hydrological model from which simulated runoff and other components of the catchment water balance can be obtained. Thus, with regard to Aim 2, the objective of the hydrological modelling is to estimate accumulated runoff from each Quaternary Catchment for use: (i) within the scope of this project, to calculate hydrological yield for different climate change scenarios, and (ii) by DWS to calculate system yield for different climate change scenarios using the WRYM. It is important to understand that, for the purposes of this study, the hydrological modelling is not intended to estimate actual streamflows, which are influenced by upstream dams and engineered water flows for irrigation, urban uses and inter-catchment transfers.

The calculation of water yield, whether it be hydrological yield, reservoir yield or system yield, requires flow data as one of the main input variables. Often some form of naturalised flows are typically used for this purpose, where these naturalised flows may be determined by: (i) removing anthropogenic impacts on measured current day flows, or (ii) applying a hydrological model using some form of assumed natural land cover. The latter approach has been used in this study as it permits future climate scenarios to be evaluated. In addition, current land cover has been applied and the yield calculated.

1.4 An Outline of this Report

The reporting consists of three different reports. Report 1 (this document) consists of background, methodology and results. Report 2 consists of adaptation strategies and Report 3 consists of verification studies with the *ACRU* model.

This section outlines Report 1. First is the background and introduction to this study. Then, in Chapter 2, "Establishing climate scenario projections", a review and selection of climate projections for this study is provided, followed by a description of the revised Quinary Catchments Climate Database in order to

provide a baseline observed climate database against which projections can be evaluated. Then the bias correction of rainfall and temperature projections is described. While originally both the RCP4.5 and RCP8.5 scenarios were planned for evaluation, the reasons why the RCP4.5 dataset was excluded from further analyses in this study are outlined. Chapter 2 relates to Aim 1.

In Chapter 3, "The land cover configuration – methods", the inputs into the hydrological model for land cover, as well as the configuration are described. This includes two scenarios, one for assumed natural vegetation and a scenario for actual land cover (as of 2018). This relates to integrating non-climatic factors that can impact hydrological responses and hydrological yield.

Chapter 4, "Projections of rainfall, temperature and potential evaporation", describes the results of statistics for potential climate change impacts on rainfall, temperature and potential evaporation for southern Africa, for the selected climate projections and periods. The daily datasets serve as inputs into the hydrological model. The outcomes relate to Aim 1.

The results of the hydrological modelling are then discussed in Chapter 5 for the hydrological responses under climate change for the RCP8.5 emission scenario, both for assumed natural vegetation actual land cover. The outcomes are related to Aim 3.

The outcomes related to Aim 2 are reported in Chapter 6, "Projected impacts of climate change on the hydrological yield", both for assumed natural vegetation as well as for actual land cover (as of 2018).

Projected climate change impacts per hydro-climatic zones in South Africa are summarised in Chapter 7 for each of South Africa's six hydro-climatic zones.

In Chapter 8, a case study with more detailed analysis for the Limpopo MA is provided.

In Chapter 9, "General conclusions, recommendations and future research", a synthesis and way forward are provided.

The appendices are covered in a separate report. Appendix A consists of tables related to the *ACRU* configuration with actual land cover, related to Chapter 3. An outline of the training programme, to address Aim 5 is presented in Appendix B. To be able to visualise and further analyse results from this study, a software utility has been developed, which is described in Appendix C.

While the previous chapters are all relevant to Aim 4 (Adaptation), this aim is more specifically addressed in Report 2, "Perspectives on Adaptation to Climate Change in the South African Water Sector". Lastly part of this project, verification studies for the *ACRU* model were complied, which is addressed in Report 3, "South African and International Verification Studies of the *ACRU* Daily Time-Step Model across a Range of Processes, Applications a and Spatial Scales".

2   ESTABLISHING CLIMATE SCENARIO PROJECTIONS

**P. Wolski, T. Lumsden, R.P. Kunz, D.J. Clark, K.R. Gwena, M.L. Toucher, S. Schütte,
R.E. Schulze**

This section relates to Aim 1: Establish appropriate climate scenario projections for short-, medium- and long term.

A review of available climate projections and the selection of projections for this study are presented first. Thereafter a revised baseline historical dataset of climate data for the Quinary Catchments Database (QCDB) is discussed, required for the bias correction of the projections. Bias correction of the selected CCAM rainfall and temperature projections are then discussed. The final section outlines why analyses with the available dataset of RCP4.5 CCAM projections provided by the CSIR were not pursued.

2.1   Review and Selection of Climate Projections for this Study

2.1.1   Introduction

Over the past few decades, as the issue of climate change has garnered more recognition, a need arose to provide projections of future climate for analyses of impacts on various elements of natural and socio-economic systems. Developing of climate projections begins with development of scenarios of future greenhouse gas emissions. These scenarios capture the main anthropogenic drivers of greenhouse gas emission, reflecting possible future trajectories of global socio-economic system and various levels of emission mitigation policies. Subsequently, future climates are simulated for each of the emission scenarios using an ensemble of global climate models. Since global climate models provide climate data of relatively coarse spatial resolution (150-300km), to be applied to drive local or regional impact models (e.g. hydrological or agricultural models), their projections need to be downscaled to appropriate spatial resolution.

Global climate models are the main tools to generate climate projections. Contemporary global climate models are typically Earth System Models that encompass a General Circulation Model, representing the dynamics of atmosphere, ocean and cryosphere, and a number of sub-models representing climate and bio-geo-chemical processes on land and in the oceans, in particular carbon cycle. Climate models build on fundamental laws of physics (e.g. Navier-Stokes or Clausius-Clapeyron equations) and empirical relationships established from observations, and, when possible, constrained by fundamental laws (e.g. mass and energy).

Climate models are complex, but they are able to capture global climate system only in a relatively simple manner, resulting in (model-related) uncertainty of projections. An unequivocally accepted way to capture that uncertainty is through the use of multi-model ensembles (Tebaldi and Knutti, 2007). Recently, the use of such ensembles has been questioned, but that is on the basis of the large cost of the ensemble approach in human and computational resources, and challenges associated with the interpretation of multi-model ensembles and not on the basis of their scientific principles (Palmer and Stevens, 2019; Touzé-Peiffer et al. 2020).

The landscape of climate projections is ever evolving, with climate models increasing in comprehensiveness and complexity and progressive updates of possible trajectories of future socio-economic development and associated greenhouse gas emissions. Initially, projections were generated in an uncoordinated manner by individual climate modelling groups, but coordinated initiatives encompassing numerous GCMs run under identical forcing are available since early 2000s, notably:

- CMIP3 (Meehl et al., 2000, Meehl et al., 2007) available ~2006, projections run under SRES (IPCC, 2000) greenhouse gas emission scenarios,
- CMIP5 projections (Taylor et al. 2012), available ~2013, run under RCP (van Vuuren et al., 2011, Moss et al., 2010) greenhouse gas emission scenarios.
- CORDEX (Giorgi et al. 2009) dynamically downscaled projections (available ~2017) that comprised an ensemble of combinations of 10 regional climate models and 20 CMIP5 GCMs
- CMIP6 (Eyring et al. 2016) GCM projections run under SSP greenhouse gas emissions scenarios (Riahi et al. 2017), available ~2021, include not just climate projections, but also a series of dedicated experiments with high-resolution models (HiResMIP), or large ensemble initial conditions simulations that allow evaluation of different sources of uncertainty of future climate.

In the South African context, one has to add to these the dedicated dynamical downscaling simulations with CSIR CCAM model, carried out in several versions since late 2000s.

Downscaling then bridges the disparity between the spatially coarse-scaled GCM output and the finer-scaled input needs of hydrological simulation models, with two types of downscaling performed routinely, *viz.* dynamical downscaling (with regional climate models, RCMs) and statistical (empirical) downscaling. The advantages of using downscaled climate projections are well recognised, but it is also recognised that downscaling introduces additional uncertainties, which are sometimes not adequately quantified. While the potential benefits of downscaling are of particular importance for South Africa as many of the GCMs fail to adequately capture the detailed spatial gradients and strong topographical forcing that influence South Africa's climate (Hewitson and Tadross, 2011), downscaled projections need to be contextualised within a broader understanding of atmospheric dynamics and their physical consistency with the parent GCMs. However, a major characteristic of any downscaling and modelling is the reliance on past climate data (e.g. Engelbrecht et al., 2011; Landman et al., 2017). Data availability in South Africa is a significant challenge (Archer et al., 2018). For example, where first world countries are likely to have daily and sometimes hourly climate data from numerous weather stations over long periods, South Africa's current climate station network is relatively sparse spatially and often plagued by missing data (Lynch, 2004; Schulze and Maharaj, 2004; Tadross et al., 2011).

In this section, climate projections (including downscaling) are first reviewed, before considering the projections that have been used in past hydrological impact studies for South Africa, and those that are currently available for this purpose.

2.1.2   Understanding future climate scenarios

To produce climate projections, climate models require data on GHG emissions over time, or concentrations of radiative forcing constituents, as well as changes in land use/land cover over time. In the early 2000s, the Special Report on Emission Scenarios (SRES, IPCC 2000) pathways of emissions scenarios were used. Later, the IPCC adopted the Representative Concentration Pathways (RCPs, van Vuuren et al., 2011, Moss et al., 2010) approach, which are plausible pathways to reaching a specific radiative forcing trajectory and include data on GHG emissions and land use/land cover over time. Following an intensive selection process, four RCPs were adopted that map a broad range of climate outcomes which span a range of radiative forcing scenarios into the future (Moss et al., 2010). The RCPs range from RCP2.6 to RCP8.5 (**Table 2.1**), where RCP2.6 is the scenario with low radiative forcing which begins to decline after 2100 while RCP4.5 and RCP6.0 show a stabilization of radiative forcing after 2100. RCP8.5 has continued increases in radiative forcing due to rising GHG emissions, notwithstanding declines in emissions growth rates in the second half of the century (IPCC, 2014).

More recently, in the process of generation of IPCC AR6 (with the report on physical climate science released in July 2021), a new set of scenarios were introduced – Shared Socioeconomic Pathways (SSP, Riahi et al. 2017). These scenarios are based on integrative RCP-SSP framework, where climate

projections are generated using GCMs as earlier, i.e. based on RCP greenhouse gas emissions or concentrations, but these projections can be analysed against the backdrop of various socio-economic scenarios that lead to a particular emission trajectory. The "pathways" capture five different trajectories of socioeconomic factors such as population, economic growth, education, urbanisation, the rate of technological development and globalization. Each of those trajectories offers different challenges to climate change adaptation and mitigation, and may lead to a different level of emissions, depending on the level of mitigation policies. In effect, the SSP framework is a "mix-and-match" of different emission pathways, socio-economic realities and mitigation efforts. Importantly, only certain emission trajectories (RCPs) are possible for individual socio-economic paths, as these paths allow only certain level of mitigation efforts.

The SSP scenarios are by design conceptually compatible with the previous generation RCP scenarios, as they incorporate RCP emission trajectories at their core. Thus, even though the SSP scenarios are not used in this project due to the unavailability of GCM projections generated under these scenarios at the time this project was initiated, it is possible to conceptually link and compare SSP and CMIP5 RCP projections.

Table 2.1   The RCP scenarios adopted by the IPCC (Moss et al., 2010)

Name	Radiative forcing	Concentration (p.p.m.)	Pathway	Model providing RCP*	Reference
RCP8.5	$>8.5\,\mathrm{W\,m^{-2}}$ in 2100	$>1,370\ CO_2$-equiv. in 2100	Rising	MESSAGE	55,56
RCP6.0	$\sim6\,\mathrm{W\,m^{-2}}$ at stabilization after 2100	$\sim850\ CO_2$-equiv. (at stabilization after 2100)	Stabilization without overshoot	AIM	57,58
RCP4.5	$\sim4.5\,\mathrm{W\,m^{-2}}$ at stabilization after 2100	$\sim650\ CO_2$-equiv. (at stabilization after 2100)	Stabilization without overshoot	GCAM	48,59
RCP2.6	Peak at $\sim3\,\mathrm{W\,m^{-2}}$ before 2100 and then declines	Peak at $\sim490\ CO_2$-equiv. before 2100 and then declines	Peak and decline	IMAGE	60,61

* MESSAGE, Model for Energy Supply Strategy Alternatives and their General Environmental Impact, International Institute for Applied Systems Analysis, Austria; AIM, Asia-Pacific Integrated Model, National Institute for Environmental Studies, Japan; GCAM, Global Change Assessment Model, Pacific Northwest National Laboratory, USA (previously referred to as MiniCAM); IMAGE, Integrated Model to Assess the Global Environment, Netherlands Environmental Assessment Agency, The Netherlands.

When these RCP pathways are used as input to the various GCMs a picture of the plausible global average surface temperatures into the future is created (**Figure 2.1**). The projected increase of global mean surface temperature, as determined by multi-model simulations, is likely to be 0.3-1.7°C higher by the end of the 21st century (2081-2100) relative to 1986-2005 under RCP2.6, 1.1-2.6°C under RCP4.5, 1.4-3.1°C under RCP6.0 and 2.6-4.8°C under RCP8.5 (**Figure 2.1**). However, the divergence in the projected changes in temperature, especially considering the uncertainty bands, is only strongly evident from approximately 2050 onwards.
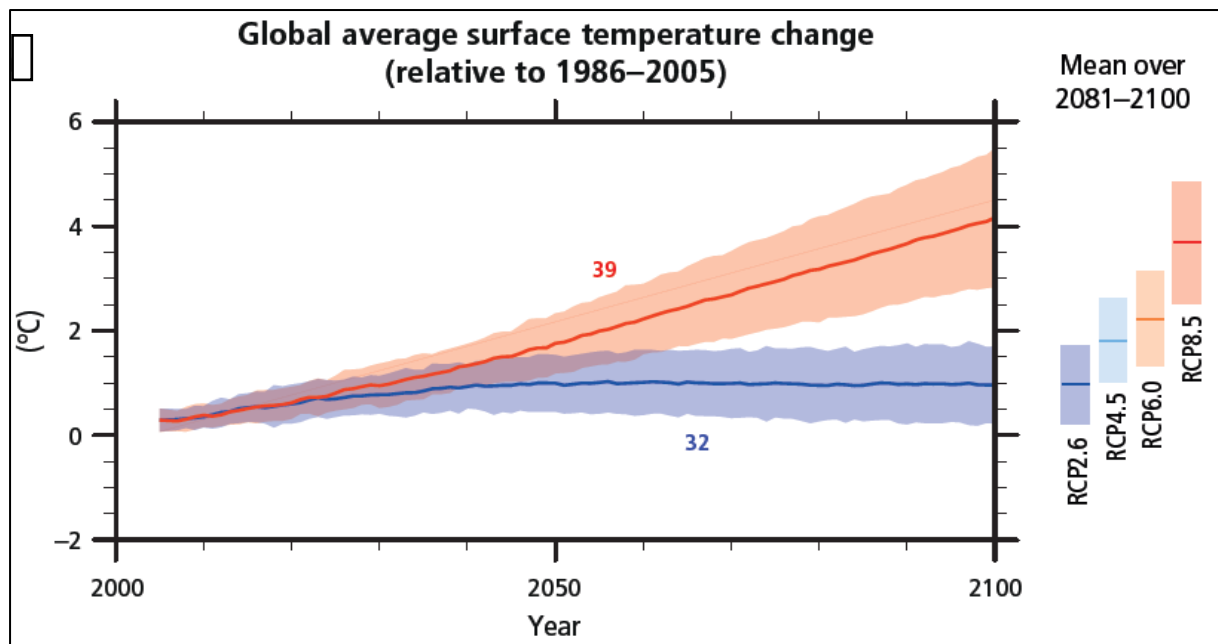
Figure 2.1   Global average surface temperature change from 2006-2100, relative to 1986-2005, as determined by multi-model simulations, with time series of projections and a measure of uncertainty (shading) shown for scenarios RCP2.6 (blue) and RCP8.5 (red), and the mean and associated uncertainties averaged over 2081-2100 given for all RCP scenarios as coloured vertical bars at the right-hand side (IPCC (2014)

Assessment of the output from the 63 simulations in the CMIP5 ensemble indicates that land temperatures over Africa are projected to rise faster than the global land average (Niang et al., 2014). This faster rise in temperature is likely to be more apparent in arid regions and, as such, temperature changes in northern and southern Africa are likely to be larger than those in central Africa (Niang et al., 2014). Increases of 3-6°C above the 1986-2005 mean average land surface temperature for the SADC region under the RCP8.5 scenario are projected by 2100 (**Figure 2.2**). A similar picture of divergence, as evident at the global scale, in the projected changes after 2050 is also evident when considering the SADC region.
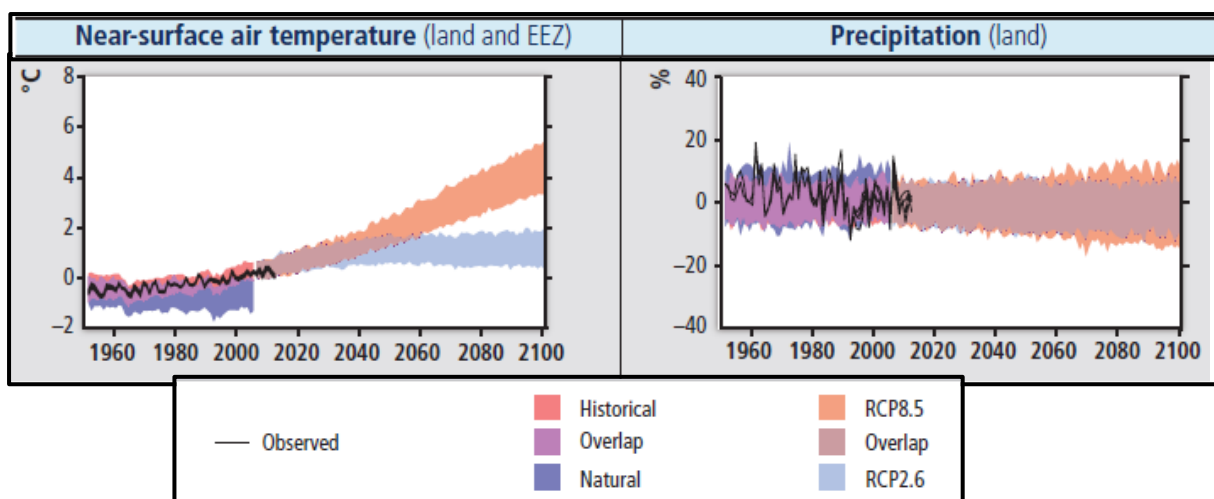
Figure 2.2   Observed and simulated variations in past and projected future annual average temperature over the Southern African Development Community (SADC), with black lines showing estimates from observational measurements and shading denoting 5th to 95th percentile range of climate model simulations (Niang et al., 2014)

GCMs generate relatively accurate projection of changes in temperatures owing to their ability to model physical processes responsible for heating and the clear physical link between greenhouse gas concentrations and air temperature (Archer et al., 2018). Unfortunately, these strengths do not transfer to the projections of changes in rainfall and other climatic variables within a region, because of the large spatial scale of approximately 150-300 km at which the GCMs are applied, which imposes the need to parameterize (describe by empirical functions with coefficients that cannot directly be measured) processes leading to formation of precipitation (Garland et al., 2015).This leads to the well-known characteristic of climate projections, whereby temperature projections are relatively precise and constrained, but rainfall projections are highly uncertain.

Projected climate changes over southern Africa depend on the future period that is being assessed. However, the general pattern from the GCMs and downscaled models show that there will be a combination of changes in average temperature and rainfall, as well as changes in the frequency and intensity of occurrence of extreme events. For the period 2041-2070, simulations of means by GCMs, both statistically and dynamically downscaled models for RCP scenarios collectively indicate a reduction in rainfall and an increase in temperatures (Davis-Reddy and Vincent, 2017).

In terms of temperature, CCAM downscaling project rising temperatures of 2-4°C by the end of the century (Garland et al., 2015). In agreement with the global GCM simulations, an analysis of the regions' projections show a rapid increase in surface temperatures at a rate approximate 1.5-2 times faster than that of the global rate, with the interior trends ranging 2.0-3.6°C warmer (Engelbrecht et al., 2015). More recent CCAM projections continue to agree with the more rapid warming relative to other areas, and temperature increases of up to 6°C by the end of the century in the interior of the country were shown (Archer et al., 2018; **Figure 2.3**). Such high temperature increases suggest the region will become drier (Niang et al., 2014).

Rainfall projections are not as straightforward and are far less certain than those of temperature, with some models suggesting an increase over some parts and decrease over others of southern Africa. However, there is a general consensus that the north will become predominantly wetter and the south drier (Jury, 2013). For example, in a study to project temperatures in the region using 14 GCMs, significant negative differences in rainfall only become apparent in three models around 2016, with 10 models indicating mean drying by 2050 (Davis-Reddy and Vincent, 2017). Similarly, Archer et al. (2018) showed drying over South Africa by 2100, relatively consistent across the analysed ensemble (**Figure 2.4**). The southwestern Cape emerged as an area of consistent rainfall decreases across all six downscaled GCM projections, with this drying being associated with a poleward displacement of the westerlies and frontal systems (e.g. Christensen et al., 2007; Engelbrecht et al., 2009). Five of the downscaled GCMs agreed on drier conditions along the eastern coast and interior by 2100 (Archer et al., 2018; **Figure 2.4**). Analyses of a broader ensemble of global and downscaled projections reveal consistent drying in the western part of the country, but possible wetter conditions in DJF in the east (Fig. 4 in Dosio et al. 2021). The latter is indicated consistently by medians of CORDEX, CMIP5 and CMIP6 ensembles, but importantly the range of projected rainfall changes span both increases and decreases in the future. Similar results emerge from analyses by Almazroui et al. (2020) (see Fig. 10 in that paper).
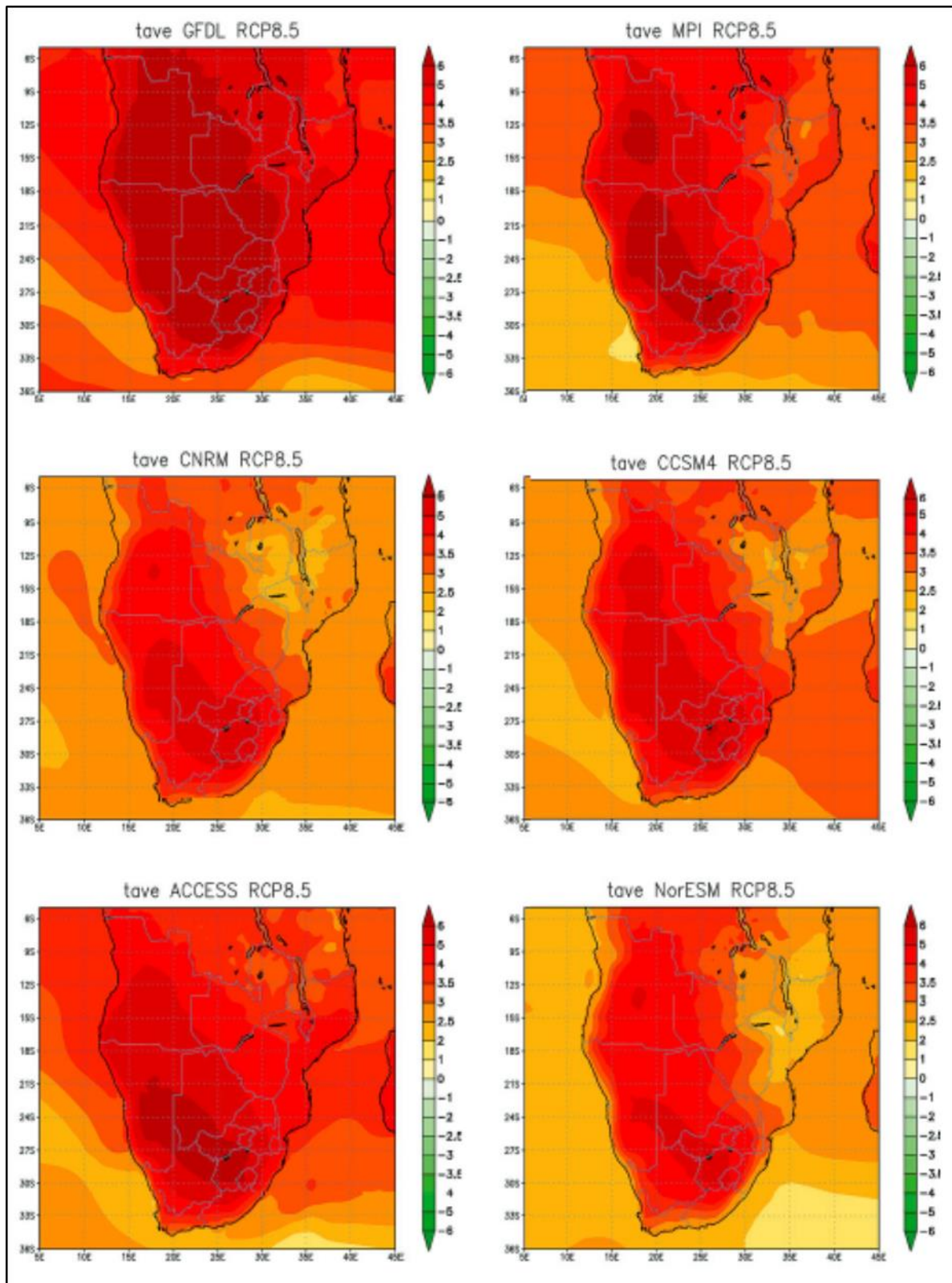
Figure 2.3   CCAM (50 km resolution, six different GCMs) projected changes in the annual average temperatures (°C) over southern Africa for the time period 2080-2099 relative to 1971-2000 under RCP8.5 (Archer et al., 2018)
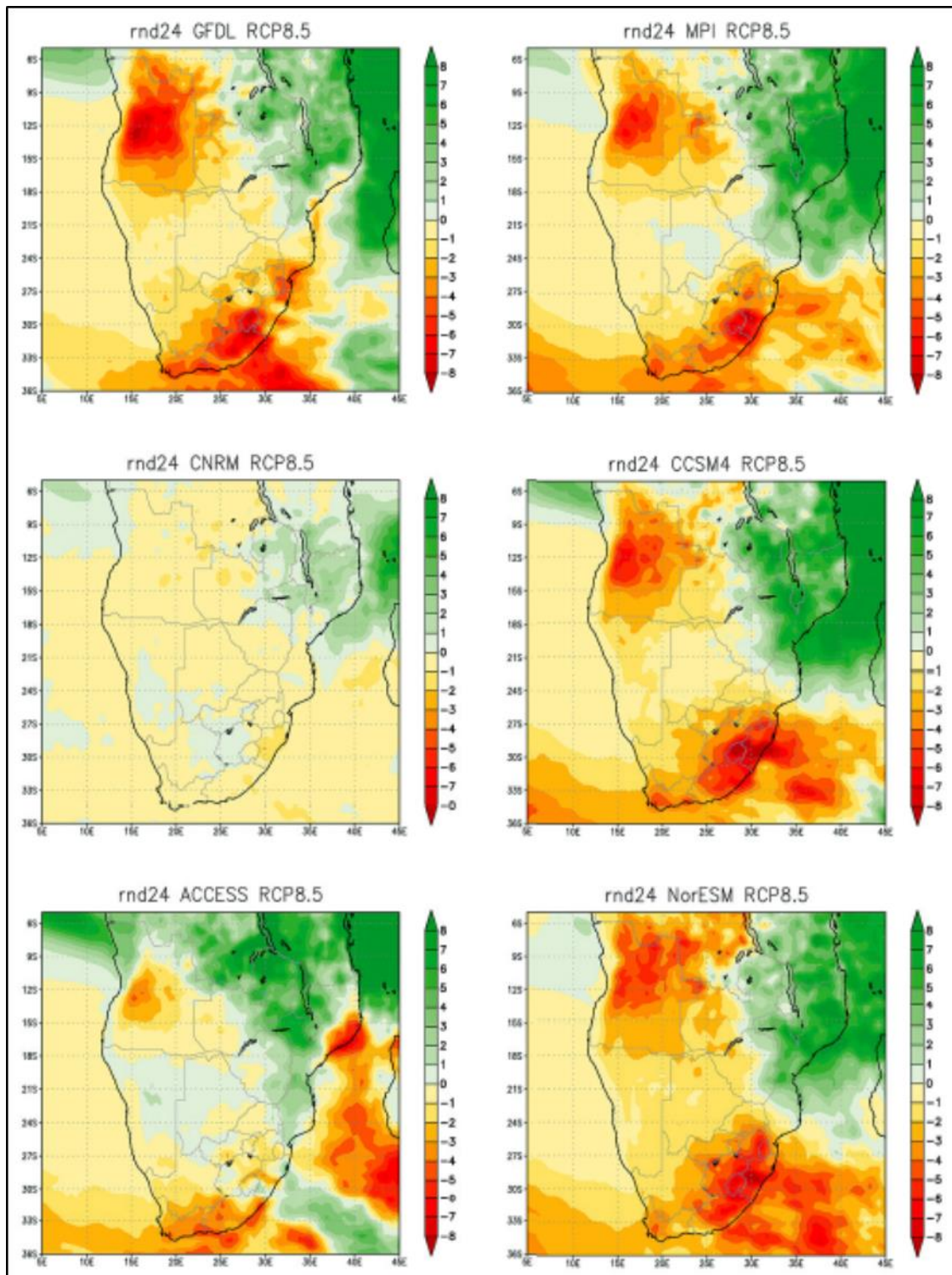
Figure 2.4   CCAM (50 km resolution, six different GCMs) projected changes in annual average rainfall totals (units *10 mm/day) over southern Africa for the time period 2080-2099 relative to 1971-2000 under RCP8.5 (Archer et al., 2018)

The changes in temperature and rainfall have a direct relationship to the frequency and magnitude of extreme events such as high temperatures and heavy rainfall events. For example, tropical cyclone tracks are projected to shift northward, bringing more flood events to northern Mozambique and fewer to the Limpopo province in South Africa (Malherbe et al., 2013). Poleward displacement of the westerly wind regime could cause a decrease in the occurrence of cut-off low related flood events over South

Africa. It is plausible that intense thunderstorms may occur more frequently over South Africa in a generally warmer climate (Archer et al., 2018). The regional changes in circulation that are plausible over southern Africa, in particular an increase in the frequency and intensity of mid-level high-pressure systems, may plausibly induce the more frequent occurrence of heat wave events over the region (Engelbrecht et al., 2015; Garland et al., 2015). It is well recognized that anthropogenic climate change and transformation of the mid-latitude westerlies was underlying the 2015-2017 Cape Town "Day Zero" drought (Otto et al. 2018).

2.1.3   Climate projections used in past South African hydrological impact studies

A number of national hydrological impact studies have been conducted in South Africa. These commenced with the US-funded South African Country Studies on Climate Change which was conducted from 1998 to 2000 (Kiker, 2000). This project utilised climate projections based on four GCMs that had been downscaled using scale transfer functions derived from observational data.

This was followed over the next 18 years by a series of WRC funded projects (Schulze, 2005; Schulze et al., 2010; Schulze, 2012) as well as a DAFF and a GIZ funded project (Schulze, 2017; Schulze and Davis, 2018). During this period, there were also hydrological impact studies covering specific catchments, but where climate projections had been developed at a national level (e.g. Malherbe et al., 2013; Schulze et al., 2013; Warburton et al., 2010; Schulze and Davis, 2015; Schulze and Davis, 2018).

In all of the WRC funded studies, the approach to developing regional climate projections involved statistical downscaling (employed by CSAG) and dynamical downscaling (employed by CSIR) of GCM projections produced in the third, fourth and fifth IPCC assessment reports (termed the TAR, AR4 and AR5), mostly based on the CMIP3 archive of GCM outputs. The CSAG approach was based on Self Organizing Map Downscaling (SOMD), which classified observed synoptic drivers of weather into different states and then characterised local station responses (observed rainfall or temperature) for each of the states. These statistical relationships were then applied to GCM projected fields to develop the downscaled projections. The CSIR approach was based on the application of the variable resolution Conformal-Cubic Atmospheric Model (CCAM) which was used to downscale the coarse resolution GCM projections.

Other climate projections that have been used in large scale hydrological impacts studies in South Africa include those developed for the Treasury and the National Planning Commission (2013) and summarised in the Long Term Adaptation Scenarios (2013) project. These were derived from a Hybrid Frequency Distribution (HFD) analysis of all possible general circulation model (GCM) outputs (+6 000 scenarios) for an unconstrained emissions scenario (UCE) and a level 1 stabilisation (L1S) emissions scenario. The large number of GCM outputs considered in the approach allowed for a robust estimate of the range of uncertainty in projected future climate to be made.

2.1.4   Climate projections available for current hydrological impact studies

The downscaled climate projections available for current hydrological impact studies are based on the CMIP5 archive of GCM simulations. These projections are discussed below in more detail.

Coordinated Regional Downscaling Experiment (CORDEX) Projections
The CORDEX programme has recently focused on Africa, resulting in a large number of downscaled projections being available for the continent. These projections are mostly dynamically downscaled and have been developed by research groups around the world. While the CORDEX data sets are a valuable resource, it is important to note that participation in the programme required all groups to develop projections for Africa in addition to any other region of interest to them. This implies that many of the research groups may have had little experience in modelling regional African climates.

CSAG Projections

In recent years the CSAG downscaling approach has moved away from the SOMD approach to downscaling, which was motivated by several factors. One is that the development of statistical downscaling procedures was driven by the very urgent need for this type of information during the end of 1990s and early 2000s, but was not necessarily supported by a good understanding of the limitations and constraints of the approach. Results emerging from recent comprehensive projects focusing on assessments of the value of statistical downscaling, such as VALUE-COST, highlighted these. While there is a value in generating statistically downscaled information at a point scale, capturing of spatial aspects of projections remains a challenge. This, in hydrological or similar applications, may counter gains obtained from site specific assessments.

It is important to note that dynamical downscaling approaches, as represented by CORDEX, are currently at the stage where statistical downscaling was some 10-15 years ago, i.e. at the stage where downscaled data started being used by a broader community in a variety of contexts, and are thus increasingly subject to scrutiny and evaluation. Whether these projections carry the anticipated value, or share the fate of statistical downscaling, will remain to be seen.

In view of the above, CSAG has adopted a more conservative, but likely a more robust approach, and now uses a stochastic delta factor method. This involves using a stochastic rainfall generator to modify observational time series of weather variables according to changes in means, variances, autocorrelations and spatial correlations between stations/ catchments. The approach essentially preserves the GCM signal, but because of the stochastics involved, provides a slightly better idea of the uncertainty of indices that are not explicitly accounted for in the process. The approach yields downscaled projections at a monthly time-step, but not yet at a daily time-step. However, the SOMD approach has not been abandoned altogether, however, and plans are in the pipeline to re-develop it with a view to possible re-introduction. Due to the character and nature of the hydrological modelling envisaged for this project, however, neither of the approaches could be used.

CSIR Projections

An ensemble of very high-resolution climate model simulations of present-day climate and projections of future climate changes over South Africa were produced by the CSIR (Engelbrecht, 2019; Engelbrecht et al., 2020), from now on called CSIR CCAM projections. As in previous work at the CSIR, the CCAM regional climate model was used to develop the downscaled projections. This model was developed by the Commonwealth Scientific and Industrial Research Organisation, CSIRO (McGregor, 2005; McGregor and Dix, 2001; 2008). CCAM runs are coupled to a dynamic land-surface model CABLE (CSIRO Atmosphere Biosphere Land Exchange model). Six GCM simulations from the CMIP5 archive based on the emission scenarios described by RCPs 4.5 and 8.5 were first downscaled to a 50 km spatial resolution globally. The selection of these six GCMs was based on their ability to provide a reasonable representation of the El Nino-Southern Oscillation (ENSO) phenomenon for the region. The simulations span the period 1961-2100 and RCP4.5 is a high mitigation scenario, whilst RCP8.5 is a low mitigation scenario. The six downscaled GCMs are the:

- Australian Community Climate and Earth System Simulator (ACCESS1-0);
- Geophysical Fluid Dynamics Laboratory Coupled Model (GFDL-CM3);
- National Centre for Meteorological Research Coupled Global Climate Model, v5 (CNRM-CM5);
- Max Planck Institute Coupled Earth System Model (MPI-ESM-LR);
- Norwegian Earth System Model (NorESM1-M); and the
- Community Climate System Model (CCSM4).

The simulations were performed on supercomputers located in the Centre for High Performance Computing (CHPC) based at the CSIR's Meraka Institute. In these simulations CCAM was forced with the bias-corrected daily sea-surface temperatures (SSTs) and sea-ice concentrations of each host GCM

model, and with CO_2, sulphate and ozone forcing consistent with the RCP4.5 and RCP8.5 scenarios. The model's ability to realistically simulate present-day southern African climate has been extensively demonstrated (e.g. Engelbrecht et al., 2009; Engelbrecht et al., 2011; Malherbe et al., 2013; Winsemius *et al*., 2014; Engelbrecht et al., 2015).

Most of the current coupled GCMs do not employ flux corrections between the atmosphere and ocean, which contributes to the existence of biases in their simulations of present-day SSTs, with these being more than 2ºC along the West African coast. An important feature of the downscaling with the CCAM model, however, was that the model was forced with bias-corrected sea-surface temperatures (SSTs) and sea-ice fields from the GCMs. The bias is computed by subtracting for each month the Reynolds (1988) SST climatology (for 1961-2000) from the corresponding CGCM climatology. The bias-correction is applied consistently throughout the simulation. Through this procedure the climatology of the SSTs applied as lower boundary forcing is the same as that of the Reynolds SSTs. However, the intra-annual variability and climate change signal of the CGCM SSTs are preserved (Katzfey et al., 2009).

For the CSIR CCAM projections, a multiple-nudging strategy was followed to obtain 8 km resolution downscalings. After completion of the 50 km resolution simulations described above, CCAM was integrated in stretched-grid mode over South Africa at a resolution of about 8 km (~ 0.08° degrees in latitude and longitude). The high-resolution component of the model domain was about 2000 x 2000 km^2 in size. The higher resolution simulations were nudged within the quasi-uniform global simulations, through the application of a digital filter using a 600 km length scale. The filter was applied at six-hourly intervals and from 900 hPa upwards (Engelbrecht, 2019; Engelbrecht et al., 2020).

To enhance the plausibility of projections of changes in extreme temperature events and the water balance, it is useful to first bias-correct the model simulations of temperature and rainfall, to remove any systematic errors in the simulation of the amplitudes of these fields (e.g. Teutschbein and Seibert, 2012). Leaving such biases unchecked may otherwise, for example, affect the calculation of the frequencies of exceedance of thresholds. A simple monthly scale mean bias-correction procedure was applied (Winsemius et al., 2014; Engelbrecht and Engelbrecht, 2015). The monthly climatologies for average temperature (defined as the average of minimum and maximum temperature for the month) and rainfall over the period 1961-1990 were used as reference climatologies. Each of the six downscalings was subsequently interpolated to a 0.5° latitude-longitude grid in order to facilitate the generation of gridded bias-corrected simulations (Winsemius et al., 2014; Engelbrecht and Engelbrecht, 2015). After calculation of the monthly climatologies of average temperature and rainfall totals for each downscaling, the corresponding monthly biases were calculated for all variables (with respect to the corresponding monthly climatologies). The simulated daily precipitation values over the full period 1961-2100 were subsequently bias-corrected for each downscaling (using a multiplicative factor unique to each month of the year, defined as the ratio of the observed monthly rainfall climatology for 1961-1990 to the corresponding simulated climatology of the particular downscaling).

The daily minimum and maximum temperatures were bias corrected using a similar procedure, with the only difference being that the monthly correction factor was additive. In this case, the temperature correction factor for a specific month is simply the relevant monthly climatology of the downscaling subtracted from the corresponding observed monthly climatology (the same additive correction is applied to the maximum temperatures). The net result of this bias correction procedure is that the monthly climatologies of each of the bias-corrected downscalings exactly represent the climatologies for rainfall, temperature and humidity for the period 1961-1990, i.e. the period over which the biases are calculated. However, the inter-annual variability in the monthly climatologies of the host GCMs is preserved, and the daily statistics of average temperature, maximum temperature and rainfall will remain to differ from one downscaling to the next (depending on the internal variability of the respective downscaled climatologies). Climate change anomalies are therefore calculated separately for each downscaling with respect to its own present-day climatology. It should be noted that the simulated

trends in annual average temperature for the bias-corrected data correspond closely to those calculated for the raw (non-bias-corrected) data.

2.1.5   Climate projections used for this study

Given the wealth of expertise in climate modelling over South Africa that is represented in the project team, and the advancement in the skill and nature of dynamical projections, it was decided that the projections developed by CSIR would be used in the project in preference to those in the CORDEX repository and statistically downscaled ones. Apart from the benefit of local climate knowledge that is represented in the CSIR projections, the resource-intensive nature of assessing hydrological impacts at national scale also limits the number of climate projections that can be considered in the project.

The daily CCAM climate projections were applied in the *ACRU* daily time-step hydrological model (Schulze, 1995; Smithers and Schulze, 2004 and updates) to develop the hydrological projections for this project. The results are shown later in Chapter 4 for the climatic variables of rainfall, temperature and potential evaporation, and the results for the hydrological responses in Chapter 5. Projections for both RCP4.5 and RCP8.5 mitigation scenarios were considered for this study. It is noted that the RCP scenarios only diverge significantly in their projections after approximately 2050. Until 2050, the variation among the available GCM projections is greater than the difference between the RCP scenarios considered. This is illustrated in **Figure 2.5** which shows WMA rainfall anomalies for ensemble GCM simulations from the CMIP5 archive, under RCP4.5 and RCP 8.5 scenarios.
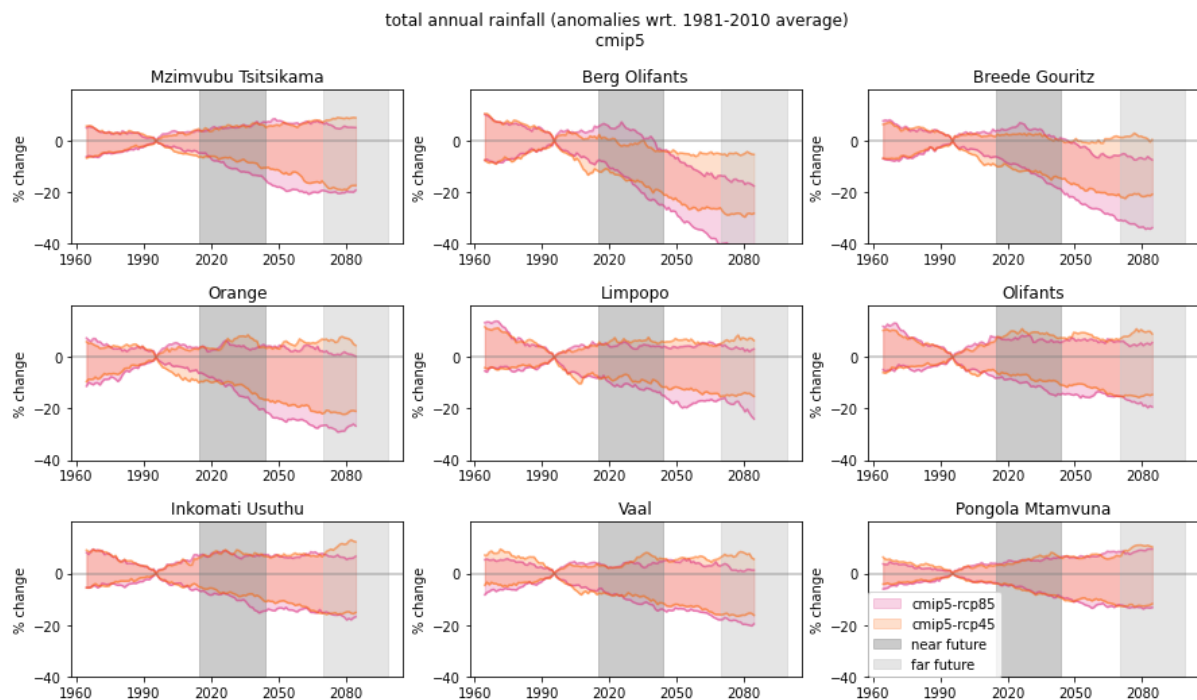
Figure 2.5   90-percentile range of 30-year running means of anomalies in total annual rainfall relative to 1981-2010 based on multi-model historical simulations and projections from CMIP5 archive, under two RCP scenarios, *viz.* 4.5 and 8.5 , for each of the WMAs

Recognizing that the ensemble of projections implemented in this study is relatively small (6 members, compared to ~33 members in CMIP5, 24 in CORDEX and ~34 members in CMIP6), and thus likely underestimates the level of uncertainty of projections, in **Figure 2.6** we illustrate how the adopted projections compare with projections from broader ensembles, including the most recent, CMIP6 archive.

It is clear from that figure, that indeed, the six models selected as a basis for climate projections in this project span a much narrower range of future rainfall changes than other, larger ensembles. They do, however, capture the principal tenets of the overall direction of future change as robustly projected across the three other ensembles – the strong drying in the Western Cape WMAs, weak drying in Limpopo, Olifants and Mzimvubu-Tsitsikama, and lack of clear signal elsewhere.

While the narrower spread of the CSIR CCAM ensemble might be disconcerting, one has to consider that the 6 GCM models that the basis for CSIR CCAM ensemble were selected because they represented historical climate best. An argument can thus be made that the narrower uncertainty of projections by that ensemble is actually a better representation of the future than that of the entire CMIP5 GCM ensemble.
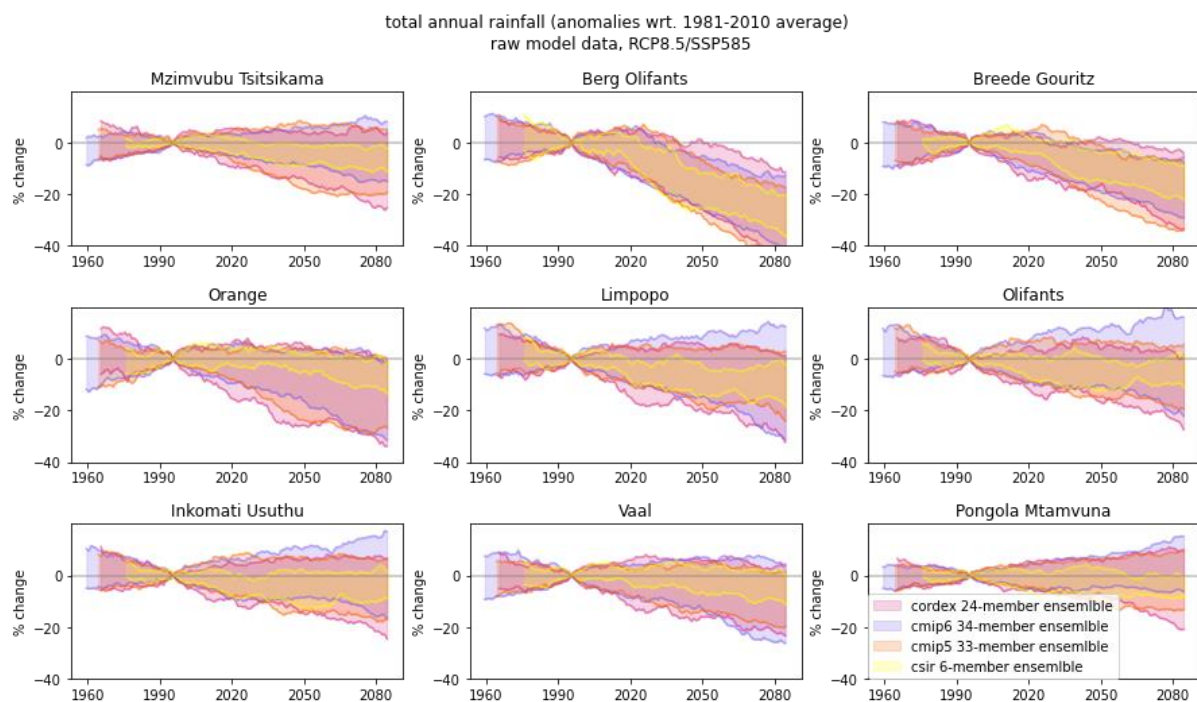
Figure 2.6   90-percentile range of 30-year running means of anomalies in total annual rainfall relative to 1981-2010 based on multi-model historical simulations and projections under RCP 8.5 and comparable SSP5-85 scenario, from CMIP5, CMIP6, and CORDEX archives, and CSIR CCAM projections adopted in this project

2.2   Revised Quinary Catchments Climate Database

2.2.1   Background to the Quaternary Catchment driver rainfall stations

The *ACRU* agrohydrological model (Schulze, 1995; Smithers and Schulze, 2004; and updates) has previously been applied in South Africa to evaluate the hydrological impacts of climate change (e.g. Schulze, 2005; 2008; Schulze et al., 2010; Schulze, 2012; Warburton et al., 2010; Schulze, 2013; Schulze et al., 2013; Schulze, 2017; Schulze and Davis, 2015; 2018). These applications made use of the Southern African Quaternary Catchments Database, QCDB, (Schulze et al., 2005) and subsequently the Southern African Quinary Catchments Database, QnCDB (Schulze et al., 2010; Schulze, 2012) to configure the *ACRU* model for the whole of South Africa and including Lesotho and Eswatini (formerly Swaziland). The Department of Water and Sanitation (DWS) uses a hierarchical system of catchments, composed of 22 Primary Catchments containing nested sets of Secondary,

Tertiary and Quaternary Catchments. The QCDB contains, for each of the 1 946 Quaternary Catchments, a set of default climate, land cover and soils data for use in the *ACRU* model. The land cover information is for natural vegetation only and relates to the Acocks' (1988) Veld Types. In the QnCDB each Quaternary Catchment has been sub-delineated into three altitude-based zones termed "Quinary Catchments", based on natural breaks in altitude, resulting in 5 838 Quinary Catchments. These altitude-based Quinary Catchments enable the differences in climates between the upper, middle and lower portions of Quaternary Catchments to be represented.

A typical approach to using historical rain gauge measurements in the *ACRU* model is to assign a so-called "driver" rain gauge to each catchment and then to apply a set of 12 month-by-month rainfall correction factors to the rainfall values at the driver rain gauge to provide an estimate of catchment rainfall. These rainfall correction factors are determined by calculating the ratio of the median monthly rainfall in a catchment to the median monthly rainfall at the driver rain gauge. A driver rain gauge was assigned to each Quaternary Catchment, and the same driver rain gauge assigned to a Quaternary Catchment was assigned to the three Quinary Catchments within it. The 1 946 Quaternary Catchments are represented by 1 240 driver rain gauges. However, a different set of 12 month-by-month rainfall correction factors was derived for each individual Quinary Catchment. The historical rainfall data used in both the QCDB and the QnCDB were obtained from the rainfall database developed by, and described in, Lynch (2004) containing 50 years (1950-1999) of historical daily rainfall data for rain gauges in South Africa. The reliability of the daily rainfall data at the driver stations used in the QCDB and QnCDB is shown in **Figure 2.7**.

The Quinary level Climate Database (QnCDB) was originally developed in 2010 as described by Schulze et al. (2011). Since 2011, this database has been used extensively to simulate hydrological and agricultural response under historical climate conditions from 1950 to 1999. Recently, the climate database was significantly revised, especially the temperature and reference evapotranspiration data, which is summarised below. For more detail, the reader is referred to Kunz et al. (2020).
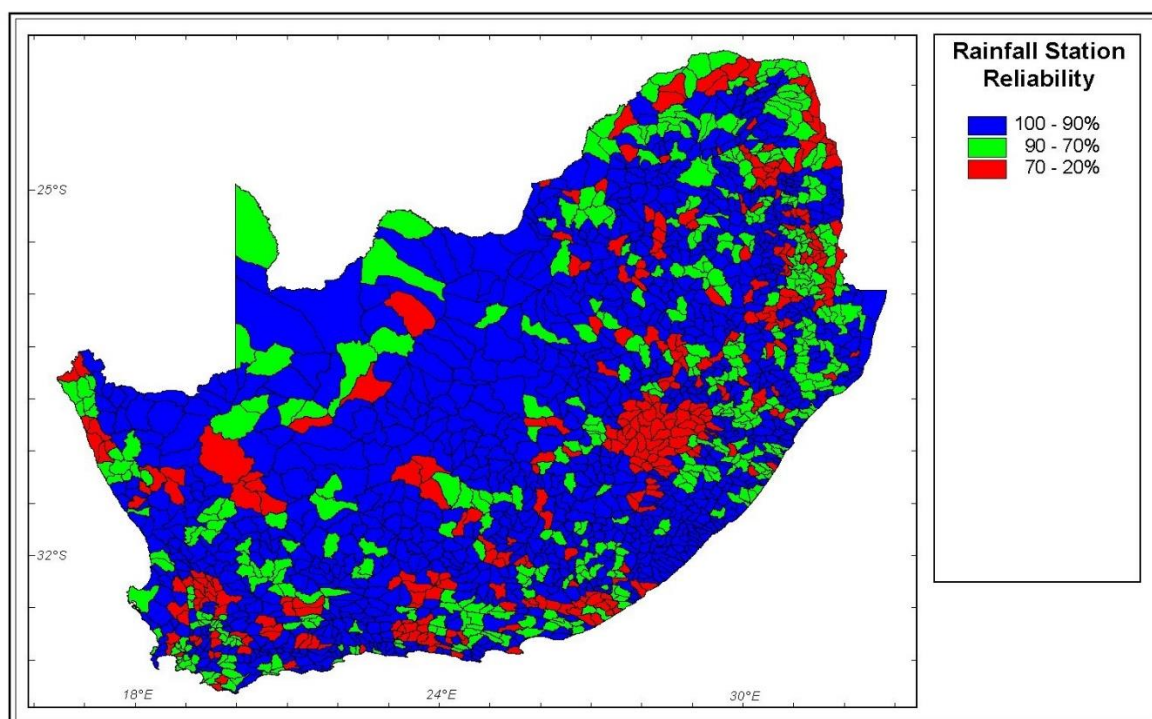
Figure 2.7   Reliability of the daily rainfall data at the driver stations used in the QCDB and the QnCDB (Warburton and Schulze, 2005)

2.2.2 Rainfall

Schulze et al. (2011) described the selection of a representative driver rainfall station from the Lynch (2004) dataset for each Quaternary Catchment. In total, 1 240 stations were selected to represent all 1 946 Quaternaries, of which the majority are owned by SAWS. The rain gauge selected to drive each Quaternary was chosen for each of the three Quinaries. For each Quinary, monthly adjustment factors were derived to enable estimation of catchment rainfall from driver station rainfall. This was done by comparing the driver station's median monthly rainfall to that derived for each Quinary using spatial estimates of median monthly rainfall developed by Lynch (2004). The monthly adjustment factors are used to derive rainfall estimates deemed more representative of each Quinary catchment (Schulze et al., 2011).

More recently, the observed daily rainfall data selected to represent each quinary was scanned to identify extreme rainfall events exceeding 400 mm. Each of the 13 extreme events was manually compared to rainfall data from 10 neighbouring rain gauges, which resulted in four daily events being adjusted downward, e.g. from 440 to 44 mm and 585 to 85.5 mm (Kunz et al., 2020).

2.2.3 Temperature

The original QnCDB utilised daily data extracted from a modelled temperature dataset developed by Schulze and Maharaj (2004) for over 437 000 grid points (each point representing one minute by one minute of a degree arc) across southern Africa. The grid point selected to represent each quinary exhibited a similar altitude to the catchment mean that was closest to the catchment centroid. Temperature data for each grid point was determined from two stations selected from a dataset of 973 stations with observed daily values.

Recently, observed temperature data was determined for each quinary as follows (Kunz et al., 2020):

- The observed temperature database developed by Schulze and Maharaj (2004) was screened to remove 275 "duplicate" stations (at similar locations and altitudes), which reduced the total number of stations from 973 to 698.
- The distance from each rainfall driver station to surrounding temperature stations was computed, together with the altitude difference between the two locations (i.e. stations).
- An algorithm then used these two metrics to determine the best temperature station to represent each rainfall driver station. In other words, a "pseudo" temperature station was assigned to each rain gauge.
- Of the 698 unique temperature stations, 543 were chosen to represent all 1 240 driver rain gauges. This means that the same temperature station was selected for up to 10 rain gauges.

Ideally, 114 temperature stations had the same SAWS ID as the rain gauge, meaning that both rainfall and temperature were measured at the same climate station. Similarly, a total of 184 temperature stations were within 1 minute (~1.7 km) of the rain gauge, with altitude differences ranging from 1 to 338 m. Approximately 95% of the selected temperature stations were situated within 30 minutes (~51 km) of the rainfall driver stations, with the furthest station being 52.5 minutes (~89 km) away (Kunz et al., 2020).

Lapse rate adjustment
The altitudinal differences between the temperature stations selected to represent a particular driver rain gauge (DALT) are shown in the **Table 2.2** below, with the worst case exceeding 950 m for two stations.

Table 2.2   Histogram of altitude difference from each rain gauge to the selected (best) temperature station (Kunz et al., 2020)

DALT (m)	Count	% of Total	Accumulated %
< 50	524	42.26	42.26
050-100	256	20.65	62.90
100-150	148	11.94	74.84
150-200	91	7.34	82.18
200-250	65	5.24	87.42
250-300	43	3.47	90.89
300-350	25	2.02	92.90
350-400	24	1.94	94.84
400-450	20	1.61	96.45
450-500	6	0.48	96.94
500-550	14	1.13	98.06
550-600	9	0.73	98.79
600-650	4	0.32	99.11
650-700	4	0.32	99.44
700-750	4	0.32	99.76
750-800	1	0.08	99.84
800-850	0	0.00	99.84
850-900	0	0.00	99.84
900-950	0	0.00	99.84
> 950	2	0.16	100.00
Total	1 240	100.00	

A lapse rate adjustment was applied to account for the altitude difference between the pseudo temperature station selected for each rain gauge. This dataset was used for bias correction of GCM climate projections (cf. Section 2.3).

Thereafter, a second lapse rate adjustment was applied to account for the altitude difference between the selected temperature station and the average altitude across each Quinary it represents. This dataset was then used to develop the revised QnCDB.

2.2.4   Reference evapotranspiration

Daily solar radiation, as well as relative humidity (maximum and minimum) values, were then generated from the lapse-rate adjusted temperatures using the method described by Schulze et al. (2011). Owing to the lack of available wind speed data, a daily default value of 2 m s^{-1} was used, as suggested by Allen et al. (1998). Daily reference evapotranspiration values (ET$_O$) were then calculated using the FAO56 version of the Penman-Monteith equation (Allen et al., 1998). Monthly adjustment factors developed by Kunz et al. (2015) were used to derive A-pan equivalent evaporation estimates as required by the *ACRU* model.

2.2.5   Summary

The recently revised QnCDB consists of 50 years of observed rainfall and temperature (maximum and minimum) data that were adjusted to better represent each Quinary Catchment. This database also contains reference evapotranspiration (FAO56 and A-pan equivalent) for each Quinary. For this project, the QnCDB was used to determine baseline hydrological conditions against which potential impacts of climate change were assessed. A modified version was used to bias correct the projected climate data.

2.3   Bias Correction of Daily CCAM Rainfall and Temperature Projections

The bias correction of the selected daily time step climate projections (derived from the CCAM model) is addressed in this section with a focus on rainfall and temperature. An outline of the CCAM projected datasets is first given. This is followed by the development and evaluation of the rainfall bias correction methodology. Finally, a brief discussion of the proposed methodology to perform bias and lapse rate corrections of temperature is provided.

2.3.1   Outline of CCAM projection datasets

In the introduction to this Report (Section 2.1) it was stated that six GCM simulations from the CMIP5 archive based on the Representative Concentration Pathway (RCP) scenarios 8.5 and 4.5 would be considered for use in hydrological modelling with the *ACRU* hydrological model, with ideally all six GCMs to be applied in hydrological modelling, but at minimum three would be used, depending on resource availability. To recap, the six GCMs are the:

- Australian Community Climate and Earth System Simulator (ACCESS1-0);
- Community Climate System Model (CCSM4);
- National Centre for Meteorological Research Coupled Global Climate Model, v5 (CNRM-CM5);
- Geophysical Fluid Dynamics Laboratory Coupled Model (GFDL-CM3);
- Max Planck Institute Coupled Earth System Model (MPI-ESM-LR); and the
- Norwegian Earth System Model (NorESM1-M).

The CCAM variable resolution climate model was applied by the CSIR to each of the six selected GCM datasets to develop very high-resolution (0.1º) climate model simulations of present-day climate and projections of future climate changes over South Africa for 140 years from years 1961-2099. The GCM data values for RCP4.5 and RCP8.5 are the same for the period 1961-2004, as emissions do not diverge during this period. The datasets were stored in NetCDF format, with one NetCDF file representing each month in the time series that contains daily data for that month in grids consisting of 231 columns and 161 rows (representing longitude and latitude, respectively). Each NetCDF file contained three dimensions, used to locate data values in space and time as follows:

- *Time* (indicating the day of the month),
- *Lat* (the latitude of the centre of the pixel), and
- *Long* (the longitude of the centre of the pixel).

The six variables stored in each NetCDF file were as follows:

- *rnd24*   - precipitation (mm),
- *tmaxscr*   - maximum screen temperature (°K),
- *tminscr*   - minimum screen temperature (°K),
- *rhmaxscr*   - maximum screen relative humidity (%),
- *rhminscr*   - minimum screen relative humidity (%), and
- *u10*   - wind speed at 10 meters (m s^{-1}).

2.3.2   Bias correction of rainfall

The Approach to Determining Catchment Rainfall from GCM Datasets
To determine catchment rainfall from the downscaled grid-based GCM datasets for use as input to the *ACRU* daily time-step model, an approach that facilitated localised bias correction of the daily time step downscaled GCM datasets using point rain gauge data and compatibility with the QnCDB was selected. In this approach the following steps were followed:

- Step (i): Each of the 1 240 driver rain gauges was associated with the closest pixel in the CCAM-downscaled GCM datasets. In some cases, more than one driver rain gauge was associated with a pixel. Thus, 1 207 GCM pixels were associated with the 1 240 driver rain gauges.
- Step (ii): Daily time series of GCM variables were then extracted for each of the GCM pixels selected in Step (i). The extraction of data from the NetCDF files is described in a section to follow.
- Step (iii): For each driver rain gauge, the historical quality-controlled measured rainfall data were used to undertake a localised bias correction of the extracted GCM rainfall time series from Step (ii) for the associated closest pixel determined in Step (i). The bias correction method is described in a section to follow.
- Step (iv): For each catchment the time series of bias corrected GCM rainfall values for the driver rain gauge associated with the catchment, was then used to create a time series input file for the catchment in *ACRU* Composite File Format (Smithers and Schulze, 1995).

The Extraction of Data from NetCDF Files

As indicated in Step (ii) above, a daily time series of GCM variables was extracted for each of a set of 1207 selected GCM pixels selected for each of the six GCM datasets listed previously. A Python script was developed to undertake the data extraction and the extracted time series of GCM variables for each GCM pixel was saved to a separated Comma Separated Value (CSV) file. Thus, a set of 1207 CSV files was created, one for each representative pixel, for each of the six GCM datasets. An example of a portion of a CSV file containing data extracted for a representative GCM pixel is shown in **Figure 2.8**. The six variables stored in each CSV file are as follows:

- *rnd24* - precipitation (mm),
- *tmaxscr* - maximum screen temperature (°C),
- *tminscr* - minimum screen temperature (°C),
- *rhmaxscr* - maximum screen relative humidity (%),
- *rhminscr* - minimum screen relative humidity (%), and
- *u2* - windrun at 2 metres (km d^{-1}).

```
Date,rnd24,tmaxscr,tminscr,rhmaxscr,rhminscr,u2
1961-01-01,0.0157187,27.3881,14.7181,72.5618,50.473,0.393950
1961-01-02,0.314198,28.5357,18.4709,70.2625,45.6859,19.952495
1961-01-03,0.769772,29.9881,17.7396,69.2279,39.3699,7.613547
1961-01-04,0.8169,30.8818,18.3084,65.0065,35.8751,475.443473
1961-01-05,2.19148,25.9408,17.5467,69.6831,57.4098,38.723450
1961-01-06,0.0314281,26.1592,17.4553,71.2673,54.8369,101.074524
1961-01-07,0.8169,25.8392,17.2877,72.4767,49.3578,91.0983489
1961-01-08,0.125685,24.3158,16.1807,73.5642,56.6487,90.704549
1961-01-09,1.32746,25.626,15.1904,73.4838,56.989,187.0533697
1961-01-10,26.0777,20.8474,17.8971,73.0239,66.6987,71.408539
```

Figure 2.8   Example of a portion of a CSV file containing data extracted for a representative GCM pixel

The GCM datasets do not contain records for 29 February in leap years, thus the following assumptions are made, on such days, to produce a full time series for input to the *ACRU* model:

- *rnd24* = 0 mm,
- *tmaxscr* = mean of values for 28 Feb and 1 March,
- *tminscr* = mean of values for 28 Feb and 1 March,
- *rhmaxsc* = mean of values for 28 Feb and 1 March,
- *rhminscr* = mean of values for 28 Feb and 1 March, and
- *u2* = mean of values for 28 Feb and 1 March.

The units of measure for the values of the *tmaxscr* and *tminscr* variables were converted from °Kelvin to °Celsius. The units of measure for the values of the *u10* variable was converted from m/s at a height of 10 m to km/day at a height of 2 m, as required by the *ACRU* model, using Equation 2.1 from Allen et al. (1998), *viz.*

$$u_2 = u_z \frac{4.87}{\ln(67.8\ z - 5.42)}$$
Equation 2.1

where:

u₂   = wind speed at 2 m above ground surface (m/s),

uᵤ   = measured wind speed at z m above ground surface (m/s), and

z   = height of measurement above ground surface (m).

The Need for Bias Correction of GCM Rainfall Estimates

For application in hydrological modelling at a local scale it is necessary to correct for systematic and localised biases in the rainfall estimates produced by GCMs. The downscaled GCM datasets provided by the CSIR, when compared to observed rain gauge data, were also found to have a substantially larger number of raindays, with many raindays having very small rainfall depths (i.e < 0.1 mm). The selection of a bias correction method and its application to the daily time step GCM rainfall estimates for application in this project are discussed in the following two sub-sections.

Selection of a Bias Correction Method for Rainfall

Numerous methods have been applied to reduce the bias of GCM and RCM estimates. Simpler methods aim to correct the mean or both the mean and the variance of the climate estimates. However, more advanced methods, referred to as Quantile Mapping (QM) methods, aim to apply corrections at all quantiles such that the full distribution of values is corrected to match a reference distribution. Various studies (e.g. Gudmundsson et al*., 2012*; Teutschbein and Seibert, 2012; Chen et al*., 2013*; Räty et al*., 2014*) have shown QM to perform better than simpler methods, although the performance of the bias corrections can vary between regions. A useful review and comparison of many QM techniques was provided by Gudmundsson et al. (2012), who classified the statistical transformations used to reduce bias into:

- distribution derived transformations,
- parametric transformations, and
- non-parametric transformations.

However, these statistical transformations aim to provide a function that maps an estimated variable such that its new distribution matches the distribution of the observed variable. Gudmundsson et al. (2012) noted that the three classes of statistical transformations differed substantially in their underlying assumptions, despite the fact that they were all designed to reduce the bias in the modelled datasets such that their distribution matched the distribution of observed historical data. Their evaluation showed that most of the statistical transformation methods were capable of reducing bias in the modelled datasets, although the performance of the methods differed substantially. Gudmundsson et al. (2012) concluded that the non-parametric methods had the best skill in reducing the bias over the entire range of the distribution. They also concluded that an additional advantage of the non-parametric methods was that they did not require specific assumptions to be made about the distribution of the data and "*are thus recommended for most applications of statistical bias correction*".

Based on the conclusions by Gudmundsson et al. (2012), non-parametric bias correction methods were investigated further. As described in Feigenwinter et al. (2018), these methods typically involve a two-step process, as shown in **Figure 2.9**, *viz.*

- the development and calibration of a transfer function using a historical calibration period, in which the observed time series overlaps with the time series of downscaled GCM data, and
- the application of the transfer function to the entire time series of downscaled GCM data.
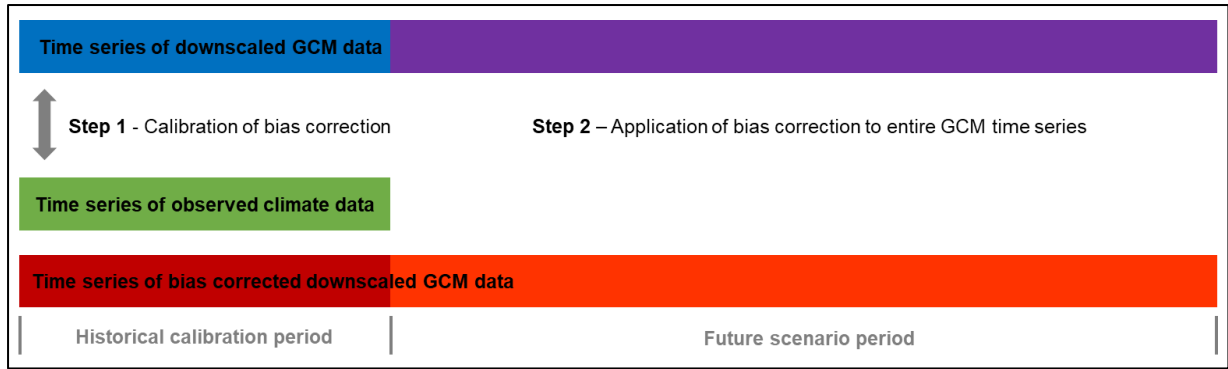
Figure 2.9   Simplified overview of non-parametric bias correction approach (after Feigenwinter et al., 2018)

The QM method is described and evaluated by, among others, Bóe et al. (2007), Gudmundsson et al. (2012), Themeßl et al. (2012) and Cannon et al. (2015). In this method cumulative distribution functions (CDFs) are calculated, as shown in **Figure 2.10** for:

- the observed time series (CDFo), and
- the downscaled GCM time series for the historical calibration period (CDFc).

The CDF curves have data values (x) (e.g. rainfall) on the x-axis and probability (P) on the y-axis. The subscripts represent the observed data in the calibration period (o), the downscaled GCM data in the calibration period (c) and the downscaled GCM data in the future period (f). For a day (d) in the future period, the data value $x_f(d)$ is used with the CDF_c curve to find the associated probability $P_c(x_f(d))$. This same probability value is then used with the CDF_o curve to find the associated observed data value x_o, which is used as the bias corrected data value for the day $x_{f-corrected}(d)$. This approach uses empirical cumulative distribution functions (in place of theoretical distributions) which are approximated using tables of associated data values and empirical percentile values. The values in between the discrete percentile values are approximated using linear interpolation.

One shortcoming of the QM approach is that extrapolation of the CDF curve is required if there are data values in the future period of the downscaled GCM data that exceed the maximum data value in the calibration period of the downscaled GCM data. Related to this is the limitation in the QM method of the assumption of a stationary statistical relationship between the observed data and the downscaled GCM data (Gudmundsson et al., 2012; Themeßl et al., 2012; Cannon et al., 2015; Rajczak et al., 2016). In addition, QM has been found to overcorrect the magnitude of relative trends in precipitation extremes compared to the uncorrected downscaled GCM data (Cannon et al., 2015).
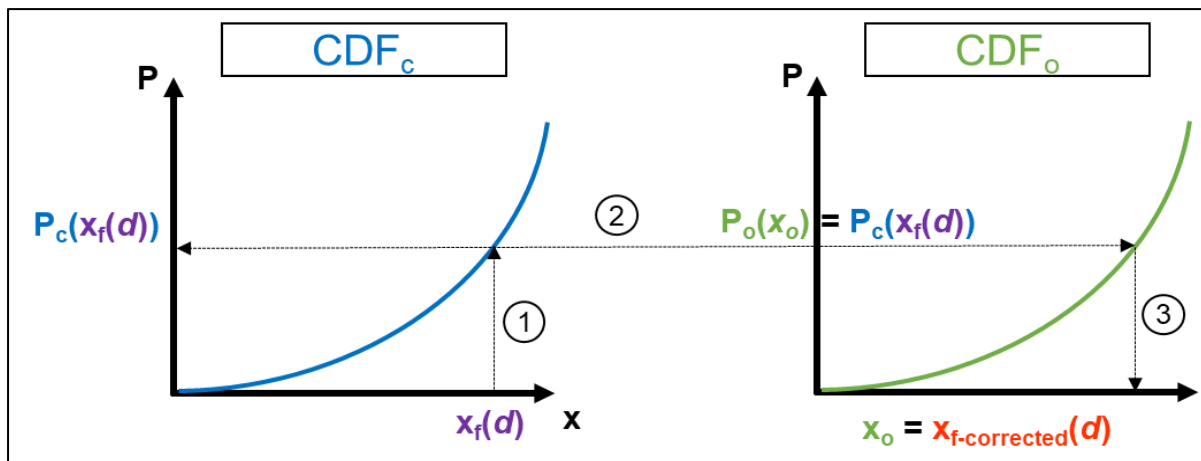
Figure 2.10   Description of QM bias correction method (after Bóe et al., 2007)

To address the limitation of the QM method relating to the assumption of stationarity the Quantile Delta Mapping (QDM) method was proposed for application in this project. The QDM methodology is described and assessed by Cannon et al. (2015). In this method CDFs are calculated, as shown in **Figure 2.11**, for

- the observed time series (CDF_o),
- the downscaled GCM time series for the historical calibration period (CDF_c) and, thirdly, for
- the downscaled GCM time series for the future period (CDF_f).

For a day (d) in the future period the data value $x_f(d)$ is used with the CDF_f curve to find the associated probability $P_f(x_f(d))$. This same probability value is then used

- with the CDF_c curve to find the associated observed data value x_c, and
- with CDF_o curve to find the associated observed data value x_o.

If the bias correction is to be done additively, then the difference between $x_f(d)$ and x_c is added to x_o to calculate the bias corrected data value for the day, i.e. $x_{f\text{-}corrected}(d)$. Similarly, if the bias correction is to be done multiplicatively, then the ratio of $x_f(d)$ to x_c is multiplied with x_o to calculate the bias corrected data value for the day.

Cannon et al. (2015) found that the QDM method of bias correction did not overcorrect the magnitude of relative trends in precipitation extremes as much as the QM method. However, when applying the QDM method in this project, it was found that the multiplicative correction of rainfall data resulted in a few unrealistically high rainfall values for uncorrected rainfall in quantiles close to the 100th percentile. This problem was addressed by limiting the bias correction factors for quantiles above the 99th percentile, to the bias correction factor for the 99th percentile of non-exceedance.

One potential difficulty in applying the QDM is deciding on the time period for which to calculate the CDF_f curve. For the purposes of this project a 39-year moving window was used to calculate the CDF_f curve. The choice of 39 years was based on the calibration period being 39 years, *viz*. 1961 to 1999. Thus, for each year in the future period 2000-2080 a different CDF_f curve was calculated (using 39-year window around that year) and used for the bias correction of the rainfall data in that year. For example, for the year 2000, the CDF_f curve would be for the period 1981 to 2019. For each year in the future period 2061-2099 (beyond which a 39-year window is not possible) the CDF_f curve for the period 2061-2099 was used for the bias correction of the rainfall data in that year.
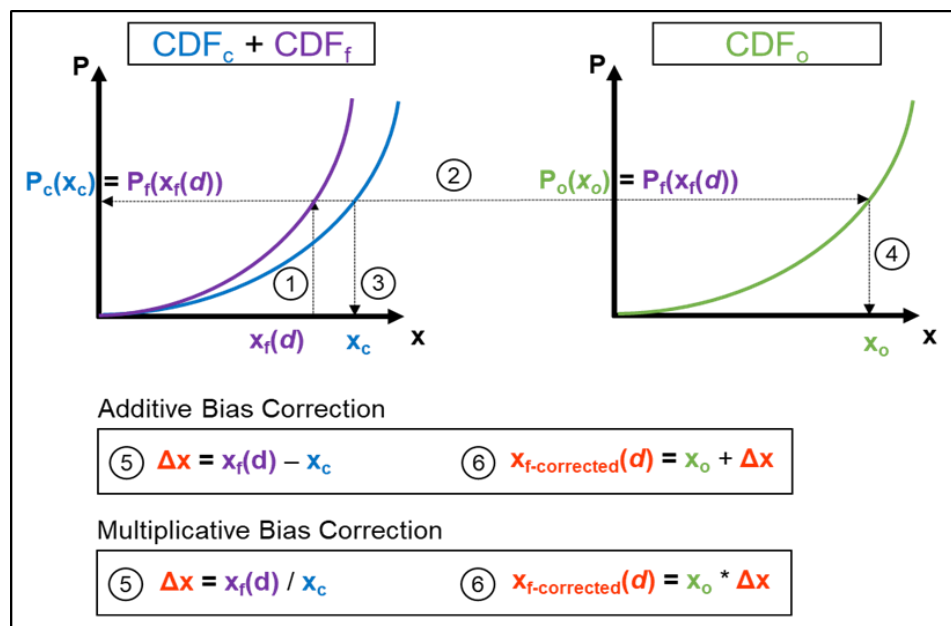
Figure 2.11   Description of the QDM bias correction method

Application of the QDM Bias Correction Method for Rainfall

As indicated in Step (iii) above, a daily time series of bias corrected GCM rainfall values was extracted for each of the 1 240 driver rain gauges for each of the six GCM datasets. A Python script was developed to undertake the bias correction using the QDM method and the bias corrected time series of GCM rainfall values for each rain gauge was saved to a separated Comma Separated Value (CSV) file. Thus, a set of 1 240 CSV files was created, one for each rain gauge, for each of the six GCM datasets. An example of a portion of a CSV file containing rainfall data for a driver rain gauge is shown in **Figure 2.12**. The three variables stored in each CSV file are as follows:

- *obs_rf* - observed rainfall (mm),
- *rnd24* - downscaled GCM rainfall (mm), and
- *rnd24_BC* - bias corrected downscaled GCM rainfall (mm).

```
Date,obs_rfl,rnd24,rnd24_BC
1961-01-01,0.0,0.0157187,0.0
1961-01-02,0.0,0.314198,0.0
1961-01-03,0.0,0.769772,0.0
1961-01-04,0.0,0.8169,0.0
1961-01-05,0.0,2.19148,0.000324
1961-01-06,0.0,0.031428,0.0
1961-01-07,0.0,0.8169,0.0
1961-01-08.0.0.0.125685.0.0
```

Figure 2.12 Example of a portion of a CSV file containing observed rain gauge rainfall, GCM pixel rainfall and bias corrected GCM pixel rainfall

An example of the effectiveness of the QDM bias correction method, at rain gauge 0002069W for the ACCESS1-0 GCM for RCP8.5, is shown in **Figure 2.13**. In **Figure 2.13**, the percentage of daily rainfall values in selected ranges are shown for the calibration period (1960-1999) to demonstrate the correction to the distribution of the rainfall values. The first three ranges on the left demonstrate the correction to increase the number of rain days and to reduce the large number of very small daily rainfall values. In the upper ranges the number of larger daily rainfall values has increased. In **Figure 2.14** and **Figure 2.15**, the annual rainfall totals for the period 1961-2099 are shown for RCP4.5 and RCP8.5 respectively, indicating the magnitude of the correction made to the annual totals. The trends in annual rainfall totals are also shown for the downscaled GCM data before and after bias correction to demonstrate that the trend has been maintained. For purposes of comparison the same graphical analysis was done at the same rain gauge for the other 5 GCMs (**Figures 2.16** to **2.30**). For all six GCMs, the application of bias corrections improves the representation of the daily rainfall distribution in the calibration period (see equivalent graphs to **Figure 2.13** for the other GCMs).
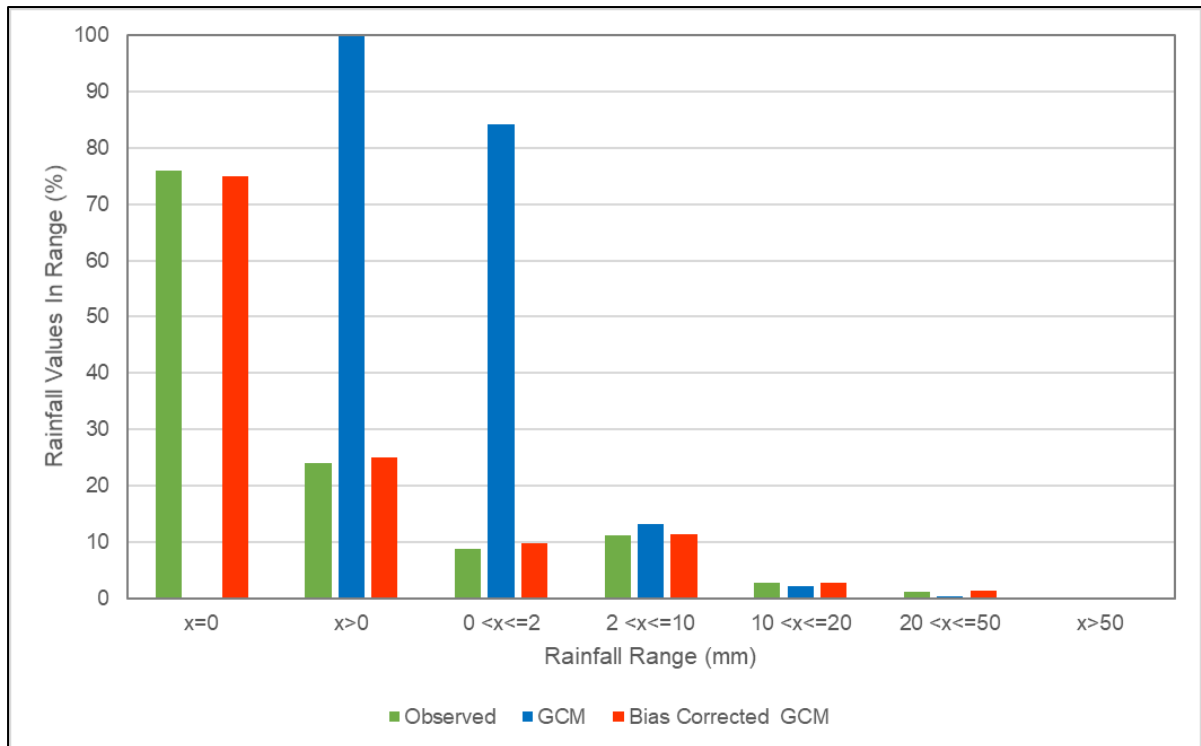
Figure 2.13 Comparison of distribution of daily rainfall in the calibration period (1961-1999) at rain gauge 0002069W for the ACCESS1-0 GCM for RCP4.5 and RCP8.5
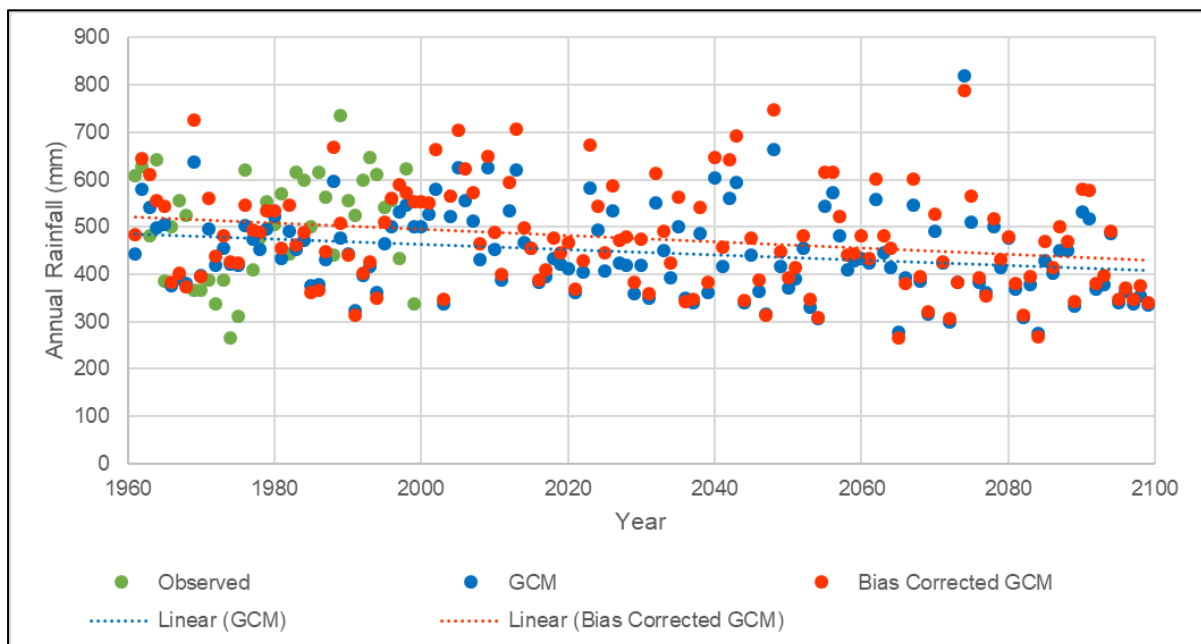
Figure 2.14 Comparison of annual rainfall totals for the period 1961-2099 (including trends) at rain gauge 0002069W for the ACCESS1-0 GCM for RCP4.5
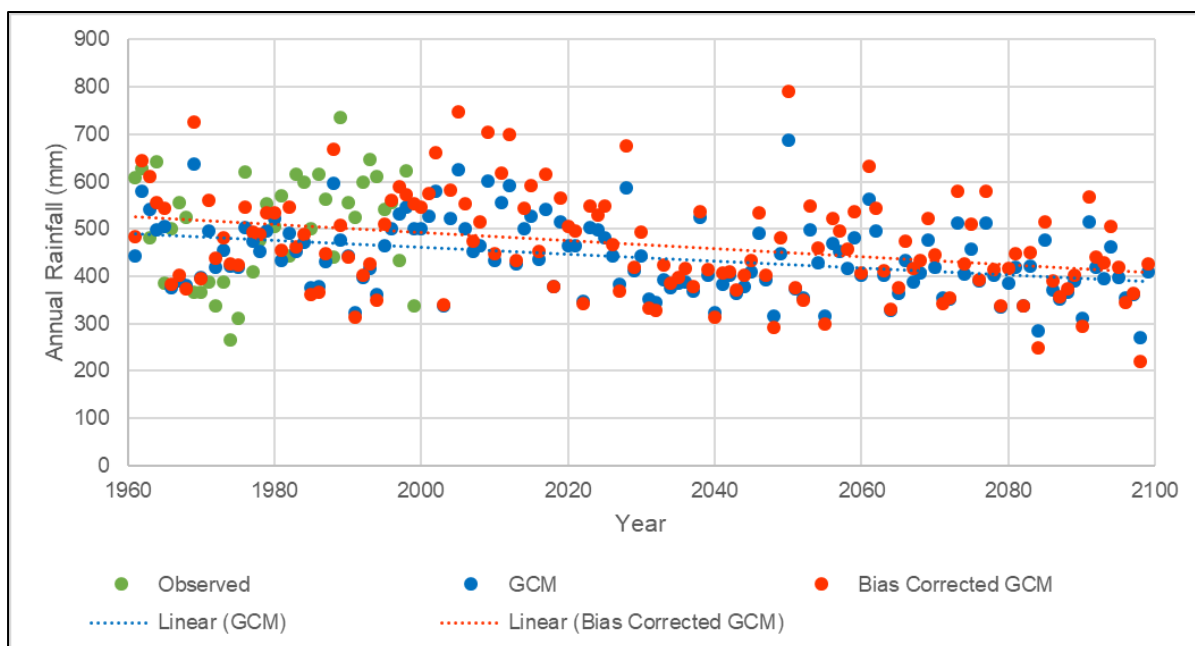
Figure 2.15 Comparison of annual rainfall totals for the period 1961-2099 (including trends) at rain gauge 0002069W for the ACCESS1-0 GCM for RCP8.5
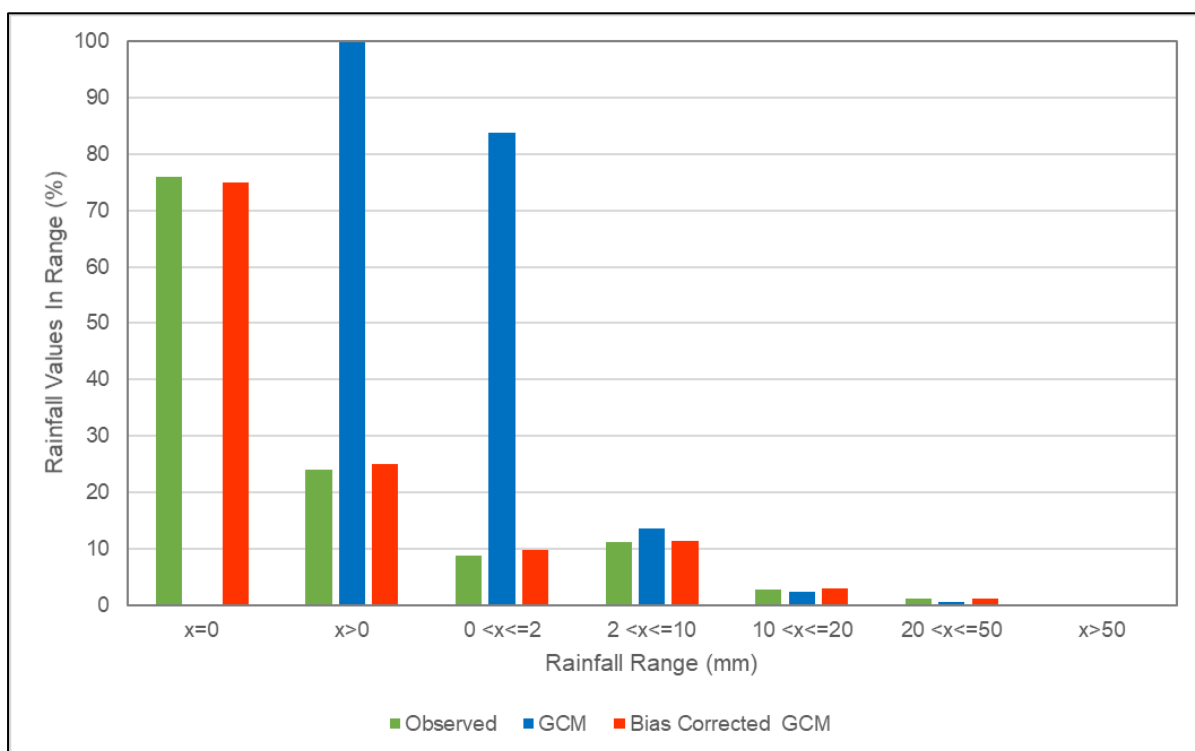
Figure 2.16 Comparison of distribution of daily rainfall in the calibration period (1961-1999) at rain gauge 0002069W for the CCSM4 GCM for RCP4.5 and RCP8.5
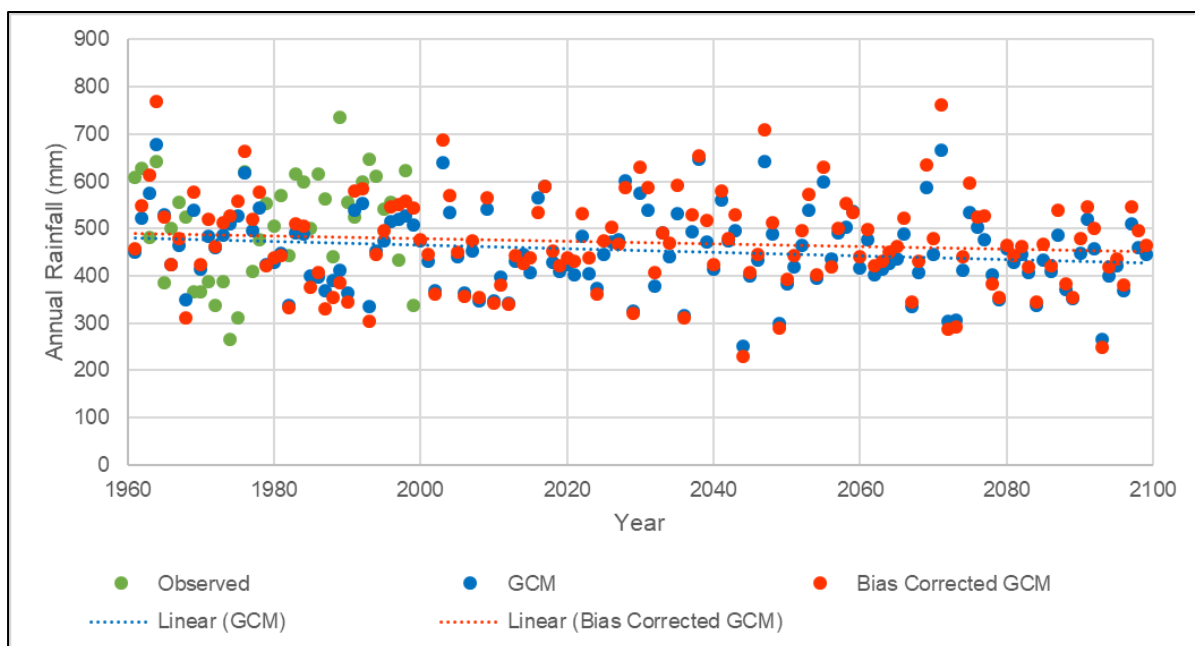
Figure 2.17 Comparison of annual rainfall totals for the period 1961-2099 (including trends) at rain gauge 0002069W for the CCSM4 GCM for RCP4.5
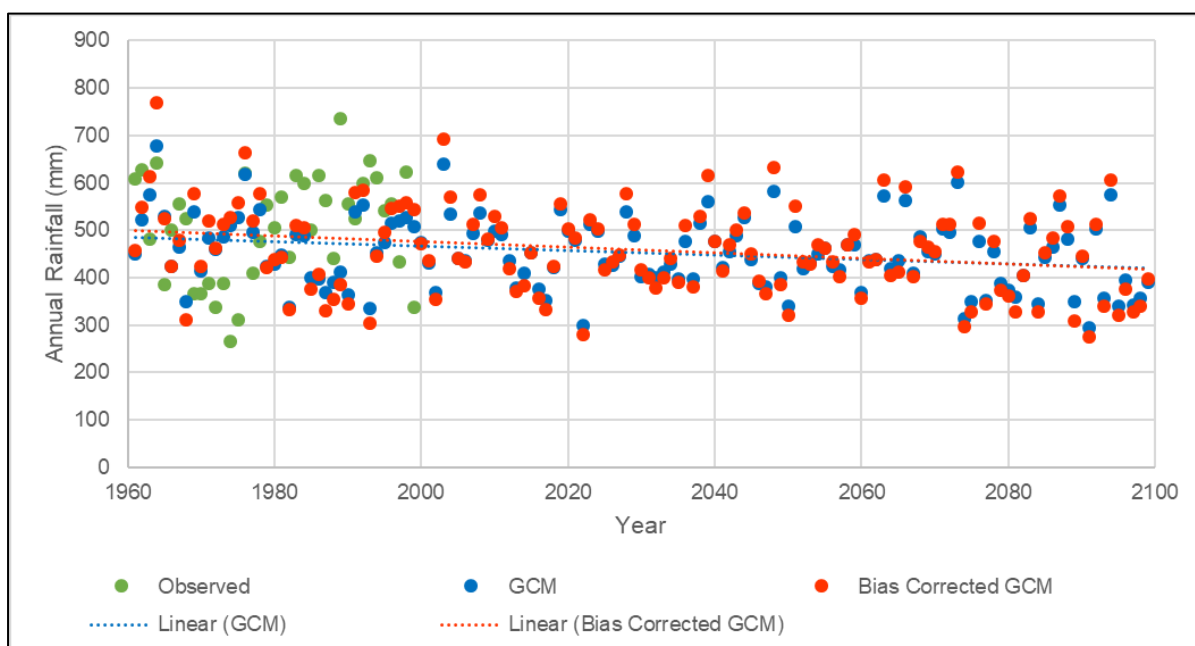
Figure 2.18 Comparison of annual rainfall totals for the period 1961-2099 (including trends) at rain gauge 0002069W for the CCSM4 GCM for RCP8.5
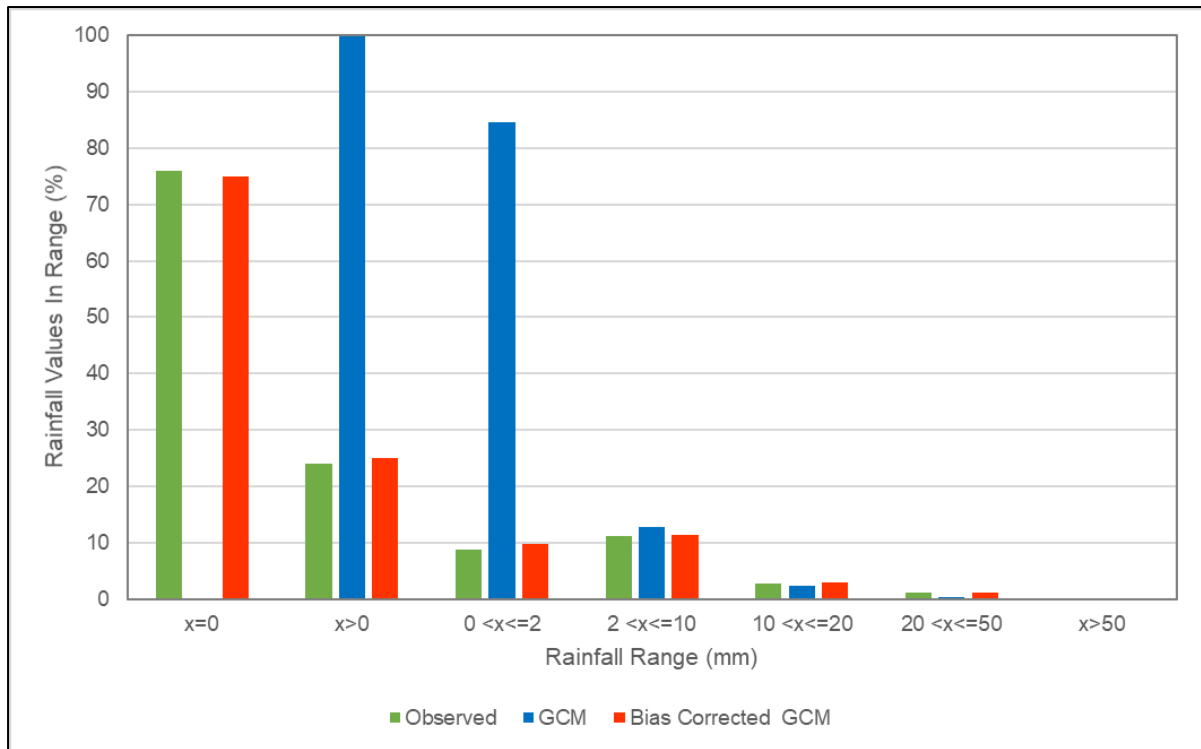
Figure 2.19 Comparison of distribution of daily rainfall in the calibration period (1961-1999) at rain gauge 0002069W for the CNRM-CM5 GCM for RCP4.5 and RCP8.5
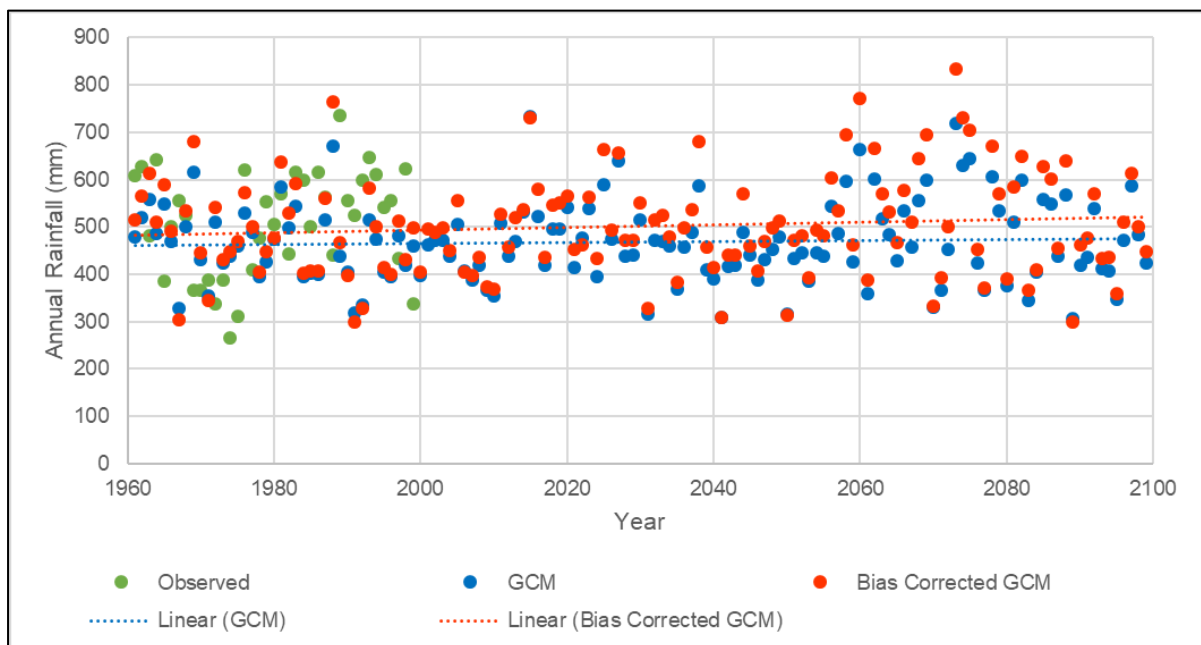
Figure 2.20 Comparison of annual rainfall totals for the period 1961-2099 (including trends) at rain gauge 0002069W for the CNRM-CM5 GCM for RCP4.5
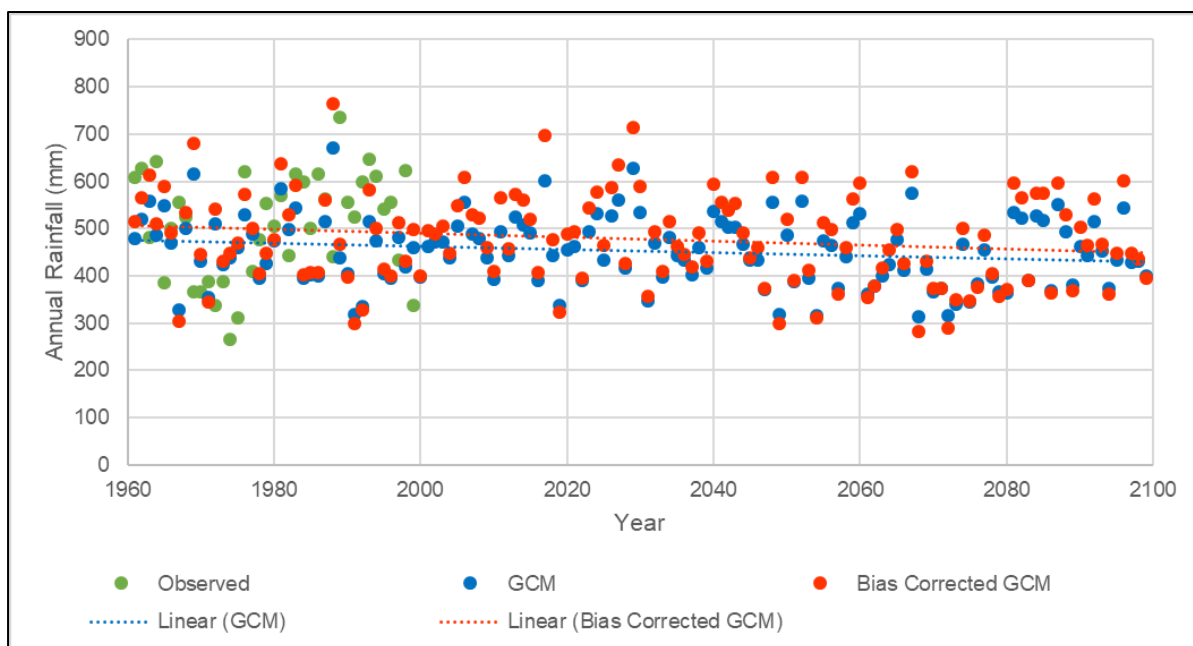
Figure 2.21 Comparison of annual rainfall totals for the period 1961-2099 (including trends) at rain gauge 0002069W for the CNRM-CM5 GCM for RCP8.5
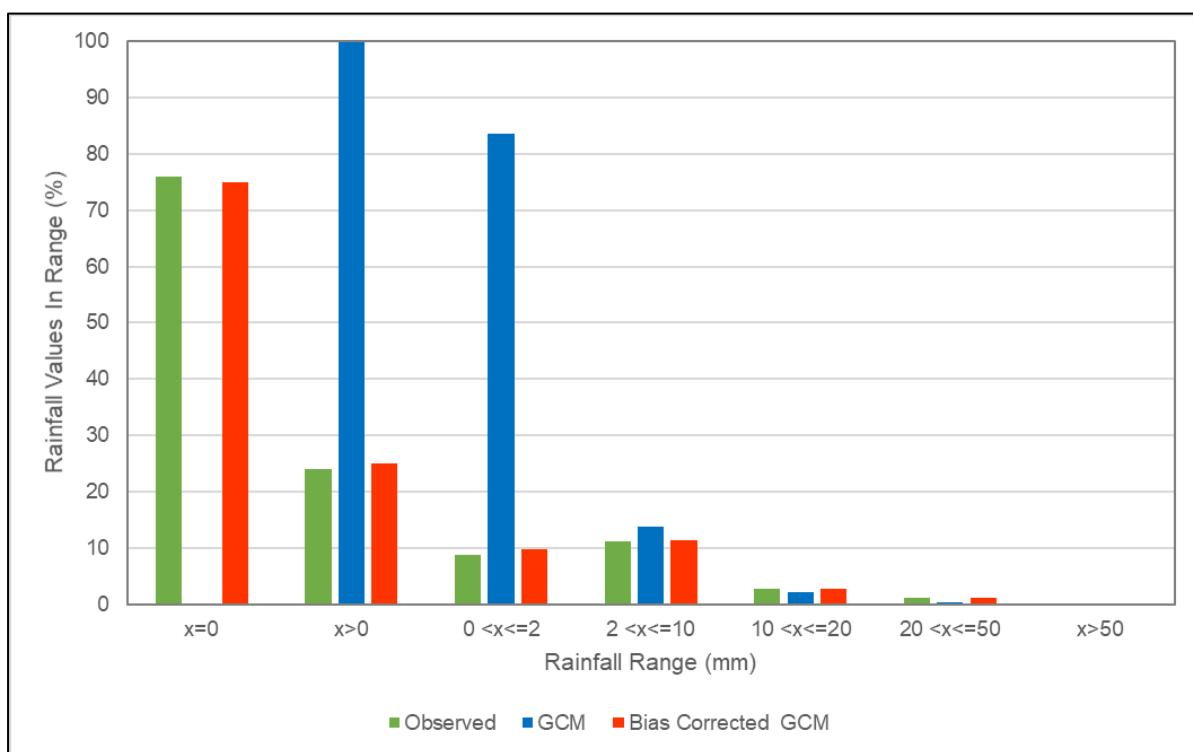
Figure 2.22 Comparison of distribution of daily rainfall in the calibration period (1961-1999) at rain gauge 0002069W for the GFDL-CM3 GCM for RCP4.5 and RCP8.5

29
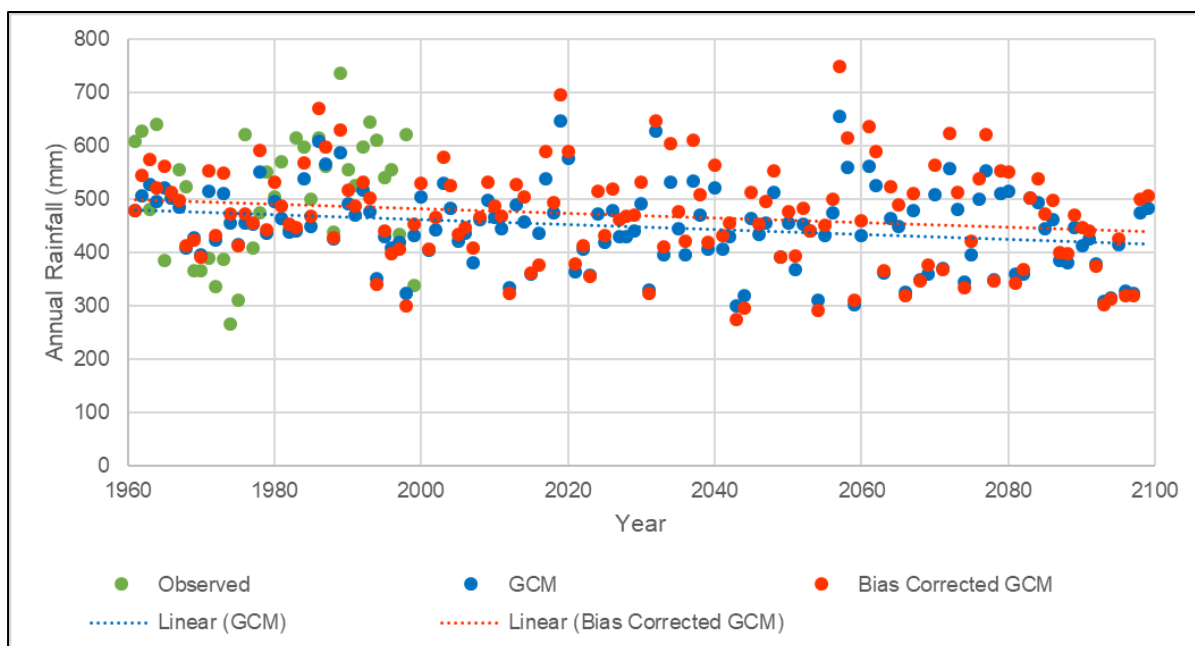
Figure 2.23 Comparison of annual rainfall totals for the period 1961-2099 (including trends) at rain gauge 0002069W for the GFDL-CM3 GCM for RCP4.5
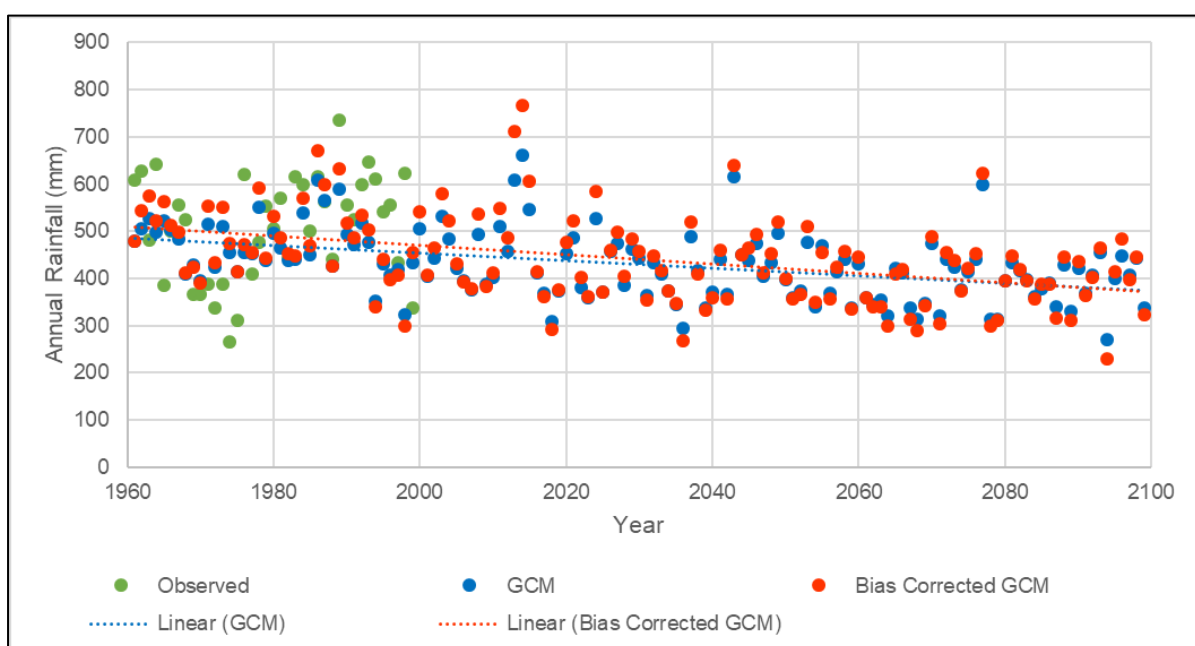
Figure 2.24 Comparison of annual rainfall totals for the period 1961-2099 (including trends) at rain gauge 0002069W for the GFDL-CM3 GCM for RCP8.5
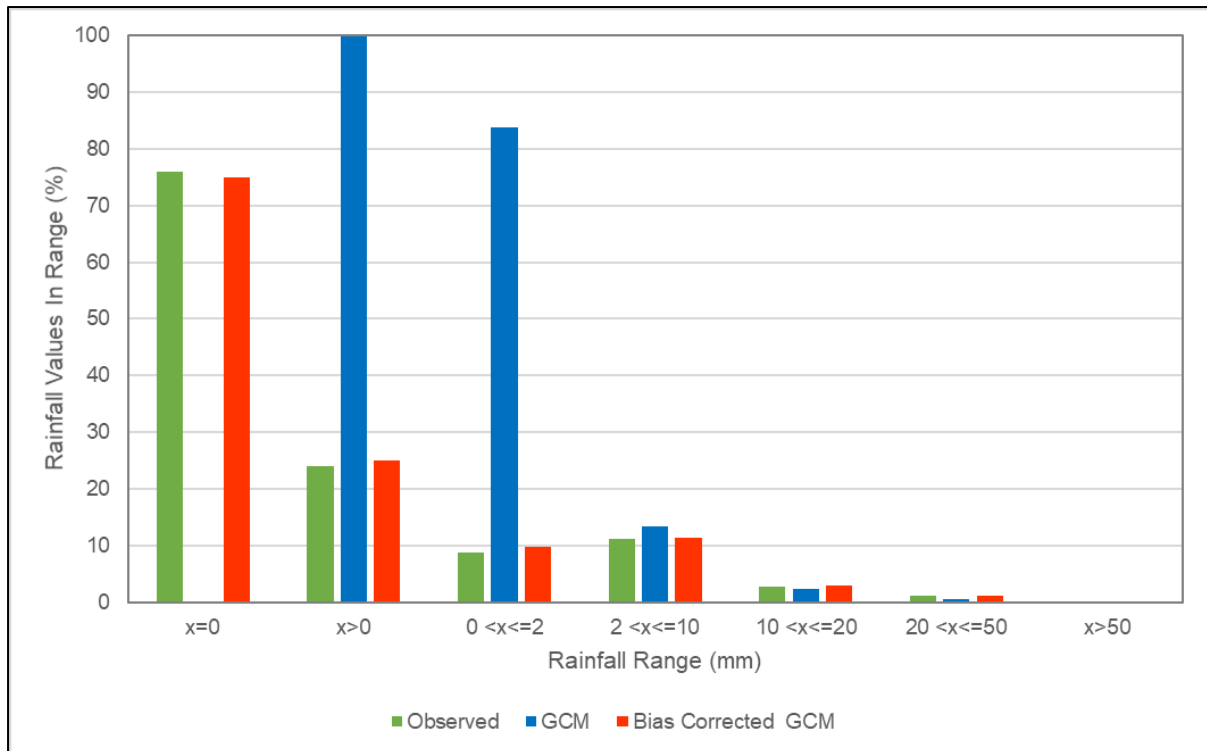
Figure 2.25 Comparison of distribution of daily rainfall in the calibration period (1961-1999) at rain gauge 0002069W for the MPI-ESM-LR GCM for RCP4.5 and RCP8.5
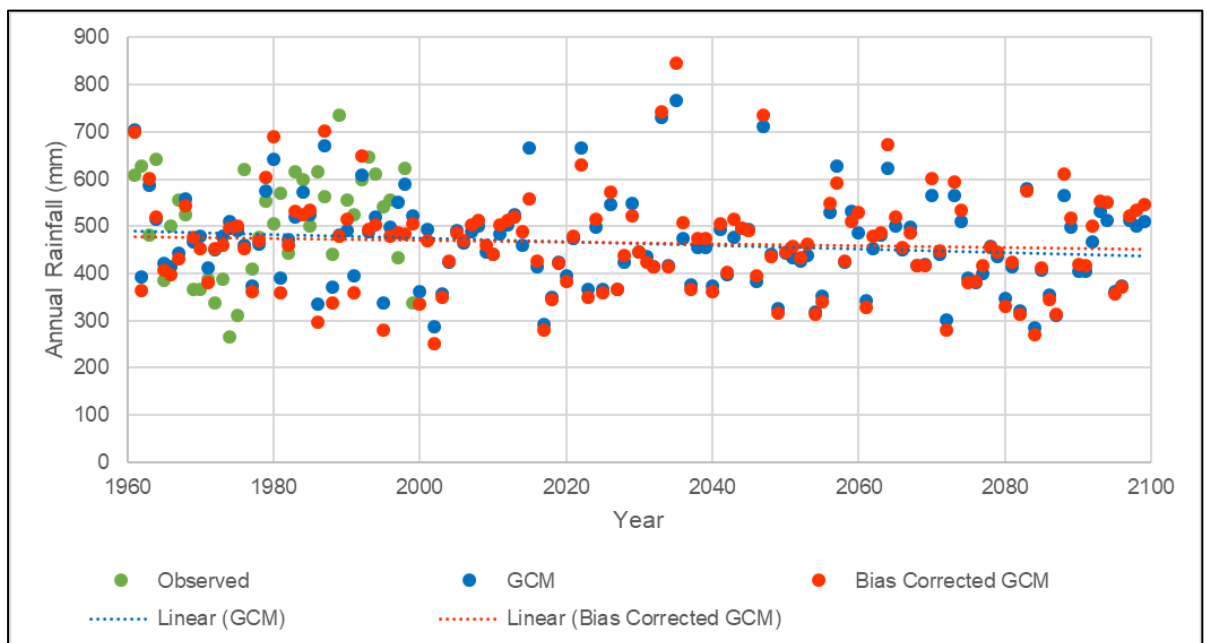
Figure 2.26 Comparison of annual rainfall totals for the period 1961-2099 (including trends) at rain gauge 0002069W for the MPI-ESM-LR GCM for RCP4.5
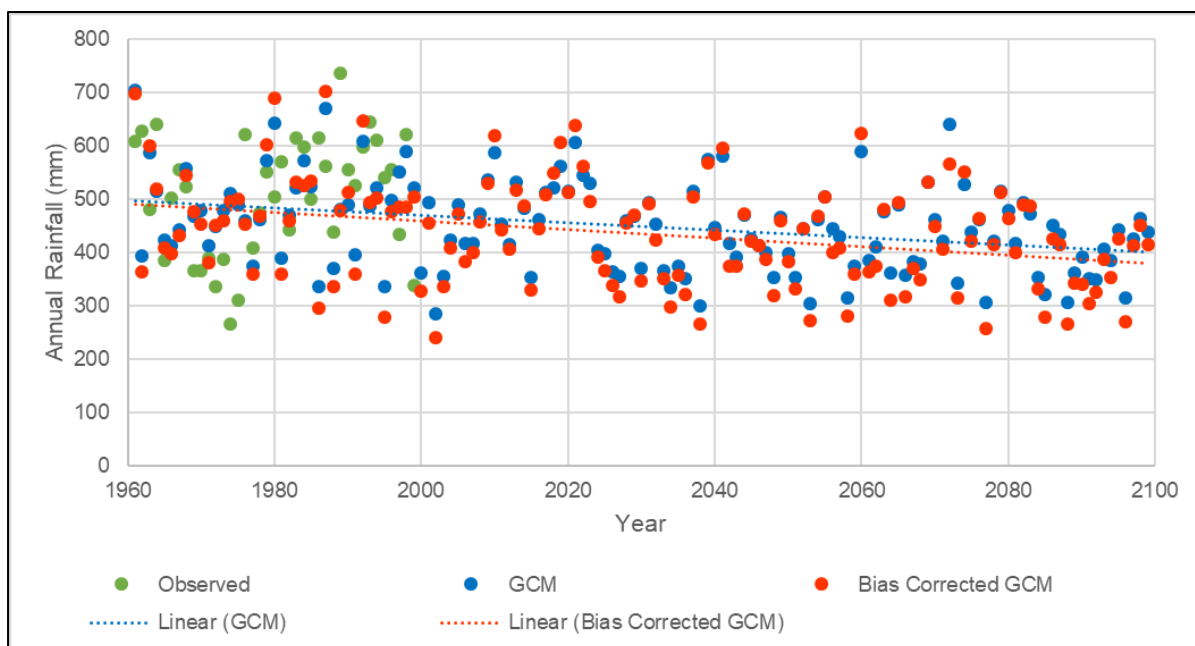
Figure 2.27 Comparison of annual rainfall totals for the period 1961-2099 (including trends) at rain gauge 0002069W for the MPI-ESM-LR GCM for RCP8.5
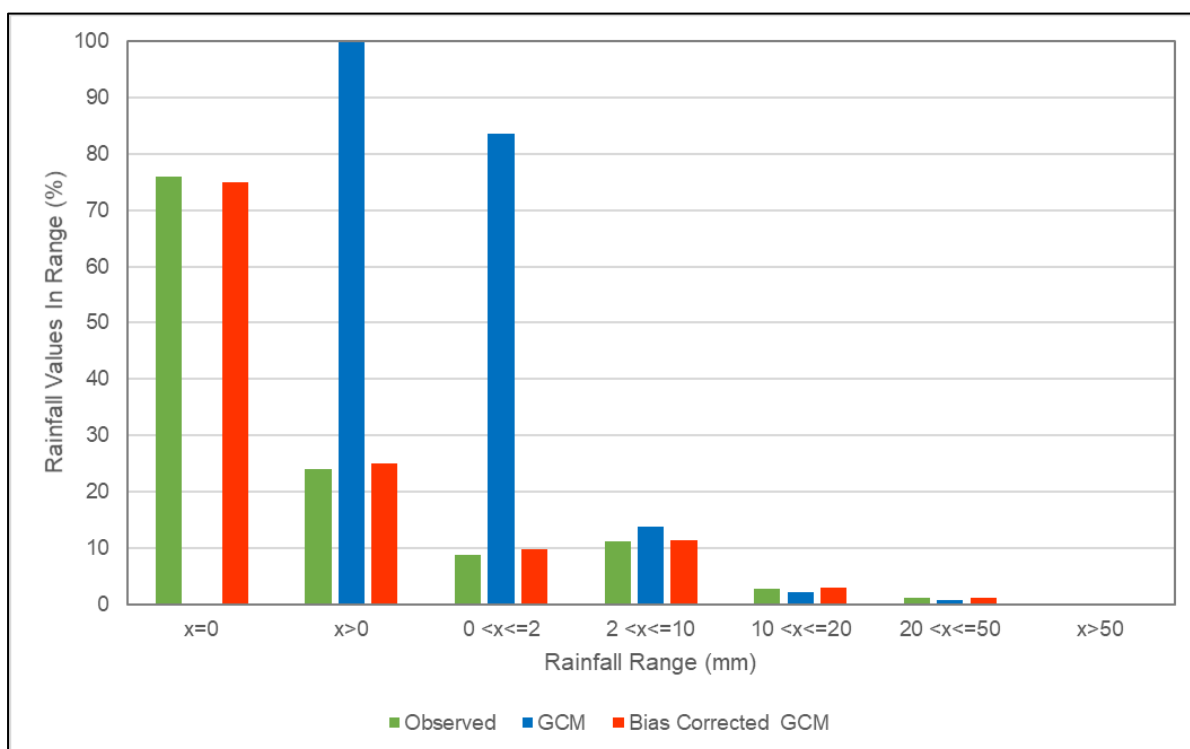
Figure 2.28 Comparison of distribution of daily rainfall in the calibration period (1961-1999) at rain gauge 0002069W for the NorESM1-M GCM for RCP4.5 and RCP8.5
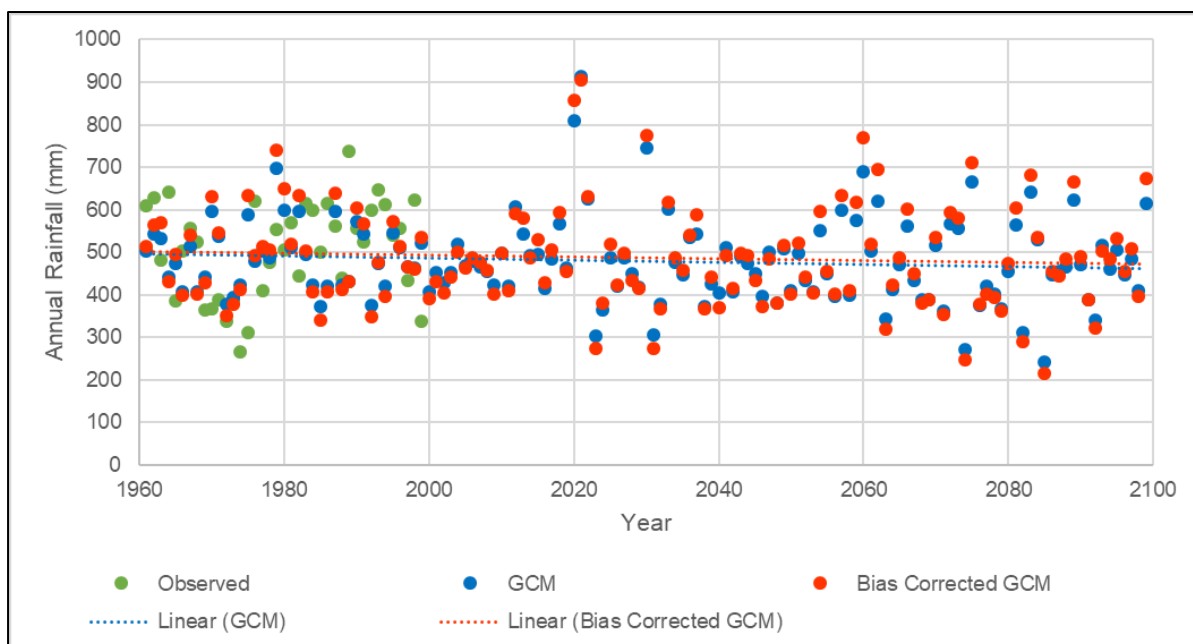
Figure 2.29 Comparison of annual rainfall totals for the period 1961-2099 (including trends) at rain gauge 0002069W for the NorESM1-M GCM for RCP4.5
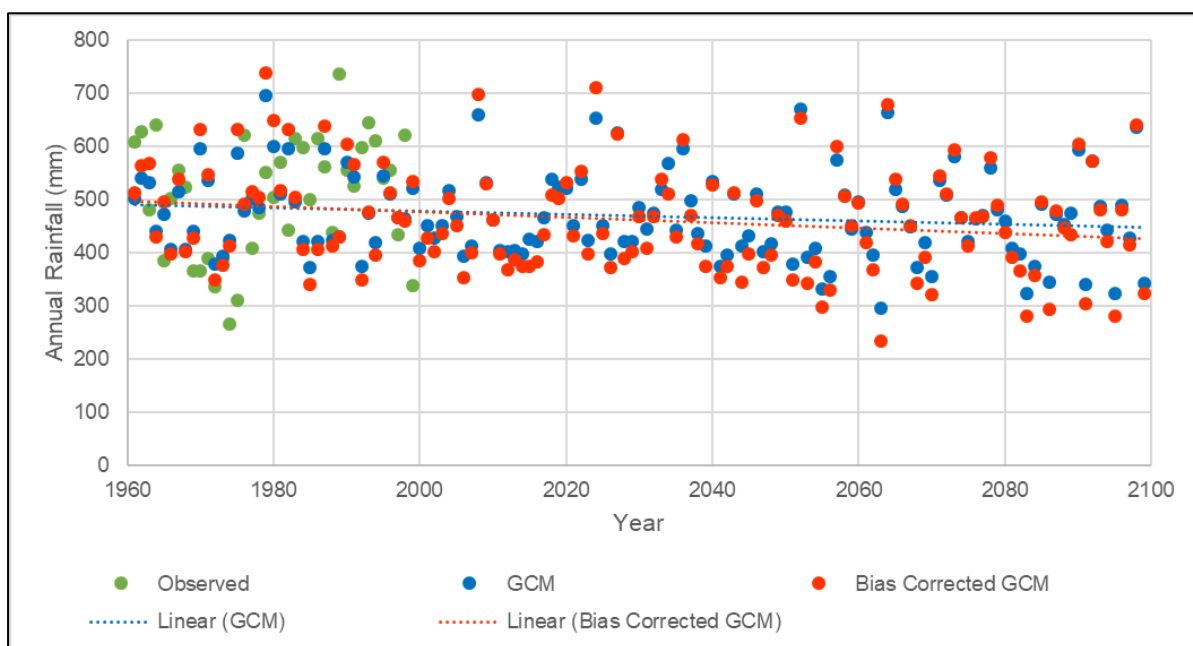
Figure 2.30 Comparison of annual rainfall totals for the period 1961-2099 (including trends) at rain gauge 0002069W for the NorESM1-M GCM for RCP8.5

2.3.3   Bias and lapse rate corrections for air temperature

The Approach to Determining Catchment Air Temperature from GCM Datasets
To determine maximum and minimum air temperature for catchments from the downscaled grid-based GCM datasets for use as input to the *ACRU* daily time-step model, an approach that facilitated bias

correction using measured point temperature data was selected. In this approach the following four steps were followed:

- Step (i): Each of the 1 240 driver temperature stations was associated with the closest pixel in the CCAM-downscaled GCM datasets. In some cases, more than one driver temperature station was associated with a pixel, and ultimately 1207 GCM pixels were associated with the 1 240 driver temperature stations.
- Step (ii): Daily time series of GCM variables were then extracted, as described in Deliverable 4, for each of the GCM pixels selected in Step 1.
- Step (iii): For each driver temperature station the historical quality-controlled measured temperature data were used to undertake a localised bias correction of the extracted GCM temperature time series from Step 2 above for the associated closest pixel determined in the first step. The Quantile Delta Mapping (QDM) bias correction method, described in Section 3 of Deliverable 4, was applied. For bias correction of temperature data an *additive* correction is applied in the QDM method, as opposed to the *multiplicative* correction applied for rainfall data.
- Step (iv): For each catchment the time series of bias corrected GCM maximum and minimum temperature values for the driver temperature station associated with the catchment is then used to create a time series input file for the catchment in *ACRU* Composite File Format (Smithers and Schulze, 1995).

The Need for Bias Correction of GCM Temperature Estimates

For application in hydrological modelling at a local scale it is necessary to correct for systematic and localised biases in the maximum and minimum air temperature estimates produced by GCMs. In an initial investigation involving 156 temperature stations, the downscaled GCM datasets provided by the CSIR were found to be biased when compared to observed temperature data.

Application of the QDM Bias Correction Method for Temperature

The derivation of an observed temperature dataset for bias-correction of GCM temperature projections is described in Section 0. This dataset of observed daily maximum and minimum air temperature data was used to adjust the maximum and minimum temperature datasets in downscaled GCM projections to reduce the bias in the GCM predictions. As indicated in Step (iii) above, a daily time series of bias corrected GCM maximum and minimum temperature values was generated for each of the 1 240 driver temperature stations, for each of the six GCM datasets, and for each of the 2 RCPs. A Python script was developed to perform the bias correction using the QDM method described above, and the bias corrected time series of GCM maximum and minimum temperature values for each temperature station was saved to a separated Comma Separated Value (CSV) file. Thus, a set of 1 240 CSV files was created, one for each temperature station, for each of the six GCM datasets, for each of the 2 RCPs. An example of a portion of a CSV file containing rainfall data for a driver temperature station is shown in **Figure 2.31**. The six variables stored in each CSV file are as follows:

- *obs_tmax*   - observed maximum daily temperature (°C),
- *tmaxscr*   - downscaled GCM maximum temperature (°C),
- *tmaxscr_BC*   - bias corrected downscaled GCM maximum temperature (°C),
- *obs_tmin*   - observed minimum daily temperature (°C),
- *tminscr*   - downscaled GCM minimum temperature (°C), and
- *tminscr_BC*   - bias corrected downscaled GCM minimum temperature (°C).

```
Date,       obs_tmax, tmaxscr  tmaxscr_BC, obs_tmin, tminscr, tminscr_BC
1961-01-01, 28.6,     23.5,    22.2,       14.2,     18.0,    18.7
1961-01-02, 25.8,     36.4,    32.1,       17.4,     17.8,    18.6
1961-01-03, 18.6,     21.1,    20.3,       14.7,     16.6,    17.4
1961-01-04, 17.2,     19.4,    19.1,       15.7,     15.4,    16.2
1961-01-05, 16.9,     23.7,    22.4,       11.3,     15.4,    16.2
```

Figure 2.31 Example of a portion of a CSV file containing observed temperature, GCM pixel temperature and bias corrected GCM pixel temperature

An example of the effectiveness of the QDM bias correction method, at the temperature station corresponding to rain gauge 0002069W for the ACCESS1-0 GCM for RCP8.5, is shown in **Figure 2.32**. In **Figure 2.32**, the percentage of daily rainfall values in selected ranges are shown for the calibration period (1960-1999) to demonstrate the correction to the distribution of both the maximum and minimum temperature values. The first three ranges on the left demonstrate the correction to the minimum temperature values. For this temperature station there was a small change in the number of days with daily minimum temperatures below 0°C, but a substantial reduction in the number of days with values less than 10°C and corresponding increase in the number of days with values greater than 10°C. For this temperature station the distribution of the GCM maximum temperatures was similar to that of the observed maximum temperatures. The bias correction of the maximum temperatures resulted in an increase in the number of days with values less than 20°C, and a decrease in the number of days in the other higher temperature ranges. The distribution of the maximum and temperature values was similar for all six GCMs. For all six GCMs, the application of the bias corrections improves the representation of the daily maximum and minimum distributions in the calibration period.

To demonstrate the result of applying the QDM bias correction methodology over the full GCM time series (historical calibration period and future scenario period), the daily maximum and minimum temperature values were used to calculate mean daily temperature values for each day. These mean daily temperatures were then used to calculate a mean annual temperature for each of the 139 years. In **Figure 2.33** and **Figure 2.34**, the annual mean temperatures for the period 1961-2099 are shown for RCP4.5 and RCP8.5 respectively, indicating the magnitude of the correction made to the annual means. For this temperature station the GCMs underestimated the temperatures in the historical calibration period, thus the bias correction resulted in an increase in the annual mean temperature values. The trends in annual mean temperatures are also shown for the downscaled GCM data, before and after bias correction, demonstrating that the trend of increasing temperatures has been maintained. For purposes of comparison, the same graphical analysis was done at the same temperature station for the other five GCMs (**Figure 2.35** to **Figure 2.49**).
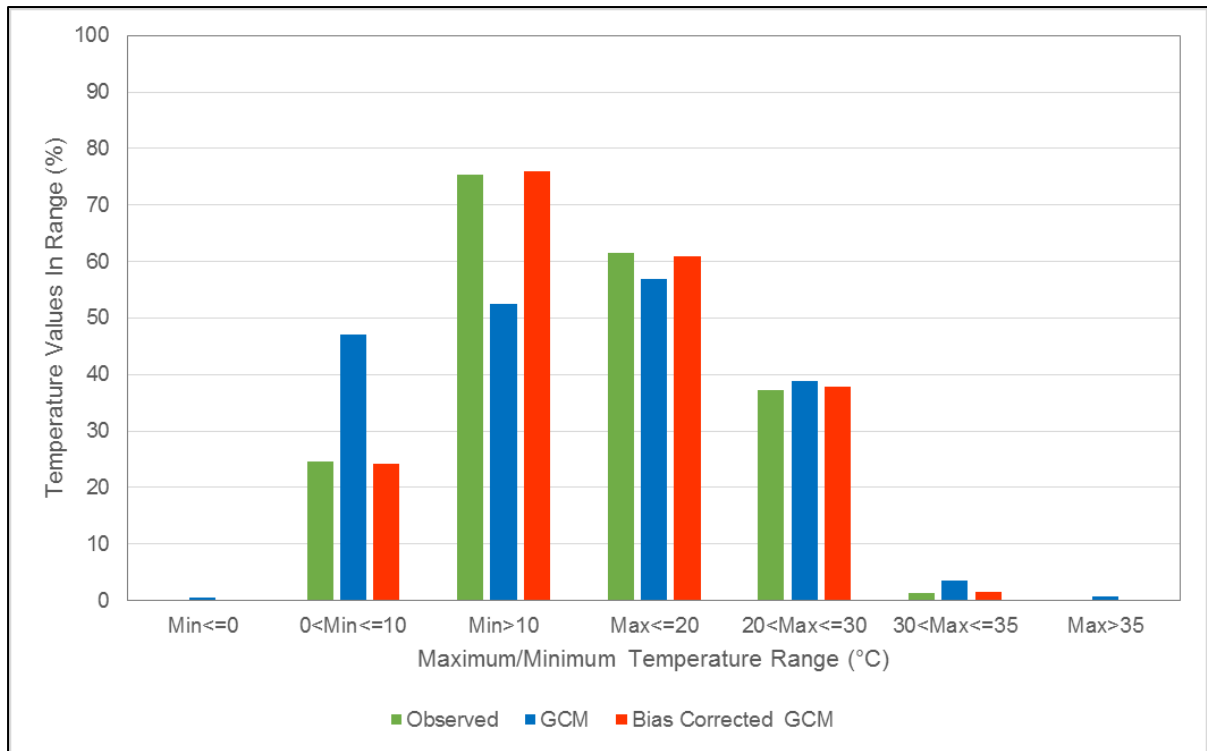
Figure 2.32 Comparison of distribution of daily maximum and minimum temperatures in the calibration period (1961-1999) at the temperature station corresponding to rain gauge 0002069W for the ACCESS1-0 GCM for RCP4.5 and RCP8.5
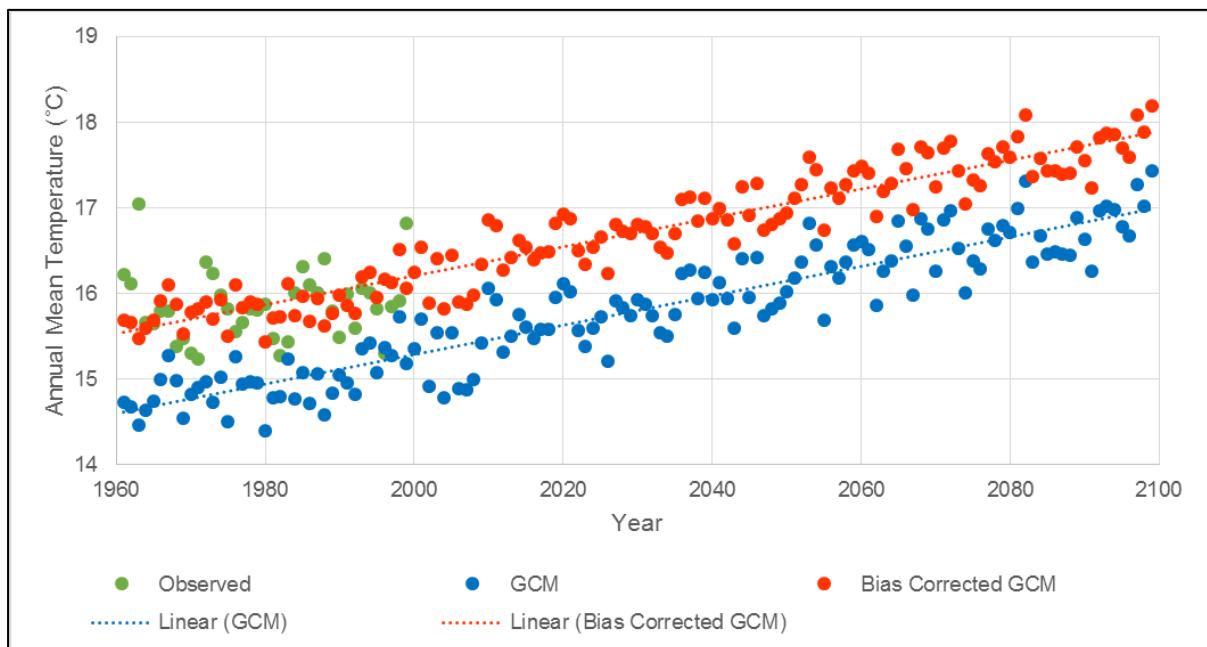
Figure 2.33 Comparison of annual mean temperatures for the period 1961-2099 (including trends) at the temperature station corresponding to rain gauge 0002069W for the ACCESS1-0 GCM for RCP4.5
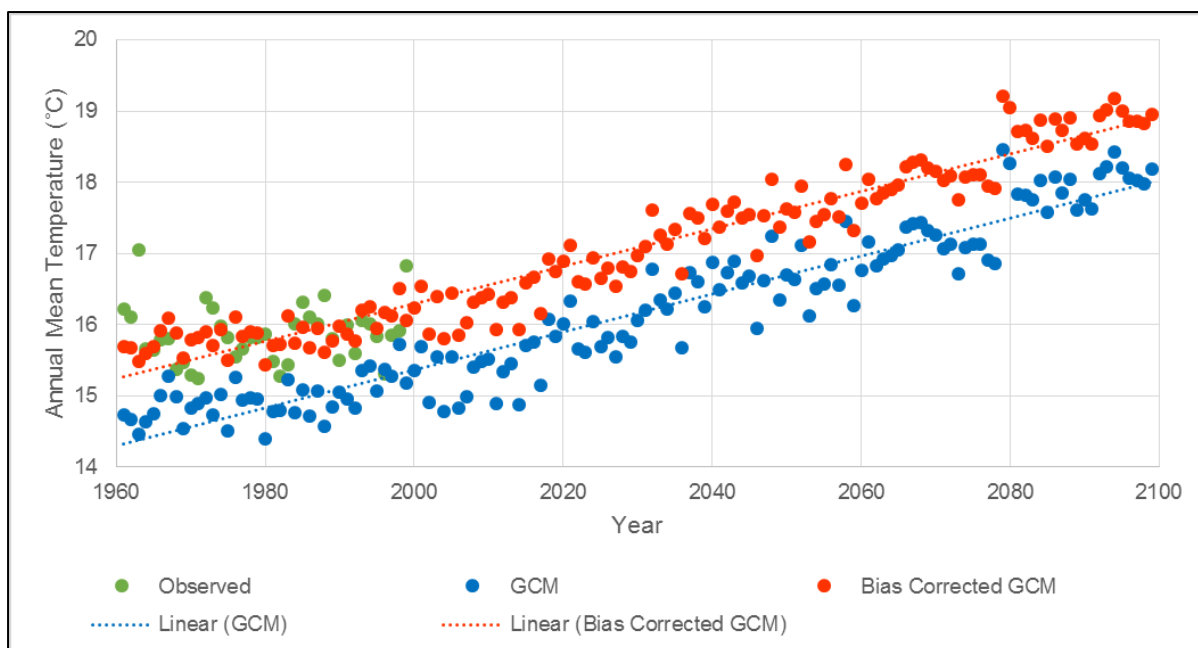
Figure 2.34 Comparison of annual mean temperatures for the period 1961-2099 (including trends) at the temperature station corresponding to rain gauge 0002069W for the ACCESS1-0 GCM for RCP8.5
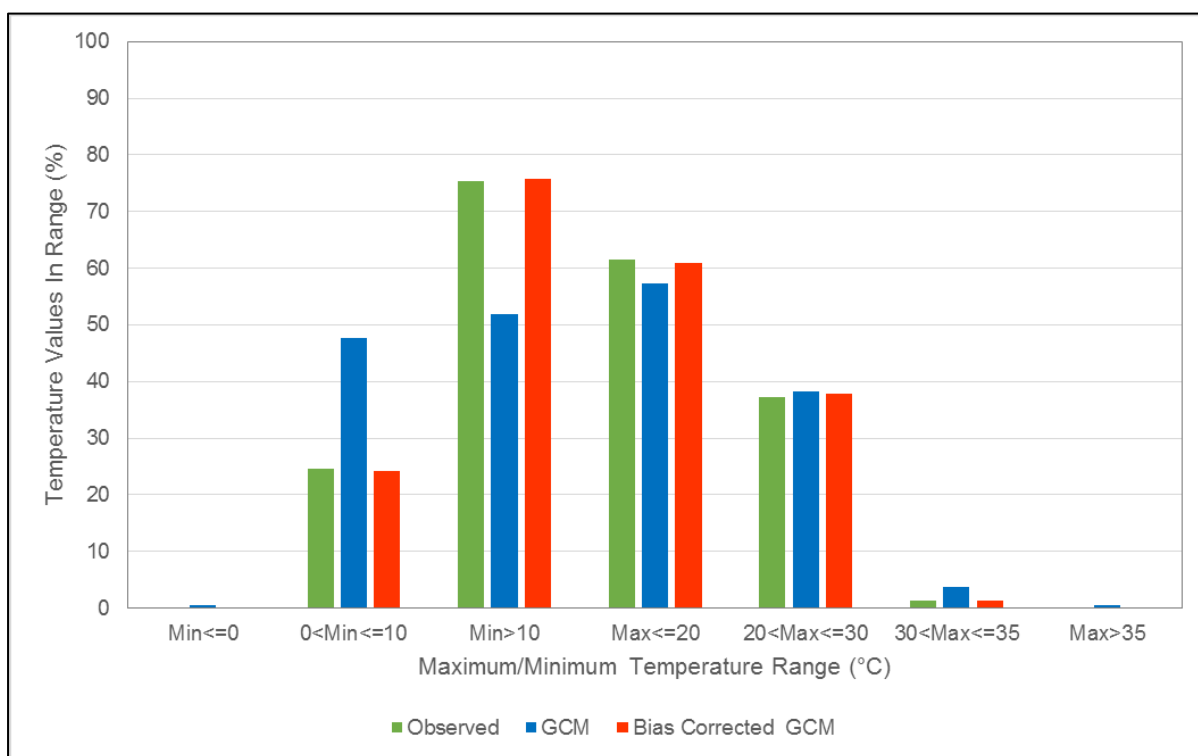
Figure 2.35 Comparison of distribution of daily maximum and minimum temperatures in the calibration period (1961-1999) at the temperature station corresponding to rain gauge 0002069W for the CCSM4 GCM for RCP4.5 and RCP8.5
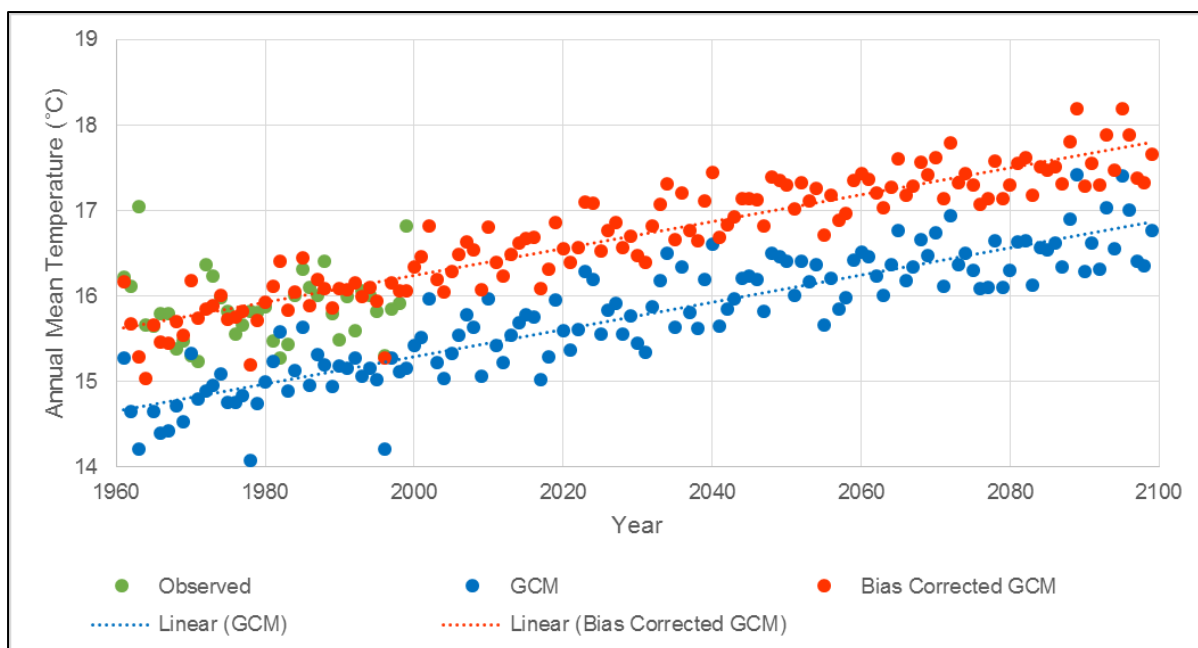
Figure 2.36 Comparison of annual mean temperatures for the period 1961-2099 (including trends) at the temperature station corresponding to rain gauge 0002069W for the CCSM4 GCM for RCP4.5
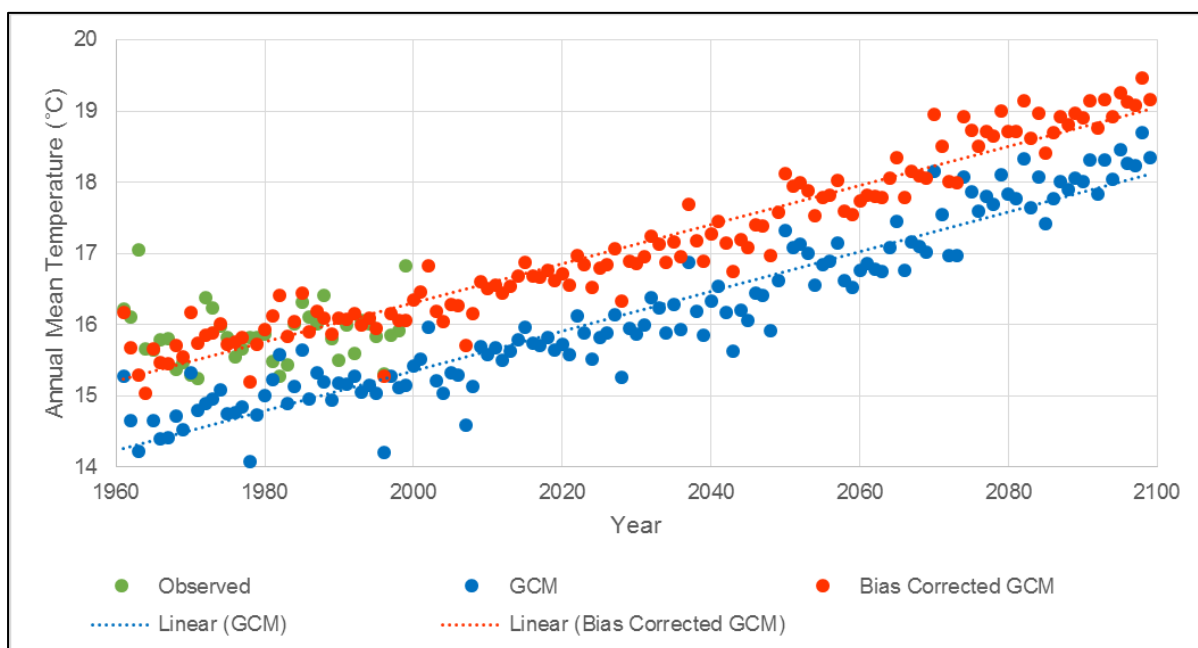
Figure 2.37 Comparison of annual mean temperatures for the period 1961-2099 (including trends) at the temperature station corresponding to rain gauge 0002069W for the CCSM4 GCM for RCP8.5
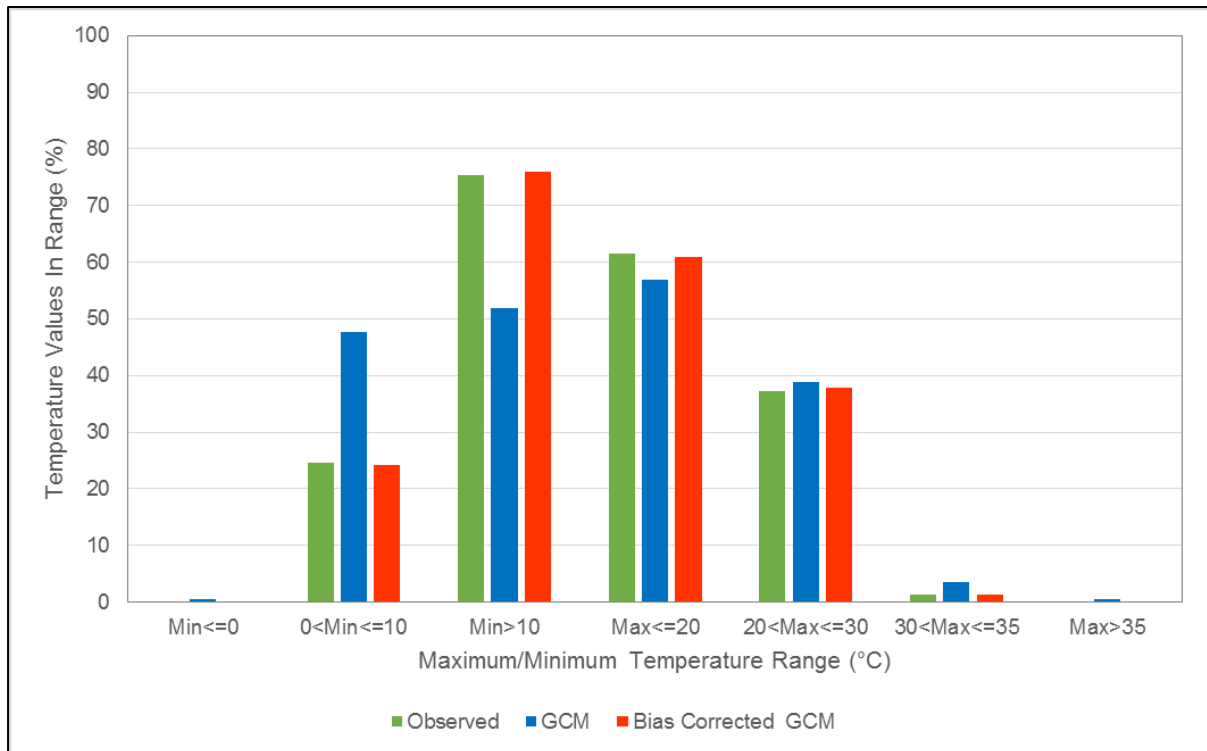
Figure 2.38 Comparison of distribution of daily maximum and minimum temperatures in the calibration period (1961-1999) at the temperature station corresponding to rain gauge 0002069W for the CNRM-CM5 GCM for RCP4.5 and RCP8.5
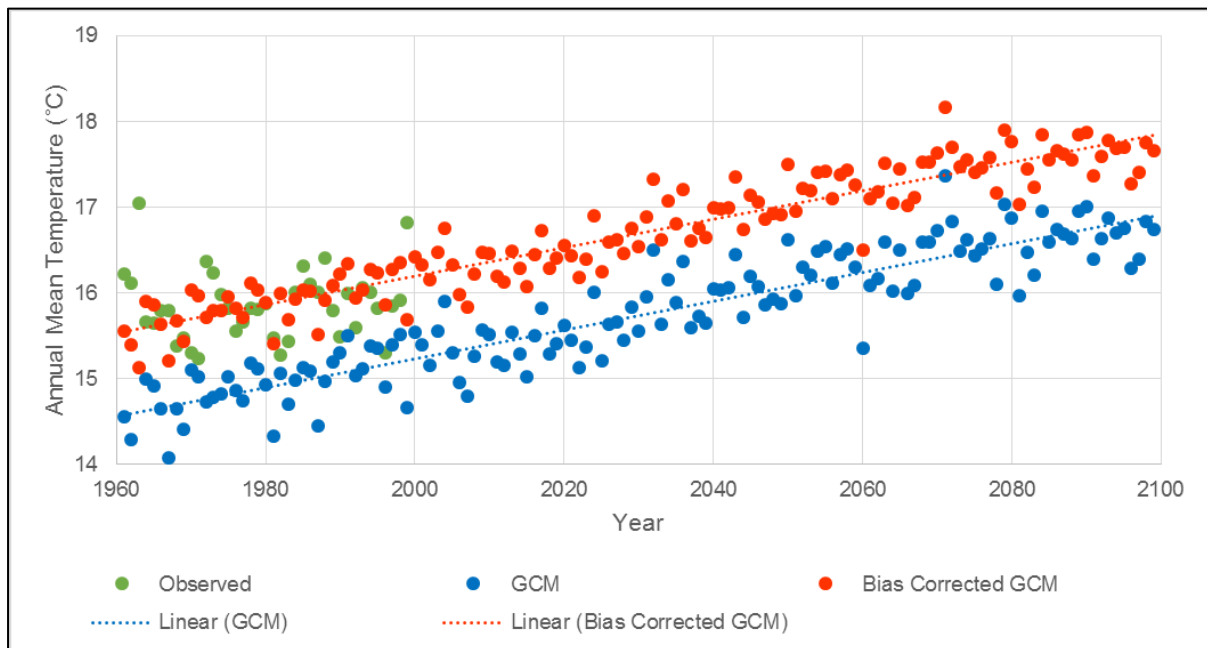
Figure 2.39 Comparison of annual mean temperatures for the period 1961-2099 (including trends) at the temperature station corresponding to rain gauge 0002069W for the CNRM-CM5 GCM for RCP4.5
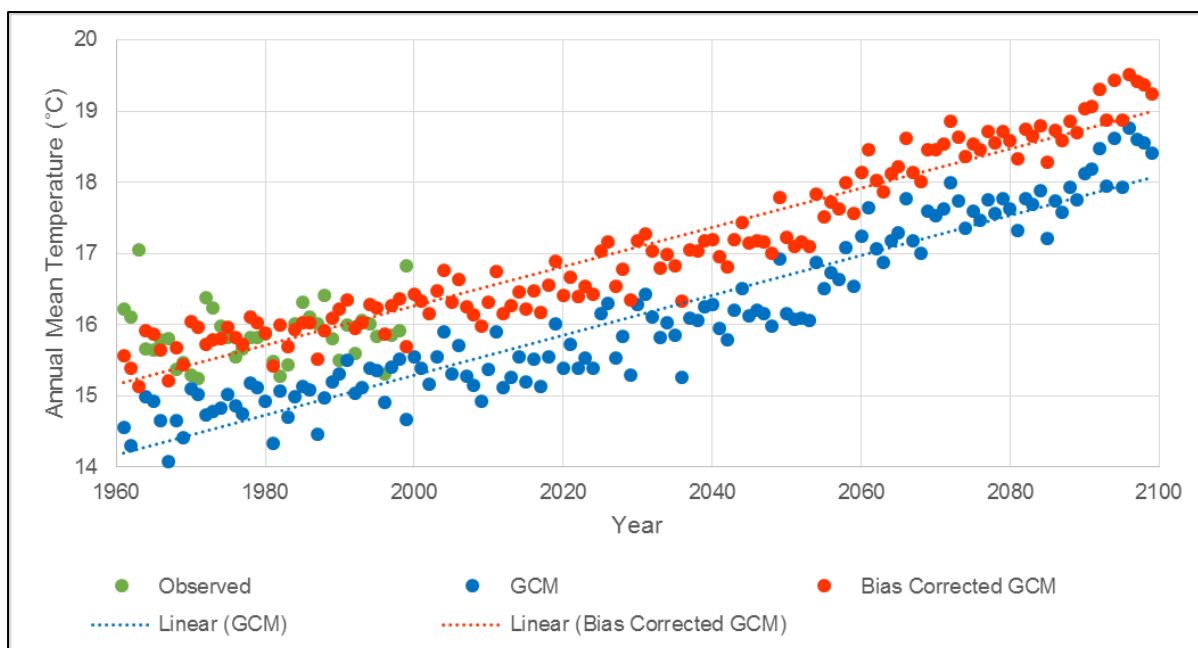
Figure 2.40 Comparison of annual mean temperatures for the period 1961-2099 (including trends) at the temperature station corresponding to rain gauge 0002069W for the CNRM-CM5 GCM for RCP8.5
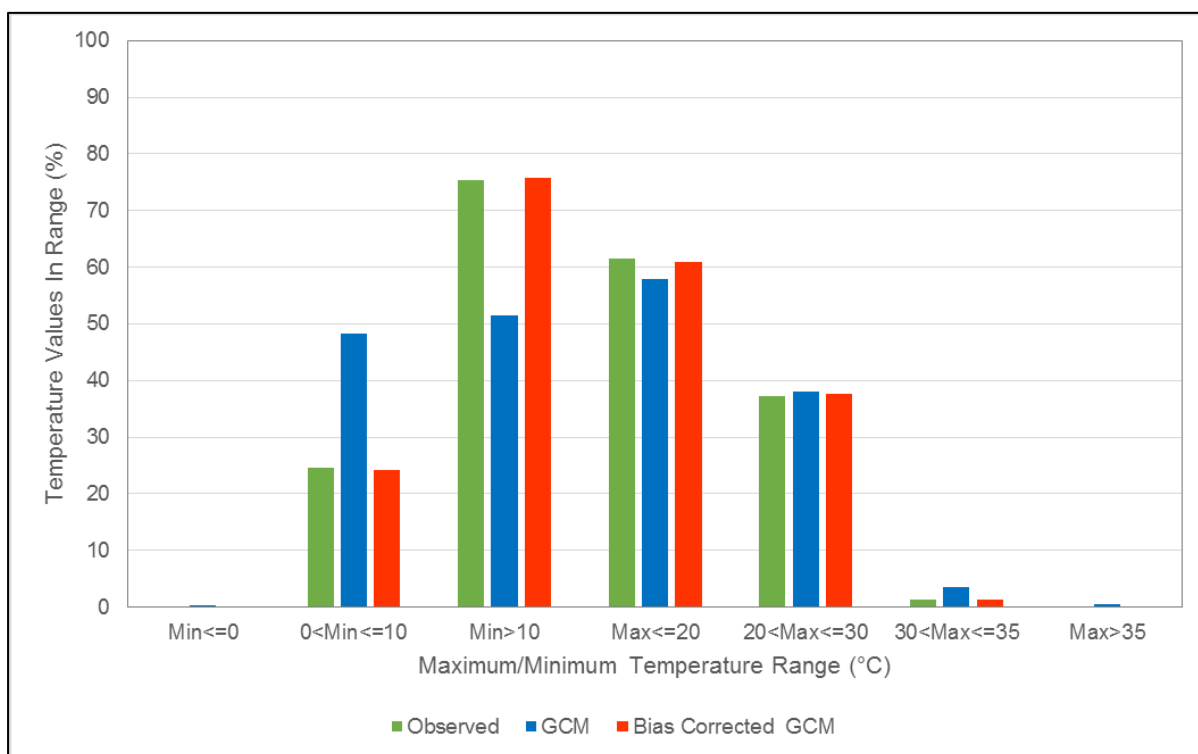
Figure 2.41 Comparison of distribution of daily maximum and minimum temperatures in the calibration period (1961-1999) at the temperature station corresponding to rain gauge 0002069W for the GFDL-CM3 GCM for RCP4.5 and RCP8.5
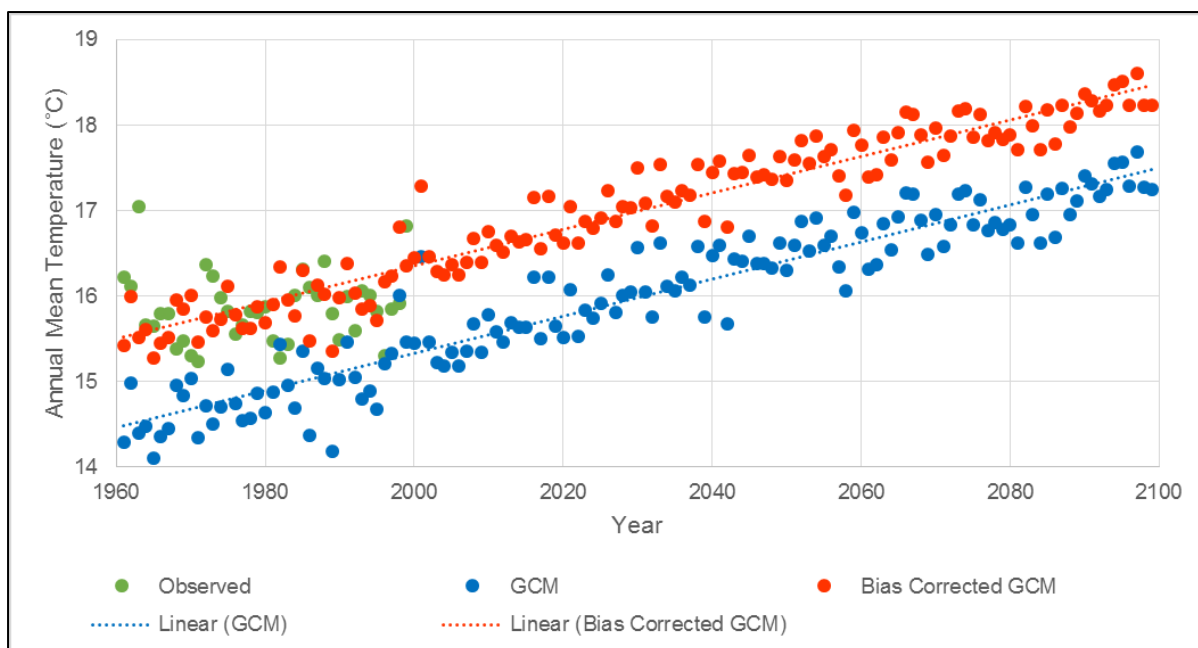
Figure 2.42 Comparison of annual mean temperatures for the period 1961-2099 (including trends) at the temperature station corresponding to rain gauge 0002069W for the GFDL-CM3 GCM for RCP4.5
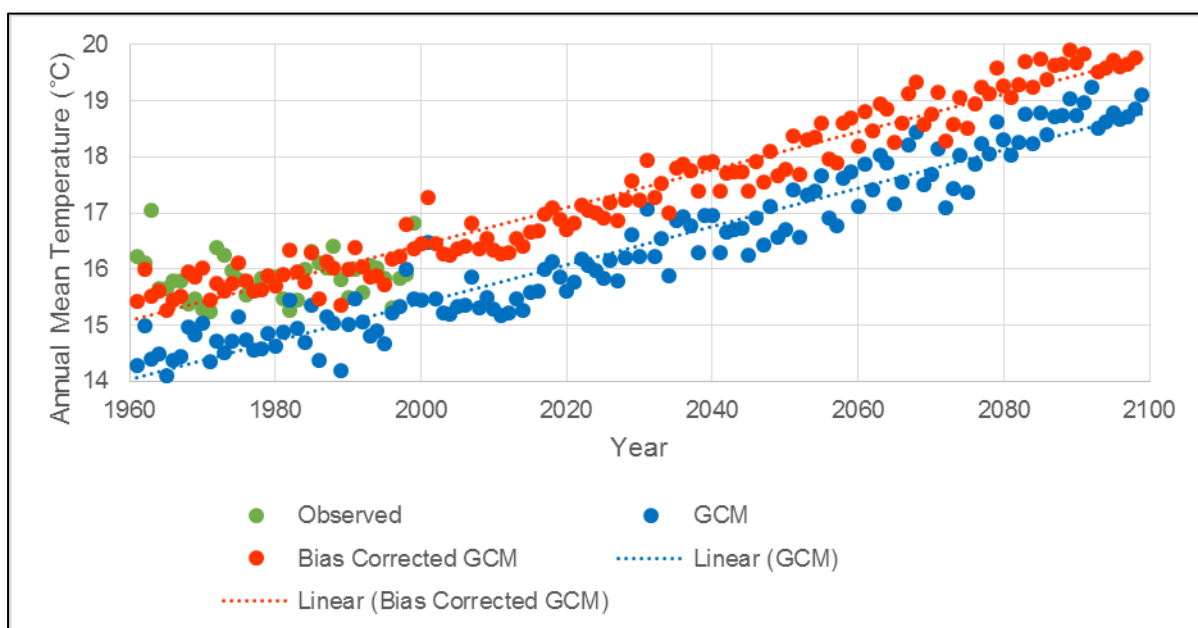
Figure 2.43 Comparison of annual mean temperatures for the period 1961-2099 (including trends) at the temperature station corresponding to rain gauge 0002069W for the GFDL-CM3 GCM for RCP8.5
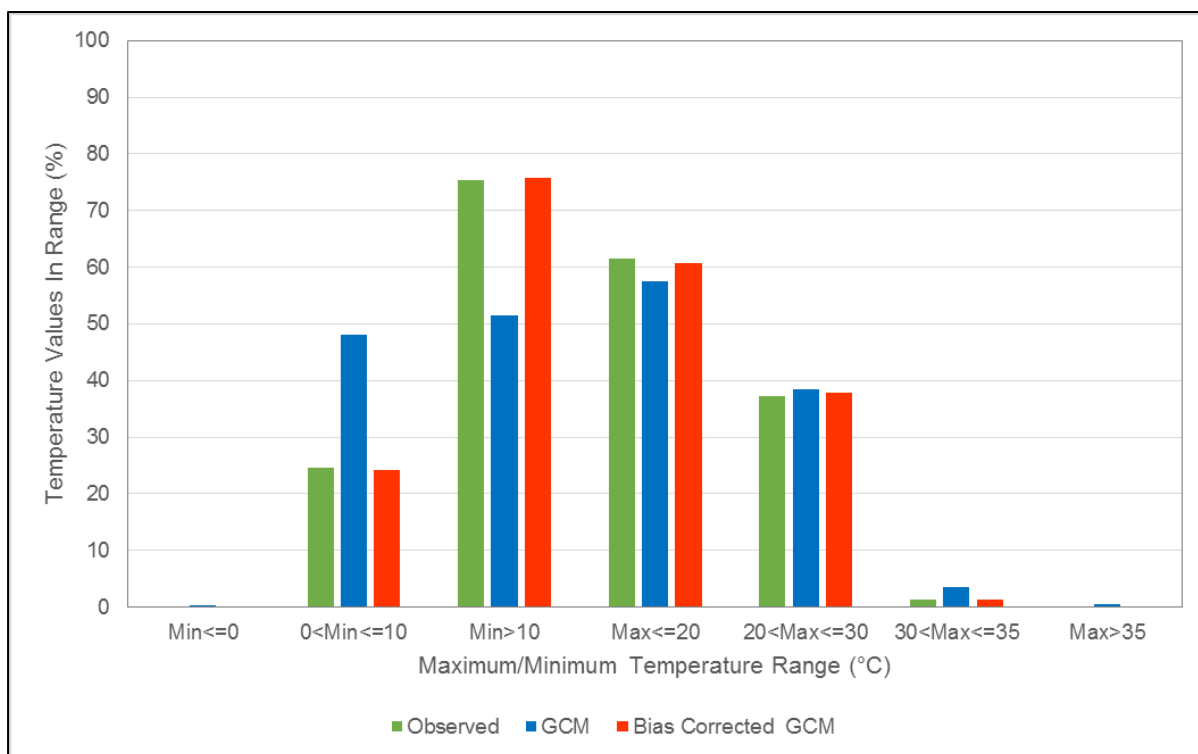
Figure 2.44 Comparison of distribution of daily maximum and minimum temperatures in the calibration period (1961-1999) at the temperature station corresponding to rain gauge 0002069W for the MPI-ESM-LR GCM for RCP4.5 and RCP8.5
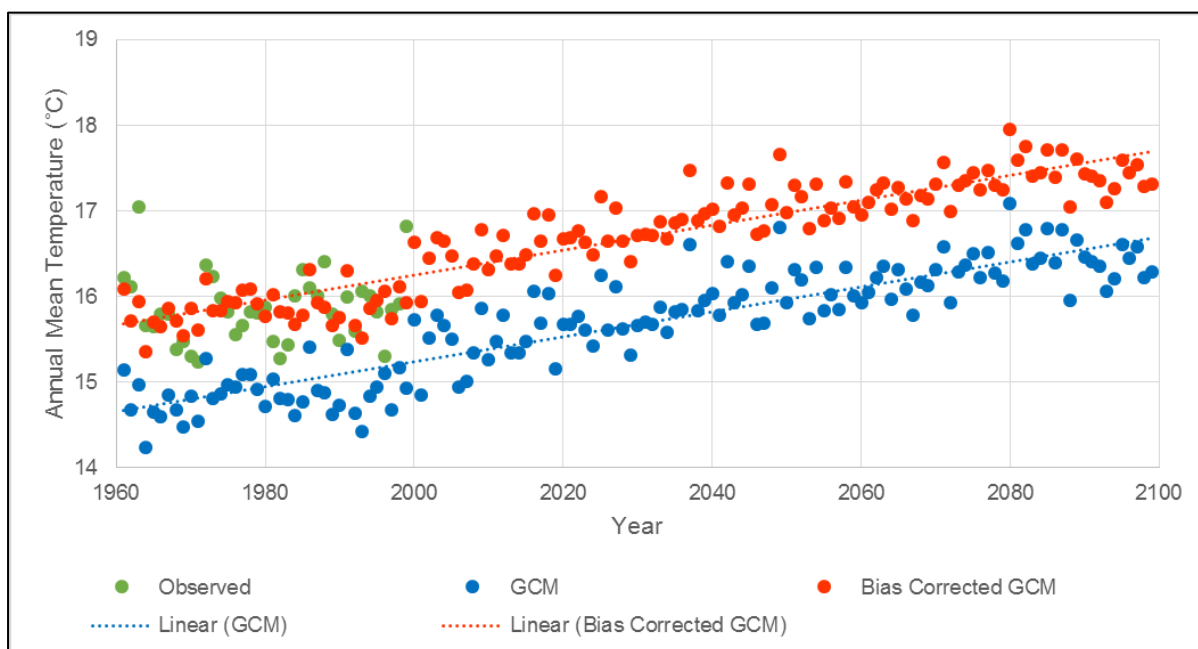
Figure 2.45 Comparison of annual mean temperatures for the period 1961-2099 (including trends) at the temperature station corresponding to rain gauge 0002069W for the MPI-ESM-LR GCM for RCP4.5
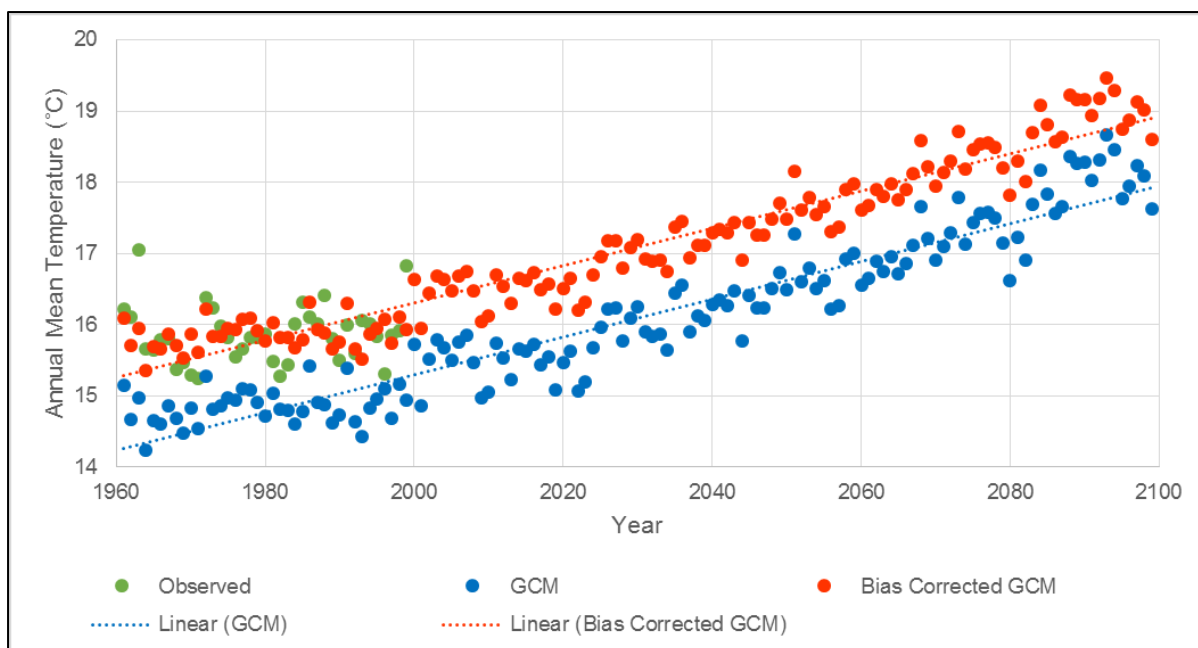
Figure 2.46 Comparison of annual mean temperatures for the period 1961-2099 (including trends) at the temperature station corresponding to rain gauge 0002069W for the MPI-ESM-LR GCM for RCP8.5
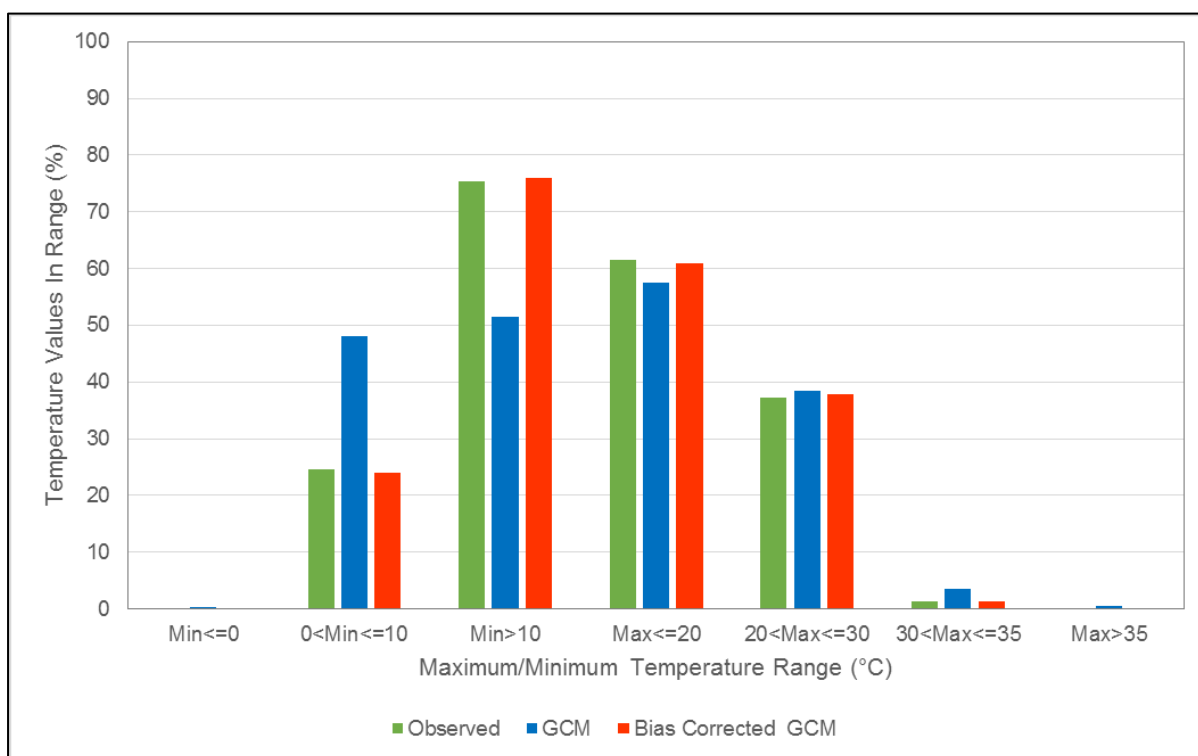
Figure 2.47 Comparison of distribution of daily maximum and minimum temperatures in the calibration period (1961-1999) at the temperature station corresponding to rain gauge 0002069W for the NorESM1-M GCM for RCP4.5 and RCP8.5
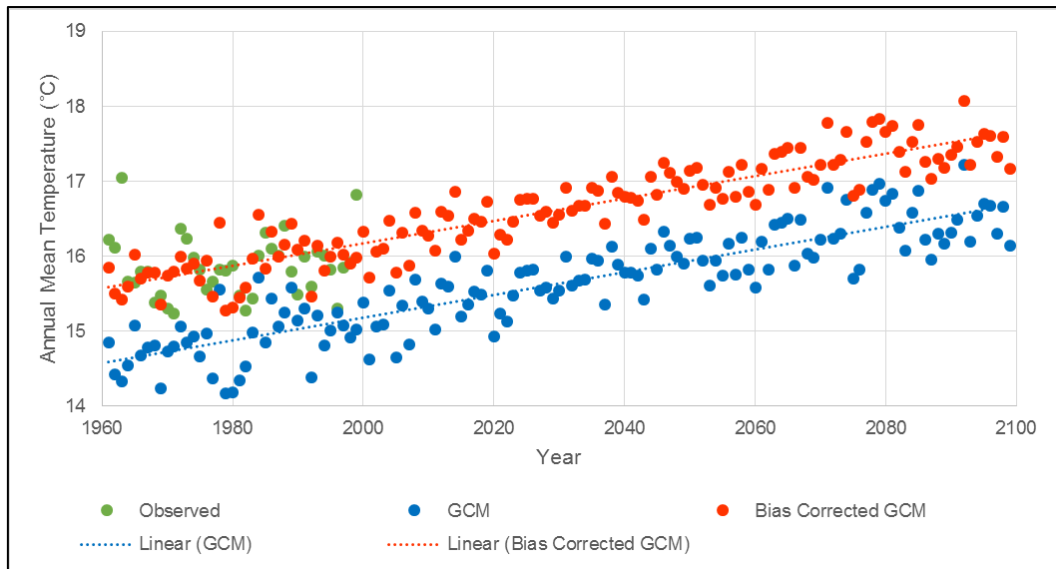
Figure 2.48 Comparison of annual mean temperatures for the period 1961-2099 (including trends) at the temperature station corresponding to rain gauge 0002069W for the NorESM1-M GCM for RCP4.5
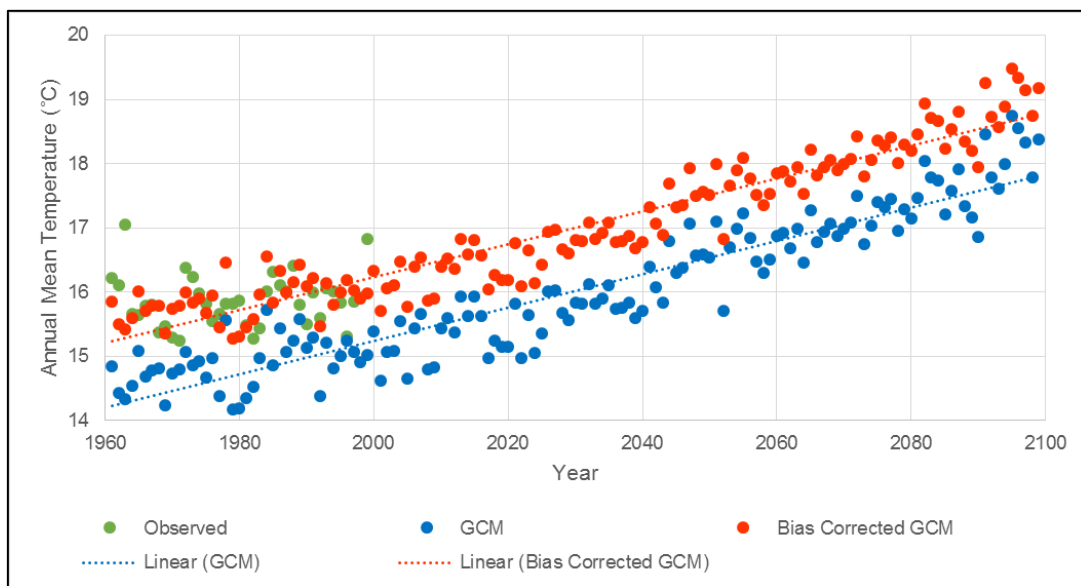
Figure 2.49 Comparison of annual mean temperatures for the period 1961-2099 (including trends) at the temperature station corresponding to rain gauge 0002069W for the NorESM1-M GCM for RCP8.5

The results shown above are for one temperature station only. The CCAM climate projections were also contextualized within a larger set of coarser scale CMIP5 projections to assess how well they represent the overall range of possible futures. This assessment was done for each of South Africa's nine Water Management Areas. The CCAM climate projections were also contextualized within CSAG downscalings of the CMIP5 projections for selected individual catchments.

Summary of Temperature Bias Correction Results Per Water Management Area for Each GCM and Both RCPs

In order to display a summary of the results of the bias correction of the temperature data, the annual mean maximum and minimum temperature values for each temperature station were used to calculate 20-year running mean values for each WMA for each RCP and each GCM. The summarised maximum temperature data is shown in **Figure 2.50 f**or RCP4.5 and in **Figure 2.51** for RCP8.5. The summarised minimum temperature data are shown in **Figure 2.53** for RCP4.5 and in **Figure 2.54** for RCP8.5. Each graph in these figures shows three datasets:

- observed data ("Obs" in green),
- raw CCAM downscaled GCM data ("Raw" in blue), and
- bias corrected CCAM downscaled GCM data ("BC" in red).

These results demonstrate that the bias correction of the temperature data worked as anticipated. The GCM projections of maximum and minimum temperature were underestimated in the historical period for all GCMs and in all WMAs. The bias in the maximum temperatures is greater than the bias in the minimum temperatures. Both the maximum and minimum projected temperatures are greater for RCP8.5 than for RCP4.5 as expected. It should be noted that there is not a similar problem with the RCP4.5 daily air temperature projections as was found with the RCP4.5 rainfall projections.
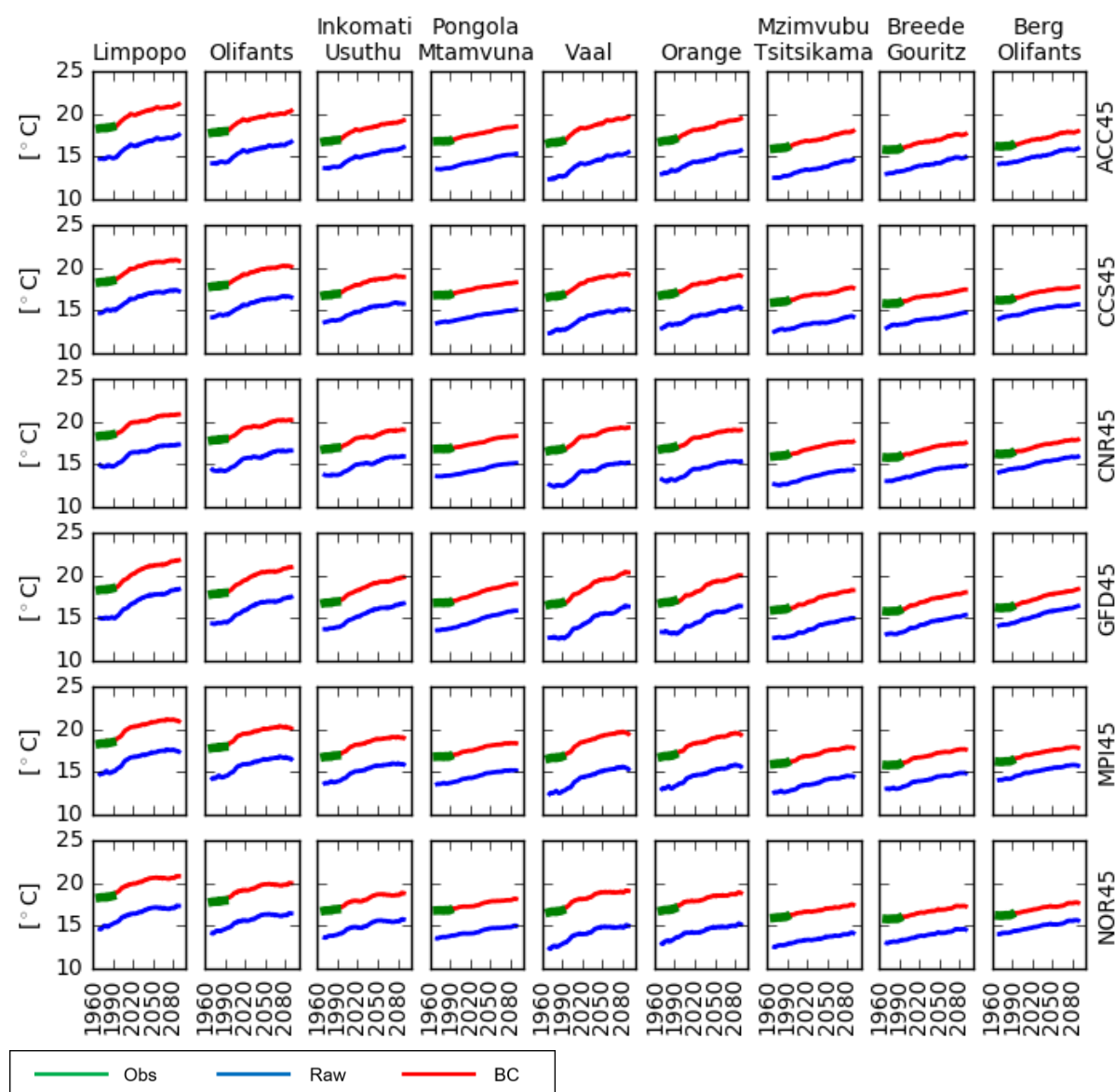
Figure 2.50   The summarised maximum temperature data for RCP4.5
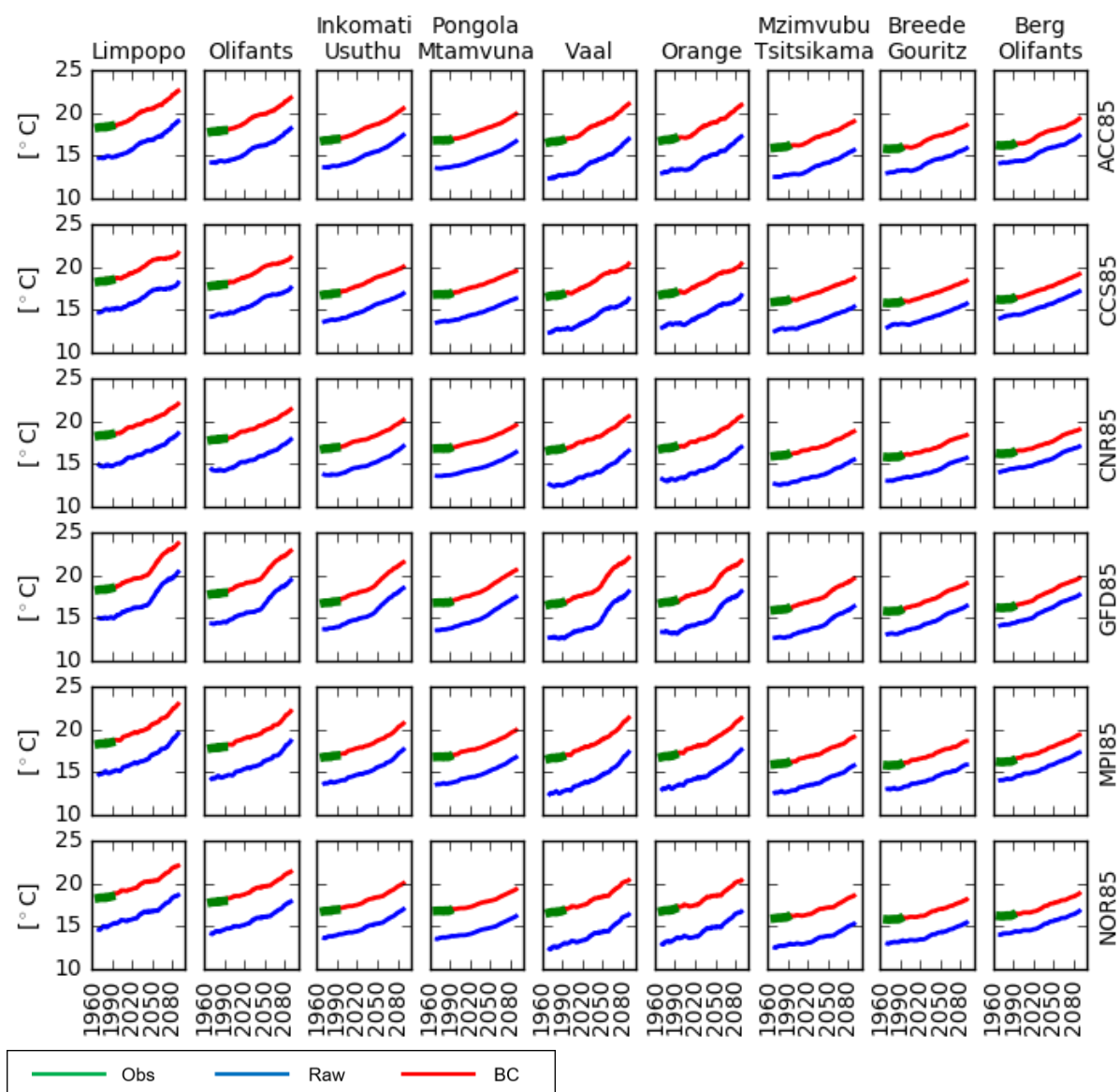
Figure 2.51 The summarised maximum temperature data for RCP8.5
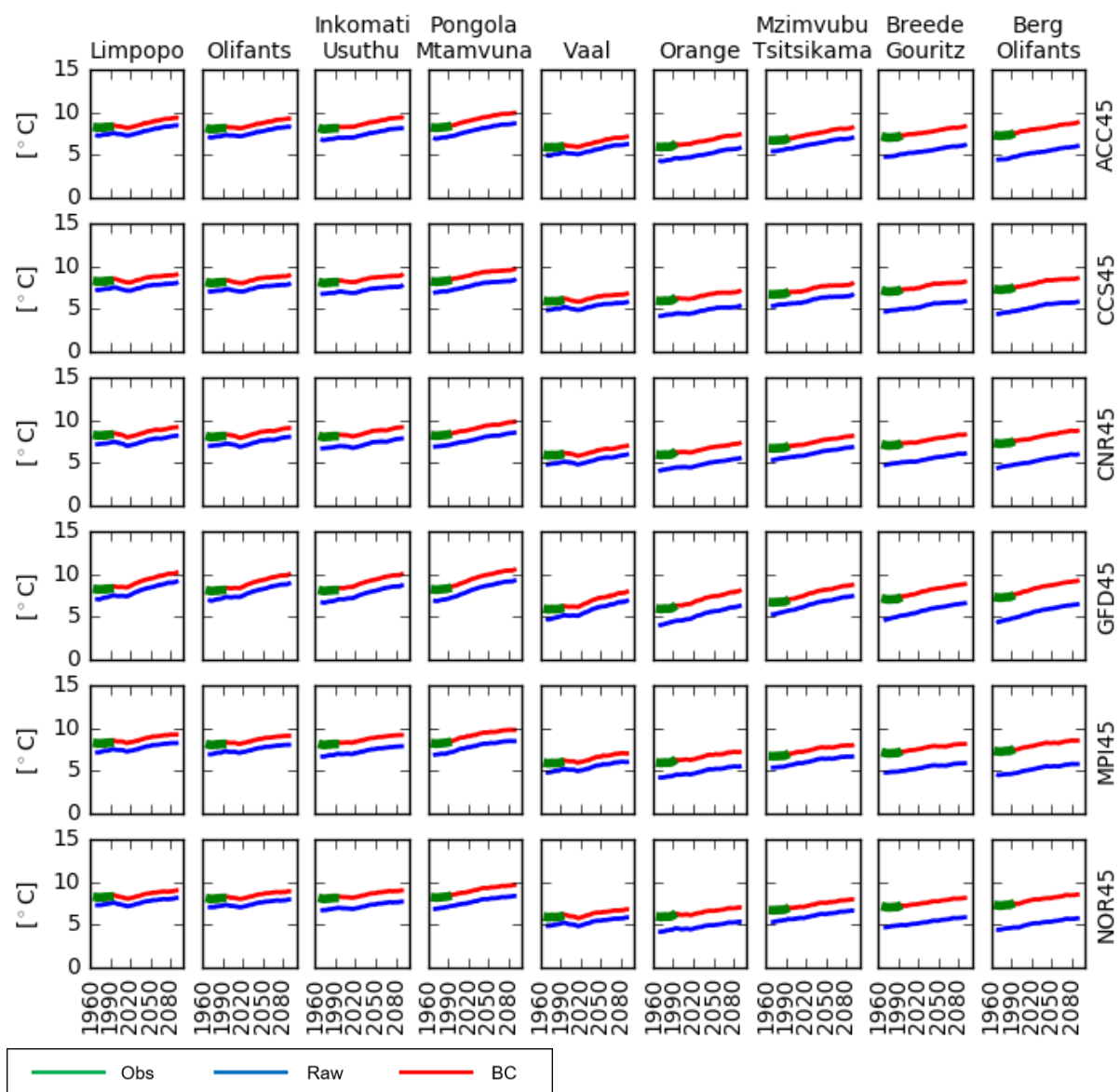
Figure 2.52 The summarised minimum temperature data for RCP4.5
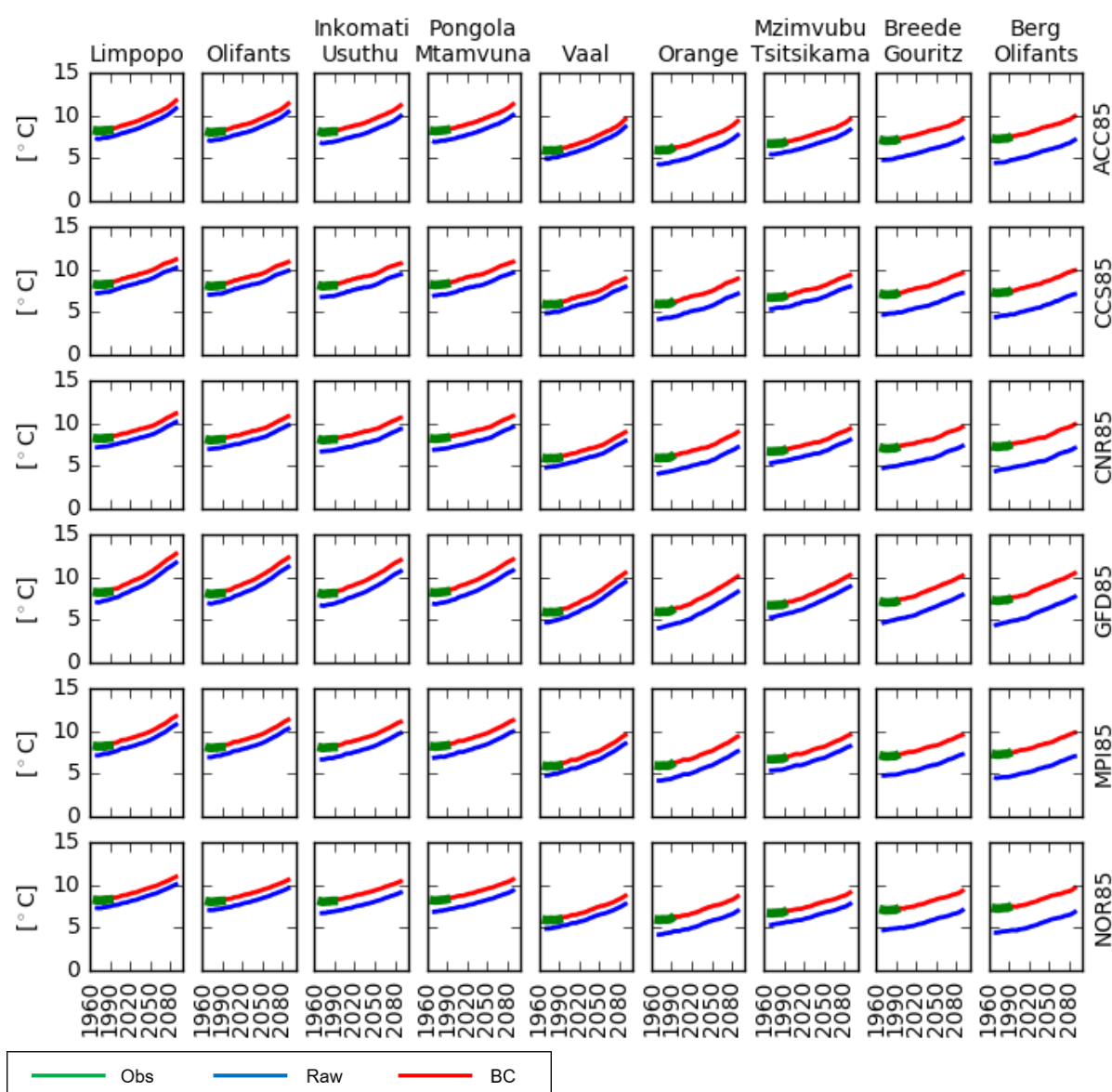
Figure 2.53 The summarised minimum temperature data for RCP8.5

2.4 Reasons that the RCP4.5 CCAM Projections were not Applied Further in the Study

While working with the CCAM climate change projection data provided to this project, rainfall patterns were detected in the RCP4.5 dataset that were not consistent with expectations when comparing them to the RCP8.5 projections. These inconsistencies are described initially in this section. Following this, a comparison of the projected patterns with that presented in previous projects where these projections were developed and documented, is presented. Conclusions drawn from these comparisons are then presented, and the implications for this project discussed.

2.4.1 Inconsistencies in the supplied RCP4.5 CCAM projection data

Inconsistencies were first detected in the RCP4.5 CCAM projection data when comparing them to the CMIP5 ensemble. This comparison was initially performed to check that the CCAM projections

adequately reflected the range and direction of change in the CMIP5 ensemble. This comparison was undertaken by developing regional (per Water Management Area) aggregate time series anomaly plots for the 6-member CCAM ensemble, as well as for the CMIP5 ensemble. Comparisons were performed for both RCP8.5 and RCP4.5 and are presented in **Figures 2.54** and **2.55**, respectively. In each case, results are presented for both raw and daily bias corrected CCAM simulation data.

There is general agreement between RCP8.5 CCAM rainfall projections and the CMIP5 ensemble projections in all regions in South Africa in terms of the sign of future change, and in the range of uncertainty. This applies to both raw and bias-corrected projections. However, there is a lack of such agreement in the RCP4.5 projections. This applies to both the raw and bias-corrected data. While the differences are relatively minor in the raw RCP4.5 CCAM data (**Figure 2.55a**), they are magnified through the process of bias correction.

To ensure that the bias correction procedures were implemented correctly, an independent implementation of the QDM bias correction algorithm was carried out and the results compared to the original set. It was found that the procedures were implemented robustly and correctly, and in an identical way for both the RCP8.5 and RCP4.5 datasets. This eliminated the possibility that the bias-correction process had introduced the unexpected patterns in the RCP4.5 CCAM rainfall projections.

To further explore the inconsistencies in the RCP4.5 data, the structure of daily rainfall in the raw CCAM data for the baseline (pre-2005) and projected (2005 onwards) periods was analysed for both RCP4.5 and RCP8.5 datasets. The simulation data for the baseline period was identical for both RCP scenarios, as observed GHG forcing was assumed for this period in the development of the climate simulations. The analysis was conducted over the whole country and is presented in map form in **Figure 2.6**. **Figure 2.6a** shows the ratio of future to baseline rainfall event frequency (mean number of rain days per annum). For RCP4.5 the dominant trend is a strong increase in the number of rain days over the Northern Cape and adjacent areas, while for RCP8.5 most areas exhibit fairly minimal change. **Figure 2.6b** shows the ratio of future to baseline mean daily rainfall. For RCP4.5 there are strong reductions in the mean daily rainfall over the Northern Cape and adjacent areas, while for RCP8.5 there are slight increases over this area, and slightly stronger increases over the Drakensberg.

The more intense trends in the RCP4.5 data set are not consistent with a scenario that is expected to be less severe than the RCP8.5 (business-as-usual) scenario. In time series plots for selected locations (not shown here) it was found that there was an abrupt change in the above daily rainfall characteristics for the RCP4.5 dataset when transitioning from the baseline (pre-2005) to projected time periods (2005 onwards). This abrupt transition was not evident in the RCP8.5 simulation data and suggests that the RCP4.5 dataset had a different daily rainfall structure to the baseline period. The abruptness of this change appeared to be artificial in nature. The differences in daily rainfall characteristics suggest that the raw RCP4.5 CCAM dataset (future) might have been subject to different pre-processing than that of the RCP8.5 (future) and baseline datasets. Alternatively, the RCP4.5 data could have been generated by a differently configured CCAM model.
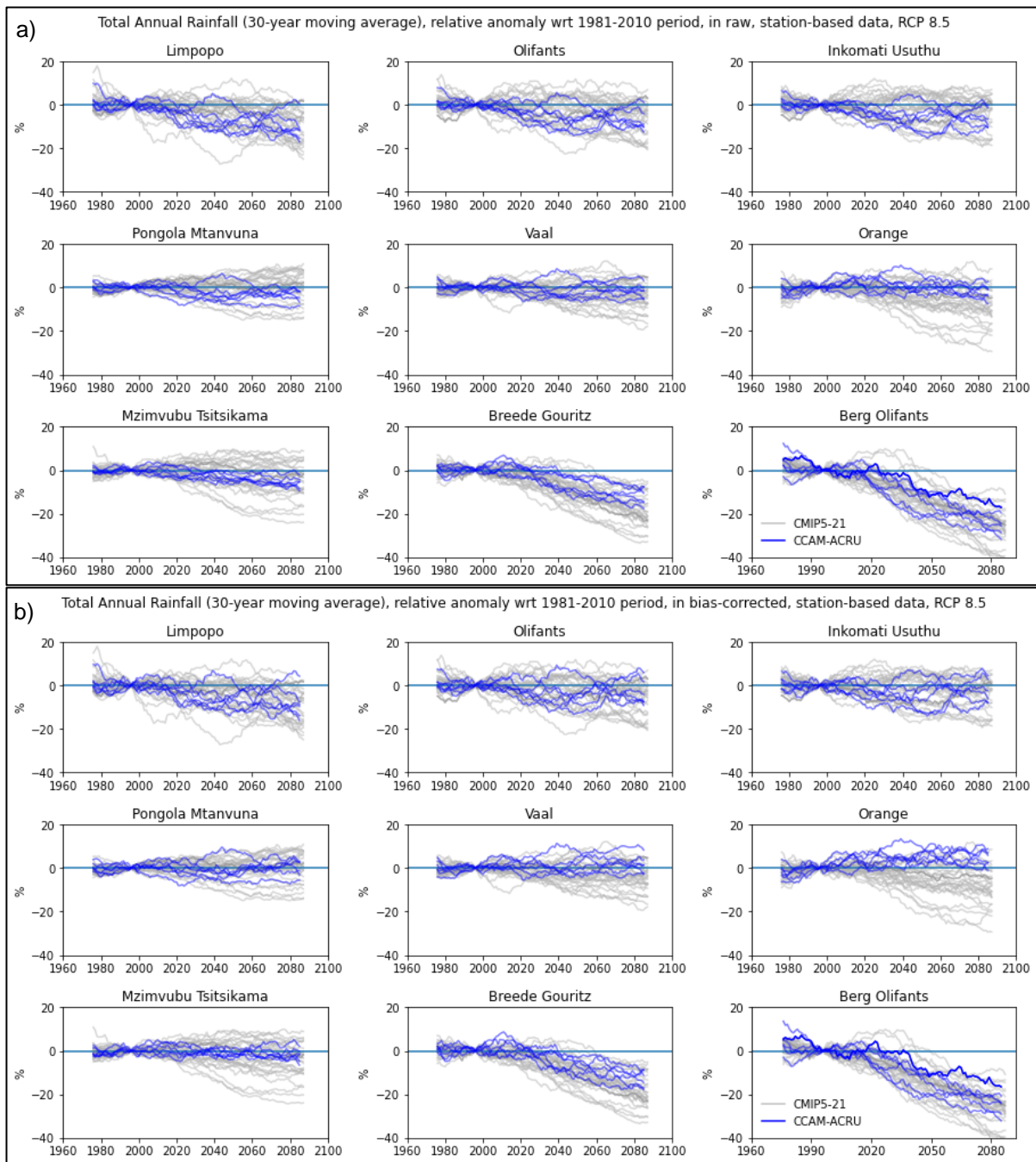
Figure 2.54 Comparison of the time series of region-aggregate rainfall anomalies with respect to the 1981-2010 period in raw (a) and bias-corrected (b) CCAM ensembles and in the CMIP5 ensemble for RCP8.5 projections
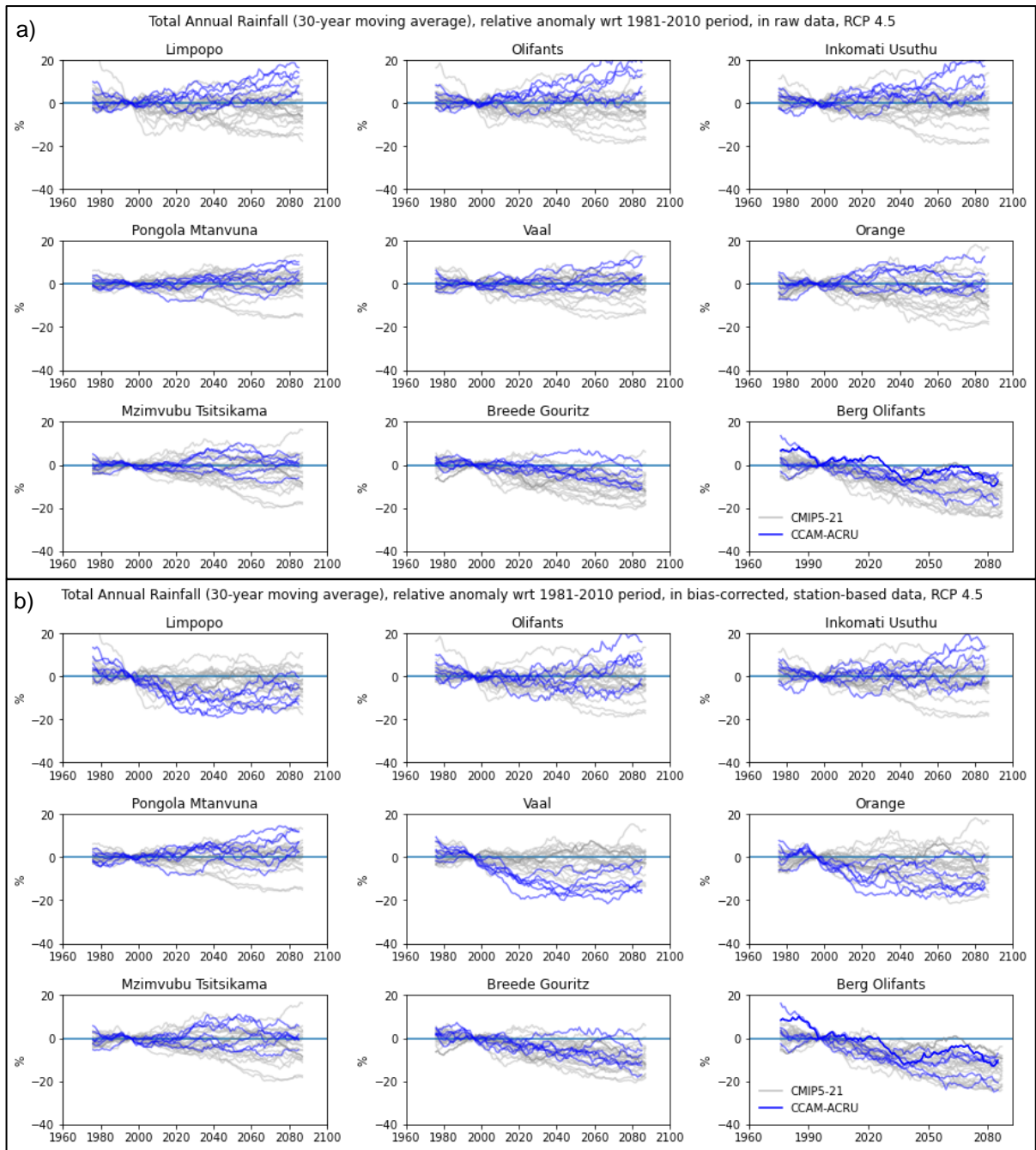
Figure 2.55   Comparison of the time series of region-aggregate rainfall anomalies with respect to the 1981-2010 period in raw (a) and bias-corrected (b) CCAM ensembles and in the CMIP5 ensemble for RCP4.5 projections
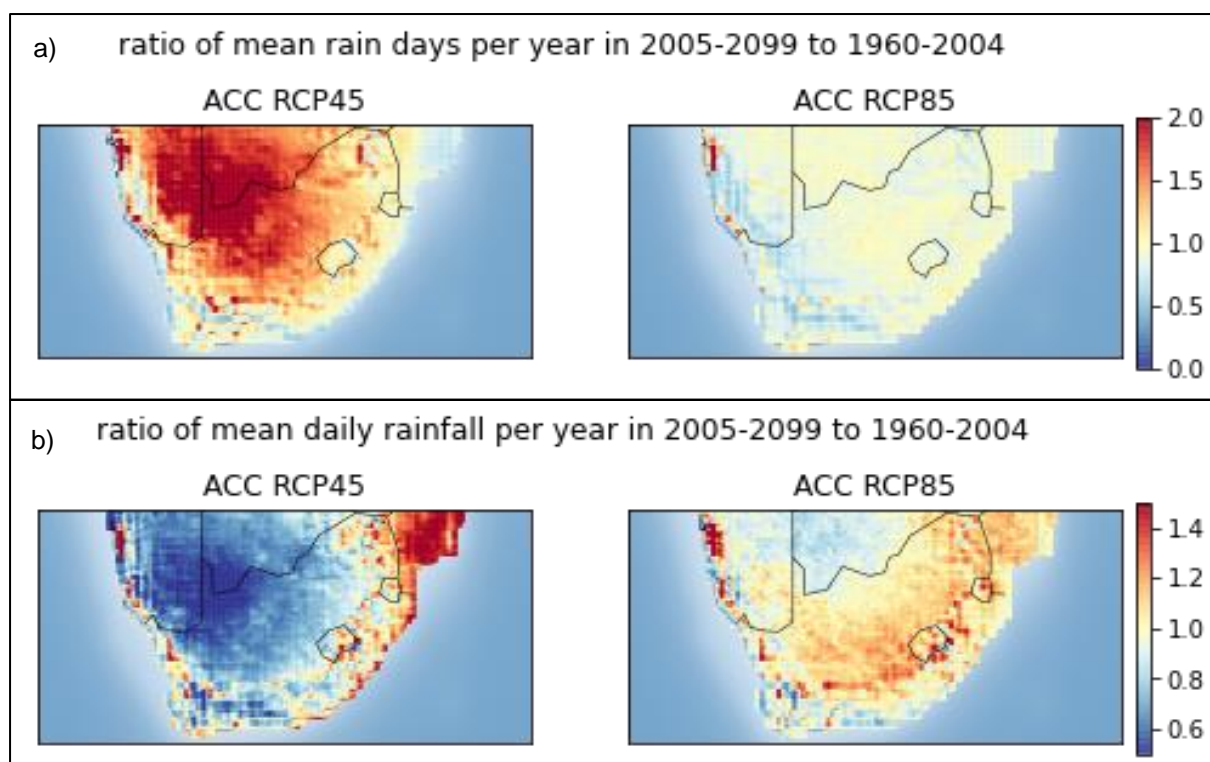
Figure 2.56   Comparison of the ratio of future to historical rainfall event frequency (a) and daily rainfall event intensity (b) in raw RCP4.5 and RCP8.5 CCAM data for a selected ensemble member (ACC GCM model). Other ensemble members are characterized by similar differences

2.4.2   Contrast with previously reported patterns for CCAM climate projections

The development and characteristics of the CCAM climate projections have been described previously (Engelbrecht, 2019; Engelbrecht et al., 2020). The patterns in the projections as they were reported in those publications were analysed and compared with the patterns as they were found in this project. The maps in the previous publications are similar, except that that in Engelbrecht et al. (2020) the domain of the maps is restricted to eastern parts of the country, whereas Engelbrecht (2019) presented maps of the whole country.

Engelbrecht (2019) presented maps of the change in annual average rainfall totals for near (**Figure 2.57**) and distant (**Figure 2.58**) futures relative to a baseline period (1961-1990). These maps were based on 8 km resolution gridded data and represented 50th percentile maps of the ensemble of the six GCMs under RCP4.5 and RCP8.5. Similar maps produced using the CCAM data provided to this project are presented in **Figure 2.59** for both RCP4.5 and RCP8.5. It is noted that there are differences in how these maps are prepared (**Figure 2.59** shows daily bias-corrected catchment-level maps that represent changes in the ensemble means), however, the broad patterns in the maps should still be comparable.

The maps in **Figures 2.57** and **2.58** portray a relationship between RCP4.5 and RCP8.5 that is more plausible than what is found for the maps produced using data supplied to this project (**Figure 2.59**). For the distant future, **Figure 2.58** clearly shows more severe impacts for RCP8.5 than RCP4.5, as would be expected. For the near future, **Figure 2.57** shows more mixed signals for RCP4.5 and RCP8.5. While the areas projected to experience drying show more intense changes in RCP4.5, the opposite is true for areas projected to experience wetting i.e. more intense wetting is projected in RCP8.5. Arguably, these mixed signals may be justified for a period during which the difference between RCP4.5 and RCP8.5 in terms of emissions and associated climate response, is relatively small.
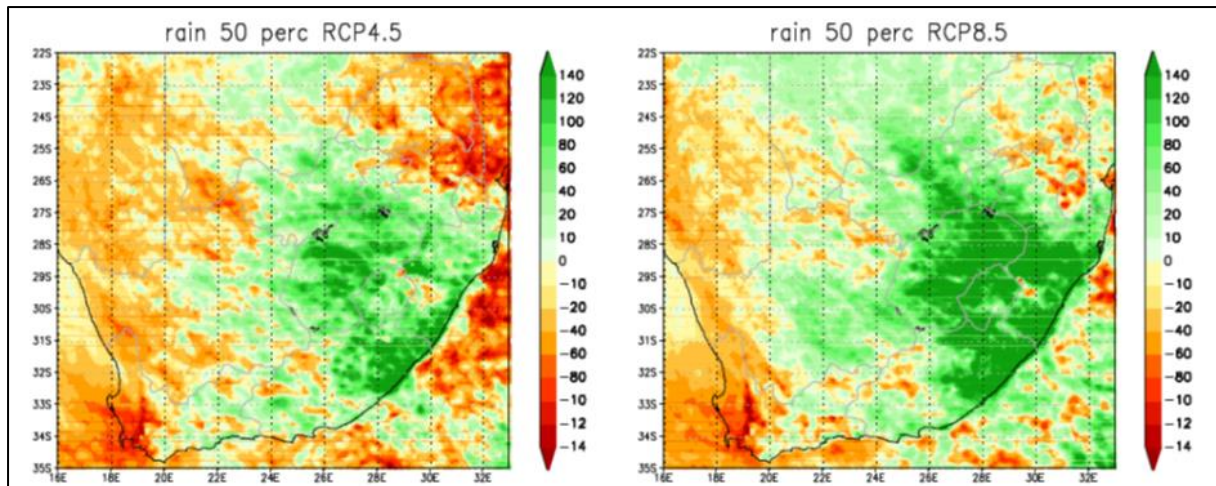
Figure 2.57 Change in mean annual rainfall (mm) for 2021-2050 relative to 1961-1990. These are the 50th percentile maps of the ensemble of six GCMs under RCP4.5 and RCP8.5 (Engelbrecht, 2019).
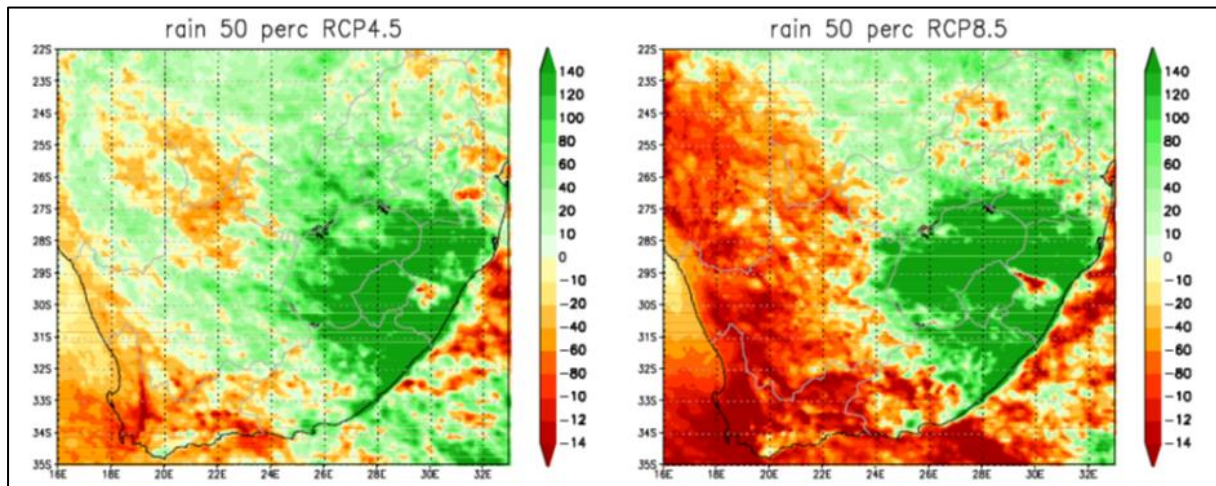
Figure 2.58 Change in mean annual rainfall (mm) for 2071-2100 relative to 1961-1990. These are the 50th percentile maps of the ensemble of six GCMs under RCP4.5 and RCP8.5 (Engelbrecht, 2019).
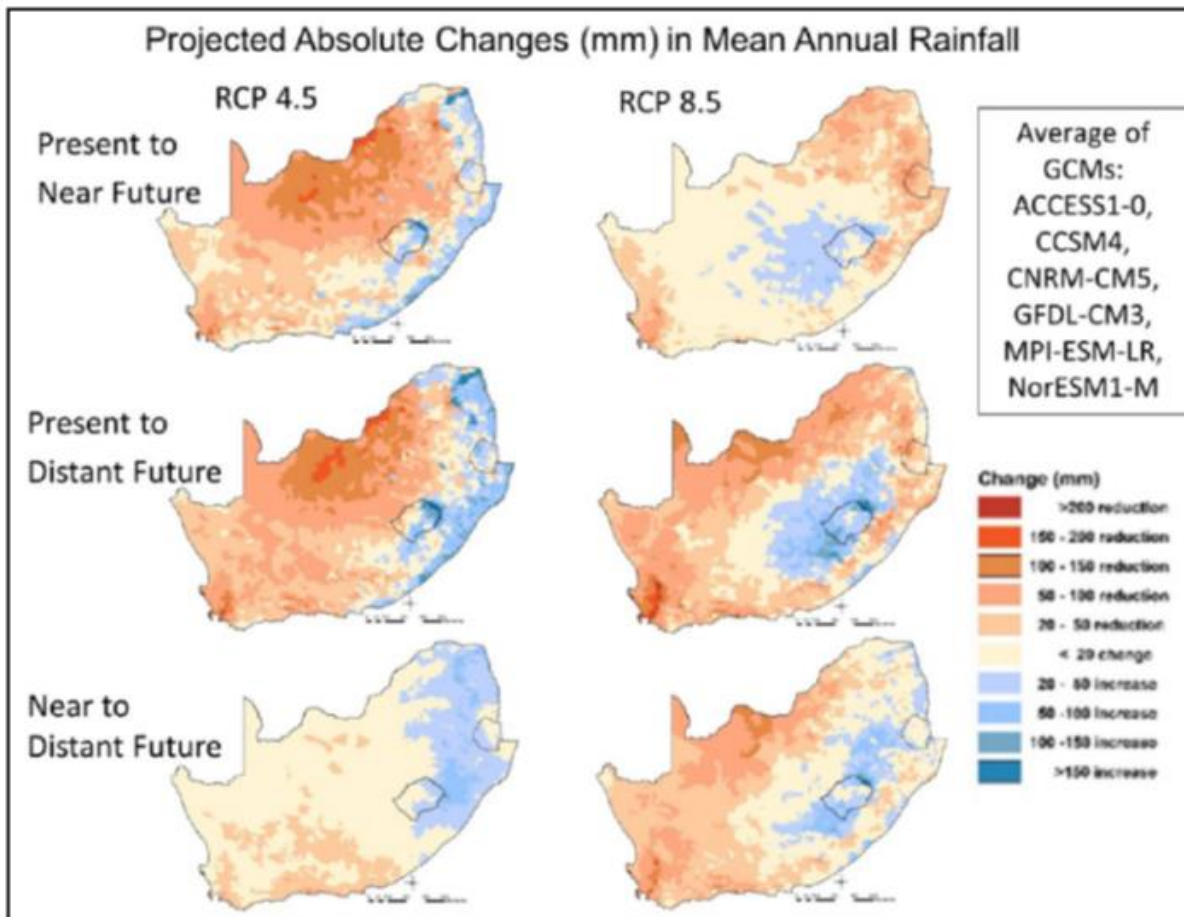
Figure 2.59 Averaged absolute change (in mm) in mean annual rainfall for each Quinary Catchment from the a) present (1961-1990) to near future (2015-2044: top), b) present to distant future (2070-2099: middle), and c) near to distant future (bottom), as projected by six GCM's forced by the RCP4.5 (left) and RCP8.5 (right) scenarios, based on data available in this study

In contrast, the maps in **Figure 2.59** show more severe patterns of change for RCP4.5 than RCP8.5. This is particularly true for drying trends and applies to both near and distant futures. This does not follow expected trends in terms of the differences between RCP4.5 and RCP8.5 scenarios. In addition, the RCP4.5 maps show a wetting pattern over KwaZulu-Natal, Mpumalanga and parts of Limpopo that is completely absent in the RCP8.5 maps. This appears to be another inconsistency between the two scenarios as it seems unlikely that such a striking difference would exist, particularly for the near future where differences in emissions are relatively small.

When comparing the maps based on data supplied to this project (**Figure 2.59**) to those produced in the previous publications, broad agreement in the spatial patterns is evident for RCP8.5. However, this is not the case for RCP4.5. For example, there is strong drying shown over the North West province in **Figure 2.59**, which is contrasted with wetting in **Figure 2.57** and **2.58**. Similarly, there is drying over Mpumalanga and Limpopo in **Figure 2.57** (near future), which is contrasted with wetting in **Figure 2.59** over the same period (eastern and northern Limpopo is referred to in this instance).

2.4.3   Conclusions

The analyses presented above led the project team to conclude that the RCP4.5 dataset supplied to this project was not the same as that presented in previous publications where the data were originally developed and described. Attempts were made by the CSIR team to locate the correct RCP4.5 dataset to accompany the RCP8.5 dataset supplied to this project. However, this dataset could unfortunately

not be located. It is believed that the data from the appropriate simulation run may have been accidentally deleted when storage space needed to be urgently cleared on the CSIR servers.

When this project was proposed it was intended that existing available climate projection data would be used. It was, therefore, beyond the scope and budget of the project to re-produce the appropriate RCP4.5 CCAM simulation run. Computing constraints would also not have allowed the simulation run to be reproduced in time for use in this project. Repeating hydrological simulations with a different set of projections (e.g. CORDEX) was also not possible, considering time frames and funding available in the project. For these reasons, it was unfortunately not possible to further consider the RCP4.5 scenario in this project.

2.5 References

ACOCKS JPH (1988) *Veld Types of South Africa,* ACOCKS JPH, Memoirs of the Botanical Survey of South Africa, Vol.*57*, 3rd ed., South African National Biodiversity Institute (SANBI) Pretoria, South Africa.

ALLEN RG, PEREIRA LS, RAES D and SMITH M (1998) Crop evapotranspiration – Guidelines for computing crop water requirements. Food and Agriculture Organization of the United Nations (FAO), Rome, Italy. FAO Irrigation and drainage paper 56, Chapter 6.
http://www.fao.org/ag/agl/aglw/cropwater/docs/method.pdf (Accessed 10th October 2007).

ALMAZROUI M, SAEED F, SAEED S, NAZRUL ISLAM M, ISMAIL M, KLUTSE NAB, and SIDDIQUI M H (2020). Projected Change in Temperature and Precipitation Over Africa from CMIP6. Earth Systems and Environment, 4(3), 455-475. https://doi.org/10.1007/S41748-020-00161-X/FIGURES/14

ARCHER E, ENGELBRECHT F, HÄNSLER A, LANDMAN W, TADROSS M and HELMSCHROT J (2018) Seasonal prediction and regional climate projections for southern Africa. In: *Climate change and adaptive land management in southern Africa – assessments, changes, challenges, and solutions*, REVERMANN R, KREWENKA KM, SCHMIEDEL U, OLWOCH JM, HELMSCHROT J and JÜRGENS N,14-21, Biodiversity and Ecology, 6, Klaus Hess Publishers, Göttingen and Windhoek. doi:10.7809/b-e.00296.

BOÉ J, TERRAY L, HABETS F and MARTIN E (2007) Statistical and dynamical downscaling of the Seine basin climate for hydro-meteorological studies. International Journal of Climatology, 2007, 27 (12) 1643-1655. doi.org/10.1002/joc.1602.

BURKHART HE, BROOKS EB, DINON-ALDRIDGE H, SABATIA CO, GYAWALI N, WYNNE RH and THOMAS VA (2018) Regional simulations of loblolly pine productivity with CO_2 enrichment and changing climate scenarios. Forest Science, 64 (4) 349-357. doi:10.1093/forsci/fxy008.

CANNON AJ, SOBIE SR and MURDOCK TQ (2015) Bias Correction of GCM Precipitation by Quantile Mapping: How Well Do Methods Preserve Changes in Quantiles and Extremes? Journal of Climate 28 (17) 6938-6959. doi:10.1175/JCLI-D-14-00754.1.

CHEN J, BRISSETTE FP, CHAUMONT D and BRAUN M (2013) Finding appropriate bias correction methods in downscaling precipitation for hydrologic impact studies over North America. Water Resources Research 49 (7) 4187-4205. doi:10.1002/wrcr.20331.

CHRISTENSEN JH, HEWITSON BC, BUSUIOC A, CHEN A, GAO X, HELD I, JONES R, KOLLI RK,KWON W-T, LAPRISE R, MAGAÑA RUEDA V, MEARNS L, MENÉDEZ CG, RÄISÄNEN J, RINKE A, SARR A and WHETTON P (2007) Regional climate projections. In: *Climate Change 2007:The Physical Science Basis* (SOLOMON S, QIN D, MANNING M, CHEN Z, MARQUIS M, AVERYT KB, TIGNOR M and MILLER HL (Eds) Contribution of Working Group I to the Fourth Assessment Report of the Intergovernmental Panel on Climate Change. Cambridge University Press, Cambridge, UK.

DAVIS-REDDY and VINCENT K (2017) *Climate Risk and Vulnerability*: *A Handbook for Southern Africa.* Council for Scientific and Industrial Research, 2nd ed., Pretoria, South Africa.

DOSIO A, JURY MW, ALMAZROUI M, ASHFAQ M, DIALLO I, ENGELBRECHT FA, KLUTSE NAB, LENNARD C, PINTO I, SYLLA MB, and TAMOFFO AT (2021) Projected future daily characteristics of African precipitation based on global (CMIP5, CMIP6) and regional (CORDEX, CORDEX-CORE) climate models. Climate Dynamics, 57(11-12), 3135-3158. https://doi.org/10.1007/s00382-021-05859-w

ENGELBRECHT CJ and ENGELBRECHT FA (2015) Shifts in Köppen-Geiger climate zones over southern Africa in relation to key global temperature goals. Theoretical and Applied Climatology. doi:10.1007/s00704-014-1354-1.

ENGELBRECHT F (2019). Green Book – Detailed Projections of Future Climate Change over South Africa. Workstream 2: Research report, CSIR, Pretoria, South Africa.

ENGELBRECHT F, DEDEKIND Z, MUTHIGE M, MALHERBE J, BERAKI A, ENGELBRECHT C, NGWANA I, LUMSDEN T, LANDMAN W, MAISHA R, MPHESHEA L, VAN DER MERWE J and EATWELL K (2020) Predictability of hydroclimatic variability over eastern South Africa under climate change. Research Report No. 2457/1/19, Water Research Commission, Pretoria, South Africa.

ENGELBRECHT FA, ADEGOKE J, BOPAPE MM, NAIDOO M, GARLAND R, THATCHER M, MCGREGOR J, KATZFEY J, WERNER M, ICHOKU C and GATEBE C (2015) Projections of rapidly rising surface temperatures over Africa under low mitigation. Environmental Research Letters 10 (8). doi:10.1088/1748-9326/10/8/085004.

ENGELBRECHT FA, LANDMAN WA, ENGELBRECHT CJ, LANDMAN S, ROUX B, BOPAPE MM, MCGREGOR JL and THATCHER M (2011) Multi-scale climate modelling over southern Africa using a variable resolution global model. Water SA 37 (5) 647-658. doi:10.4314/wsa.v37i5.2.

ENGELBRECHT FA, MCGREGOR JL and ENGELBRECHT CJ (2009) Dynamics of the conformal-cubic atmospheric model projected climate-change signal over southern Africa. International Journal of Climatology 29 (7) 1013-1033. doi:10.1002/joc.1742.

EYRING V, BONY S, MEEHL GA, SENIOR CA, STEVENS B, STOUFFER RJ and TAYLOR KE (2016) Overview of the Coupled Model Intercomparison Project Phase 6 (CMIP6) experimental design and organization. Geoscientific Model Development, 9(5), 1937-1958. https://doi.org/10.5194/GMD-9-1937-2016

FEIGENWINTER I, KOTLARSKI S, CASANUEVA A, FISCHER AM, SCHWIERZ C and LINIGER MA (2018) *Exploring quantile mapping as a tool to produce user-tailored climate scenarios for Switzerland.* Technical Report MeteoSwiss no. 270, Federal Office of Meteorology and Climatology MeteoSwiss, Zürich, Switzerland.

GARLAND R, MATOOANE M, ENGELBRECHT FA, BOPAPE M, LANDMAN W, NAIDOO M, VAN DER MERWE J and WRIGHT C (2015) Regional projections of extreme apparent temperature days in Africa and the related potential risk to human health. International Journal of Environmental Research and Public Health 12 (10) 12577-12604. doi:10.3390/ijerph121012577.

GIORGI F, JONES C and ASRAR GR (2009) Addressing climate information needs at the regional level: the CORDEX framework. WMO Bulletin, 58(3). http://wcrp.ipsl.

GUDMUNDSSON L, BREMNES JB, HAUGEN JE and ENGEN-SKAUGEN T (2012) Technical Note: Downscaling RCM precipitation to the station scale using statistical transformations – a comparison of methods. Hydrology and Earth System Sciences (16) 3383-3390.

HARGREAVES GH and SAMANI ZA (1985) Reference crop evapotranspiration from temperature. Journal of Applied Engineering in Agriculture (1) 96-99. doi:10.13031/2013.26773.

HAYHOE K, EDMONDS J, KOPP RE, LEGRANDE AN, SANDERSON BM, WEHNER MF and WUEBBLES DJ (2017) Climate models, scenarios, and projections. In: *Climate Science Special Report: Fourth National Climate Assessment* WUEBBLES DJ, FAHEY DW, HIBBBARD KA, DOKKEN DJ, STEWART BC, and MAYCOCK TK, U.S. Global Change Research Program, V, (1) 133-160, Washington DC. doi:10.7930/JOWH2N54.

IPCC, 2014: *Climate Change 2014: Synthesis Report. Contribution of Working Groups I, II and III to the Fifth Assessment Report of the Intergovernmental Panel on Climate Change.* Report no.AR5, (Core writing team, PACHAURI RK and MEYER LA, IPCC, Geneva, Switzerland, 151pp.

IPCC, 2007: *Climate change 2007. Synthesis report. Contribution of Working Groups I, II and III to the Fourth assessment report* of the Intergovernmental Panel on Climate Change. PACHAURI RK, and REISINGER A, IPCC, Geneva, Switzerland.

IPCC, 2000: *Special Report on Emissions Scenarios, Working Group III* of the Intergovernmental Panel for Climate Change.

JURY MR (2013) Climate trends in southern Africa. South African Journal of Science, 109 (1/2) 1-11. doi:10.1590/sajs.2013/980.

KUNZ RP, MENGISTU MG, STEYN JM, DOIDGE IA, GUSH MB, DU TOIT ES, DAVIS NS, JEWITT GPW and EVERSON CS (2015) *Assessment of biofuel feedstock production in South Africa: Technical report on the field-based measurement, modelling and mapping of water use of biofuel crops (Volume 2).* Research Report No.1874/2/15,Water Research Commission, Pretoria, South Africa. ISBN 978-1-4312-0749-7

KUNZ R, MASANGANISE J, REDDY K, MABHAUDHI T, LEMBEDE L, NAIKEN V AND FERRER S (2020) *Water use and yield of soybean and grain sorghum for biofuel production*. Research Report No. 2491/1/20, Water Research Commission, Pretoria, South Africa.

LANDMAN WA, ENGELBRECHT FA, HEWITSON B, MALHERBE J, and VAN DER MERWE J (2017) Towards bridging the gap between climate change projections and maize producers in South Africa. Theoretical and Applied Climatology 132 (4) 11-17. doi:10.1007/s00704-017-2168-8.

LUMSDEN TG, KUNZ RP, SCHULZE, RE, KNOESEN DM and BARICHIEVY KR (2011) Methods 4: Representation of grid and point scale regional climate change scenarios for national and catchment level hydrological impacts assessments. In: *Methodological Approaches to Assessing Eco-Hydrological*

Responses to Climate Change in South Africa SCHULZE RE, HEWITSON BC, BARICHIEVY KR, TADROSS M, KUNZ RP, HORAN MJC and LUMSDEN TG. Research report no.1562/1/10. Water Research Commission, Pretoria, South Africa.

LYNCH SD (2004) *Development of a Raster Database of Annual, Monthly and Daily Rainfall for Southern Africa.* Research report no.1156/1/04, Water Research Commission, Pretoria, South Africa.

MALHERBE J, ENGELBRECHT FA and LANDMAN WA (2013) Projected changes in tropical cyclone climatology and landfall in the Southwest Indian Ocean region under enhanced anthropogenic forcing. Climate Dynamics 40 (11-12) 2867-2886. doi:10.1007/s00382-012-1635-2.

MCGREGOR JL (2005) C-CAM geometric aspects and dynamical formulation, CSIRO Atmospheric Research technical paper, no 70, CSIRO Atmospheric Research, Victoria, Australia.

MCGREGOR JL and DIX MR (2008) An updated description of the Conformal-Cubic Atmospheric Model in: *High Resolution Simulation of the Atmosphere and Ocean* HAMILTON K and OHFUCHI W, Springer, New York, NY. doi:10.1007/978-0-387-49791-4_4.

MCGREGOR JL and DIX MR (2001) The CSIRO conformal-cubic atmospheric GCM In: HODNETT PF *IUTAM Symposium on Advances in Mathematical Modelling of Atmosphere and Ocean Dynamics: proceedings* Limerick Ireland, 2000. Fluid mechanics and its applications (61) 307-315 Kluwer Academic, Dordrecht.

MEEHL GA, BOER GJ, COVEY C, LATIF M and STOUFFER RJ (2000) The Coupled Model Intercomparison Project (CMIP). Bulletin of the American Meteorological Society, 81(2), 313-318, doi:10.1175/1520-0477(2000)081<0313:tcmipc>2.3.co;2.

MEEHL GA, COVEY C, DELWORTH T, LATIF M, MCAVANEY B, MITCHELL JF, STOUFFER RJ and TAYLOR KE (2007) The WCRP CMIP3 multimodel dataset: A new era in climate change research. *Bulletin of the American meteorological society*, *88*(9), pp.1383-1394, doi:10.1175/bams-88-9-1383.

MEINSHAUSEN M, SMITH SJ, CALVIN K, DANIEL JS, KAINUMA MLT, LAMARQUE JF, MATSUMOTO K, MONTZKA SA, RAPER SCB, RIAHI K and THOMSON AGJMV (2011) The RCP greenhouse gas concentrations and their extensions from 1765 to 2300. Climatic change, 109 (1-2) 213. doi:10.1007/s10584-011-0156-z.

MOSS RH, EDMONDS JA, HIBBARD KA, MANNING MR, ROSE SK, VAN VUUREN DP, CARTER TR, EMORI S, KAINUMA M, KRAM T, MEEHL GA, MITCHELL JFB, NAKICENOVIC N, RIAHI K, SMITH SJ, STOUFFER RJ, THOMSON AM, WEYANT JP and WILBANKS TJ (2010) The Next Generation of Scenarios for Climate Change Research and Assessment. Nature (463) 747-756.doi:10.1038/nature08823.

NIANG I, RUPPEL OC, ABDRABO MA, ESSEL A, LENNARD C, PADGHAM J and URQUHART P (2014) Africa. Climate Change 2014: Impacts, Adaptation, and Vulnerability: Part B: Regional Aspects. In: *Contribution of Working Group II to the Fifth Assessment Report of the Intergovernmental Panel on Climate Change* BARROS VR, FIELD CB, DOKKEN DJ et al, (22) 1199-1265, Cambridge University Press, Cambridge, United Kingdom and New York, NY,USA.

OTTO FEL, WOLSKI P, LEHNER F, TEBALDI C, VAN OLDENBORGH GJ, HOGESTEEGER S, SINGH R, HOLDEN P, FUČKAR NS, ODOULAMI RC and NEW M (2018) Anthropogenic influence on the drivers of the Western Cape drought 2015-2017. Environmental Research Letters, 13(12), 124010. https://doi.org/10.1088/1748-9326/aae9f9

PALMER T and STEVENS B (2019) The scientific challenge of understanding and estimating climate change. Proceedings of the National Academy of Sciences of the United States of America, 116(49), 34390-34395. https://doi.org/10.1073/PNAS.1906691116/ASSET/13FD8CCF-520C-4729-BD09-FC61D7C0FCD9/ASSETS/GRAPHIC/PNAS.1906691116FX02.JPEG

PIKE A (2004) CalcPPTCor: A utility to assist in the selection of rainfall stations and adjustment of rainfall data. In: *Development and Evaluation of an Installed Hydrological Modelling System* SCHULZE RE and PIKE A (2004) Research report no. 1155/1/04, Water Research Commission, Pretoria, South Africa.

RAJCZAK J, KOTLARSKI S and SCHÄR C (2016) Does Quantile Mapping of Simulated Precipitation Correct for Biases in Transition Probabilities and Spell Lengths? Journal of Climate 29 (5) 1605-1615. doi:10.1175/JCLI-D-15-0162.1.

RÄTY O, RÄISÄNEN J and YLHÄISI JS (2014) Evaluation of delta change and bias correction methods for future daily precipitation: Intermodel cross-validation using ENSEMBLES simulations. Climate Dynamics (42) 2287-2303. doi:10.1007/s00382-014-2130-8.

RIAHI K, VAN VUUREN DP, KRIEGLER E, EDMONDS J, O'NEILL BC, FUJIMORI S, BAUER N, CALVIN K, DELLINK R, FRICKO O, LUTZ W, POPP, A., CUARESMA, JC, SAMIR KC, LEIMBACH M, JIANG L, KRAM T, RAO S, EMMERLING J, et al. (2017). The Shared Socioeconomic Pathways and their energy, land use, and greenhouse gas emissions implications: An overview. Global Environmental Change, 42, 153-168. https://doi.org/10.1016/J.GLOENVCHA.2016.05.009

SCHULZE RE (1995) *Hydrology and Agrohydrology*. Research Report no.TT69/95, Water Research Commission, Pretoria, South Africa.

SCHULZE RE (1995) *Hydrology and Agrohydrology: A Text to Accompany the ACRU 3.00 Agrohydrological Modelling System*. Water Research Commission, Pretoria, South Africa.

SCHULZE RE (2005) *Climate Change and Water Resources in Southern Africa: relevant statistics Impacts, Vulnerabilities and Adaptation*. Research Report no.1430/1/05, Water Research Commission, Pretoria, South Africa.

SCHULZE RE (2005) *Climate Change and Water Resources in Southern Africa: Studies on Scenarios, Impacts, Vulnerabilities and Adaptation*. Research Report no.1430/1/05, Water Research Commission, Pretoria, South Africa.

SCHULZE RE (2008) *South African Atlas of Climatology and Agrohydrology*. Research Report no. 1489/1/08, Water Research Commission, Pretoria, South Africa. (On interactive DVD).

SCHULZE RE (2012) A 2011 *Perspective on Climate Change and the South African Water Sector*. Research Report no. TT 518/12, Water Research Commission, Pretoria, South Africa.

SCHULZE RE (2013) *Climate Baseline and Climate Change Assessment for KwaDukuza. Schulze and Associates.* Prepared for Mott MacDonald RSA, Report 307958/RSA/ENV/01/A.

SCHULZE RE (2017) *Handbook for Farmers, Officials and Others on Adaptation to Climate Change in the Agricultural Sector of South Africa*. Department of Agriculture, Forestry and Fisheries, Pretoria, South Africa.

SCHULZE RE and DAVIS NS (2015) *Climate change adaptation strategy for Komati River Basin*. Schulze and Associates Report to Mott Macdonald PDNA, Johannesburg.

SCHULZE RE and DAVIS NS (2018) *Development of a Framework and Methodology for Undertaking a Risk and Vulnerability Assessment in All Nine Water Management Areas of South Africa*. Schulze and Associates Report to GIZ, Pretoria, South Africa.

SCHULZE RE, DAVIS NS, SNYMAN N-M and KNOESEN DR (2013) *Hydrological Modelling in the Waterberg Catchment Area.* ESKOM Report RES/RR/09/30892.

SCHULZE RE, HEWITSON BC, BARICHIEVY KR, TADROSS M, KUNZ RP, HORAN MJC and LUMSDEN TG (2010) *Methodological Approaches to Assessing Eco-Hydrological Responses to Climate Change in South Africa*. Research Report no.1562/1/10. Water Research Commission, Pretoria, South Africa.

SCHULZE RE and HORAN MJC (2011) Methods 1: Delineation of South African Lesotho and Swaziland into Quinary catchments. In: *Methodological Approaches to Assessing Eco-Hydrological Responses to Climate Change in South Africa*. SCHULZE RE, HEWITSON BC, BARICHIEVY KR, TADROSS M, KUNZ RP, HORAN MJC and LUMSDEN TG, Research Report no.1562/1/10, Water Research Commission, Pretoria, South Africa. ISBN:978-1-4312-0050-4.

SCHULZE RE, HORAN MJC, KUNZ RP, LUMSDEN TG and KNOESEN DM (2011) Methods 2: Development of the southern African Quinary catchments database. In: *Methodological approaches to assessing eco-hydrological responses to climate change in South Africa.* SCHULZE RE, HEWITSON BC, BARICHIEVY KR, TADROSS M, KUNZ RP, HORAN MJC and LUMSDEN TG, Research Report no.1562/1/10, Water Research Commission, Pretoria, South Africa. ISBN:978-1-4312-0050-4.

SCHULZE RE and KUNZ RP (2011) Climate Change and Annual Temperature Statistics: A 2011 Perspective. In: *A 2011 Perspective on Climate Change and the South African Water Sector*. SCHULZE RE (2011) Research Report no.TT518/12, Water Research Commission, Pretoria, South Africa.

SCHULZE RE and MAHARAJ M (1994) Monthly means of daily maximum and minimum temperatures for southern Africa. University of Natal, Pietermaritzburg, Department of Agricultural Engineering. Unpublished documents and maps.

SCHULZE RE and MAHARAJ M (2004) *Development of a database of gridded daily temperatures for Southern Africa.* Research Report no. 1156/2/04, Water Research Commission, Pretoria, South Africa.

SCHULZE RE, WARBURTON ML, LUMSDEN TG and HORAN MJC (2005) The Southern African Quaternary Catchments Database: Refinements to, and Links with, the *ACRU* System as a Framework for Modelling Impacts of Climate Change on Water Resources. In: Climate Change and Water Resources in Southern Africa: Studies on Scenarios, Impacts, Vulnerabilities and Adaptation. SCHULZE RE, Research Report no.1430/1/05, Water Research Commission, Pretoria, South Africa.

SMITHERS JC and SCHULZE RE (2004) *ACRU* Agrohydrological Modelling System, User Manual Version 4.00, University of KwaZulu-Natal, Pietermaritzburg, South Africa, p.302.

TADROSS M, DAVIS C, ENGELBRECHT FA, JOUBERT A and ARCHER VAN GARDEREN E (2011) Regional scenarios of future climate change over southern Africa. In: *Climate Risk and Vulnerability: A Handbook for Southern Africa* DAVIS CL et al, Council for Scientific and Industrial Research, Pretoria, South Africa.

TAYLOR KE, STOUFFER ERJ, and MEEHL GA (2012) An Overview of CMIP5 and the Experiment Design. Bulletin of the American Meteorological Society, 93(4), doi:10.1175/bams-d-11-00094.1.

TEBALDI C and KNUTTI R (2007) The use of the multi-model ensemble in probabilistic climate projections. Philosophical Transactions of the Royal Society A: Mathematical, Physical and Engineering Sciences, 365(1857), 2053-2075. https://doi.org/10.1098/RSTA.2007.2076

TEUTSCHBEIN C and SEIBERT J (2012) Bias correction of regional climate model simulations for hydrological climate-change impact studies: Review and evaluation of different methods. Journal of Hydrology, (12) 29 456-457. doi:10.1016/j.jhydrol.2012.05.052.

THEMESSL, MJ, GOBIET A and HEINRICH G (2012) Empirical-statistical downscaling and error correction of regional climate models and its impact on the climate change signal. Climatic Change, 112 (2) 449-468. doi:10.1007/s10584-011-0224-4.

THERON AK (2011) Climate Change: Sea level rise and the southern African coastal zone. In: *Observations on Environmental Change in South Africa,* ZIETSMAN L, Sun Press, Stellenbosch, South Africa.

TOUZÉ-PEIFFER L, BARBEROUSSE A and LE TREUT H (2020) The Coupled Model Intercomparison Project: History, uses, and structural effects on climate research. Wiley Interdisciplinary Reviews: Climate Change, 11(4), e648. https://doi.org/10.1002/WCC.648

VAN VUUREN DP, EDMONDS J, KAINUMA M, RIAHI K, THOMSON A, HIBBARD K, HURTT GC, KRAM T, KREY V, LAMARQUE J-F, MASUI T, MEINSHAUSEN M, NAKICENOVIC, N, SMITH SJ and ROSE SK (2011). The representative concentration pathways: an overview. Climatic Change, 109(1-2), 5-31. https://doi.org/10.1007/s10584-011-0148-z

WARBURTON ML and SCHULZE RE (2005) On the Southern African Rainfall Station Network and its Data for Climate Change Detection and Other Hydrological Studies. In: *Climate Change and Water Resources in Southern Africa: Studies on Scenarios, Impacts, Vulnerabilities and Adaptation.* SCHULZE RE, Research Report no.1430/1/05, Water Research Commission, Pretoria, South Africa.

WARBURTON ML, SCHULZE RE and JEWITT GPW (2010) Confirmation of *ACRU* model results for applications in land use and climate change studies. Hydrology and Earth System Sciences (14) 2399-2414.

WINSEMIUS HC, DUTRA E, ENGELBRECHT FA, ARCHER E, WETTERHALL F, PAPPENBERGER F and WERNER MGF (2014) The potential value of seasonal forecasts in a changing climate in southern Africa. Hydrology and Earth System Sciences (18) 1525-1538. doi:10.5194/hess-18-1525-2014.

3   THE LAND COVER CONFIGURATION – METHODS

D.J. Clark, R.E. Schulze, M.J.C. Horan, R.P. Kunz, J.C. Smithers, S. Schütte, M.L. Toucher and S.L.C. Thornton-Diabb

3.1   Introduction

Next to climate impacts, there are other, non-climatic factors that can impact hydrological responses, compared to baseline conditions. These non-climatic factors include land cover change that has occurred from past natural land cover and also land cover and land use change over time. For this study, both a new natural vegetation baseline was used in the modelling scenarios as well as actual present-day (2018) land cover for other scenarios. The configuration of the *ACRU* model with natural and actual land cover is explained in this chapter. Water abstractions, irrigation, dams and inter-basin transfers were not taken into account in the configuration of the *ACRU* hydrological model as different scenarios of engineered flows are typically addressed separately in the hydrological yield calculations. Land cover and land use change projections did not form part of this study. Rather it was assumed that the whole time period (1961-2099) is either under natural land cover or under actual land cover conditions based on 2018, and kept static, while the climate changes.

The calculation of water yield, whether it be hydrological yield, reservoir yield or system yield, requires flow data as one of the main input variables. Often some form of naturalised flows are typically used for this purpose, where these naturalised flows may be determined by (i) removing anthropogenic impacts on measured current-day flows, or (ii) applying a hydrological model using some form of assumed natural land cover. However, land cover and land use change as a result of anthropogenic activities could potentially have a significant effect on the hydrological response of a catchment and these should thus be taken into account in the runoff from catchments that is used in the calculation of yield. Thus, in this project, the impact of climate change on hydrological yield will be evaluated under two land cover scenarios:
(i)   natural land cover based on the CWRR Clusters (Toucher et al., 2019), and
(ii)   actual land cover/use based on NLC2018 (DEA and GTI, 2019).

In this project, the intention is not to model land cover/use change over the 139 years (1961-2099) of the GCM datasets or to model the impact of climate change on land cover/use. The intention of the actual land cover/use scenario is simply to evaluate whether the use of simulated runoff based on actual land cover/use has a significant impact on the yield estimates under different climate change scenarios.

Until recently the Acocks Veld Types dataset (Acocks, 1988) was used with the *ACRU* model, together with the associated hydrological characteristics developed by Schulze (2004), to simulate naturalised flows.   In the recently completed WRC Project K5/2437 (Toucher et al., 2019), hydrological characteristics were derived for the SANBI 2012 Vegetation Types (SANBI, 2012). In Toucher et al. (2019) the Vegetation Types were assigned to clusters (termed "the CWRR Clusters"), where the Vegetation Types within each cluster were assessed as having similar hydrological characteristics. A set of variables was derived for each CWRR Cluster to describe the hydrological characteristics of the cluster for use in hydrological modelling.

In recent years, a number of national land cover (NLC) datasets of actual land cover have been produced, including:
(i)   NLC1990 (DEA and GTI, 2016),
(ii)   NLC2000 (ARC and CSIR, 2005),
(iii)   NLC2013-2014 (DEA and GTI, 2015), and
(iv)   NLC2018 (DEA and GTI, 2019).

These NLC datasets not only represent actual land cover and land use at different points in time, but are based on different classifications, except for NLC1990 and NLC2013-2014 which are based on the same classification. The NLC2018 dataset was selected as it is the most recent national scale dataset representing current land cover/use. However, of these datasets, only the NLC2000 dataset includes the countries of Lesotho and Eswatini (formerly Swaziland), which have catchments that drain directly into catchments in South Africa. Thus the NLC2000 dataset was used in conjunction with the NLC2018 dataset. The NLC2000 dataset was also used to provide information on forest plantation genus which is not included in the NLC2018 classification.

3.2   Background to *ACRU* Configuration for Quinary Catchments

For many years the Southern African Quinary Catchments Database (QnCDB) (Schulze et al., 2010) and its predecessor, the Southern African Quaternary Catchments Database, QNDB (Hallowes et al., 2004; Schulze et al., 2005) have been used in conjunction with the *ACRU* model and other models for hydrological assessments. The South African Department of Water and Sanitation (DWS) maintains Primary, Secondary, Tertiary and Quaternary Catchment boundary datasets. For the purpose of the QnCDB each Quaternary Catchment was subdivided into three zones based on natural breaks in altitude in order to better account for variability in climate, land cover and soils, as there are often strong links between the spatial distribution of these characteristics and changes in altitude. These quinary level zones within Quaternary Catchments were termed 'Quinary Catchments' by Schulze and Horan (2010) and will be referred to as such in this chapter, though they are not strictly catchments but more altitudinal zones.

The QnCDB includes a 50-year (1950-1999) database of daily climate data including rainfall from Lynch (2004) and air temperature from Schulze and Maharaj (2004). This climate database was used in the bias correction of the GCM outputs (*cv.* Chapter 2).

The QnCDB includes information on soil hydrological characteristics, per Quinary Catchment, derived from the Land Types dataset (SIRI, 1987) by Schulze and Horan (2007) using the AUTOSOILS decision support tool (Pike and Schulze, 1995). For each Quinary Catchment and for each hydrological soil variable an area weighted average value was calculated from the characteristics derived from the Land Types identified in that Quinary Catchment.

The QnCDB uses the Acocks' Veld Types (Acocks, 1988) to represent naturalised land cover for the whole region. The spatially modal Veld Type in each Quinary Catchment was determined and hydrological characteristics assigned to each Veld Type, based on the work of Schulze (2004). However, for the purposes of this study the CWRR Clusters (Toucher et al*.,* 2019) based on the SANBI 2012 Vegetation Types (SANBI, 2012) were used in place of the Acocks' Veld Types, as described in Section 3.3.

3.3 Natural Land Cover Configuration

In the recently completed WRC Project K5/2437 titled "Resetting the baseline land cover against which streamflow reduction activities and the hydrological impacts of land use change are assessed" (Toucher et al., 2019) the SANBI 2012 Vegetation Types (SANBI, 2012) were assigned to clusters (termed "the CWRR Clusters"), where the Vegetation Types within each cluster were assessed as having similar hydrological characteristics. A set of variables and parameters was derived for each CWRR Cluster to describe the hydrological characteristics. These monthly variables and parameters used in the *ACRU* model were the crop coefficient (CAY), the coefficient of initial abstraction before runoff commences (COIAM), the root colonisation in the subsoil horizon (COLON), the fraction of plant available water at which plant stress commences (CONST), the percentage surface cover by litter/detritus (PCSUCO), the fraction of roots in the topsoil horizon (ROOTA) and the interception of rainfall on a day with rain (VEGINT). Toucher et al. (2019) determined the spatially modal CWRR Cluster for each Quinary Catchment and used this to configure the *ACRU* model to provide a naturalised land cover configuration of the model where the CWRR Clusters were used in place of the Acocks' Veld Types in the *ACRU* QnCDB. It was this configuration of the *ACRU* model based on the CWRR Clusters that was used in this study, together with GCM projected climate values, to provide what has been termed the land cover "baseline" (naturalised) hydrological projections of runoff, as described later in Chapter 5. In total, 132 CWRR Clusters have been identified. The location and extent of the biomes into which both the SANBI (2012) vegetation types and CWRR Clusters derived from them are grouped, are shown in **Figure 3.1**.
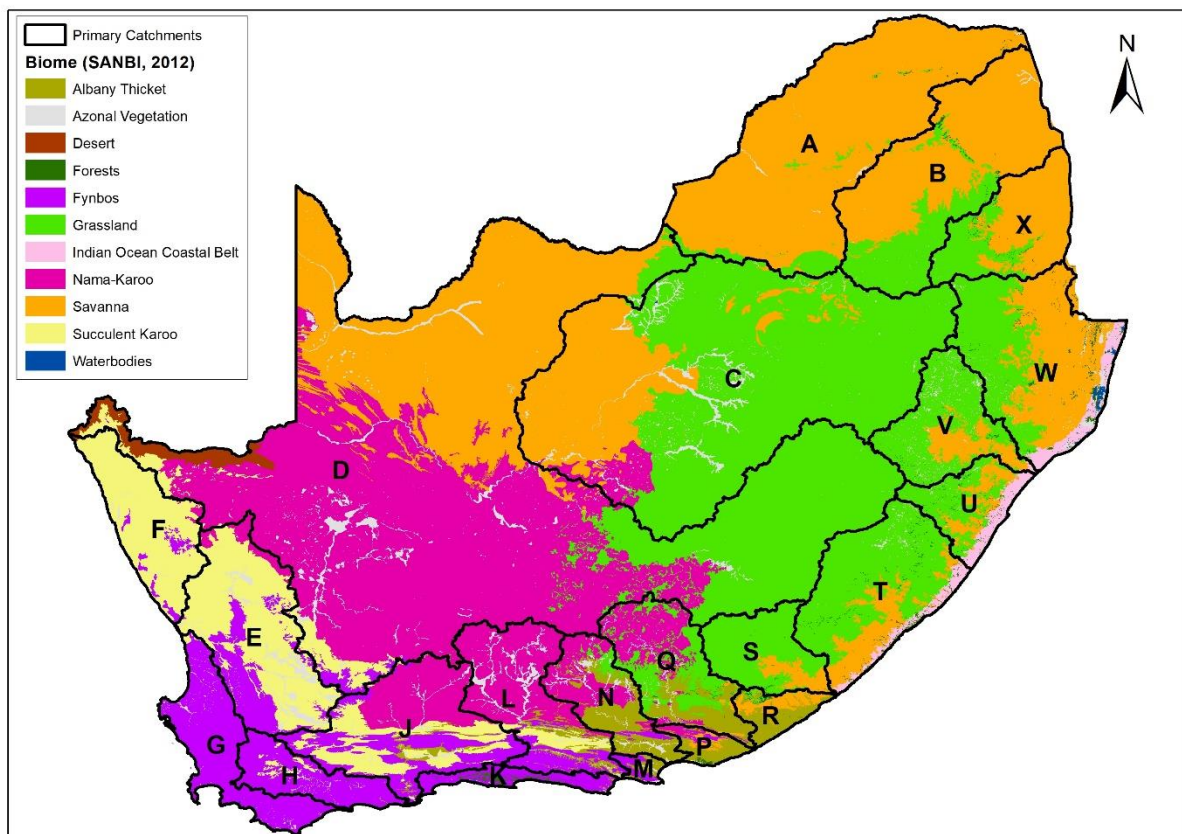
Figure 3.1   Map of the biomes into which the natural vegetation types are grouped (SANBI, 2012)

3.4 Actual Land Cover Configuration

The *ACRU* model has been used for many years to undertake national level hydrological assessments based on naturalised land cover. The *ACRU* model has, however, not previously been configured for actual land cover for the whole of South Africa, together with Lesotho and Eswatini, at Quinary Catchment scale. Configuring *ACRU* with actual land cover at Quinary Catchment level within the constraints presented by availability of data and computer processing power, was challenging, but also an exciting step forward for *ACRU* and South Africa. To put this in context, there are 5 838 Quinary Catchments, across which 73 different NLC2018 land cover/use classes are represented, for which a physical conceptual hydrological model is to be run for 139 years for six GCMs for two RCPs as well as for 50 years of historical climate. As with the "Baseline" *ACRU* configuration, the "Actual" land cover/use configuration of *ACRU* is built upon the QnCDB using the same Quinary Catchments and soils information.

The NLC2018 land cover/use dataset (DEA and GTI, 2019) was selected as the main source of information on the spatial distribution of actual land cover/use, based on its 73 classes. The NLC2018 dataset does not cover Lesotho and Eswatini, and thus the NLC2000 dataset (ARC and CSIR, 2005) was used to provide a representation of land cover/use in these countries. Although the information in NLC2000 is now somewhat dated, with possible land cover/use change having occurred in the period 2000-2018, this is a better alternative to simply assuming modal natural vegetation in Lesotho and Eswatini. The area of South Africa, Lesotho and Eswatini is represented by a total of 1 946 Quaternary Catchments, subdivided into a total of 5 838 Quinary Catchments. An initial investigation was conducted for South Africa only, using NLC2018, to determine the number of land cover/use classes present in each Quinary Catchment. It was found that even at the Quinary Catchment scale there is a high degree of heterogeneity in land cover/use. This is demonstrated in the cumulative frequency distribution shown in **Figure 3.2**. Most Quinaries contain more than one land cover/use class and half the catchments contain 28 or more classes.
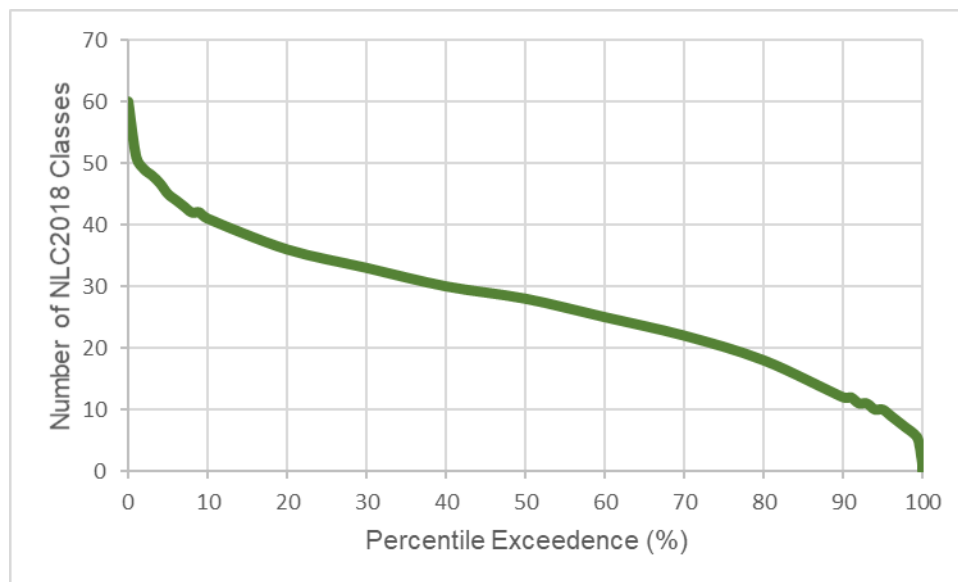
Figure 3.2   Cumulative frequency distribution of the number of NLC2018 land cover/use classes present in each Quinary Catchment

Based on further analysis of the land cover/use classes, and taking into consideration the various modelling constraints, it was decided that each Quinary Catchment would be modelled using a fixed set

of six hydrological response unit (HRU) types. These six HRUs, and the way in which they would conceptually be configured to flow within each Quinary Catchment, are shown in **Figure 3.3**.
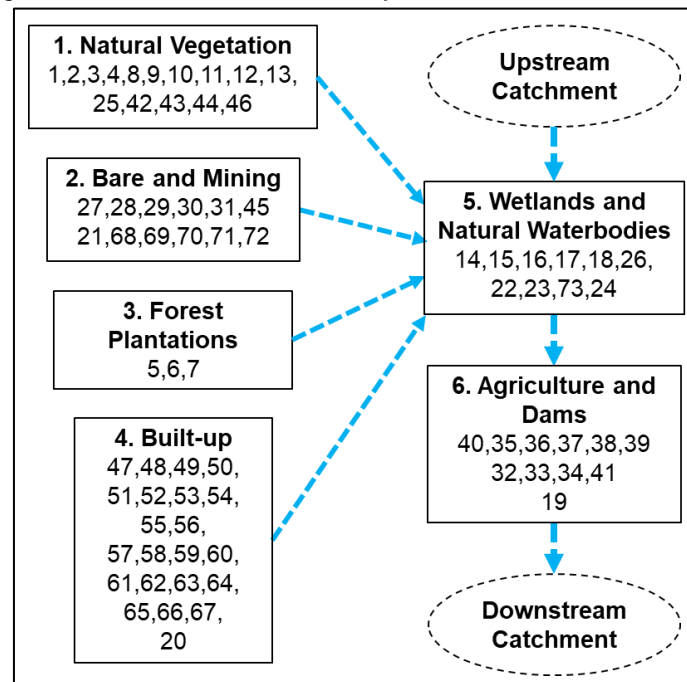
Figure 3.3   Schematic diagram of the six HRU types modelled within each Quinary Catchment and the flow links between them, with the NLC2018 classes represented in each HRU listed using the integer ID of each class

The flow connectivity between HRUs in different Quinary Catchments is demonstrated in **Figure 3.4**. Natural vegetation and natural rock are modelled in HRU 1, bare (non-vegetated, pervious) surfaces and mining are modelled in HRU 2, forest plantations are modelled in HRU 3, built-up areas are modelled in HRU 4, wetlands and natural waterbodies are modelled in HRU 5, and agriculture and dams are modelled in HRU 6. HRU 5 and HRU 6 are conceptualised as being part of the river flow network, with HRU 1, HRU 2, HRU 3 and HRU 4 contributing runoff to HRU 5 in the same Quinary Catchment.

Each HRU within each Quinary Catchment is configured uniquely in the *ACRU* model, depending on which of the 73 land cover/use classes are present, which is the modal class, and depending also on a number of other assumptions made which are based on supplementary datasets, such as the CWRR Clusters, rainfall seasonality, and cropping regions. To achieve this, the 73 NLC2018 land cover/use classes were grouped, first to arrive at a set of 33 groups, which were then further grouped to a set of 13 groups, which in turn are grouped into the six HRU types. These HRU types and land cover/use groupings, used to configure the *ACRU* model, are shown in **Table 3.**1. A map of the six land cover/use HRUs is shown in **Figure 3.5**.
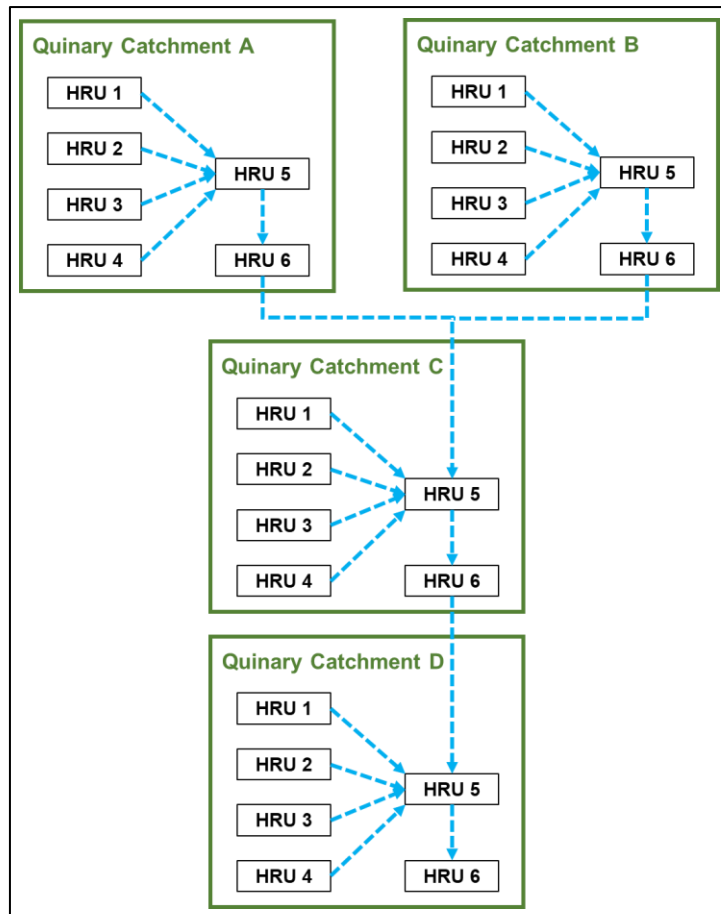
Figure 3.4   Schematic diagram of the flow links between HRU types in different Quinary Catchments

Table 3.1   HRUs and land cover/use groupings used in configuring the *ACRU* model

6 HRUs		13 Groups		33 Groups	
1	Natural Vegetation and Rock	1	Natural - Vegetated	1	Natural - Relatively Unmodified
1	Natural Vegetation and Rock	1	Natural - Vegetated	2	Natural - Modified
1	Natural Vegetation and Rock	2	Natural - Bare Rock	3	Natural - Bare Rock
2	Bare and Mining	3	Bare	4	Bare - Sand
2	Bare and Mining	3	Bare	5	Bare - Soil
2	Bare and Mining	3	Bare	6	Bare - Riverbed
2	Bare and Mining	4	Mining - General	7	Mining - General
2	Bare and Mining	4	Mining	8	Mining - Water
3	Forest Plantations	5	Forest Plantations	9	Forest Plantations
4	Built-up	6	Built-up - Urban	10	Built-up - Urban - Residential - Formal
4	Built-up	6	Built-up - Urban	11	Built-up - Urban - Residential - Informal
4	Built-up	6	Built-up - Urban	12	Built-up - Urban - Smallholdings
4	Built-up	6	Built-up - Urban	13	Built-up - Urban - Recreational
4	Built-up	6	Built-up - Urban	14	Built-up - Urban - Commercial
4	Built-up	6	Built-up - Urban	15	Built-up - Urban - Industrial
4	Built-up	6	Built-up - Urban	16	Built-up - Urban - Transport
4	Built-up	6	Built-up - Urban	17	Built-up - Urban -Waterbodies
4	Built-up	7	Built-up - Rural	18	Built-up - Rural
5	Wetlands and Natural Waterbodies	8	Wetlands	19	Wetlands - Herbaceous
5	Wetlands and Natural Waterbodies	8	Wetlands	20	Wetlands - Mangrove
5	Wetlands and Natural Waterbodies	9	Waterbodies - Natural	21	Waterbodies - Flooded Pans
5	Wetlands and Natural Waterbodies	10	Waterbodies - Dry Pans	22	Waterbodies - Dry Pans
5	Wetlands and Natural Waterbodies	9	Waterbodies - Natural	23	Waterbodies - Lakes
5	Wetlands and Natural Waterbodies	9	Waterbodies - Natural	24	Waterbodies - Rivers
5	Wetlands and Natural Waterbodies	9	Waterbodies - Natural	25	Waterbodies - Coastal Water
6	Agriculture and Dams	11	Agriculture - Commercial	26	Agriculture - Commercial - Annual
6	Agriculture and Dams	11	Agriculture - Commercial	27	Agriculture - Commercial - Sugarcane
6	Agriculture and Dams	11	Agriculture - Commercial	28	Agriculture - Commercial - Pineapples
6	Agriculture and Dams	11	Agriculture - Commercial	29	Agriculture - Commercial - Orchards
6	Agriculture and Dams	11	Agriculture - Commercial	30	Agriculture - Commercial - Vines
6	Agriculture and Dams	12	Agriculture - Subsistence	31	Agriculture - Subsistence - Annual
6	Agriculture and Dams	12	Agriculture - Subsistence	32	Agriculture - Subsistence - Sugarcane
6	Agriculture and Dams	13	Waterbodies - Dams	33	Waterbodies - Dams
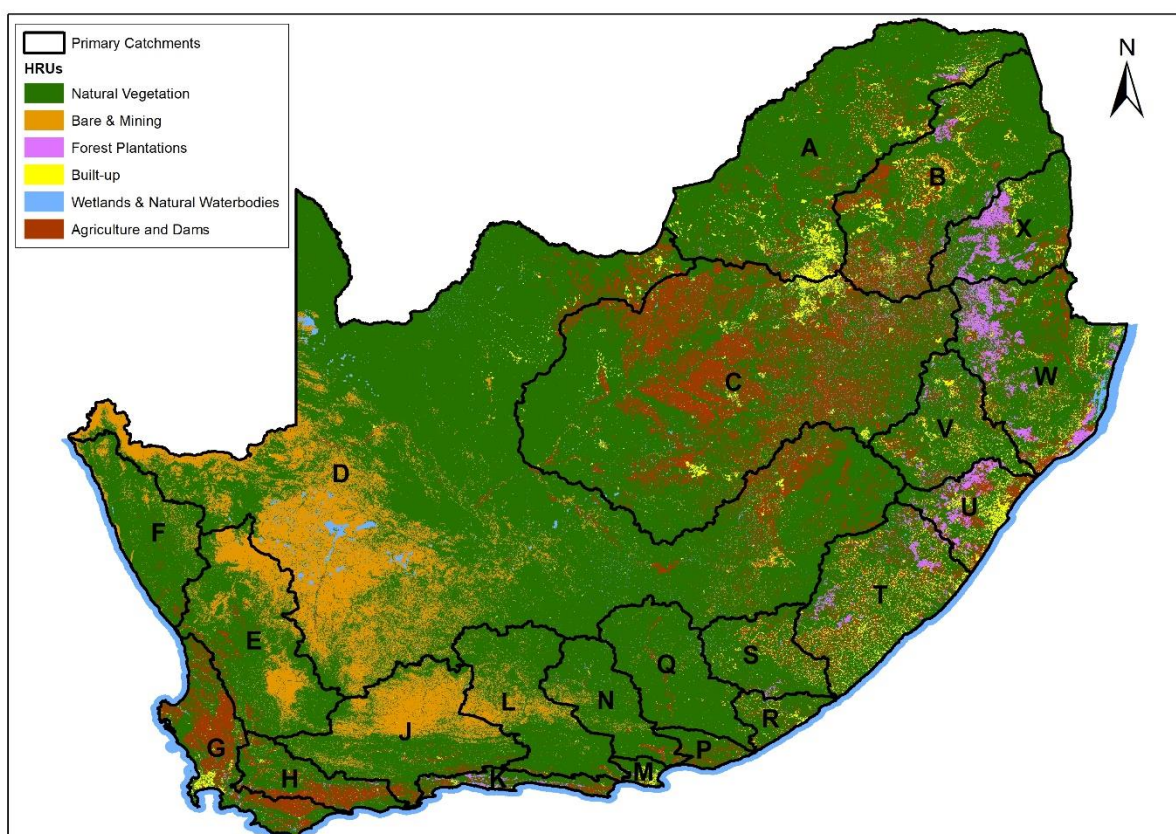
Figure 3.5   Map of the six land cover/use HRUs used to configure the *ACRU* model (derived from ARC and CSIR, 2005; DEA and GTI, 2019)

The 73 NLC 2018 land cover/use classes and these groupings are shown in the Appendices, **Table A.1** (33 groups), **Table A.2** (13 groups) and **Table A.3** (6 HRU types). The NLC2018 dataset does not include data for the countries of Lesotho and Eswatini, thus the NLC2000 dataset was used in conjunction with the NLC2018 dataset to represent land cover/use in these countries which form part of Quinary Catchments in Primary Catchments D, W and X. The 49 NLC 2000 land cover/use classes and the class groupings are shown in **Table A.4** (33 groups), **Table A.5** (13 groups) and **Table A.6** (6 HRU types) in the Appendices.

The configuration and parameterisation of the *ACRU* model for each of the six HRU types is described below. The parameterisation is based largely on recommendations in the *ACRU* Theory and User Manuals (Schulze, 1995; Smithers and Schulze, 1995), the Compoveg database that accompanies the *ACRU* model, and revised recommendations in Schulze (2013) and Schulze and Davis (2018).

3.4.1   Natural vegetation and rock (HRU 1)

HRU 1 (Natural Vegetation and Rock) represents naturally vegetated areas, which may be interspersed with rocky areas. The NLC2018 classes represented by HRU1 are shown in **Table 3.2** and the configuration of the HRU 1 components is summarised in **Table 3.3**. The classes have been grouped as: (i) relatively unmodified natural vegetation, (ii) modified natural vegetation, and (iii) natural rock. The NLC2018 dataset does not specifically identify the condition of natural vegetation, but based on the class description in DEA and GTI (2019), some of the "fallow land and old fields classes" have been considered here to be essentially repopulated with some form of natural vegetation, but in a poorer condition than would have occurred there previously.

Table 3.2   HRU1 land cover/use classes and suggested groupings for NLC 2018

Grouping	National Land Cover 2018	
	ID	Description
Natural Relatively Unmodified	1	contiguous (indigenous) forest
	2	contiguous low forest & thicket
	3	dense forest & woodland
	4	open woodland
	8	low shrubland (other)
	9	low shrubland (fynbos)
	10	low shrubland (succulent karoo)
	11	low shrubland (nama karoo)
	12	sparsely wooded grassland
	13	natural grassland
Natural - Modified	42	fallow land & old fields (trees)
	43	fallow land & old fields (bush)
	44	fallow land & old fields (grass)
	46	fallow land & old fields (low shrub)
Natural - Rock	25	natural rock surfaces

Table 3.3   Summary of configuration of HRU 1 components

HRU Components	Description
Pervious portion	Modal of: • Relatively Unmodified • Modified Use modal CWRR Cluster for parameterisation
Adjunct impervious	Natural - Rock (80%), STOIMP=5 mm
Disjunct impervious	Natural - Rock (20%), STOIMP=5 mm

The NLC2018 dataset includes 10 very general classes representing natural vegetation. Thus, the CWRR Clusters were used instead of these classes as (i) this enables better representation of the natural vegetation that is present in each individual Quinary Catchment, and (ii) ensures compatibility with the baseline (naturalised) configuration of *ACRU*. If HRU 1 is predominantly relatively unmodified natural vegetation, then it is parameterised using the modal CWRR Cluster (Toucher et al., 2019) for the naturally vegetated portion of HRU 1. The CWRR Clusters are parameterised in the *ACRU* model using the parameter values derived by Toucher et al. (2019).

If the HRU is predominantly modified natural vegetation, then it is parameterised using the modal CWRR Cluster (Toucher et al., 2019) for the modified naturally vegetated portion of HRU 1, with adjustments being made to the parameters to account for the assumed poorer condition, as suggested by Schulze and Davis (2018) for areas degraded by overgrazing. These adjustments are listed in **Table A.7** in the Appendices.

Class 25 (natural rock surfaces) in NLC 2018 could possibly have been included as part of HRU 2 (Bare and Mining). However, bare rock is a natural phenomenon, is often found interspersed with natural vegetation and, due to the presence of rock, land use change in these areas is not common. Thus, in this configuration of *ACRU*, bare rock is modelled as impervious land cover as part of HRU 1. As suggested by Schulze and Davis (2018), part of the impervious area (80%) is assumed to discharge directly to a stream and the remainder (20%) is assumed to contribute to runoff to the surrounding vegetation.

3.4.2 Bare ground and mining (HRU 2)

HRU 2 (Bare Ground and Mining) represents non-vegetated pervious surfaces, either naturally bare, eroded areas or mining related bare areas such as excavated areas and tailings dumps. While some of these land cover classes are naturally bare, these have been included in HRU 2 so that in *ACRU* they can be modelled differently to naturally vegetated areas and natural rock. Bare riverbed material has been included here as it would be modelled in a similar way to other bare pervious areas, which may be better than including it in HRU5 (Wetlands and Natural Waterbodies). Landfill is combined here with mining as they will be modelled in a similar way. Dry pans could potentially have been modelled here in HRU 2, however, as these may not always be dry, even if flooded for very short periods, and have characteristics that differentiate them from other bare (and possibly more pervious) land cover classes, they are modelled as part of HRU 5 (Wetlands and Natural Waterbodies). The classes represented by HRU 2 are shown in **Table 3.4** and the configuration of HRU 2 is summarised in **Table 3.5**.

The land cover parameters use to represent bare pervious surfaces in *ACRU* are shown in **Table A.8** in the Appendices. One of the challenges in HRU 2 was the representation of mining waterbodies, such as tailing dams, which may not receive runoff from a large catchment area, but may be required to retain a 1:50-year or 1:100-year design rainfall event, which is subsequently depleted slowly by evaporation. These areas were represented in *ACRU* as an impervious area with a storage capacity of 999 mm (the largest value permitted by *ACRU*).

Table 3.4   HRU 2 land cover/use classes and suggested groupings for NLC 2018

Grouping	National Land Cover 2018	
	ID	Description
Bare - Sand	28	sand dunes (terrestrial)
	29	coastal sand & dunes
Bare - Soil	45	fallow land & old fields (bare)
	27	eroded lands
	31	other bare
Bare - Riverbed	30	bare riverbed material
Mining - General	68	mines: surface infrastructure
	69	mines: extraction pits, quarries
	70	mines: salt mines
	71	mine: tailings and resource dumps
	72	land-fills
Mining - Water	21	artificial flooded mine pits

Table 3.5.   Summary of configuration of HRU 2 components

HRU Components	Description
Pervious portion	Model all bare (non-vegetated) pervious surface land cover parameters for all three classes
Adjunct impervious	Used to represent mining water using STOIMP=999
Disjunct impervious	None

3.4.3 Forest plantations (HRU 3)

HRU 3 (Forest Plantations) represents forest plantations as a separate land cover/use HRU, as forest plantations are a streamflow reduction activity (SFRA) according to the National Water Act (1998) and also need to be modelled differently to other vegetated land cover in *ACRU*. The classes represented by HRU 3 are shown in **Table 3.6**.

The NLC2018 dataset includes three forest plantation classes related to the density of the land cover which effectively represent mature plantations (Class 5), young plantations (Class 6) and clear-felled areas (Class 7). Forest plantations have a long growth cycle compared to other cultivated land cover, and each Quinary Catchment with plantations is likely to contain blocks of plantation forests with a range of maturity levels. However, only mature trees are modelled in this configuration of the *ACRU* model, and thus a range of maturity levels is not represented. However, the NLC2018 dataset does not include classes that indicate the genus of the forest plantation trees, where each genus has different water use characteristics, different typical growing cycle lengths and may be better suited for growth in certain areas of South Africa. The NLC2000 dataset does, however, include classes that represent the three main different genera of forest plantations classes grown in South Africa, and also includes a "catch-all" class representing other genera or mixed genera. The NLC2000 forest plantation classes are shown in **Table 3.7**. Class 12 in NLC2000, representing clear-felled areas, was combined with Class 11 where the specific genus is not known. Thus effectively 4 different forest plantation classes were used: (i) *Eucalyptus*, (ii) Pinus, (iii) Acacia (Wattle), and (iv) Other/Mixed. Although there is an 18 year difference in the points in time represented by the NLC2000 and NLC2018 datasets, it is assumed that the modal forest plantation genus would remain the same in most Quinary Catchments, even if the area of each genus in a catchment may have changed to some degree over this period. The modal genus in each catchment containing forest plantations was determined and used to parameterise HRU 3. The modal forest plantation genus in each Quinary Catchment is shown in **Figure 3.6**. The configuration of HRU 3 is summarised in **Table 3.8**. If NLC2018 indicated that forest plantations existed in a catchment, but no forest plantations were indicated by the NLC2000 dataset, then the parameters for the generalised class termed "Other/Mixed" were used. The forest plantation parameter values used to configure the *ACRU* model are shown in **Table A.9** in the Appendices, and were based on recommendations in Schulze (2013) and Schulze and Davis (2018) which were based on Jewitt et al. (2009), Schulze and Schütte (2014) and Schulze and Schütte (2016). Different parameters are provided in **Table A.9** for *Eucalyptus* plantations grown in coastal and inland regions. The coastal and inland regions were defined based on Jewitt et al. (2009) and (Schulze, 2013), and are shown in **Figure 3.7**. In the absence of more detailed data it was assumed that Pinus plantations are grown on a 15-year rotation for pulp.

Table 3.6   HRU 3 land cover/use classes and suggested groupings for NLC 2018

Grouping	National Land Cover 2018	
	ID	Description
Forest Plantations	5	contiguous & dense plantation forest
	6	open & sparse plantation forest
	7	temporary unplanted (clear-felled) plantation forest

Table 3.7   Forest plantation classes and suggested groupings for NLC 2000

National Land Cover 2000	
ID	Description
8	Forest Plantations (*Eucalyptus* spp)
9	Forest Plantations (*Pinus* spp)
10	Forest Plantations (*Acacia* spp)
11	Forest Plantations (Other/mixed spp)
12	Forest Plantations (Clearfelled)

Table 3.8   Summary of configuration of HRU 3 components

HRU Components	Description
Pervious portion	Modal of: • Pinus • Eucalyptus • Acacia (Wattle) • Other Use modal forest plantation genus for parameterisation.
Adjunct impervious	None
Disjunct impervious	None
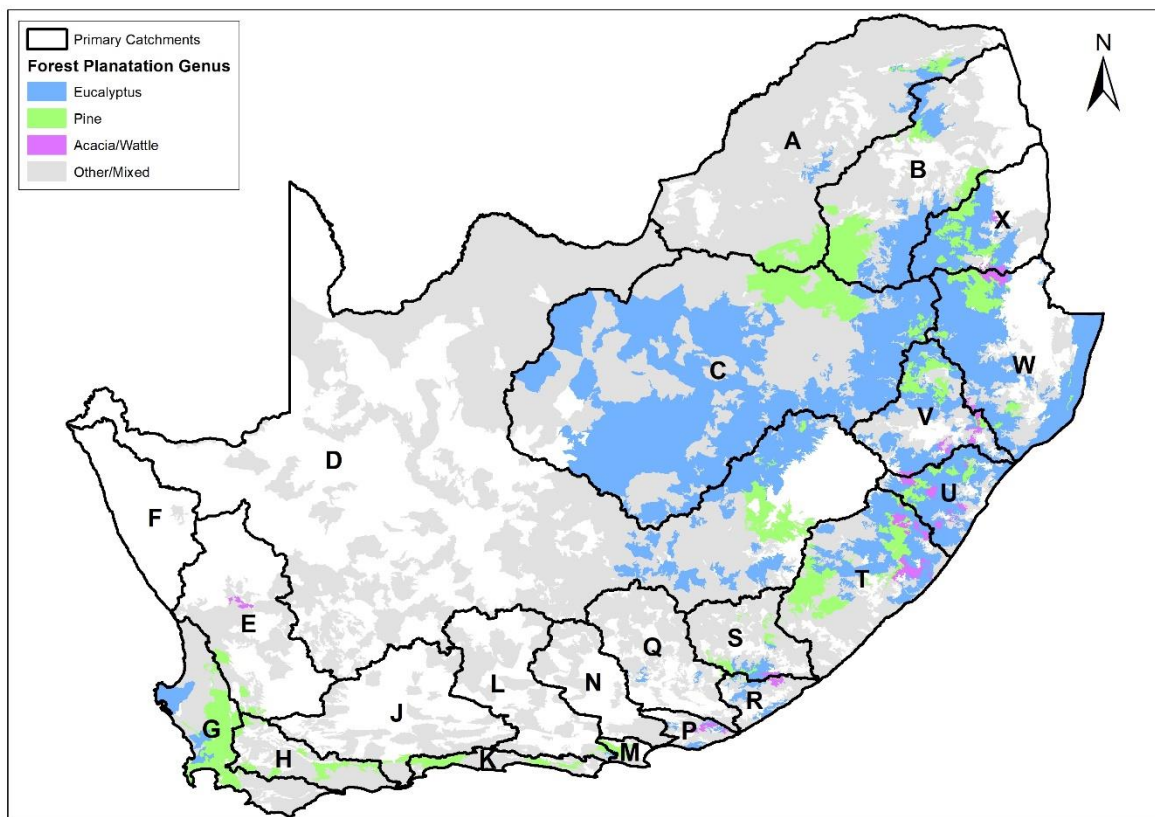
Figure 3.6   Map of model forest plantation genus based on NLC2000 (after ARC and CSIR, 2005)
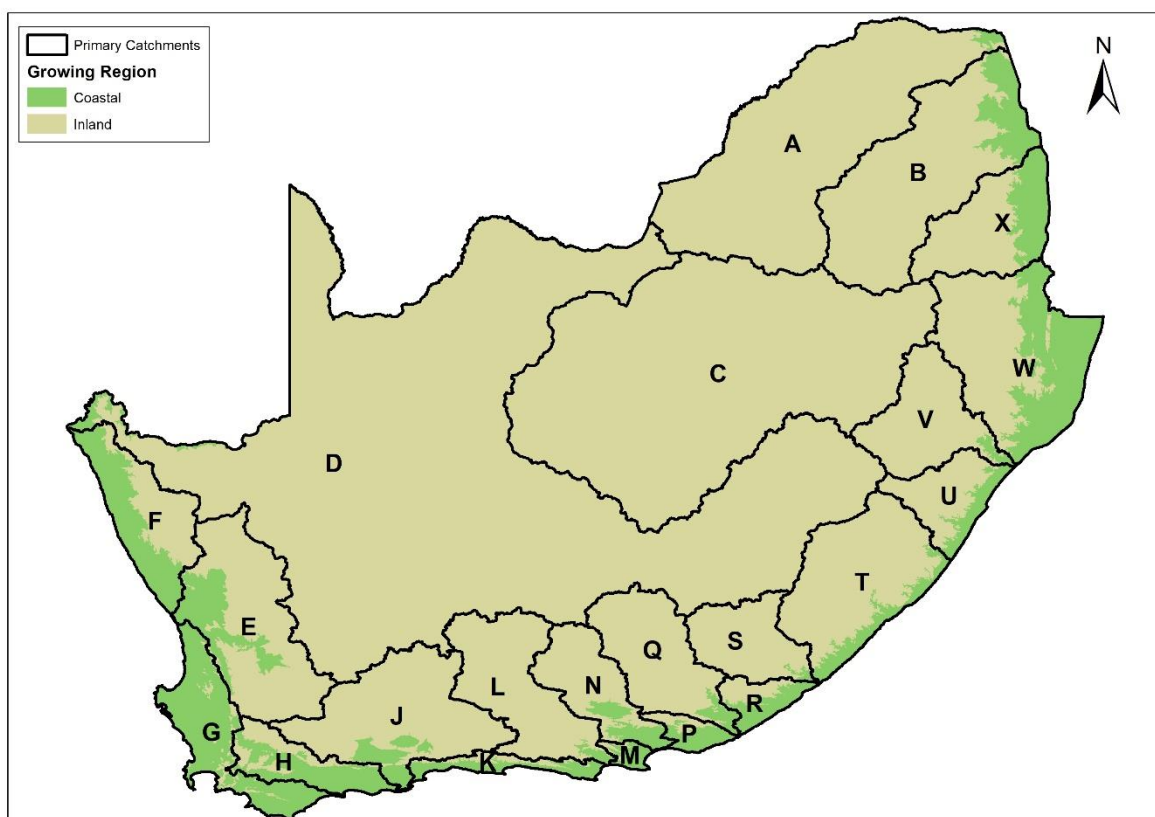
Figure 3.7   Map of inland and coastal growing regions for *Eucalyptus* plantations (Jewitt et al., 2009; Schulze, 2013)

3.4.4 Built-up areas (HRU 4)

HRU 4 (Built-up) represents a variety of built-up land cover/use classes. The classes represented by HRU 4 are shown in **Table 3.9**. The NLC2018 dataset not only includes different categories of built-up area, but also different types of vegetated pervious land cover for some categories. In the *ACRU* model, built-up areas are modelled as a combination of vegetated pervious surface, adjunct impervious areas (e.g. roads and parking lots connected to some form of stormwater system) and disjunct impervious areas (e.g. roofs of buildings, especially in residential areas from which runoff may be directed onto a pervious surface). The proportions of pervious and impervious areas differ for the different categories of built-up area. In other HRUs the modal land cover was modelled. However, a wide range different categories of built-up area may exist within a single catchment, where the runoff characteristics of these areas may differ substantially. Thus, in HRU 4 an area weighted average of the proportions of pervious area, adjunct impervious area and disjunct impervious area was calculated and used in the configuration of the *ACRU* model. These proportions for each of the three areas, for each class of built up area, were based on work by Tarboton and Schulze (1992), as recommended by Schulze and Davis (2018), and are shown in **Table A.10** in the Appendices. The configuration of HRU 4 is summarised in **Table 3.10**. It was not feasible to model a range of vegetation types in a single HRU. Thus two types of vegetation were modelled for urban areas: (i) unimproved grassland in poor condition, for informal residential areas and rural built-up areas, and (ii) improved grassland in good condition in all other built-up areas. The modal type of these two grassland types was used to parameterise the pervious vegetated portion of HRU4, using the parameter values shown in **Table A.11** in the Appendices.

Table 3.9   HRU 4 land cover/use classes and suggested groupings for NLC 2018

Grouping	National Land Cover 2018	
	ID	Description
Built-up - Urban - Residential - Formal	47	residential formal (tree)
	48	residential formal (bush)
	49	residential formal (low veg / grass)
	50	residential formal (bare)
Built-up - Urban - Residential - Informal	51	residential informal (tree)
	52	residential informal (bush)
	53	residential informal (low veg / grass)
	54	residential informal (bare)
Built-up - Urban - Smallholdings	57	smallholdings (tree)
	58	smallholdings (bush)
	59	smallholdings (low veg / grass)
	60	smallholdings (bare)
Built-up - Urban - Recreational	61	urban recreational fields (tree)
	62	urban recreational fields (bush)
	63	urban recreational fields (grass)
	64	urban recreational fields (bare)
Built-up - Urban - Commercial	65	commercial
Built-up - Urban - Industrial	66	industrial
Built-up - Urban - Transport	67	roads & rails (major linear)
Built-up - Urban - Waterbodies	20	artificial sewage ponds
Built-up - Rural	55	village scattered (bare & low veg/ grss combo)
	56	village dense (bare & low veg / grss combo)

Table 3.10   Summary of configuration of HRU 4 components

HRU Components	Description
Pervious portion	Area weighted fraction of the HRU based on pervious fraction for the different groupings present. Parameterisation assumed (i) informal and rural built-up groupings vegetated with degraded unimproved grassland, and (ii) other groupings vegetated with improved grassland. The modal grouping of these two was used in parameterisation.
Adjunct impervious	Area weighted fraction of the HRU, based on adjunct impervious fraction for the different groupings present. Waterbodies in built-up areas modelled as adjunct impervious areas.
Disjunct impervious	Area weighted fraction of the HRU, based on disjunct impervious fraction for the different groupings present.

3.4.5   Wetlands and natural waterbodies (HRU 5)

HRU 5 (Wetlands and Natural Waterbodies) represents vegetated pervious wetland areas and the natural waterbodies often associated with them. The documentation for NLC 2018 (DEA and GTI, 2019) states the following, which was the basis for grouping the wetland and pan classes: "*Note that the full spatial extent of any pan landscape feature is often represented by a combination of both flooded pans, dry pans, and/or herbaceous wetland vegetation classes; although this may not still represent the full extent of the physical pan depression, especially if the pan depression has been grass covered for a long time without flooding*". Dry pans have been included in HRU 5, rather than HRU 2 (Bare and Mining), as they may not always be dry, even if flooded for very short periods. The classes represented by HRU 5 are shown in **Table 3.11**, and the suggested configuration of HRU 5 is shown in **Table 3.12**.

In *ACRU* wetlands are typically modelled in one of two ways: (i) as a shallow dam, or (ii) using the *ACRU* Wetland routine (IVLEI=1). The second option was selected for the purpose of this configuration of the *ACRU* model. Using the Wetland routine, wetlands are modelled as "wet land", i.e. a vegetated pervious land unit onto which water spills from an adjacent river reach when the flow exceeds a user specified flow rate (CAPM3S). This makes the assumption that the majority of the wetland area in a catchment is a floodplain type wetland, as the NLC2018 datasets does not differentiate between different types of herbaceous wetland. In this national scale configuration of the *ACRU* model, the values for the CAPM3S variable were estimated as the median daily average flow rate modelled for the historical period 1950-1999 using the baseline (naturalised) configuration of the *ACRU* model. Given that it is often difficult to distinguish between the flooded (i.e. the class Natural Pans – Flooded) and unflooded herbaceous wetland areas, these were modelled together using the *ACRU* LYSIM option, such that these areas do not generate any surface runoff until both the topsoil and subsoil horizons are saturated. In addition, these wetland areas were assumed to be underlain by an impervious layer, such that there is not percolation to groundwater and only surface runoff is generated into the adjacent river reach. The previous vegetated wetland area was modelled using the vegetation parameters shown in **Table A.12** in the Appendices. It is acknowledged that Mangrove wetlands would have different vegetation characteristics to herbaceous wetlands, however, the area of Mangrove wetlands within a catchment (if they occur at all), is typically small compared to herbaceous wetland, and thus Mangrove wetlands are combined with herbaceous wetlands for the purpose of this configuration.

Natural waterbodies, which included the groupings Lakes, Rivers and Coastal Water were modelled as adjunct impervious areas with variable STOIMP=0 mm such that all rainfall on these surfaces contributes to runoff.

The Dry Pans class represented a challenge in configuring *ACRU* at a national scale. These areas of dry pan are assumed to be endorheic (i.e. internally drained) in most instances and under most runoff

conditions. Initially dry pans were represented in *ACRU* as disjunct impervious areas, to initially retain runoff on the surface of the catchment and, once an assumed storage depth was reached, to flood onto adjacent wetland areas where these exist. However, in catchments where dry pans exist these often form a large portion of the catchment resulting in excessive runoff depths onto the pervious wetland portion of the catchment which caused an instability in *ACRU*. Thus dry pans were modelled as adjunct impervious areas with variable STOIMP=50 mm such that runoff, even from significant rainfall events, is retained on the surface of the catchment. The retained runoff is depleted gradually by evaporation and runoff in excess of the assumed surface storage contributes to streamflow.

Table 3.11   HRU 5 land cover/use classes and suggested groupings for NLC 2018

Grouping	National Land Cover 2018	
	ID	Description
Herbaceous Wetlands	22	herbaceous wetlands (currently mapped)
	23	herbaceous wetlands (previously mapped)
	73	fallow land & old fields (wetlands)
Mangrove Wetlands	24	mangrove wetlands
Flooded Pans	18	natural pans (flooded at observation times)
Dry Pans	26	dry pans
Lakes	17	natural lakes
Rivers	14	natural rivers
Coastal Water	15	natural estuaries & lagoons
	16	natural ocean & coastal

Table 3.12   Summary of configuration of HRU 5 components

HRU Components	Description
Pervious portion	Herbaceous Wetlands, Mangrove Wetlands and Flooded Pans. Model using both the IVLEI and LYSIM options turned on. Parameterised with wetland vegetation characteristics
Adjunct impervious	Lakes, Rivers and Coastal Water modelled with STOIMP=0. Dry Pans modelled with STOIMP=50. The STOIMP values area weighted if both groupings exist in the same catchment.
Disjunct impervious	None

3.4.6   **Agriculture and Dams (HRU 6)**

HRU 6 (Agriculture and Dams) represents agricultural land cover/use classes and dams. Dams were included in this HRU as dams, in addition to being the primary water source for urban water supply, are also an important water source for irrigated agricultural crops. The classes represented by HRU 6 are shown in **Table 3.13** and the suggested configuration of HRU 6 is shown in **Table 3.14**. The NLC2018 dataset includes several classes representing various annual and perennial crops and crop types. The parameterisation of these crops and the assumptions made are discussed below. In each Quinary Catchment the modal crop or crop type is modelled. No distinction is made between dryland and irrigated crops in this configuration of the *ACRU* model, as engineered water use is not being modelled for the purpose of this study.

Table 3.13   HRU 6 land cover/use classes and suggested groupings for NLC 2018

Grouping	National Land Cover 2018	
	ID	Description
Agriculture - Commercial - Annual	40	commercial annual crops rain-fed / dryland
	38	commercial annual crops pivot irrigated
	39	commercial annual crops non-pivot irrigated
Agriculture - Commercial - Sugarcane	36	cultivated commercial sugarcane non-pivot
	34	cultivated commercial sugarcane pivot irrigated
Agriculture - Commercial - Pineapples	35	cultivated commercial permanent pineapples
Agriculture - Commercial - Orchards	32	cultivated commercial permanent orchards
Agriculture - Commercial - Vines	33	cultivated commercial permanent vines
Agriculture - Subsistence - Annual	41	subsistence / small-scale annual crops
Agriculture - Subsistence - Sugarcane	37	cultivated emerging farmer sugarcane non-pivot
Waterbodies - Dams	19	artificial dams (including canals)

Table 3.14   Summary of configuration of HRU 6 components

HRU Components	Description
Pervious portion	Modal agricultural crop. Parameterise according to modal class
Adjunct impervious	Lakes, Rivers and Coastal Water modelled with STOIMP=0.
Disjunct impervious	None

The NLC2018 dataset has classes representing commercial annual crops, but does not identify specific annual crop types. This required some assumptions to be made regarding the crop type, where the seasonality of the assumed crop is important and it assumed that the difference in total evaporation and runoff for different crop types grown in the same rainfall seasonality region will not be significant. The rainfall seasonality dataset produced by Schulze and Maharaj (2008) was used. A map of the rainfall seasonality regions is shown in **Figure 3.8**. In the Winter and All Seasons rainfall seasonality regions the annual crop was assumed to be winter wheat. In all other rainfall seasonality regions the annual crop was assumed to be summer maize. For maize, different planting dates were used in different parts of the country with different rainfall regimes, based on work reported in Kunz et al. (2020). These maize planting data regions are shown in **Figure 3.9**. Annual crops grown for subsistence were assumed to be maize grown in summer. The NLC2018 dataset does differentiate between irrigated and dryland commercial annual dryland crops, but no distinction was made between dryland and irrigated commercial crops in this configuration of the *ACRU* model as engineered water use is not being modelled for the purpose of this study. The parameters used to configure annual crops in the *ACRU* model are shown in **Table A.13** in the Appendices.

In NLC2018 sugarcane is included as a specific crop and is modelled as such in this configuration of the *ACRU* model. The sugarcane parameter values used to configure the *ACRU* model are shown in **Table A.14** in the Appendices, and were based on recommendations in Schulze (2013) and Schulze and Davis (2018) which were based on Jewitt et al. (2009) and Schulze and Schütte (2014). Different parameters are provided in **Table A.14** for sugarcane grown in four different regions of South Africa: (i) KwaZulu-Natal inland, (ii) KwaZulu-Natal south coast, (iii) KwaZulu-Natal north coast, and (iv) far north coast of KwaZulu-Natal and also Mpumalanga and Eswatini. The sugarcane growing regions were defined based on Jewitt et al. (2009) and (Schulze, 2013), and are shown in **Figure 3.10**. In NLC2018

there is a class for emerging farmer sugarcane, however, this was not the modal agricultural crop in any of the Quinary Catchments and thus was not included in the *ACRU* configuration.
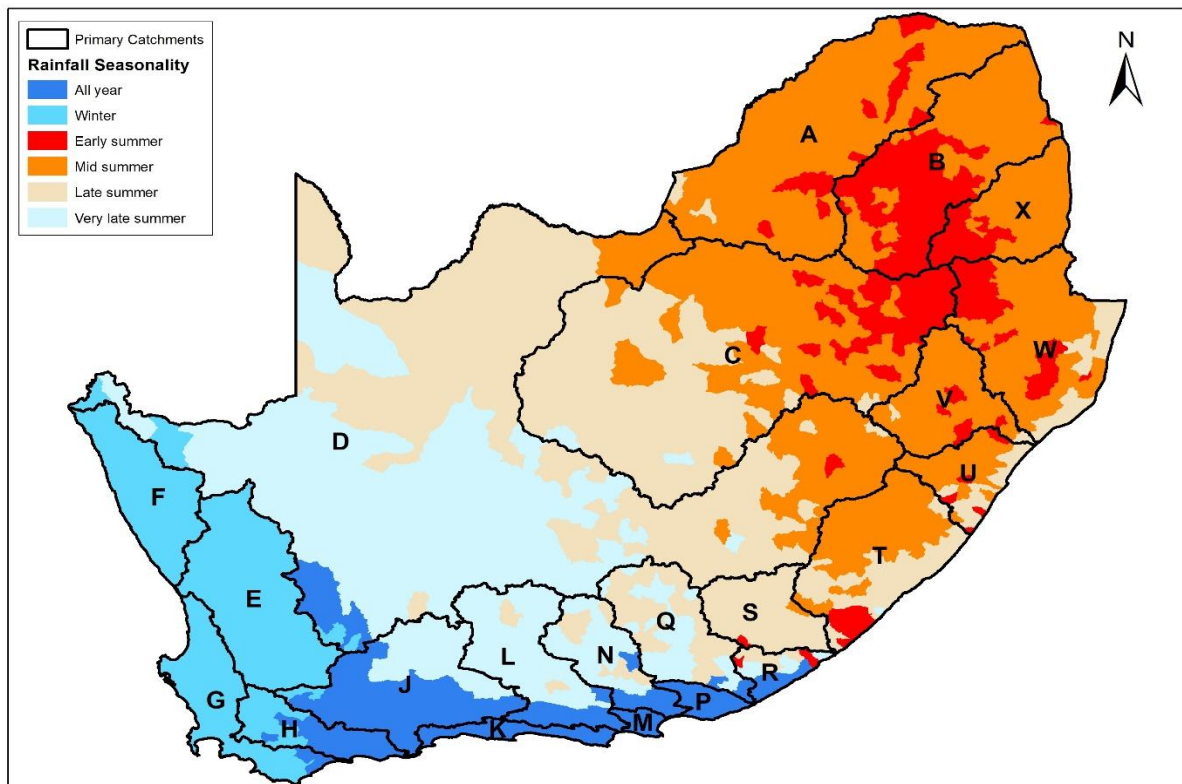
Figure 3.8   Map of rainfall seasonality (Schulze and Maharaj, 2008)
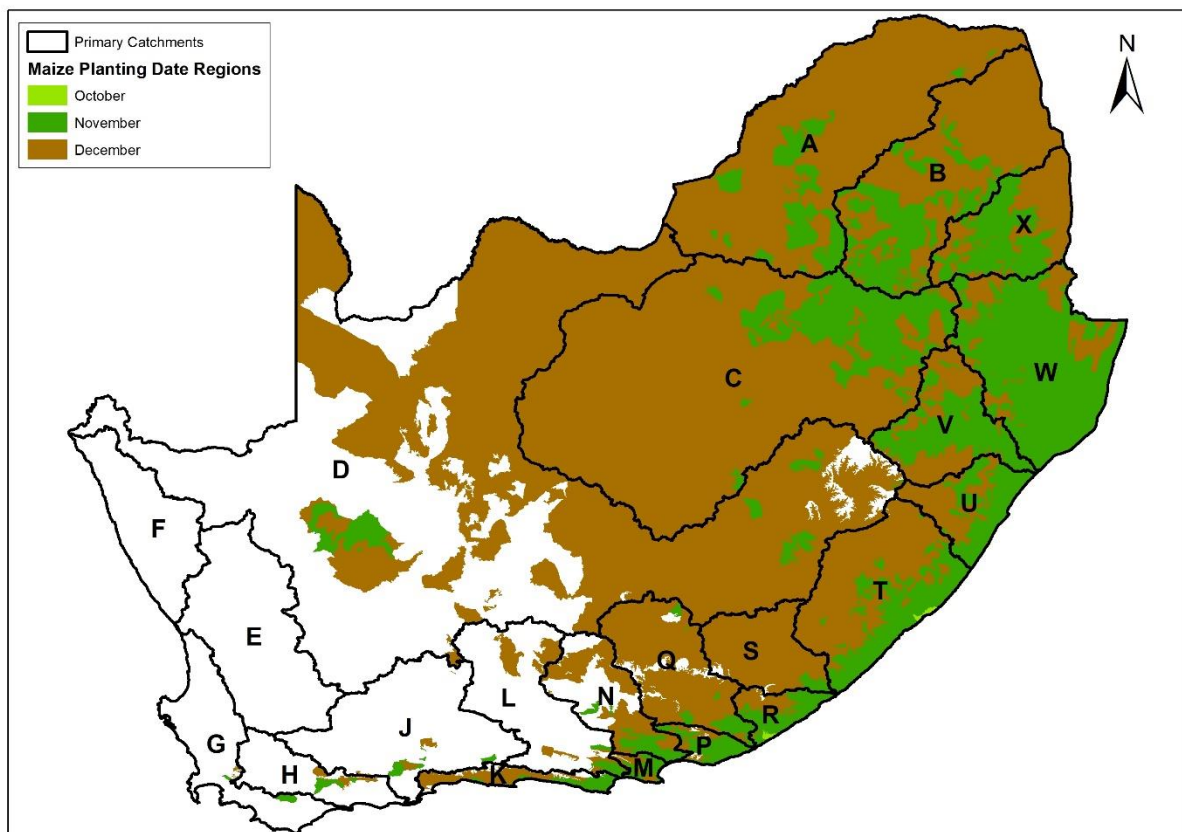
Figure 3.9   Map of maize planting date regions (after Kunz et al., 2020)
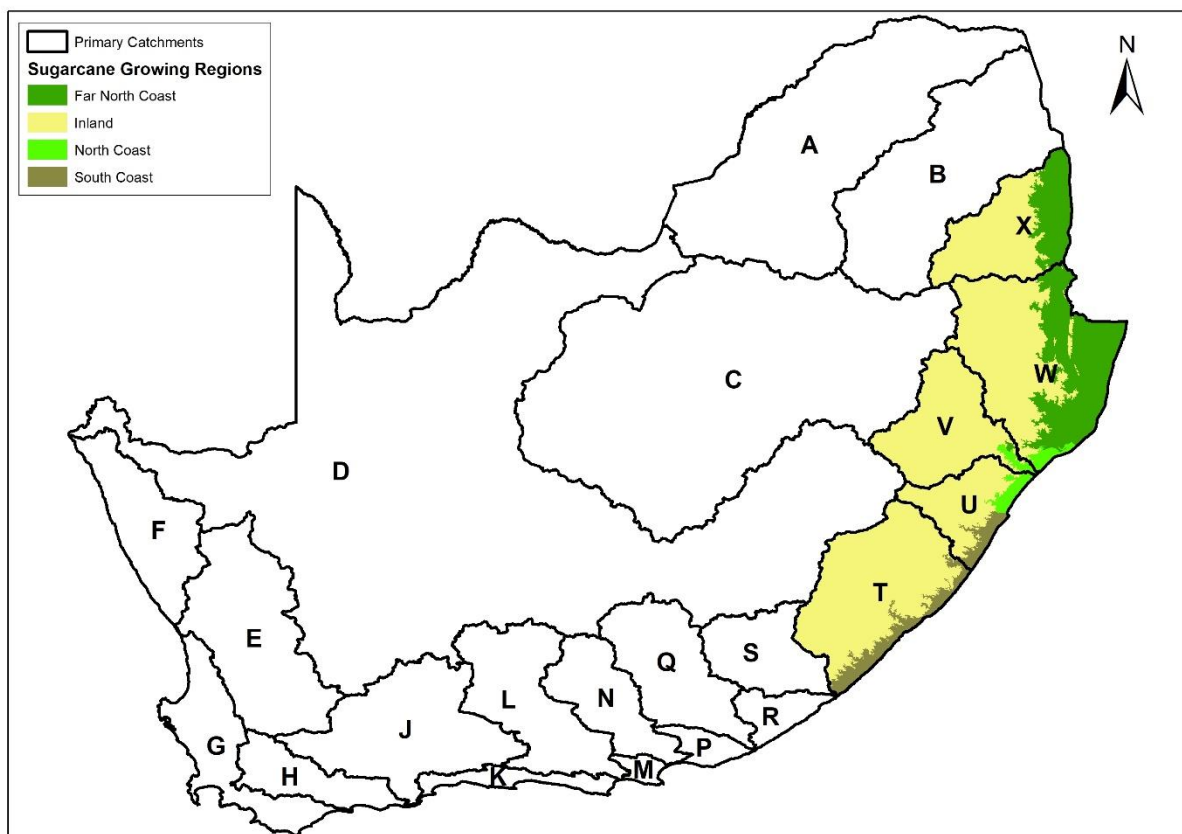
Figure 3.10 Map of growing regions for sugarcane (Jewitt et al., 2009; Schulze, 2013)

The NLC2018 dataset includes classes representing horticultural crops. One class specifically represents pineapples. Pineapples are the modal crop in 11 Quinary Catchments in this configuration of the *ACRU* model. The parameters used to represent pineapples were estimated from various sources and are shown in **Table A.15** in the Appendices. There is one class representing vine crops, which for the purpose of this configuration are assumed to be grapes for wine making. The parameters used to represent wine grapes are shown in **Table A.15** in the Appendices. There is one class representing orchards, which for the purpose of this configuration orchards were assumed to be citrus orchards (which are evergreen), except in the winter rainfall region, where the orchards were assumed to be deciduous fruit orchards. The parameters used to represent citrus and deciduous fruit orchards are shown in **Table A.15** in the Appendices.

Dams were modelled as adjunct impervious areas, for the purpose of this *ACRU* configuration, with the variable STOIMP=0 mm, such that all rainfall on these surfaces contributes to runoff.

3.5 Discussion and Conclusions

Configuring a hydrological model with actual land cover/use for the whole of South Africa has been a significant undertaking. This is the first time that the *ACRU* model has been configured with actual land cover/use at Quinary Catchment level for the whole of South Africa, Lesotho and Eswatini. This is an exciting and important step forward for *ACRU* and South Africa. Such a configuration, by its nature, requires some compromises and many assumptions to be made. It also needs to be remembered that, for the purposes of this study, actual water use, especially engineered water use, and dams were not modelled. These cautions need to be considered when applying the simulated runoff values produced through the use of this configuration of the *ACRU* model. The simulated runoff values are thus better suited to comparative analyses, such as (i) comparing runoff produced by actual land cover/use with runoff produced under naturalised land cover, (ii) comparing runoff produced based on different GCMs, (iii) comparing runoff produced using different RCPs, and (iv) comparing runoff produced in different time periods.

3.6 References

ACOCKS, JPH (1988) *Veld Types of South Africa.* Botanical Research Institute, Memoirs of the Botanical Survey of South Africa, 57, 3rd ed., Government Printer, Pretoria, South Africa.

ARC and CSIR. 2005. *National Land Cover (2000).* Consortium of the Council for Scientific and the Industrial Research (CSIR) and the Agricultural Research Council (ARC): Pretoria, South Africa [Dataset].

Department of Environmental Affairs (DEA) (2015) *2013-14 SA national land-cover – broad parent classes* [Dataset]*.* Produced by GeoTerraImage Pty Ltd (GTI) for Department of Environmental Affairs (DEA): Pretoria, South Africa. doi:10.15493/DEA.CARBON.10000015

DEA and GTI. 2016. 1990 *South African National Land Cover Dataset* [Dataset]. Produced by GeoTerraImage Pty Ltd (GTI) for the Department of Environmental Affairs (DEA): Pretoria, South Africa.

DEA and GTI. 2019. 73 *Class GTI South African National Land Cover Dataset* (2018) [Dataset]. Produced by GeoTerraImage Pty Ltd (GTI) for the Department of Environmental Affairs (DEA): Pretoria, South Africa.

HALLOWES, LA, SCHULZE, RE, HORAN, MJC and PIKE, A. 2004. South African National Quaternary Catchments Database : Refinements to, and links with, the *ACRU* model as a framework for installed hydrological modelling systems. In: eds. SCHULZE, RE and PIKE, A, *Development and Evaluation of an Installed Hydrological Modelling System*. WRC Report 1155/1/04. Chapter 6. Water Research Commission, Pretoria, South Africa.

JEWITT, GPW, LORENTZ, SA, GUSH, MB, THORNTON-DIBB, SLC, KONGO, V, WILES, L, BLIGHT, J, STUART-HILL, SI, VERSVELD, D and TOMLINSON, K. 2009. *Methods and guidelines for the licensing of SFRAs with paticular reference to low flows*. WRC Report 1428/1/09. Water Research Commission, Pretoria, South Africa.

KUNZ, R, MASANGANISE, J, REDDY, K, MABHAUDHI, T, LEMBEDE, L, NAIKEN, V and FERRER, S. 2020. *Water use and yield of soybean and grain sorghum for biofuel production*. WRC Report 2491/1/20. Water Research Commission, Pretoria, South Africa.

LYNCH, S. 2004. *Development of a Raster Database of Annual, Monthly and Daily Rainfall for Southern Africa*. WRC Report 1156/1/04. Water Research Commission, Pretoria, South Africa.

PIKE, A AND SCHULZE, RE. 1995. AUTOSOIL Version 3: A Soils Decision Support System for South African Soils [Software], in :*Handbook on adaptation to climate change for farmers, officials and others in the agricultural sector of South Africa.* Department of Agricultural Engineering, University of Natal, Pietermaritzburg, South Africa.

South African National Biodiversity Institute (SANBI (2012) Vegetation Map of South Africa, Lesotho and Swaziland. NVM2012beta2_wgs84_Geo. [Dataset]. Pretoria, South Africa.

SCHULZE, R AND HORAN, M. 2010. Methods 1: Delineation Of South Africa, Lesotho And Swaziland Into Quinary Catchments. In: *Methodological Approaches to Assessing Eco-Hydrological Responses to Climate Change in South Africa*, SCHULZE, R, HEWITSON, B, BARICHIEVY, K, TADROSS, M, KUNZ, R, HORAN, M AND LUMSDEN, T, WRC Report 1562/1/10. Water Research Commission, Pretoria, South Africa.

SCHULZE, R, HORAN, M, KUNZ, R, LUMSDEN, T AND KNOESEN, D. 2010. Methods 2: Development Of The Southern African Quinary Catchments Database. In: *Methodological Approaches to Assessing Eco-Hydrological Responses to Climate Change in South Africa*, SCHULZE, R, HEWITSON, B, BARICHIEVY, K, TADROSS, M, KUNZ, R, HORAN, M AND LUMSDEN, T, WRC Report 1562/1/10. Water Research Commission, Pretoria, South Africa.

SCHULZE, RE (1995) *Hydrology and Agrohydrology: A Text to Accompany the ACRU 3.00 Agrohydrological Modelling System.* Water Research Commission, Pretoria, South Africa.

SCHULZE, RE (2004) Determination of Baseline Land Cover Variables for Applications in Assessing Land Use Impacts on Hydrological Responses in South Africa. In: Development and Evaluation of an Installed Hydrological Modelling System, SCHULZE RE and PIKE A, WRC Report 1155/1/04. Water Research Commission, Pretoria, South Africa.

SCHULZE, RE (2013) Modelling Impacts Of Land Use On Hydrological Responses In South Africa With The *ACRU* Model By Sub-Delineation Of Quinary Catchments Into Land Use Dependent Hydrological Response Units. Internal Report. Centre for Water Resources Research, University of KwaZulu-Natal, Pietermaritzburg, South Africa.

SCHULZE RE and DAVIS NS (2018) Practitioners' Handbook for Undertaking Current and Projected Future Climate Related Risk and Vulnerability Assessments. GIZ Contract Number 83259369 on "Development of a Framework and Methodology for Undertaking a Risk and Vulnerability Assessment in all Nine Water Management Areas of South Africa". Schulze and Associates, Pietermaritzburg, South Africa.

SCHULZE RE and HORAN, MJC (2007) Hydrological Modelling as a Tool for Ecosystem Services Trading: Case Studies from the Drakensberg Region of South Africa. *.ACRU*cons Report 56. School of Bioresources Engineering and Environmental Hydrology, University of KwaZulu-Natal, Pietermaritzburg, South Africa.

SCHULZE RE and MAHARAJ, M (2004) Development of a Database of Gridded Daily Temperatures for Southern Africa. WRC Report 1156/2/04. Water Research Commission, Pretoria, South Africa.

SCHULZE RE and MAHARAJ M (2008) Section 6.5: Rainfall Seasonality. In: *African Atlas of Climatology and Agrohydrology* Schulze, RE. WRC Report 1489/1/06. Water Research Commission, Pretoria, South Africa.

SCHULZE RE and SCHÜTTE S (2014) Complexities of streamflow reductions by commercial plantation forests under varying climatic scenarios. 17th SANCIAHS National Hydrology Symposium, University of the Western Cape, Bellville, South Africa.

SCHULZE RE and SCHÜTTE S (2016) Assessment of Sediment Yields from Post-Harvest Burn vs No-Burn Management Scenarios using the *ACRU* Model with Land Type Soils Data on all Forested Areas for Mondi Holdings within South Africa. Report by Schulze and Associates for Mondi Project Phase 2. Mondi, Hilton, South Africa.

SCHULZE RE, WARBURTON M, LUMSDEN TG and HORAN MJC (2005) The Southern African Quaternary Catchments Database: Refinements to, and Links with, the *ACRU* System as a Framework for Modelling Impacts of Climate Change on Water Resources. In: *Climate Change and Water Resources in Southern Africa: Studies on Scenarios, Impacts, Vulnerabilities and Adaptation. African Atlas of Climatology and Agrohydrology,* SCHULZE RE,WRC Report 1430/1/05. Chapter 8. Water Research Commission, Pretoria, South Africa.

SIRI. 1987. Land Type Series. Memoirs on the Agricultural Natural Resources of South Africa. [Dataset]. Soil and Irrigation Research Institute, Pretoria, South Africa.

SMITHERS JC and SCHULZE RE (1995) *ACRU* Agrohydrological Modelling System : User Manual Version 3.00. WRC Report No. TT70/95. Water Research Commission, Pretoria, South Africa.

TARBOTON KC and SCHULZE RE (1992) Distributed hydrological modelling system for the Mgeni catchment. WRC Report 234/1/92. Water Research Commission, Pretoria, South Africa.

TOUCHER ML, RAMJEAWON M, MCNAMARA MA, ROUGET M, BULCOCK H, KUNZ RP, MOONSAMY J, MENGISTU M, NAIDOO T, VATHER T and ALDWORTH TA (2019) Resetting The Baseline Land Cover Against Which Streamflow Reduction Activities And The Hydrological Impacts Of Land Use Change Are Assessed. WRC Report 2437/1/19. Water Research Commission, Pretoria, South Africa.

4 PROJECTIONS OF RAINFALL, TEMPERATURE AND POTENTIAL EVAPORATION

S. Schütte, R.E. Schulze, D.J. Clark, R.P. Kunz, Z. Jele

Maps of projected mean annual rainfall, followed by monthly rainfall for selected month are shown and discussed. Then design rainfall events are presented, followed by means of daily temperature and mean annual reference evaporation for future periods for RCP8.5, followed by conclusions.

4.1 Results for Historical Observed and Projected Future Rainfall, Temperature and Reference Evaporation under RCP8.5

4.1.1 Rainfall

Annual rainfall (precipitation) will be discussed first, followed by selected monthly rainfall and design rainfall.

Mean annual rainfall
Projected changes in mean annual rainfall for the individual GCMs (**Figure 4.1**) show broad overall similarities amongst the GCMs, with reduced rainfall in the west, especially towards the distant future, and increases in the Drakensberg and more central parts of South Africa. Differences in the severity of increases (darker shades of purple) and reductions (darker shades of red) can be seen, with the magnitudes of decreases and increases depending on the GCM. The confidence in the results is discussed later, in Section 5.2.11.
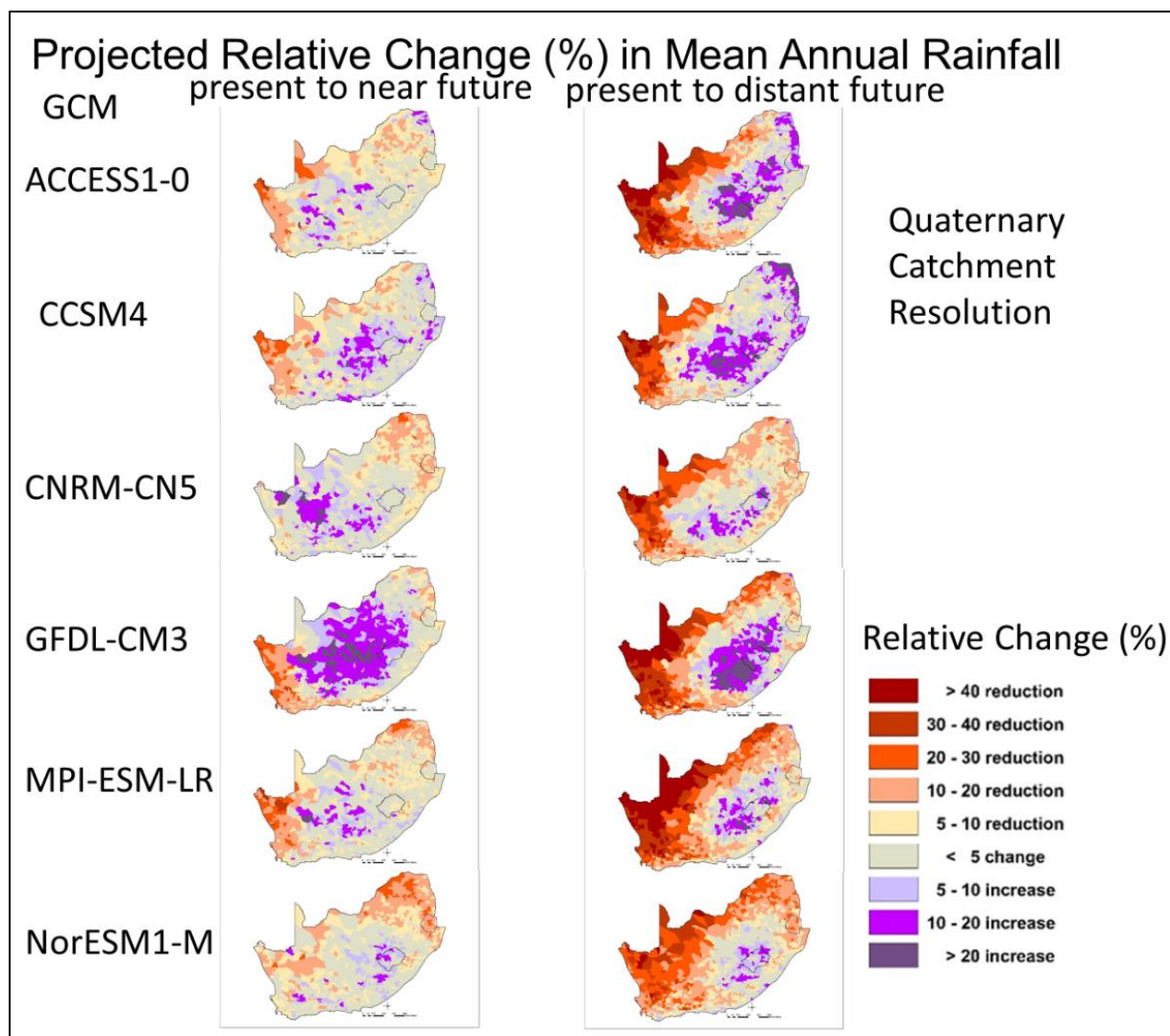
Figure 4.1   Projected changes in mean annual rainfall for the individual GCMs used, showing relative changes (%) from the present (1961-1990) to the near future (2015-2044) in the left column, and from the present to the distant future (2070-2099) in the right column, at a Quaternary Catchment resolution

Correlations between observed mean annual rainfall for the 1961-1990 time period (termed 'historical') and GCM derived mean annual rainfall for the same (1961-1990) period (termed 'present') show relatively good fits for all 6 GCMs (**Figure 4.2**). This highlights the success of the bias correction applied to the GCM rainfall data. It also shows that bias corrected GCM derived data (present) can be used to represent the observed (historical) for that period.
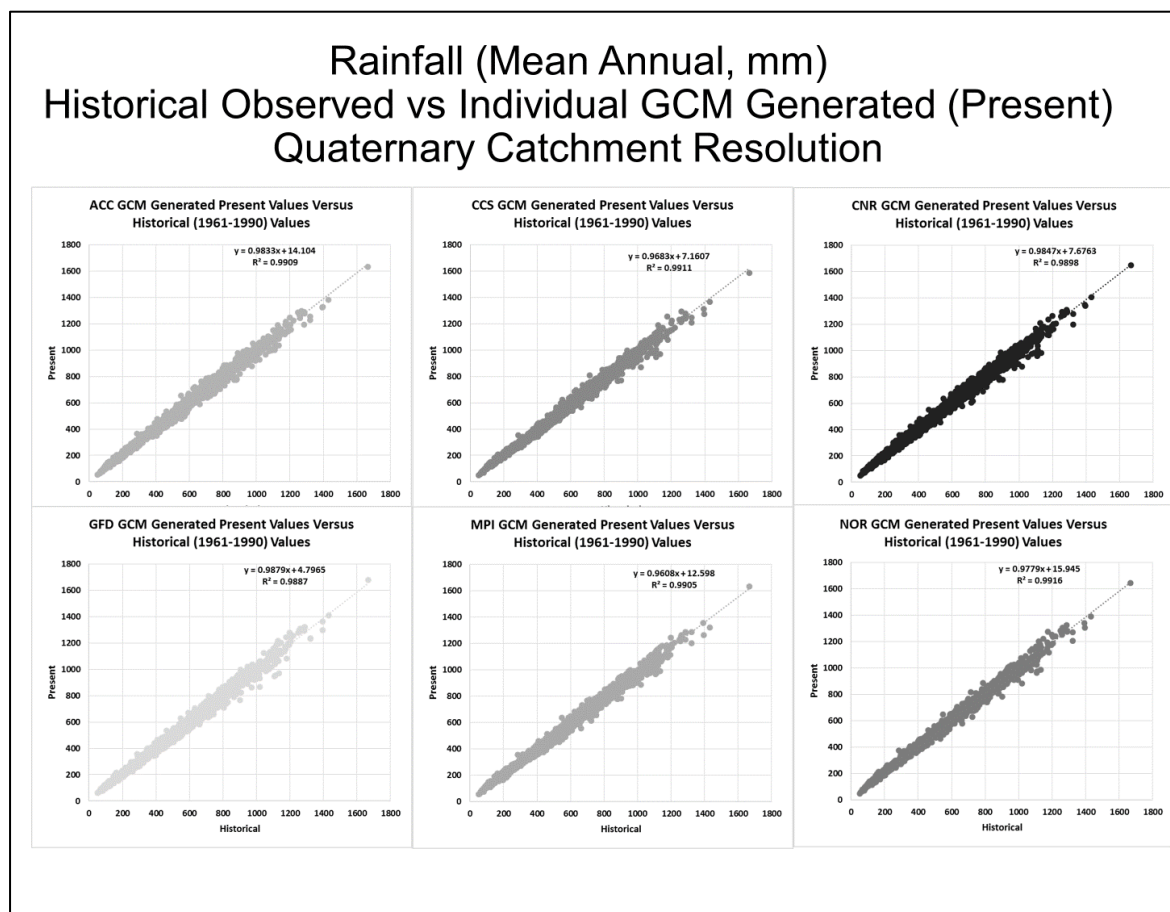
Figure 4.2   Correlations between observed (historical) and GCM derived mean annual rainfall for the individual GCMs (present) for the period 1961-1990, at a Quaternary Catchment resolution

A comparison of the observed historical and the average of the six GCM generated and bias corrected mean annual rainfalls at Quaternary Catchment resolution (**Figure 4.3**) shows similar results for both scenarios, with more rainfall in the east and along the coast in the east and south, and much less rainfall in the west and north-west.

Mean annual GCM derived rainfall distributions for the present (1961-1990), the near future (2015-2044) and the distant future periods (2070-2099) are shown in **Figure 4.4** for the RCP8.5 emission scenario, indicating a drier west into the future. Projected changes in mean annual rainfall, when expressed as absolute and relative changes (**Figure 4.5**), show a reduction in rainfall in the west and north, especially into the distant future. Along the east coast the changes are mixed. In the eastern interior, in the Drakensberg area more rainfall than at present is projected for the near future and even more for the distant future.
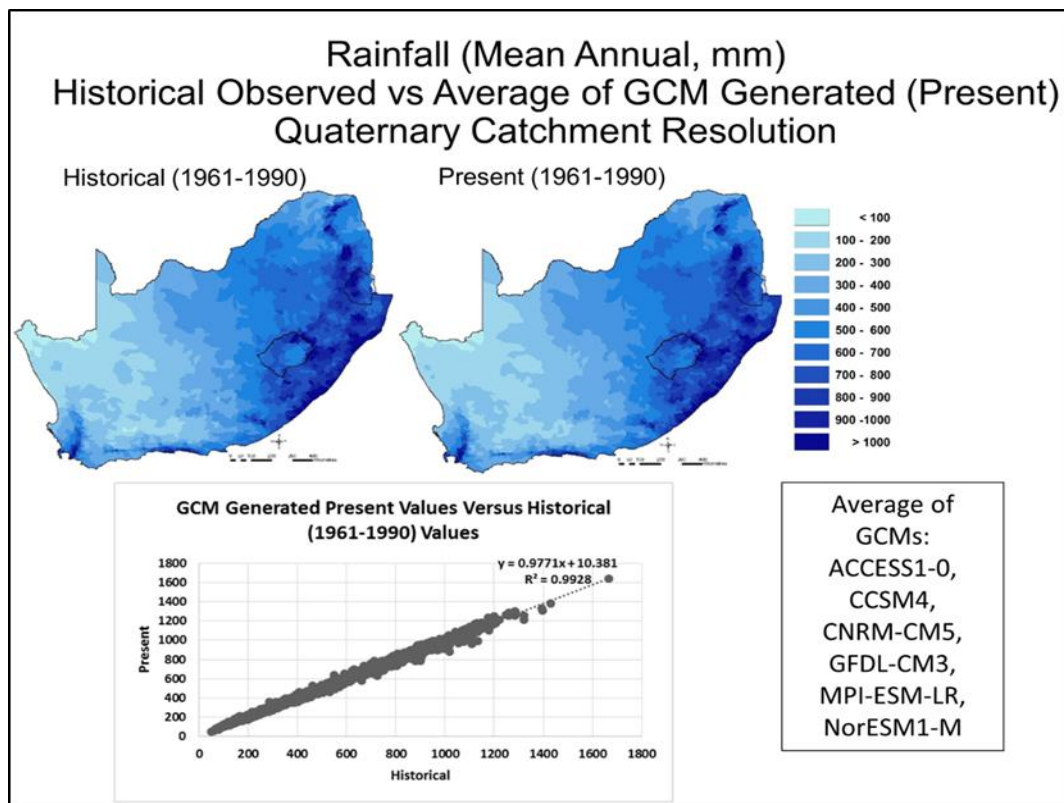
Figure 4.3   A comparison of mean annual observed rainfall [left] and the GCM generated and bias corrected mean annual rainfall for the concurrent period 1961-1990, as well as a correlation between the two, on a Quaternary Catchment resolution
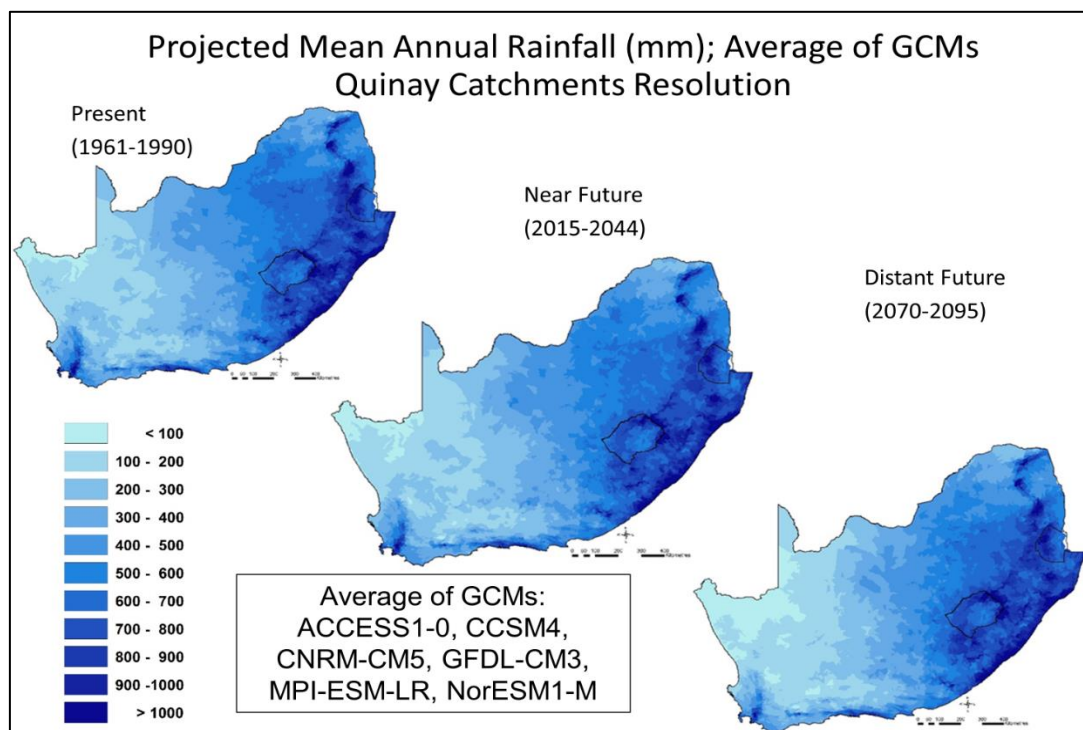
Figure 4.4   GCM generated mean annual rainfall for the present (1961-1990) [left] and projected MAP for the near future (2015-2044) [middle] and the distant future (2070-2099) [right] time periods, at Quinary Catchment Resolution
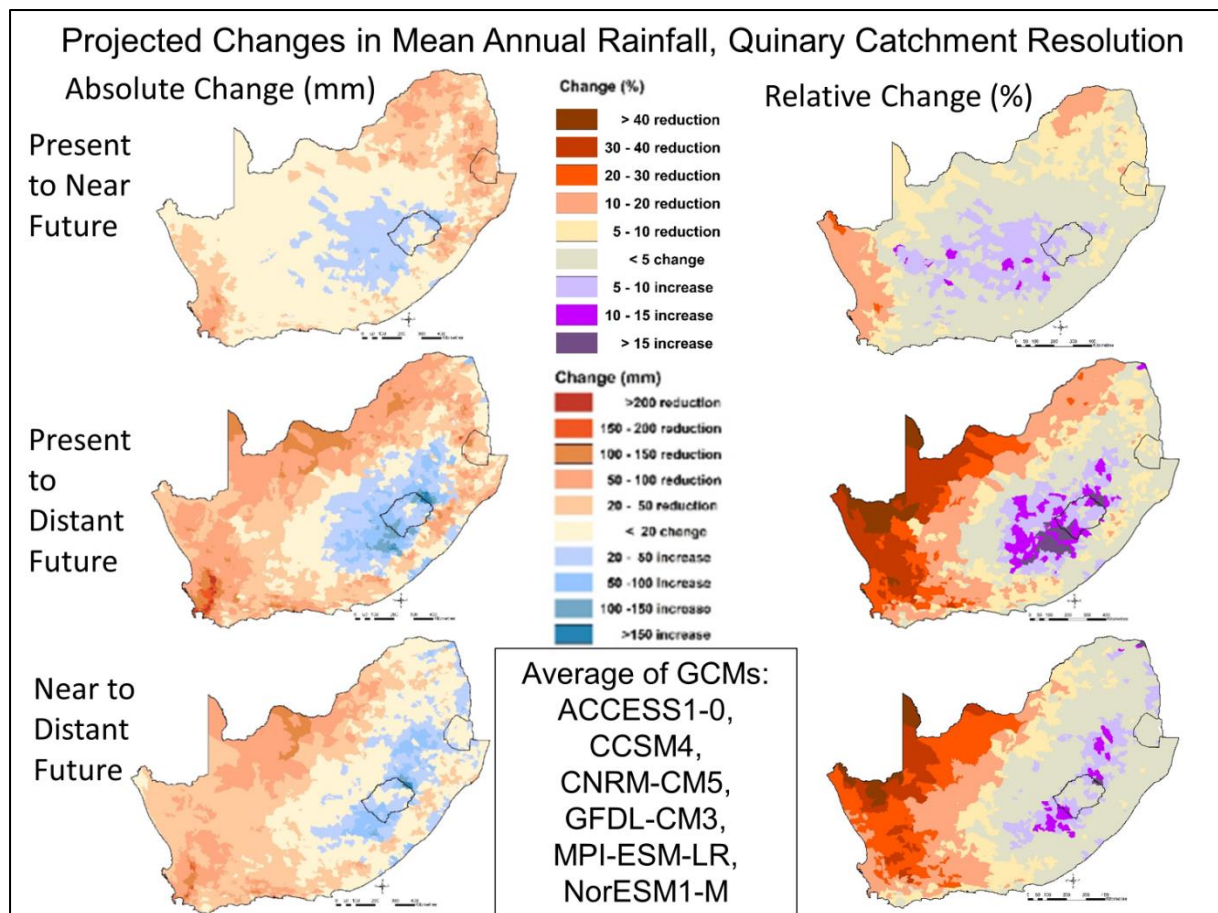
Figure 4.5   Projected changes in mean annual rainfall showing absolute changes (mm) on the left and relative changes (%) on the right, with changes from the present (1961-1990) to the near future (2015-2044) [top row], from the present to the distant future (2070-2099) [middle row] and changes from the near to the distant future [bottom row], at Quinary Catchment resolution

For the annual rainfall statistics of the 1:10-year low, the median annual and the 1:10 high year, ratio changes of average GCM generated rainfall for the near future divided by average of GCM generated rainfall of the present period, as well as rainfall for the distant future divided by rainfall of the present period show ratio changes being highest in a 1:10 low year, compared to a median and 1:10 high year (**Figure 4.6**).
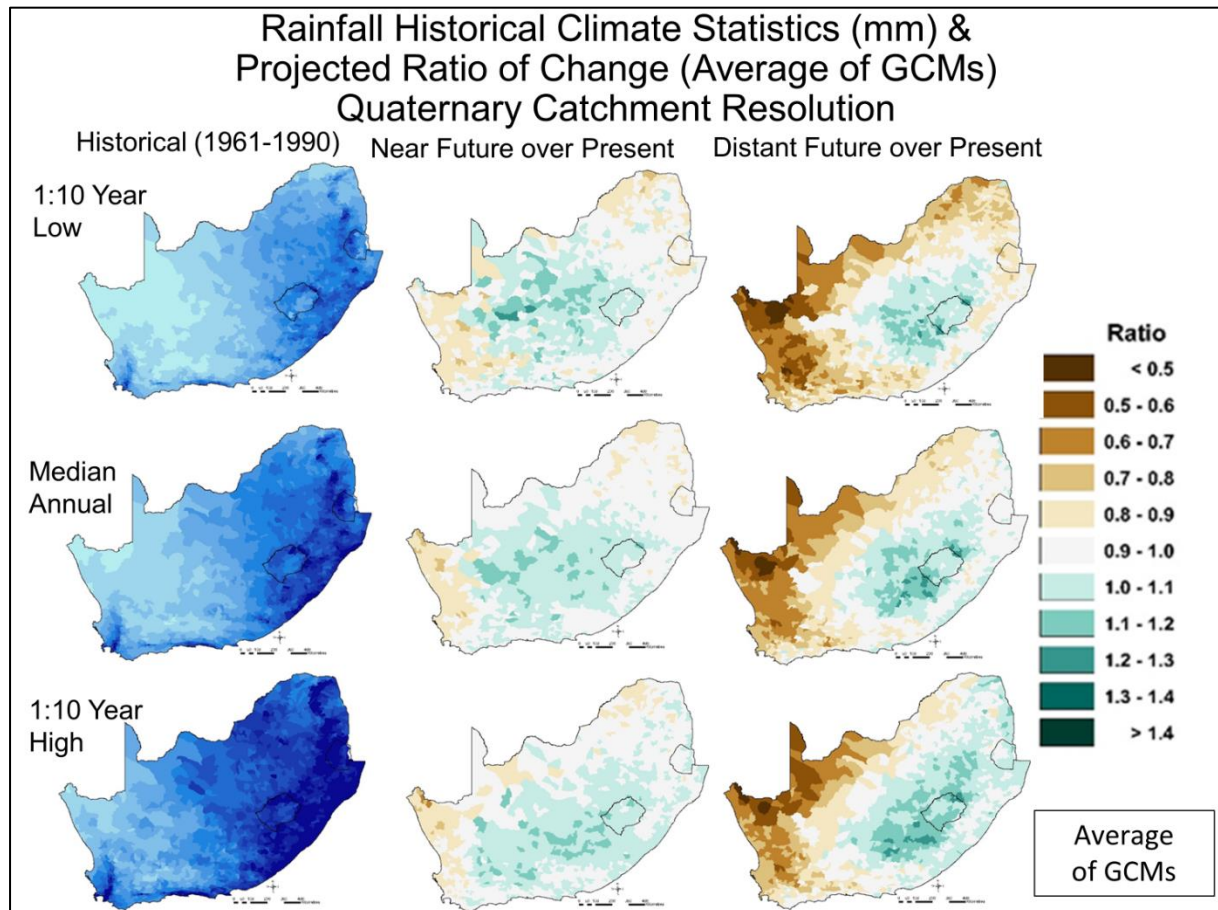
Figure 4.6   Statistics of annual rainfall for a 1:10-year low [top], a median [middle] and a 1:10-year high annual rainfall [bottom] for observed historical climate (1961-1990) [left column] and for projected GCM generated ratio changes of the near future to present [middle column] and distant future to present ratios [right column], at Quaternary Catchment resolution

Monthly rainfall

Median monthly rainfall for January, representing summer, April, representing autumn, July, representing winter and October, representing spring. The selected month are called cardinal month as they are representative for the season. **Figure 4.7** shows GCM generated monthly rainfall for 1961-1990.
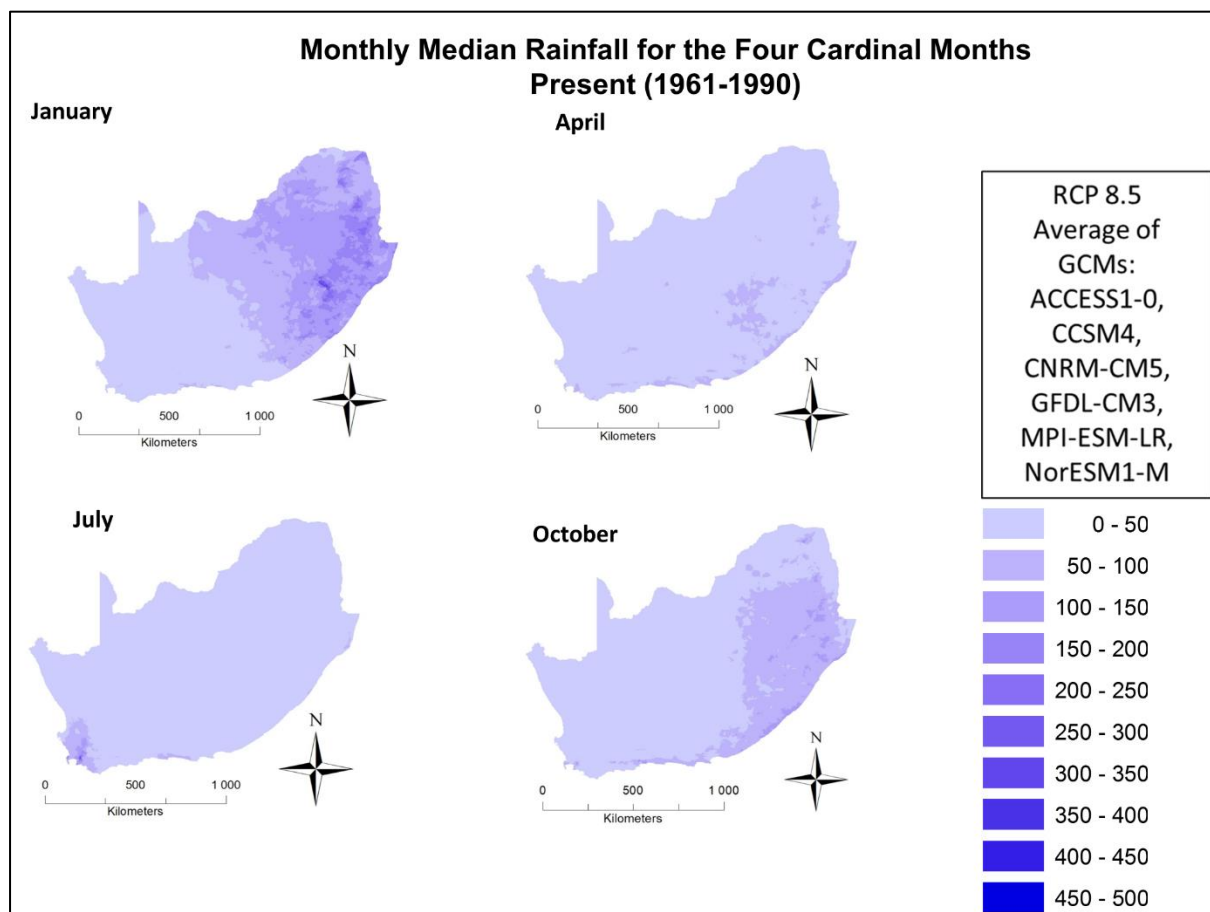
Figure 4.7　Median monthly rainfall for the present (1961-1990) for January (top left), April (top right), July (bottom left) and October (bottom right), average of GCMs, Quinary Catchments resolution

Projected changes to median monthly rainfall in mm and %, relative to the present are shown for October, January, April and July (**Figure 4.8** to **Figure 4.11**). October rainfall generally shows small decreases over most of the country with small increases over some areas in the interior, but quite severe decreases are projected over the north-east especially into the distant future (**Figure 4.8**). January rainfall generally shows increases in the interior and decreases in the south and mixed changes along the east coast (**Figure 4.9**). April rainfall generally shows decreases in the west and north and increases in the east (**Figure 4.10**). July rainfall generally show small decreases in the north and the interior, with small increases along the east (**Figure 4.11**). The north-east seems to have a decrease in spring rain but an increase in rainfall in summer, thus a shift in the onset of rain later towards summer. Spring rains generally show reductions over nearly all of southern Africa.
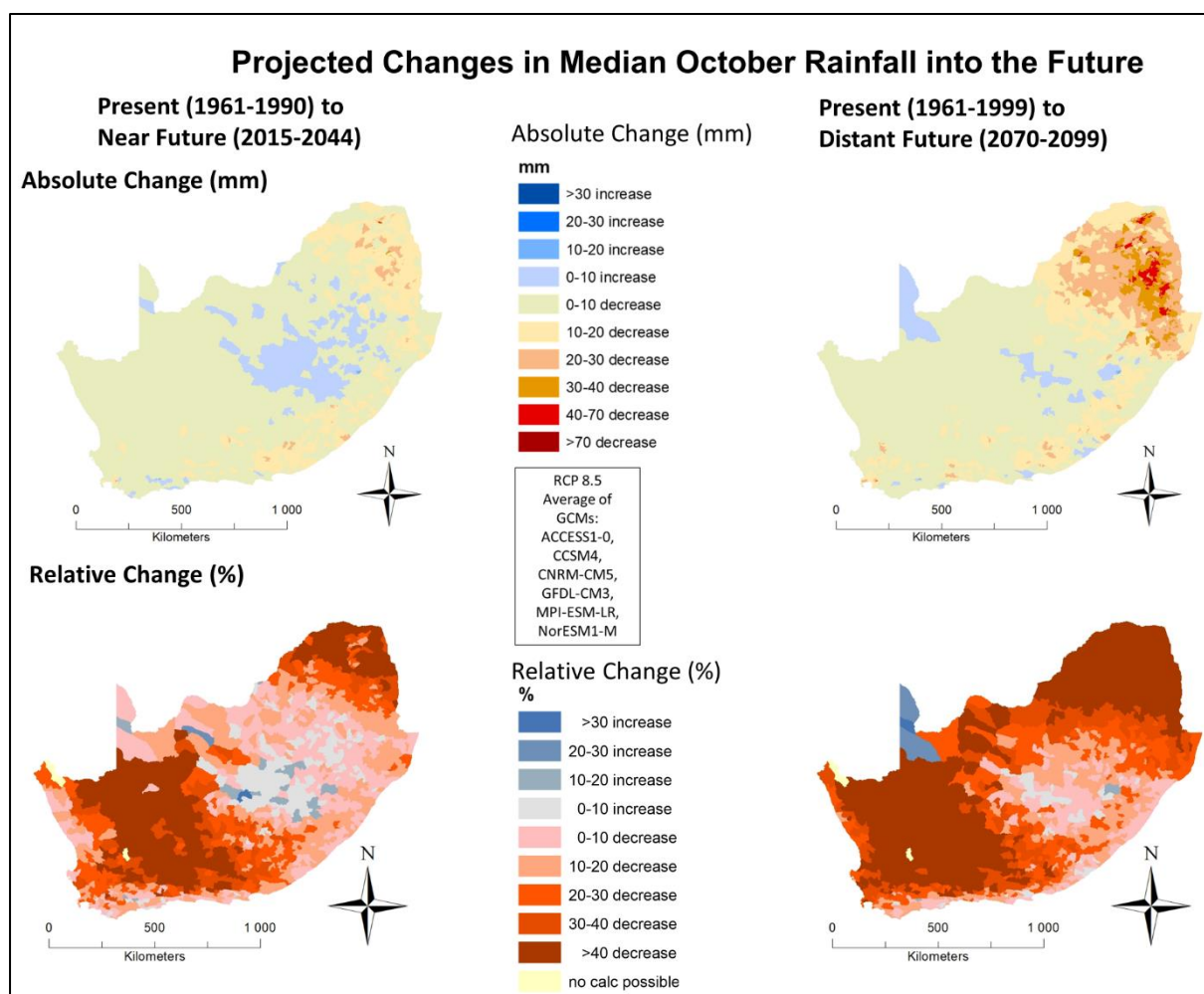
Figure 4.8   Projected change in median October rainfall from the present (1961-1990) to the near future (2015-2044) shown in the left column and from the present to the distant future (2070-2099) in the right column. Absolute change (mm) in the top row and relative change (%) in the bottom row, with relative change not calculated for very small (<10 mm) present rainfall values. Average of GCMs, at Quinary Catchment resolution
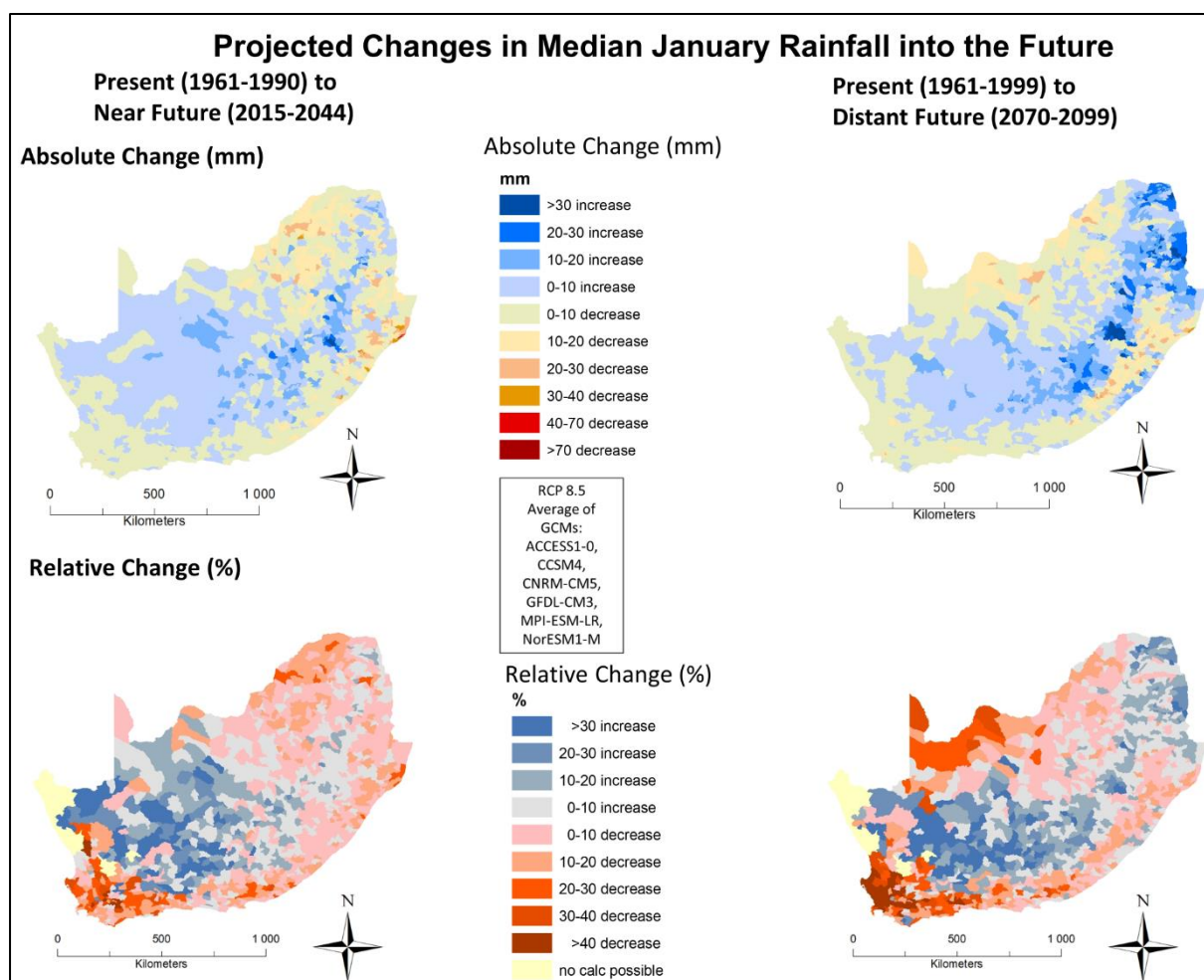
Figure 4.9   Projected change in median January rainfall from the present (1961-1990) to the near future (2015-2044) shown in the left column and from the present to the distant future (2070-2099) in the right column. Absolute change (mm) in the top row and relative change (%) in the bottom row, with relative change not calculated for very small (<10 mm) present rainfall values. Average of GCMs, at Quinary Catchment resolution
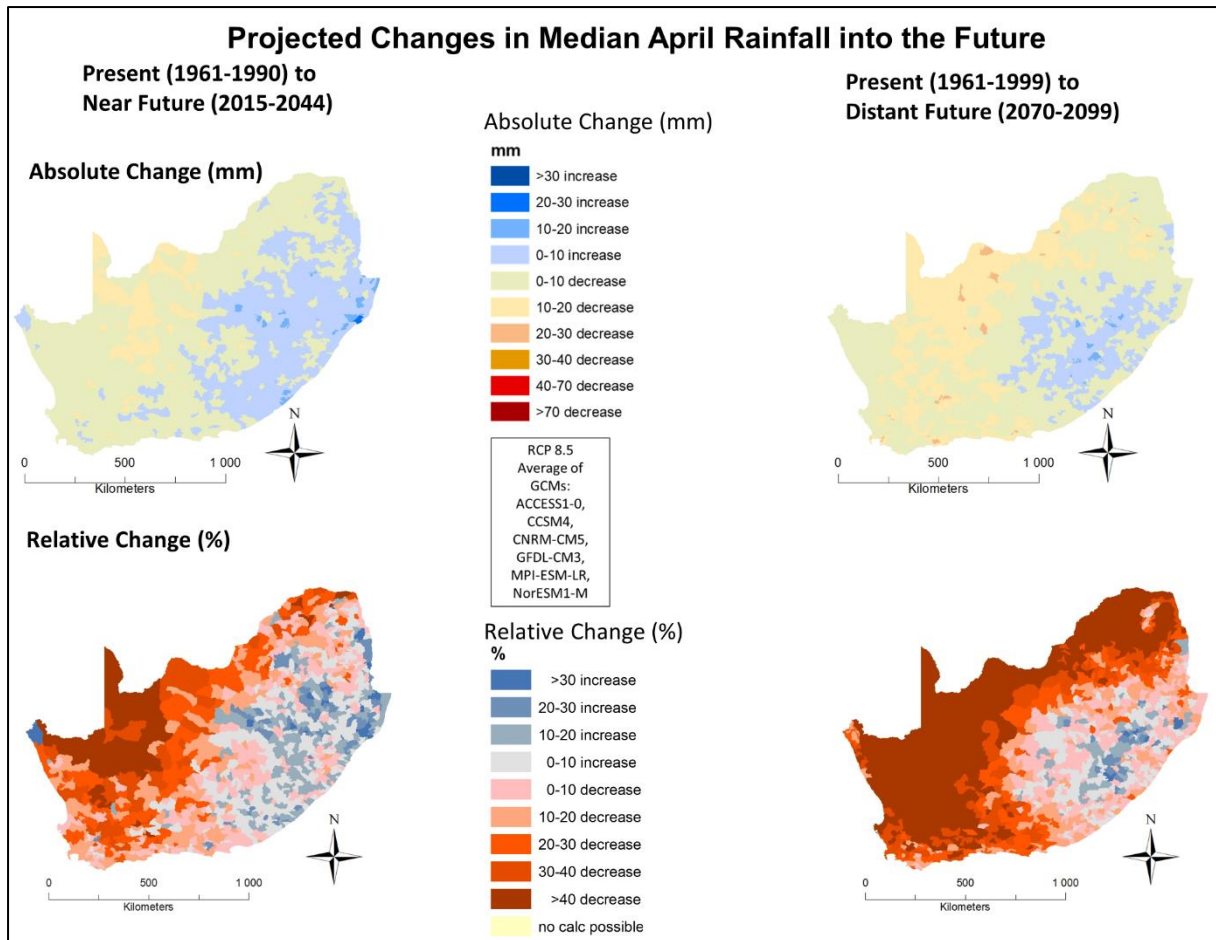
Figure 4.10 Projected change in median April rainfall from the present (1961-1990) to the near future (2015-2044) shown in the left column and from the present to the distant future (2070-2099) in the right column. Absolute change (mm) in the top row and relative change (%) in the bottom row, with relative change not calculated for very small (<10 mm) present rainfall values. Average of GCMs, at Quinary Catchment resolution
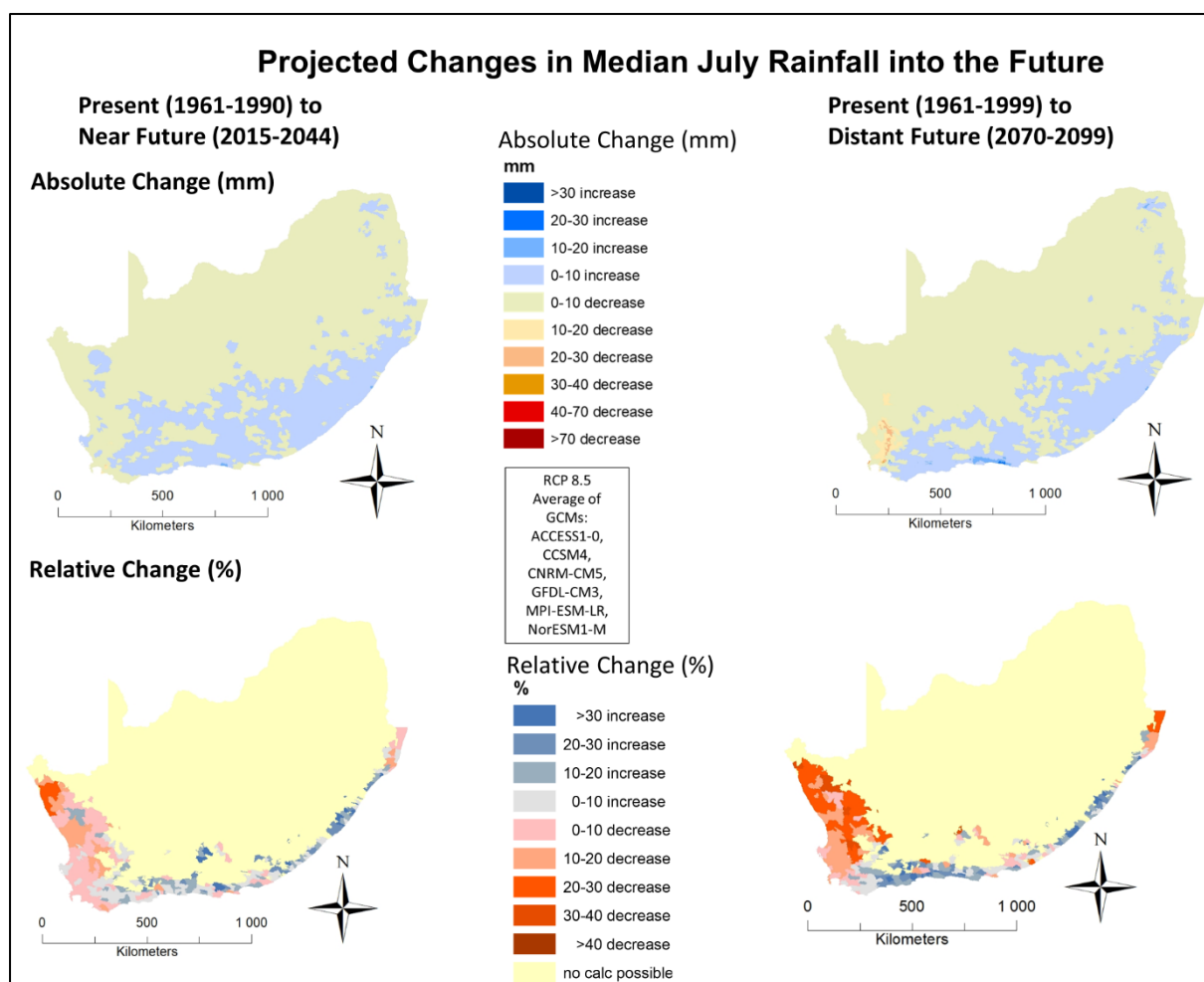
Figure 4.11 Projected change in median July rainfall from the present (1961-1990) to the near future (2015-2044) shown in the left column and from the present to the distant future (2070-2099) in the right column. Absolute change (mm) in the top row and relative change (%) in the bottom row, with relative change not calculated for very small (<10 mm) present rainfall values. Average of GCMs, at Quinary Catchment resolution

Design rainfall events

From Annual to "Extreme" Daily Rainfalls: Background to and Importance of Design Rainfalls
Hydraulic engineering structures and conservation structures such as dams, bridges, culverts and stormwater systems need to be designed to accommodate peak floods of a certain magnitude in order to function safely at a given level of risk. Climate change, by expected alterations to the temperature and rainfall regimes as well as possible increases to rainfall variability, may lead to increases in the intensity and frequency of extreme rainfall events and associated flooding. Consequently, this might have serious repercussions on the design of hydraulic structures. Since the failure of such structures can have potential economic, environmental and societal repercussions, including loss of life, it can be appreciated why flood frequency analysis is of great importance.

With reliable flood estimates from good quality observed streamflow data seldom available at the site of interest, it is common for rainfall-based methods of flood frequency estimations to be used. To derive such "design rainfalls" one needs to know the depth (i.e. magnitude, in mm) of rainfall, for a critical duration (e.g. of long duration such as 1-7 days, which are important for designs on larger catchments, for multiple day flooding and for regional damage assessments), for a desired frequency of recurrence (e.g. statistically once in 10 or 20 or 50 years), depending on the size and economic importance of the structure, and where frequency of recurrence is commonly referred to as the return period (RP), with a RP of, say, 10 years implying a statistical probability of recurrence once in 10 years or 10 times in 100 years.

An estimate of design rainfall can then be used to generate design flood hydrographs when combined with catchment characteristics such as slope, size, land use and soils.

Design Rainfalls under Historical Climatic Conditions
One day design rainfalls under historical climatic conditions are shown in **Figure 4.12** for the 1 in 10 and the 1 in 50-year return periods, with low values in light blue at < 50 mm grading through to darker blues at > 200 mm rainfall per day for the highest values, a marked increase in design rainfall from the 1:10 to the 1:50-year "extreme" daily events and with highest values along the coast. Such extreme daily rainfalls have the potential to do considerable damage, as such, to properties for example, and even more so when converted to extreme runoff.
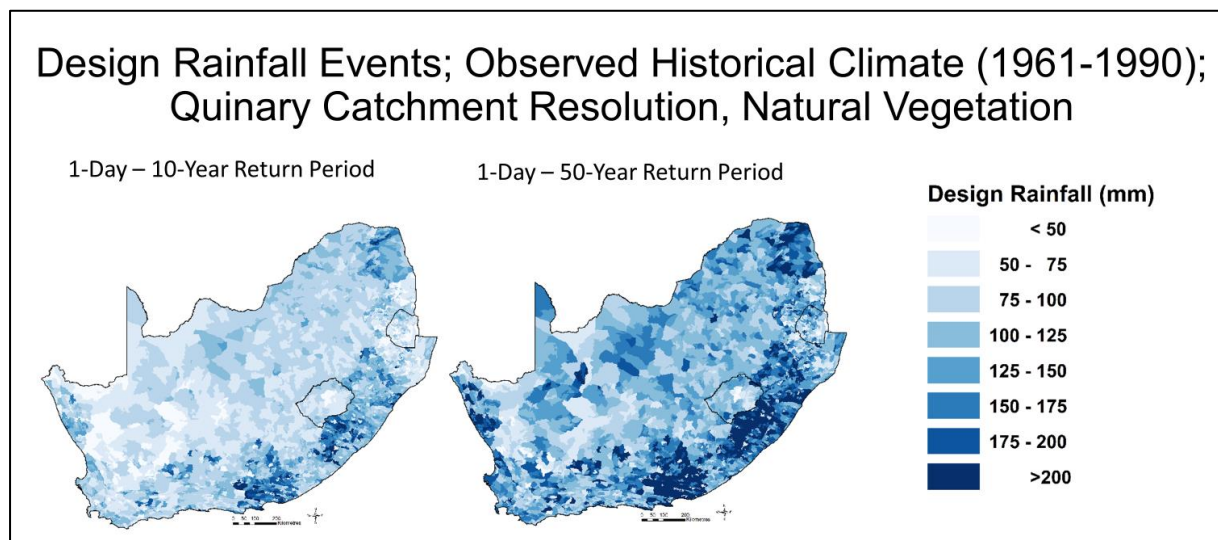
Figure 4.12   Design rainfalls under historical climatic conditions for the 1:10-year return period 1-day rains (left) and the 1:50-year 1-day rains (right)

Projected changes in design rainfall events from the present to the near future are shown in **Figure 4.13** and show increases over most of southern Africa. The increases in general look larger for the rainfall events for 1-day 50-year return period compared to the 1-day 10-year return period.
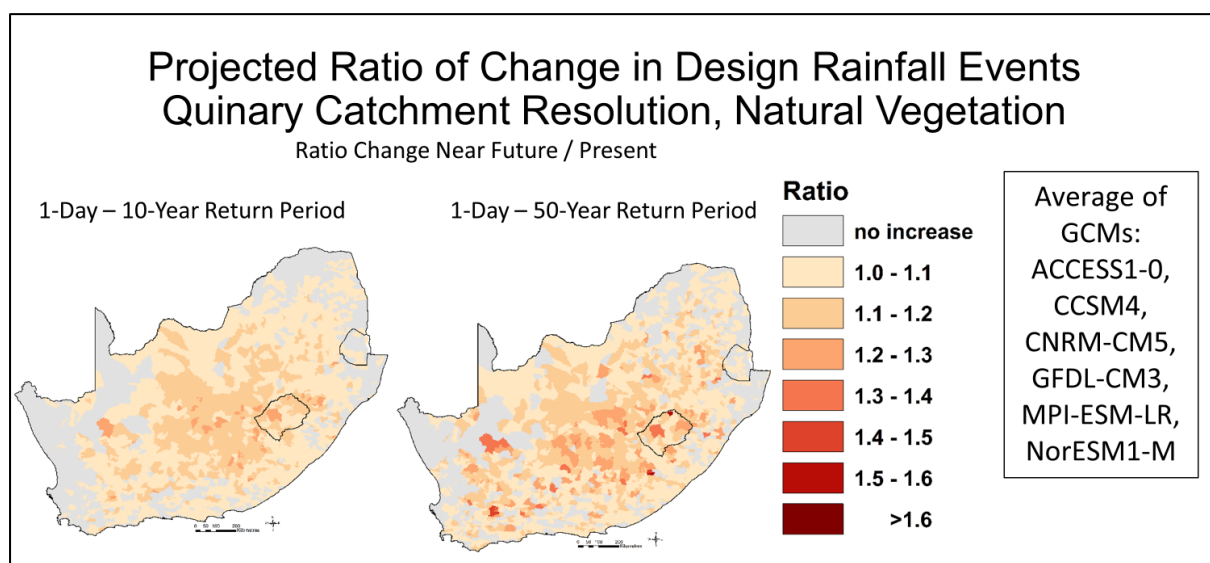
Figure 4.13   Projected changes from the present to the near future in design rainfalls for the 1:10-year return period 1-day rains (left) and the 1:50-year 1-day (right), derived from outputs from multiple GCMs

4.1.2   Temperature

Temperature is a climatological variable used frequently as an index of the energy status of the environment. It is the one climatic variable for which there is a high degree of certainty that it will increase with climate change. Temperature has a direct effect on all forms of life on earth, impacting on a wide range of processes which, in the context of crops and natural vegetation, includes biomass production, areas within which crops can grow optimally or where a given natural vegetation type can occur in regard to temperature thresholds and limits, under both current as well as projected future climates. This affects hydrological responses indirectly. More directly, temperature affects evaporation rates both now and under projected climate change (Schulze and Kunz, 2011).

Of the various statistics of temperature, the annual mean of daily maximum temperatures, as well as annual mean of daily minimum temperatures, represent broad indices of the environmental status of a location. While in themselves these are not particularly useful statistics because they have integrated and smoothed the effects of monthly and seasonal patterns, they are nevertheless commonly used as a descriptor of the climate of a location or region and as a point of departure in climate change studies (Schulze and Kunz, 2011).

Where maps of temperature from GCMs are shown later in this section, these are generated as averages from the six GCMs used in this project. Annual means of daily maximum and minimum temperature statistics are shown in **Figure 4.14** and **Figure 4.15**. This shows temperature from the observed historical data and from the bias corrected GCM generated data for the present period (1961-1990), as well as the correlation between historically observed and GCM generated temperatures for, respectively, maxima and minima. Overall, the correlations match excellently, both spatially and statistically, the north-west and north in general show higher means of daily maximum temperatures compared to further south. The means of daily minimum temperatures are the lowest in the high lying areas of the Drakensberg / Lesotho.
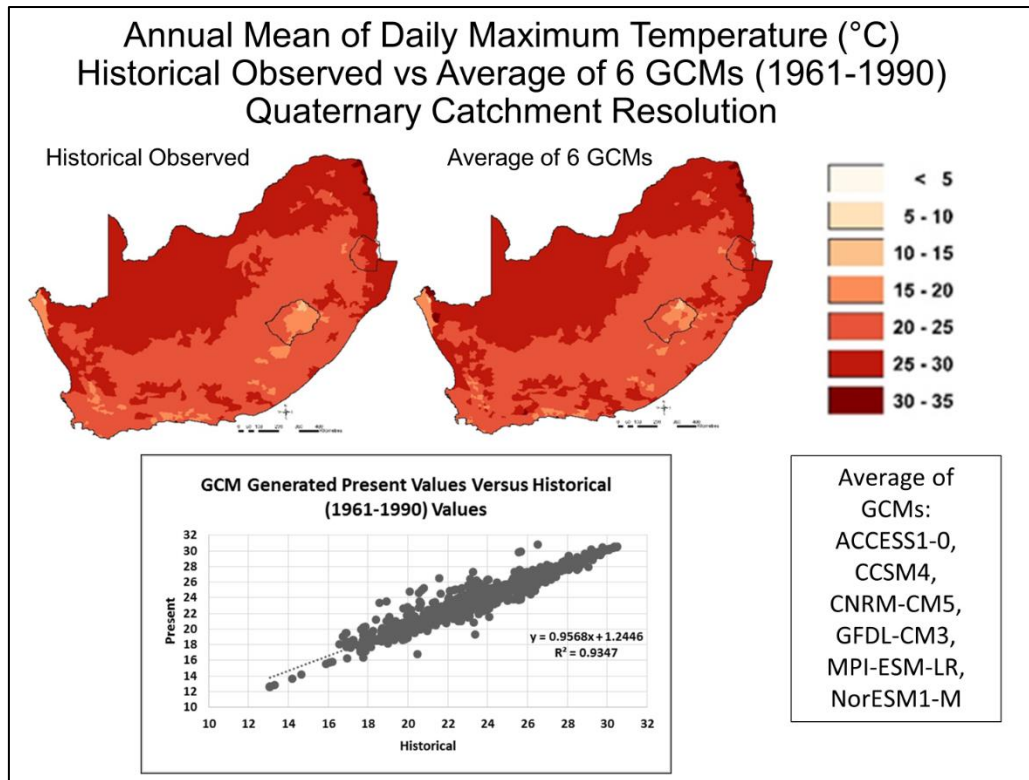
Figure 4.14 Annual means of daily maximum temperature (°C) showing the observed historical pattern [left] and [right] the pattern generated from the average of six GCMs for the period 1961-1990, as well as the correlation between the two, at a Quaternary Catchment resolution
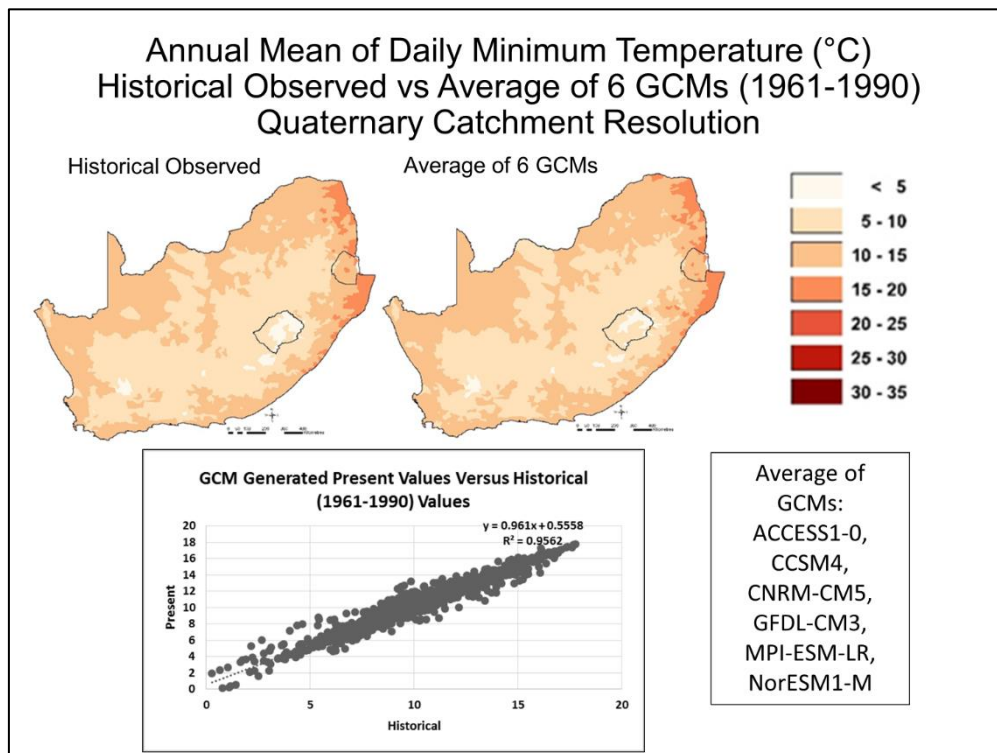
Figure 4.15 Annual means of daily minimum temperature (°C) showing the observed historical [pattern [left] and [right] the pattern generated from the average of six GCMs for the period 1961-1990, as well as the correlation between the two, at a Quaternary Catchment resolution

Projected GCM generated changes show increases throughout South Africa, Lesotho and Eswatini of between 1°C along the coast and 3°C in the north-west from the present to the near future of the 2030s, both for maximum and minimum daily temperatures. From the present to the distant future of the 2070s, projected changes are between 3°C at the coast to more than 6°C in the north-west for daily maximum temperatures, while the minimum temperatures are also projected to increase by between 3°C at the coast and to up to 6°C in the north-west (**Figure 4.16**).
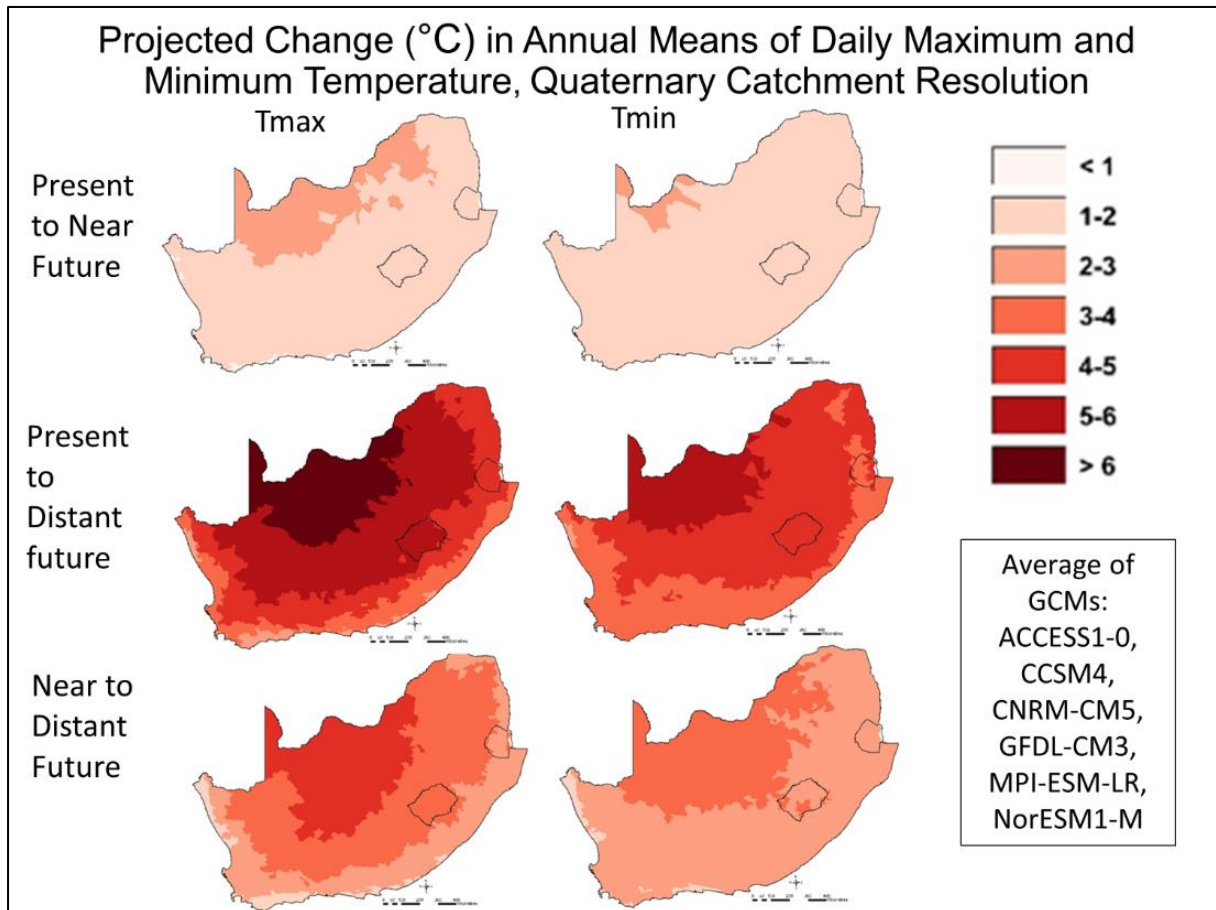
Figure 4.16   Projected changes in GCM generated annual means of daily maximum [left] and minimum [right] temperatures (°C) from the present to near future [top], the present to distant future [middle] and the near to distant future [bottom], at a Quaternary Catchment resolution

4.1.3   Potential evaporation

Potential evaporation (also termed "reference potential evaporation") is the amount of water that is evaporated from wet surfaces from which water is not a limiting factor. The *ACRU* model uses the 'A-Pan' equivalent as reference evaporation. Mean annual potential evaporation from the observed historical time period (1961-1990) is compared to that from the GCM derived values for the same time period, with the latter being the average from multiple GCMs (**Figure 4.17**). The results for the two datasets are similar, with the GCMs thus representing the potential evaporation well. Ratios of changes in GCM generated mean annual potential evaporation (**Figure 4.18**) show small increases by a factor of up to 1.1 (i.e. 10%) over most of the RSA for the near future compared to the present, while larger increases are projected for changes from the present to the distant future, by a factor of between 1.1 and 1.2 along the coast and 1.2-1.3 (i.e. 20-30%) over most of the interior, with some areas showing an even larger factor of increase. Absolute and relative changes for mean annual evaporation (**Figure 4.19**) similarly show increases throughout the area, with a change from the present to near future of less than 100 mm along the coast up to 250 mm in the north, with much larger annual increases from the present to the distant future of over 500 mm.

The statistics of the 1:10-year low, median and the 1:10-year high annual potential evaporation (**Figure 4.20**) show fairly comparable ratio increases when compared to the results for mean annual potential evaporation shown previously (**Figure 4.18**).

The confidence in the results is discussed later, in Section 5.2.11.
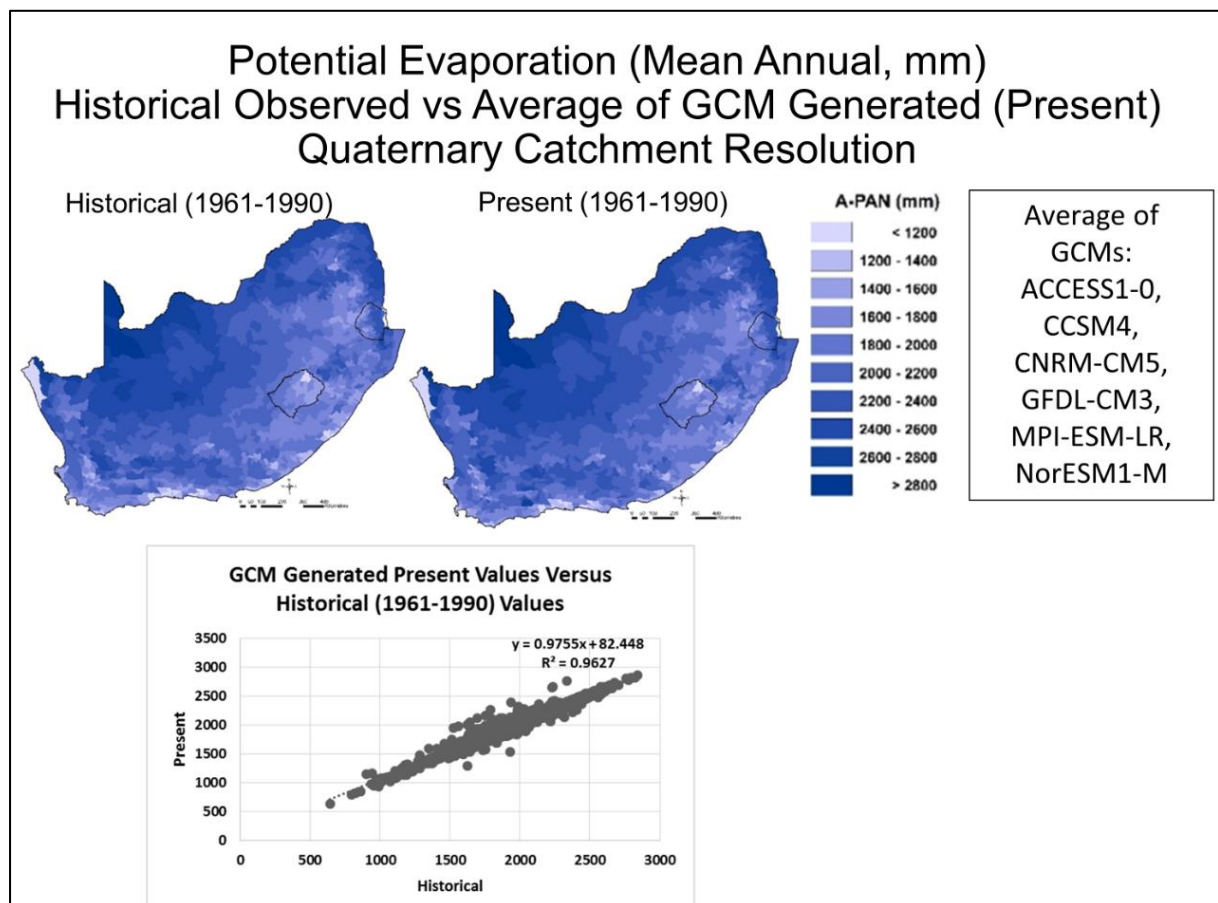
Figure 4.17   Mean annual reference potential evaporation (mm) derived from historical climate data (1961-1990) [left] versus that generated from multiple GCM climate values for the present (1961-1990) [right], as well as the correlation between the two, at Quaternary Catchment resolution
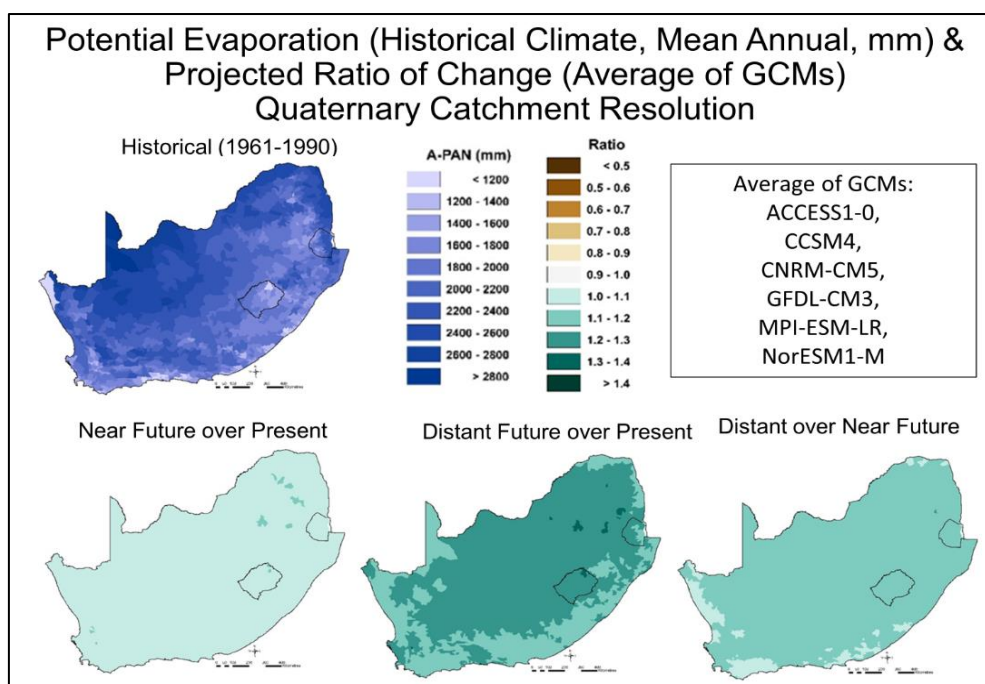
Figure 4.18 Mean annual reference potential evaporation (mm) derived from historical observed climate (1961-1990) [top row left map] versus GCM generated ratios of change for the near future over present (1961-1990) [bottom left], the distant future over present [bottom middle] and distant future over near future [bottom, right map], at Quaternary Catchment resolution
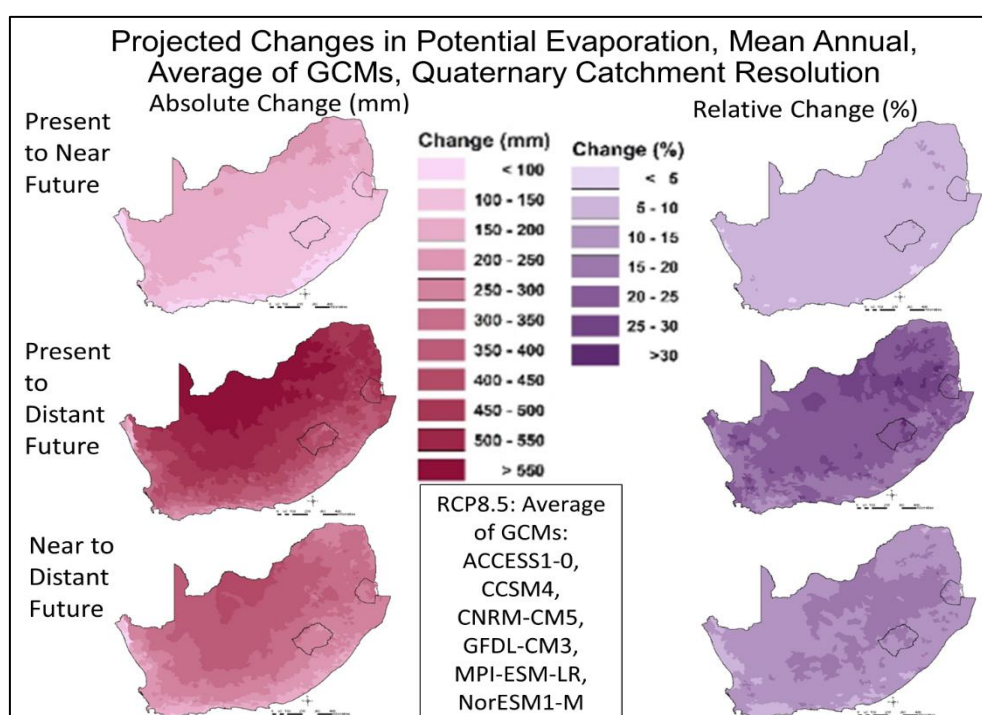
Figure 4.19   Projected changes in mean annual reference potential evaporation in absolute (mm) [left] and relative changes (%) [right] terms, with changes from the present (1961-1990) to the near future (2015-2044) [top row], from the present to the distant future (2070-2099) [middle row] and from the near to the distant future [bottom row], all at Quaternary Catchment resolution
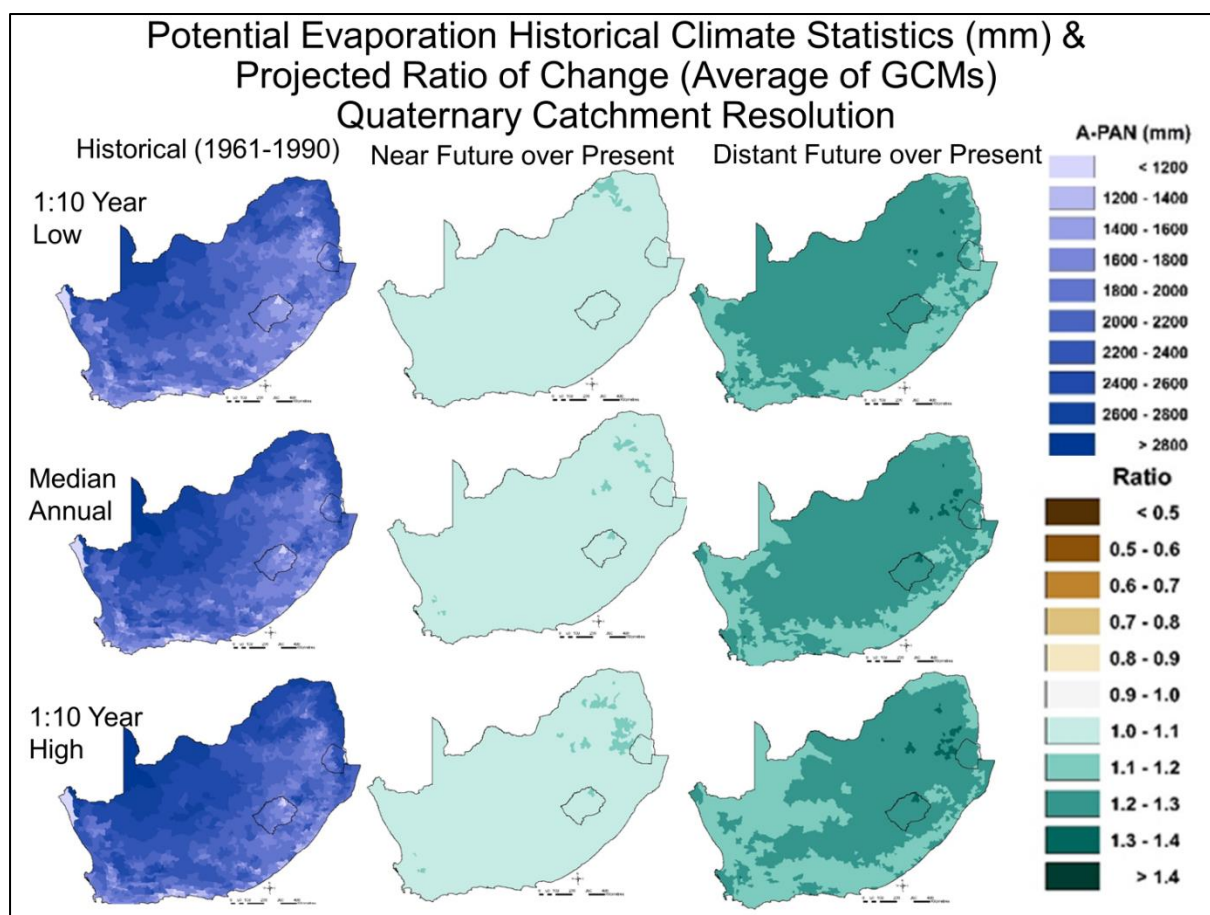
Figure 4.20   Statistics of annual reference potential evaporation for the 1:10-year low [top row], the median annual [middle row] and the 1:10-year high [bottom row] for observed historical climate (1961-1990) [left column] and for projected GCM generated ratio changes showing near future to present [middle column] and distant future to present ratios [right column], all at Quaternary Catchment resolution

4.2   Conclusions from Projected Climate Scenarios under RCP8.5

Based on the approach outlined in applying outputs from 6 GCMs under CMIP5, with the RCP8.5 that were previously regionalised by the CSIR using CCAM, and then further localised and bias corrected, as part of this study, the results are discussed.

Projected mean annual rainfall shows a reduction in the west and north, especially towards the distant future. Along the east coast the changes are mixed. In the eastern interior, in the Drakensberg and eastern interior area more rainfall is projected for the near future and even more for the distant future. October rainfall (representing spring) generally shows small decreases over most of the country with small increases over some areas in the interior, but quite severe decreases are projected over the north-east especially into the distant future. January rainfall (representing summer rainfall) generally shows increases in the interior and decreases in the south and mixed changes along the east coast. April rainfall (representing autumn rainfall) generally shows small to medium decreases in the west and north and small increases in the east. July rainfall (representing winter rainfall) generally show small decrease in the north and the interior, with small increases along the east. The north-east seems to have a decrease in spring rain but an increase in rainfall in summer, thus a shift in the onset of rain later towards summer. Spring rains generally show reductions over nearly all of southern Africa. Projected changes

101

in design rainfall events from the present to the near future show increases over most of southern Africa. The increases in general are larger for the rainfall events for 1-day 50-year return period compared to the 1-day 10-year return period.

Projections for temperature show increases throughout southern Africa of between 1°C along the coast and 3°C in the north-west from the present to the near future, both for maximum and minimum daily temperatures. From the present to the distant future, projected changes are between 3° at the coast to more than 6°C in the north-west for daily maximum temperatures, while the minimum temperatures are also projected to increase by between 3° at the coast and to up to 6°C in the north-west.

Projections for potential evaporation show increases throughout and larger increases towards the distant future, especially in the north-west, the north and the interior. The east coast in general shows a smaller increase in potential evaporation.

Projected temperature changes alone are showing a bleak picture for the future climate in southern Africa. Therefore, greenhouse gas emissions globally need to be reduced, to ensure this is not the future that we leave behind for future generations. Climate change mitigation thus needs to be given high priority, globally as well as in South Africa.

5 PROJECTED HYDROLOGICAL RESPONSES TO CLIMATE CHANGE

S. Schütte, R.E. Schulze, D.J. Clark and R.P. Kunz

This section addresses Aim 3, "Assess the hydrological response to those climate impacts".

5.1 Introduction

Hydrological responses to projected climate change, based on the RCP8.5 emission scenario, were modelled using the *ACRU* model. The climate projections were previously described in Chapter 2. The six GCMs used in this study are abbreviated here as ACCESS1-0, CCSM4, CNRM-CM5, GFDL-CM3, MPI-ESM-LR and NorESM1-M. The analysis of climatic variables of temperature, rainfall and potential evaporation and their projected changes under climate change were described in Chapter 4.

The spatial resolution is based on Quinary level altitudinal response zones within Quaternary Catchments, i.e. by South Africa, Lesotho and Eswatini having been delineated into 5 838 relatively homogeneous hydrological response units (Schulze and Horan, 2010). To derive the Altitudinal Quinaries, each Quaternary Catchment was sub-delineated into three altitudinally relatively homogenous zones to better represent more local homogeneity in regard to temperature and rainfall, and hence runoff, within Quaternary Catchments which are often hydrologically relatively heterogeneous. This has previously been described in Section 2.2.

Simulations were run for land cover inputs for both, natural vegetation as well as for actual land cover. The *ACRU* model configured with land cover representing natural vegetation was made up of CWRR Clusters (Toucher et al., 2019) that were recently developed (see Section 3.3). Actual land cover were as of 2018 (NLC2018; DEA and GTI, 2019) and the configuration has been previously described in Section 3.4. Not included in the model setup were water abstractions for, e.g. irrigation or urban land uses, inter-basin transfers, return flows or dams.

A statistical analysis of mean annual, 1:10-year low, median year, and 1:1-year high for various *ACRU* outputs was undertaken for the different climatic, time period and land cover scenarios. While most of the analysis and some of the mapping of results was undertaken at Quinary Catchment resolution, other mapping was at Quaternary Catchment resolution. The Quaternary results were calculated by area weighting the Quinary results, while for accumulated streamflow the outflow of the lower altitude Quinary Catchment was used.

The results of projected climate change impacts on the hydrological responses are presented first for the natural land cover simulations, followed by selected hydrological responses under the actual land cover scenarios. The hydrological responses presented here are actual evapotranspiration, individual catchment runoff, streamflow (depth and volume), soil water content, soil water drainage to the groundwater zone, baseflow. This is followed by a section on confidence in the results and then design streamflow events. Then selected hydrological responses under actual land cover are presented, namely individual catchment runoff, streamflow and baseflow. This is followed by a discussion and recommendations.

While only selected results can be presented in this report, a part of this project is the development of a software utility (Appendix C), which should give the user the possibility to interrogate most variables of their interest, for different areas, climate scenarios, time periods and land cover scenarios, either at Quinary or Quaternary Catchment resolution.

5.2 Results

The results of climate change impacts on various hydrological responses are presented in this section. This includes actual evapotranspiration, individual catchment runoff, streamflow (in mm and as volume), soil water content, soil water drainage to the groundwater zone, baseflows. The results presented are for natural vegetation, actual land cover, or both. Also included in this section is an evaluation into the confidence in the result, as well as design streamflow events.

5.2.1   Actual evapotranspiration

Actual evapotranspiration is made up of plant transpiration and evaporation from soil surface, but for the purpose of this report does not include rainfall intercepted by vegetation. It is a water-limited process with values usually much lower than those of potential evaporation. The actual evapotranspiration values reported here were simulated using the *ACRU* model. The results shown in this section assume that the land cover is natural vegetation, as per the CWRR Clusters (Toucher et al., 2019).

The comparison of mean annual evapotranspiration modelled using observed historical climate inputs to the *ACRU* model with that using GCM generated climate inputs (**Figure 5.1**) presents a similar picture for both scenarios. Evapotranspiration is much higher in the wetter east and lower in the drier west of the region.
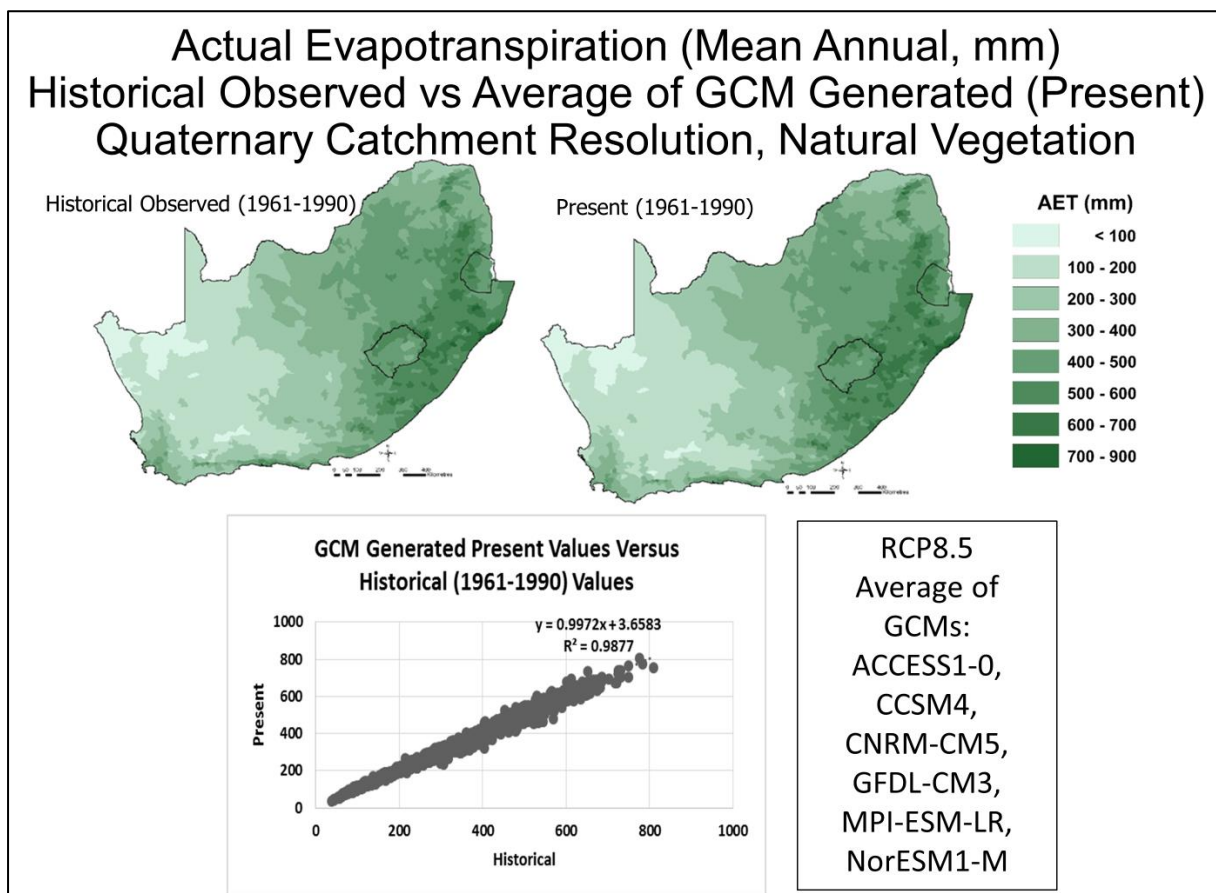
Figure 5.1   Mean annual actual evapotranspiration (mm) using historical [left] versus GCM generated climates for the present time period (1961-1990) [right], as well as the correlation between the two, at Quaternary Catchment resolution

The actual evapotranspiration statistics for historical observed climate inputs show overall values are lower for 1:10-year low and higher for a 1:10-year high (**Figure 5.2**).
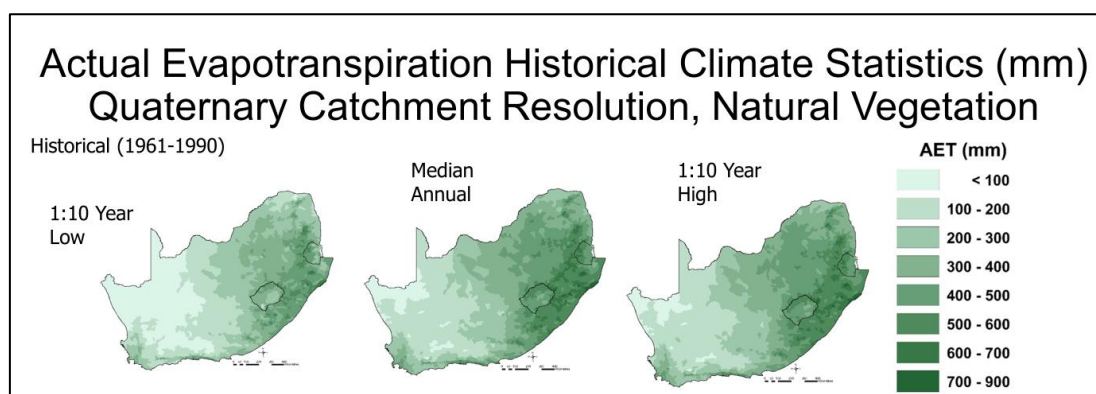
Figure 5.2   Annual actual evapotranspiration (mm) statistics for 1:10-year low [left], median [middle] and 1:10-year high [right] situations, using historical observed climates for 1961-1990, all at Quaternary Catchments resolution

Projected changes in actual evapotranspiration into the future for absolute and relative changes at Quaternary Catchment resolution (**Figure 5.3**) show milder changes into the near future and more extreme changes into the distant future. The west and north of the region have projected reductions in evapotranspiration while the interior shows little to no changes, but the Drakensberg area shows increases in evapotranspiration. The east coast yields mixed results.
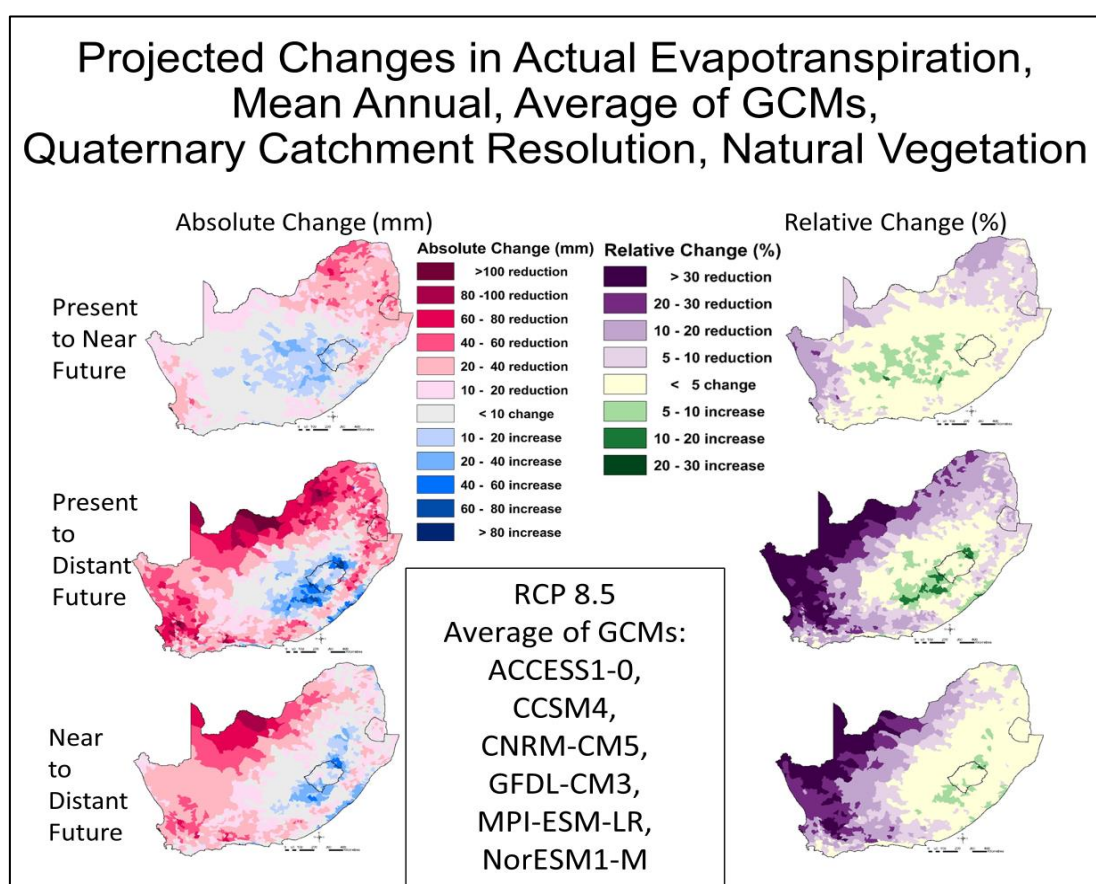
Figure 5.3   Projected absolute changes (mm) [left column] and relative changes (%) [right column] in mean annual actual evapotranspiration, from the present (1961-1990) to the near future (2015-2044) [top left], from the present to the distant future (2070-2099) [top right] and from the near to the distant future periods [bottom], all at Quaternary Catchment resolution

In relative terms, the changes into the future are more pronounced for the 1:10-year low case (**Figure 5.4**), but in absolute terms more pronounced for a 1:10-year high situation (**Figure 5.5**).
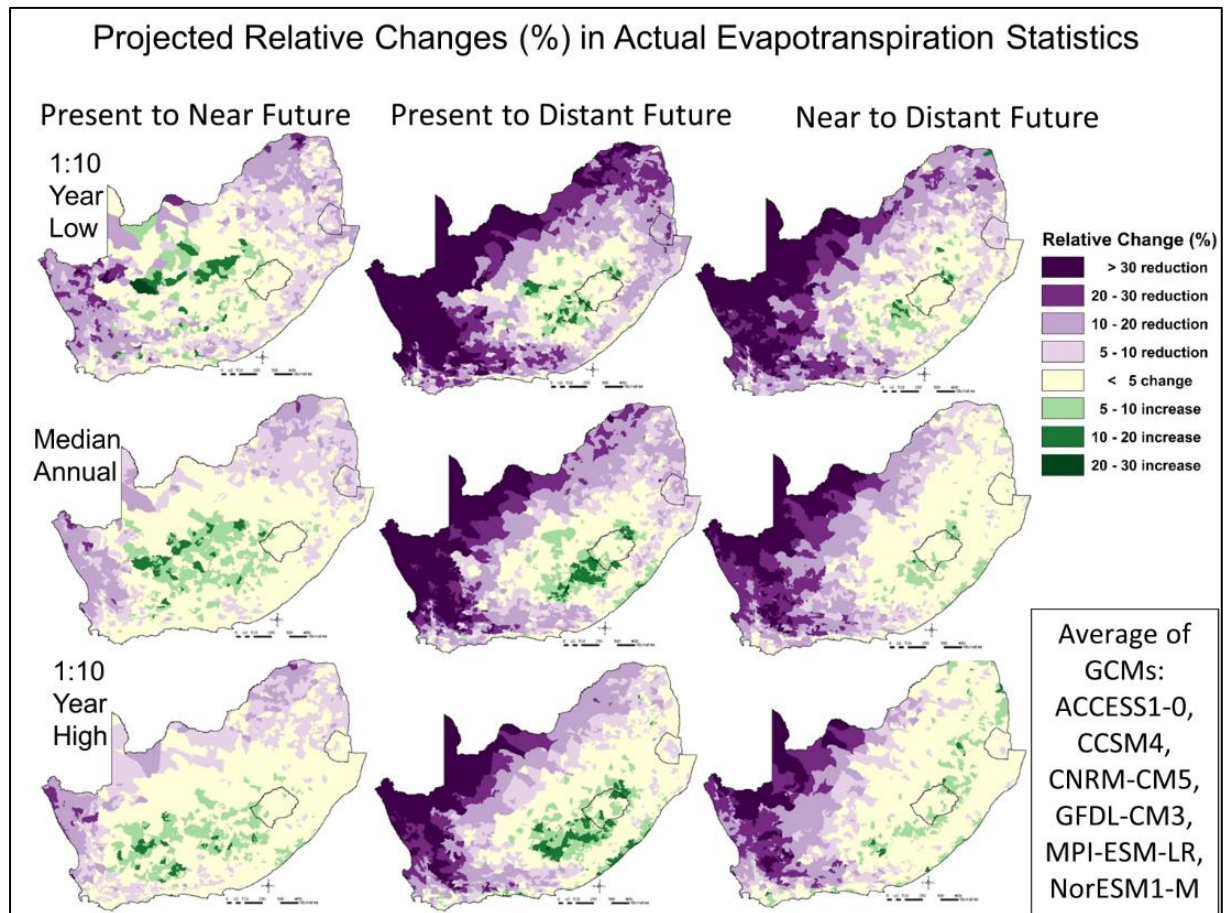
Figure 5.4   Projected relative changes (%) in annual actual evapotranspiration for a 1:10-year low [top row], a median [middle row] and a 1:10-year high [bottom row], from the present (1961-1990) to the near future (2015-2044) [left column], from the present to the distant future (2070-2099) [middle column] and the from near to the distant future [right column], natural vegetation, at Quinary Catchment Resolution
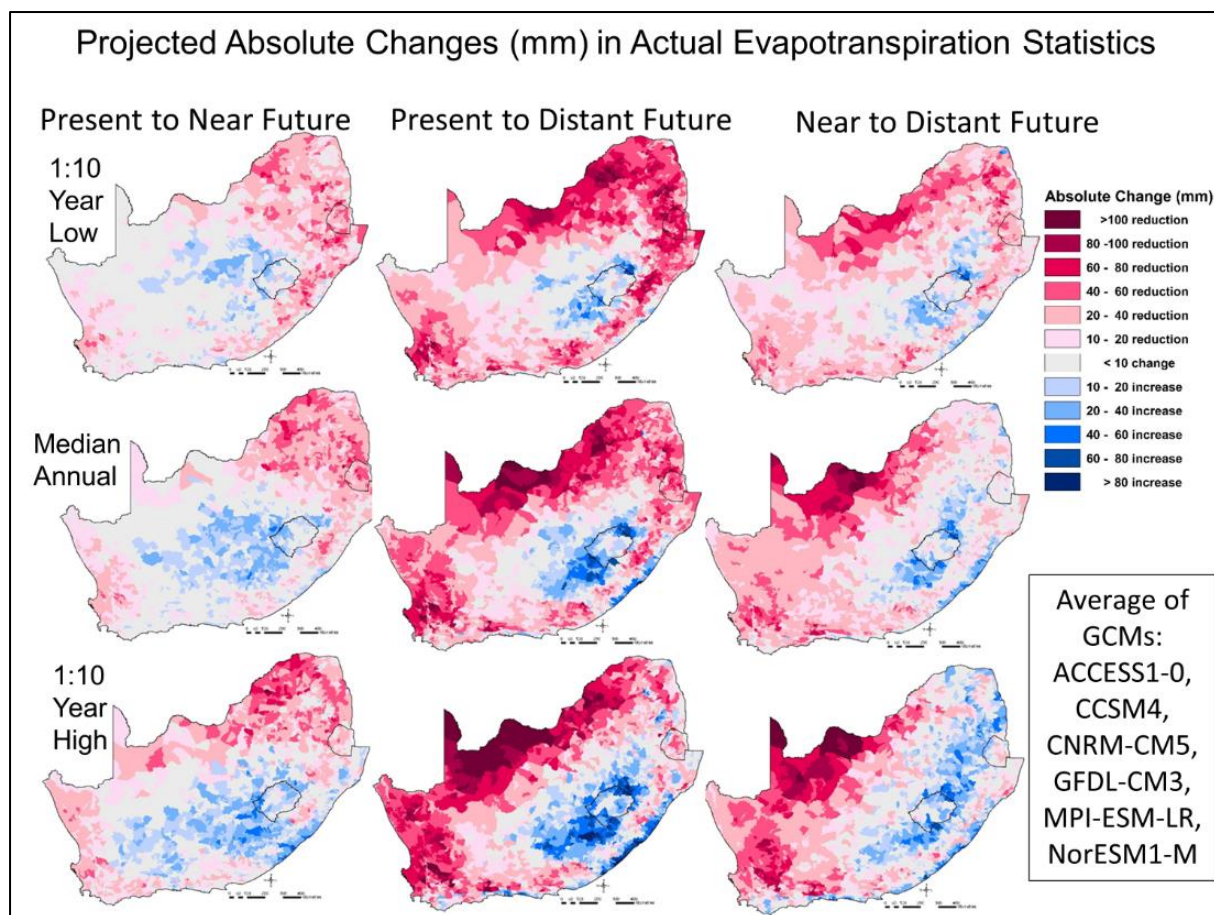
Figure 5.5   Projected absolute changes (mm) in annual actual evapotranspiration for the 1:10-year low [top row], the median [middle row] and the 1:10-year high [bottom row] case, from the present (1961-1990) to the near future (2015-2044) [left column], from the present to the distant future (2070-2099) [middle column] and from the near to distant future periods (right column), all at Quinary Catchment resolution

5.2.2   Individual catchment runoff

Runoff is defined here as the channelled water from an individual Quinary or Quaternary Catchment. The *ACRU* model output variable name is SIMSQ, and is made up of on/near surface stormflow and subsurface generated baseflow.

Individual catchment runoff under natural vegetation

The results under assumed natural vegetation (cv. Section 3.3) is shown first. A comparison of mean annual individual Quaternary Catchment runoff simulated using observed historical climate with that derived from multiple GCM generated climate inputs (**Figure 5.6**) displays similarities for both scenarios, with the GCM results possibly showing less runoff in the interior. Catchment runoff is much higher in the wetter east and lower in the drier north-west of the region.
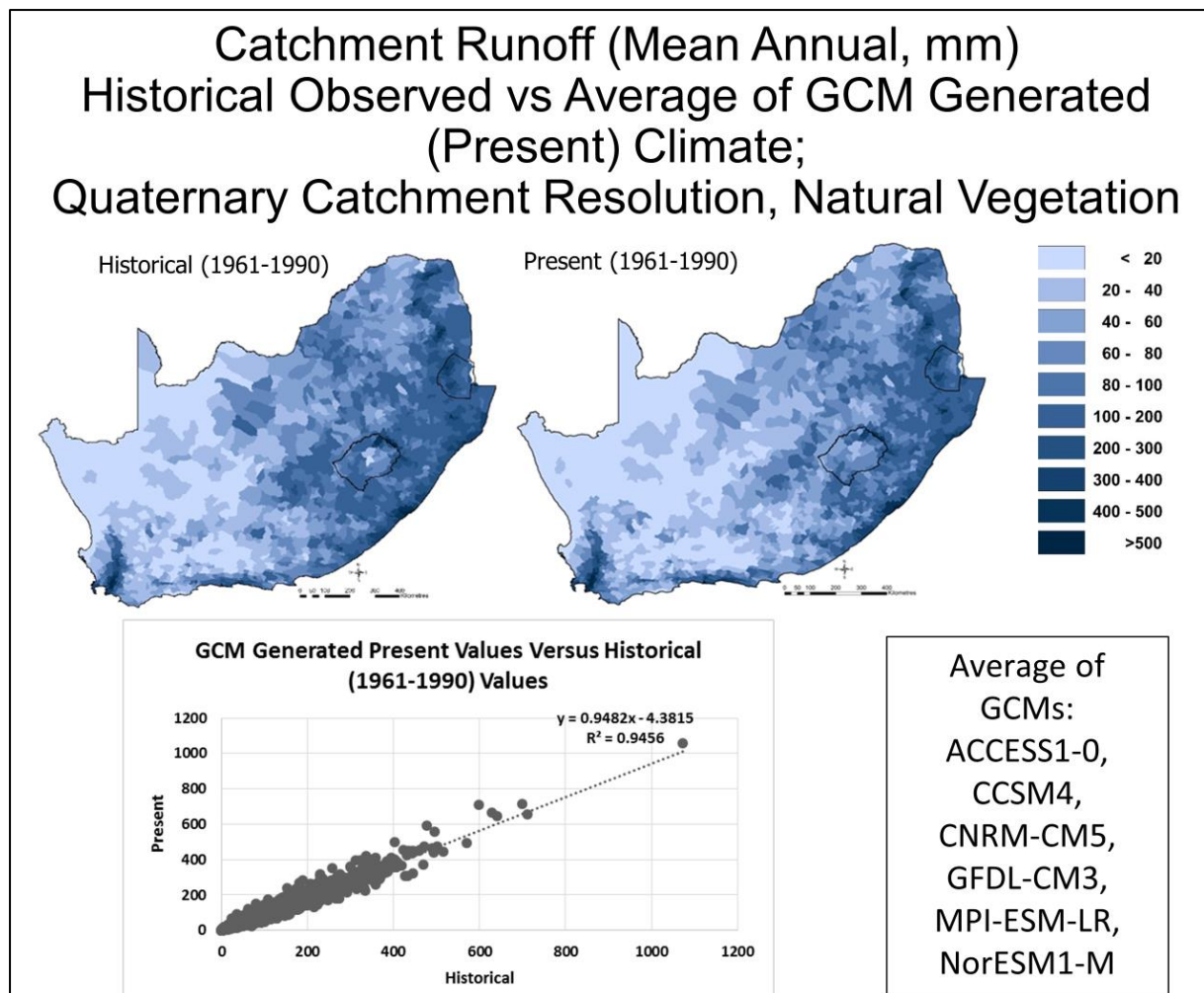
Figure 5.6   Mean annual catchment runoff (mm) derived from historical observed [left] versus GCM generated [right] climates for 1961-1990, as well as the correlation between the two, at Quaternary Catchment resolution

The same holds true for the statistics when comparing runoff derived from historical with that derived from GCM generated climate input, with overall lower results for 1:10-year low and higher results for a 1:10-year high flows. The GCM results again show slightly less runoff for a 1:10 high year compared to that generated with historical climate inputs (**Figure 5.7**).
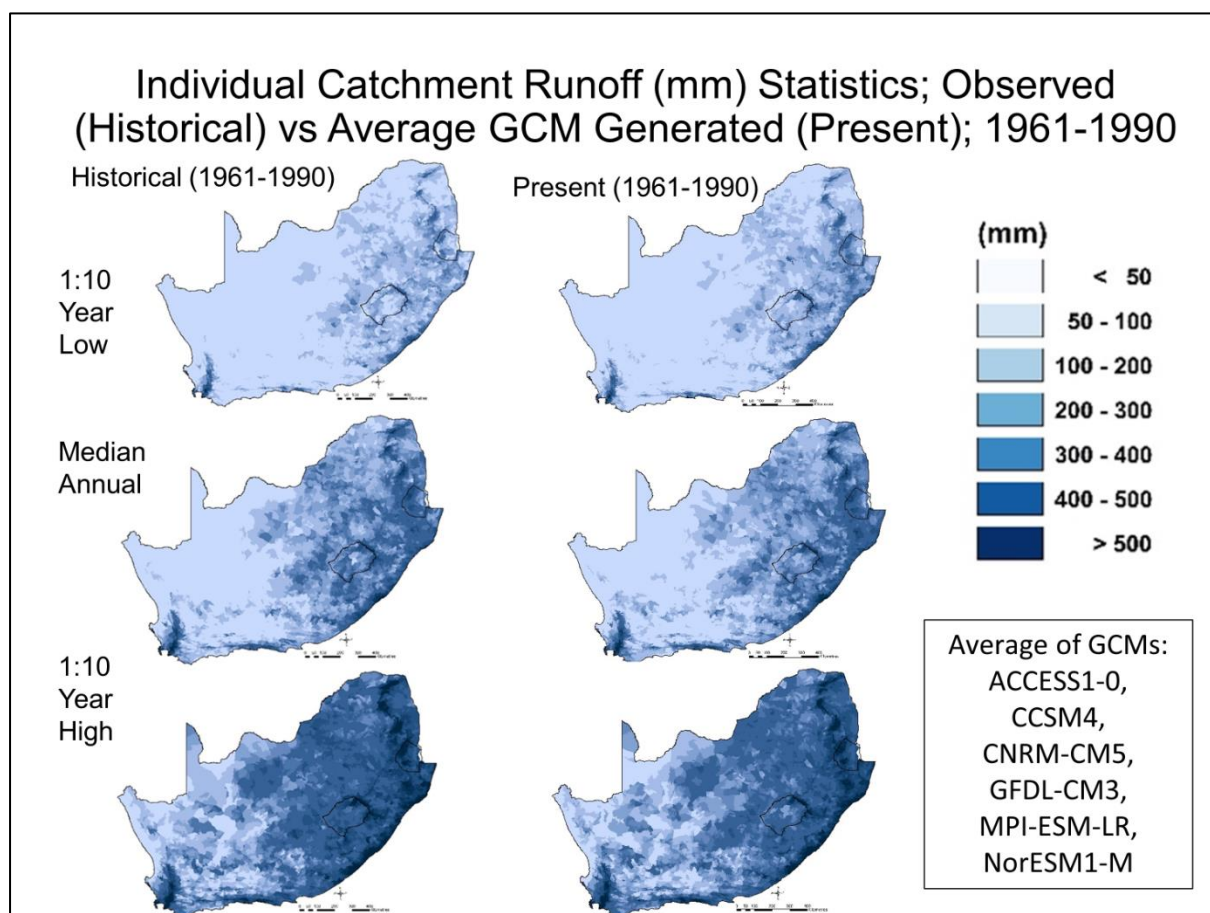
Figure 5.7   Annual Quinary Catchment runoff (mm) statistics for 1:10-year lows [top row], median years [middle row] and 1:10-year highs [bottom row], derived from historical (1950-1999) [left column] versus multiple GCM generated climates for the present period (1961-1990) [right column]

Projected GCM derived Catchment runoff from the present and into the future is shown in **Figure 5.8**. It is however not easy to detect changes in these maps. Therefore change maps are presented next.
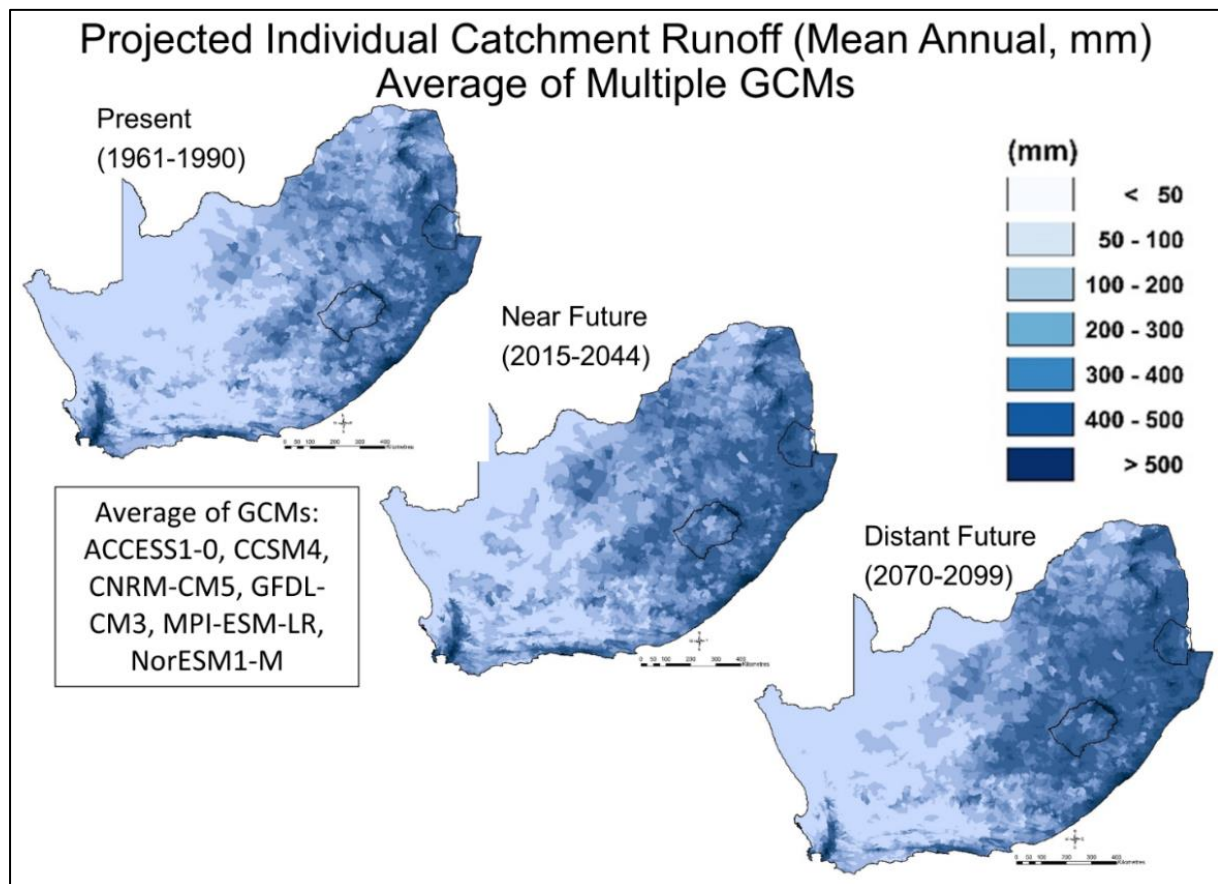
Figure 5.8   Projected mean annual Quinary Catchment runoff averaged from multiple GCM generated runoff for the present (1961-1990) [left], the near future (2015-2044) [middle] and the distant future (2070-2099) [right] periods

Ratios of change (**Figure 5.9**) generally show a decrease in the west and an increase in the eastern interior.
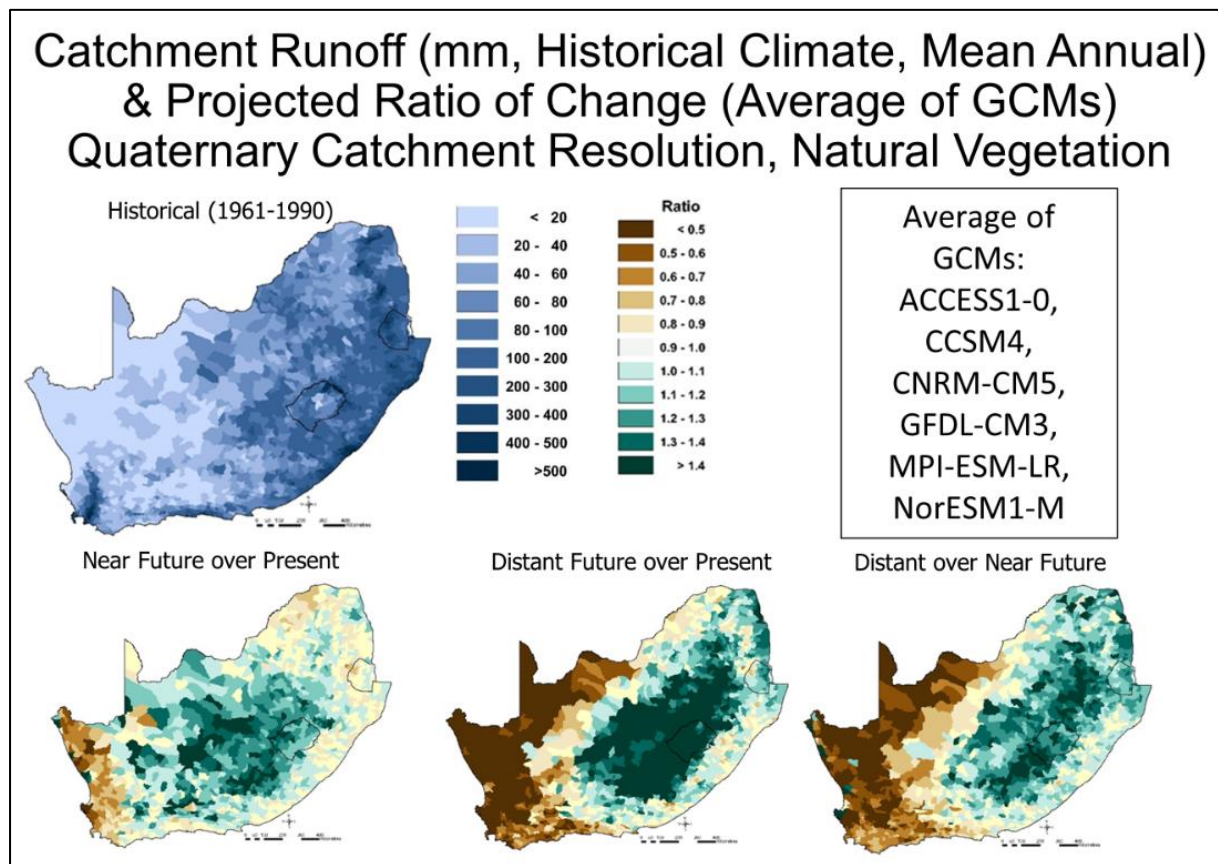
Figure 5.9   Mean annual Quaternary Catchment runoff derived from historical climate (top), and ratios of projected changes of GCM generated runoff for the near future (2015-2044) over present (1961-1990) [bottom left map], the distant future (2070-2099) over present [bottom middle map] and the distant over the near future [bottom right map]

Relative changes (in %) and absolute changes (in mm), for mean annual runoff at Quaternary Catchment resolution (**Figure 5.10**) and ratio changes for 1:10-year low, median annual and 1:10-year high flows (**Figure 5.11**) show differences in magnitude and direction over South Africa, with smaller changes for the near future and more extreme changes for the distant future being projected. For the west, a relative reduction in runoff is projected, with this being especially severe for the distant future, and more so for a 1:10-year low. However, in absolute terms the changes are small, because the area experiences very low catchment runoff and the changes are thus calculated off a low base. However, the area around Cape Town shows both sizeable relative and absolute reductions in annual runoff. The interior and (to a lesser extent) the north-east are projected to receive relatively more runoff compared to present conditions, especially for the distant future, which also translates into more runoff in absolute terms. The east coast generally shows no marked relative changes, with a few patches of small changes in either direction, translating in absolute terms to either quite insignificant to significant local changes in either direction.
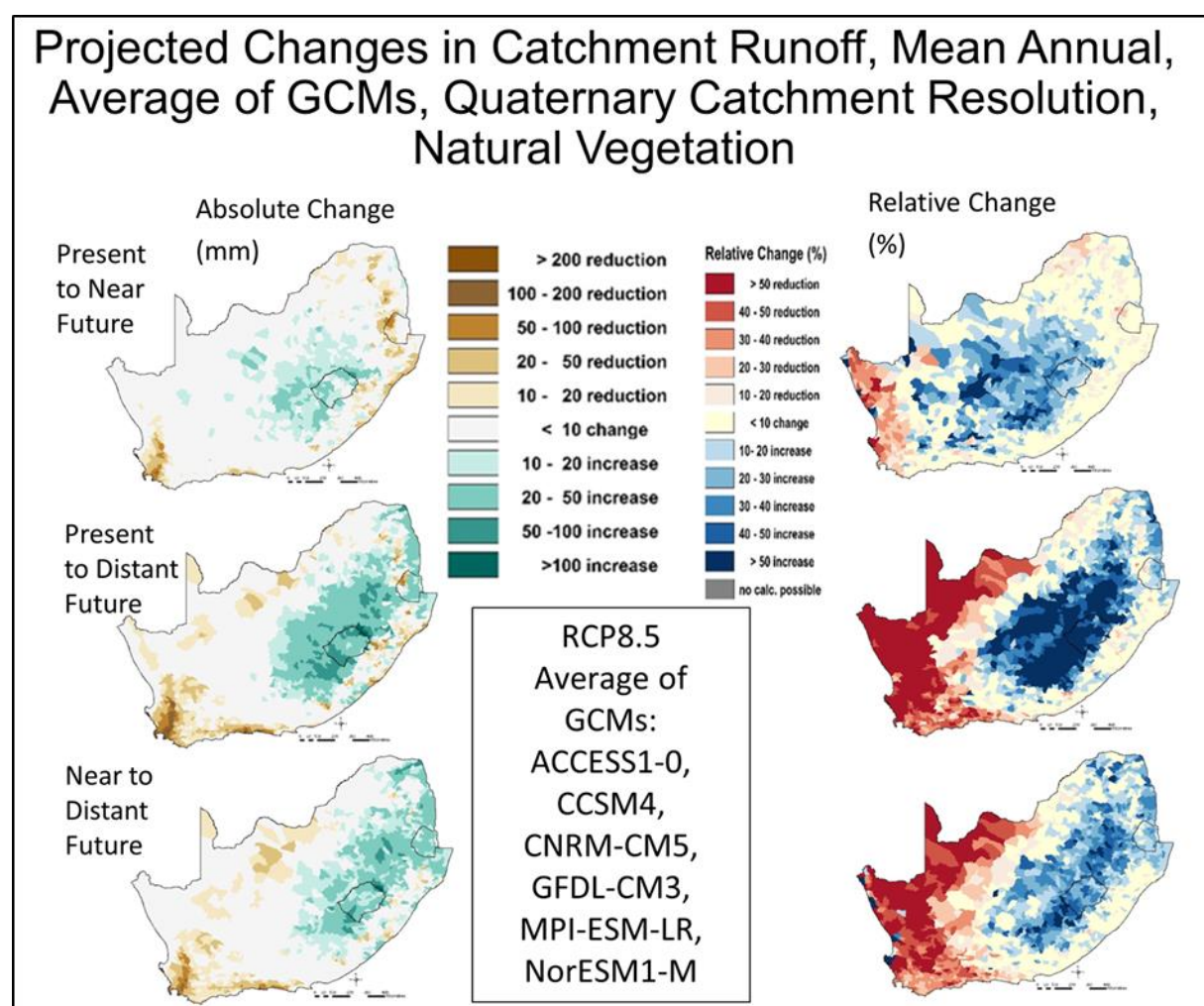
Figure 5.10 Projected absolute (mm) [left] and relative (%) [right] changes in mean annual individual Catchment runoff, from the present (1961-1990) to the near future (2015-2044) [top row], from the present to the distant future (2070-2099) [middle row] and from the near to the distant future [bottom row]
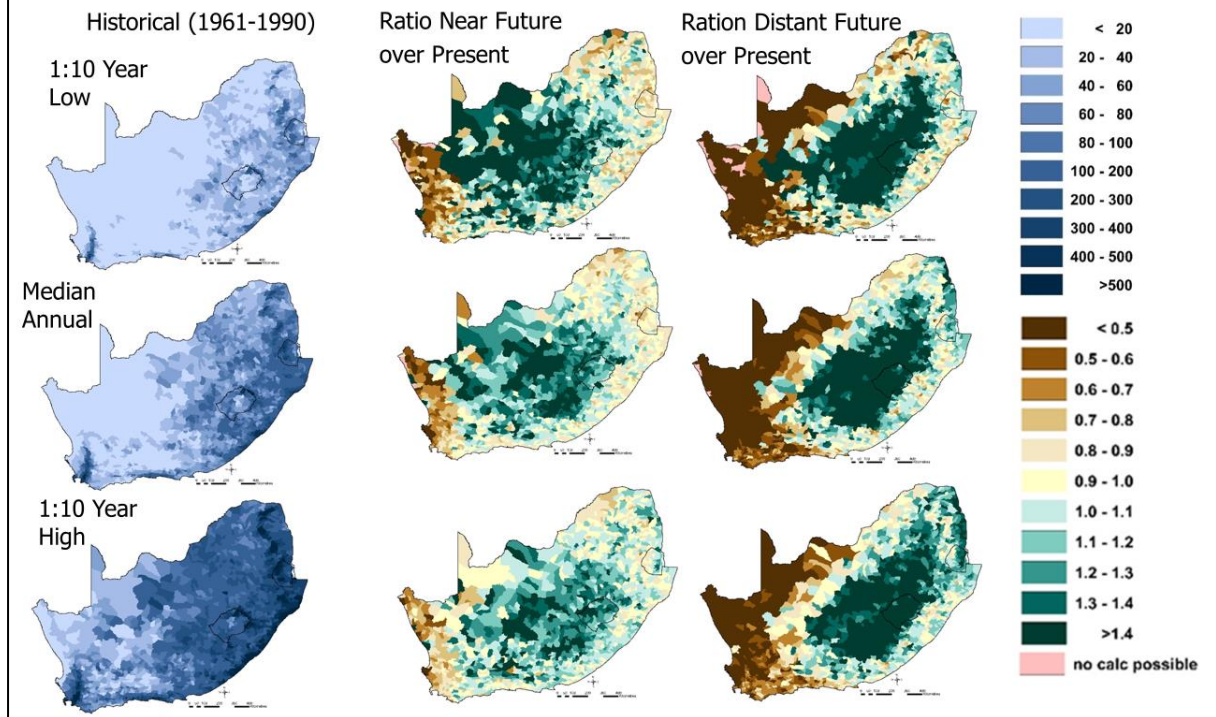
Figure 5.11 Runoff statistics of 1:10-year low [top row], median [middle row] and 1:10-year high [bottom row] annual flows under historical climatic conditions [left column] and ratios of projected changes of multiple GCM generated runoff for the near future (2015-2044) to the present (1961-1990) [middle column] and the distant future (2070-2099) to the present [right column], at Quaternary Catchment resolution

Individual catchment runoff under actual land cover

The results under assumed actual land cover as of 2018 (cv. Section 3.4) is shown next. Mean annual individual Quaternary Catchment runoff simulated using observed historical climate shows that catchment runoff is much higher in the wetter east and lower in the drier north-west of the region (**Figure 5.12**, top).

Ratios of change (**Figure 5.12**, bottom) from the present (1961-1990) to the near future (2015-2044) generally show a decrease in mean annual runoff in the west and an increase in the eastern interior, with higher magnitude into the distant future.
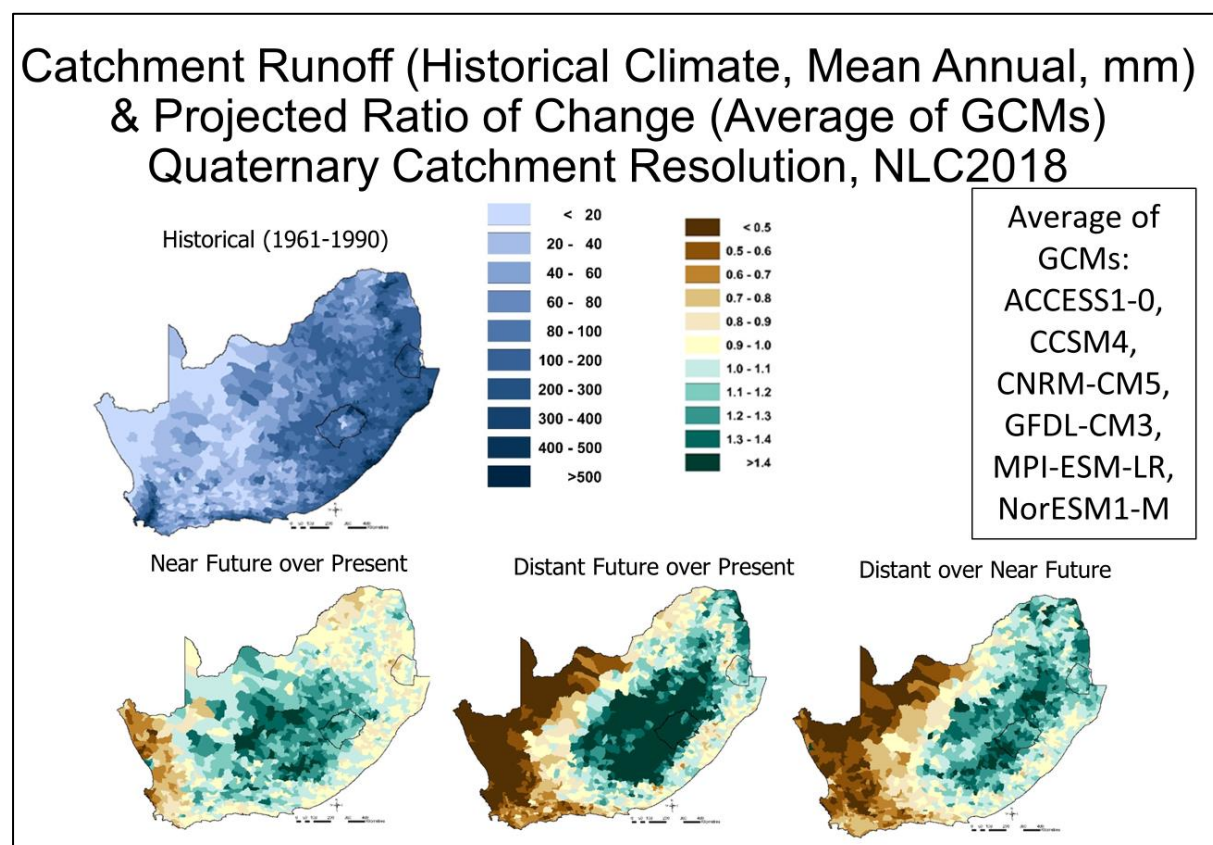
Figure 5.12   Mean annual catchment runoff under historical climate and ratios of projected change of GCM generated runoff for the near future (2015-2044) over present (1961-1990) [bottom left], distant future (2070-2099) over present [bottom middle] and distant over near future [bottom right] at Quaternary Catchment resolution under land cover of NLC2018

A decrease in mean annual runoff in the west and an increase in the eastern interior, with higher magnitude into the distant future is also shown when expressed as absolute changes (mm) and relative changes (%), shown in **Figure 5.13**.
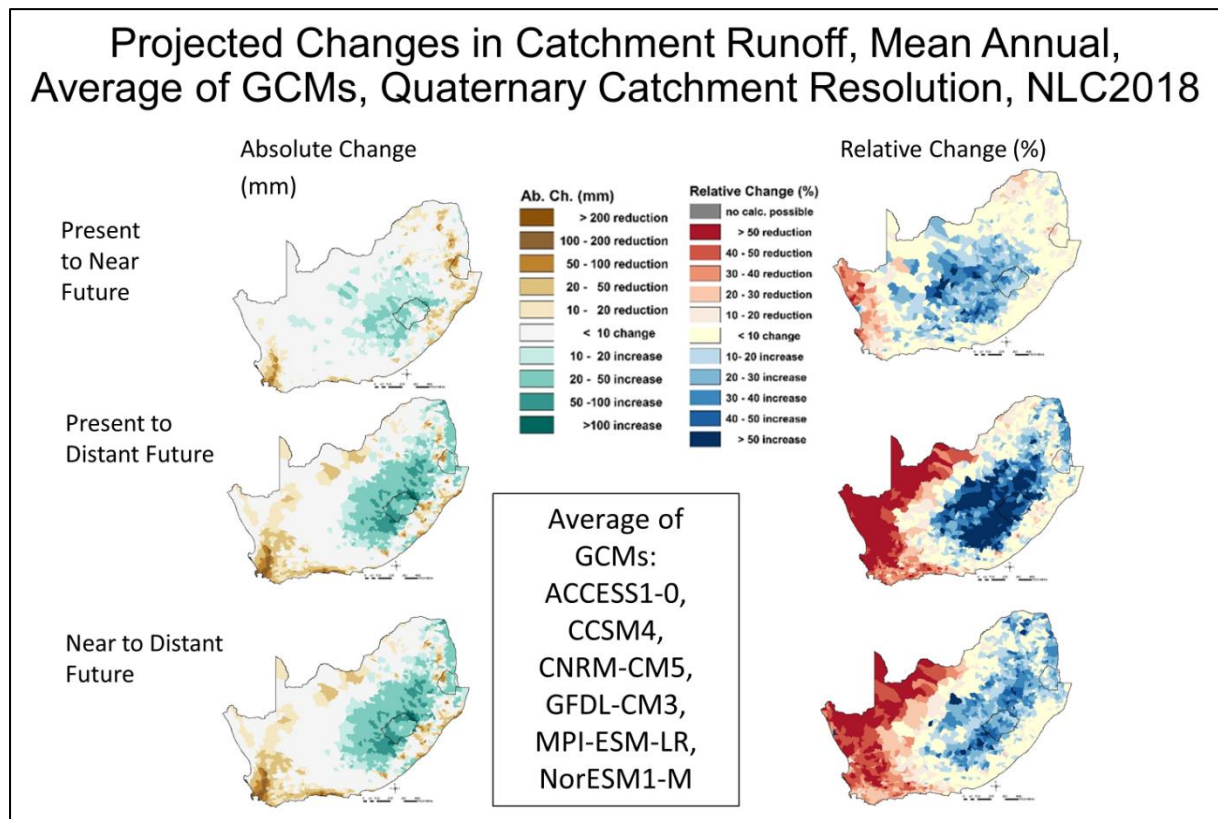
Figure 5.13 Projected absolute (mm) [left] and relative (%) [right] of mean annual individual catchment runoff, from present (1961-1990) to near future (2015-2044) [top], from present to distant future (2070-2099) [middle] and from near to the distant future [bottom] at Quaternary Catchment resolution under land cover of NLC2018

The runoff statistics of 1:10-year low, median annual and 1:10-year high are shown in **Figure 5.14**. Ratios of change for project climate change are also shown in **Figure 5.14**. Compared to the ratio changes of the mean (*cv.* Figure 5.12), ratio changes are similar, but are higher in a 1:10-year low, compared to a 1:10-year high.
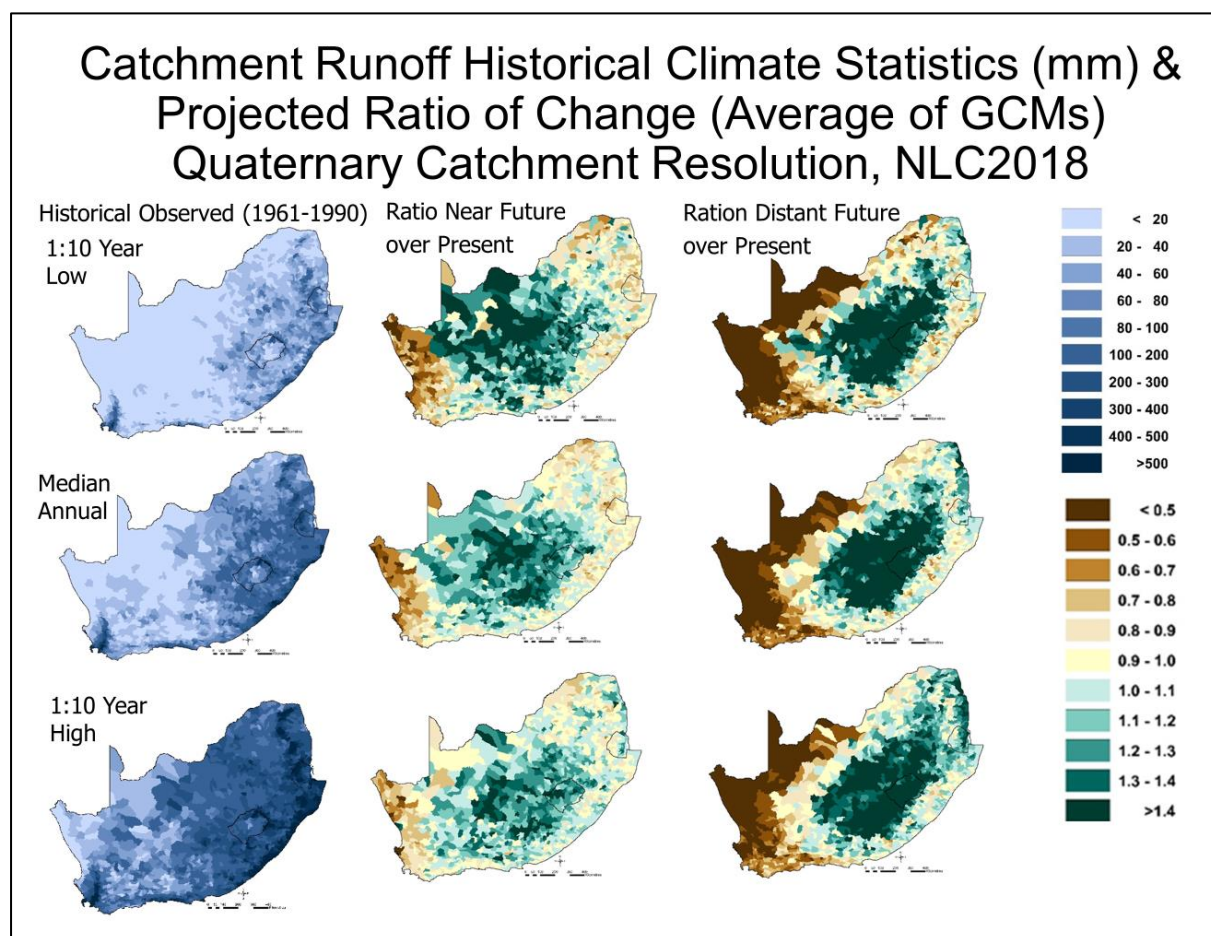
Figure 5.14   Annual catchment runoff statistics of a 1:10-year low [top], median annual [middle] and 1:10-year high [bottom] under historical climate [left] and ratios of projected change in runoff for the near future (2015-2044) over present (1961-1990) [middle column] and distant future (2070-2099) over present [right column], at Quaternary Catchment resolution, under land cover of NLC2018

When comparing the results with the results from natural vegetation (*cv.* Figure 5.9, Figure 5.10 and Figure 5.11) these look similar, with some localised differences. Any land cover impacts thus would need to be analysed on a finer scale.

5.2.3   Streamflow (mm)

Streamflow is defined here as the accumulated runoff from a catchment which includes contributions from upstream catchments. The *ACRU* model variable name for streamflow is CELRUN and it is provided as a depth equivalent in mm. Streamflow volume results will be shown later and these include the catchment area as a factor.

Accumulated streamflow (mm) under natural vegetation
The results under assumed natural vegetation (cv. Section 3.3) is shown first. A comparison between mean annual streamflow modelled using historical climate input and that modelled from the average of multiple GCM generated streamflows for the present climate period (**Figure 5.15**) and provides a similar picture for both scenarios, of higher streamflows in the east as well as the south around Cape Town, but very little in the west, except for the catchments that contain the large rivers flowing west. Both the Quaternary Catchment resolution, as well as altitudinal Quinary Catchment resolution (**Figure 5.16**) are shown, because for this variable, the finer resolution shows a lot more detail, showing up the areas with rivers.
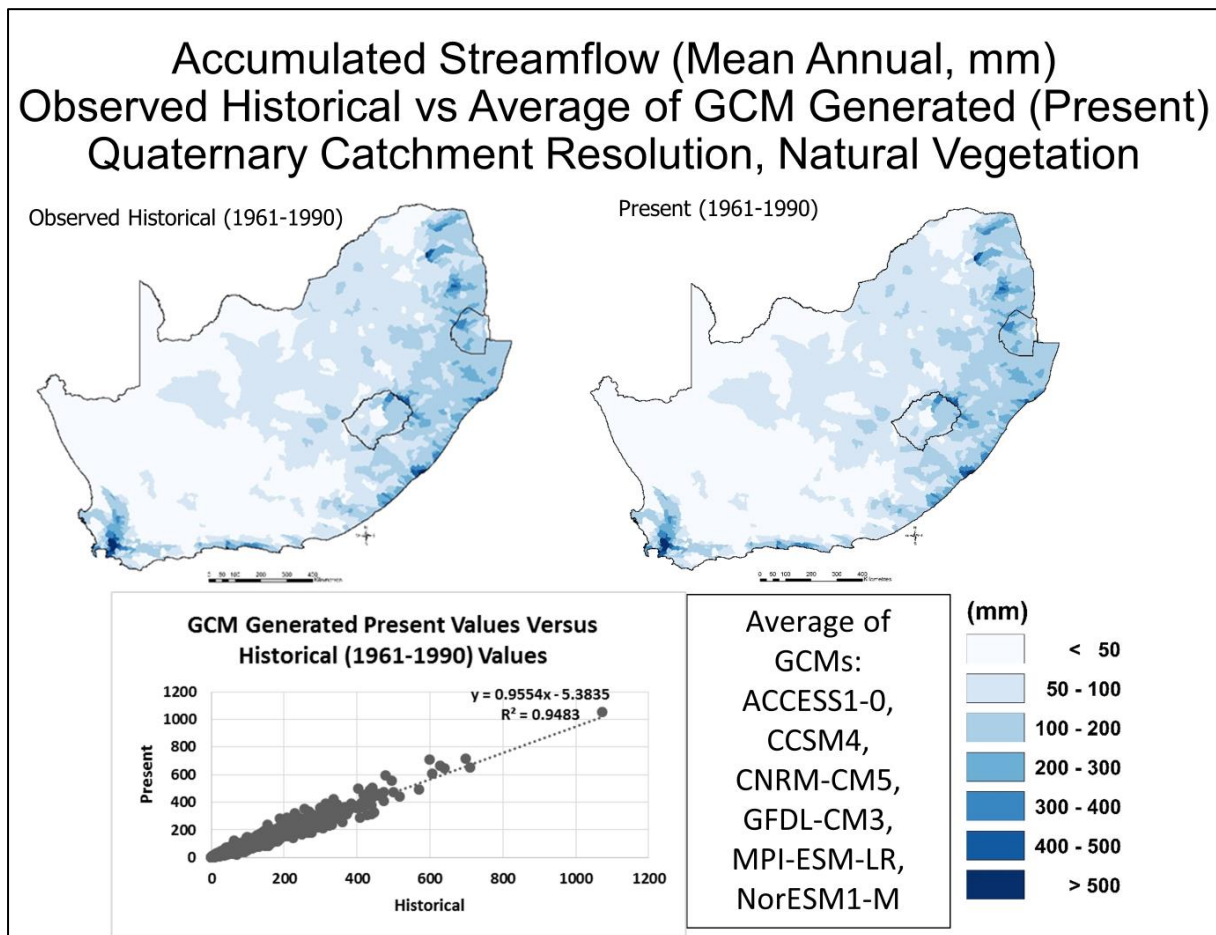
Figure 5.15 Mean annual streamflows (mm) derived using historical [left] versus GCM generated climates for the present (1961-1990) [right] at Quaternary Catchment resolution
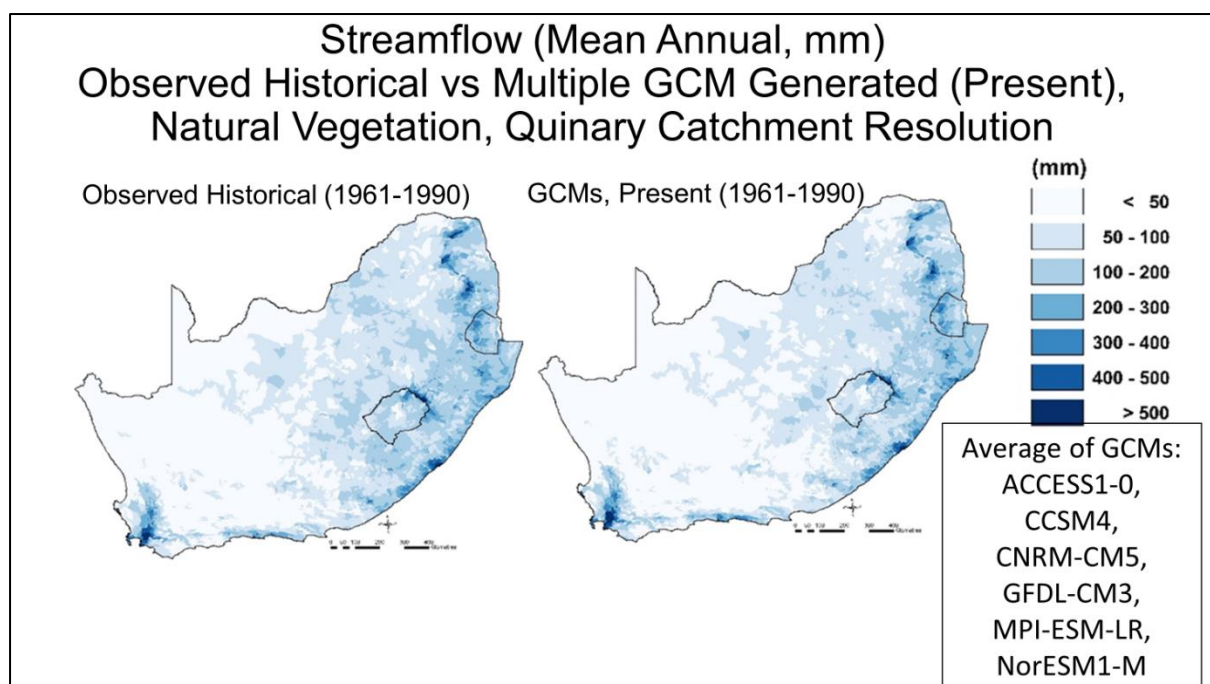
Figure 5.16   Mean annual streamflows (mm) derived using historical (1950-1999) [left] versus GCM
                generated climates for the present (1961-1990) [right] at Quinary Catchment resolution

The statistics of the 1:10-year low shows low streamflow in mm over most of South Africa, while for a 1:10-year high there is considerably more streamflow, with a small under-estimation in the interior when using the GCM generated climate in the present scenario (**Figure 5.17**).
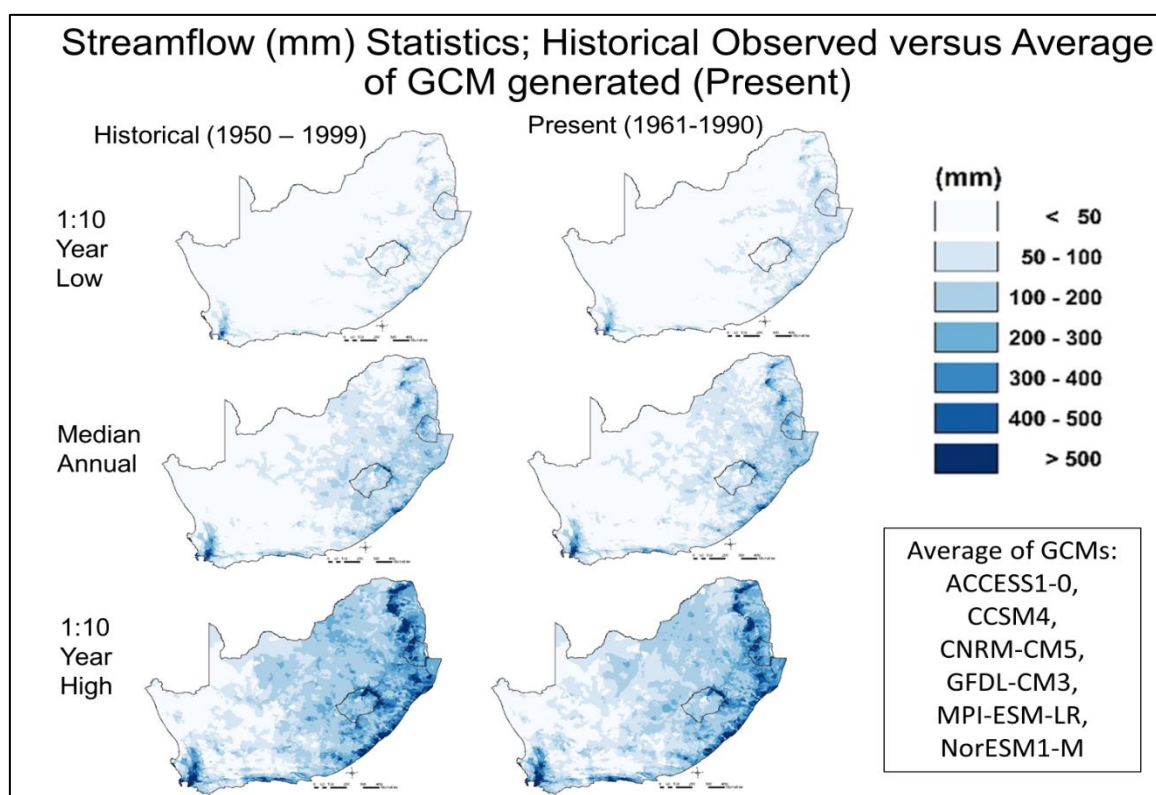
Figure 5.17 Streamflows (mm) for a statistically 1:10-year low [top row], median annual [middle row]
             and 1:10-year high [bottom row], derived using historical [left column] versus multiple GCM
             generated climates for the present period (1961-1990) [right column], at Quinary
             Catchment Resolution

Projected relative and absolute changes in mean annual streamflows into the future from the present to the near future show mixed changes (**Figure 5.18** at Quaternary Catchment and **Figure 5.19** at altitudinal Quinary Catchment resolution). For relative changes, there is a general reduction in the west, a lesser reduction in the far north, and an increase in the interior which continues downstream from there. The area around the eastern coast and central north of South Africa shows very little relative changes. This relative change becomes more extreme towards the distant future. Mean annual absolute changes display a similar, but more muted, result with the north-west not standing out with large absolute changes because of the general low streamflow in the present period, as was shown previously. Again, the finer-scaled altitudinal Quinary Catchment resolution follows the river reaches more closely and provides more details.
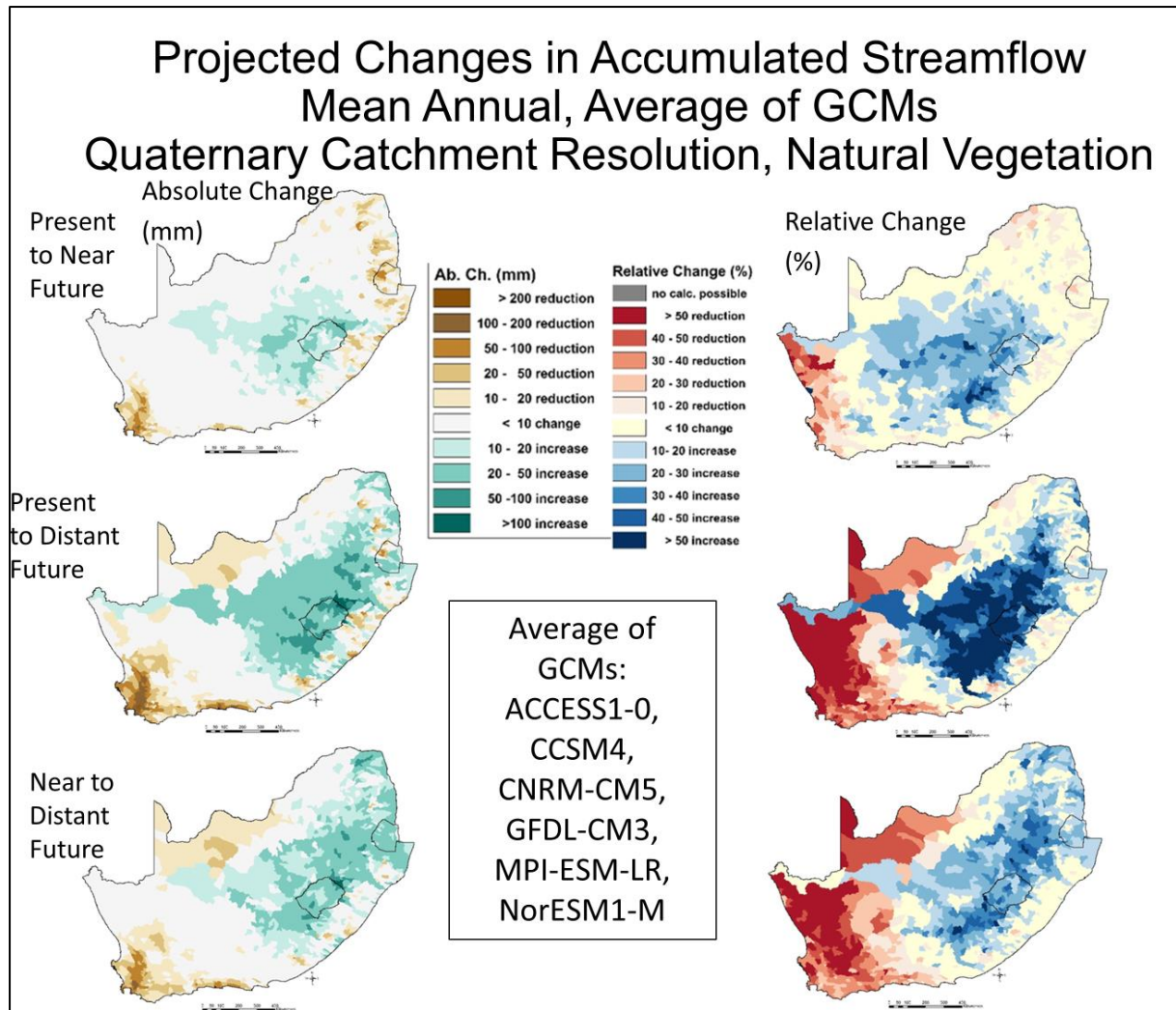
Figure 5.18 Changes (mm [left] and % [right]) in mean annual streamflows derived using GCM generated climate input, with projected changes from the present (1961-1990) to the near future (2015-2044) [top] and from the present (1961-1990) to the distant future (2070-2099) [bottom], at Quaternary Catchment resolution
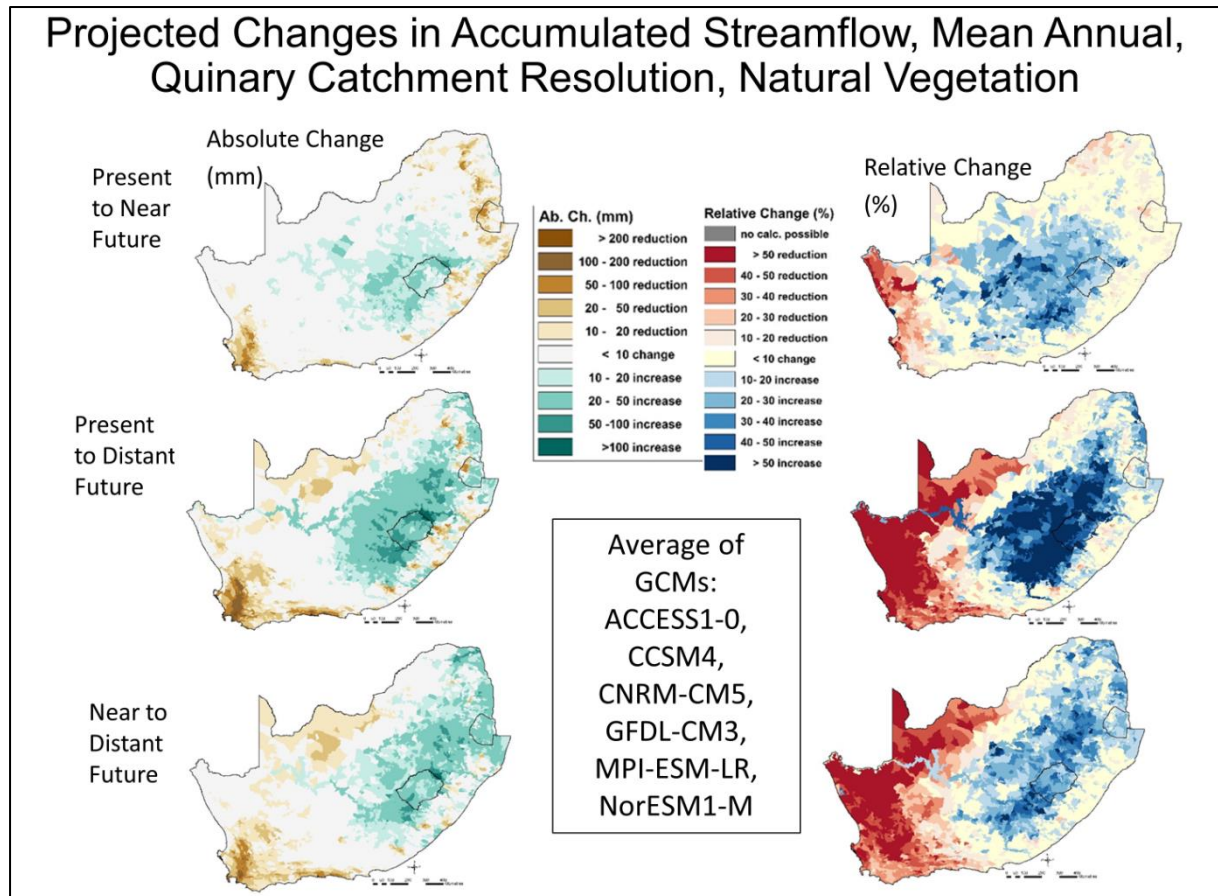
Figure 5.19 Changes (mm [left] and % [right]) in mean annual streamflows derived using GCM generated climate input, with projected changes from the present (1961-1990) to the near future (2015-2044) [top] and from the present (1961-1990) to the distant future (2070-2099) [bottom], at Quinary Catchment resolution

The relative changes in streamflow for the statistics of 1:10-year low, median annual and 1:10-year high show a similar trend compared to that of mean annual, but in relative terms the changes are higher in 1:10-year low, compared to 1:10-year high (**Figure 5.20**).
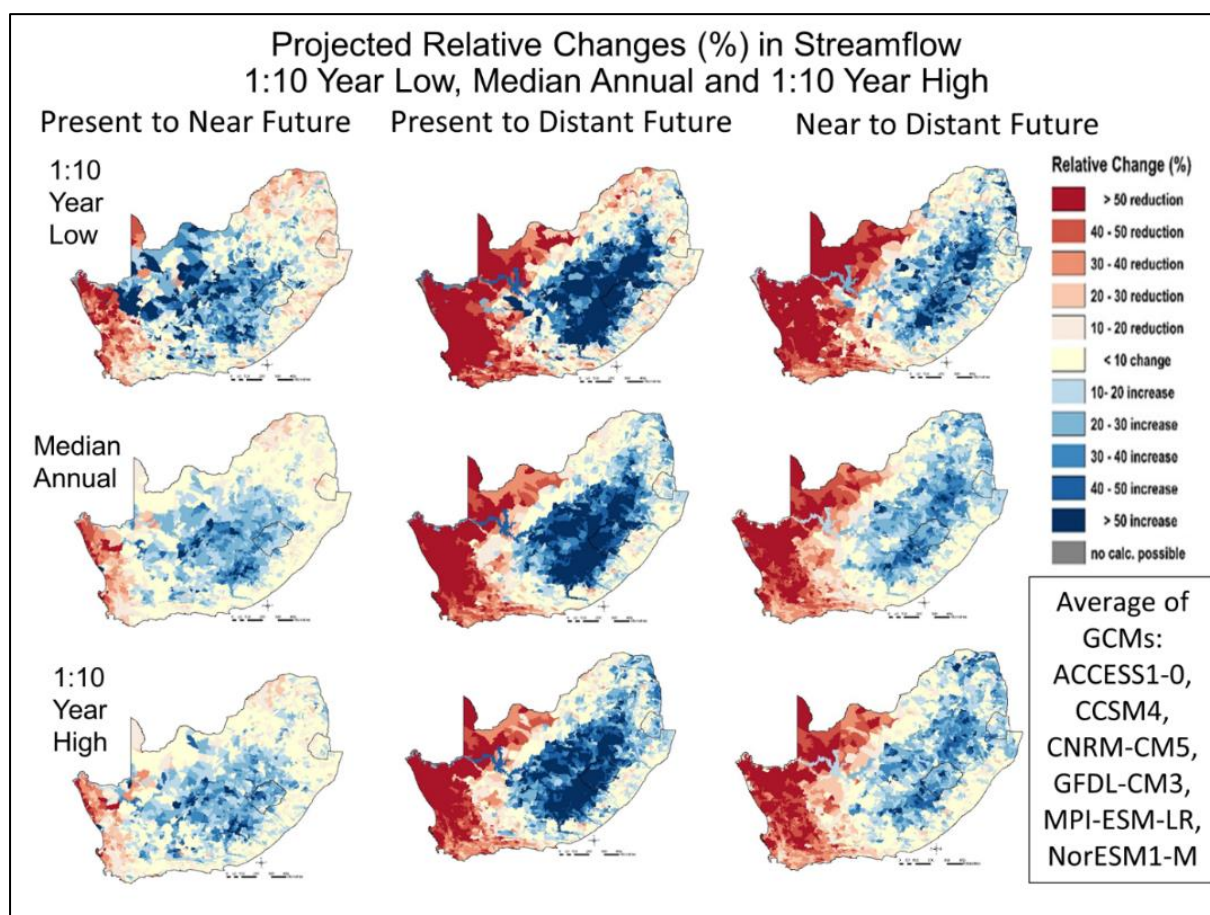
Figure 5.20 Relative changes (%) of Quinary Catchment 1:1-year low, median annual and 1:10-year high streamflows using GCM generated climate input, with projected changes from the present (1961-1990) to the near future (2015-2044) [left], from the present (1961-1990) to the distant future (2070-2099) [middle] and from the near to distant future [right]

Projected changes into the future for median seasonal streamflows are shown next, all under assumed natural vegetation. Projected changes for the spring period (September to November) shows small absolute changes, with small increases in the interior and small decreases along the coast and bigger decreases around the western part of the Western Cape (**Figure 5.21**).
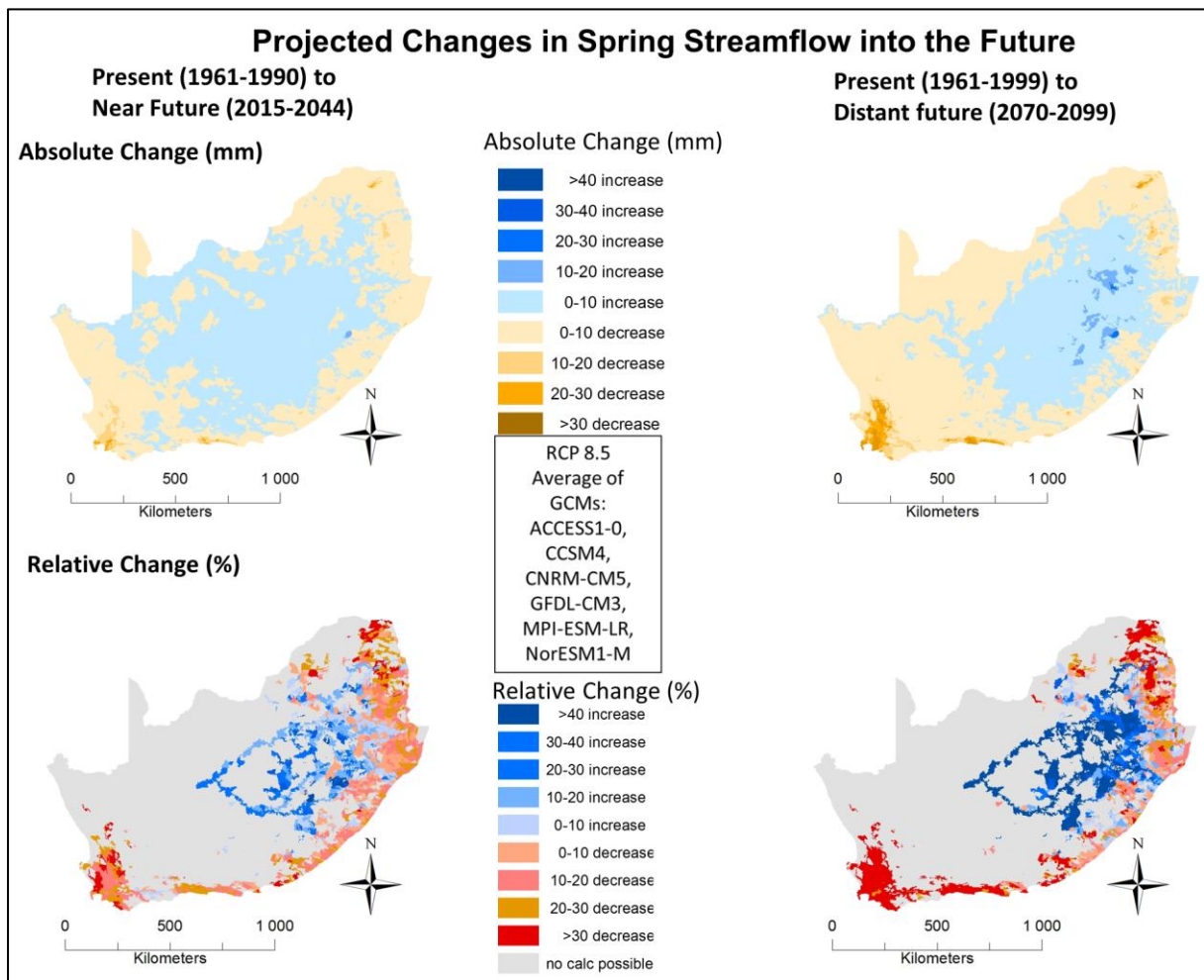
Figure 5.21 Projected change in median spring (September to October) streamflow from the present (1961-1990) to the near future (2015-2044) shown in the left column and from the present to the distant future (2070-2099) in the right column. Absolute change (mm) in the top row and relative change (%) in the bottom row, with relative change not calculated for small (<10 mm) present streamflow values. Average of GCMs, at Quinary Catchment resolution

Changes for summer (December to February) streamflow (**Figure 5.22**) shows small absolute increases in the interior, more towards the distant future. Small decreases can be seen in patches in the west, with the patches increasing towards the distant future.
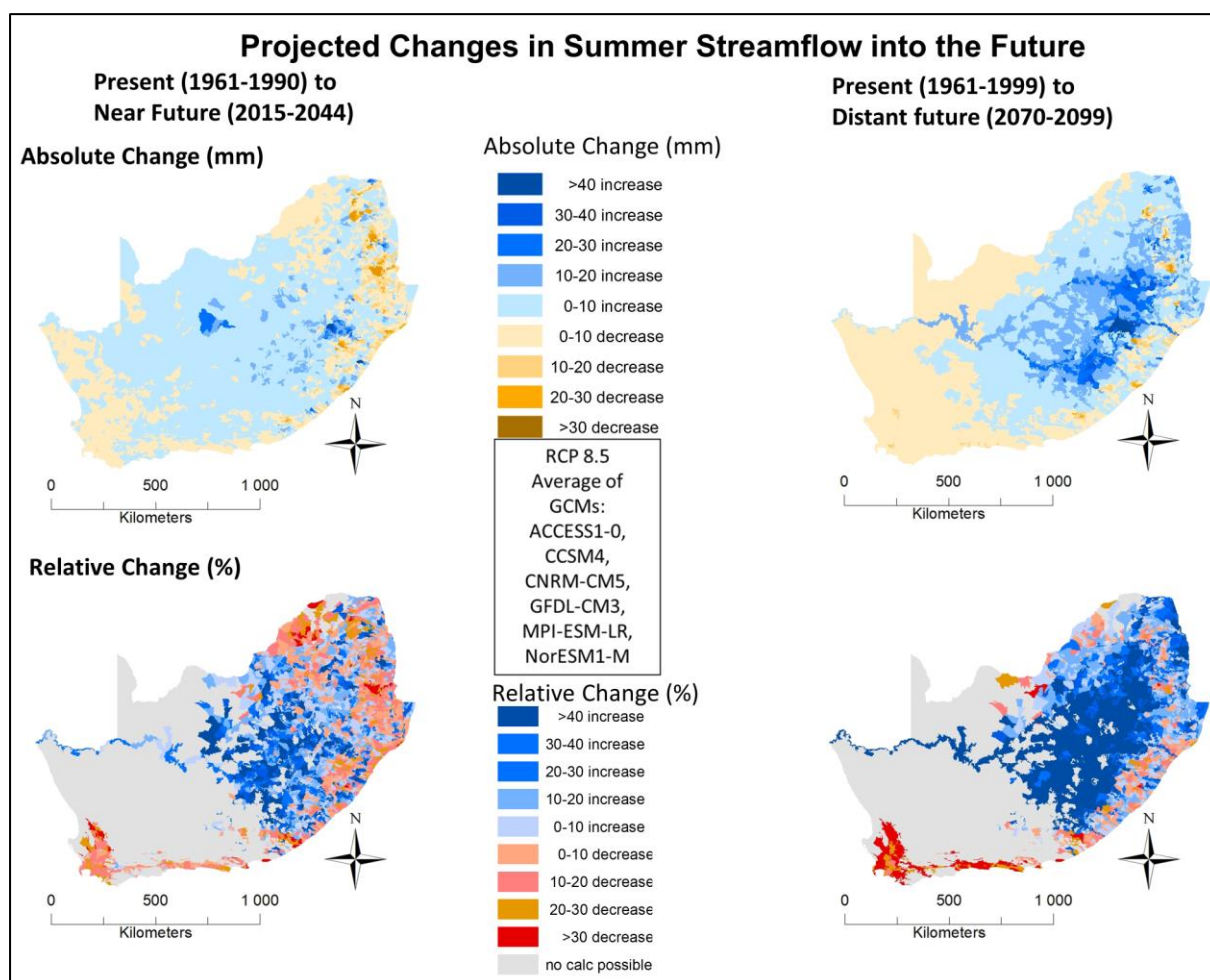
Figure 5.22 Projected change in median summer (December to February) streamflow from the present (1961-1990) to the near future (2015-2044) shown in the left column and from the present to the distant future (2070-2099) in the right column. Absolute change (mm) in the top row and relative change (%) in the bottom row, with relative change not calculated for small (<10 mm) present streamflow values. Average of GCMs, at Quinary Catchment resolution

Projected changes in median streamflows for autumn (March to May) shows small increases in the interior, more towards the distant future for the Orange catchment, and decreases along the coast and north-west (**Figure 5.23**).
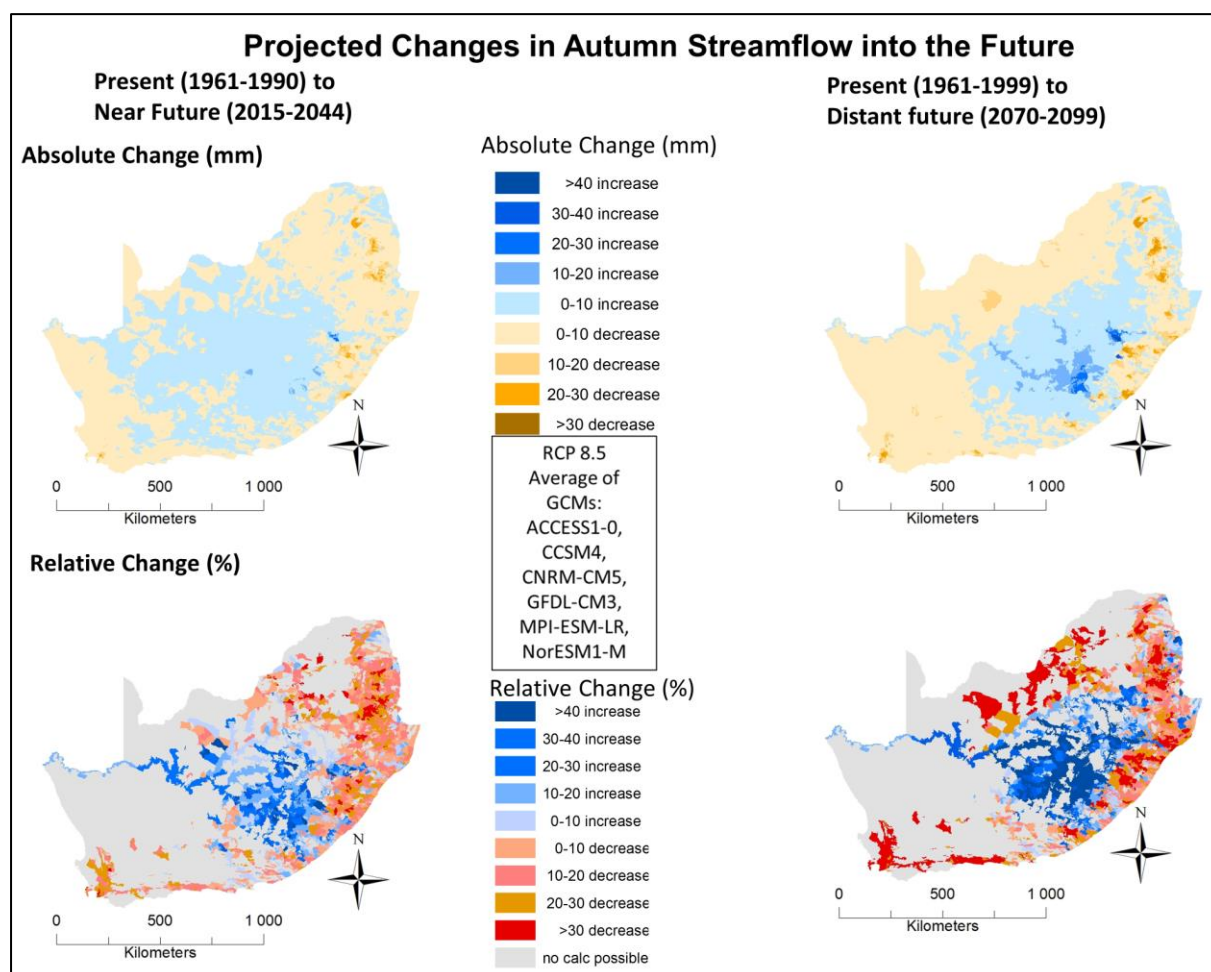
Figure 5.23 Projected change in median autumn (March to May) streamflow from the present (1961-1990) to the near future (2015-2044) shown in the left column and from the present to the distant future (2070-2099) in the right column. Absolute change (mm) in the top row and relative change (%) in the bottom row, with relative change not calculated for very small (<10 mm) present streamflow values. Average of GCMs, at Quinary Catchment resolution

Projected changes in median winter (June to August) streamflows (**Figure 5.24**) shows small increases in the interior and small decreases along the coast and the north-west, with larger decreases in the western part of the Western Cape. This winter rainfall area stands out with projected reductions in winter streamflow, and the same can also be seen to a lesser degree for spring streamflow (cv. Figure 5.21). For future research, it would be beneficial to determine changes in streamflow volume, as that might be more important to the water management and planning sector.
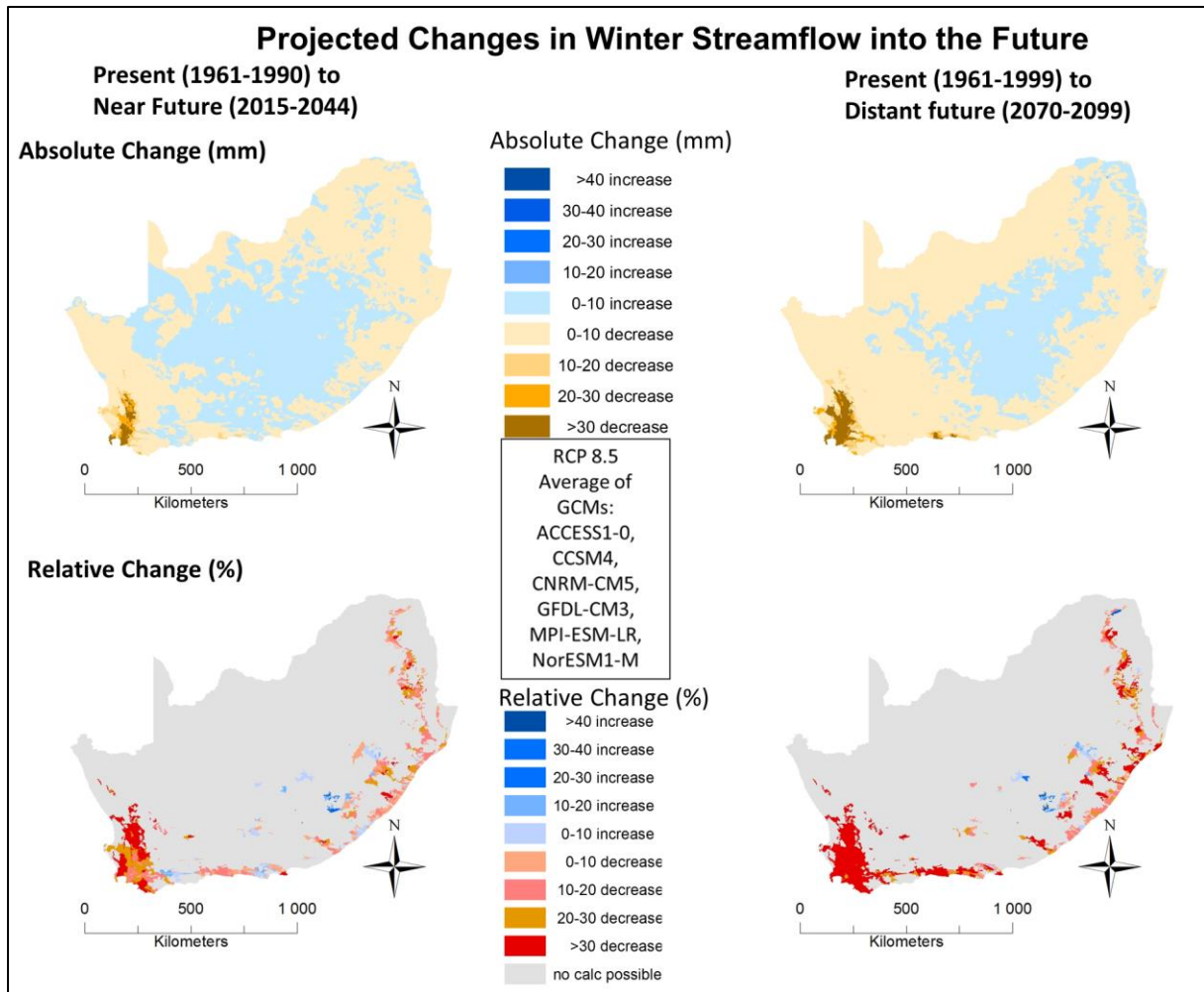
Figure 5.24 Projected change in median winter (June to August) streamflow from the present (1961-1990) to the near future (2015-2044) shown in the left column and from the present to the distant future (2070-2099) in the right column. Absolute change (mm) in the top row and relative change (%) in the bottom row, with relative change not calculated for very small (<10 mm) present streamflow values. Average of GCMs, at Quinary Catchment resolution

Accumulated streamflow (mm) under actual land cover
The results under assumed actual land cover as of 2018 (cv. Section 3.4) is shown next. Mean annual streamflow modelled using historical climate input show higher streamflows in the east as well as the south around Cape Town, but very little in the west, except for the Orange River Catchment, that originated in Lesotho, flowing west (**Figure 5.25**, top).

Projected changes in mean annual streamflows into the future are shown as ratios of change (**Figure 5.25**, bottom) and also as absolute (mm) and relative (%) changes (**Figure 5.26**). The results are mixed. For relative changes, there is a general reduction in the west, a lesser reduction in the far north, and an increase in the interior which continues downstream from there. The area around the eastern coast and central north of South Africa shows very little relative changes. This relative change becomes more extreme towards the distant future. Mean annual absolute changes display a similar, but more muted, result with the north-west not standing out with large absolute changes because of the general low streamflow in the present period, as was shown previously. Generally in the west there is either no to very little change, or a reduction in streamflow projected, especially into the distant future. There is an increase in flows in the interior, and also for rivers flowing either towards the east or west, if the rivers have their origin in the higher altitude interior where more streamflow is projected by the GCMs. There are mixed changes projected for the areas along the eastern coast.
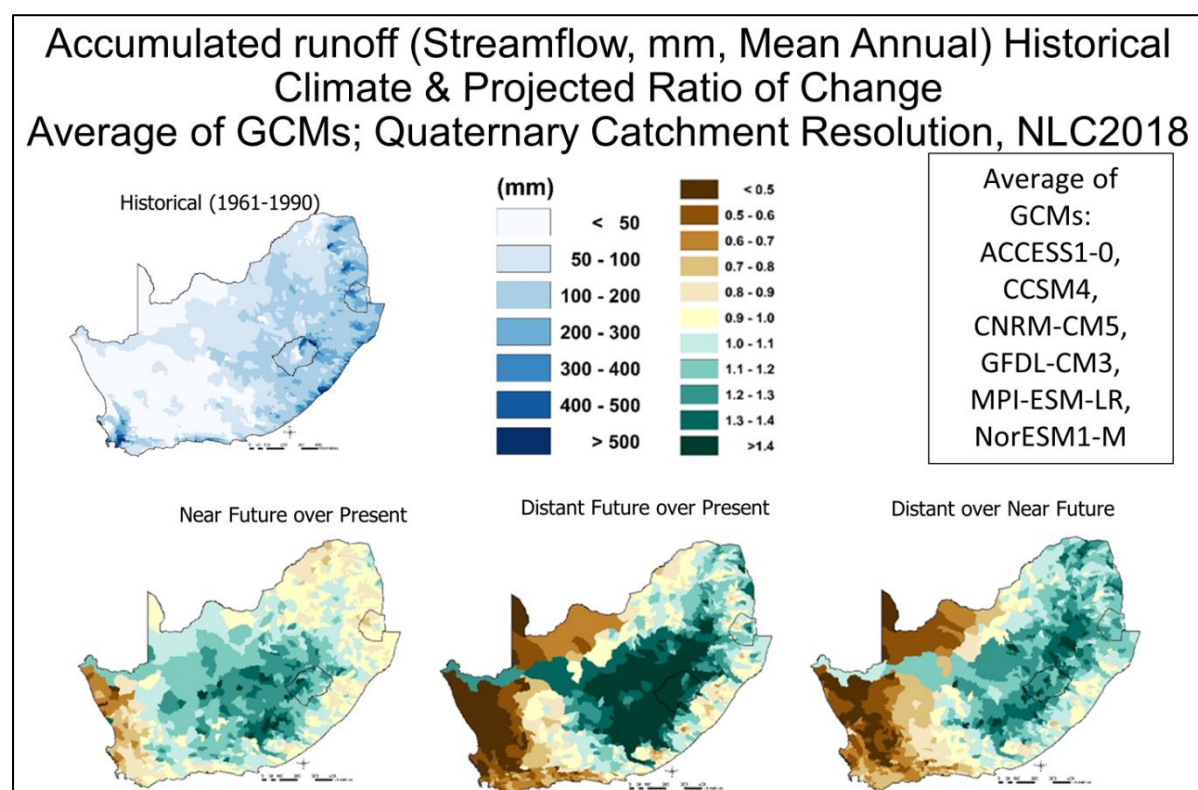
Figure 5.25   Mean annual streamflow under historical climate and ratios of projected change for the near future (2015-2044) over present (1961-1990) [bottom left], distant future (2070-2099) over present [bottom middle] and distant over near future [bottom right] at Quaternary Catchment resolution, under land cover of NLC2018
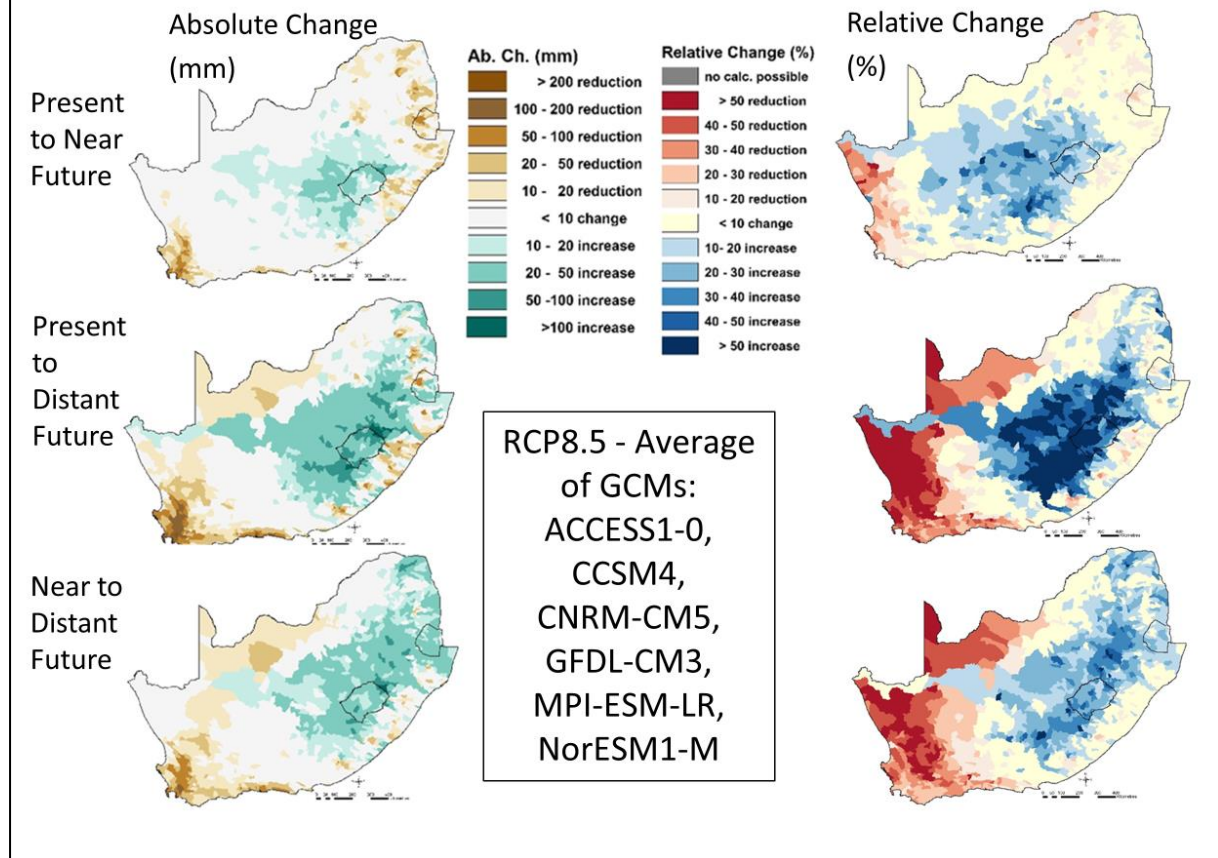
Figure 5.26   Projected absolute changes in mm [left] and relative changes in % [right] in mean annual streamflow using projected GCM generated climate input, with projected changes from the present (1961-1990) to the near future (2015-2044) [top] and from the present (1961-1990) to the distant future (2070-2099) [bottom], at Quaternary Catchment resolution, under NLC2018

The annual streamflow statistics under historical climate of 1:10-year low, median and 1:10-year high show low streamflow in mm over most of South Africa, while for a 1:10-year high there is considerably more streamflow (**Figure 5.27**, top). Projected changes into the future (**Figure 5.27**, bottom) are similar to those of mean annuals (*cv.* Figure 5.25), but show that relative impacts are higher in a 1:10-year low, compared to a 1:10-year high.
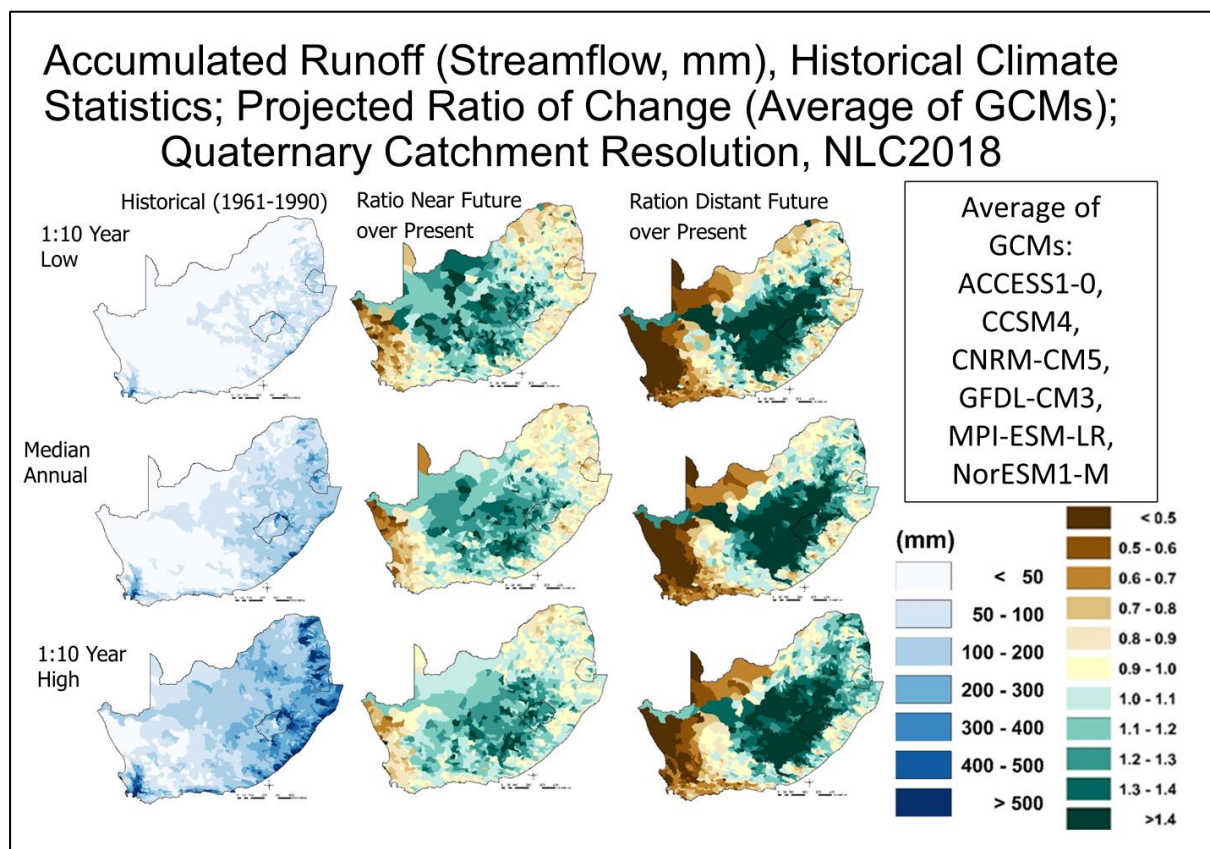
Figure 5.27   Annual streamflow statistics of a 1:10-year low [top], median annual [middle] and 1:10-year high [bottom] under historical climate [left column] and ratios of projected change of GCM generated runoff for the near future (2015-2044) over present (1961-1990) [middle column] and distant future (2070-2099) over present [right column], at Quaternary Catchment resolution and NLC2018

When comparing the results with the results from natural vegetation these look similar, with some localised differences. Any land cover impacts thus would need to be analysed on a finer scale.

5.2.4   Streamflow volume

The results under assumed natural vegetation (cv. Section 3.3) is shown. Streamflow volume is calculated by multiplying the *ACRU* runoff (mm) from a Quinary Catchment by its area to obtain an answer in m^3, and then accumulating the volumes from all the Quinaries upstream of the point of interest. A comparison between mean annual streamflow volumes shows up the Quinary Catchments containing the major rivers in South Africa. Generally, the results derived from observed historical climate data and those from GCM generated values for the present time period match well (**Figure 5.28**). The streamflow statistics (**Figure 5.29**) similarly match well for a 1:10-year low, median and a 1:10-year high annual streamflows.
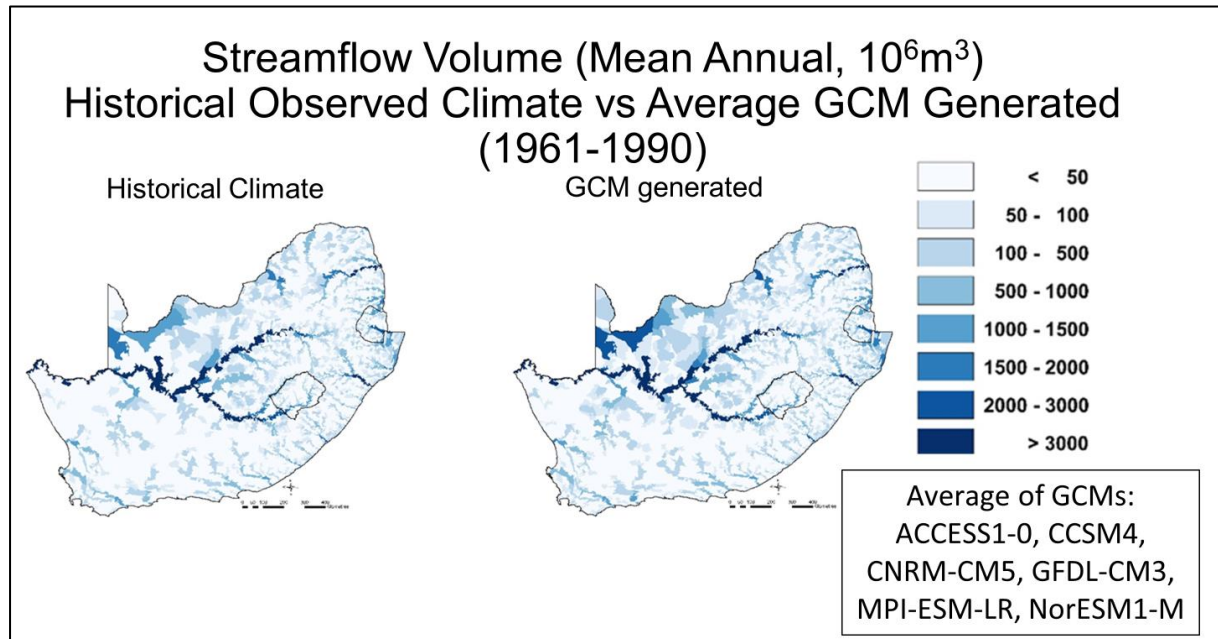
Figure 5.28   Mean annual streamflow volumes (10^6m^3) derived using historical observed climate [left] versus GCM generated climates [right] for the time period 1961-1990, natural vegetation, at Quinary Catchment resolution
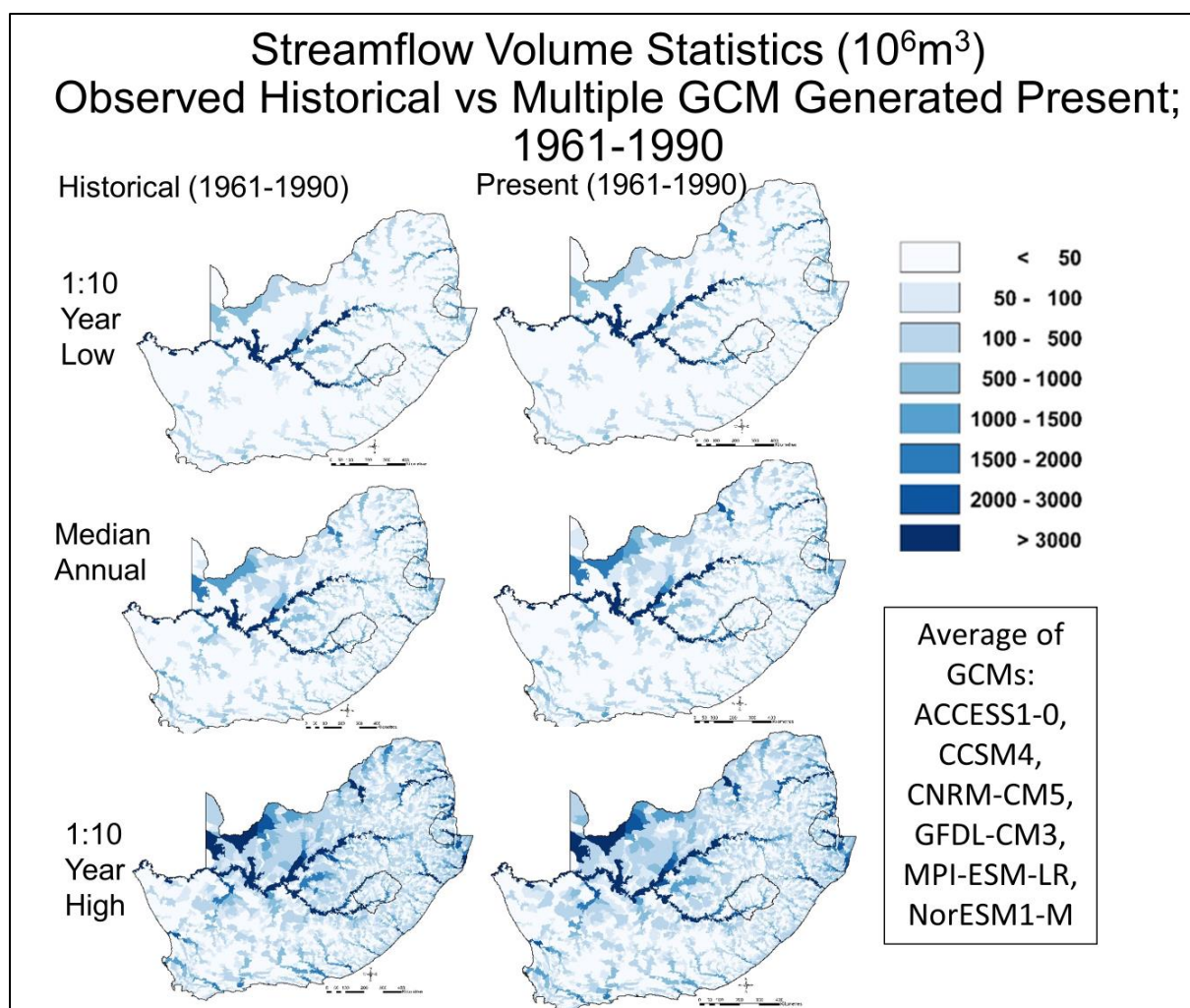
Figure 5.29   Annual streamflow volumes, (10^6m^3) for a statistically 1:10-year low [top], a median [middle] and a 1:10-year high flow year [bottom], derived using historical (1961-1990) [left] versus GCM generated climates for the present (1961-1990) [right], natural vegetation, Quinary Catchment resolution

Projected GCM generated mean annual streamflows for the present, near future and distant future (**Figure 5.30**) show a similar picture. The differences are shown as absolute as well as relative changes (**Figure 5.31**) and are also shown at Quaternary Catchment resolution (**Figure 5.32**). Again, for streamflow volume, it is recommended to use the finer resolution of altitudinal Quinary Catchments, as this closely follows river reaches and more relevant details can be seen. Generally in the west there is either no to very little change, or a reduction in streamflow projected, with increasing magnitude into the distant future. There is an increase in flows in the interior, and also for rivers flowing either towards the east or west, if the rivers have their origin in the higher altitude interior where more streamflow is projected by the GCMs. There are mixed changes projected for the areas along the eastern coast.
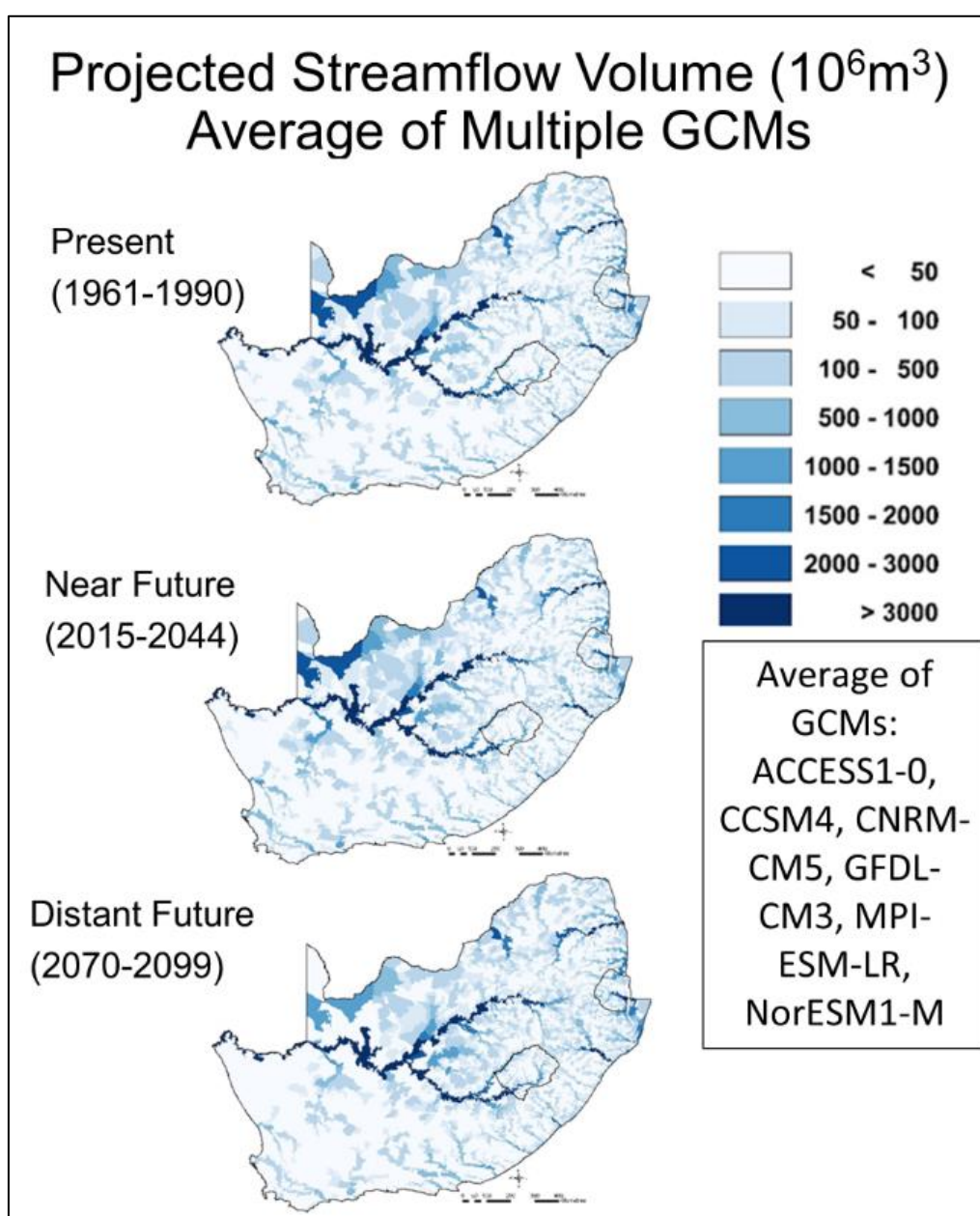
Figure 5.30 Projected mean annual accumulated Quinary Catchment streamflow volume (10^6m^3), derived from the average of GCM outputs used, showing results for the present (1961-1990) [left], the near future (2015-2044) [middle] and the distant future (2070-2099) [right], natural vegetation
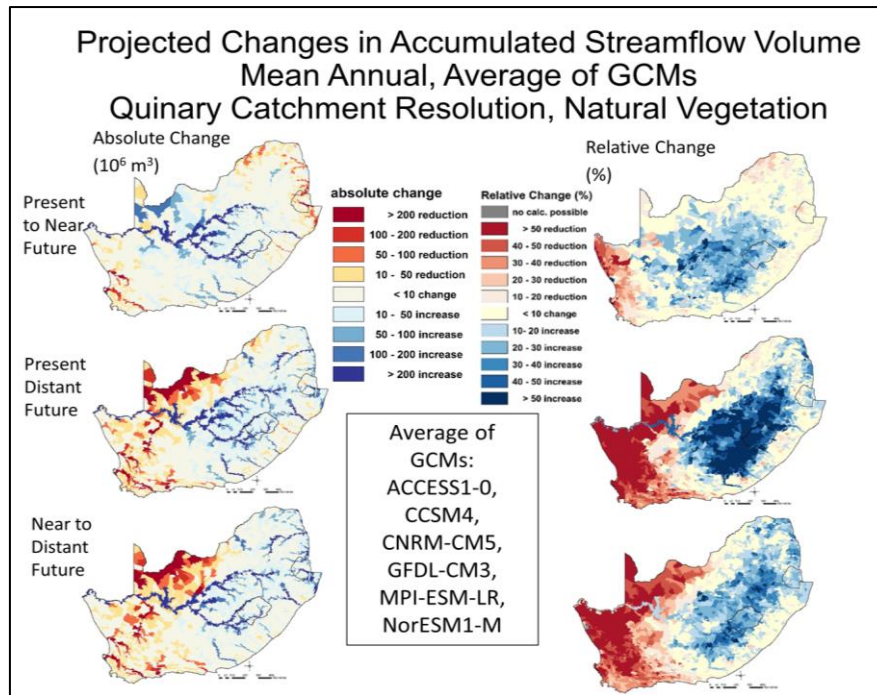
Figure 5.31 Projected changes in mean annual accumulated streamflow volume (10^6m^3 [left] and % [right]), with changes from the present (1961-1990) to the near future (2015-2044) [top], from the present to the distant future (2070-2099) [middle] and from the near to the distant future [bottom], derived as an average of changes from the 6 GCMs used, at Quinary Catchment resolution
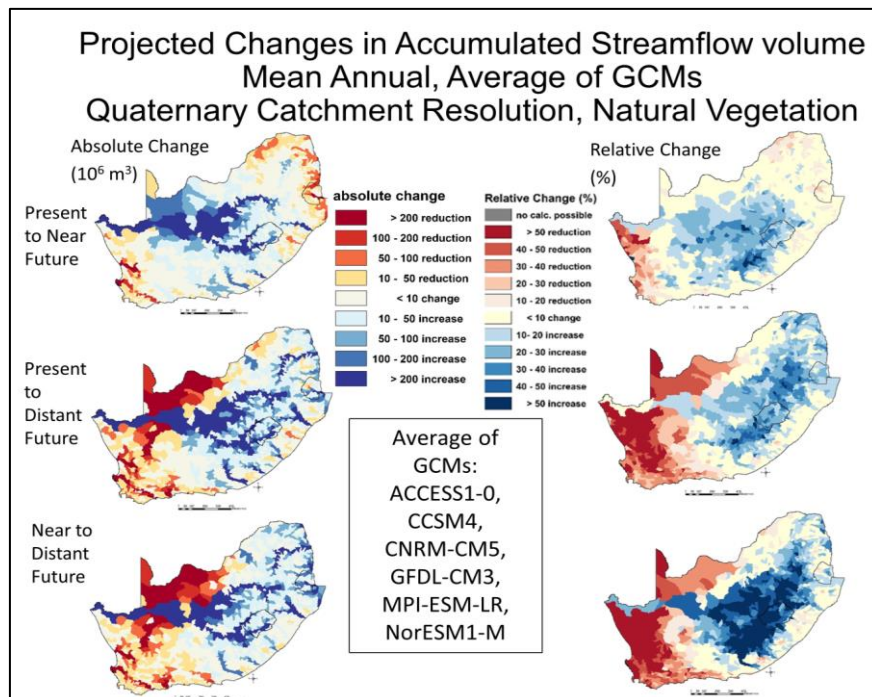
Figure 5.32 Projected changes in mean annual accumulated streamflow volume (10^6m^3 [left] and % [right]), with changes from the present (1961-1990) to the near future (2015-2044) [top], from the present to the distant future (2070-2099) [middle] and from the near to the distant future [bottom], derived as an average of changes from the 6 GCMs used, at Quaternary Catchment resolution

Changes in projected GCM generated mean annual streamflow statistics for the present, near future and distant future (**Figure 5.33**) show greater absolute changes for the 1:10-year high, compared for the 1:10-year low.
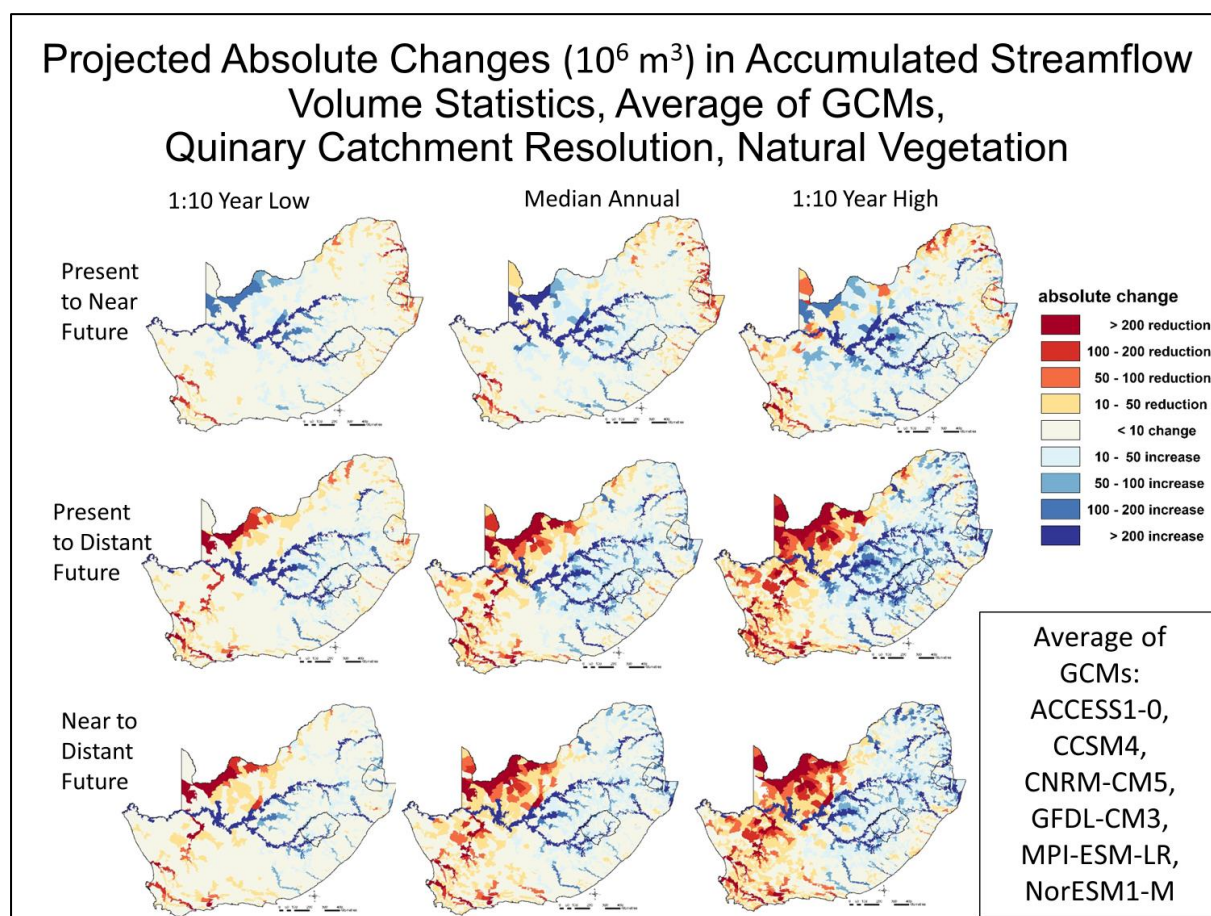
Figure 5.33 Projected changes in accumulated streamflow volume statistics ($10^6 m^3$, with changes from the present (1961-1990) to the near future (2015-2044) [top], from the present to the distant future (2070-2099) [middle] and from the near to the distant future [bottom], for a 1:10-year low [left], a median year [middle column] and for a 1:10-year high [right], derived as an average of changes from the 6 GCMs used, at Quinary Catchment resolution

5.2.5   Soil water content

The results under assumed natural vegetation (cv. Section 3.3) is shown. Soil water holding capacity is dependent on soil depth and soil type and, as such, next to climate it is also very location dependent. Therefore, here, the finer scale altitudinal Quinary Catchment resolution, instead of the Quaternary Catchment resolution was used. Even that is a coarse resolution and large variation is likely to occur on a more local scale. Annual soil water is also likely to be varied during the year. More meaningful would be to map monthly and seasonal changes, rather than annual changes, and even more meaningful would be for future analyses to calculate changes in days with different levels of soil water content.

Nevertheless, mean annual soil water content (**Figure 5.34**) shows variations being generally lower in the south-west compared to the north-east.
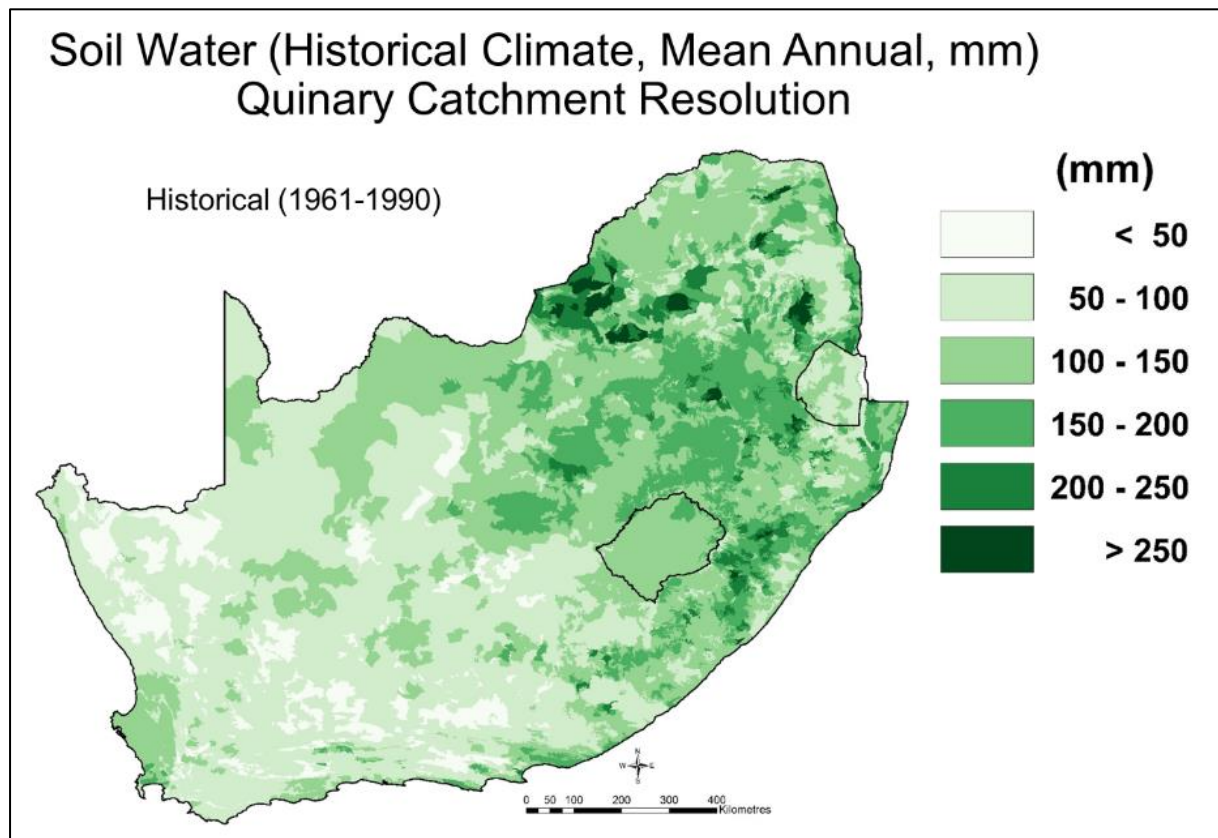
Figure 5.34 Mean annual soil water (mm) at Quinary Catchment resolution, derived using historical (1961-1990) climates

Climate change impacts on soil water content, when shown as relative changes (**Figure 5.35**) show less than 2% changes in either direction for most of the region from the present to the near future, with small reductions towards some coastal areas. Into the more distant future the changes are more severe, with increasing reductions towards the coastal reaches and the north, but especially in the north-west, with up to 8% reductions in mean annual soil water content.
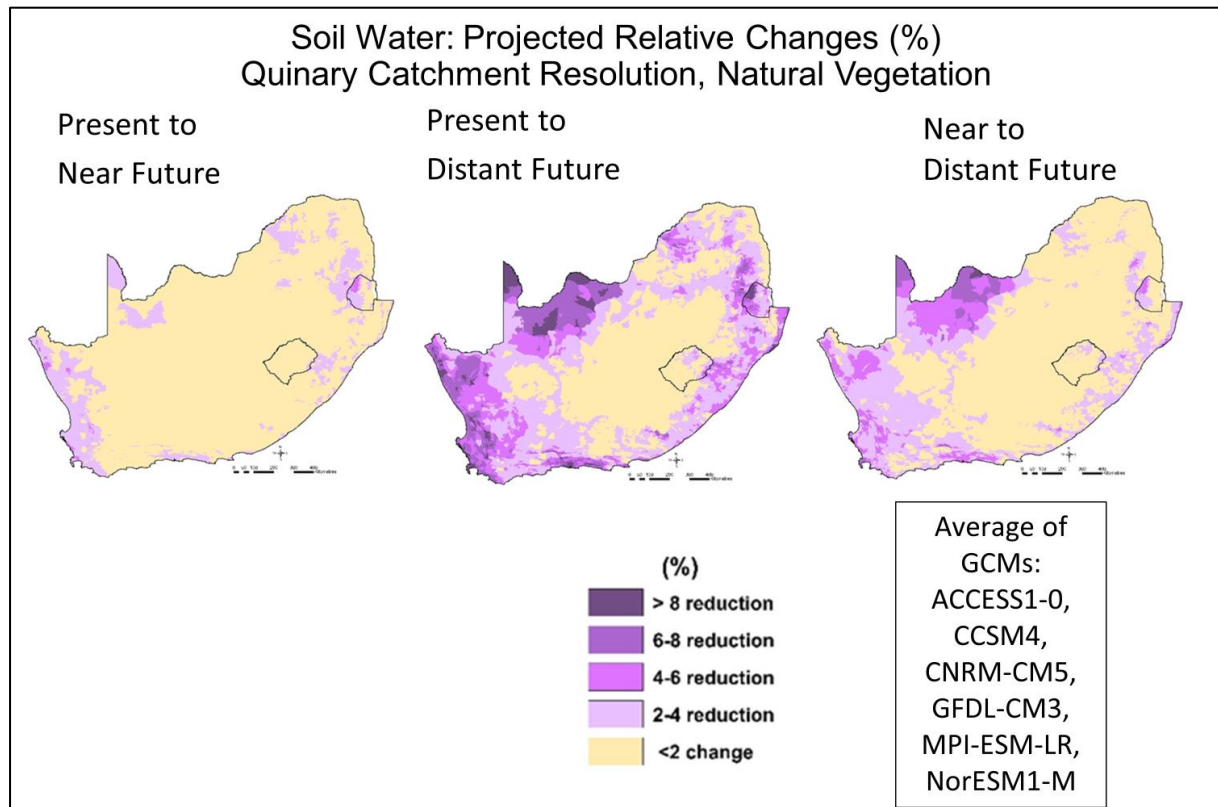
Figure 5.35 Relative changes (%) in mean annual soil water (mm) at Quinary Catchment resolution, from the present to near future [left], from the present to the distant future [middle] and from the near to the distant future [right]

5.2.6 Soil water drainage to the groundwater zone

The results under assumed natural vegetation (cv. Section 3.3) is shown. When the soil water content of the subsoil horizon exceeds its drained upper limit (field capacity), drainage into the groundwater zone takes place, at a rate depended on the soil texture of the subsoil horizon. Water from this groundwater zone then enters the stream as baseflow, which is further explained later in the next section.

Mean annual soil water drainage to the groundwater zone is shown for historical and GCM generated present conditions (**Figure 5.36**), showing higher magnitudes of drainage in the wetter parts of the region. Note that values in Lesotho are not as accurate as elsewhere, because soil information is not at the same spatial resolution as for the rest of the region.
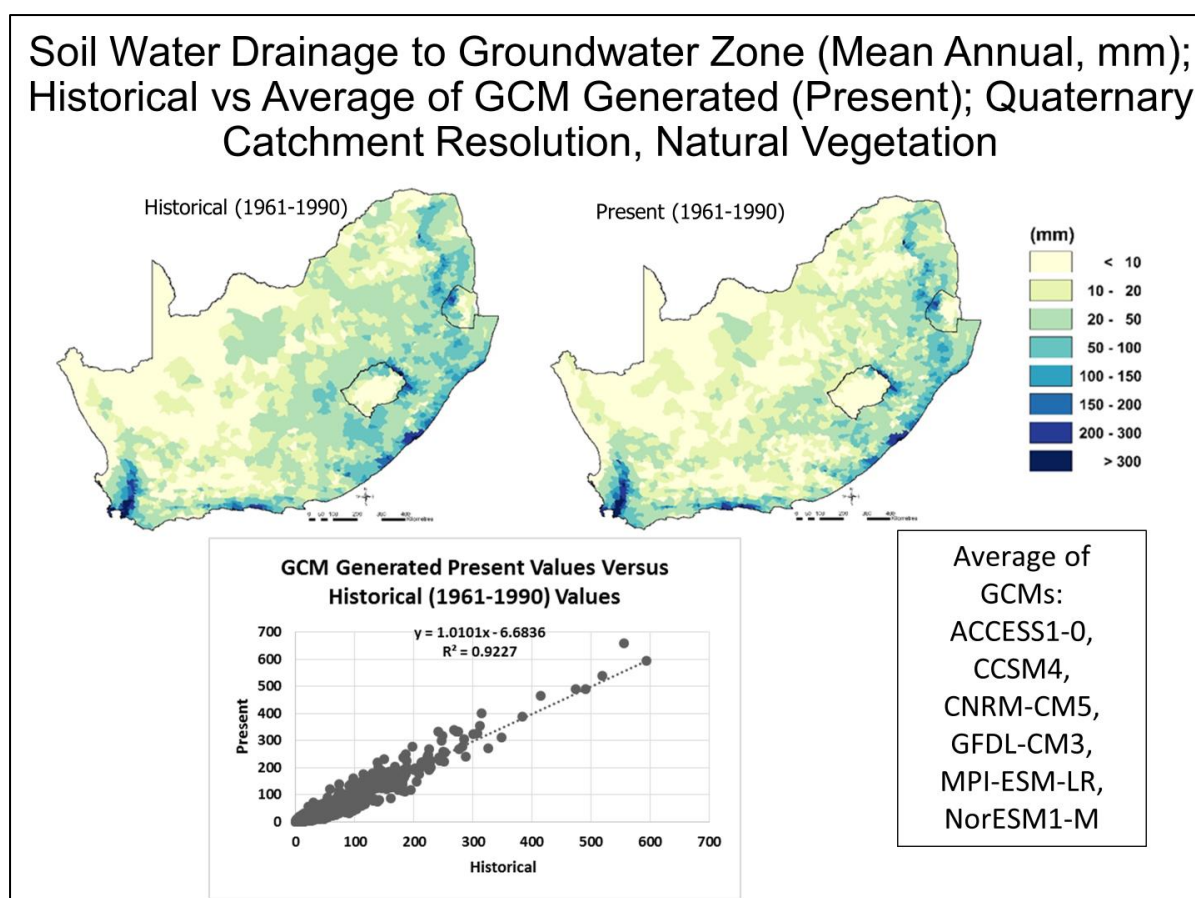
Figure 5.36   Mean annual soil water drainage to the groundwater zone (mm) at Quaternary Catchment resolution, derived using observed historical [left] versus multiple GCM generated climates for the present time period (1961-1990) [right]

Projected changes of mean annual drainage of soil water into the groundwater zone into the future is shown as ratios (**Figure 5.37**), as well as absolute (in mm) and relative (%) changes (**Figure 5.38**). Absolute changes are small for most of the region, but especially into the distant future a reduction can be seen in areas of the Western Cape and along some eastern regions and some increases along the Drakensberg. In relative terms the generally a reduction can be seen especially towards the distant future in the west as well as along the east coast, but increases in the eastern interior and the far north.
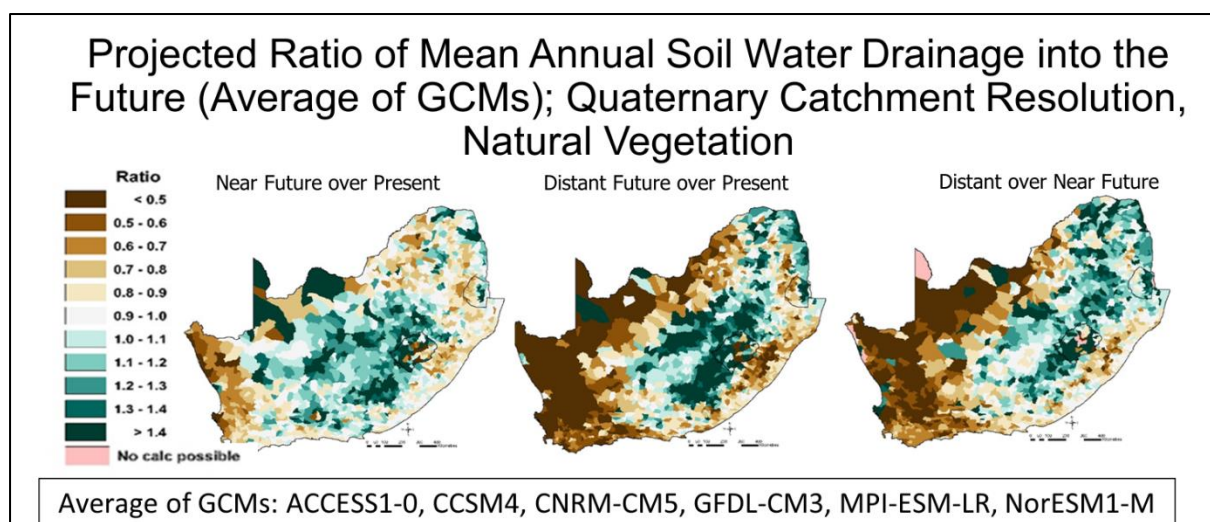
Figure 5.37 Projected ratios of mean annual soil water drainage to the groundwater zone of the near future (2015-2044) over present (1961-1990) [left], the distant future (2070-2099) over present [middle] and the distant over the near future [right], at Quaternary Catchment resolution
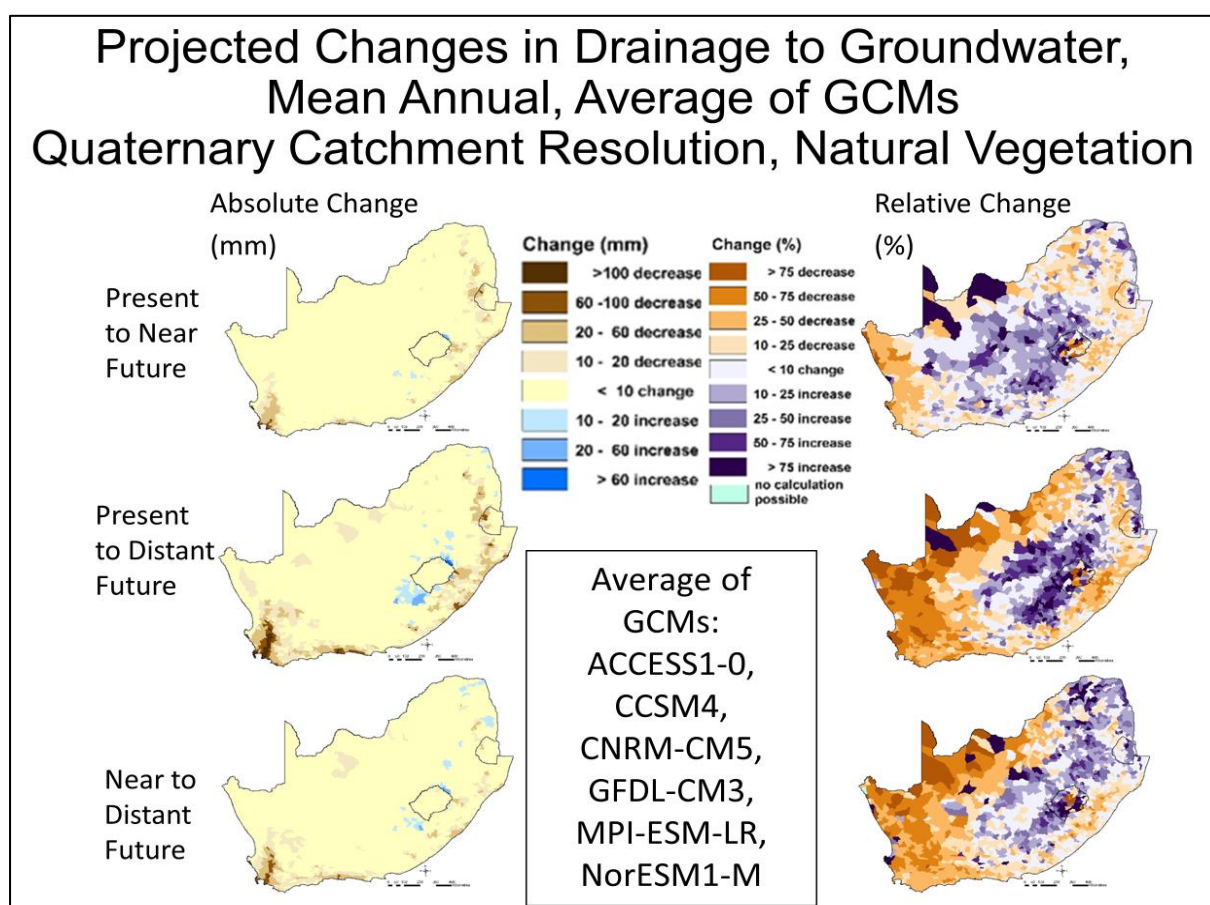
Figure 5.38 Projected changes (mm [left] and % [right]), at Quaternary Catchment resolution, in mean annual soil water drainage to the groundwater zone derived from GCM generated climate input, with projected changes from the present (1961-1990) to the near future (2015-2044) [top] and from the present (1961-1990) to the distant future (2070-2099) [bottom]

Statistics of change for 1:10-year low, median annual and 1:10 year high (**Figure 5.39**) show a fairly patchy picture, with limitations in the calculation in the dry areas and years, often because of errors of dividing by zero.
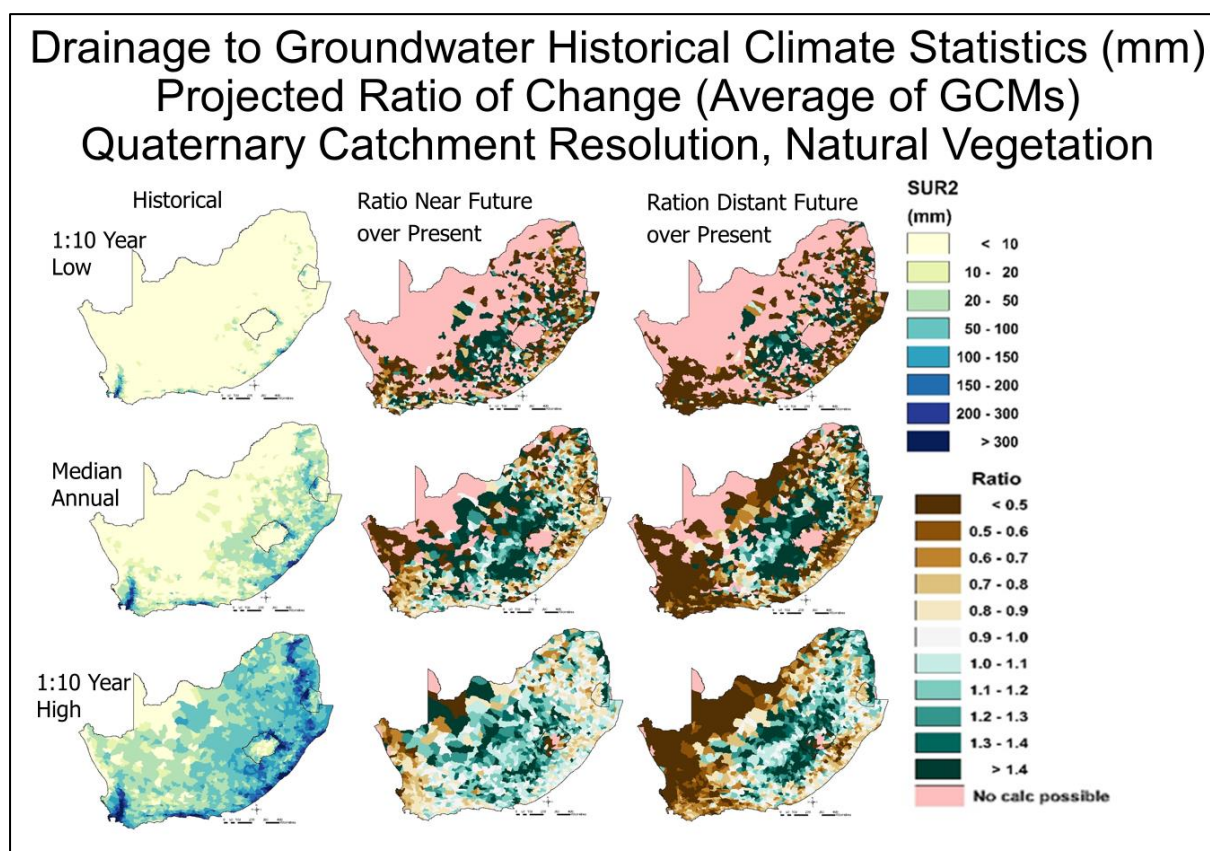
Figure 5.39 Statistics of annual soil water drainage to the groundwater zone at Quaternary Catchment resolution for a 1:10 year of low drainage [top row], a median [middle row] and 1:10 year of high drainage [bottom row] for observed historical climate (1961-1990) [left column] and GCM generated ratio changes showing near future to present ratios [middle column] and distant future to present ratios [right column]

5.2.7 Baseflows

In the *ACRU* model baseflow is generated from excess rainwater having drained through the topsoil into the subsoil and then out of the subsoil into a groundwater store (see previous section), from which this water is then released very slowly back into the stream as baseflow at a rate determined by the magnitude of the groundwater store and on topographic conditions.

Baseflows under natural vegetation

The results under assumed natural vegetation (cv. Section 3.3) is shown first. Mean annual baseflow (**Figure 5.40**) for historical and GCM generated present (1961-1990) generally show low baseflow values except for the far-east and extreme south.
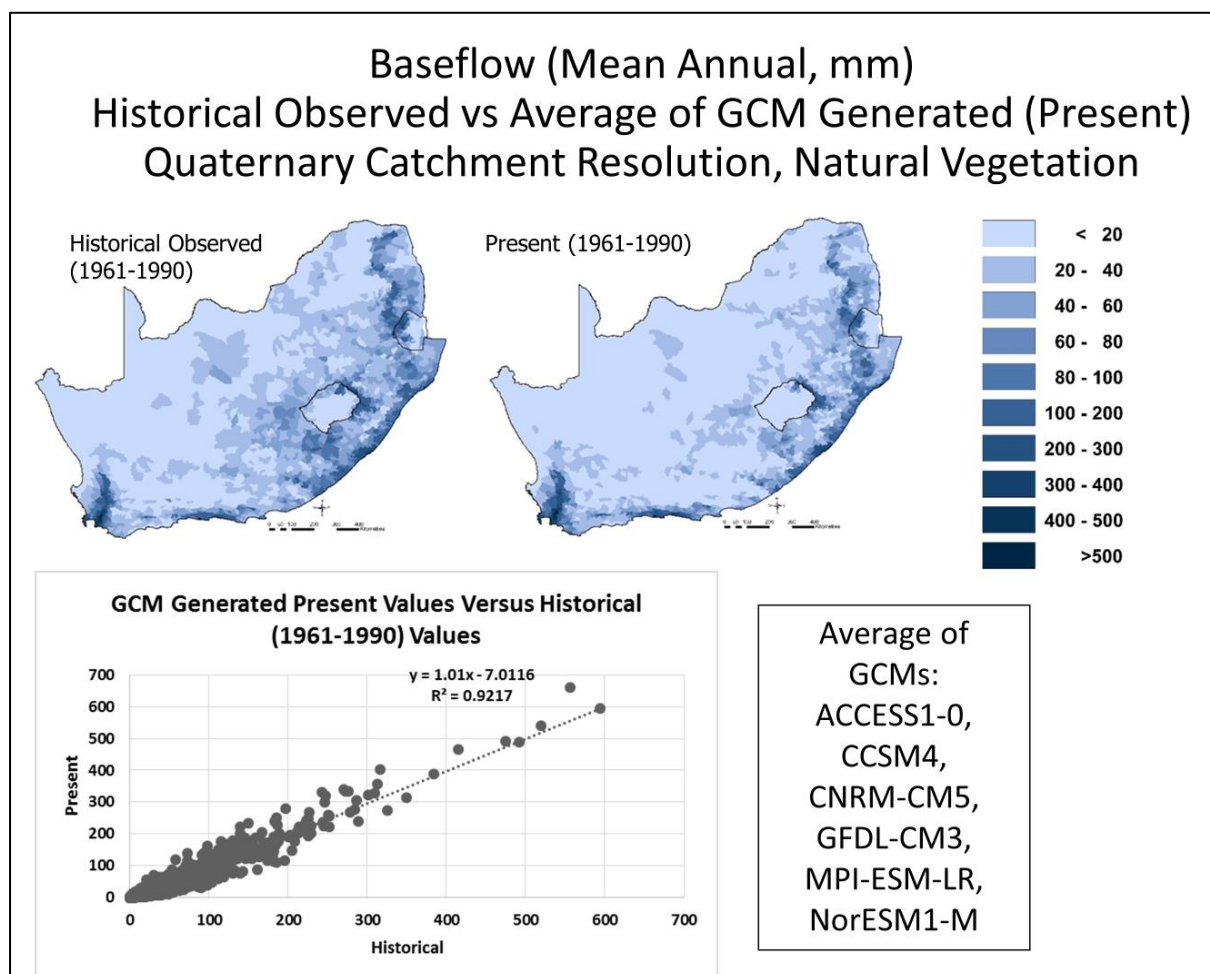
Figure 5.40   Mean annual baseflow (mm) using observed historical [left] versus GCM generated climate (present) [right] for 1961-1990, under natural vegetation land cover at Quaternary Catchment resolution

Projected changes in mean annual Baseflow into the future (**Figure 5.41**) show low absolute change for most of the region, with decreases in areas of the Western Cape and parts of the far-east. Relative changes show up higher changes (but coming from a general low base), generally showing a reduction in the west, a, increase in certain sections of the interior and a patchy picture for the rest.
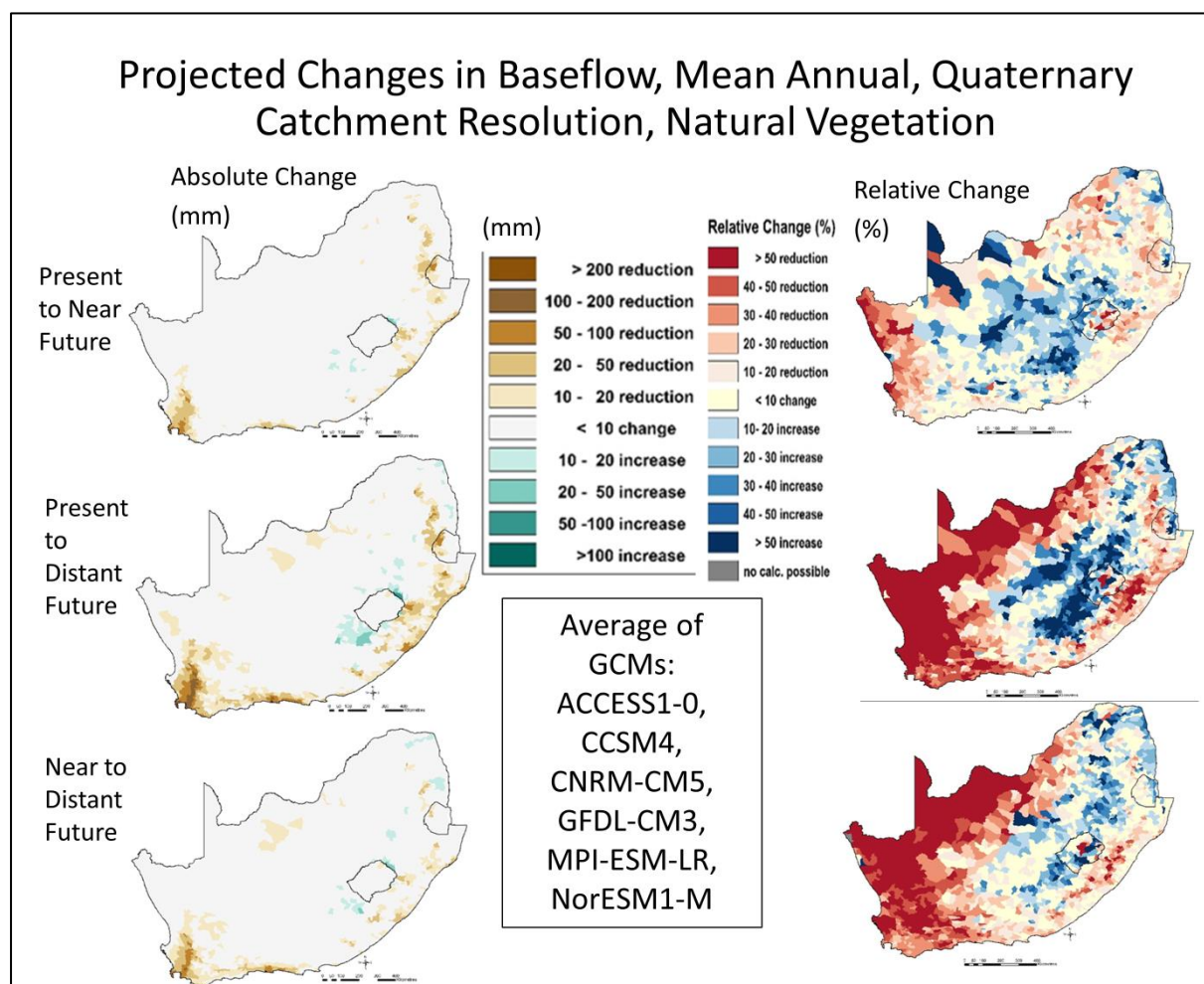
Figure 5.41 Projected absolute (mm) [left] and relative (%) [right] Quaternary Catchment mean annual baseflow, from the present (1961-1990) to the near future (2015-2044) [top], from the present to the distant future (2070-2099) [middle] and from the near to the distant future [bottom], under natural vegetation cover

Baseflows under actual land cover

Mean annual baseflow (**Figure 5.42**) for historical and GCM generated present climate (1961-1990) generally show low baseflow values except for the far-east and extreme south.
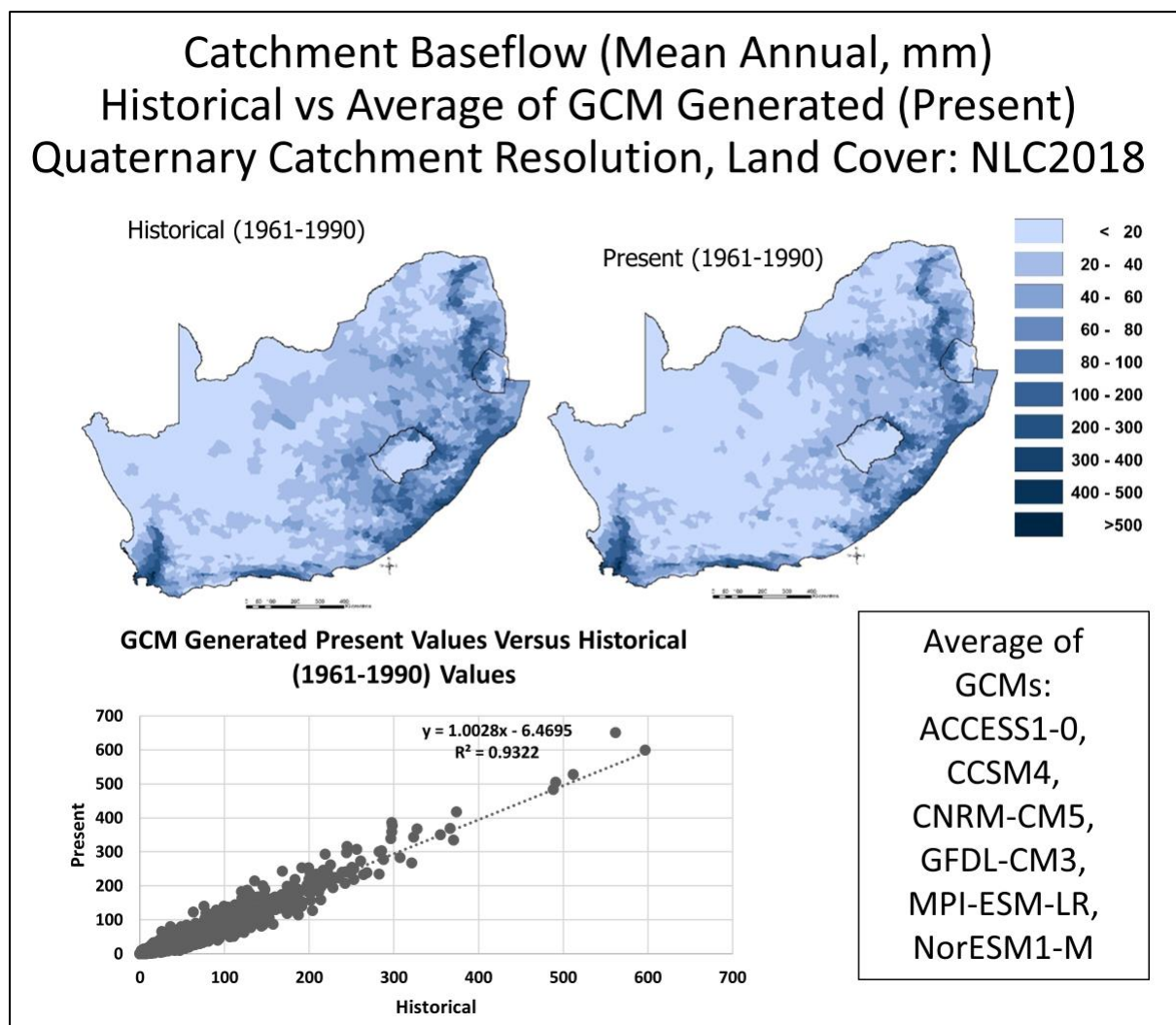
Figure 5.42   Mean annual catchment baseflow (mm) using historical [left] versus GCM generated climate for the present time period (1961-1990) [right] at Quaternary Catchment resolution and NLC2018

Projected changes in mean annual baseflow into the future (**Figure 5.43**) show low absolute change for most of the region, with decreases in areas of the Western Cape and parts of the far-east. The relative changes are greater (but coming from a general low base), generally showing a reduction in the west, an increase in certain sections of the interior and a patchy picture for the rest.
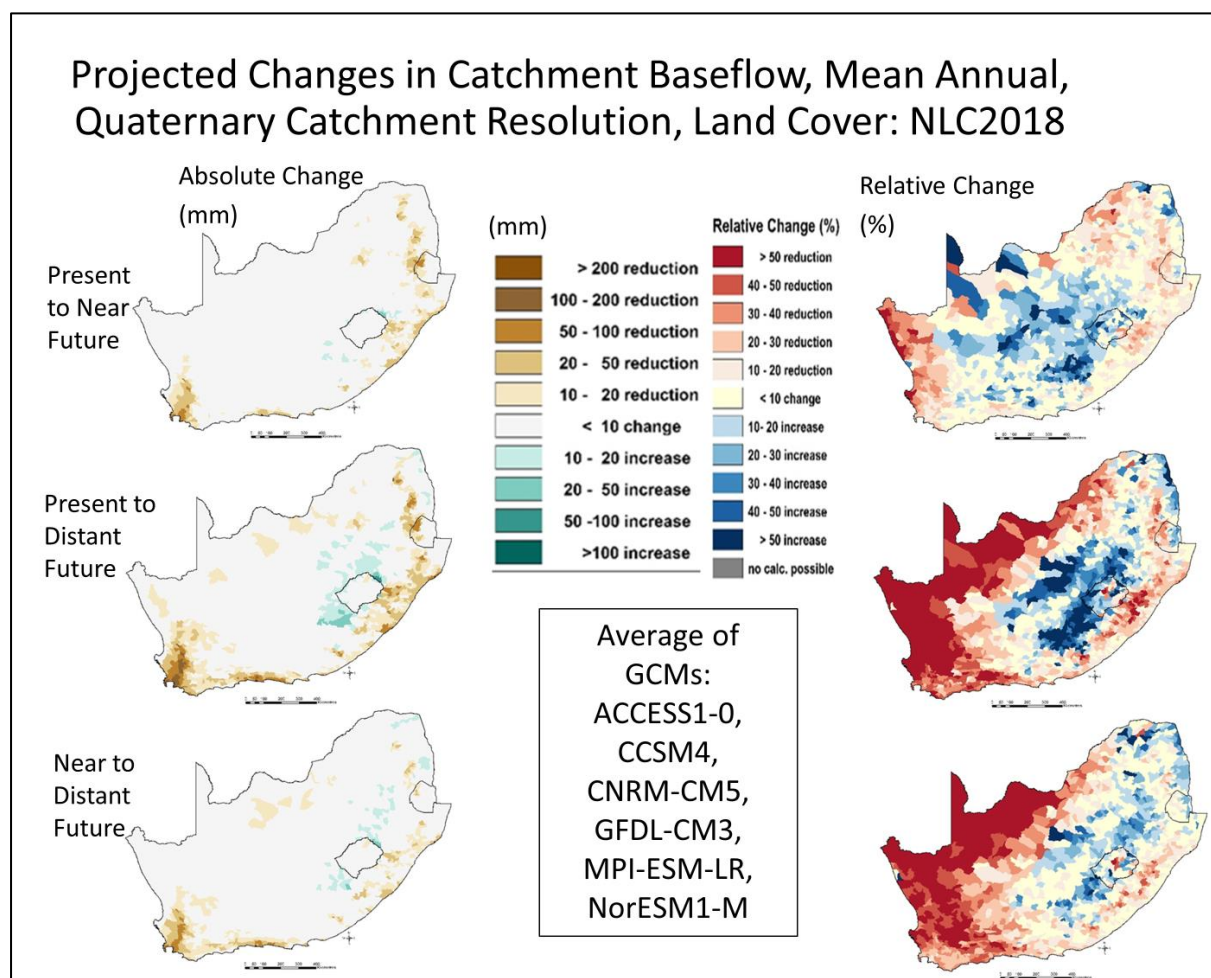
Figure 5.43 Projected absolute (mm) [left] and relative (%) [right] of mean annual baseflow, from present (1961-1990) to near future (2015-2044) [top], from present to distant future (2070-2099) [middle] and from near to the distant future [bottom] at Quaternary Catchment resolution and NLC2018

As for the previous variables, when comparing the results with the results from natural vegetation these look similar, with some localised differences. Any land cover impacts thus would need to be analysed on a finer scale.

5.2.8   Confidence in the results

It is not possible to verify the model results projected climate at this point in time. This will only be possible in the future, when looking back at the past. However, the projected hydrological responses using the various GCMs used can be compared for similarities and differences. A method of doing this is to calculate the ratio of the results of the relevant time periods for each GCM, for example, the results of the near future to the present. Then the coefficient of variation, CV%, among the ratios from all GCMs is calculated, with CV% being the standard deviation over the mean, expressed as a %. This is calculated for mean annual rainfall for the altitudinal Quinary Catchment No 1 (A10A1) in **Table 5.1** as a clarification of the method.

Table 5.1   Standard deviation and coefficient of variation calculated from mean annual projected rainfall of six GCMs, for Altitudinal Quinary Catchment 1 (A10A1)

GCM abbreviation	Mean annual Rainfall 1961-1990	Mean annual Rainfall 2015-2044	Ratio	Average of ratios	Standard Deviation of ratios	Coefficient of Variation (%) of ratios
acc	600.98	576.59	0.96	0.98	0.07	7.37
ccs	595.45	548.35	0.92			
cnr	575.24	578.78	1.00			
gfd	575.74	641.37	1.11			
mpi	561.71	563.25	1.00			
nor	591.75	525.67	0.89			

A low CV% thus implies that the individual GCMs give similar ratios, while a higher CV% implies that there is a large discrepancy among the ratios obtained from the different GCMs. By providing categories of the CV%, a confidence index (CI) can be obtained (**Table 5.2**). While the categorisation is somewhat subjective, it gives an indication of the relative confidence in the results obtained.

Table 5.2   Confidence index: categorising the coefficient of variation (%)

Coefficient of Variation (CV%) Classes	Confidence Index
0- 5	Very High
5-10	High
10-20	Medium-High
20-30	Medium
30-40	Medium-Low
40-50	Low
> 50	Very Low

The confidence indices for projected ratio changes to the near future (values of the near future over values of the present) for various variables under natural vegetation are shown in **Figure 5.44**. The confidence indices for projected ratio changes to the distant future (values of the distant future over values of the present) are shown in **Figure 5.45**. This includes the mean annual variables of rainfall, individual catchment runoff, accumulated streamflow, soil water drainage to groundwater zone, potential evaporation and actual evapotranspiration, at Quinary Catchment resolution, with the hydrological responses being modelled under the natural vegetation scenario.
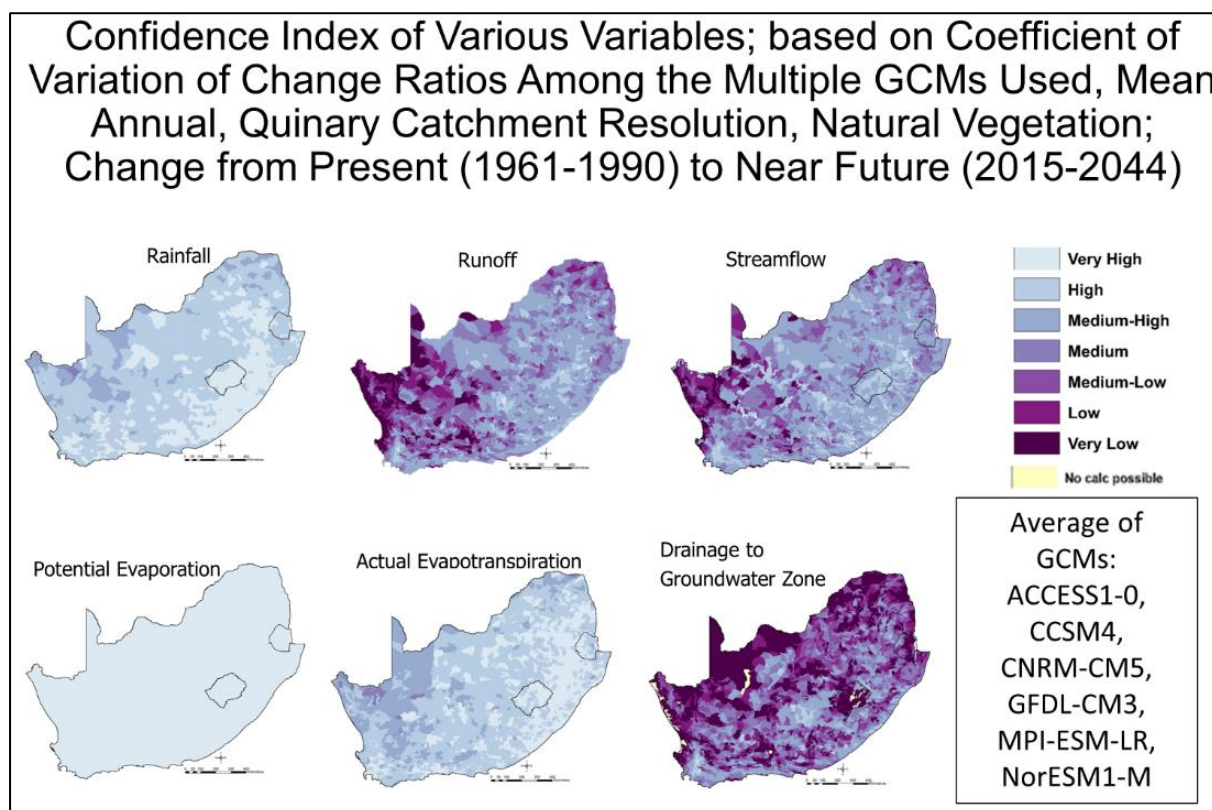
Figure 5.44 A comparison of the Confidence Index of GCM projected ratios of changes in mean annual rainfall [top left], individual catchment runoff [top middle], accumulated streamflow [top right], potential evaporation [left bottom], evapotranspiration [bottom middle] and soil water drainage to the groundwater zone [bottom right] between the near future and present for natural vegetation, at Quinary Catchment resolution
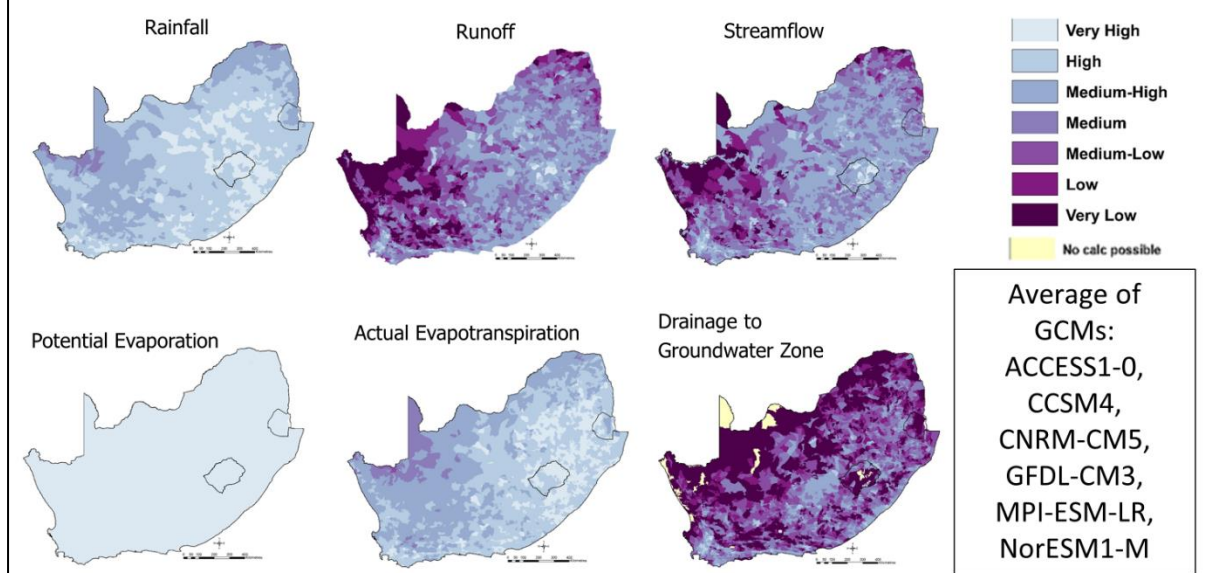
Figure 5.45   A comparison of the Confidence Index of GCM projected ratios of changes in mean annual rainfall [top left], individual catchment runoff [top middle], accumulated streamflow [top right], potential evaporation [left bottom], evapotranspiration [bottom middle] and soil water drainage to the groundwater zone [bottom right] between the near future and present for natural vegetation, at Quinary Catchment resolution

The CI of rainfall for the ratio of near future over present ranges between very high in parts of the east to medium-high and medium confidence in the more arid west. The CI of rainfall for the ratio of distant future over present shows a reduction in areas with very high confidence and an increase in areas of medium or medium-high confidence.

The CI of individual catchment runoff is much lower, being generally very low, low, medium low to medium in the west, medium and medium-low in the north and mainly medium high in the east. The reason for the much lower confidence is that runoff is dependent not only on the total amount of rainfall, but rather on the sequencing of wet days, on individual rain event characteristics (e.g. magnitude, intensity), on antecedent soil water conditions on a day of rain as well as on soil and slope characteristics and on the vegetation type on which the rain falls before being converted to runoff. The CI for the change to the near future is generally higher than that to the distant future. The runoff CI is less than that of rainfall, showing an amplification of differences among GCMs.

The CI of streamflow is also fairly low, but is higher compared to that of Catchment runoff, especially for the Quinary Catchments containing major rivers which moderate flow variability and dampen the effects of individual catchment runoff.

The CI of soil water drainage to the groundwater store is fairly low because of the various thresholds that have to be exceeded before drainage commences.

The CI of reference potential evaporation, in being temperature based and temperatures being consistently projected to increase by similar amounts among the GCMs, is very high throughout the region for both sets of ratios from near future to present and from distant future to present.

The CI of actual evapotranspiration in general is medium and medium-high in the west and high to very high in the east, with higher confidence in the change to the near future than to the distant future.

A comparison of CI of various variables shows in general that the confidence in the results are highest for potential evaporation, followed by actual evapotranspiration and rainfall, then accumulated streamflow, then runoff, with soilwater drainage to groundwater zone being the lowest.

5.2.9   Design streamflow events

Hydraulic engineering and conservation structures such as dams, bridges, culverts and stormwater systems need to be designed to accommodate floods of a certain magnitude and duration in order to function safely at a given level of risk. Climate change, by expected alterations to the temperature and rainfall regimes as well as increases to rainfall variability, may lead to increases in the intensity, duration and frequency of extreme rainfall events and associated flooding. Consequently, this might have serious repercussions on the design of hydraulic structures. Since the failure of such structures can have potential economic, environmental and societal repercussions, including loss of life, it can be appreciated why flood frequency analysis is of great importance.

Reliable estimates of flood frequencies derived from long time series of good quality observed streamflow data are seldom available in South Africa at the site of interest because of the lack of such streamflow data. Therefore, it is common for rainfall-based methods of flood frequency estimations to be used. In this study a continuous modelling approach to flood frequency analysis has been used, whereby floods are generated using sequences of daily rainfall which are input into the daily time-step *ACRU* hydrological model.

The term "design streamflow" is used to describe the depth (i.e. magnitude, in m³ or in mm equivalents) of streamflow, for a critical duration (where longer durations are important when considering designs on larger catchments, as well as for multiple day flooding and for regional damage assessments), for a desired frequency of recurrence (e.g. once in 10 or 50 years, depending on the size and economic importance of the structure), where the frequency is commonly referred to as the return period and where a return period of, say, 20 years implies a statistical probability of recurrence once in 20 years or 5 times in 100 years, and not that it will recur regularly every 20 years. Design streamflows can be expressed either in mm equivalents or, as below, as a volume in m^3.

One day design streamflows in thousands of m^3 for the 10 year return period (**Figure 5.46** left) and the 50 year return period (**Figure 5.46** right) under historical climatic conditions show clearly the increase in flow magnitudes for the 50 year event, and the increase in accumulated flow magnitudes as one moves downstream large river systems.
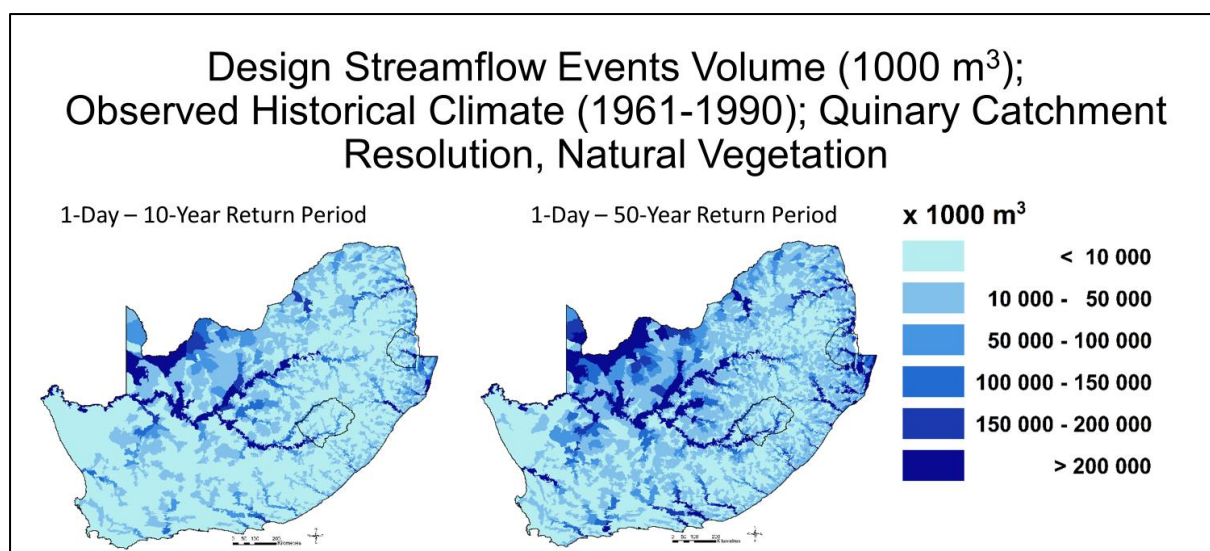
Figure 5.46   Design streamflows under historical climatic conditions for the 1:10-year return period 1-day (left) and the 1:50-year 1-day (right)

Projected changes into the near future (**Figure 5.47**) show an increase over most of the country, of between 1 to 1.6 times. Generally the 1 day 50-year return event shows bigger increases compared to the 1 day 10 year return event. A more localised analysis is required for more detailed results. Future research could also include changes in design streamflow into the distant future.
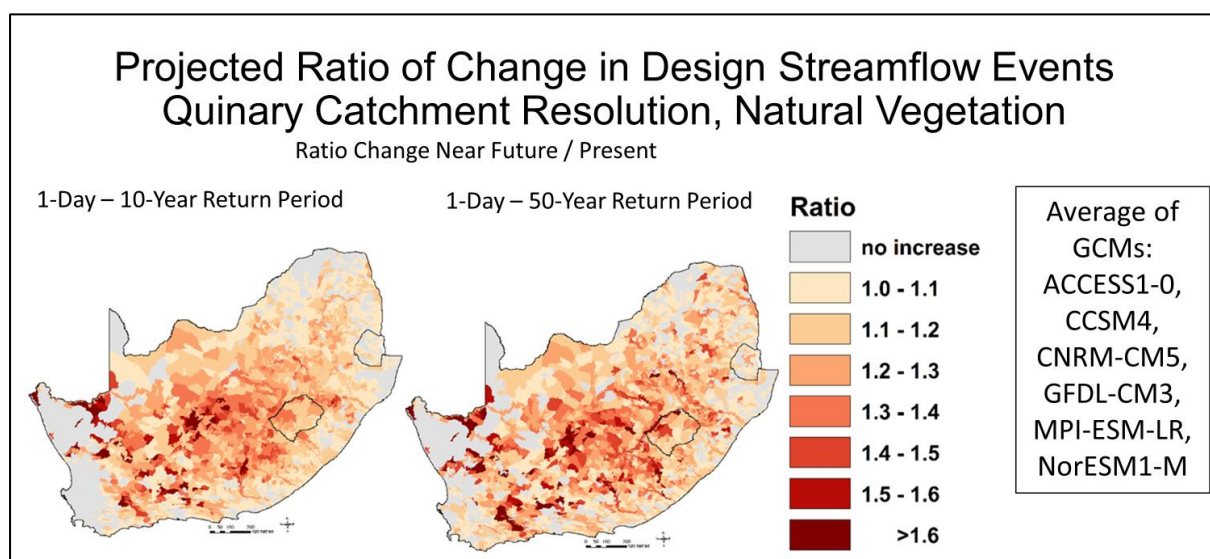
Figure 5.47   Projected changes from the present to the near future in design streamflow for the 1:10-year return period 1-day (left) and the 1:50-year 1-day (right), derived from outputs of multiple GCMs

5.3   Discussion

The results of hydrological drivers and responses to projected climate change are summarised in **Table 5.3.** The projected changes found are of mixed severity and direction and can be further analysed, e.g. on a more local level and/or for monthly and/or seasonal changes. Also more emphasis could be put on comparing the results under actual land cover versus those under natural vegetation.

Table 5.3   Summary of results of hydrological drivers and responses to projected climate change

Hydrological Variable	Summary of Results
	Spatial Distribution: under Historical Climate Conditions Projected Changes: from the Present to the Near and Distant Future Confidence in Results: The six GCMs project similarly or differently
Potential Evaporation	Spatial Distribution: Higher reference potential evaporation in the north and lower potential evaporation around the coast and adjacent interior. Projected Changes: Increases throughout and larger increases towards the distant future, especially in the north-west, the north and the interior. The east coast in general shows a smaller increase in potential evaporation. Confidence in Results: Very high throughout the region.
Rainfall	Spatial Distribution: More rainfall in the east and along the coast in the east and south and much less rainfall for the west and north-west. Projected Changes: Reduction in rainfall in the west and north, especially towards the distant future. Along the east coast the changes are mixed. In the eastern interior, in the Drakensberg area more rainfall is projected for the near future and even more for the distant future. Confidence in Results: Generally very high to high, with a higher confidence in higher rainfall regions.
Actual Evapo-transpiration	Spatial Distribution: Evapotranspiration is much higher in the wetter east and lower in the drier west of the country. Projected Changes: Projected changes in evapotranspiration into the future show milder changes for the near future and more extreme changes for the distant future. The west and north of the country have a projected reduction in evapotranspiration, the interior shows no changes, but the Drakensberg area show increases in evapotranspiration. Confidence in Results: Generally from very high through high to medium, with lower confidence in the drier regions.

Individual Catchment Runoff (both under natural vegetation and actual land cover)	<u>Spatial Distribution</u>: Catchment runoff is much higher in the wetter east and lower in the drier north-west of the country. <u>Projected Changes</u>: Smaller changes for the near future and more extreme changes for the distant future are projected. For the west, a reduction in runoff is projected, but this more severe for the distant future. The area around Cape Town shows sizeable relative and absolute reductions. The interior and to a lesser extent the north-east are projected to produce more runoff, compared to present conditions, especially for the distant future. The east coast generally shows little to no changes, though there are a few patches with more significant local changes in either direction. <u>Confidence in Results</u>: Ranges from high to very low, generally lower in the west and the extreme north, with patchy spatial pattern.
Accumulated Streamflow (both under natural vegetation and actual land cover)	<u>Spatial Distribution</u>: More streamflow in the east and south around Cape Town, but very little in the west, except for the Quinary Catchments that contain the large rivers flowing west. <u>Projected Changes</u>: Projected streamflow into the near future show mixed changes. There is a general reduction in the west, a lesser reduction in the far north, an increase in the interior and little change around the eastern coast. The changes are more extreme towards the distant future. <u>Confidence in Results</u>: Similar to runoff, except for the bigger river systems, which have a higher confidence than that of the surrounding catchments.
Soil Water Drainage into the Groundwater Zone (under actual land cover)	<u>Spatial Distribution:</u> Higher magnitudes of drainage in the wetter parts of the region is seen. <u>Projected Changes:</u> Absolute changes are small for most of the region, but especially into the distant future a reduction can be seen in areas of the Western Cape and along some eastern regions and some increases along the Drakensberg. In relative terms the generally a reduction can be seen especially towards the distant future in the west as well as along the east coast, but increases in the eastern interior and the far north. <u>Confidence in Results:</u> The confidence index of soil water drainage to the groundwater store is fairly low compared to other variables because of the various thresholds that have to be exceeded before drainage commences.
Baseflow (under actual land cover)	<u>Spatial Distribution:</u> Higher magnitudes of baseflow in the wetter parts of the region is seen. <u>Projected Changes:</u> Absolute changes are small for most of the region, but especially into the distant future a reduction can be seen in areas of the Western Cape and along some eastern regions and some increases along the Drakensberg. In relative terms generally a reduction can be seen, especially towards the distant future in the west as well as along the east coast, but increases in the eastern interior and the far north.

Projected changes to median monthly rainfall show mixed results. October rainfall generally shows small decreases over most of the country with small increases over some areas in the interior, but quite severe decreases are projected over the north-east especially into the distant future. January rainfall generally shows increases in the interior and decreases in the south and mixed changes along the east coast. April rainfall generally shows decreases in the west and north and increases in the east. July rainfall generally show small decreases in the north and the interior, with small increases along the east. The north-east seems to have a decrease in spring rain but an increase in rainfall in summer, thus a shift in the onset of rain later towards summer. Spring rains generally show reductions over nearly all of southern Africa.

Seasonal changes in median streamflow (mm) for the spring period (September to November) shows small absolute changes, with small increases in the interior and small decreases along the coast and bigger decreases around the western part of the Western Cape. Changes for summer (December to February) streamflow shows small absolute increases in the interior, more towards the distant future. Small decreases can be seen in patches in the west, with the patches increasing towards the distant future. Projected changes in median streamflows for autumn (March to May) shows small increases in the interior, more towards the distant future for the Orange catchment, and decreases along the coast and north-west. Projected changes in median winter (June to August) streamflows shows small increases in the interior and small decreases along the coast and the north-west, with larger decreases in the western part of the Western Cape. This winter rainfall area stands out with projected reductions in winter streamflow, and the same can also be seen to a lesser degree for spring streamflow. For future research, it would be beneficial to determine changes in streamflow volume, as that might be more important to the water management and planning sector.

Projected changes in design streamflow into the near future show an increase over most of the country, of between 1 to 1.6 times. Generally the 1 day 50-year return event shows bigger increases compared to the 1 day 10-year return event. A more localised analysis is required for more detailed results. Future research could also include changes in design streamflow into the distant future.

The confidence with which the different GCMs give similar projections of change is very high for potential evaporation, in general high for rainfall and evapotranspiration, but overall much lower for individual catchment runoff and for accumulated streamflow as well as for soil water drainage into the groundwater zone. The confidence in streamflow is higher than that of individual catchment runoff, but lower than the first order inputs. In general the confidence in the results is lower in the west and higher in the east. Furthermore, the confidence is generally higher for the change from present to near future compared to present to distant future. The ratios of change among the six GCMs between the present and the immediate future and the present and distant future in the hydrological drivers of reference potential evaporation and rainfall, as well as in the hydrological responses of actual evapotranspiration, individual catchment runoff, accumulated streamflow and soil water drainage into the groundwater zone display progressively lower confidence. This must be borne in mind when developing adaptation strategies.

5.4   Recommendations

Projected climate change impacts on runoff, streamflow and baseflow were shown for the southern African region of South Africa, Eswatini and Lesotho. Climate change impacts result in projected changes of mixed severity and direction within the region. This allows for general adaptation strategies.

While modelling was done for natural vegetation and actual land cover, the comparison of results due to land cover impact was beyond this study, but could be done using the outputs from this study.

The results presented, inclusive the confidence analysis in the projected results, thus far, is based only on annual values, except for rainfall and streamflow, where some monthly and seasonal analysis was undertaken. It would be beneficial to examine monthly and/or seasonal changes for the other variables.

The results of projected changes found are of mixed severity and direction and thus require further in-depth analysis, if local recommendations are required. Risk determination is required on a more local basis. This could be in the form of a more detailed analysis for the individual Water Management Areas or Primary Catchments. A summary of results per Hydro-Climatic Zone is provided later in Chapter 7.

For a more detailed localised approach, analysis on a more local level is recommended. This could be for individual primary catchments or Water Management areas. A case study of the Limpopo Primary Catchment is presented in Chapter 8.

5.5   References

DEA and GTI (2019) *73 Class GTI South African National Land Cover Dataset (2018)* [Dataset]. Produced by GeoTerraImage Pty Ltd (GTI) for the Department of Environmental Affairs (DEA), Pretoria, South Africa.

SCHULZE RE and HORAN M (2010) Methods 1: Delineation Of South Africa, Lesotho And Swaziland Into Quinary Catchments. In: *Methodological Approaches to Assessing Eco-Hydrological Responses to Climate Change in South Africa,* SCHULZE R, HEWITSON B, BARICHIEVY K, TADROSS M, KUNZ R, HORAN M and LUMSDEN T. Research report no. 1562/1/10, Water Research Commission, Pretoria, South Africa.

SCHULZE RE and KUNZ RP (2011) Climate Change and Annual Temperature Statistics: A 2011 Perspective. In: *A 2011 Perspective on Climate Change and the South African Water Sector,* SCHULZE RE, Research report 1843/2/11, Chapter 3.1, 73-77, Water Research Commission, Pretoria, South Africa.

TOUCHER ML, RAMJEAWON M, MCNAMARA MA, ROUGET M, BULCOCK H, KUNZ RP, MOONSAMY J, MENGISTU M, NAIDOO T, VATHER T and ALDWORTH TA (2019) *Resetting The Baseline Land Cover Against Which Streamflow Reduction Activities And The Hydrological Impacts Of Land Use Change Are Assessed.* Research report 2437/1/19, Water Research Commission, Pretoria, South Africa

6   PROJECTED IMPACTS OF CLIMATE CHANGE ON HYDROLOGICAL YIELD

S. Schütte, J.C. Smithers and D.J. Clark

This section addresses Aim 2, 'Assess impacts of climate change on the hydrological yield within hydro-climatic zones based on medium to short-, medium- and long-term climate projections and taking into consideration the attribution of non-climatic factors'.

6.1   Introduction

It is important for water resource planning to be able to take into account impacts of climate change on future water yield. The assessment of the potential impacts of climate change on hydrological yield is a primary objective for this project. A detailed literature study on yield models was undertaken and a comparison of historical firm yields for the Midmar and Albert Falls Dams estimated using the Gould-Dincer and WRYM approaches was undertaken by Ramchandra and Clark (2020) as Chapter 2 in Deliverable 5 for this project. This chapter contains an overview of the approach adopted to determine yield and some results.

6.2   Methods

As proposed to and agreed by the Reference Group, a simple approach was adopted to determine hydrological yield. This approach is the same as that used to calculate historical firm yield, i.e. yield based on a single period of "historical" simulated runoff. The methodology adopted to determine the hydrological yield for a given sequence of flow is summarised as follows:

(i)   Three time periods were used in the analysis, i.e. present (1961-1990), near future (2015-2044) and distant future (2070-2099), i.e. 30 years of simulated runoff was used in each scenario.
(ii)   For each period, the Mean Annual Runoff (MAR) was computed using the spatially accumulated catchment runoff (CELRUN) simulated by the *ACRU* model.
(iii)   A dam with a storage capacity equal to the MAR for the present climate (1961-1990) was assumed to be located at the outlet of the catchment. This dam storage capacity remained the same for all three periods analysed.
(iv)   A simple dam water balance was computed using monthly runoff into the dam with overflow occurring when the volume exceeded the assumed dam capacity.
(v)   It was assumed that the dam was at full capacity at the start of every scenario simulated.
(vi)   A monthly demand (extraction) was included in the monthly dam water balance calculations and this demand was incrementally increased until only one failure (i.e. dam not able to meet monthly demand for one month) occurs in the 30 years of data. The hydrological yield for the time period is then computed from the monthly demand which results in the single failure.

The above procedures were repeated for all scenarios, i.e. all six individual GCMs and at the outlet from all Quaternary Catchments. The GCMs used in this project were previously described in Section 2.1.5 and the abbreviations used here are ACCESS1-0, CCSM4, CNRM-CM5, GFDL-CM3, MPI-ESM-LR, and NorESM1-M. The methods of downscaling the GCMs to regional catchment levels and bias correction was previously explained in Section 2.3. The modelling was first for naturalised flows, meaning no impact of land cover changes was taken into account, thus assuming natural vegetation, using the CWRR Clusters (Toucher et al., 2019, see Section 3.3). A second set of model runs was to repeat the above exercise, but for a land cover scenario as per National Land Cover 2018, from here on abbreviated as NLC2018 (DEA and GTI, 2019.). The modelling using actual land cover (NLC2018), however, did not include dams or water abstractions (e.g. for irrigation or urban water supply) as runoff based on actual land cover was required as an input for estimating hydrological yield. This modelling setup was previously described in Section 3.4.

The above method was coded in FORTRAN enabling the calculation of yield for all the 1 946 Quaternary Catchments in South Africa, Eswatini and Lesotho and the various climate scenarios and time periods of analysis. Absolute and relative changes from one time period to another were then calculated as per Eq.6.1 and Eq. 6.2 for each GCM and then averaged.

$$\text{Actual Change}_{GCMi,TP1to2} = Y_{GCM1,TP2} - Y_{GCMi,TP1} \qquad \text{(Eq.6.1)}$$

$$\text{Relative Change}_{GCMi,TP1to2} = 100 * (\text{Actual Change}_{GCMi,TP1to2} / Y_{GCMi,TP1}) \qquad \text{(Eq. 6.2)}$$

where

Actual Change$_{GCMi,TP1to2}$	:	change in yield (mm/annum),
Relative Change $_{GCMi,TP1to2}$	:	relative change in yield (%),
Y	:	hydrological yield (mm/annum),
GCMi	:	each of the six's GCMs (ACCESS1-0, CCSM4, CNRM-CM5, GFDL-CM3, MPI-ESM-LR, NorESM1-M),
TP1	:	baseline time period,
TP2	:	new time period,
TP1to2	:	from the baseline time period to the new time period, and
TP	:	either the present (1961-1990), the near future (2015-2044) or the distant future (2070-2099) time period.

Note: Relative change is undefined, if the divisor is zero.

Both, absolute and relative changes are useful when analysing data. Note that relative changes on small numbers often give large relative differences, while relative changes on big numbers are generally small. Actual changes on small values often look small, while absolute changes on big numbers often look large.

6.3   Results

6.3.1   Projected climate change impacts on hydrological yield under natural vegetation

Results for estimated hydrological yields using naturalised flows (for a land cover of natural vegetation using CWRR Clusters (Toucher et al., 2019) and on a national level for the selected periods of present (1961-1990), near future (2015-2044) and distant future (2070-2099), for the average of the six GCMs used for RCP8.5, are shown in **Figure 6.1**. In runoff depth terms (mm/year), the yield is higher in the east and along the east coast and towards the south, and lower in the north-west.
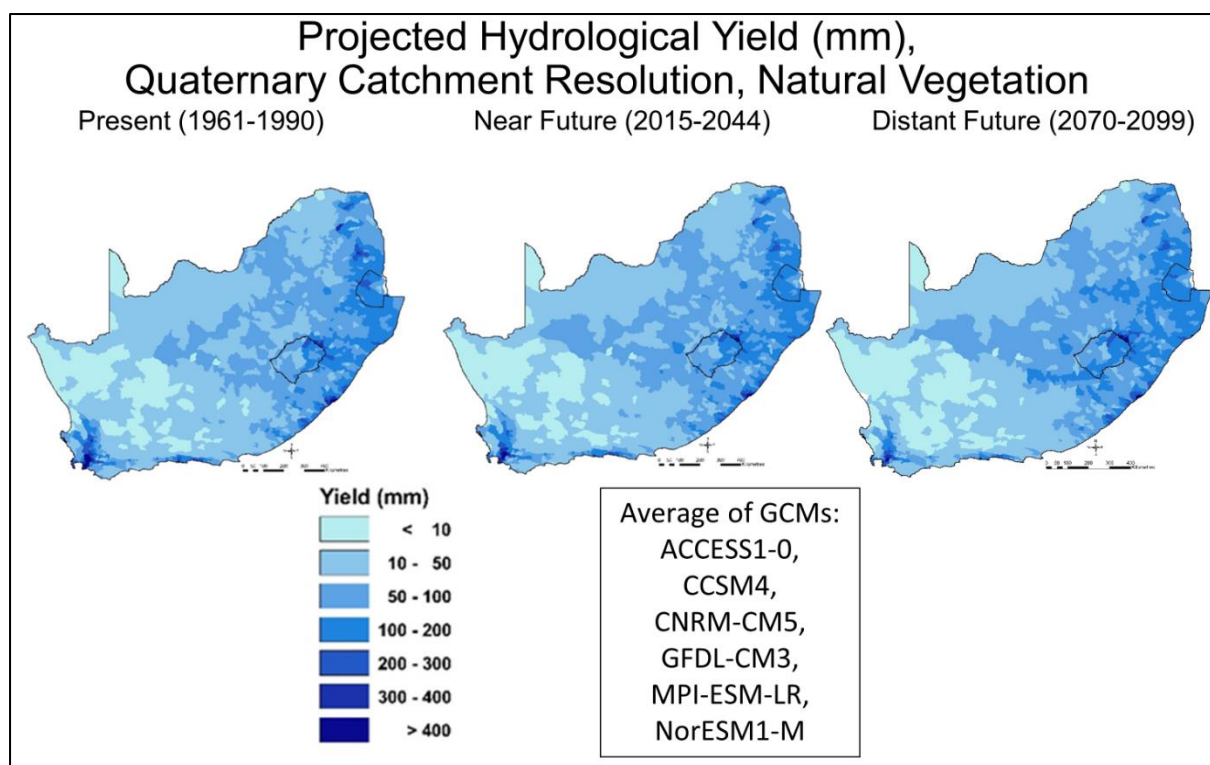
Figure 6.1   Projected yield (mm) at Quaternary Catchment resolution under natural land cover, for the present (1961-1990) [left], the near future (2015-2044) [middle] and distant future (2070-2099) [right], average of six GCMs, assuming natural vegetation

The results for the different time periods paint a similar picture for the hydrological yield at a national scale. The results are shown as absolute and relative differences in yield between two time periods in **Figure 6.2**.

The average changes in yield from multiple GCMs (**Figure 6.2**) show strong regional differences, with little or no projected change in yield for many areas, large relative reductions in yield in the west and smaller relative reductions in the north-east. The middle part of the country show relative increases in yield of up to 50%. The absolute changes in yield (in mm) for the average of the six GCMs also show large areas with little or no changes, but large reductions in parts of the Western Cape, and some areas in the north-east and east. Increases in yield are also evident in the middle of the country and for catchments where the rivers originate in this area (i.e. the Orange River system).
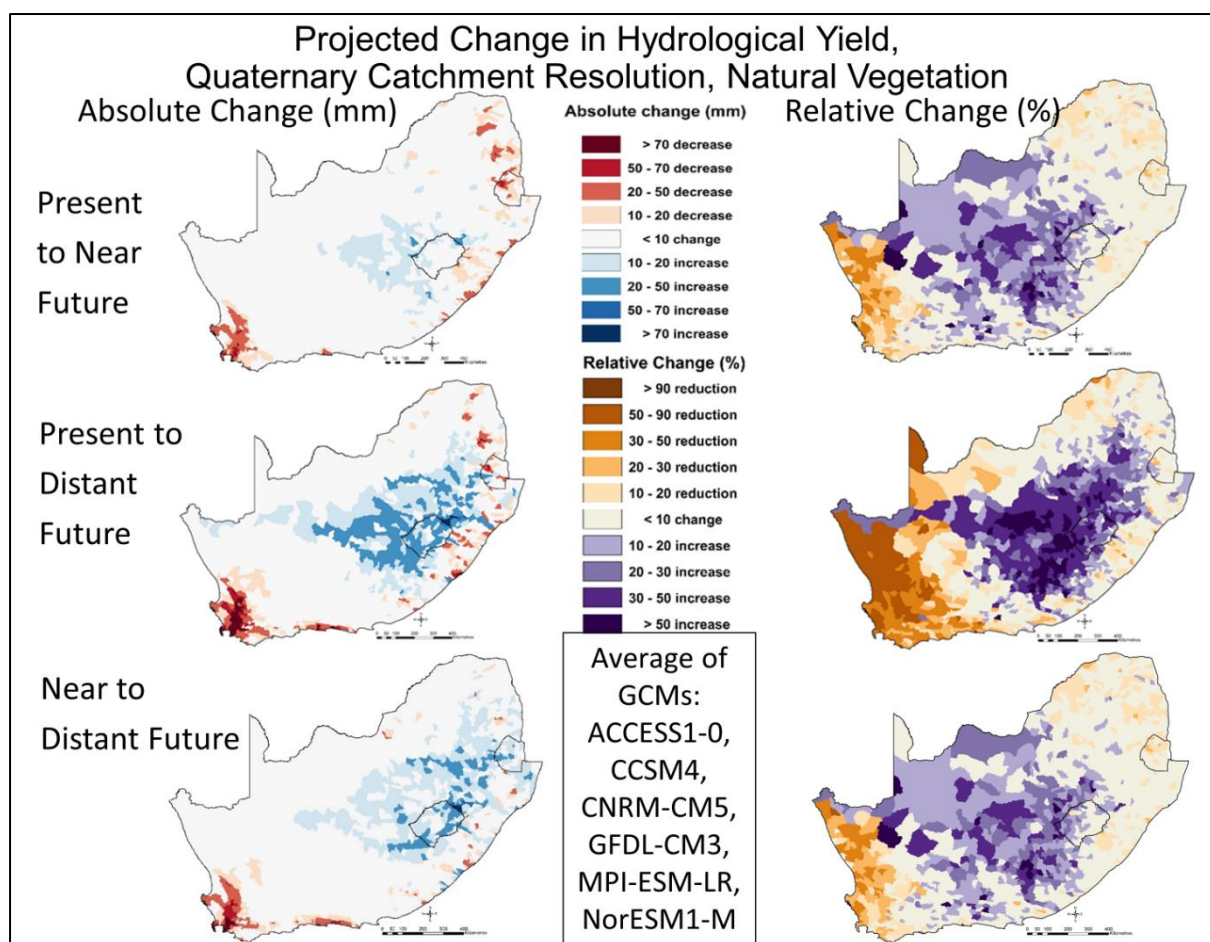
Figure 6.2   Projected absolute changes (mm) [left] and relative changes (%) [right] in hydrological yield at Quaternary Catchment resolution, for the present (1961-1990) to near future (2015-2044) [top], the present (1961-1990) to distant future (2070-2099) [middle] and near future (2015-2044) to distant future (2070-2099) [bottom], average of six GCMs, under natural vegetation land cover conditions

When zooming in, as was done for Primary Catchments U and V as an example (**Figure 6.3**), differences are evident. For example, the differences range from zero to a marked reduction in hydrological yield for Primary Catchment U, but range from zero to marked increases for Primary Catchment V, with much of the yield originating in the Drakensberg area. These changes are especially marked into the distant future period. For clarification, Primary Catchment U and V's river network is shown in **Figure 6.4**.
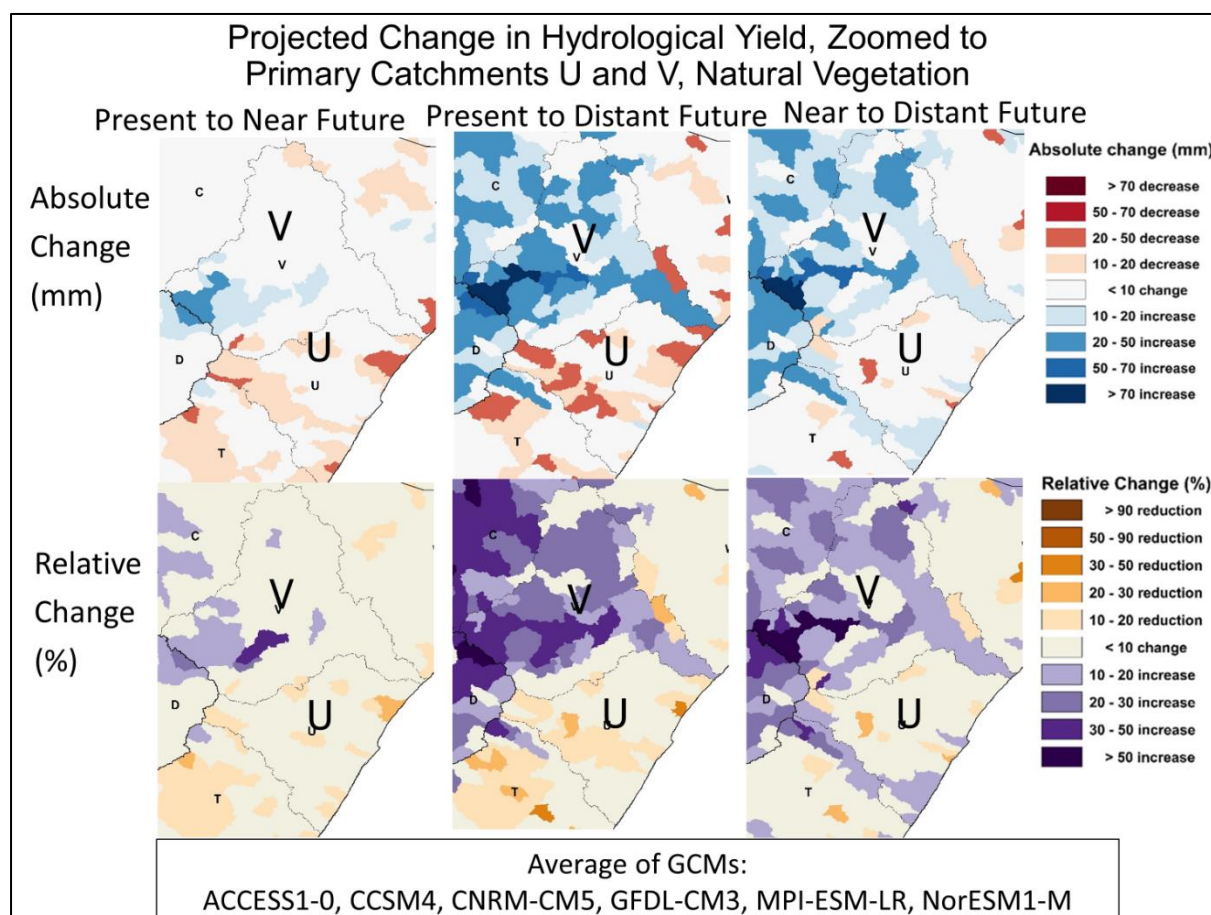
Figure 6.3   Projected absolute changes (mm) [top] and relative changes (%) [bottom] in hydrological yield of Primary Catchment U and V as examples, at Quaternary Catchment Resolution, for the present (1961-1990) to near future (2015-2044) [left], the present (1961-1990) to distant future (2070-2099) [middle] and near future (2015-2044) to distant future (2070-2099) [right], average of six GCMs, under natural vegetation land cover conditions
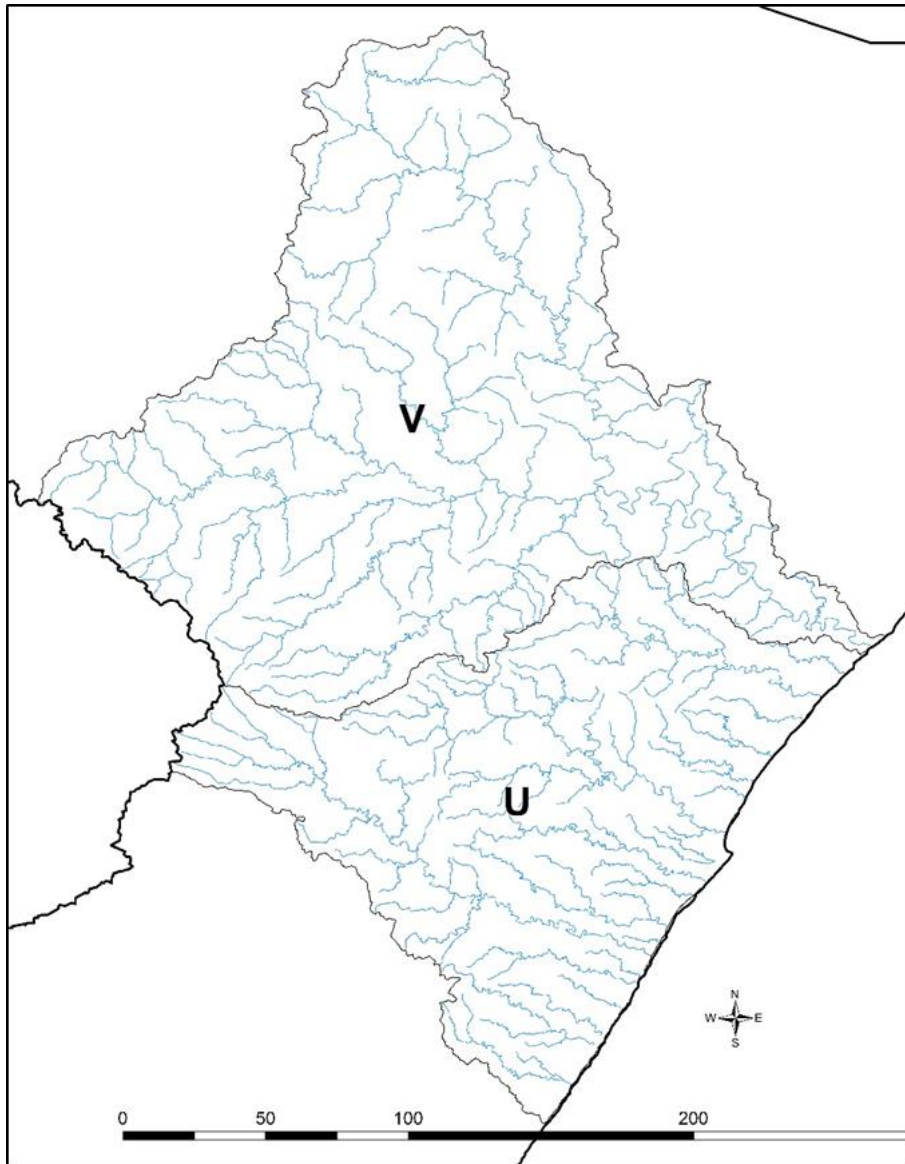
Figure 6.4   Primary Catchment U and V, with river network shown

It is not possible to verify the results for the projected future at this point in time. This will only be possible in the future, looking back at the past. However, the projected changes in yield from the various GCMs used can be compared for similarities or differences (for more details see Chapter 6). A confidence index (CI, *cv.* Chapter 6), expressed as a categorization of the coefficient of variation of the ratio of change from the individual GCMs for the hydrological yield is shown in **Figure 6.5**.

Generally, the CI is lower for Primary Catchment D, E, F, G, J and L, compared to the other Primary Catchments. This means that the projections differ more amongst the GCMs for those catchments.
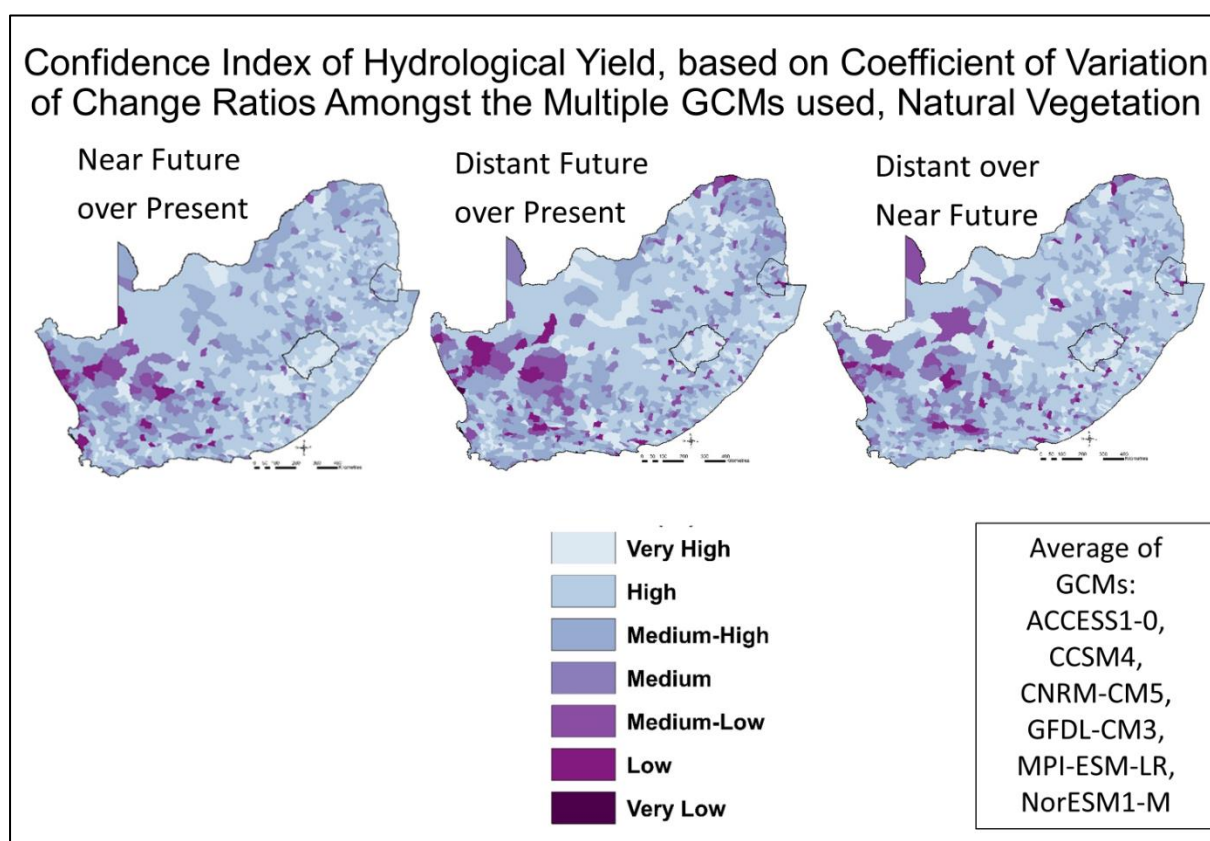
Figure 6.5   Confidence Index of projected ratios of the yield into the future, under natural vegetation land cover conditions, at Quaternary Catchment resolution

6.3.2 Projected climate change impacts on hydrological yield under actual land cover

In many places, natural vegetation has been replaced with certain anthropogenic land uses, which may impact the hydrological yield. While land use is unlikely to remain static, for this project and scenario analysis, the national land cover as per NLC2018 (DEA and GTI, 2019) was assumed and applied in the modelling setup, for all time periods.

Results for hydrological yields under NLC2018 for the selected periods of present (1961-1990), near future (2015-2044) and distant future (2070-2099), for the average of the six GCMs used for RCP8.5 are shown in **Figure 6.6**. In runoff depth terms, the yield is higher in the east and along the east coast and towards the south, and lower in the north-west.
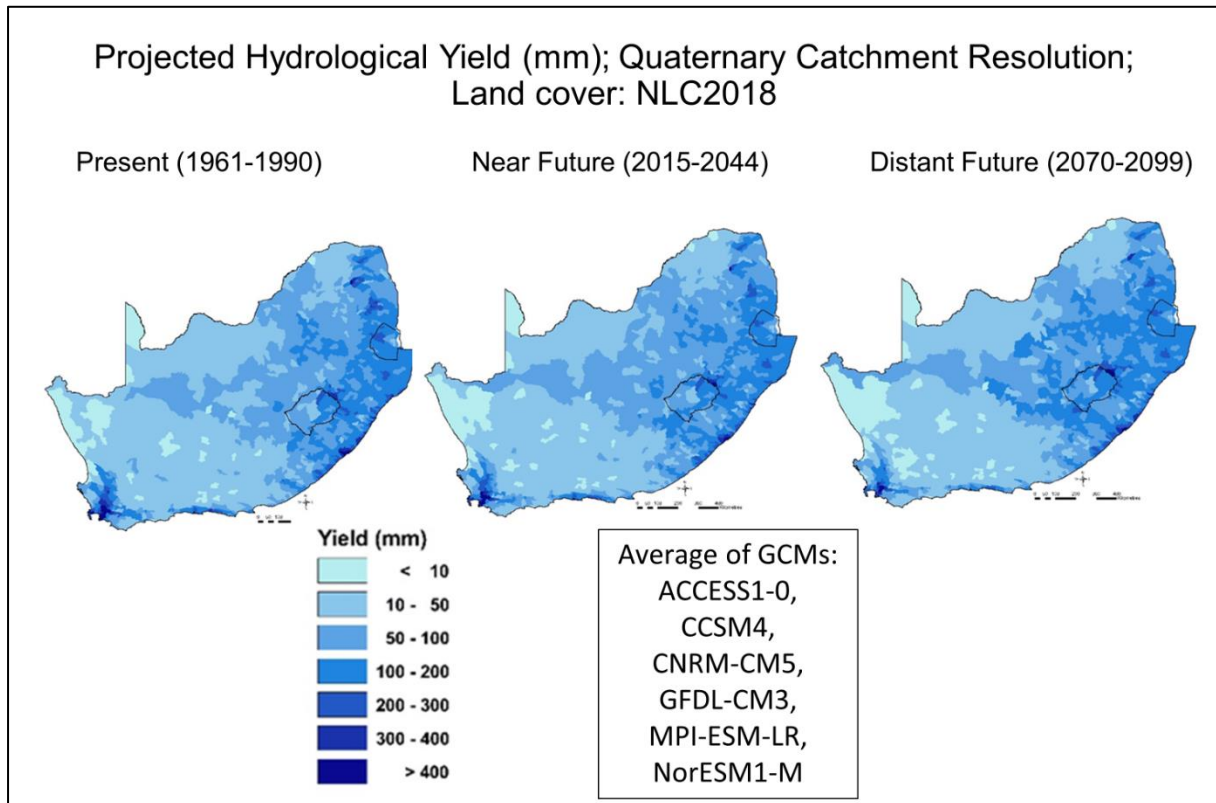
Figure 6.6   Projected hydrological yield (mm) at Quaternary Catchment resolution under natural land cover, for the present (1961-1990) [left], the near future (2015-2044) [middle] and distant future (2070-2099) [right], average of six GCMs, under actual land cover

The average projected changes from multiple GCM results (**Figure 6.7**) show both, strong regional differences, as well as no projected change in yield for many areas. Large relative reductions in yield in the west and smaller relative reductions in the north-east parts of the region are evident. The middle part of the country show relative increases in yield of up to 50%. The absolute changes in yield (in mm) for the average of the six GCMs also show large areas with no changes, but large reductions in parts of the Western Cape, and some areas in the north-east and east. Increases in yield are also evident in the middle of the country and where the rivers originate in this area.
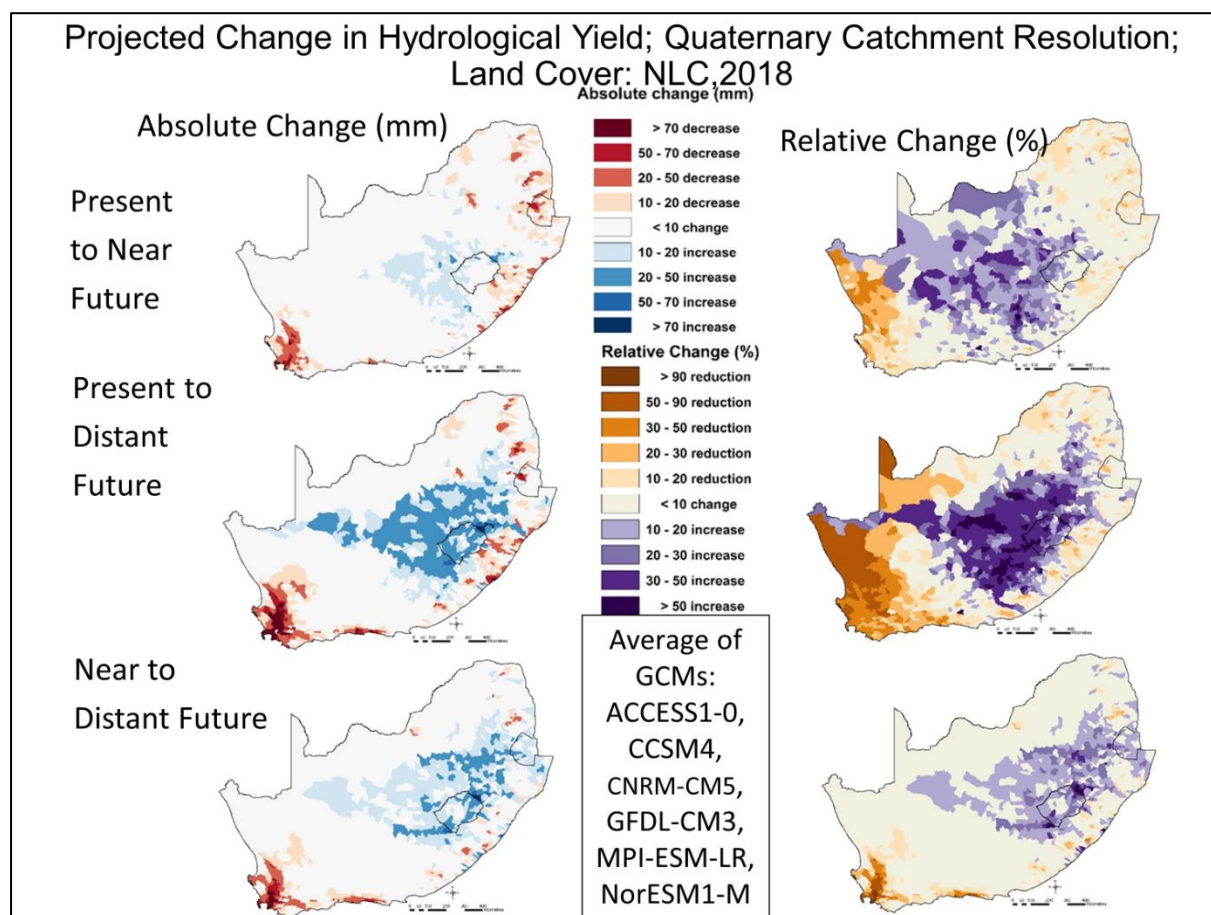
Figure 6.7   Projected absolute changes (mm) [left] and relative changes (%) [right] in hydrological yield at Quaternary Catchment resolution, for the present (1961-1990) to near future (2015-2044) [top], the present (1961-1990) to distant future (2070-2099) [middle] and near future (2015-2044) to distant future (2070-2099) [bottom], average of six GCMs, under actual land cover

Again, Primary Catchments U and V were zoomed in as an example (**Figure 6.8**). Differences can be seen, ranging from a zero to marked reduction in hydrological yield for Primary Catchment U, and from zero to marked increases in Primary Catchment V, with much of the yield originating in the Drakensberg area.
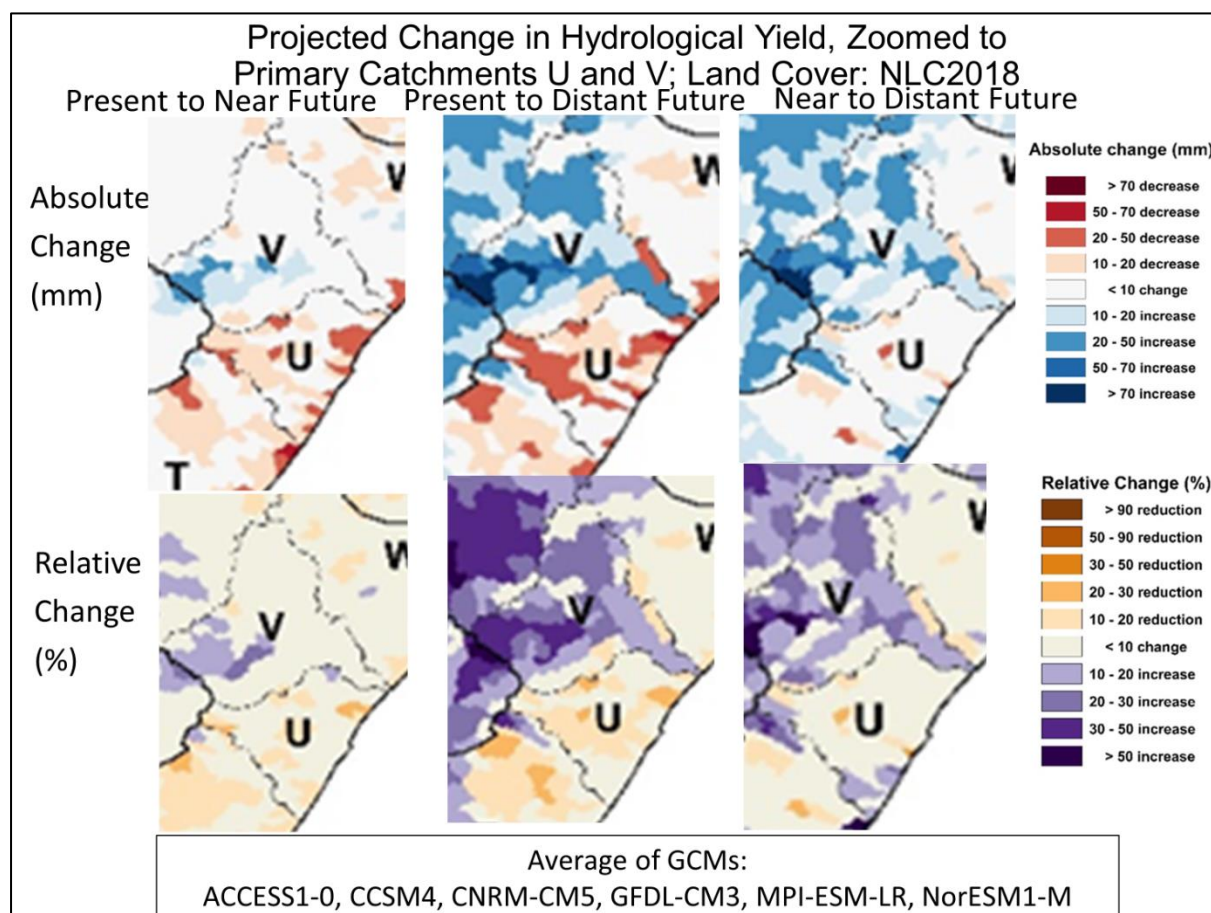
Figure 6.8   Projected absolute changes (mm) [top] and relative changes (%) [bottom] in hydrological yield of Primary Catchment U and V as examples, at Quaternary Catchment Resolution, for the present (1961-1990) to near future (2015-2044) [left], the present (1961-1990) to distant future (2070-2099) [middle] and near future (2015-2044) to distant future (2070-2099) [right], average of six GCMs, under actual land cover

6.3.3 Comparing projected climate change impacts on hydrological yield under natural vegetation to those under actual land uses

When comparing projected climate change impacts under natural vegetation to those under actual land uses, projected absolute changes (**Figure 6.9)**, relative changes (**Figure 6.10**) and actual changes zoomed to Primary Catchments U and V (**Figure 6.11**), the overall picture looks similar. However, localised changes may be magnified or muted. In some areas the yield is greater when modelled with actual (NLC2018) land cover. To understand localized changes would require further investigation, beyond the scope of this project.
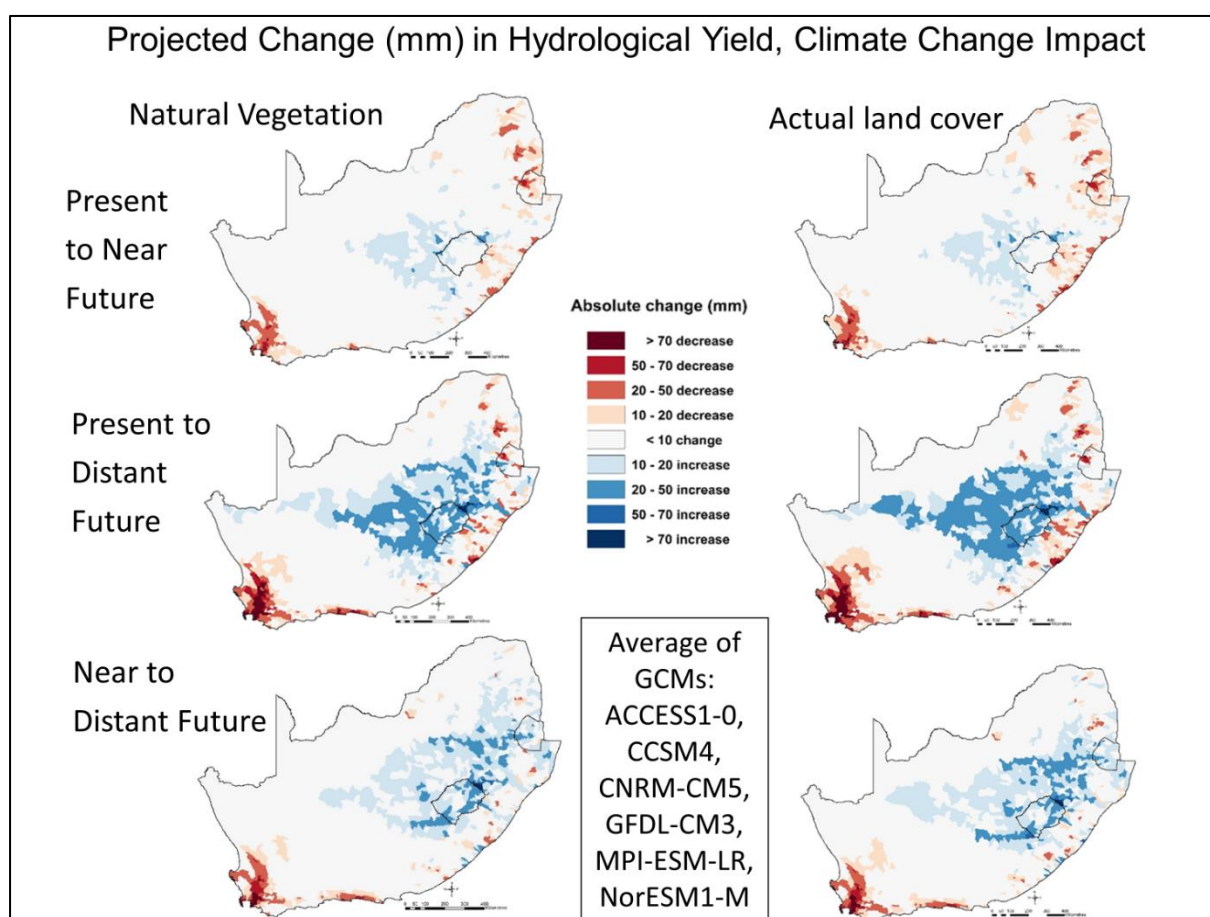
Figure 6.9   Projected absolute changes (mm) in hydrological yield for the present (1961-1990) to near future (2015-2044) [top], the present (1961-1990) to distant future (2070-2099) [middle] and near future (2015-2044) to distant future (2070-2099), under natural vegetation [left] and under actual land cover [right], at Quaternary Catchment resolution, average of six GCMs
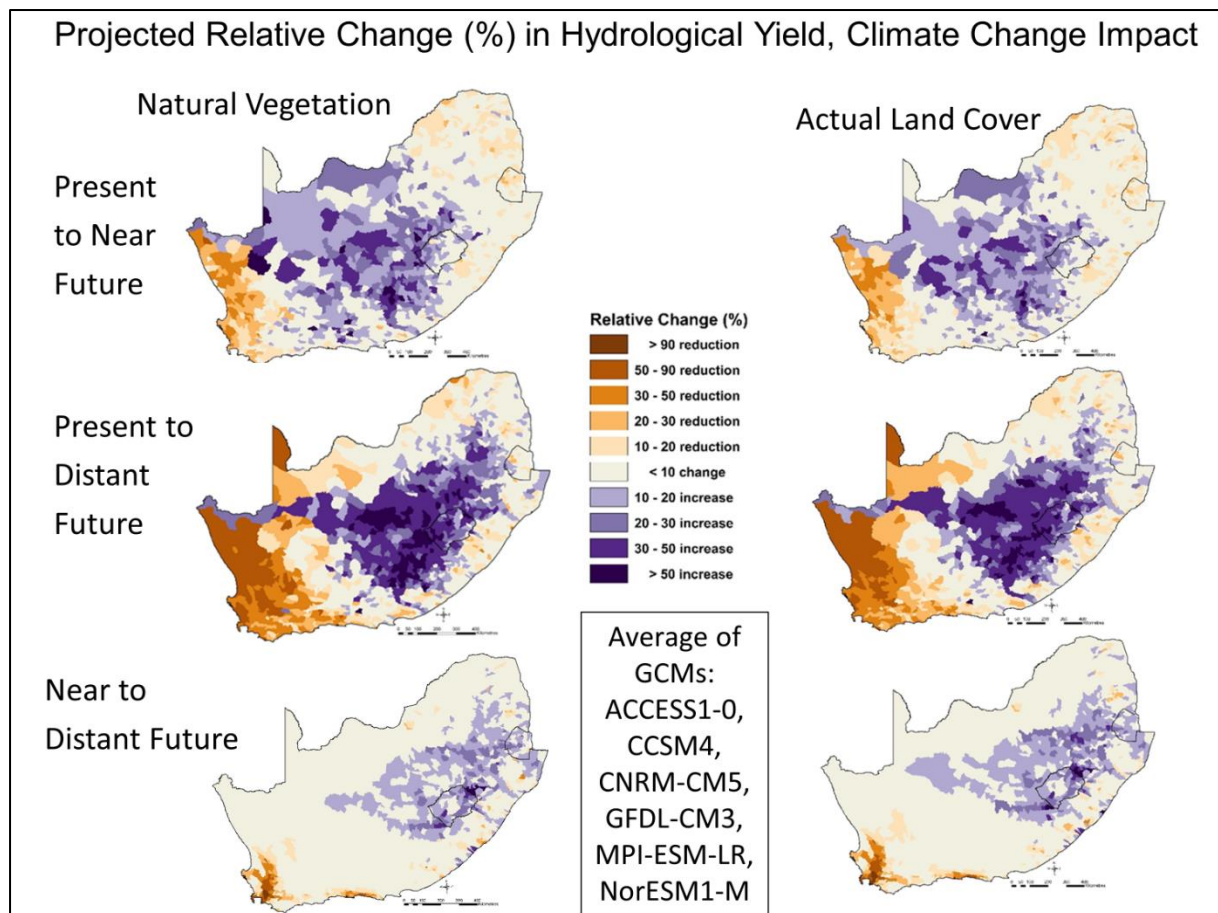
Figure 6.10   Projected relative changes (%) in hydrological yield for the present (1961-1990) to near future (2015-2044) [top], the present (1961-1990) to distant future (2070-2099) [middle] and near future (2015-2044) to distant future (2070-2099) [bottom], under natural vegetation [left] and under actual land cover [right], at Quaternary Catchment resolution, average of six GCMs
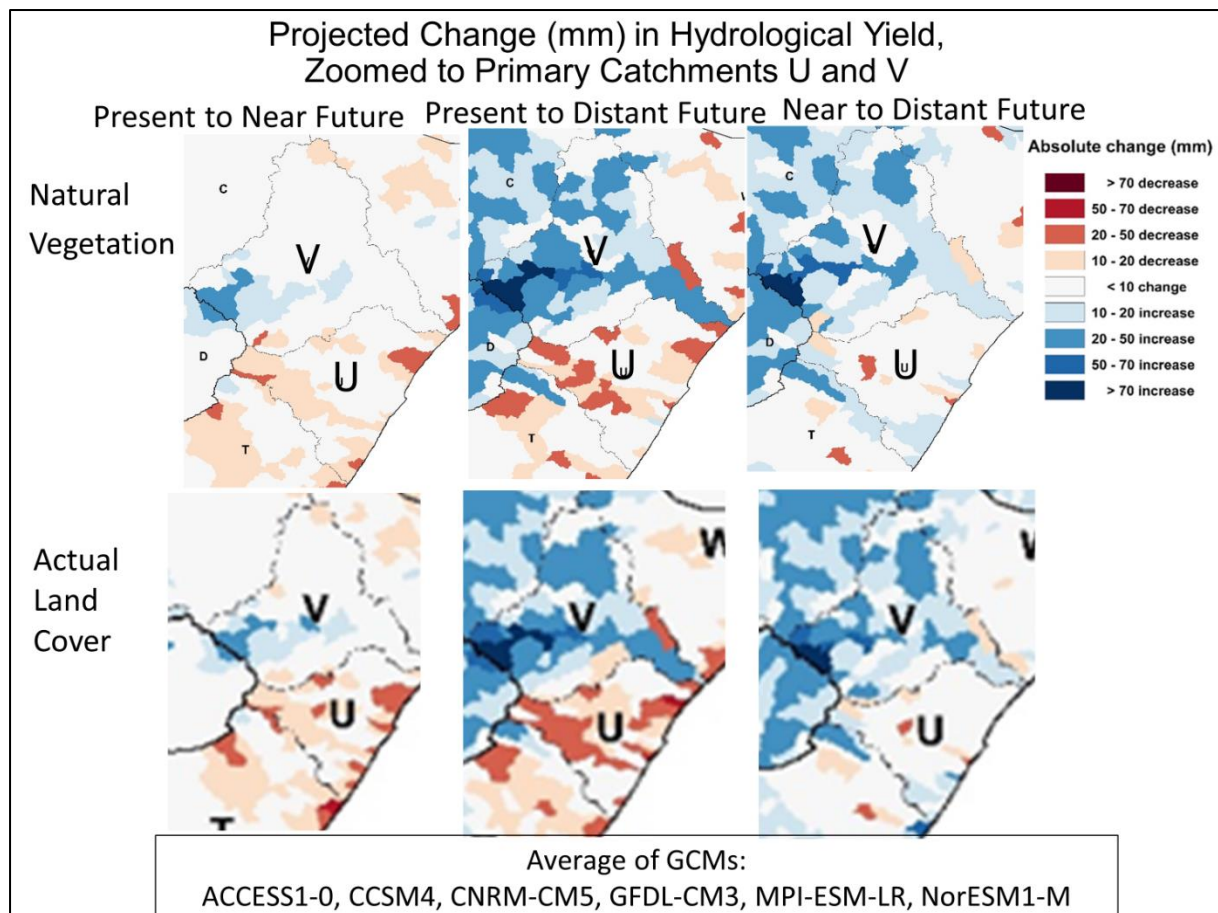
Figure 6.11 Projected absolute changes (mm) in hydrological yield of Primary Catchment U and V as examples, for the present (1961-1990) to near future (2015-2044) [left], the present (1961-1990) to distant future (2070-2099) [middle] and near future (2015-2044) to distant future (2070-2099) [right], average of six GCMs, under natural vegetation [left] and under actual land cover [right], at Quaternary Catchment resolution, average of six GCMs

Actual land cover impacts on yield, compared to natural vegetation (**Figure 6.12**), for the present, for the near future and for the distant future, in general show either zero to small absolute changes, while several areas in the south west, the east and the interior show an increase of up to 30 mm in hydrological yield, with only very small areas in the east show a decrease. Relative changes show generally large increase in the south-west, where most areas have relatively low yields, and increases in parts of the eastern interior, with other areas showing less than 10% change.
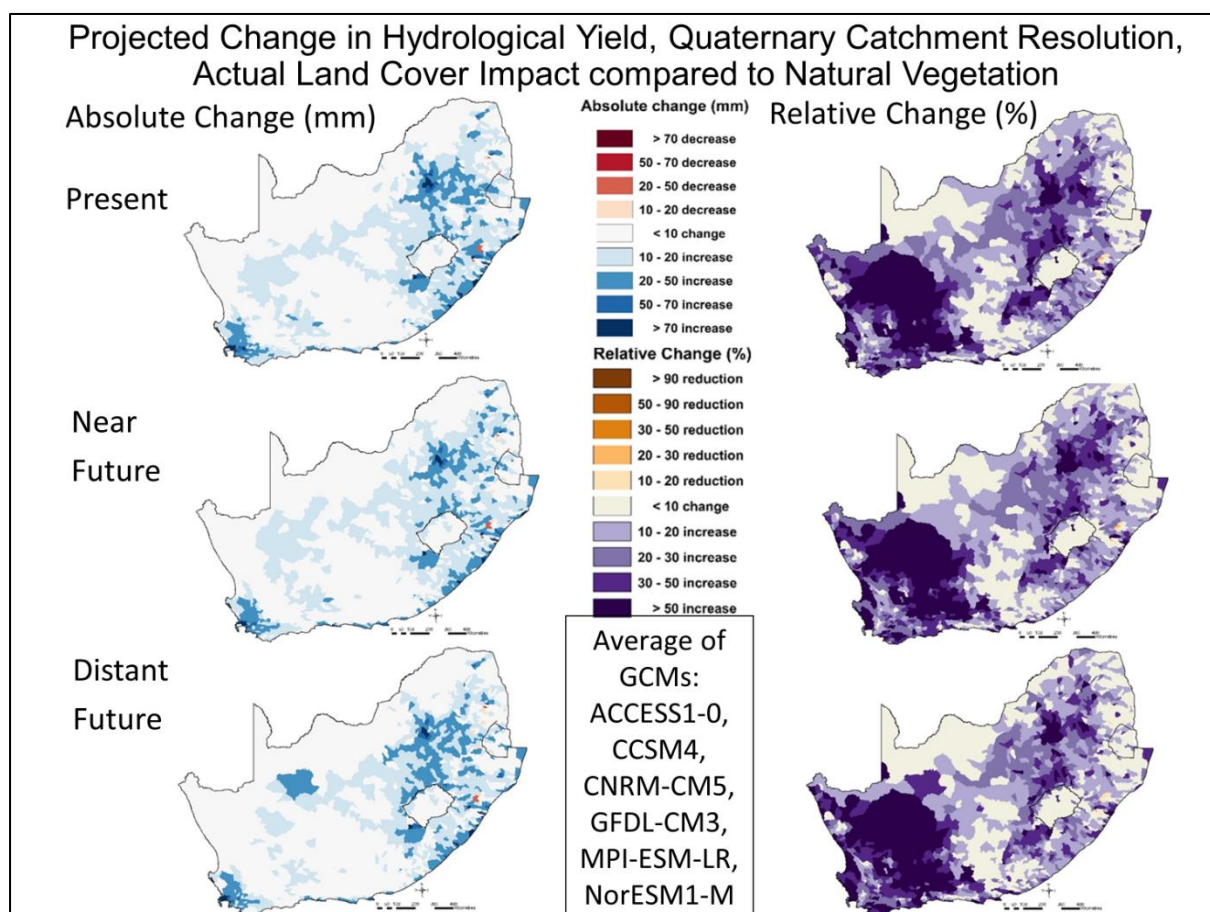
Figure 6.12 Projected absolute changes (mm) [left] and relative changes (%) [right] in hydrological yield, from natural vegetation to actual land cover, for the present (1961-1990) [top], the near future (2015-2044) [middle] and distant future (2070-2099), average of six GCMs, at Quaternary Catchment resolution

6.4   Discussion and Conclusions

The results for both naturalised flows as well as flows under actual land cover conditions (as at 2018), indicate that the western areas, especially around the Western Cape, show a decrease in yield for the near future, and further decreases in the more distant future. A large relative change might not translate in large absolute changes in yield, if the yield is very small. A decrease in yield is also projected for some areas in the east, especially north-east. This needs to be considered in future water resources planning. Conversely, areas where the rivers originate from the Drakensberg areas are projected to have an increase in yield. When zooming in to Primary Catchments U and V, as examples, this shows a projected decrease in yield for part of Primary Catchment U, where the origin is mainly in the KwaZulu-Natal Midlands, but a projected increase in yield for Primary Catchment V, where the origin is in the Drakensberg area is much the projection is bigger than for Primary U.

Looking at land cover impacts, overall, projected climate change impacts look similar when comparing natural vegetation versus NLC2018, however, the impacts on a local level might be either magnified or muted. Increases in runoff are usually expected from degraded and urban areas and where low biomass replaces larger biomass under natural vegetation cover. There might also be increased runoff when cultivated land might be lying fallow in the off season, with no transpiration compared to natural vegetation which may be transpiring during the off season. Reductions in hydrological yield would be expected from, for example, forest plantations, which are known to reduce streamflow. Thus decreased yield would have been expected in forest plantation dominated areas, where these replaced grasslands, e.g. in the KwaZulu-Natal Midlands and in Mpumalanga. To understand the differences between the natural vegetation and actual land cover scenarios better would require a more detailed, further investigation to Quaternary Catchment and even HRU level, as well as a comparison of catchment runoff.

One needs to be aware that this is the first attempt to model land use impacts on a national scale and is very useful to be able to see a broad picture of the whole region. However, anthropogenically modified land cover had to be simplified for national scale modelling and the approach to representing actual land cover at national scale may need to be refined. For example, currently no deep rooting of forest trees is modelled, while this is often the case in reality, which is likely to result in an under estimation of the modelled water use of forest plantation. It would be interesting to see whether climate change or land use has a larger impact on yield, and if the impact differs at a large scale compared to a local scale. However, this project is focussed on climate change impacts and not at detailed land use impacts.

Even though a simplified yield model has been used to determine the hydrological yield, it is expected that the relative changes in yield would be similar to relative changes determined using a more detailed, stochastic yield model (e.g. WRYM). The results simulated to date have analysed the impacts of climate change on yield under assumed natural vegetation, as well as the impacts of climate change on yield for actual cover and the climate change impacts have been found to be similar for both land cover scenarios. Climate change impact might locally be magnified or muted because of anthropogenically altered land cover.

It is useful, to assess both relative and absolute changes of climate change on yield, because there might be large relative changes, but coming from a very low base.

With the significant differences occurring in some regions of the country, it is recommended that future analyses should include more detail at a local level, for example, to examine yields from individual Primary Catchments and/or water management areas.

6.5   References

DEA and GTI. 2019. 73 Class GTI South African National Land Cover Dataset (2018) [Dataset]. Produced by GeoTerraImage Pty Ltd (GTI) for the Department of Environmental Affairs (DEA), Pretoria, South Africa

TOUCHER, ML, RAMJEAWON, M, MCNAMARA, MA, ROUGET, M, BULCOCK, H, KUNZ, RP, MOONSAMY, J, MENGISTU, M, NAIDOO, T, VATHER, T AND ALDWORTH, TA. 2019. *Resetting The Baseline Land Cover Against Which Streamflow Reduction Activities And The Hydrological Impacts Of Land Use Change Are Assessed*. WRC Report 2437/1/19. Water Research Commission (WRC), Pretoria, South Africa

7 PROJECTED CLIMATE CHANGE IMPACTS FOR THE HYDRO-CLIMATIC ZONES IN SOUTH AFRICA

S. Schütte, R.E. Schulze

7.1 Introduction

In the South African Climate Change Response Strategy (DWS, no date) a number of Hydro-Climatic Zones (HCZs) were delineated, with general climate change impacts and adaptation strategies given for each. In this chapter a summary is provided with some of the climate change impact results from this project provided for each of the HCZs. This summary includes projected changes from what has been defined as "the present" (1961-1990) to the defined "near future" (2015-2044) and from the present to what has been defined as the "distant future" (2070-2099), assuming outputs from the RCP8.5 emission scenarios. The variables summarised here include temperature, expressed as annual means of daily maximum temperatures, as well as annual means of daily minimum temperatures, and also mean annual precipitation. Hydrological responses were modelled using the *ACRU* model configured with actual land cover as of 2018 (NLC2018; DEA and GTI, 2019), as summarised in Sections 3.4. Summarised here are changes in mean annual individual catchment runoff and changes in mean annual accumulated streamflow. Changes in hydrological yield, as described in Chapter 6 are also summarised. The spatial resolution used in the modelling was based on the Quinary level altitudinal response zones within Quaternary Catchments; i.e. where South Africa, Lesotho and eSwatini have been delineated into 5 838 relatively homogeneous hydrological response units, previously described in Section 2.2. While the modelling was done at altitudinal Quinary level resolution, the mapping resolution in this Chapter is at Quaternary Catchment resolution.

Hydro-Climatic zones can be defined in several ways, and could be as fine-scaled as the sub-catchment level, but for this Chapter, the zonation as per Climate Change Response Strategy (DWS, no date) is followed. This is with the understanding that these zones are not hydrologically uniform and may contain within each a variety of climatic responses. Nevertheless, as a summary of the results of this project the Quaternary classification will be used. In the Climate Change Response Strategy, South Africa has been divided into six so-called Hydro-Climatic Zones (**Figure 7.1**), each of which is made up of one or more Water Management Areas (WMAs). The WMAs are shown in **Figure 7.2**.
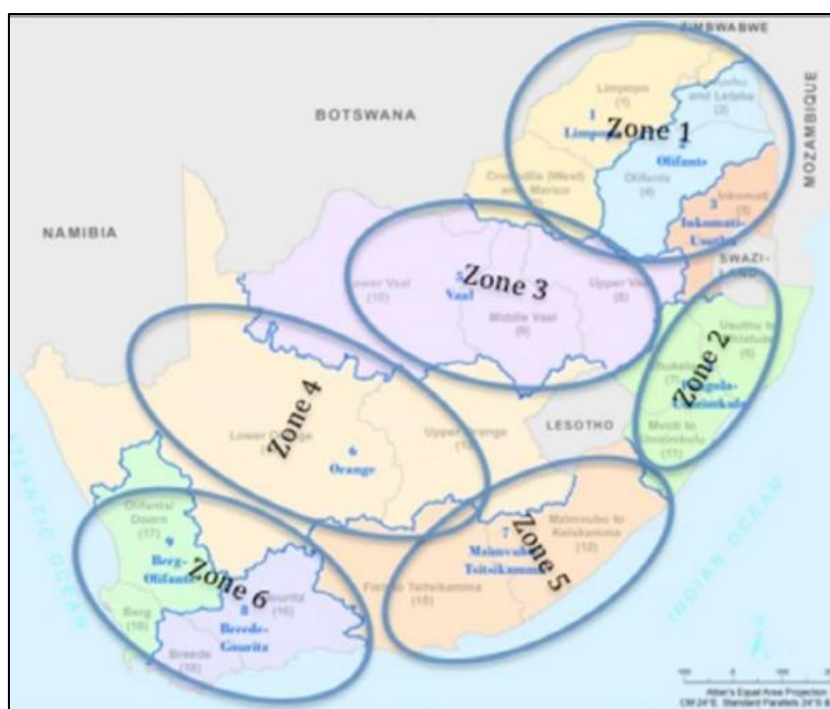
Figure 7.1   Hydro-Climatic Zonation used in the Climate Change Response Strategy (DWS, no date)

Hydro-Climatic Zone 1 is in the north-east of the country and consists of WMA 1 (Limpopo), WMA 2 (Olifants) and WMA 3 (Inkomati-Usuthu). Hydro-Climatic Zone 2 consist of the WMA 4 (Pongola-Mtamvuna), while Hydro-Climatic Zone 3 consists of WMA 5 (Vaal) and Hydro-Climatic Zone 4 consists of WMA 6 (Orange). Hydro-Climatic Zone 5 consists of WMA 7 (Mzimvubu-Tsitsikamma) and Hydro-Climatic Zone 6 consists of WMA 8 (Breede-Gouritz) and WMA 9 (Berg-Olifants)
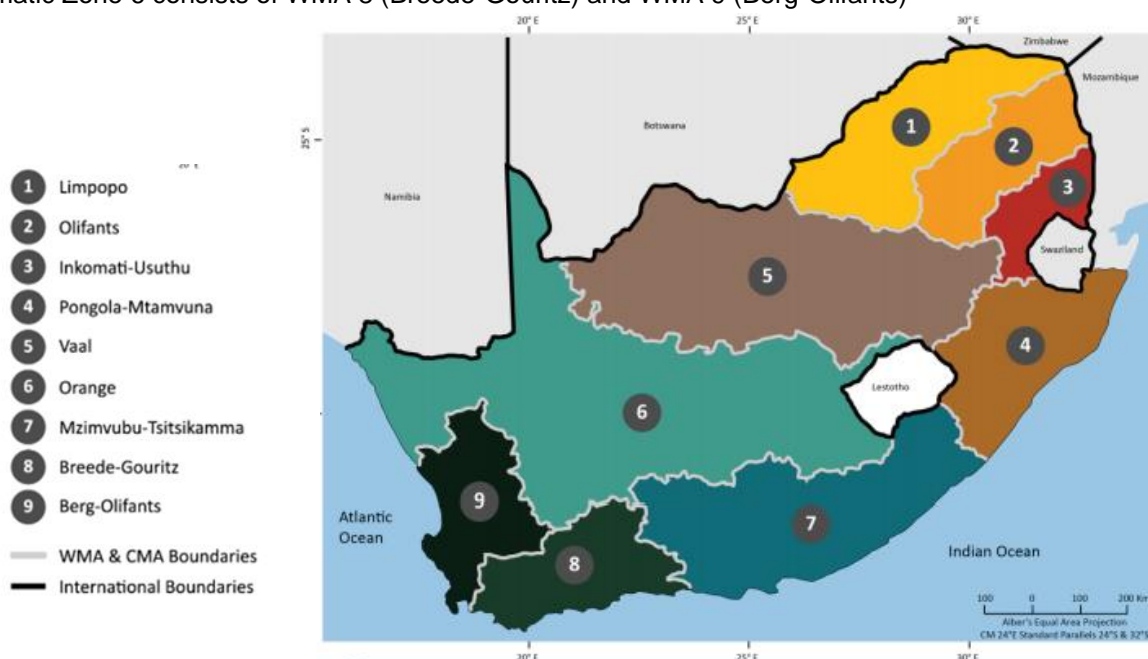
Figure 7.2   Water Management Areas in South Africa (DWS, 2016)

7.2   Summary of Results per Hydro-Climatic Zone

Results of this study are now summarised per Hydro-Climatic Zone.

7.2.1   Hydro-Climatic Zone 1

Hydro-Climatic Zone is situated in the far north-east of South Africa (**Figure 7.3**) and is made up of three Water Management Areas, namely WMA 1 (Limpopo), WMA 2 (Olifants) and WMA 3 (Inkomati-Usuthu). HCZ 1's projected changes into the future are summarised in **Table 7.1** and shows temperature increases into the future, with severe increases projected into the distant future of over 6°C (**Figure 7.4**). Change in mean annual precipitation generally shows little change to some decreases, generally more severe into the distant future (**Figure 7.5**). Mean annual catchment runoff generally shows mixed changes, as does mean annual accumulated streamflow (**Figure 7.6** and **Figure 7.7**). Hydrological yield shows mixed results with the majority of the area showing no change, but some areas also showing decreases and increases (**Figure 7.8**).
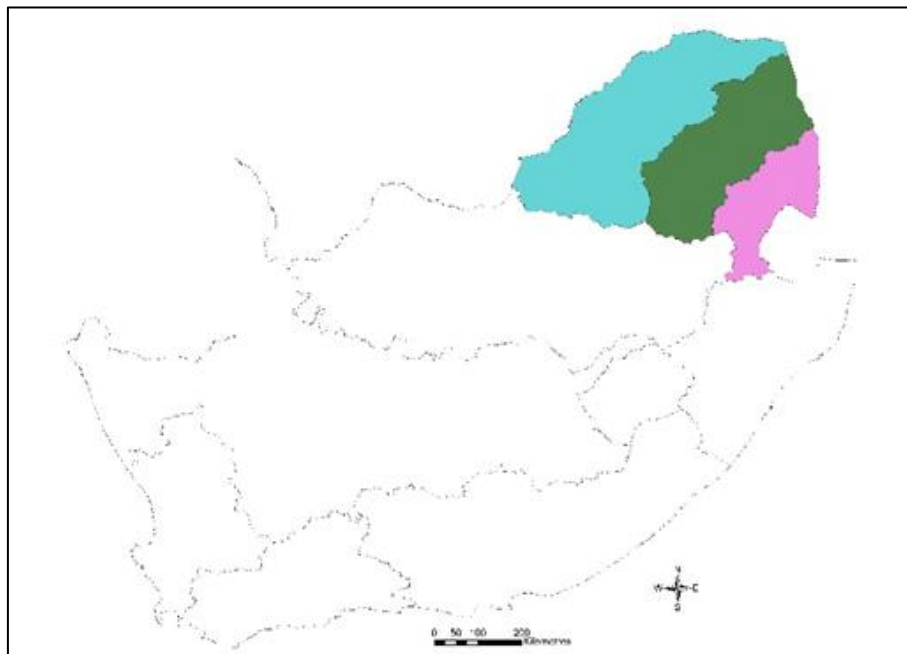
Figure 7.3   Hydro-Climatic Zone 1 is made up of 3 Water Management Areas, with WMA 1 (Limpopo) in turquoise, WMA 2 (Olifants) in green and WMA 3 (Inkomati-Usuthu) shown in purple

Figure 7.4   Hydro-Climatic Zone 1: Projected changes in annual means of daily maximum [bottom] and minimum [top] temperatures (°C) from the present to the near future [left] and the present to the distant future [right] at a Quaternary Catchment resolution

Figure 7.5   Hydro-Climatic Zone 1: Projected changes in mean annual precipitation (mm) from the present to the near future [left] and the present to the distant future [right] at a Quaternary Catchment resolution

Figure 7.6   Hydro-Climatic Zone 1: Projected changes in mean annual catchment runoff (mm) from the present to the near future [left] and the present to the distant future [right] at a Quaternary Catchment resolution

Figure 7.7   Hydro-Climatic Zone 1: Projected changes in mean annual accumulated streamflow (mm) from the present to the near future [left] and the present to the distant future [right] at a Quaternary Catchment resolution

Figure 7.8   Hydro-Climatic Zone 1: Projected changes in hydrological yield (mm) from the present to the near future [left] and the present to the distant future [right] at a Quaternary Catchment resolution

Table 7.1   Hydro-Climatic Zone 1 comprising of the Limpopo, Olifants and Inkomati WMAs:
                 Projected climate change impact on temperature, precipitation, catchment runoff,
                 accumulated streamflow and hydrological yield

Variable	Present to near future	Present to distant future
Annual mean of daily maximum temperatures	Increases: 1-3°C In the west 1-3°C, in the east 1-2°C	Large increases: In the south-west more than >6°C, the interior and south 5-6°C, in the north and east 4-5°C
Annual mean of daily minimum temperatures	Increases of 1-2°C	Large increases: The largest area 4-5°C, 3-4°C towards the east and small areas in the west 5-6°C
Mean annual precipitation	No change to small decreases: Generally < 20 mm change up to 150 mm reduction, with the majority of the area showing a 20-50 mm reduction; Some GCMs, however, show an increase towards the east.	Generally a reduction, with some exceptions: Larger reductions towards the north-west, smaller for the rest of the area. Most areas show small changes < 20 mm to decreases of up to 100 mm, with some areas displaying decreases up to 150 mm. Compared to the changes to the near future, more severe changes are shown in the west, but generally results remain similar in the middle and east. Some GCMs, however, show an increase towards the east
Catchment runoff mean annual, mean of GCMs (LU)	Mixed results: Generally, the larger part of the area shows less than 10 mm changes, but in patches also changes in both directions, with reductions mainly towards the north-west, of up to 100 mm and small areas showing increases up to 50 mm.	Mixed results, but small changes dominate, with some increases towards the east and south and patches of decreases. The west generally shows no or little change, with some decreases and localised increases up to 20 mm. Towards the east more increases up to 100 mm are projected, as well as south-east, but also decreases up to 100 mm for some areas
Accumulated streamflow (mm)	Mixed results: in the west generally no change or mainly small reductions (10-20 mm), more areas with reductions up to 100 mm in the middle and east, but also some increases	Mixed results: in the west generally little change of 20 mm in both directions, in the middle and east larger changes, generally increases, but also some decreases
Hydrological yield	Mixed results, but generally no change over most of the area, with small reductions up to 70 mm, more towards the east.	Mixed results, no or small changes for much of the area, with localised decreases, but also localised increases towards the south-east

7.2.2 Hydro-Climatic Zone 2

Hydro-Climatic Zone 2 consist of the WMA 4 (Pongola-Mtamvuna), situated in the eastern parts of South Africa, from just east of Lesotho to the East Coast (**Figure 7.9**). Hydro-Climatic Zone 2's projected changes are summarised in Table 7.2 and show temperature increases into the future, with severe increases into the distant future of up to 6°C projected (**Figure 7.10**). Change in mean annual precipitation generally shows mixed results, with no change to decreases over most of the area, but with increases in the east towards Lesotho. Changes are generally more severe into the distant future (**Figure 7.11**). Mean annual catchment runoff generally also shows mixed changes, with increases towards Lesotho, but no change or decreases for the rest of the area (**Figure 7.12**). Mean annual accumulated streamflow shows similar trends (**Figure 7.13**). Hydrological yield shows mixed results with the majority of the area showing no change or reductions, but with some also areas showing increases, generally east of Lesotho, for the Thukela catchment east up to the coast (**Figure 7.14**).
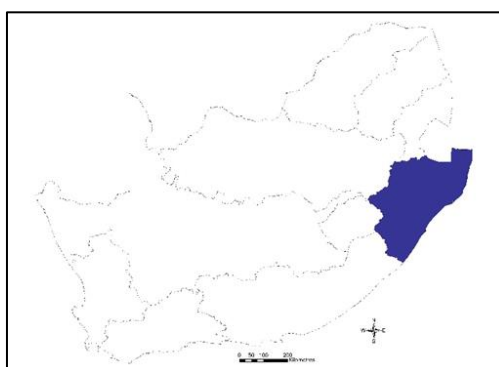
Figure 7.9   Hydro-Climatic Zone 2 is made up of WMA 4 (Pongola-Mtamvuna) and is shown in blue, situated along the east coast of South Africa, also bordering on eSwatini and Mozambique in the north and Lesotho in the south-west

Figure 7.10 Hydro-Climatic Zone 2: Projected changes in annual means of daily maximum [bottom] and minimum [top] temperatures (°C) from the present to near future [left] and the present to distant future [right] at a Quaternary Catchment resolution

Figure 7.11   Hydro-Climatic Zone 2: Projected changes in mean annual precipitation (mm) from the present to the near future [left] and the present to the distant future [right] at a Quaternary Catchment resolution

Figure 7.12 Hydro-Climatic Zone 2: Projected changes in mean annual catchment runoff (mm) from the present to the near future [left] and the present to the distant future [right] at a Quaternary Catchment resolution

Figure 7.13 Hydro-Climatic Zone 2: Projected changes in mean annual accumulated streamflow (mm) from the present to the near future [left] and the present to the distant future [right] at a Quaternary Catchment resolution

Figure 7.14 Hydro-Climatic Zone 2: Projected changes in hydrological yield (mm) from the present to the near future [left] and the present to the distant future [right] at a Quaternary Catchment resolution

Table 7.2   Hydro-Climatic Zone 2, comprising the Pongola-uMzimkhulu WMA: Projected climate change impacts on temperature, precipitation, catchment runoff, accumulated streamflow and hydrological yield

Variable	Present to near future	Present to distant future
Annual mean of daily maximum temperatures	Increases of 1-2°C	Increase of between 3-6°C, with 3-4°C along the east coast, more inland
Annual mean of daily minimum temperatures	Increases of 1-2°C	Increase of 2-5°C inland and 3-4°C along the east coast
Mean annual precipitation	Mixed results. No change or decreases in most of the area, with increases inland towards Lesotho.	Mixed results, generally more severe changes compared to the changes to the near future. Increases inland towards Lesotho and some areas in the south-east, reductions towards the middle and north-east of the study area
Catchment runoff mean annual, mean of GCMs	Mixed results. No changes or decreases across most of the area, with increases inland towards Lesotho.	Mixed results, generally more severe changes compared to the changes to the near future. Increases inland towards Lesotho and some areas in the north-east, generally reductions towards the east of the study area
Accumulated streamflow	Mixed results. Increases inland towards Lesotho, but no change or decreases across the rest of the area.	Mixed results, generally more severe changes compared to the changes to the near future. Increases inland towards Lesotho and some area in the north-east, generally reductions towards the east of the study area.
Hydrological yield	Mixed results. No changes over large areas, localised increases of up to 50 mm in the inland, in the west of the study area, towards Lesotho, some localised reductions in the north, south and south-east, up to 70 mm.	Mixed results. More severe changes compared to the changes for present to near future. Some areas (but to a decreased extent) show no change, the inland areas towards the west show increases, going through to the east coast for the Thukela River and also some increases towards the north-east and the upper reaches of the Mzimkhulu. Decreases in yield are seen, however, for the Mtamvuna, Mkomazi, Mgeni, Mdloti, Tongati, and the upper reaches of the Umfolozi rivers

7.2.3   Hydro-Climatic Zone 3

Hydro-Climatic Zone 3 consists of WMA 5 (Vaal) and covers the area just north of Lesotho and west towards Botswana (**Figure 7.15**). Hydro-Climatic Zone 3's projected changes are summarised in Table 7.3 and shows temperature increases into the future, with severe increases into the distant future of up to and over 6°C projected (**Figure 7.16**). Change in mean annual precipitation generally shows mixed results with some increases in the west, but generally no changes or decreases, getting more severe into the distant future (**Figure 7.17**). Mean annual catchment runoff generally shows mixed changes, as does mean annual streamflow (**Figure 7.18** and **Figure 7.19**), with some increases projected in the west, but no changes or decreases in the west. Hydrological yield shows mixed results with the majority of the area showing no change, but also areas showing increases in the east (**Figure 7.20**).
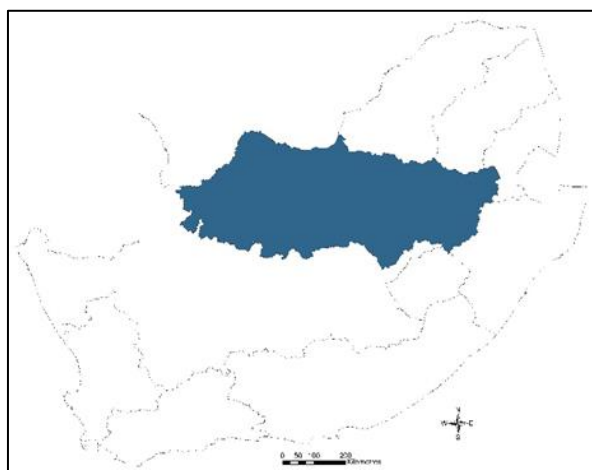
Figure 7.15 Hydro-Climatic Zone 3 is made up of WMA 5 (Vaal) shown in blue, between Lesotho in the east and Botswana in the north-west
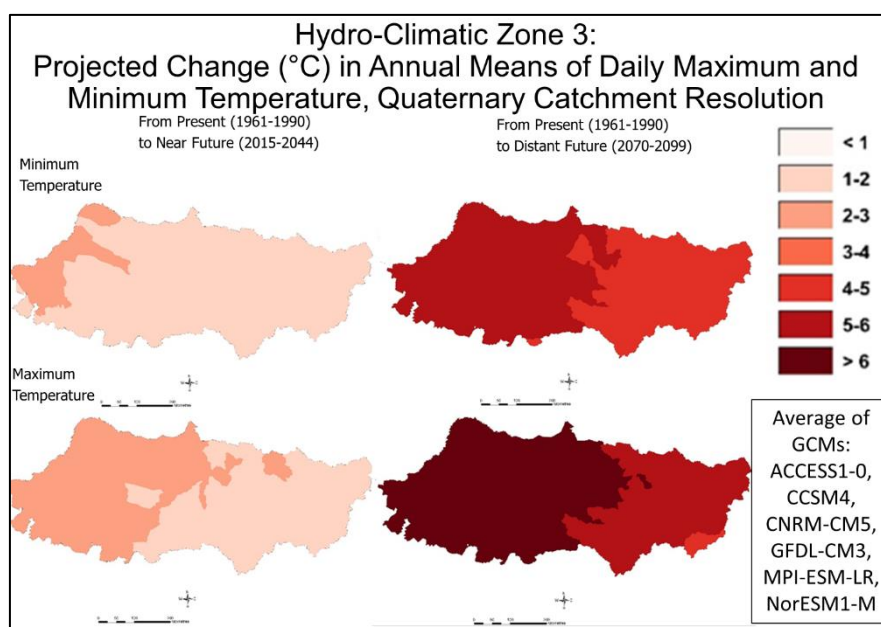
Figure 7.16   Hydro-Climatic Zone 3: Projected changes in annual means of daily maximum [bottom] and minimum [top] temperatures (°C) from the present to the near future [left] and the present to the distant future [right] at a Quaternary Catchment resolution
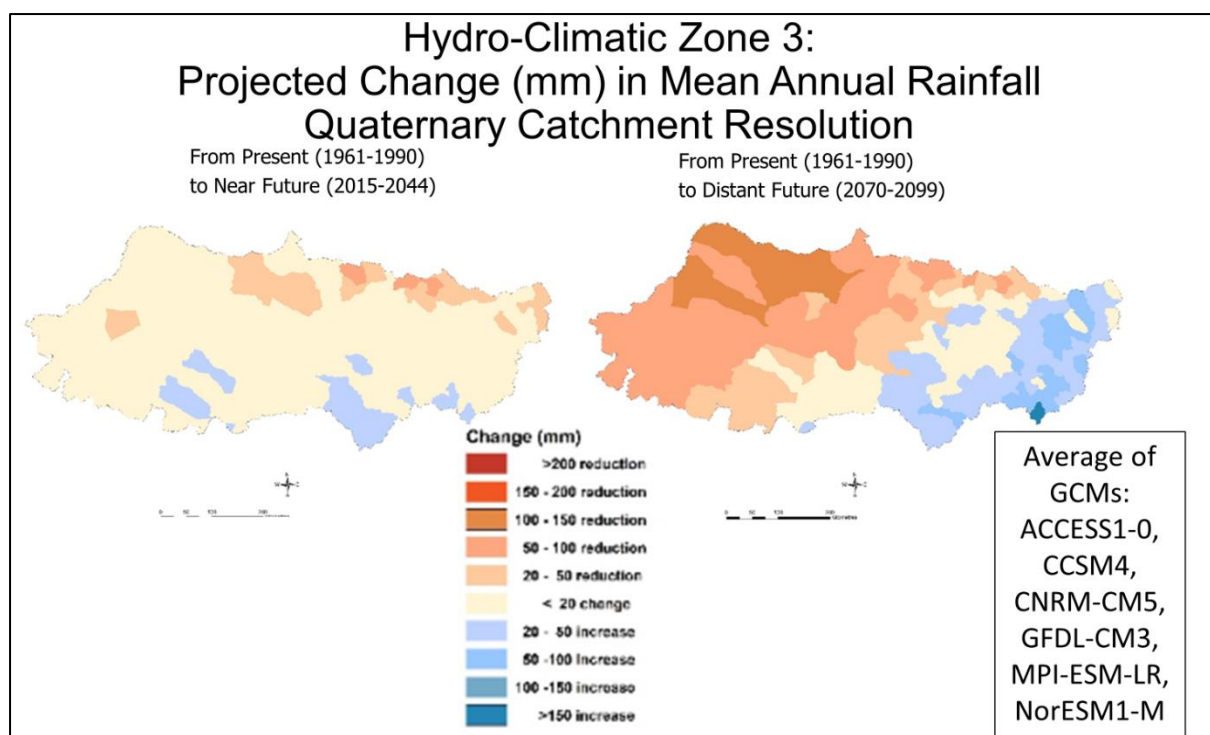
Figure 7.17   Hydro-Climatic Zone 3: Projected changes in mean annual precipitation (mm) from the present to the near future [left] and the present to the distant future [right] at a Quaternary Catchment resolution
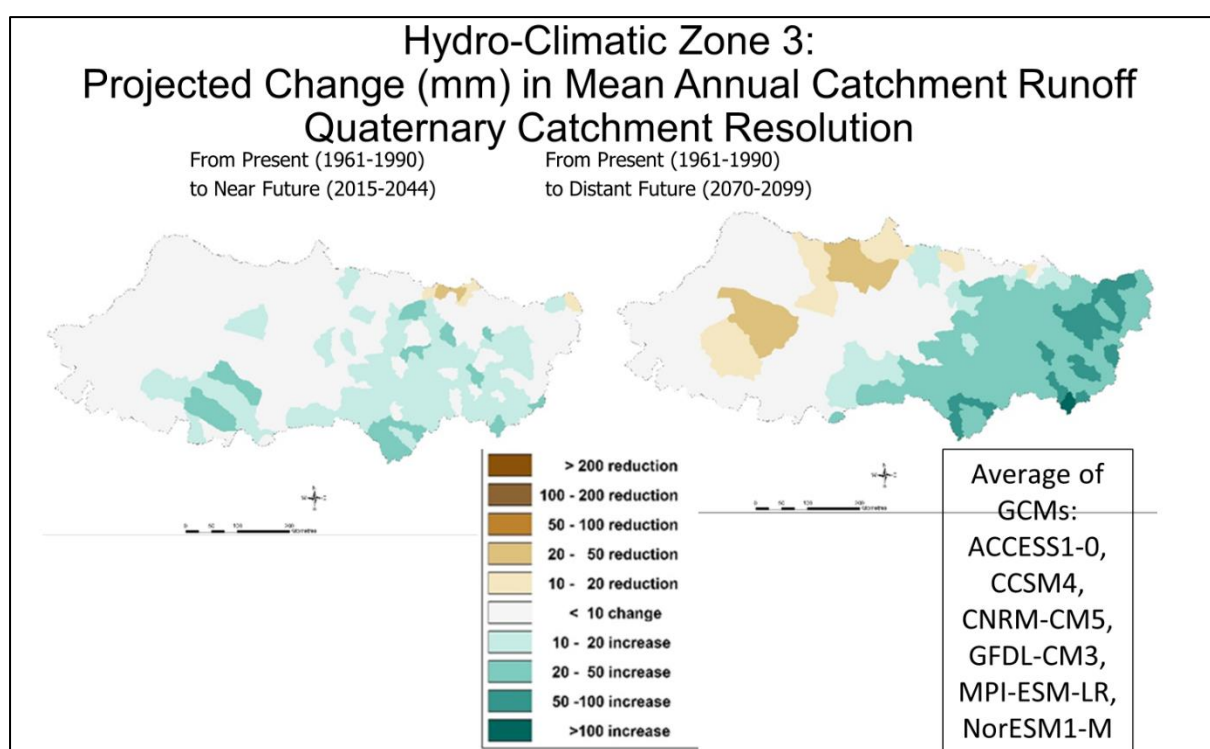
Figure 7.18   Hydro-Climatic Zone 3: Projected changes in mean annual catchment runoff (mm) from the present to the near future [left] and the present to the distant future [right] at a Quaternary Catchment resolution
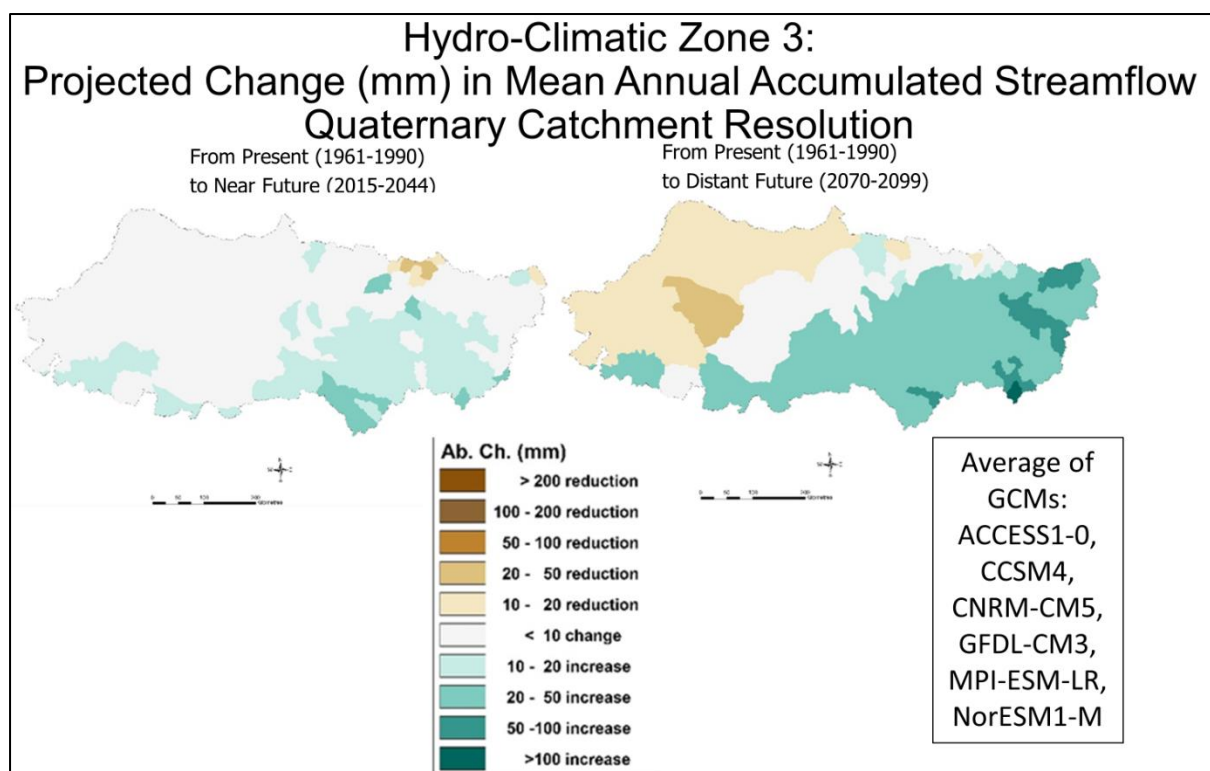
Figure 7.19 Hydro-Climatic Zone 3: Projected changes in mean annual accumulated streamflow (mm) from the present to the near future [left] and the present to the distant future [right] at a Quaternary Catchment resolution
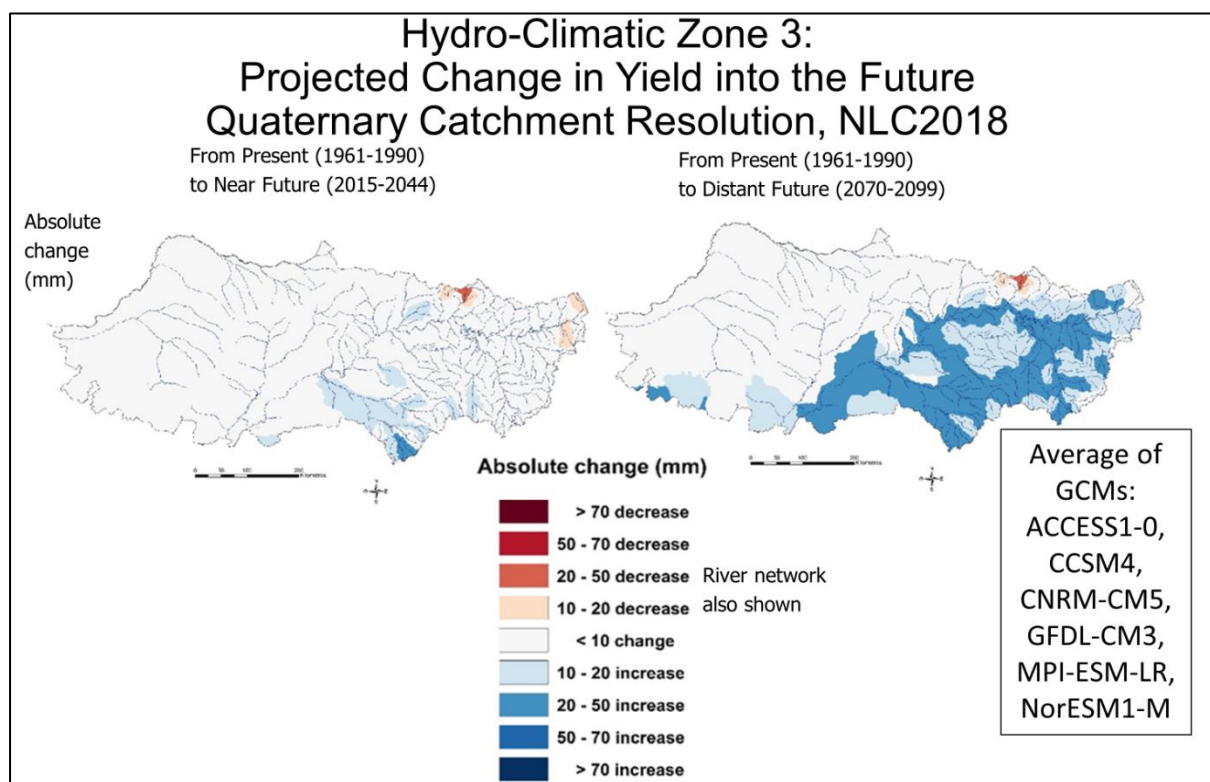
Figure 7.20 Hydro-Climatic Zone 3: Projected changes in hydrological yield (mm) from the present to the near future [left] and the present to the distant future [right] at a Quaternary Catchment resolution

Table 7.3   Hydro-Climatic Zone 3, comprising the Vaal WMA: Projected climate change impacts on temperature, precipitation, catchment runoff, accumulated streamflow and hydrological yield

Variable	Present to near future	Present to distant future
Annual mean of daily maximum temperatures	Increases of 2-4°C: Increases of between 2-3°C in the east and 3-4°C in the west.	Increases of between 4 and more than 6°C, with more severe increases in the west
Annual mean of daily minimum temperatures	Increases of 1-3°C, 1-2°C over most of the area, but 2-3°C in the far west	Increases of 4-6°C, 4-5°C in the east, 5-6°C in the west
Mean annual precipitation	Mixed results, no change over most of the area, increases in patches towards the south-east, decreases in patches towards the north-east	Mixed results, more severe changes. Increases in the east, but mainly decreases in the middle and especially towards the west (up to 100 mm) and the north-west (up to 150 mm).
Mean annual catchment runoff	Mixed results. No change over most of the area, increases in patches in the east and south, with some small areas showing a reduction in the north-east.	Mixed results, with more severe changes in places. No change over most of the area in the west, increases in the east, decreases in some area in the western interior.
Accumulated streamflow	Mixed results. No change over most of the area, but increases in patches in the east and south, with some small areas showing a reduction in the north-east.	Mixed results, with more severe changes in places. Increases in the east, but decreases in the west.
Hydrological Yield	The east shows no change, or localised increases in yield in the upper Vaal system, with no change towards the west	Mixed results, increases towards for the Vaal river in the east, no change in the middle reaches and west

7.2.4   Hydro-Climatic Zone 4

Hydro-Climatic Zone 4 consists of WMA 6 (Orange) and is situated from just west of Lesotho, bordering Botswana in the north and Namibia in the west, but reaching to the West Coast of South Africa. Projected changes are summarised in Table 7.4 and show temperature increases into the future, with severe increases into the distant future of over 6°C projected in the north (**Figure 7.21**). Change in mean annual precipitation generally shows mixed results, with increases in the east towards Lesotho, no change or decreases towards the east, with changes generally more severe into the distant future (**Figure 7.22**). Mean annual catchment runoff generally shows mixed changes, as does mean annual accumulated streamflow, with increases in the east (**Figure 7.23** and **Figure 7.24**). Hydrological yield shows mixed results with increases in the east, but mixed results in the west (**Figure 7.25**).
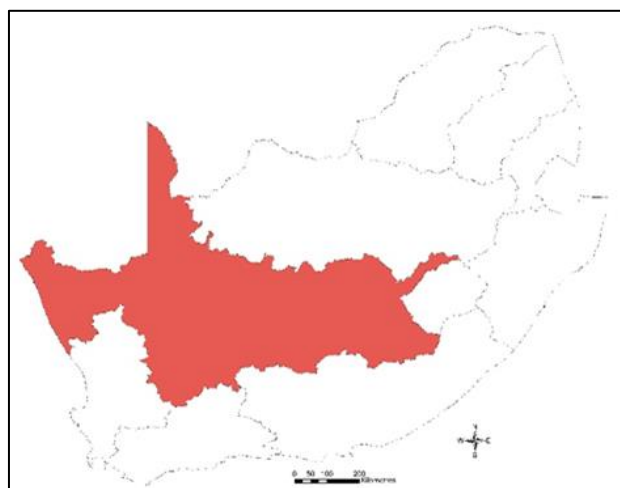
Figure 7.21 Hydro-Climatic Zone 4 is made up of WMA 6 (Orange) shown in red, between Lesotho in the east, Botswana in the north and Namibia in the north-west
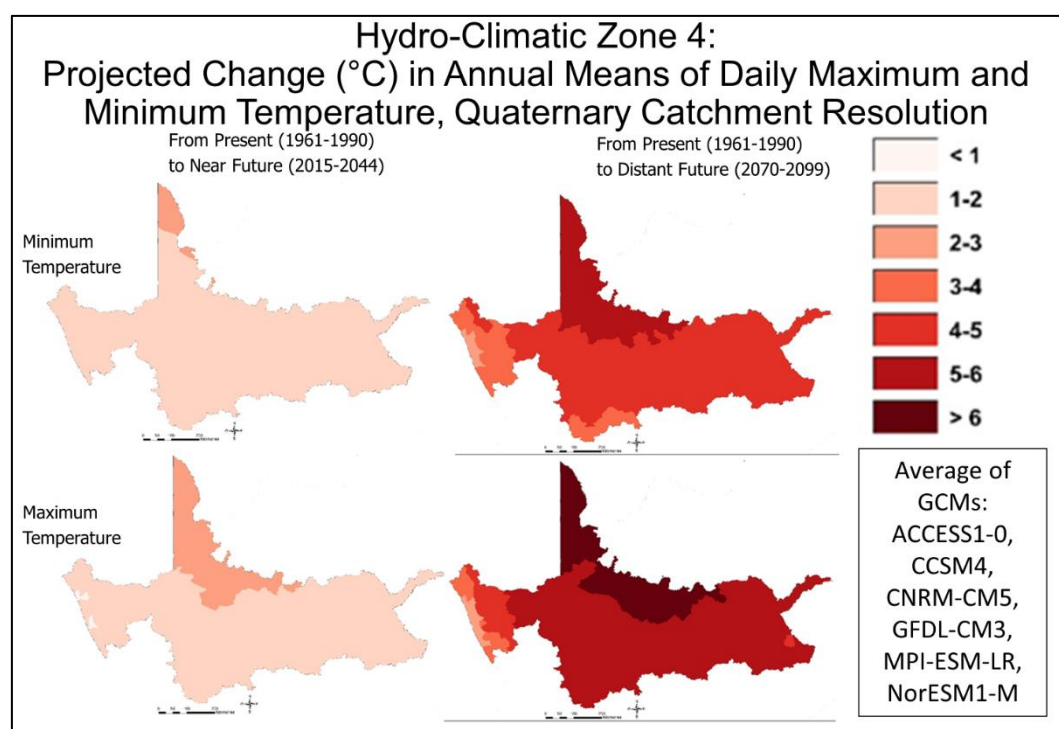
Figure 7.22 Hydro-Climatic Zone 4: Projected changes in annual means of daily maximum [bottom] and minimum [top] temperatures (°C) from the present to the near future [left] and the present to the distant future [right] at a Quaternary Catchment resolution

183
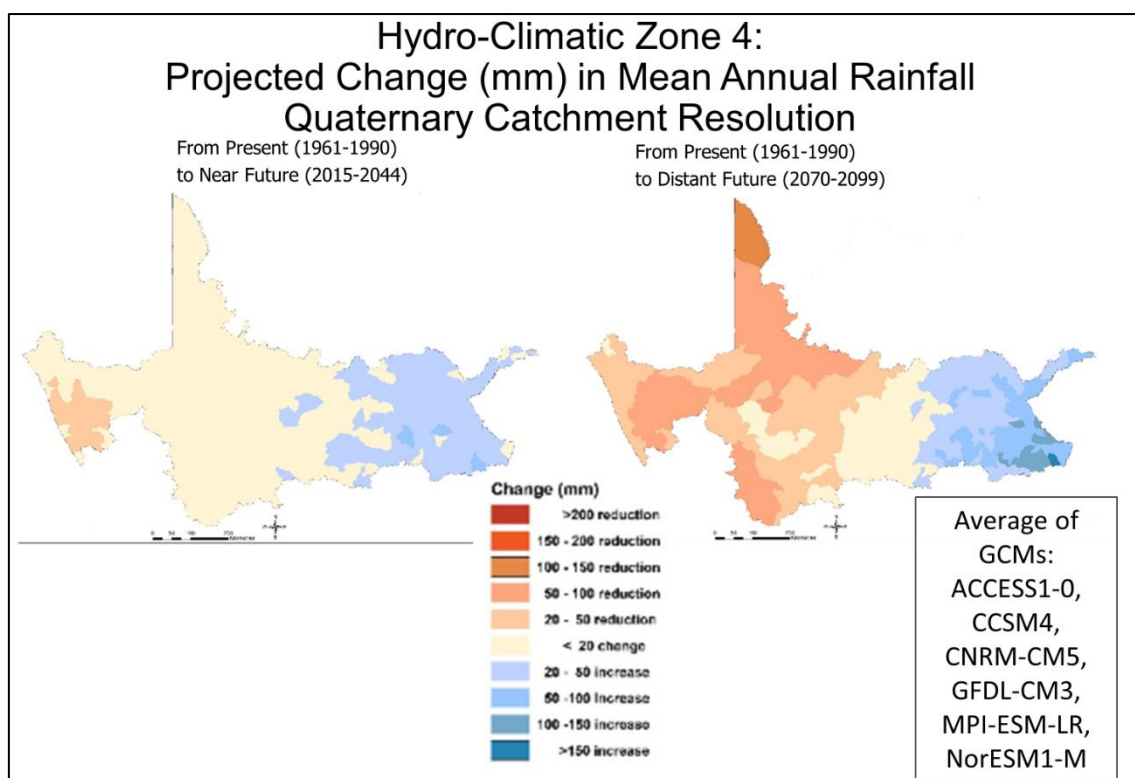
Figure 7.23 Hydro-Climatic Zone 4: Projected changes in mean annual precipitation (mm) from the present to the near future [left] and the present to the distant future [right] at a Quaternary Catchment resolution
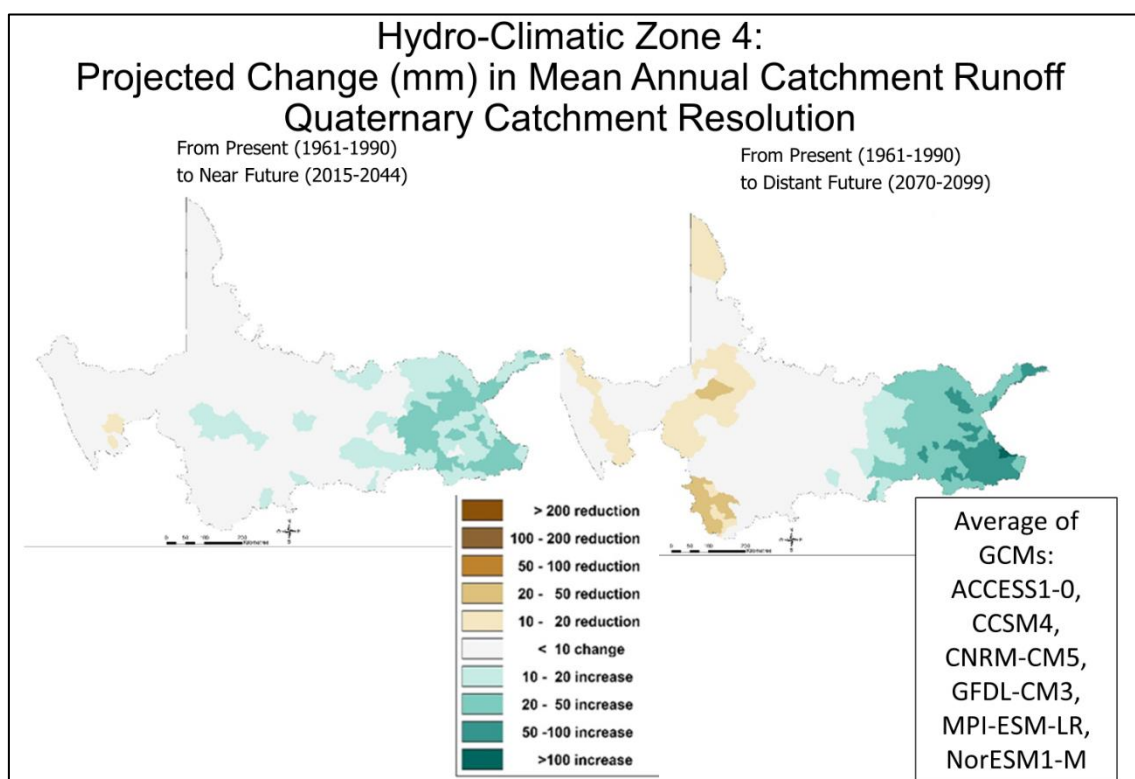
Figure 7.24 Hydro-Climatic Zone 4: Projected changes in mean annual catchment runoff (mm) from the present to the near future [left] and the present to the distant future [right] at a Quaternary Catchment resolution
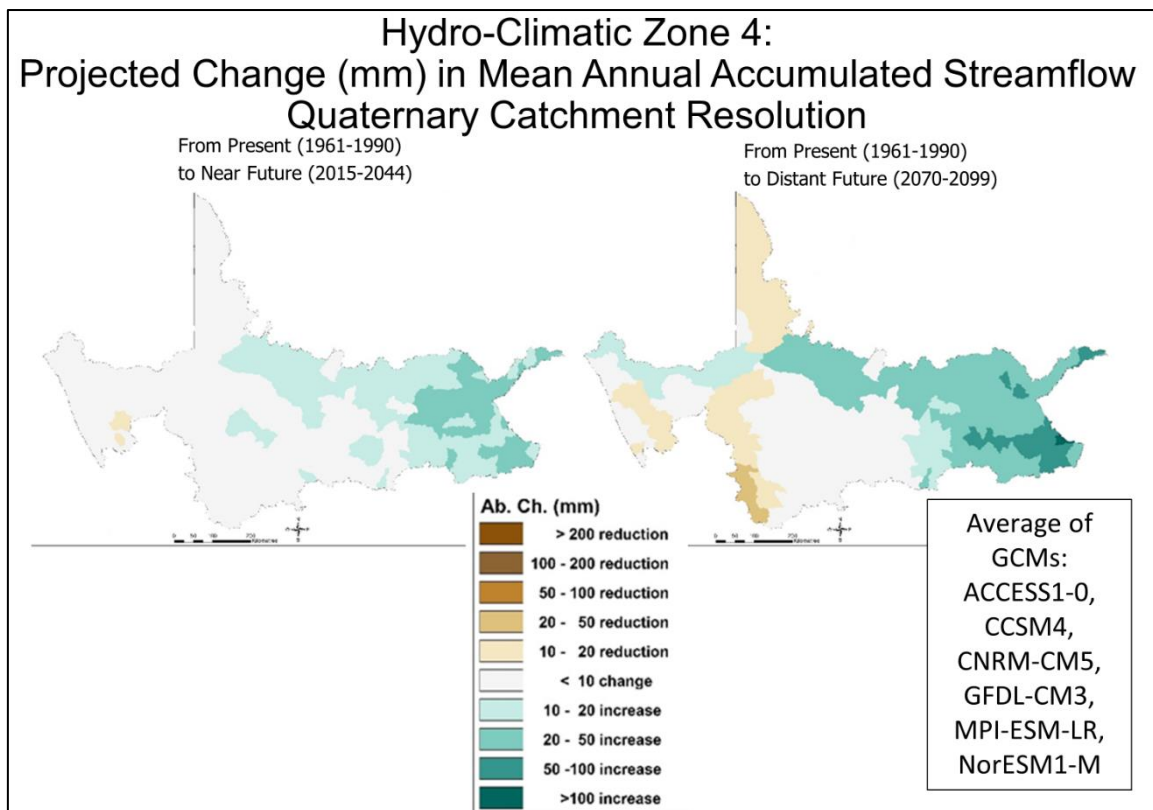
Figure 7.25 Hydro-Climatic Zone 4: Projected changes in mean annual accumulated streamflows (mm) from the present to the near future [left] and the present to the distant future [right] at a Quaternary Catchment resolution
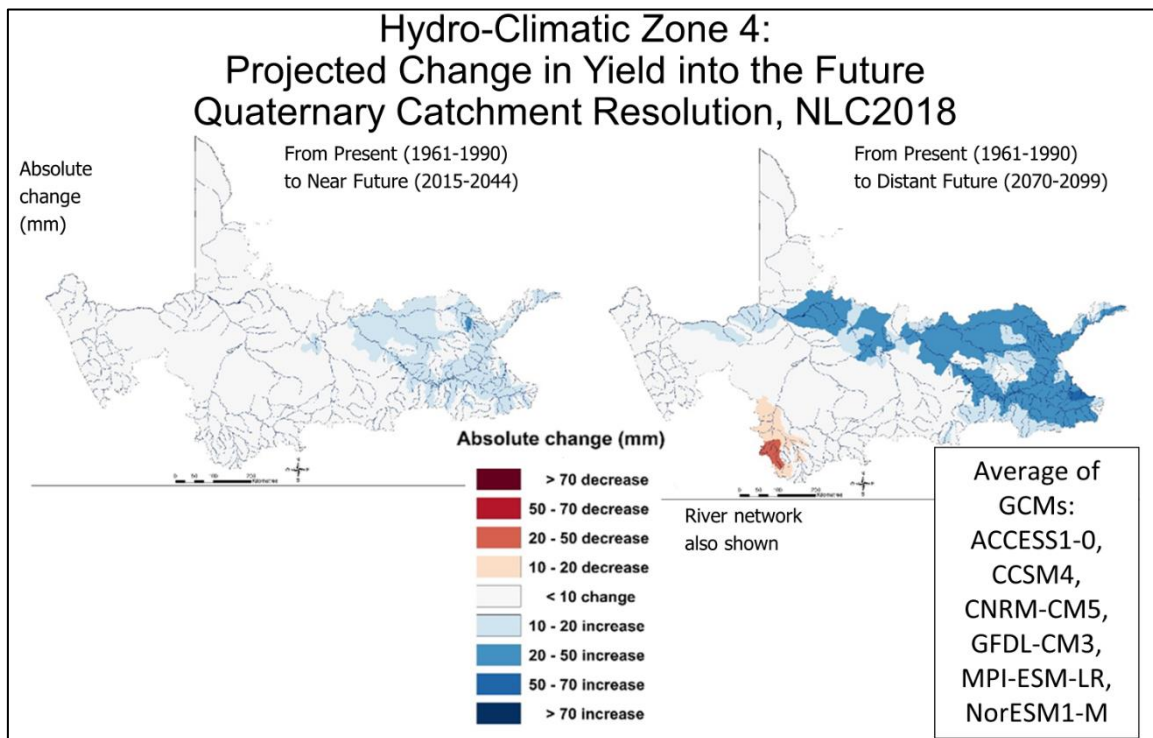
Figure 7.26 Hydro-Climatic Zone 4: Projected changes in hydrological yield (mm) from the present to the near future [left] and the present to the distant future [right] at a Quaternary Catchment resolution

Table 7.4   Hydro-Climatic Zone 4 comprising the Orange System: Projected climate change impact on temperature, precipitation, catchment runoff, accumulated streamflow and hydrological yield

Variable	Present to near future	Present to distant future
Annual mean of daily maximum temperatures	Increases throughout of 1-3°C, with 1-2°C for most of the area, and 2-3°C in the north	Increases between 2 to more than 6°C. The more severe > 6°C in the north, the majority of the area 5-6°C, lower values towards the west coast (2-3°C).
Annual mean of daily minimum temperatures	Increases between 1°C and 3°C. Most area 1-2°C, small area in the north 2-3°C.	Increases between 2 and 6°C, with the 5-6°C in the north and the less severe increases towards the coast in the west and the south.
Mean annual precipitation	Mixed results, increases inland towards Lesotho, no change for most of the area in the interior and north, with decreases of up to 50 mm in the west	Mixed results, more severe than changes to the near future. Increases inland towards Lesotho up to 150 mm, no change for some of the area in the interior and decreases of up to 100 mm in the west and up to 150 mm in the north.
Mean annual catchment runoff, mean of GCMs	Mixed results, increases in the east towards Lesotho. But no change for most of the area towards the west	Mixed results, more severe changes compared to those towards the near future. Increases in the east towards Lesotho. No changes over much of the middle and western area, decreases in the far north, and in patches in the west.
Accumulated streamflows	Mixed results, with increases inland, close to Lesotho, which carries through towards but not reaching the west coast, generally no change in the west and south	Mixed results, increases in the east inland near Lesotho, carrying through the whole Orange catchment to the coast, but with reduced increases. No changes or decreases over the other areas.
Hydrological Yield	Mixed results, small increases (10-20 mm) inland towards Lesotho, but no change for the rest of the study area.	Mixed results, increases up to 50 mm in the east inland near Lesotho, carrying through along the Orange river, but with reduced increases and no change at the Orange mouth. No changes over most of the other areas, small decrease up to 20 mm in small areas in the south.

7.2.5   Hydro-Climatic Zone 5

Hydro-Climatic Zone 5 consists of WMA 7 (Mzimvubu-Tsitsikamma) in the south-eastern part of South Africa (**Figure 7.27**). Hydro-Climatic Zone 5's projected changes are summarised in **Table 7.5** and show temperature increases into the future, with severe increases projected into the distant future of up to 6°C (**Figure 7.28**). Changes in mean annual precipitation generally show mixed results, with changes generally more severe into the distant future (**Figure 7.29**). Mean annual catchment runoff generally shows mixed changes, as does mean annual accumulated streamflow (**Figure 7.30** and **Figure 7.31**). Hydrological yield shows mixed results, with the majority of the area showing no change, but some areas showing decreases and increases (**Figure 7.32**).
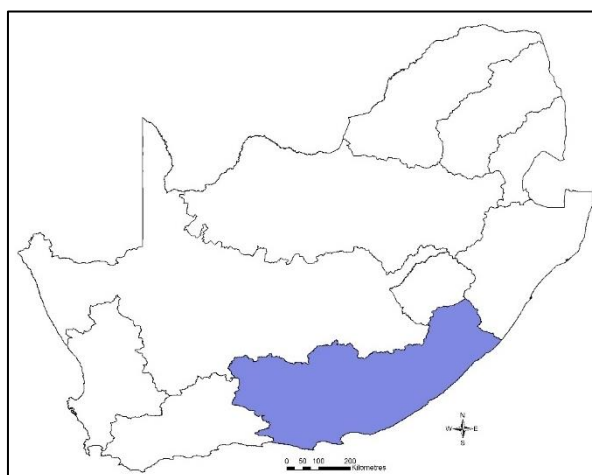

Figure 7.27 Hydro-Climatic Zone 5 consists of WMA 7 (Mzimvubu-Tsitsikamma) in the south-eastern part of South Africa, shown in blue
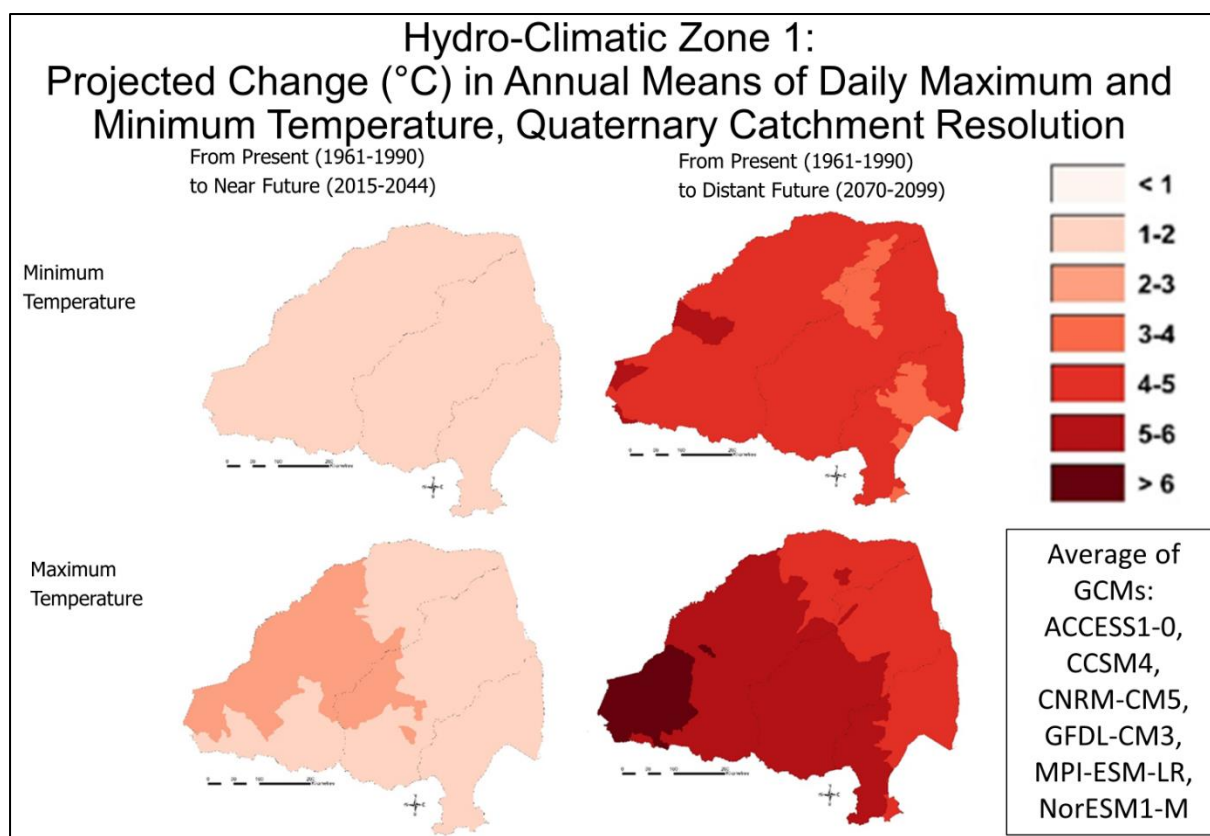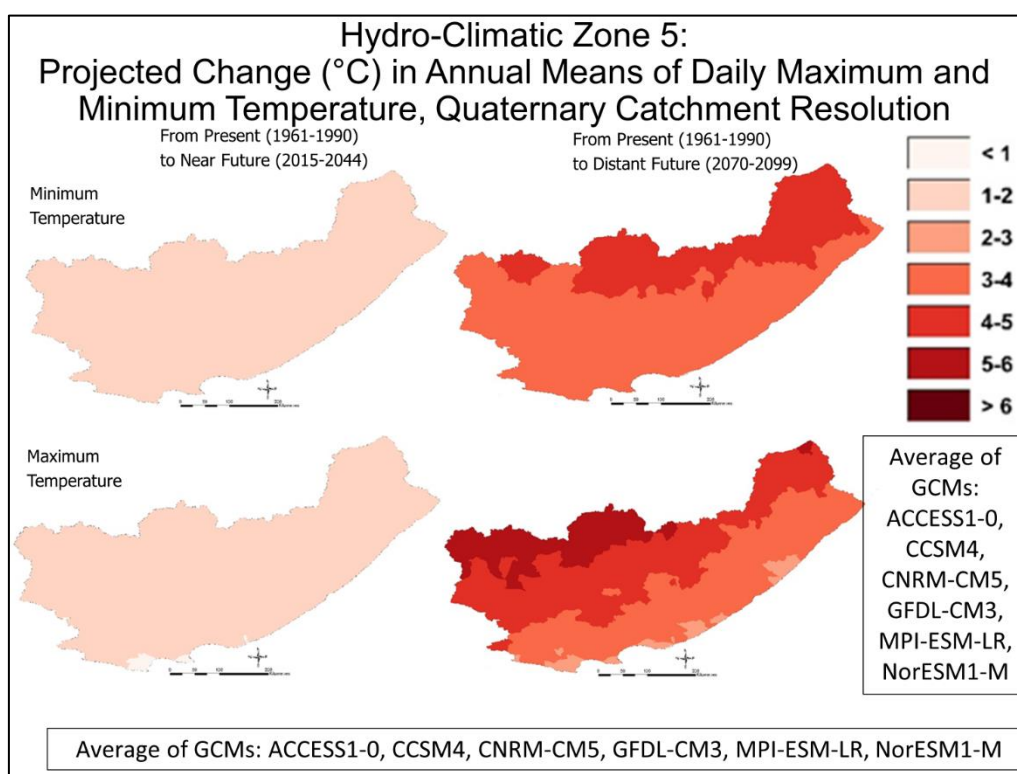

Figure 7.28 Hydro-Climatic Zone 5: Projected changes in annual means of daily maximum [bottom] and minimum [top] temperatures (°C) from the present to the near future [left] and the present to the distant future [right] at a Quaternary Catchment resolution
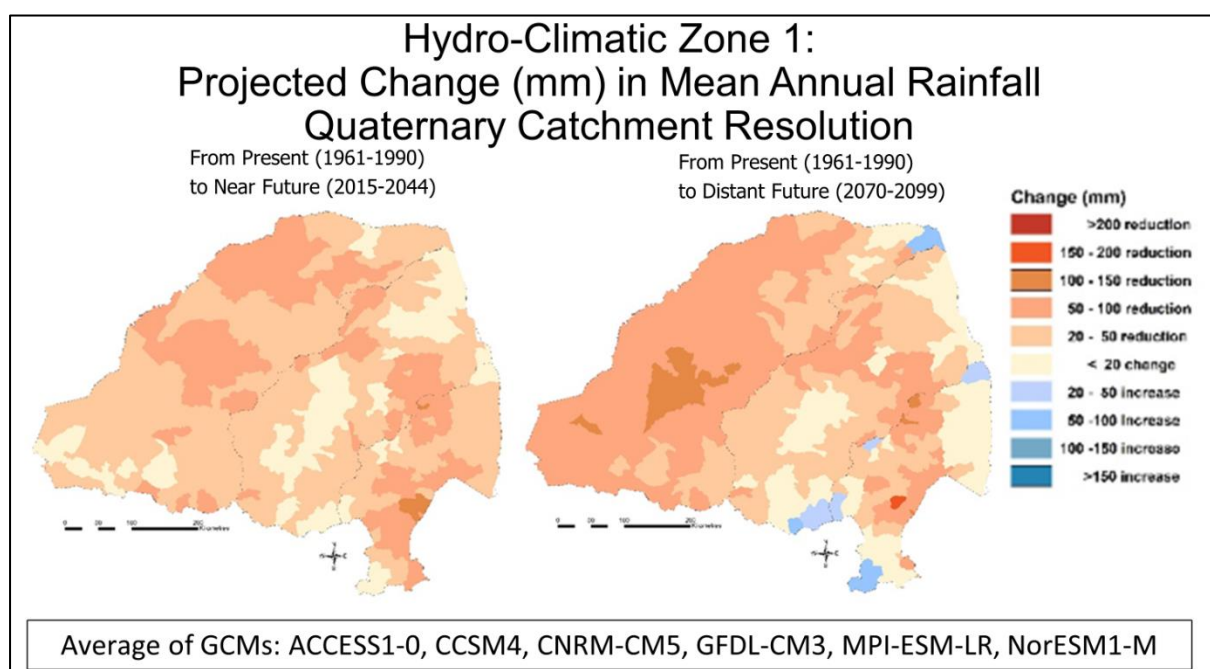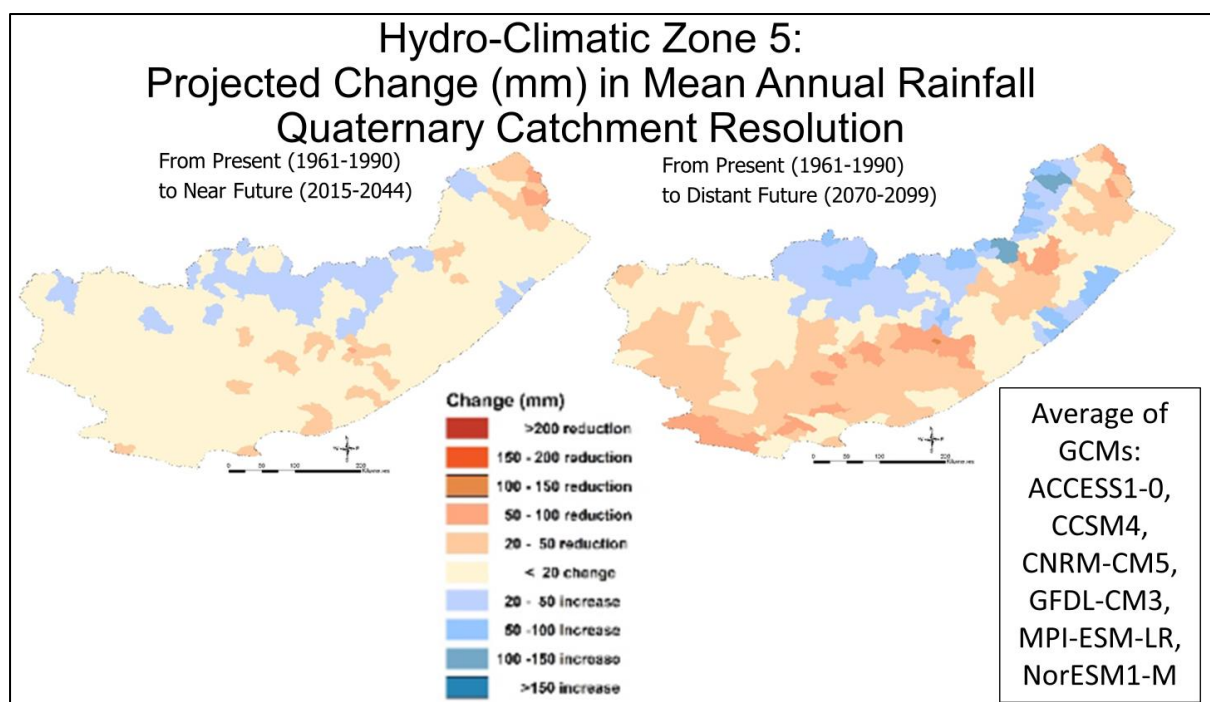
Figure 7.29 Hydro-Climatic Zone 5: Projected changes in mean annual precipitation (mm) from the present to the near future [left] and the present to the distant future [right] at a Quaternary Catchment resolution
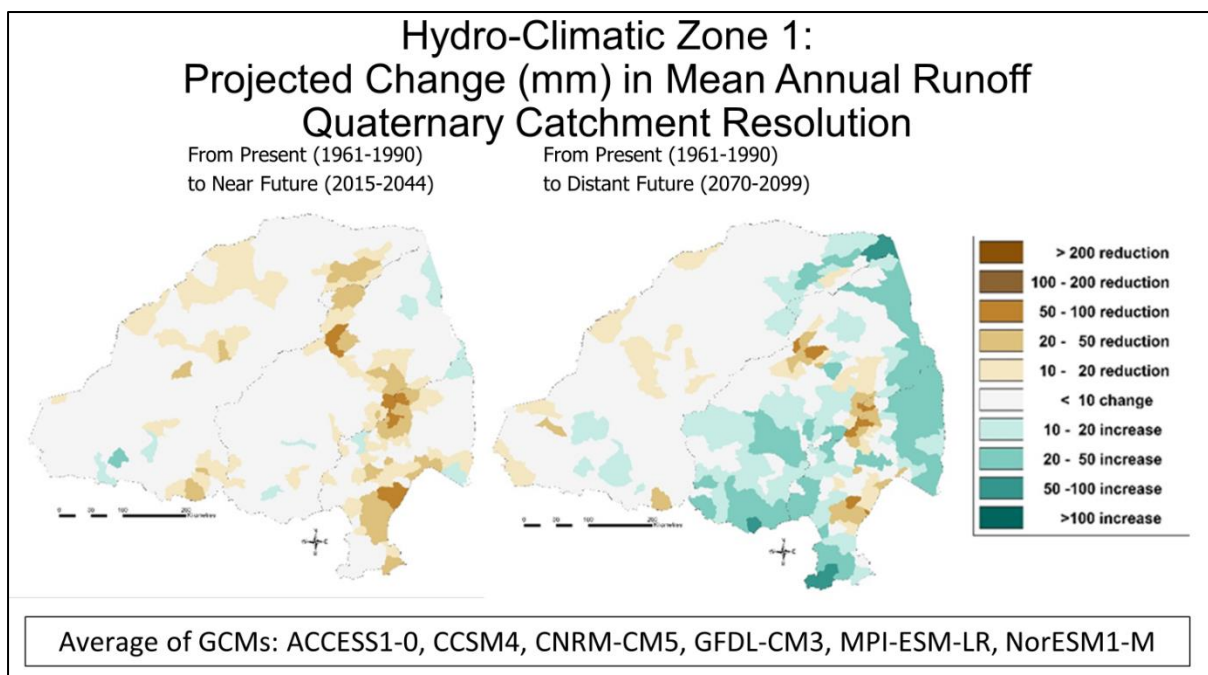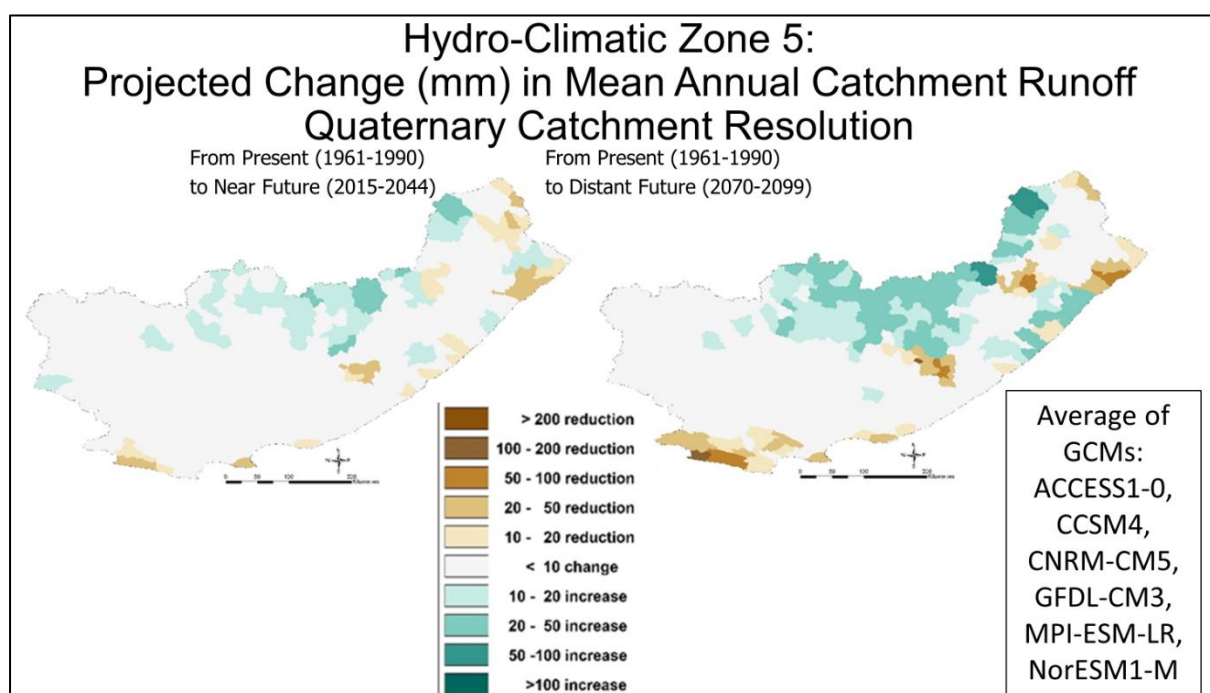

Figure 7.30 Hydro-Climatic Zone 5: Projected changes in mean annual catchment runoff (mm) from the present to the near future [left] and the present to the distant future [right] at a Quaternary Catchment resolution
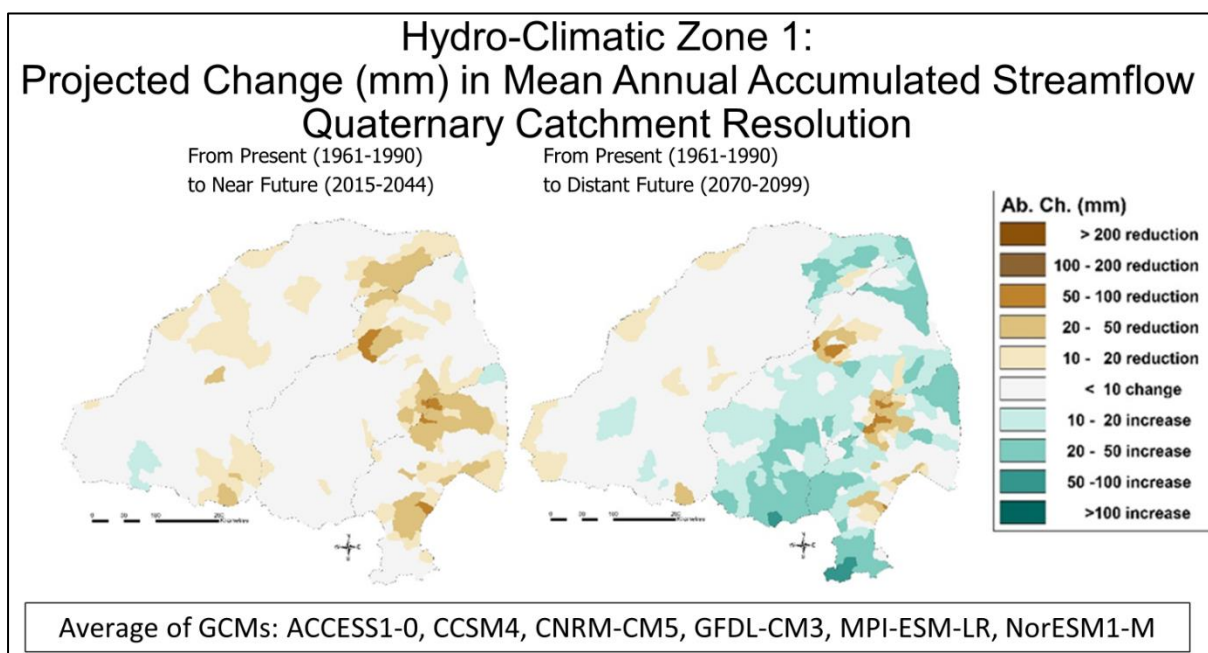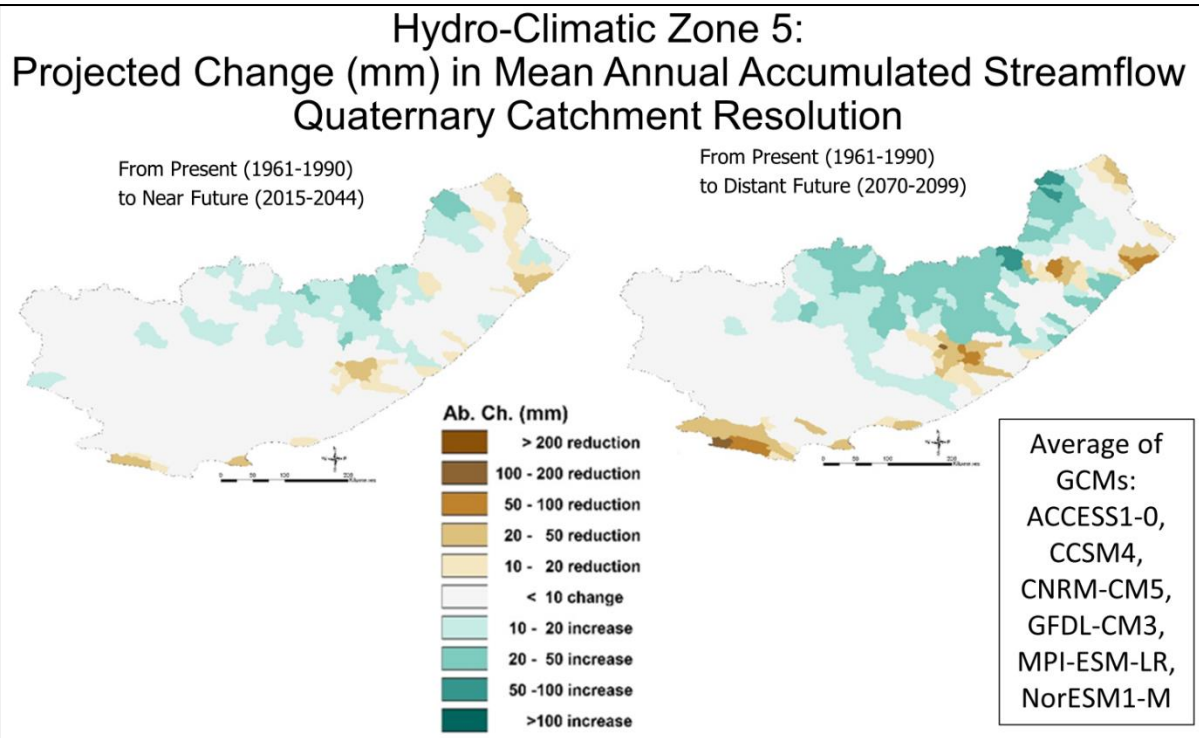
Figure 7.31 Hydro-Climatic Zone 5: Projected changes in mean annual accumulated streamflow (mm) from the present to the near future [left] and the present to the distant future [right] at a Quaternary Catchment resolution
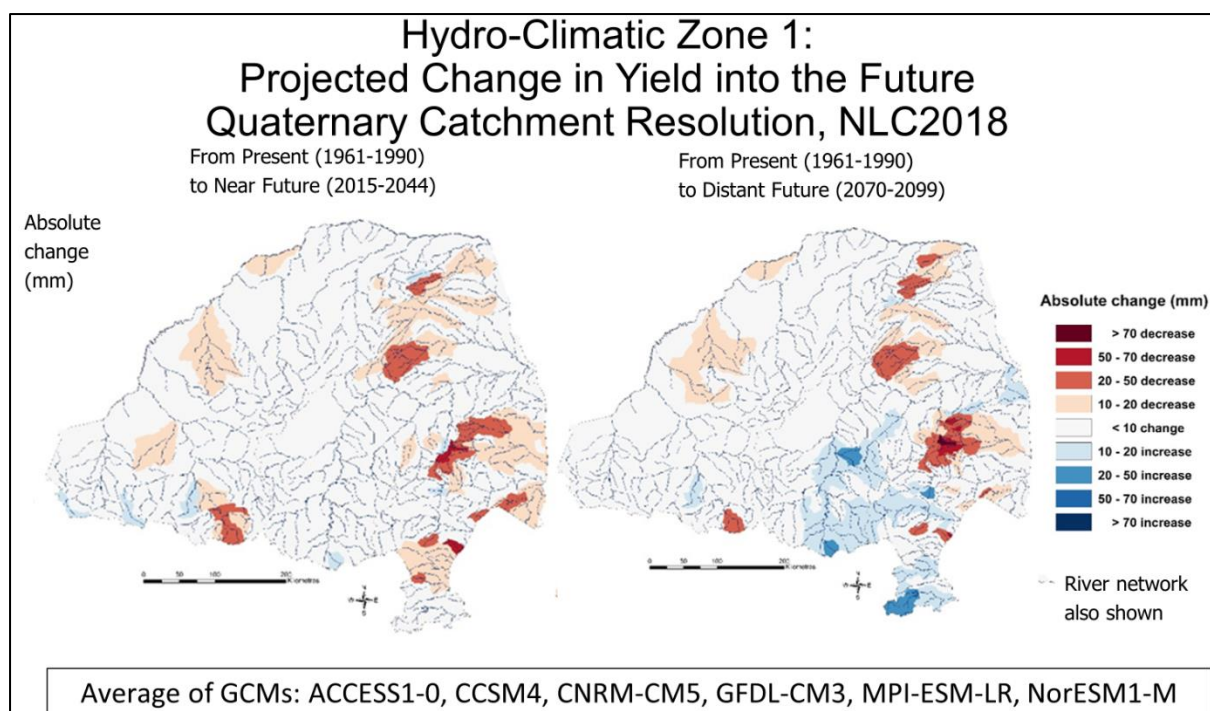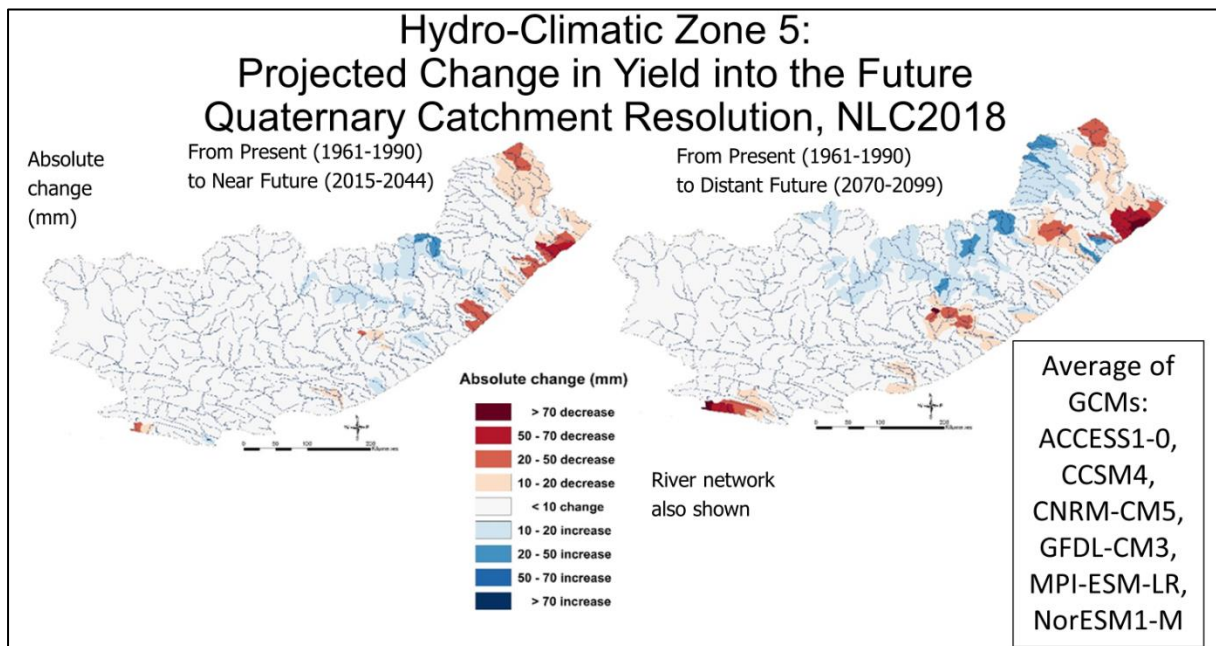

Figure 7.32 Hydro-Climatic Zone 5: Projected changes in hydrological yield (mm) from the present to the near future [left] and the present to the distant future [right] at a Quaternary Catchment resolution

Table 7.5   Hydro-Climatic Zone 5, comprising the Mzimvubu-Tsitsikamma WMA: Projected climate change impacts on temperature, precipitation, catchment runoff, accumulated streamflow and hydrological yield

Variable	Present to near future	Present to distant future
Annual mean of daily maximum temperatures	Increases of 1-2°C.	Increases of 2-6°C. Most severe (5-6°C) in the north-west, lowest increases along the coast (2-4°C).
Annual mean of daily minimum temperatures	Increases of 1-2°C.	Increases of 3-5°C. Most severe in the north (4-5°C), 3-4°C in the south and East Coast.
Mean annual precipitation	Mixed results. No change over most of the area, with patches of decreases in the north-east and south and patches of increases in the north and small areas in the east.	Mixed results, more severe compared to the changes to the near future. Some patches with increases in the north and east, patches with decreases in the south and north-east.
Mean annual catchment runoff, mean of GCMs	Mixed results. The largest area shows no change, with patches of increases in the north and patches of decreases in the north-east and along the coast towards the south	Mixed results, more severe changes compared to those towards the near future. The north generally shows increases, as do some patches in the east. No changes over much of the west. Decreases towards the south and some patches in the east.
Accumulated streamflow	Mixed results. The largest area shows no change, with patches of increases in the north and patches of decreases in the north-east and along the coast towards the south	Mixed results, more severe changes compared to those towards the near future. The north generally shows increases, as do some patches in the east. No changes over much of the west. Decreases towards the south and in some patches in the east.
Hydrological Yield	Mixed results. The largest area shows no change, with patches of increases in the northern interior and patches of decreases in the north-east and along the coast in the north.	Mixed results, more severe compared to the near future. The largest area shows no change, with patches of increases in the northern interior and patches of decrease in the north-east and along the coast in the north and to a lesser extent along the coast, towards the south.

7.2.6   Hydro-Climatic Zone 6

Hydro-Climatic Zone 6 is situated in the south of the country (**Figure 7.33**) and consists of WMA 8 (Breede-Gouritz) in the far south) and WMA 9 (Berg-Olifants) in the far south-west of the country, including Cape Town. Hydro-Climatic Zone 6's projected changes are summarised in **Table 7.6** and show temperature increases into the future, with severe increases projected into the distant future of up to 6°C (**Figure 7.34**). Change in mean annual precipitation generally shows decreases or no change, with changes more severe into the distant future (**Figure 7.35**). Mean annual catchment runoff generally shows decreases or no change, as does mean annual accumulated streamflow (**Figure 7.36** and **Figure 7.37**). Hydrological yield shows decreases or no change (**Figure 7.38**).
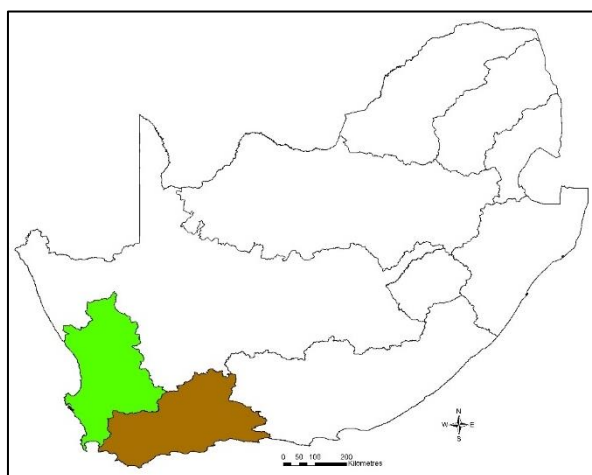
Figure 7.33 Hydro-Climatic Zone 6, in the far south of South Africa consists of WMA 8 (Breede-Gouritz) shown in brown and of WMA 9 (Berg-Olifants) shown in green
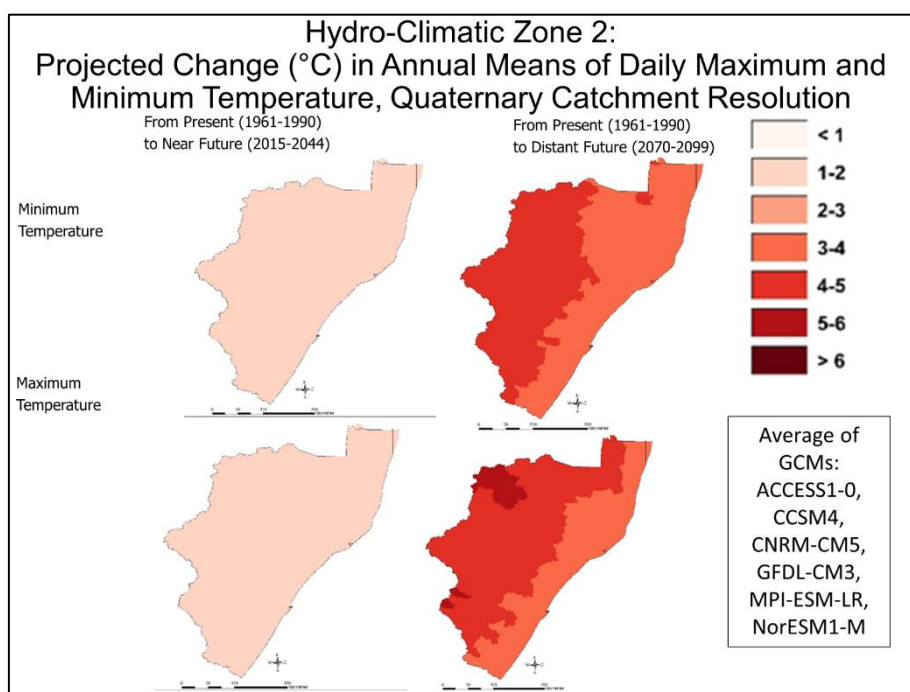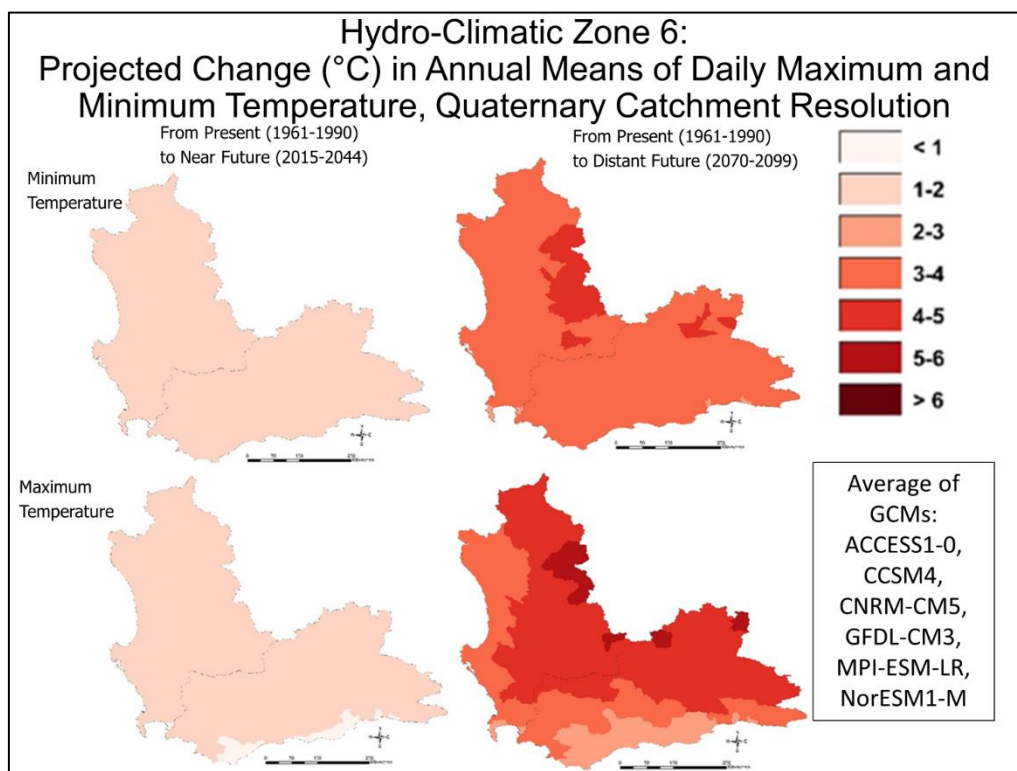

Figure 7.34 Hydro-Climatic Zone 6: Projected changes in annual means of daily maximum [bottom] and minimum [top] temperatures (°C) from the present to the near future [left] and the present to the distant future [right] at a Quaternary Catchment resolution
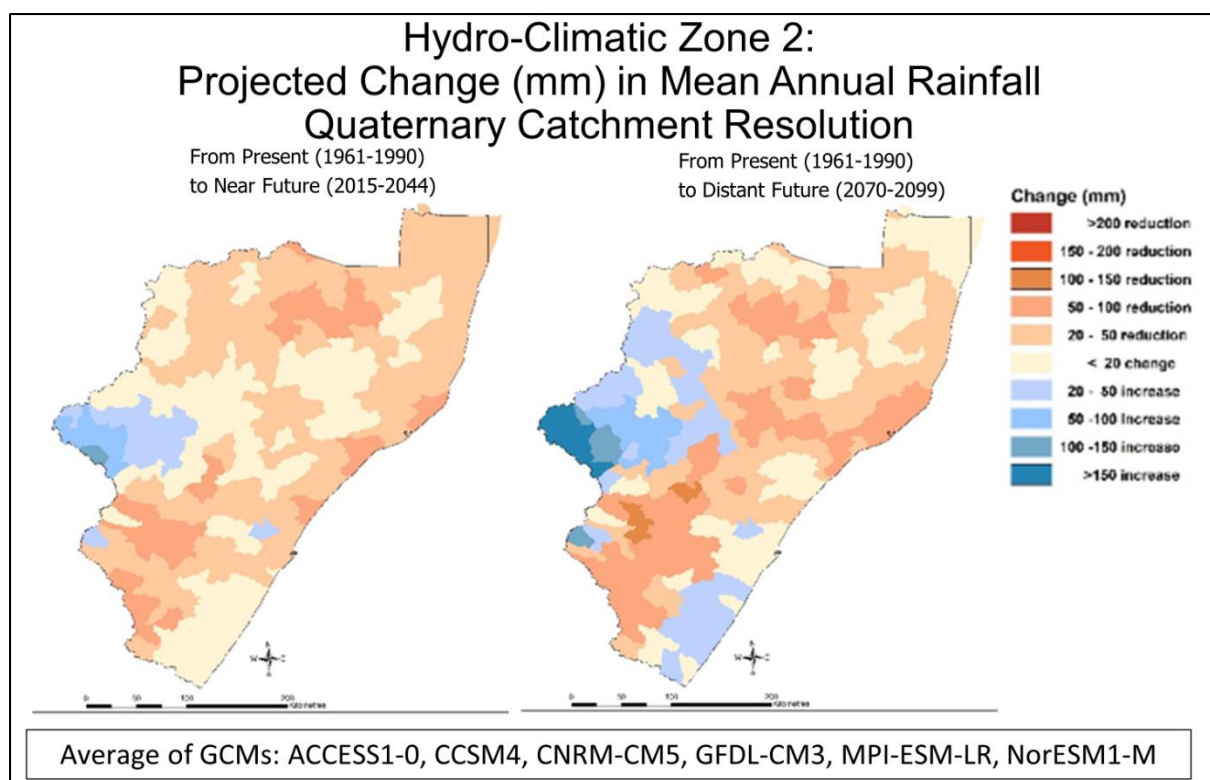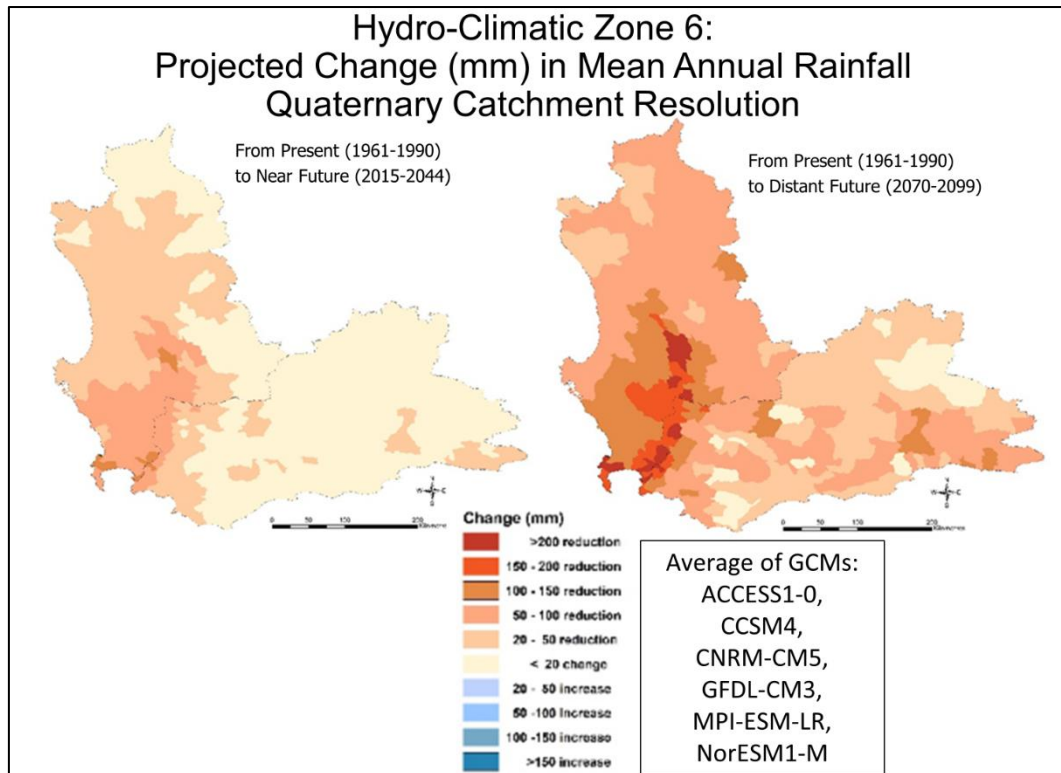
Figure 7.35 Hydro-Climatic Zone 6: Projected changes in mean annual precipitation (mm) from the present to the near future [left] and the present to the distant future [right] at a Quaternary Catchment resolution
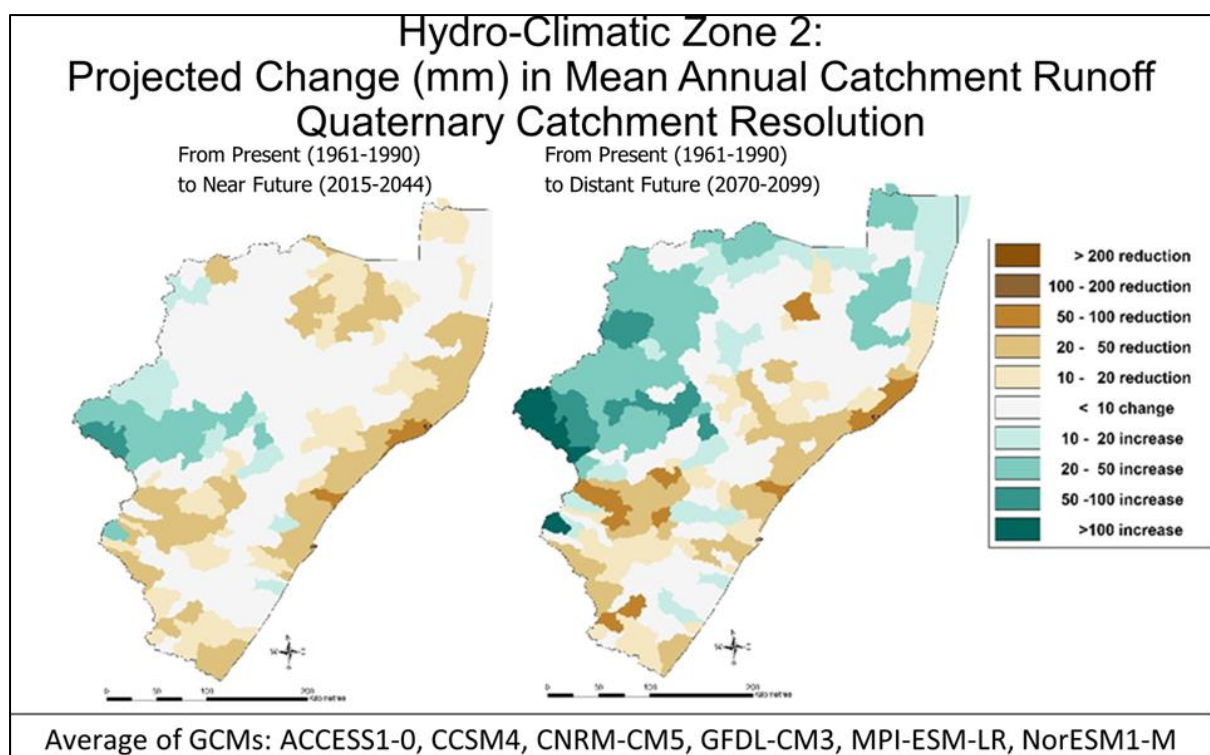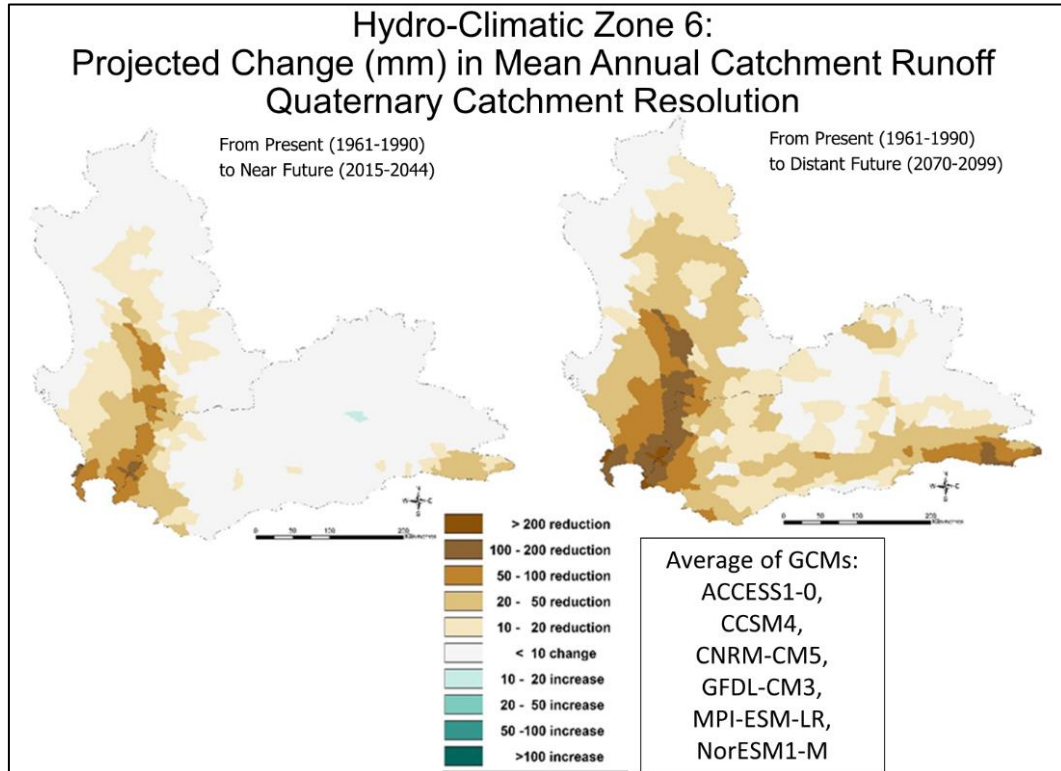

Figure 7.36 Hydro-Climatic Zone 6: Projected changes in mean annual catchment runoff (mm) from the present to the near future [left] and the present to the distant future [right] at a Quaternary Catchment resolution
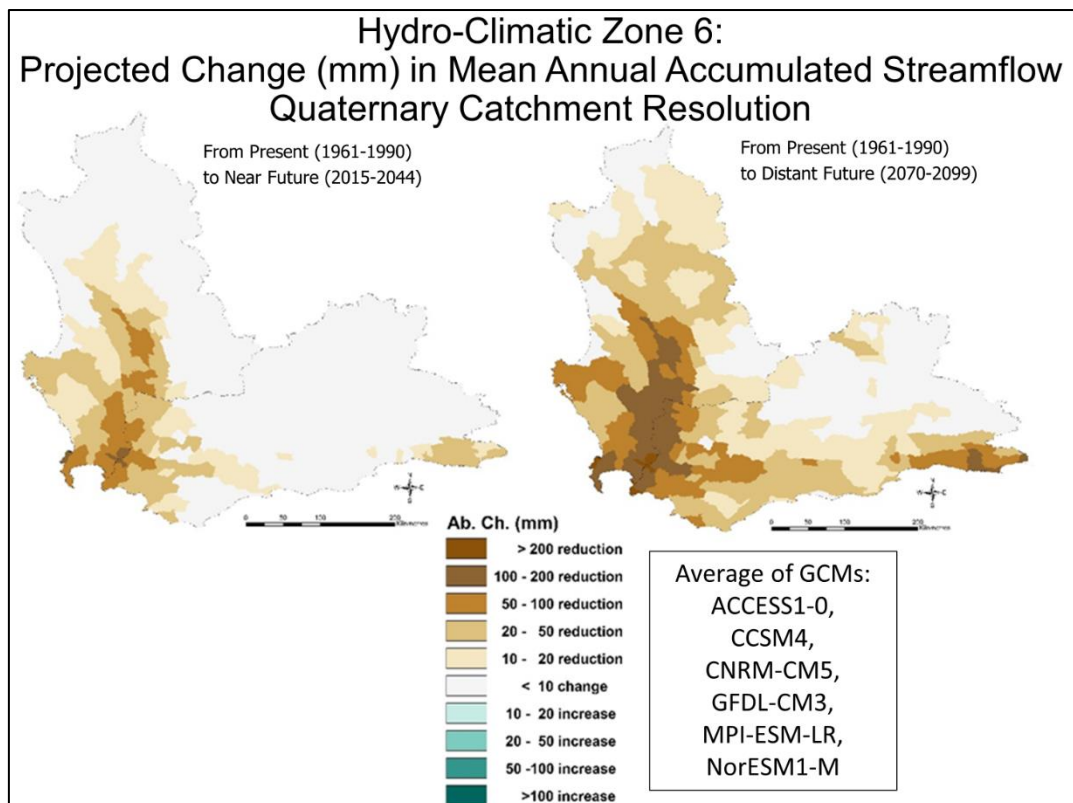
Figure 7.37 Hydro-Climatic Zone 6: Projected changes in mean annual accumulated streamflows (mm) from the present to the near future [left] and the present to the distant future [right] at a Quaternary Catchment resolution
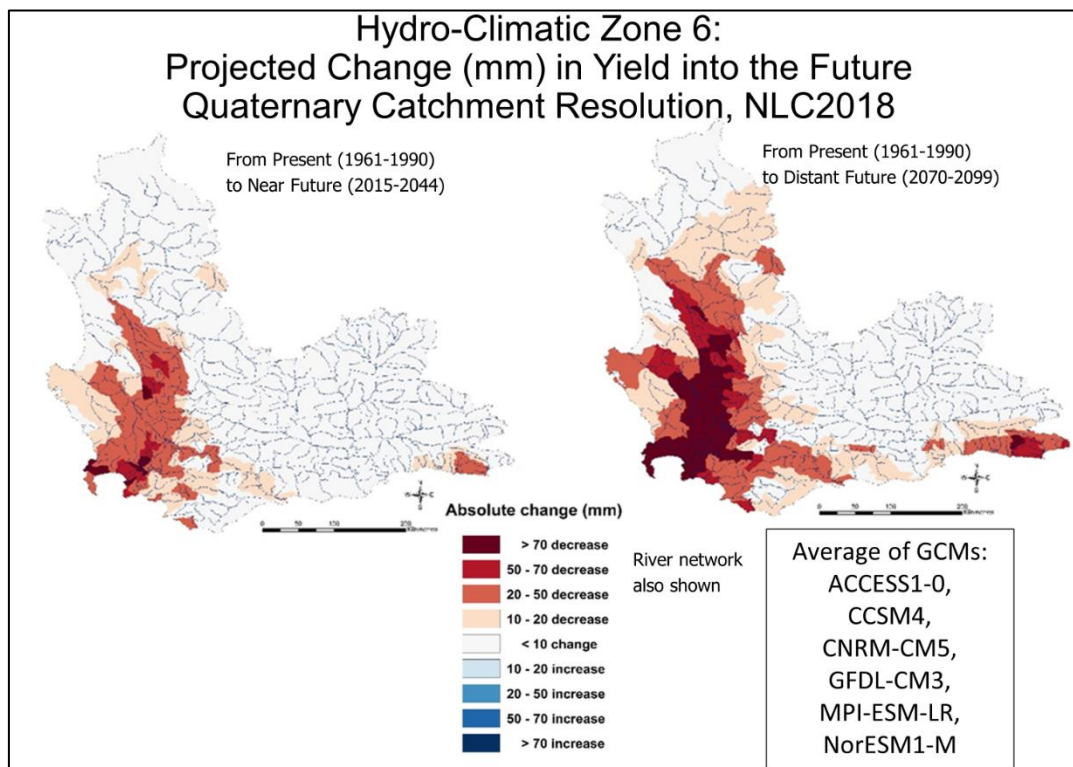
Figure 7.38 Hydro-Climatic Zone 6: Projected changes in hydrological yield (mm) from the present to the near future [left] and the present to the distant future [right] at a Quaternary Catchment resolution
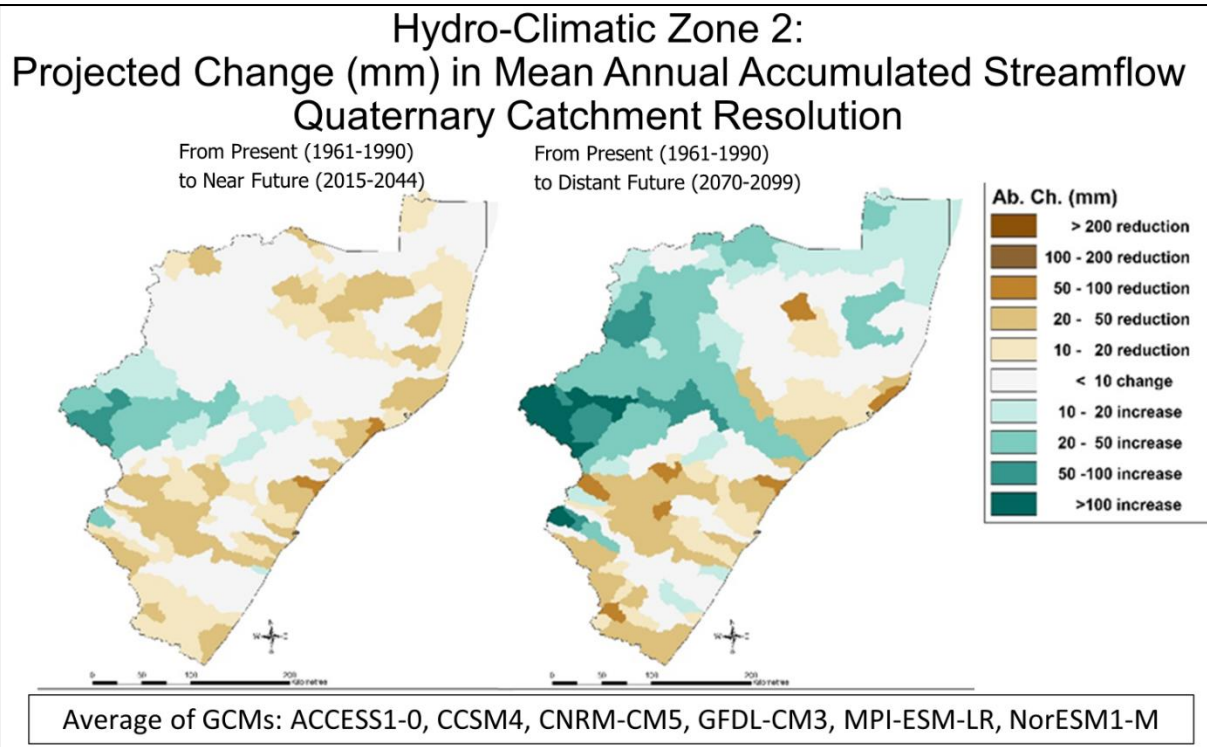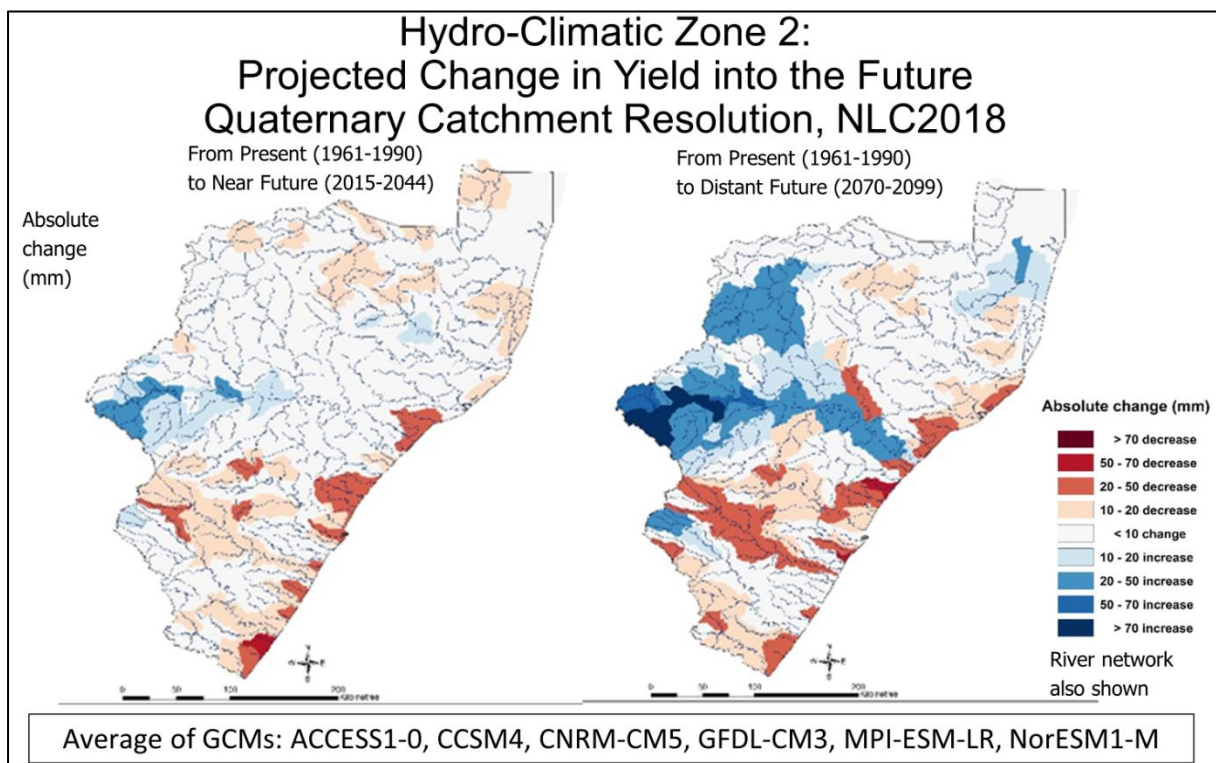
193

Table 7.6   Projected climate change impacts on temperature, precipitation, catchment runoff, accumulated streamflow and hydrological yield for the Hydro-Climatic Zone 6, comprising the Breede-Gouritz and Berg-Olifants WMAs

Variable	Present to near future	Present to distant future
Annual mean of daily maximum temperatures	Increases of 1-2°C.	Increases of 2-6 °C, with 2-3°C in the south-east, 3-4°C in the west, 4-6°C in the north.
Annual mean of daily minimum temperatures	Increases of <1-2°C.	Increases of 3-5°C. 3-4°C over most of the area, with patches of 4-5°C towards the north.
Mean annual precipitation	The whole area shows either no change or slight reductions. Generally no change in the east, with reductions in the west and south.	Most of the area shows reductions, more severe in the south-west towards Cape Town of up to and more than 200 mm. Some patches towards the east show no changes.
Mean annual catchment runoff, mean of GCMs	The whole area shows either no change or slight reductions. Generally no change in the east, with reductions in the west and south.	Most of the area shows reductions, more severe in the south-west towards Cape Town of up to 200 mm. Some patches towards the east and west show no changes.
Accumulated streamflow	The whole area shows either no change or slight reductions. Generally no change in the east, with reductions in the west and south.	Most of the area shows reductions, more severe in the south-west towards Cape Town of up to 200 mm. Some patches towards the east and west show no changes.
Hydrological Yield	The whole area shows either no change or reductions. Generally no change in the east, with reductions in the west and south.	Most of the area in the west show reductions, more severe in the south-west towards Cape Town of up to and more than 70 mm. Most of the east shows no change, but reductions in the south-west.

7.3   References

DEA and GTI (2019) *73 Class GTI South African National Land Cover Dataset (2018)* [Dataset]. Produced by GeoTerraImage Pty Ltd (GTI) for the Department of Environmental Affairs (DEA), Pretoria, South Africa

Department of Water and Sanitation (DWS) no date *National Climate Change Response Strategy for the Water Sector*. Report No. P RSA 000/00/17812-18112.

Department of Water and Sanitation (DWS) (2016) *Water Management Areas in South Africa.* Available from www.dws.gov.za/IO/Docs/Starter%20Pack%20_Final_FULL%20(00000003).pdf

SCHULZE, R AND HORAN, M. 2010. Methods 1: Delineation Of South Africa, Lesotho And Swaziland Into Quinary Catchments. In: *Methodological Approaches to Assessing Eco-Hydrological Responses to Climate Change in South Africa*, SCHULZE, R, HEWITSON, B, BARICHIEVY, K, TADROSS, M, KUNZ, R, HORAN, M AND LUMSDEN, T, WRC Report 1562/1/10. Water Research Commission, Pretoria, South Africa.

8   CLIMATE CHANGE IMPACTS IN THE LIMPOPO WATER MANAGEMENT AREA – A CASE STUDY

S. Schütte, RE Schulze

8.1   Background to the Study Area

In order to be able to recommend climate change adaptation strategies, impacts need to be analysed in further detail. Impacts on the Limpopo WMA is here analysed in more depths.

Background

The Limpopo Water Management Area (WMA) is the most northerly WMA in South Africa (**Figure 8.1**) and forms part of the international Limpopo Basin, which spans across South Africa, Botswana, Zimbabwe and Mozambique. The Limpopo River forms the borders between South Africa and Zimbabwe and Botswana in the north and further downstream between South Africa and Mozambique. The Limpopo WMA comprises of six major catchments, viz. the Matlabas, Mokolo, Lephalala, Mogalakwena, Sand and Nzhelele which, together with smaller tributaries, flow northwards into the Limpopo River. The WMA is highly water stressed through extensive development with limited water resources as well as poor management due to limited financial/human capital resources.
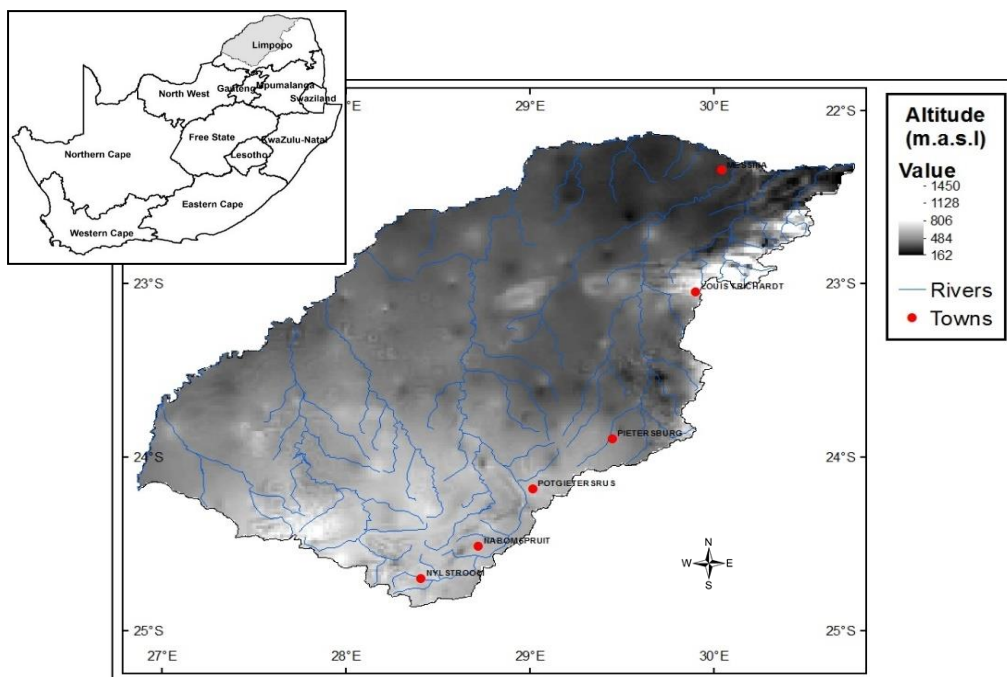
Figure 8.1   Location of the Limpopo WMA, with the river network and altitudes also shown

Physiography and Soils

The topography of the Limpopo WMA is characterised by mountains surrounded by flat plains (**Figure 8.1**). The major mountain ranges include the Waterberg in the south and east, at altitudes of over 1 800 m.a.s.l., which forms the water divide between the Lephalala and Mogalakwena catchments as well as between the Mokolo and Mogalakwena catchments; the Soutpansberg range, with altitudes of over 1 700 m.a.s.l., which forms the upper reaches of the Nzhelele and Nwanedi catchments; the Blouberg mountain, which is the highest free-standing massif in the Mogalakwena catchment at an altitude of

over 2 000 m.a.s.l., with several other massifs in this catchment and the Buffelshoek mountain range, with an altitude of over 2 000 m.a.s.l. in places, extending east from Mokopane.

The southern and western parts of the WMA are underlain mainly by sedimentary rocks, whilst metamorphic and igneous rocks are found in the northern and eastern parts. With the exception of some alluvium deposits and dolomites near Mokopane and Thabazimbi, the formations are mostly not high water-bearing. The mineral rich Bushveld Igneous Complex extends across the south-eastern part of the WMA, and precious metals are mined at various locations. Large coal deposits are found in the north-west.

Land Uses
The primary economic activities in the WMA are irrigated commercial agriculture, livestock farming and power generation, with mining becoming more important. A portion of the inhabitants are dependent on subsistence farming. The challenges are that the catchment is part of a transboundary basin, and that water demand is increasing from farming activities and mining.

Irrigation developments occur at various locations throughout the Limpopo WMA, such as in the Waterberg area, the Sand River catchment and along the Limpopo River, with much of the water being supplied from farm dams and groundwater. Small areas of commercial forest are found in the high rainfall parts of the Soutpansberg near Louis Trichardt. Most of the WMA remains under natural vegetation, with livestock and game farming as main activities. Severe overgrazing is prevalent in many areas.

Climate
The mean annual temperatures of the WMA are relatively high, with the lowest mean annual temperature of 15ºC occurring over the high mountain ranges and the highest mean annual temperatures in the north of the WMA reaching 23ºC (**Figure 8.2**). Most of the WMA experiences January means of daily maximum temperatures upwards of 26°C (**Figure 8.3**), with relatively high means of July minimum temperatures. The mean annual potential evaporation is in excess of 2 000 mm.a^{-1} over the entire WMA (Schulze et al., 2008). Annual means of daily maximum temperatures are between 25 and 30°C for most of the area and daily minimum temperatures between 10-15°C for most of the region (**Figure 8.4**).
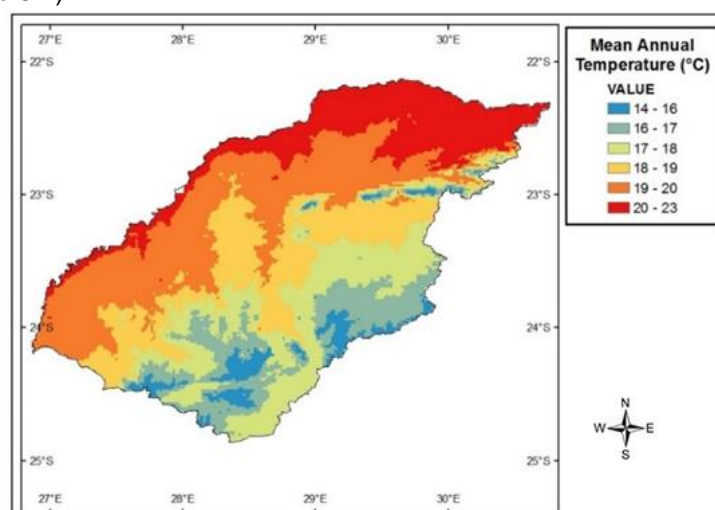
Figure 8.2   Mean annual temperatures across the Limpopo WMA (Schulze, 2008)
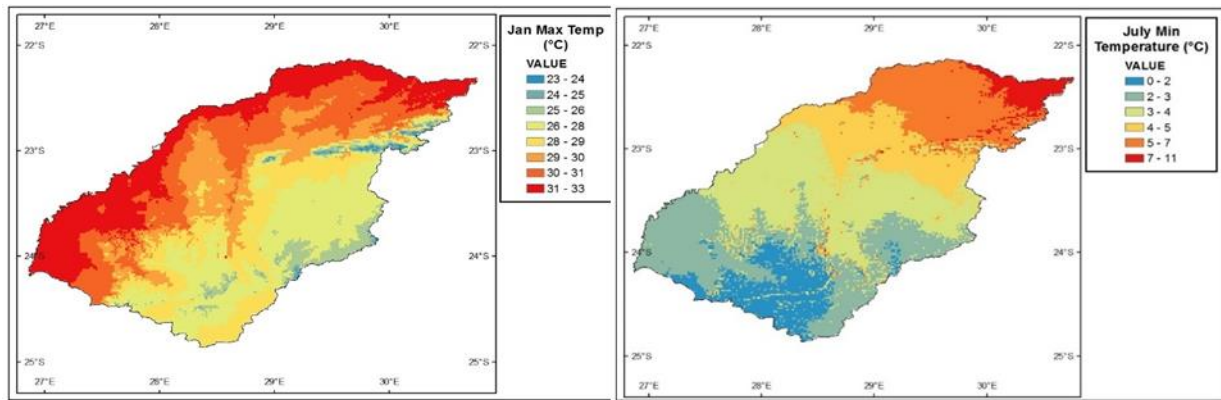
Figure 8.3   (a) Means of January daily maximum temperatures [left] and [right] means of July daily minimum temperatures across the Limpopo WMA (Schulze., 2008)
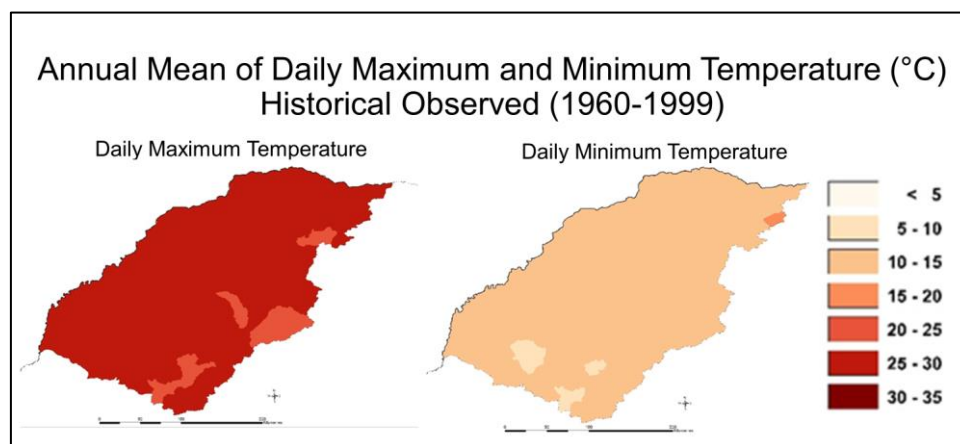
Figure 8.4   Annual means of daily maximum (left) and minimum (right) temperature for the Limpopo WMA, historical observed

The climate of the WMA is temperate to semi-arid in the drier west and prone to droughts. The WMA falls within the summer rainfall region of South Africa. Most of the WMA experiences a mean annual precipitation of less than 500 mm.a^{-1} (**Figure 8.5**) and, added to this, the rainfall is highly variable over time, with the inter-annual coefficient of variability of rainfall ranging from 30% to 50%. The wettest month in the catchment is generally January (**Figure 8.6**), with the driest month on average being July.
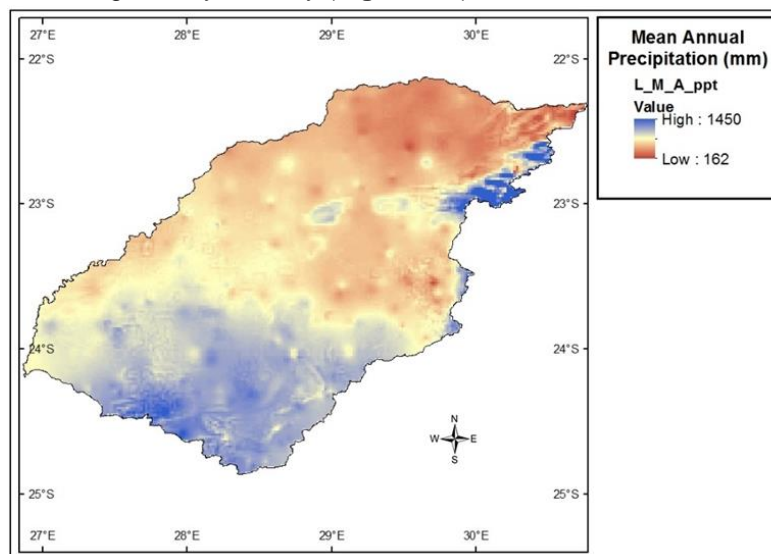
Figure 8.5   Mean annual precipitation across the Limpopo WMA (Schulze, 2008)
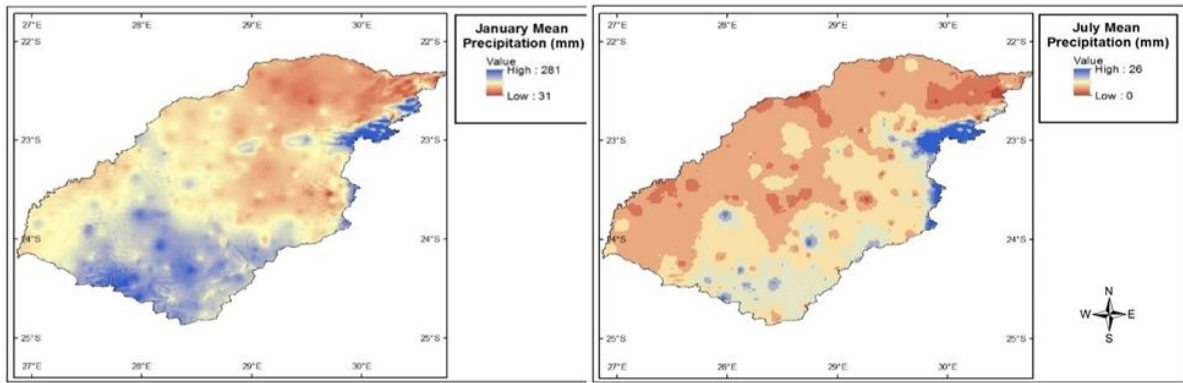
Figure 8.6   Means January precipitation [left] and [right] mean July precipitation across the Limpopo WMA (Schulze, 2008)

Hydrology

The Limpopo WMA includes the following major rivers: the Limpopo River, Matlabas River, Mokolo River, Lephalala River, Mogalakwena River, Sand River and Nzhelele River, all flowing into the Limpopo River. The catchments form part of Primary Catchment A and have been divided into Secondary Catchments A4, A5, A6, A7 and A8 (**Figure 8.7)**, as well as further into Tertiary (A41, A42, A50, A61 to A63, A71, A72 and A80), Quaternary and Quinary Catchments (Quinary Catchment No. 174-375).
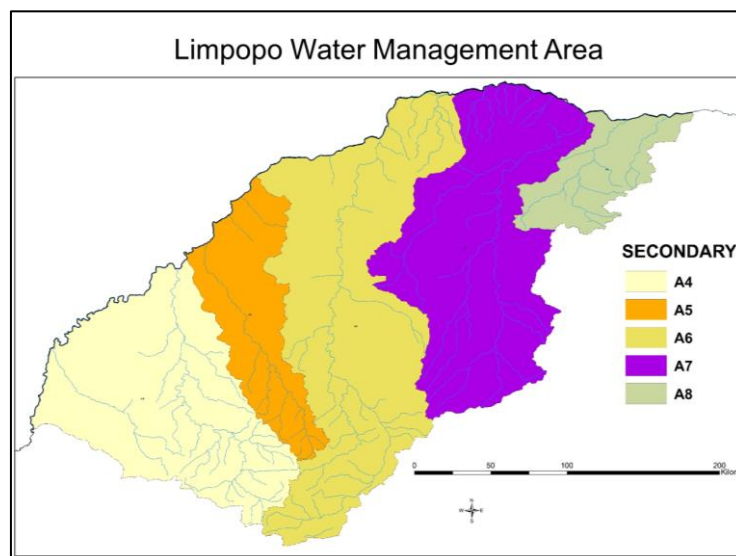
Figure 8.7   The Secondary Catchments of the Limpopo WMA, with the river network also shown

For the historical (observed) climate from 1961 to 1990, mean annual rainfall is 466 mm, with a mean annual runoff of 62 mm. This means that overall only 13% of rainfall is converted into runoff (**Figure 8.8),** which consists of ~ 70% stormflow and 30% baseflow.

The mean annual accumulated streamflows for the Limpopo are low, the greatest flows being around 100 mm.a^{-1}. However, the inter-annual coefficient of variation of accumulated streamflows is greater than 50% for all areas of the WMA. The highest streamflow month for the Limpopo WMA is January, while the lowest streamflow month is August, when the mean accumulated flows are less than 2 mm (Schulze., 2008).
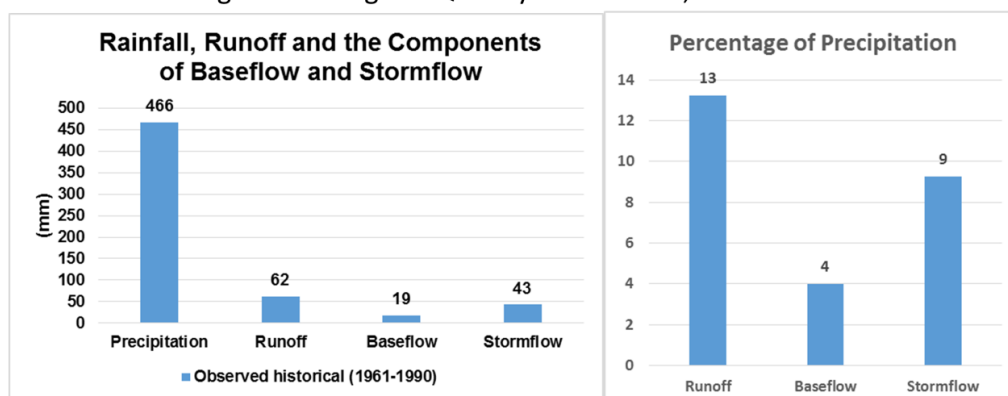
Figure 8.8   Mean annual precipitation, individual catchment runoff and its components of baseflow and stormflow, all in mm equivalent (left) and as a percentage of rainfall (%, right), computed from area weighted averages of the Quinary Catchments for the Limpopo WMA, under actual land cover

Mean annual accumulated streamflow volumes, at Quinary Catchment resolution (**Figure 8.9**   ), modelled under actual land cover conditions of 2018 (NLC2018; DEA and GTI, 2019) and described previously in Chapter 3, displaying the higher volumes of the main rivers.
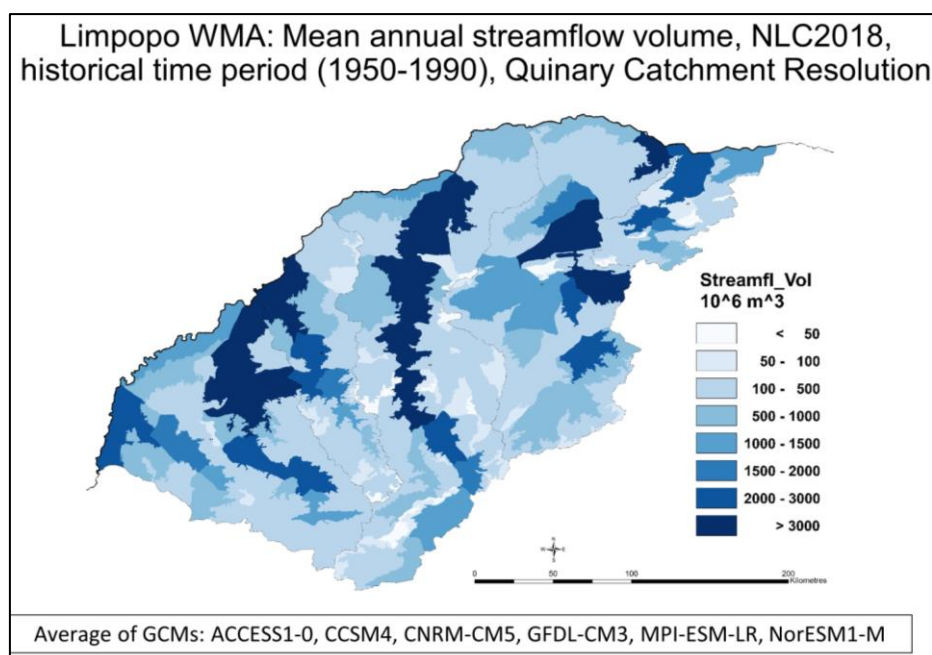
Figure 8.9   Mean annual streamflow volumes (10^6 m^3) under historical climate conditions (1950-1999) at Quinary Catchment resolution for the Limpopo WMA

8.2 Climate Change Impacts on Temperature, Rainfall, Hydrological Responses and Hydrological Yield

The methodology of modelling projected climates under the RCP8.5 emission scenario has been described previously in this report. Temperature as annual means of daily maximum and minimum temperature for three time periods for the Limpopo WMA are discussed first, followed by projected changes in mean annual rainfall. The results of these changes in climate inputs, when modelling using the *ACRU* daily agro-hydrological model, under actual land uses as of 2018 (NLC2018; DEA and GTI, 2019), but not including dams or water abstractions are analysed in detail in this section. This includes the hydrological responses of runoff and its components of stormflow and baseflow. Projected changes in hydrological yield are then discussed.

Daily means of maximum and minimum temperatures **Figure 8.10**) show temperature increases throughout the WMA, for this already hot region. Maximum temperatures are projected to increase from the present to the near future by 2-3°C in the north-east and by 3-4°C on average in the south-west. When comparing the present to the distant future, the projections show severe temperature increases of 5-6°C in the south-west and 4-5°C in the north-east.
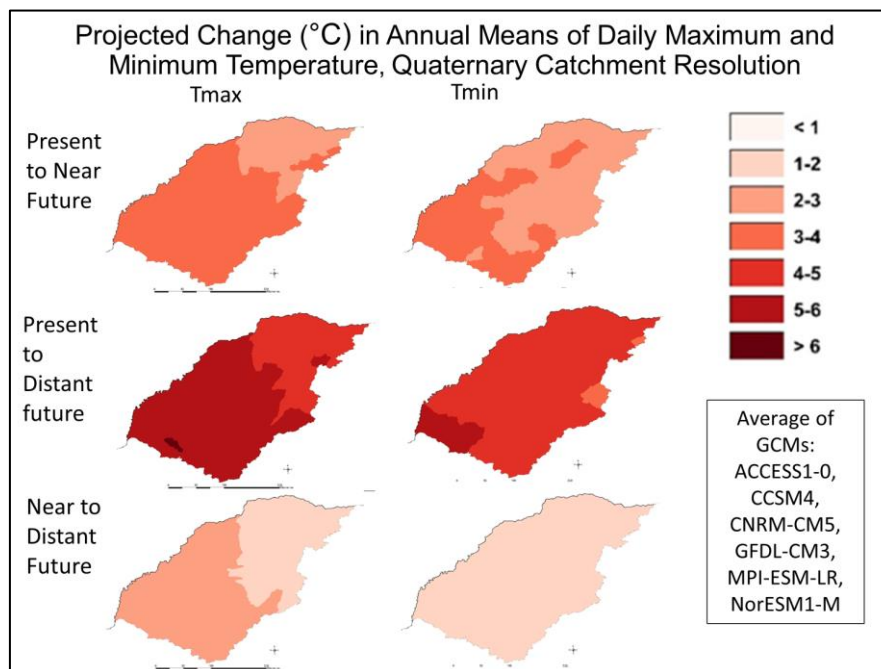
Figure 8.10 Limpopo WMA increases in projected annual means of daily maximum temperatures (left column) and minimum temperatures (right column) for the present to near future period (top row), the present to distant future (middle row) and the near to distant future (bottom row)

For the Limpopo WMA, the projected, GCM generated impacts of climate change on rainfall is shown spatially in **Figure 8.11** and graphically in **Figure 8.12**. Graphically, rainfall, runoff and its components of stormflow and baseflow calculated as averages of the Quinary Catchments of the region, show a reduction in mean annual rainfall by ~ 10% from 502 mm (present, 1961-1990) to 451 mm for the near future (2015-2044) and a further reduction to 436 mm for the distant future (2070-2099). This equates to a 13% reduction in rainfall from the present to the distant future. Runoff and its stormflow component show relatively little difference, with a small decrease in baseflows.
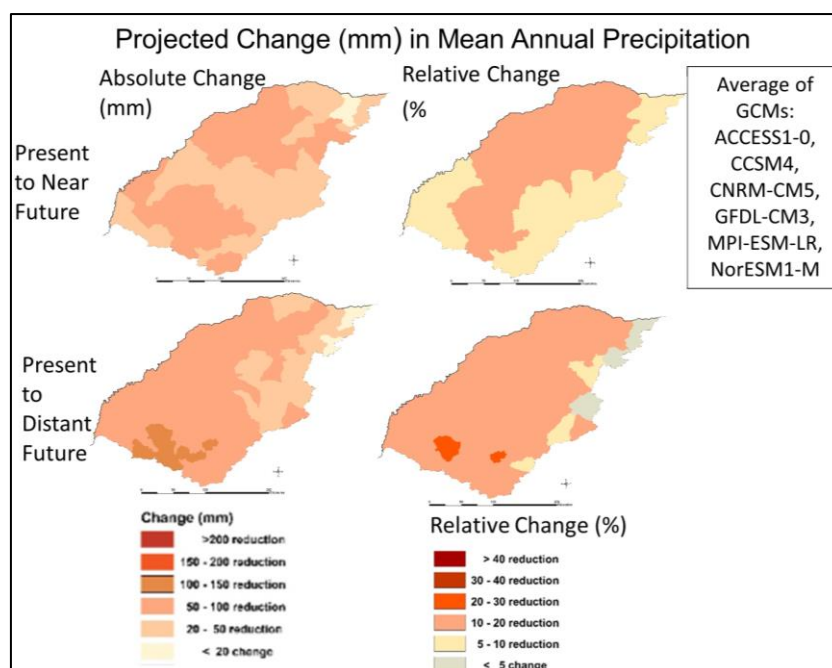
Figure 8.11 Limpopo WMA projected changes in mean annual rainfall, expressed as absolute changes (mm; left column) and relative changes (%; right column) for the present to near future period (top row) and the present to the distant future (bottom row)
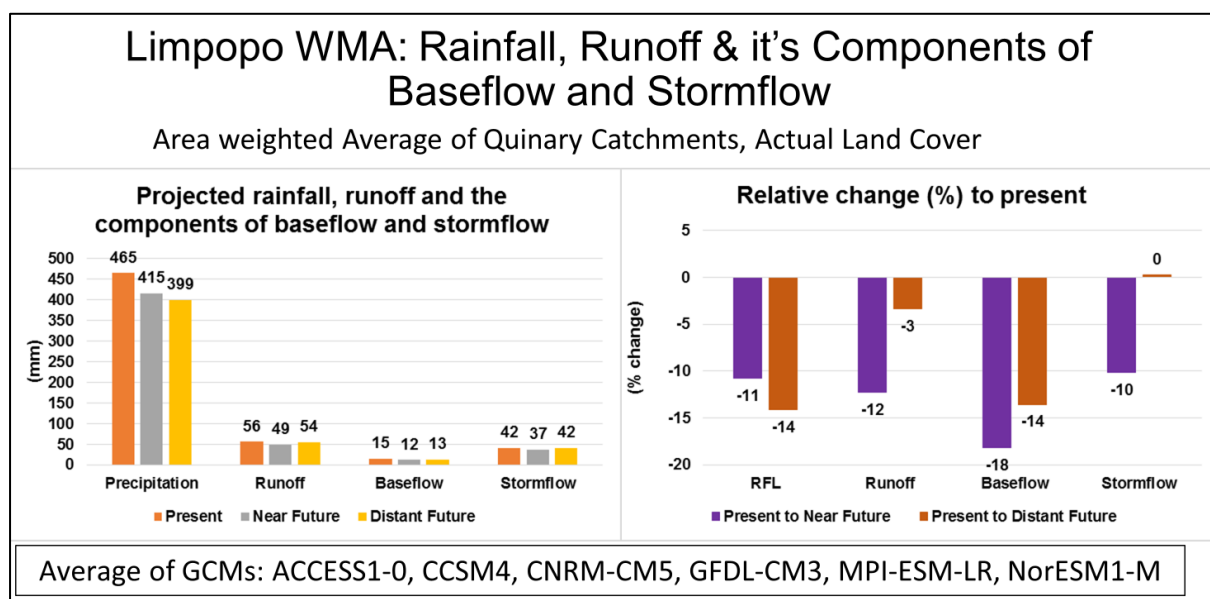
Figure 8.12 Limpopo WMA GCM projected rainfall, runoff and its components of baseflow and stormflow (left), as well as relative changes to the near and distant periods (right), with results expressed as area weighted averages of Quinary Catchments

The hydrological yield, previously described in Chapter 6), is shown spatially in **Figure 8.13** and graphically in **Figure 8.4**. The hydrological yield at major outlets of the area into the Limpopo River varies from 34 to 47 mm depth equivalent for the present. Into the future, climate change impacts are projected to reduce the hydrological yield (**Figure 8.15**) for all Secondary Catchments from the present to the near future, and further into the distant future for most Secondary Catchments. On average, the hydrological yield from all major drainage areas to the Limpopo River within South Africa is projected

to reduce due to climate change impacts. The projected reduction in hydrological yield is 11% from present (1961-1990) to near future (2015-2044) and 15% from present to distant future (2070-2099).
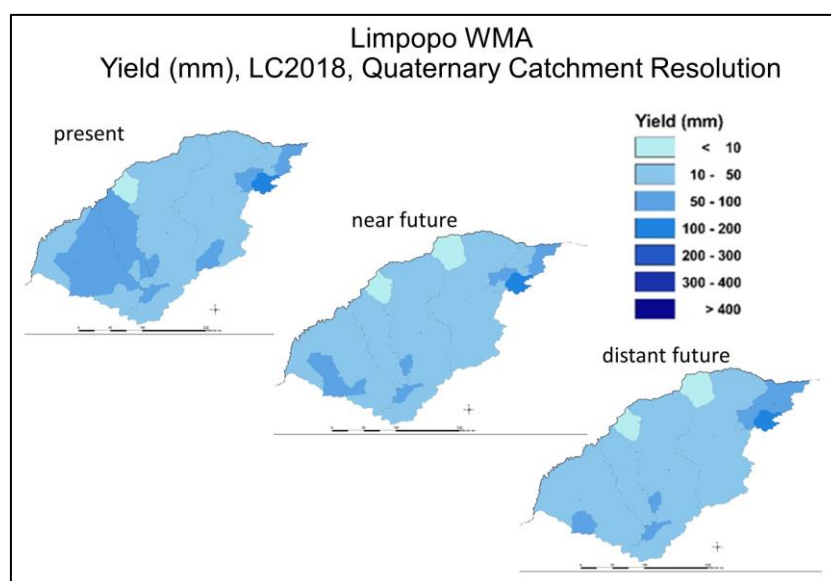
Figure 8.13 Projected hydrological yield (mm) for the present (left), the near future (middle) and the distant future (right) for the Limpopo WMA
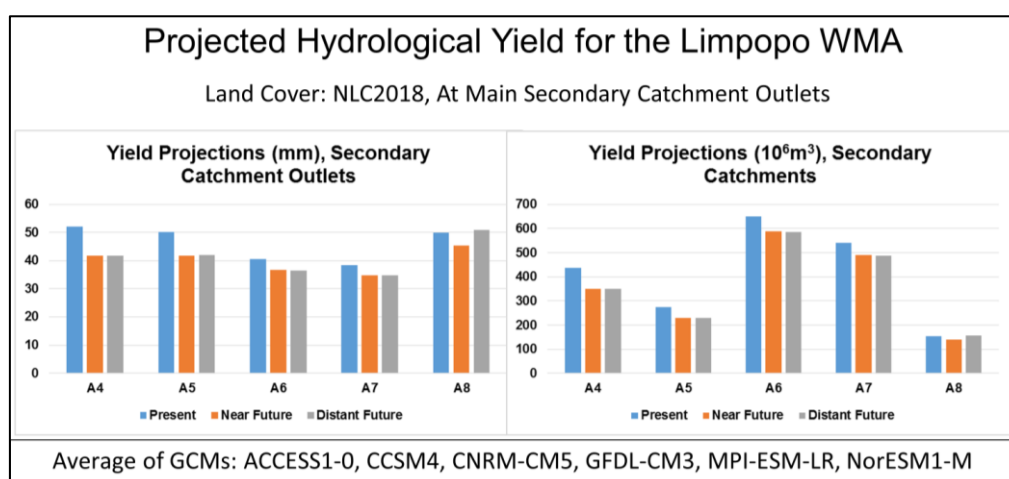
Figure 8.14 Yield projections for the Limpopo WMA in mm equivalents (left) and as a volume (10^6m^3) at the Secondary Catchment outlets, for the present (1961-1990), the near future (2015-2044) and the distant future (2070-2099)
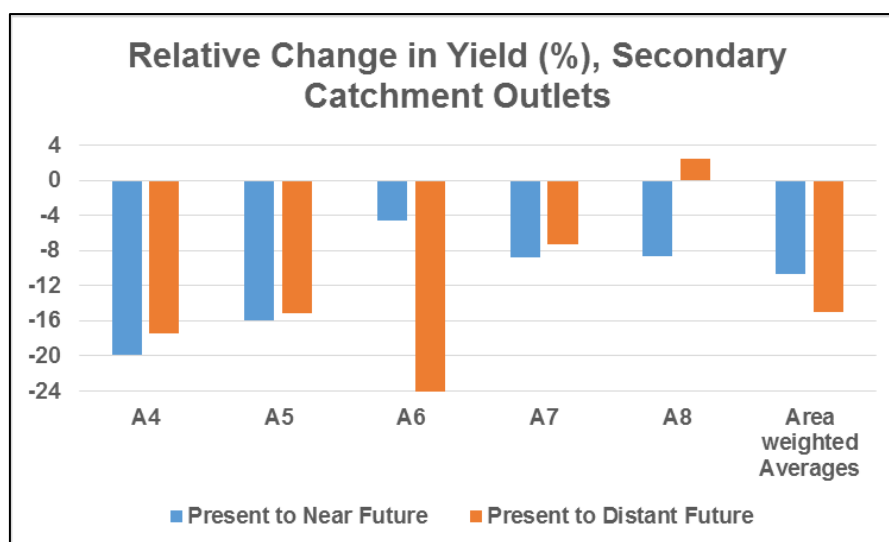
Figure 8.15 Relative changes (%) in yield within the Limpopo WMA at the Secondary Catchment outlets, and area weighted average for the present (1961-1990) to the near future (2015-2044; in blue) and to the distant future (2070-2099; in orange)
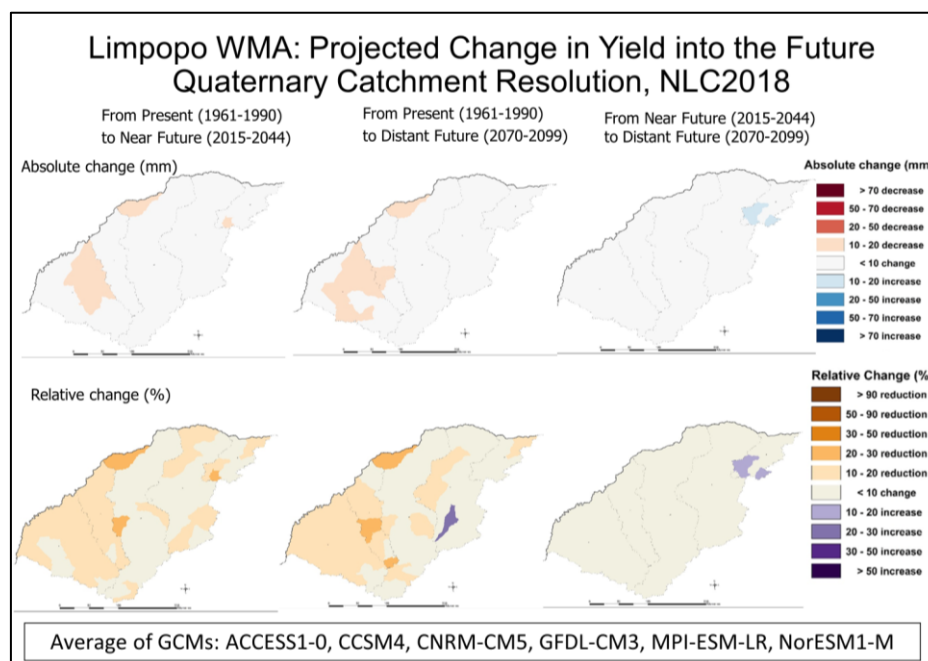
Figure 8.16   Projected changes into the future in hydrological yield for the Limpopo WMA under actual land use conditions (NLC2018) at Quaternary Catchment Resolution, showing absolute changes (mm, top row) and relative changes (%, bottom row), from present to near future (left column), from present to distant future (middle) and from the near to distant future (right) scenarios, with Secondary Catchment boundaries also shown

8.3   Summary, Discussion and the Way Forward

In summary, for the Limpopo WMA, climate change from the RCP8.5 emission scenario, when comparing averages of GCM generated climates for the periods termed the present (1961-1990), the near future (2015-2044) and the distant future (2070-2099) result in the following impacts.

Temperatures are increasing. This already hot area is getting even hotter in average, both for daily maximum, and daily minimum temperatures. Maximum daily temperatures are projected to increase by 2-4°C from the present to the near future and by 4-6°C from the present to the distant future.
Rainfall, in this already low rainfall area is projected to decrease by 11% from the present to the near future and by 14% from the present to the distant future. Most change occurs from the present to the near future, and less from the near to the distant future.
Mean annual runoff, baseflow and streamflow shows only a small change.
The hydrological yield reduces by 11% from the present to the near future and 15% from the present to the distant future. Most change occurs from the present to the near future, and less from the near to the distant future.

With a projected decline in hydrological yield, both water supply and demand needs to be carefully managed.

The above climate change impacts are likely to translate into more frequent and severe heatwaves, higher incidence of discomfort, as measured by the discomfort index, higher heat stress for livestock and wildlife. Higher plant water stress leads to a higher irrigation demand.

It is strongly recommended that **mitigation measures,** locally and globally, be urgently put in place, to reduce greenhouse gas emissions, so that severe climate change impacts are reduced.

Going forward, finer scale analysis could be done for the other WMAs.

8.4   References

SCHULZE RE (2008) *South African Atlas of Climatology and Agrohydrology*. Research Report no. 1489/1/08, Water Research Commission, Pretoria, South Africa. (On interactive DVD).

9 GENERAL CONCLUSIONS, RECOMMENTDATIONS AND FUTURE RESEARCH

S. Schütte, R.E. Schulze

9.1 Summary of Main Findings

9.1.1 Establish appropriate climate scenario projections (*cv*. Chapter 2)

Selection of appropriate climate scenario projections (cv. Chapter 2.1)
An ensemble of very high-resolution climate model simulations of present-day climate and projections of future climate changes over South Africa were produced in previous projects by the CSIR, using the CCAM regional climate model. In that effort, six GCM simulations from the CMIP5 archive based on the emission scenarios described by RCP4.5 and RCP8.5 were first downscaled to a 50 km spatial resolution globally. The selection of these six GCMs was based on their ability to provide a reasonable representation of the El Nino-Southern Oscillation (ENSO) phenomenon for the region. A multiple-nudging strategy was then followed to obtain 8 km resolution downscalings. The simulations span the period 1961-2100. The six downscaled GCMs are the:

- Australian Community Climate and Earth System Simulator (ACCESS1-0);
- Geophysical Fluid Dynamics Laboratory Coupled Model (GFDL-CM3);
- National Centre for Meteorological Research Coupled Global Climate Model, v5 (CNRM-CM5);
- Max Planck Institute Coupled Earth System Model (MPI-ESM-LR);
- Norwegian Earth System Model (NorESM1-M); and the
- Community Climate System Model (CCSM4).

Projections for both RCP4.5 and RCP8.5 mitigation scenarios were originally considered for this study, with RCP4.5 being a high mitigation scenario, whilst RCP8.5 being a low mitigation scenario. It is noted that the RCP scenarios only diverge significantly in their projections after approximately 2050. Until 2050, the variation among the available GCM projections is greater than the difference between the RCP scenarios considered. During the course of the study, it was found that the dataset supplied under RCP4.5 was not compatible with the supplied RCP8.5 dataset, due to a likely difference in the underlying modelling assumptions. The appropriate RCP4.5 dataset that would have enabled fair comparisons with the RCP8.5 dataset could not be located at the CSIR and may have been accidentally deleted during a clean-up of storage space. As it was not possible to re-generate the appropriate dataset within the scope of this project, CCAM RCP4.5 projections were not considered further in the study.

Reference database of observed climate (cv. Section 2.2)
The recently revised Quinary Catchments Database (QnCDB) consists of 50 years of observed rainfall and temperature (maximum and minimum) data that were adjusted to better represent each Quinary Catchment. This database also contains reference evapotranspiration (FAO56 and A-pan equivalent) for each Quinary. For this study, the QnCDB was used to determine baseline hydrological conditions against which potential impacts of climate change were assessed. A modified version was used to bias correct the projected climate data.

Bias Correction of daily rainfall and temperature projections (cv. Section 2.3)
Daily rainfall and minimum air temperature projections are bias corrected to the resolution of the Quinary Catchments Database (QnCDB) with the methods described, giving 5 838 datasets covering South Africa, Eswatini and Lesotho. These datasets were used as climate input into the *ACRU* Model, to be able to determine climate change impacts on hydrological responses and hydrological yield.

9.1.2 Land cover inputs for assumed natural vegetation and actual land cover

Land cover inputs for assumed natural vegetation and actual land cover are outlined in Chapter 3. Next to climate impacts, there are other, non-climatic factors that can impact hydrological responses, compared to baseline conditions. These non-climatic factors include land cover change that has occurred from past natural land cover and also land cover and land use change over time. For this study, both a new natural vegetation baseline was used in the modelling scenarios as well as actual present-day (2018) land cover for other scenarios. These were used to develop land cover inputs for the configuration of the *ACRU* model. Water abstractions, irrigation, dams and inter-basin transfers were not taken into account in the configuration of the *ACRU* hydrological model as different scenarios of engineered flows are typically addressed separately in the hydrological yield calculations. Land cover and land use change projections did not form part of this study. Rather it was assumed that the whole time period (1961-2099) is either under natural land cover or under actual land cover conditions based on 2018, and kept static, while the climate changes.

Configuring a hydrological model with actual land cover/use for the whole of South Africa has been a significant undertaking. This is the first time that the *ACRU* model has been configured with actual land cover/use at Quinary Catchment level for the whole of South Africa, Lesotho and Eswatini. This is an exciting and important step forward for *ACRU* and South Africa.

9.1.3 Projected changes for rainfall, temperature and potential evaporation

Statistics of projected changes for rainfall, means of daily minimum and maximum air temperatures as well as potential evaporation are shown and discussed for southern Africa in Chapter 5, for the selected climate projections.

Projected changes for rainfall
Projected changes in mean annual rainfall for the individual GCMs show broad overall similarities with reduced rainfall in the west, especially towards the distant future, and increases in the Drakensberg and more central parts of South Africa. Differences in the severity of increases and reductions can be seen, with the magnitudes of decreases and increases depending on the GCM.

October rainfall (representing spring rains) generally show reductions over nearly all of southern Africa. The north-east seems to have a decrease in spring rain but an increase in rainfall in summer, thus a shift in the onset of rain later towards summer. January rainfall (representing summer rainfall) generally show increases in the interior and decreases in the south and mixed changes along the east coast. April rainfall (representing autumn rainfall) generally shows small to medium decreases in the west and north and small increases in the east. July rainfall (representing winter rainfall) generally show small decrease in the north and the interior, with small increases along the east.

Design rainfall events show projected changes from the present to the near future show increases over most of southern Africa. The increases in terms of ratios in general look larger for the rainfall events for 1-day 50-year return period, compared to the 1-day 10-year return period.

Projected changes for temperature
Projections for annual means of daily temperature show increases throughout southern Africa of between 1°C along the coast and 3°C in the north-west from the present to the near future, both for maximum and minimum daily temperatures. From the present to the distant future, projected changes are between 3° at the coast to more than 6°C in the north-west for daily maximum temperatures, while the minimum temperatures are also projected to increase by between 3° at the coast and to up to 6°C in the north-west.

Projected changes for potential evaporation
Projections for potential evaporation show increases throughout and larger increases towards the distant future, especially in the north-west, the north and the interior. The east coast in general shows a smaller increase in potential evaporation.

Projected temperature changes alone are showing a bleak picture for the future climate in southern Africa. Therefore, greenhouse gas emissions globally need to be reduced, to ensure this is not the future that we leave behind for future generations. Climate change mitigation thus needs to be given high priority, globally as well as in South Africa.

9.1.4 Projected hydrological responses to climate change

Actual evapotranspiration
The spatial distribution of evapotranspiration is much higher in the wetter east and lower in the drier west of the country. Projected changes in evapotranspiration into the future show milder changes for the near future and more extreme changes for the distant future. The west and north of the country have a projected reduction in evapotranspiration, the interior shows no changes, but the Drakensberg area show increases in evapotranspiration. The confidence in results (convergence of GCMs used) is generally from very high through high to medium, with lower confidence in the drier regions.

Individual catchment runoff
The spatial distribution of catchment runoff is much higher in the wetter east and lower in the drier north-west of the country. Projected changes are smaller for the near future and more extreme changes for the distant future. For the west, a reduction in runoff is projected, but this more severe for the distant future. The area around Cape Town shows sizeable relative and absolute reductions. The interior and to a lesser extent the north-east are projected to produce more runoff, compared to present conditions, especially for the distant future. The east coast generally shows little to no changes, though there are a few patches with more significant local changes in either direction. The confidence in the results (convergence of GCMs used) ranges from high to very low, generally lower in the west and the extreme north, with patchy spatial pattern.

Accumulated streamflow
The spatial distribution show more streamflow in the east, as well as south around Cape Town, but very little in the west, except for the Quinary Catchments that contain the large rivers flowing west. Projected changes into the near future show mixed changes. There is a general reduction in the west, a lesser reduction in the far north, an increase in the interior and little change around the eastern coast. The changes are more extreme towards the distant future. The confidence in results (convergence of GCMs used) are similar to runoff, except for the bigger river systems, which have a higher confidence than that of the surrounding catchments.

Seasonal changes in median streamflow (mm) for the spring period (September to November) shows small absolute changes, with small increases in the interior and small decreases along the coast and bigger decreases around the western part of the Western Cape. Changes for summer (December to February) streamflow shows small absolute increases in the interior, more towards the distant future. Small decreases can be seen in patches in the west, with the patches increasing towards the distant future. Projected changes in median streamflows for autumn (March to May) shows small increases in the interior, more towards the distant future for the Orange catchment, and decreases along the coast and north-west. Projected changes in median winter (June to August) streamflows shows small increases in the interior and small decreases along the coast and the north-west, with larger decreases in the western part of the Western Cape. This winter rainfall area stands out with projected reductions in winter streamflow, and the same can also be seen to a lesser degree for spring streamflow. For future

research, it would be beneficial to determine changes in streamflow volume, as that might be more important to the water management and planning sector.

Soil water drainage to the groundwater zone
The spatial distribution shows higher magnitudes of drainage in the wetter parts of the region. Projected absolute changes are small for most of the region, but especially into the distant future a reduction can be seen in areas of the Western Cape and along some eastern regions and some increases along the Drakensberg. In relative terms, generally a reduction can be seen especially towards the distant future in the west as well as along the east coast, but increases in the eastern interior and the far north. The confidence in results (convergence of GCMs used) of soil water drainage to the groundwater store is fairly low compared to other variables because of the various thresholds that have to be exceeded before drainage commences.

Baseflow
The spatial distribution shows higher magnitudes of baseflow in the wetter parts of the region. Projected absolute changes are small for most of the region, but especially into the distant future a reduction can be seen in areas of the Western Cape and along some eastern regions and some increases along the Drakensberg. In relative terms, a reduction can generally be seen, especially towards the distant future in the west as well as along the east coast, but increases in the eastern interior and the far north.

Design streamflow events
The term "design streamflow" is used to describe the depth (i.e. magnitude, in m³ or in mm equivalents) of streamflow, for a critical duration (where longer durations are important when considering designs on larger catchments, as well as for multiple day flooding and for regional damage assessments), for a desired frequency of recurrence (e.g. once in 10 or 50 years, depending on the size and economic importance of the structure), where the frequency is commonly referred to as the return period and where a return period of, say, 10 years implies a statistical probability of recurrence once in 10 years or 10 times in 100 years, and not that it will recur regularly every 10 years.

One day design streamflow volumes under historical climatic conditions show clearly the increase in flow magnitudes for the 50 year event compared to the 10 year event, and the increase in accumulated flow magnitudes as one moves downstream in large river systems. Projected changes into the near future show an increase over most of the country, of between 1 to 1.6 times. Generally the 1 day 50-year return event shows bigger increases compared to the 1 day 10-year return event. A more localised analysis is required for more detailed results.

9.2   Limitations, Assumptions and Interpretation of Results

9.2.1   *ACRU* configuration

The complex *ACRU* configuration used for this study, by its nature, requires some compromises and many assumptions to be made. It also needs to be remembered that, for the purposes of this study, actual water use, especially engineered water use, and dams were not modelled. These limitations need to be considered when applying the simulated runoff values produced through the use of this configuration of the *ACRU* model. The simulated runoff values are thus better suited to comparative analyses, such as (i) comparing runoff produced by actual land cover/use with runoff produced under naturalised land cover, (ii) comparing runoff produced based on different GCMs, (iii) comparing runoff produced using different RCPs, and (iv) comparing runoff produced in different time periods.

9.2.2 Future land cover/use

Land cover/use change projections into the future did not form part of this study. Rather it was assumed that the whole time period (1961-2099) to be either under natural land cover or under actual land cover conditions based on 2018, and kept static, while the climate changes.

9.2.3 Climate projections and their input into hydrological models

Results of climate change impacts into the future on climate related variables must be interpreted on the understanding that no GCM provides "perfect" future climate scenarios, but that the projections from the suite of the six bias-corrected GCMs used in this study (where the bias correction involved matching the GCM output with observations for an overlapping historical period) fall within the spectrum of outputs from the 30 CMIP6 GCMs used in the latest IPCC Reports. Additionally, given the many factors beyond just daily rainfall that affect hydrological responses, without even considering projected climate change (e.g. rainfall intensity, soils characteristics, as well as land use, its seasonal changes and management), and the fact that errors and variability in hydrology are amplified as we move from potential evaporation to rainfall to runoff and then to groundwater recharge. Hence, uncertainty analyses have been undertaken to assess the extent to which the hydrological outputs resulting from the 6 GCMs used vary among one another. Note that the projected changes shown in the maps are in places at variance in the direction and magnitude of changes from GCMs used in previous studies in South Africa, and that the next generation of GCMs is likely to give results that are different again to the ones found here.

9.3 Recommendations

9.3.1 Climate change mitigation

There is a need for climate change mitigation. Projected temperature changes alone are showing a bleak picture for the future climate in southern Africa, while yield and hydrological responses show mixed responses. Greenhouse gas emissions globally need to be reduced, to ensure this is not the future that we leave behind for future generations. Climate change mitigation thus needs to be given high priority, globally as well as in South Africa.

9.3.2 Climate change adaptation

There is a need for climate change adaptation. Climate change impacts are already there and will become more severe into the future. There is, therefore, a need to understand potential impacts to be resilient and to be able to adapt to them. More on adaptation will be in Report 2.

9.3.3 Recommendations for future research

This project produced a wealth of model outputs and statistics. This includes separate scenarios of climate change impacts under land cover of natural vegetation and under actual land cover. A comparison of results under natural vegetation and those under actual land cover does require a more detailed analysis, as the impacts are likely to be localised.

The climate science is evolving and this study should be repeated as and when new climate projections become available. Also, the confidence in the projections can be improved if a longer time period of observed climate variables can be compared with GCM derived climate variables.

Further improvements can be made in the *ACRU* model configurations. In this project, water abstractions, irrigation, dams, inter-basin transfers and urban return flows were not taken into account in the configuration of the *ACRU* hydrological model. To be able to model streamflows more realistically, these should be taken into account in a future project, where information is available.

APPENDIX A – LAND COVER INPUTS FOR THE ACRU MODEL

By
D.J. Clark

Appendix A consists of various tables related to .actual land cover used in the hydrological modelling for this study (cv. Report 1, Chapter 3)

Table A.1.　　　Mapping of 73 NLC2018 classes to 33 groups for use in model configuration

NLC2018 ID	NLC2018 Description	Group ID	Group Name
1	contiguous (indigenous) forest	1	Natural – Relatively Unmodified
2	contiguous low forest & thicket	1	Natural – Relatively Unmodified
3	dense forest & woodland	1	Natural – Relatively Unmodified
4	open woodland	1	Natural – Relatively Unmodified
5	contiguous & dense plantation forest	9	Forest Plantations
6	open & sparse plantation forest	9	Forest Plantations
7	temporary unplanted (clear-felled) plantation forest	9	Forest Plantations
8	low shrubland (other)	1	Natural – Relatively Unmodified
9	low shrubland (fynbos)	1	Natural – Relatively Unmodified
10	low shrubland (succulent karoo)	1	Natural – Relatively Unmodified
11	low shrubland (nama karoo)	1	Natural – Relatively Unmodified
12	sparsely wooded grassland	1	Natural – Relatively Unmodified
13	natural grassland	1	Natural – Relatively Unmodified
14	natural rivers	24	Waterbodies – Rivers
15	natural estuaries & lagoons	25	Waterbodies – Coastal Water
16	natural ocean & coastal	25	Waterbodies – Coastal Water
17	natural lakes	23	Waterbodies – Lakes
18	natural pans (flooded @ observation times)	21	Waterbodies – Flooded Pans
19	artificial dams (including canals)	33	Waterbodies – Dams
20	artificial sewage ponds	17	Built-up – Urban -Waterbodies
21	artificial flooded mine pits	8	Mining – Water
22	herbaceous wetlands (currently mapped)	19	Wetlands – Herbaceous
23	herbaceous wetlands (previously mapped)	19	Wetlands – Herbaceous
24	mangrove wetlands	20	Wetlands – Mangrove
25	natural rock surfaces	3	Natural – Bare Rock
26	dry pans	22	Waterbodies – Dry Pans
27	eroded lands	5	Bare – Soil
28	sand dunes (terrestrial)	4	Bare – Sand
29	coastal sand & dunes	4	Bare – Sand
30	bare riverbed material	6	Bare – Riverbed
31	other bare	5	Bare – Soil
32	cultivated commercial permanent orchards	29	Agriculture – Commercial – Orchards
33	cultivated commercial permanent vines	30	Agriculture – Commercial – Vines
34	cultivated commercial sugarcane pivot irrigated	27	Agriculture – Commercial – Sugarcane

35	cultivated commercial permanent pineapples	28	Agriculture – Commercial – Pineapples
36	cultivated commercial sugarcane non-pivot	27	Agriculture – Commercial – Sugarcane
37	cultivated emerging farmer sugarcane non-pivot	32	Agriculture – Subsistence – Sugarcane
38	commercial annual crops pivot irrigated	26	Agriculture – Commercial – Annual
39	commercial annual crops non-pivot irrigated	26	Agriculture – Commercial – Annual
40	commercial annual crops rain-fed / dryland	26	Agriculture – Commercial – Annual
41	subsistence / small-scale annual crops	31	Agriculture – Subsistence – Annual
42	fallow land & old fields (trees)	2	Natural – Modified
43	fallow land & old fields (bush)	2	Natural – Modified
44	fallow land & old fields (grass)	2	Natural – Modified
45	fallow land & old fields (bare)	5	Bare – Soil
46	fallow land & old fields (low shrub)	2	Natural – Modified
47	residential formal (tree)	10	Built-up – Urban – Residential – Formal
48	residential formal (bush)	10	Built-up – Urban – Residential – Formal
49	residential formal (low veg / grass)	10	Built-up – Urban – Residential – Formal
50	residential formal (bare)	10	Built-up – Urban – Residential – Formal
51	residential informal (tree)	11	Built-up – Urban – Residential – Informal
52	residential informal (bush)	11	Built-up – Urban – Residential – Informal
53	residential informal (low veg / grass)	11	Built-up – Urban – Residential – Informal
54	residential informal (bare)	11	Built-up – Urban – Residential – Informal
55	village scattered (bare & low veg/ grass combo)	18	Built-up – Rural
56	village dense (bare & low veg / grass combo)	18	Built-up – Rural
57	smallholdings (tree)	12	Built-up – Urban – Smallholdings
58	smallholdings (bush)	12	Built-up – Urban – Smallholdings
59	smallholdings (low veg / grass)	12	Built-up – Urban – Smallholdings
60	smallholdings (bare)	12	Built-up – Urban – Smallholdings
61	urban recreational fields (tree)	13	Built-up – Urban – Recreational
62	urban recreational fields (bush)	13	Built-up – Urban – Recreational
63	urban recreational fields (grass)	13	Built-up – Urban – Recreational
64	urban recreational fields (bare)	13	Built-up – Urban – Recreational
65	commercial	14	Built-up – Urban – Commercial
66	industrial	15	Built-up – Urban – Industrial
67	roads & rails (major linear)	16	Built-up – Urban – Transport
68	mines: surface infrastructure	7	Mining – General
69	mines: extraction pits, quarries	7	Mining – General
70	mines: salt mines	7	Mining – General
71	mine: tailings and resource dumps	7	Mining – General
72	land-fills	7	Mining – General

| 73 | fallow land & old fields (wetlands) | 19 | Wetlands – Herbaceous |

Table A.2.   Mapping of 73 NLC2018 classes to 13 groups for use in model configuration

NLC2018 ID	NLC2018 Description	Group ID	Group Name
1	contiguous (indigenous) forest	1	Natural – Vegetated
2	contiguous low forest & thicket	1	Natural – Vegetated
3	dense forest & woodland	1	Natural – Vegetated
4	open woodland	1	Natural – Vegetated
5	contiguous & dense plantation forest	5	Forest Plantations
6	open & sparse plantation forest	5	Forest Plantations
7	temporary unplanted (clear-felled) plantation forest	5	Forest Plantations
8	low shrubland (other)	1	Natural – Vegetated
9	low shrubland (fynbos)	1	Natural – Vegetated
10	low shrubland (succulent karoo)	1	Natural – Vegetated
11	low shrubland (nama karoo)	1	Natural – Vegetated
12	sparsely wooded grassland	1	Natural – Vegetated
13	natural grassland	1	Natural – Vegetated
14	natural rivers	9	Waterbodies – Natural
15	natural estuaries & lagoons	9	Waterbodies – Natural
16	natural ocean & coastal	9	Waterbodies – Natural
17	natural lakes	9	Waterbodies – Natural
18	natural pans (flooded @ observation times)	9	Waterbodies – Natural
19	artificial dams (including canals)	13	Waterbodies – Dams
20	artificial sewage ponds	6	Built-up – Urban
21	artificial flooded mine pits	4	Mining
22	herbaceous wetlands (currently mapped)	8	Wetlands
23	herbaceous wetlands (previously mapped)	8	Wetlands
24	mangrove wetlands	8	Wetlands
25	natural rock surfaces	2	Natural – Bare Rock
26	dry pans	10	Waterbodies – Dry Pans
27	eroded lands	3	Bare
28	sand dunes (terrestrial)	3	Bare
29	coastal sand & dunes	3	Bare
30	bare riverbed material	3	Bare
31	other bare	3	Bare
32	cultivated commercial permanent orchards	11	Agriculture – Commercial
33	cultivated commercial permanent vines	11	Agriculture – Commercial
34	cultivated commercial sugarcane pivot irrigated	11	Agriculture – Commercial
35	cultivated commercial permanent pineapples	11	Agriculture – Commercial
36	cultivated commercial sugarcane non-pivot	11	Agriculture – Commercial
37	cultivated emerging farmer sugarcane non-pivot	12	Agriculture – Subsistence
38	commercial annual crops pivot irrigated	11	Agriculture – Commercial

39	commercial annual crops non-pivot irrigated	11	Agriculture – Commercial
40	commercial annual crops rain-fed / dryland	11	Agriculture – Commercial
41	subsistence / small-scale annual crops	12	Agriculture – Subsistence
42	fallow land & old fields (trees)	1	Natural – Vegetated
43	fallow land & old fields (bush)	1	Natural – Vegetated
44	fallow land & old fields (grass)	1	Natural – Vegetated
45	fallow land & old fields (bare)	3	Bare
46	fallow land & old fields (low shrub)	1	Natural – Vegetated
47	residential formal (tree)	6	Built-up – Urban
48	residential formal (bush)	6	Built-up – Urban
49	residential formal (low veg / grass)	6	Built-up – Urban
50	residential formal (bare)	6	Built-up – Urban
51	residential informal (tree)	6	Built-up – Urban
52	residential informal (bush)	6	Built-up – Urban
53	residential informal (low veg / grass)	6	Built-up – Urban
54	residential informal (bare)	6	Built-up – Urban
55	village scattered (bare & low veg/ grass combo)	7	Built-up – Rural
56	village dense (bare & low veg / grass combo)	7	Built-up – Rural
57	smallholdings (tree)	6	Built-up – Urban
58	smallholdings (bush)	6	Built-up – Urban
59	smallholdings (low veg / grass)	6	Built-up – Urban
60	smallholdings (bare)	6	Built-up – Urban
61	urban recreational fields (tree)	6	Built-up – Urban
62	urban recreational fields (bush)	6	Built-up – Urban
63	urban recreational fields (grass)	6	Built-up – Urban
64	urban recreational fields (bare)	6	Built-up – Urban
65	commercial	6	Built-up – Urban
66	industrial	6	Built-up – Urban
67	roads & rails (major linear)	6	Built-up – Urban
68	mines: surface infrastructure	4	Mining – General
69	mines: extraction pits, quarries	4	Mining – General
70	mines: salt mines	4	Mining – General
71	mine: tailings and resource dumps	4	Mining – General
72	land-fills	4	Mining – General
73	fallow land & old fields (wetlands)	8	Wetlands

Table A.3.   Mapping of 73 NLC2018 classes to 6 HRU types for use in model configuration

NLC2018 ID	NLC2018 Description	HRU ID	HRU Name
1	contiguous (indigenous) forest	1	Natural Vegetation and Rock
2	contiguous low forest & thicket	1	Natural Vegetation and Rock
3	dense forest & woodland	1	Natural Vegetation and Rock
4	open woodland	1	Natural Vegetation and Rock
5	contiguous & dense plantation forest	3	Forest Plantations
6	open & sparse plantation forest	3	Forest Plantations
7	temporary unplanted (clear-felled) plantation forest	3	Forest Plantations
8	low shrubland (other)	1	Natural Vegetation and Rock
9	low shrubland (fynbos)	1	Natural Vegetation and Rock
10	low shrubland (succulent karoo)	1	Natural Vegetation and Rock
11	low shrubland (nama karoo)	1	Natural Vegetation and Rock
12	sparsely wooded grassland	1	Natural Vegetation and Rock
13	natural grassland	1	Natural Vegetation and Rock
14	natural rivers	5	Wetlands and Natural Waterbodies
15	natural estuaries & lagoons	5	Wetlands and Natural Waterbodies
16	natural ocean & coastal	5	Wetlands and Natural Waterbodies
17	natural lakes	5	Wetlands and Natural Waterbodies
18	natural pans (flooded @ observation times)	5	Wetlands and Natural Waterbodies
19	artificial dams (including canals)	6	Agriculture and Dams
20	artificial sewage ponds	4	Built-up
21	artificial flooded mine pits	2	Bare and Mining
22	herbaceous wetlands (currently mapped)	5	Wetlands and Natural Waterbodies
23	herbaceous wetlands (previously mapped)	5	Wetlands and Natural Waterbodies
24	mangrove wetlands	5	Wetlands and Natural Waterbodies
25	natural rock surfaces	1	Natural Vegetation and Rock
26	dry pans	5	Wetlands and Natural Waterbodies
27	eroded lands	2	Bare and Mining
28	sand dunes (terrestrial)	2	Bare and Mining
29	coastal sand & dunes	2	Bare and Mining
30	bare riverbed material	2	Bare and Mining
31	other bare	2	Bare and Mining
32	cultivated commercial permanent orchards	6	Agriculture and Dams
33	cultivated commercial permanent vines	6	Agriculture and Dams
34	cultivated commercial sugarcane pivot irrigated	6	Agriculture and Dams
35	cultivated commercial permanent pineapples	6	Agriculture and Dams
36	cultivated commercial sugarcane non-pivot	6	Agriculture and Dams
37	cultivated emerging farmer sugarcane non-pivot	6	Agriculture and Dams
38	commercial annual crops pivot irrigated	6	Agriculture and Dams
39	commercial annual crops non-pivot irrigated	6	Agriculture and Dams
40	commercial annual crops rain-fed / dryland	6	Agriculture and Dams
41	subsistence / small-scale annual crops	6	Agriculture and Dams

42	fallow land & old fields (trees)	1	Natural Vegetation and Rock
43	fallow land & old fields (bush)	1	Natural Vegetation and Rock
44	fallow land & old fields (grass)	1	Natural Vegetation and Rock
45	fallow land & old fields (bare)	2	Bare and Mining
46	fallow land & old fields (low shrub)	1	Natural Vegetation and Rock
47	residential formal (tree)	4	Built-up
48	residential formal (bush)	4	Built-up
49	residential formal (low veg / grass)	4	Built-up
50	residential formal (bare)	4	Built-up
51	residential informal (tree)	4	Built-up
52	residential informal (bush)	4	Built-up
53	residential informal (low veg / grass)	4	Built-up
54	residential informal (bare)	4	Built-up
55	village scattered (bare & low veg/ grass combo)	4	Built-up
56	village dense (bare & low veg / grass combo)	4	Built-up
57	smallholdings (tree)	4	Built-up
58	smallholdings (bush)	4	Built-up
59	smallholdings (low veg / grass)	4	Built-up
60	smallholdings (bare)	4	Built-up
61	urban recreational fields (tree)	4	Built-up
62	urban recreational fields (bush)	4	Built-up
63	urban recreational fields (grass)	4	Built-up
64	urban recreational fields (bare)	4	Built-up
65	commercial	4	Built-up
66	industrial	4	Built-up
67	roads & rails (major linear)	4	Built-up
68	mines: surface infrastructure	2	Bare and Mining
69	mines: extraction pits, quarries	2	Bare and Mining
70	mines: salt mines	2	Bare and Mining
71	mine: tailings and resource dumps	2	Bare and Mining
72	land-fills	2	Bare and Mining
73	fallow land & old fields (wetlands)	5	Wetlands and Natural Waterbodies

Table A.4.   Mapping of 49 NLC2000 classes to 33 groups for use in model configuration

NLC2000 ID	NLC2000 Description	Group ID	Group Name
0	Missing data	1	Natural – Relatively Unmodified
1	Forest (indigenous)	1	Natural – Relatively Unmodified
2	Woodland	1	Natural – Relatively Unmodified
3	Thicket, Bushland, Bush Clumps, High Fynbos	1	Natural – Relatively Unmodified
4	Shrubland and Low Fynbos	1	Natural – Relatively Unmodified
5	Herbland	1	Natural – Relatively Unmodified
6	Natural Grassland	1	Natural – Relatively Unmodified
7	Planted Grassland	26	Agriculture – Commercial – Annual
8	Forest Plantations (Eucalyptus spp)	9	Forest Plantations
9	Forest Plantations (Pine spp)	9	Forest Plantations
10	Forest Plantations (Acacia spp)	9	Forest Plantations
11	Forest Plantations (Other / mixed spp)	9	Forest Plantations
12	Forest Plantations (clearfelled)	9	Forest Plantations
13	Waterbodies	33	Waterbodies – Dams
14	Wetlands	19	Wetlands – Herbaceous
15	Bare Rock and Soil (natural)	3	Natural – Bare Rock
16	Bare Rock and Soil (erosion: dongas / gullies)	5	Bare – Soil
17	Bare Rock and Soil (erosion: sheet)	5	Bare – Soil
18	Degraded Forest & Woodland	2	Natural – Modified
19	Degraded Thicket, Bushland, etc.	2	Natural – Modified
20	Degraded Shrubland and Low Fynbos	2	Natural – Modified
22	Degraded Unimproved (natural) Grassland	2	Natural – Modified
23	Cultivated, permanent, commercial, irrigated	29	Agriculture – Commercial – Orchards
24	Cultivated, permanent, commercial, dryland	29	Agriculture – Commercial – Orchards
25	Cultivated, permanent, commercial, sugarcane	27	Agriculture – Commercial – Sugarcane
26	Cultivated, temporary, commercial, irrigated	26	Agriculture – Commercial – Annual
27	Cultivated, temporary, commercial, dryland	26	Agriculture – Commercial – Annual
28	Cultivated, temporary, subsistence, dryland	31	Agriculture – Subsistence – Annual
29	Cultivated, temporary, subsistence, irrigated	31	Agriculture – Subsistence – Annual
30	Urban / Built-up	10	Built-up – Urban – Residential – Formal
31	Urban / Built-up (rural cluster)	18	Built-up – Rural
32	Urban / Built-up (residential, formal suburbs)	10	Built-up – Urban – Residential – Formal
33	Urban / Built-up (residential, flatland)	10	Built-up – Urban – Residential – Formal

34	Urban / Built-up (residential, mixed)	10	Built-up – Urban – Residential – Formal
35	Urban / Built-up (residential, hostels)	10	Built-up – Urban – Residential – Formal
36	Urban / Built-up (residential, formal township)	10	Built-up – Urban – Residential – Formal
37	Urban / Built-up (residential, informal township)	11	Built-up – Urban – Residential – Informal
38	Urban / Built-up (residential, informal squatter camp)	11	Built-up – Urban – Residential – Informal
39	Urban / Built-up (smallholdings, forest & woodlands)	12	Built-up – Urban – Smallholdings
40	Urban / Built-up (smallholdings, thicket, bushland, etc.)	12	Built-up – Urban – Smallholdings
41	Urban / Built-up (smallholdings, shrubland, etc.)	12	Built-up – Urban – Smallholdings
42	Urban / Built-up (smallholdings, grassland, etc.)	12	Built-up – Urban – Smallholdings
43	Urban / Built-up (commercial, mercantile)	14	Built-up – Urban – Commercial
44	Urban / Built-up (commercial, education, health, IT)	14	Built-up – Urban – Commercial
45	Urban / Built-up (industrial / transport: heavy)	15	Built-up – Urban – Industrial
46	Urban / Built-up (industrial / transport: light)	15	Built-up – Urban – Industrial
47	Mines and Quarries (underground / subsurface mining)	7	Mining – General
48	Mines and Quarries (surface-based mining)	7	Mining – General
49	Mines and Quarries (mine tailings, waste dumps)	7	Mining – General

Table A.5.   Mapping of 49 NLC2000 classes to 13 groups for use in model configuration

NLC2000 ID	NLC2000 Description	Group ID	Group Name
0	Missing data	1	Natural – Vegetated
1	Forest (indigenous)	1	Natural – Vegetated
2	Woodland	1	Natural – Vegetated
3	Thicket, Bushland, Bush Clumps, High Fynbos	1	Natural – Vegetated
4	Shrubland and Low Fynbos	1	Natural – Vegetated
5	Herbland	1	Natural – Vegetated
6	Natural Grassland	1	Natural – Vegetated
7	Planted Grassland	11	Agriculture – Commercial
8	Forest Plantations (Eucalyptus spp)	5	Forest Plantations
9	Forest Plantations (Pine spp)	5	Forest Plantations
10	Forest Plantations (Acacia spp)	5	Forest Plantations
11	Forest Plantations (Other / mixed spp)	5	Forest Plantations
12	Forest Plantations (clearfelled)	5	Forest Plantations
13	Waterbodies	13	Waterbodies – Dams
14	Wetlands	8	Wetlands
15	Bare Rock and Soil (natural)	2	Natural – Bare Rock

16	Bare Rock and Soil (erosion: dongas / gullies)	3	Bare
17	Bare Rock and Soil (erosion: sheet)	3	Bare
18	Degraded Forest & Woodland	1	Natural – Vegetated
19	Degraded Thicket, Bushland, etc.	1	Natural – Vegetated
20	Degraded Shrubland and Low Fynbos	1	Natural – Vegetated
22	Degraded Unimproved (natural) Grassland	1	Natural – Vegetated
23	Cultivated, permanent, commercial, irrigated	11	Agriculture – Commercial
24	Cultivated, permanent, commercial, dryland	11	Agriculture – Commercial
25	Cultivated, permanent, commercial, sugarcane	11	Agriculture – Commercial
26	Cultivated, temporary, commercial, irrigated	11	Agriculture – Commercial
27	Cultivated, temporary, commercial, dryland	11	Agriculture – Commercial
28	Cultivated, temporary, subsistence, dryland	12	Agriculture – Subsistence
29	Cultivated, temporary, subsistence, irrigated	12	Agriculture – Subsistence
30	Urban / Built-up	6	Built-up – Urban
31	Urban / Built-up (rural cluster)	7	Built-up – Rural
32	Urban / Built-up (residential, formal suburbs)	6	Built-up – Urban
33	Urban / Built-up (residential, flatland)	6	Built-up – Urban
34	Urban / Built-up (residential, mixed)	6	Built-up – Urban
35	Urban / Built-up (residential, hostels)	6	Built-up – Urban
36	Urban / Built-up (residential, formal township)	6	Built-up – Urban
37	Urban / Built-up (residential, informal township)	6	Built-up – Urban
38	Urban / Built-up (residential, informal squatter camp)	6	Built-up – Urban
39	Urban / Built-up (smallholdings, forest & woodlands)	6	Built-up – Urban
40	Urban / Built-up (smallholdings, thicket, bushland, etc.)	6	Built-up – Urban
41	Urban / Built-up (smallholdings, shrubland, etc.)	6	Built-up – Urban
42	Urban / Built-up (smallholdings, grassland, etc.)	6	Built-up – Urban
43	Urban / Built-up (commercial, mercantile)	6	Built-up – Urban
44	Urban / Built-up (commercial, education, health, IT)	6	Built-up – Urban
45	Urban / Built-up (industrial / transport: heavy)	6	Built-up – Urban
46	Urban / Built-up (industrial / transport: light)	6	Built-up – Urban
47	Mines and Quarries (underground / subsurface mining)	4	Mining – General
48	Mines and Quarries (surface-based mining)	4	Mining – General
49	Mines and Quarries (mine tailings, waste dumps)	4	Mining – General

Table A.6.   Mapping of 49 NLC2000 classes to 6 HRU types for use in model configuration

NLC2000 ID	NLC2000 Description	HRU ID	HRU Name
0	Missing data	1	Natural Vegetation and Rock
1	Forest (indigenous)	1	Natural Vegetation and Rock
2	Woodland	1	Natural Vegetation and Rock
3	Thicket, Bushland, Bush Clumps, High Fynbos	1	Natural Vegetation and Rock
4	Shrubland and Low Fynbos	1	Natural Vegetation and Rock

5	Herbland	1	Natural Vegetation and Rock
6	Natural Grassland	1	Natural Vegetation and Rock
7	Planted Grassland	6	Agriculture and Dams
8	Forest Plantations (Eucalyptus spp)	3	Forest Plantations
9	Forest Plantations (Pine spp)	3	Forest Plantations
10	Forest Plantations (Acacia spp)	3	Forest Plantations
11	Forest Plantations (Other / mixed spp)	3	Forest Plantations
12	Forest Plantations (clearfelled)	3	Forest Plantations
13	Waterbodies	6	Agriculture and Dams
14	Wetlands	5	Wetlands and Natural Waterbodies
15	Bare Rock and Soil (natural)	1	Natural Vegetation and Rock
16	Bare Rock and Soil (erosion: dongas / gullies)	2	Bare and Mining
17	Bare Rock and Soil (erosion: sheet)	2	Bare and Mining
18	Degraded Forest & Woodland	1	Natural Vegetation and Rock
19	Degraded Thicket, Bushland, etc.	1	Natural Vegetation and Rock
20	Degraded Shrubland and Low Fynbos	1	Natural Vegetation and Rock
22	Degraded Unimproved (natural) Grassland	1	Natural Vegetation and Rock
23	Cultivated, permanent, commercial, irrigated	6	Agriculture and Dams
24	Cultivated, permanent, commercial, dryland	6	Agriculture and Dams
25	Cultivated, permanent, commercial, sugarcane	6	Agriculture and Dams
26	Cultivated, temporary, commercial, irrigated	6	Agriculture and Dams
27	Cultivated, temporary, commercial, dryland	6	Agriculture and Dams
28	Cultivated, temporary, subsistence, dryland	6	Agriculture and Dams
29	Cultivated, temporary, subsistence, irrigated	6	Agriculture and Dams
30	Urban / Built-up	4	Built-up
31	Urban / Built-up (rural cluster)	4	Built-up
32	Urban / Built-up (residential, formal suburbs)	4	Built-up
33	Urban / Built-up (residential, flatland)	4	Built-up
34	Urban / Built-up (residential, mixed)	4	Built-up
35	Urban / Built-up (residential, hostels)	4	Built-up
36	Urban / Built-up (residential, formal township)	4	Built-up
37	Urban / Built-up (residential, informal township)	4	Built-up
38	Urban / Built-up (residential, informal squatter camp)	4	Built-up
39	Urban / Built-up (smallholdings, forest & woodlands)	4	Built-up
40	Urban / Built-up (smallholdings, thicket, bushland, etc.)	4	Built-up
41	Urban / Built-up (smallholdings, shrubland, etc.)	4	Built-up
42	Urban / Built-up (smallholdings, grassland, etc.)	4	Built-up
43	Urban / Built-up (commercial, mercantile)	4	Built-up
44	Urban / Built-up (commercial, education, health, IT)	4	Built-up
45	Urban / Built-up (industrial / transport: heavy)	4	Built-up
46	Urban / Built-up (industrial / transport: light)	4	Built-up
47	Mines and Quarries (underground / subsurface mining)	2	Bare and Mining
48	Mines and Quarries (surface-based mining)	2	Bare and Mining
49	Mines and Quarries (mine tailings, waste dumps)	2	Bare and Mining

Table A.7.   Suggested adjustments to CWRR Cluster parameters for ACRU to represent degraded natural vegetation (Schulze and Davis, 2018)

ACRU Variable	Adjustment
CAY	Reduce by 25% with a minimum value of 0.2
COIAM	Natural forest: reduce to 0.20 for all months of the year. Other vegetation: reduce to 0.10 for the months November to March, reduce to 0.15 for April, May and October, reduce to 0.20 for the months June to September
COLON	Reduce to 60%
PCSUCO	Natural forest: reduce to 40% Other vegetation: reduce to 10%
VEGINT	Reduce by 50%

Table A.8.   The parameter values used to represent bare pervious surfaces in ACRU for HRU 2

ACRU Variable	Jan	Feb	Mar	Apr	May	Jun	Jul	Aug	Sep	Oct	Nov	Dec
CAY	0.2	0.2	0.2	0.2	0.2	0.2	0.2	0.2	0.2	0.2	0.2	0.2
COIAM	0.3	0.3	0.3	0.3	0.3	0.3	0.3	0.3	0.3	0.3	0.3	0.3
COLON	0	0	0	0	0	0	0	0	0	0	0	0
CONST	0.4	0.4	0.4	0.4	0.4	0.4	0.4	0.4	0.4	0.4	0.4	0.4
PCSUCO	0	0	0	0	0	0	0	0	0	0	0	0
ROOTA	1	1	1	1	1	1	1	1	1	1	1	1
VEGINT	0.05	0.05	0.05	0.05	0.05	0.05	0.05	0.05	0.05	0.05	0.05	0.05

Table A.9.   The parameter values used to represent forest plantations in ACRU in HRU 3 (Jewitt et al., 2009; Schulze, 2013; Schulze and Schütte, 2014; Schulze and Schütte, 2016; Schulze and Davis, 2018)

ACRU Variable	Eucalyptus grandis Inland 10 Year Rotation	Eucalyptus grandis Coastal 7 Year Rotation	Pinus patula Pulp 15 Year Rotation	Pinus patula Sawlogs 25 Year Rotation	Acacia mearnsii Wattle 10 Year Rotation	Other/Mixed
CAY	0.81	0.85	0.88	0.87	0.79	0.90
COIAM	0.32	0.33	0.33	0.34	0.29	0.32
COLON	65	82	66	80	46	60
CONST	0.17	0.13	0.78	0.80	0.50	0.5
PCSUCO	95	95	95	95	95	95
ROOTA	0.76	0.69	0.69	0.65	0.90	0.74
VEGINT	2.0	2.2	3.1	3.3	1.8	2.5

Table A.10.   The pervious and impervious fractions assumed for each of the Built-up classes an HRU 4 (Tarboton and Schulze, 1992)

Built-up Class	Pervious Fraction	Impervious Fraction	Adjunct Fraction	Disjunct Fraction
Built-up – Urban – Residential – Formal	0.35	0.65	0.15	0.50
Built-up – Urban – Residential – Informal	0.35	0.65	0.15	0.50
Built-up – Urban – Smallholdings	0.95	0.05	0.00	0.05
Built-up – Urban – Recreational	0.95	0.05	0.05	0.00
Built-up – Urban – Commercial	0.15	0.85	0.70	0.15
Built-up – Urban – Industrial	0.30	0.7	0.40	0.30
Built-up – Urban – Transport	0.00	1.00	1.00	0.00
Built-up – Rural	0.90	0.1	0	0.1

Table A.11.   The parameter values used to represent the vegetated pervious portion of built-up areas in HRU 4, based on parameter values in the ACRU Compoveg file (Smithers and Schulze, 1995)

Improved grassland (inland) – Compoveg 5070102												
ACRU Variable	Jan	Feb	Mar	Apr	May	Jun	Jul	Aug	Sep	Oct	Nov	Dec
CAY	0.55	0.55	0.55	0.55	0.35	0.2	0.2	0.2	0.35	0.45	0.55	0.55
COIAM	0.15	0.15	0.15	0.25	0.3	0.3	0.3	0.3	0.3	0.3	0.2	0.15
COLON	100	100	100	100	100	100	100	100	100	100	100	100
CONST	0.4	0.4	0.4	0.4	0.4	0.4	0.4	0.4	0.4	0.4	0.4	0.4
PCSUCO	100	100	100	100	100	100	100	100	100	100	100	100
ROOTA	0.95	0.95	0.95	0.95	0.95	1	1	1	0.95	0.95	0.95	0.95
VEGINT	0.7	0.7	0.7	0.7	0.7	0.7	0.7	0.7	0.7	0.7	0.7	0.7
Degraded unimproved grassland – Compoveg 5150102												
ACRU Variable	Jan	Feb	Mar	Apr	May	Jun	Jul	Aug	Sep	Oct	Nov	Dec
CAY	0.55	0.55	0.55	0.45	0.2	0.2	0.2	0.2	0.4	0.45	0.55	0.55
COIAM	0.1	0.1	0.1	0.15	0.15	0.2	0.2	0.2	0.2	0.15	0.1	0.1
COLON	60	60	60	60	60	60	60	60	60	60	60	60
CONST	0.4	0.4	0.4	0.4	0.4	0.4	0.4	0.4	0.4	0.4	0.4	0.4
PCSUCO	10	10	10	10	10	10	10	10	10	10	10	10
ROOTA	0.9	0.9	0.9	0.94	1	1	1	1	0.95	0.92	0.9	0.9
VEGINT	0.8	0.8	0.8	0.7	0.6	0.6	0.6	0.6	0.65	0.75	0.8	0.8

Table A.12.   The parameter values used to represent the vegetated pervious wetland areas in HRU 5, based on parameter values in the ACRU Compoveg file (Smithers and Schulze, 1995)

Wetland – Compoveg 5100102												
ACRU Variable	Jan	Feb	Mar	Apr	May	Jun	Jul	Aug	Sep	Oct	Nov	Dec
CAY	0.8	0.8	0.8	0.7	0.6	0.5	0.4	0.4	0.4	0.5	0.6	0.7
COIAM	0.2	0.2	0.2	0.2	0.3	0.3	0.3	0.3	0.3	0.3	0.2	0.2
COLON	100	100	100	100	100	100	100	100	100	100	100	100
CONST	0.4	0.4	0.4	0.4	0.4	0.4	0.4	0.4	0.4	0.4	0.4	0.4
PCSUCO	100	100	100	100	100	100	100	100	100	100	100	100
ROOTA	1	1	1	1	1	1	1	1	1	1	1	1
VEGINT	0.6	0.6	0.6	0.6	0.6	0.6	0.6	0.6	0.6	0.6	0.6	0.6

Table A.13. The parameter values used to represent commercial and subsistence annual crops in HRU 6, based on parameter values in the ACRU Compoveg file (Smithers and Schulze, 1995) and Schulze and Davis (2018)

Maize, Dryland Summer, October Planting – Compoveg 3020101												
ACRU Variable	Jan	Feb	Mar	Apr	May	Jun	Jul	Aug	Sep	Oct	Nov	Dec
CAY	0.99	0.84	0.2	0.2	0.2	0.2	0.2	0.2	0.2	0.2	0.48	0.78
COIAM	0.2	0.2	0.2	0.2	0.2	0.2	0.2	0.2	0.2	0.3	0.25	0.2
COLON	50	50	50	50	50	50	50	50	50	50	50	50
CONST	0.4	0.4	0.4	0.4	0.4	0.4	0.4	0.4	0.4	0.4	0.4	0.4
PCSUCO	50	50	50	50	50	50	50	50	50	50	50	50
ROOTA	0.78	0.91	1.0	1.0	1.0	1.0	1.0	1.0	1.0	0.92	0.79	0.74
VEGINT	1.4	1.4	1.4	1.2	1.0	1.0	1.0	0.8	0.1	0.1	0.8	1.4

Maize, Dryland Summer, November Planting – Compoveg 3020102												
ACRU Variable	Jan	Feb	Mar	Apr	May	Jun	Jul	Aug	Sep	Oct	Nov	Dec
CAY	0.78	0.99	0.84	0.2	0.2	0.2	0.2	0.2	0.2	0.2	0.2	0.48
COIAM	0.2	0.2	0.2	0.2	0.2	0.2	0.2	0.2	0.2	0.2	0.3	0.25
COLON	50	50	50	50	50	50	50	50	50	50	50	50
CONST	0.4	0.4	0.4	0.4	0.4	0.4	0.4	0.4	0.4	0.4	0.4	0.4
PCSUCO	50	50	50	50	50	50	50	50	50	50	50	50
ROOTA	0.74	0.78	0.91	1.0	1.0	1.0	1.0	1.0	1.0	1.0	0.92	0.79
VEGINT	1.4	1.4	1.4	1.4	1.2	1	1	1	0.8	0.0	0.0	0.8

Maize, Dryland, Summer, December 15 Planting Date – (derived from Compoveg 3020102)												
ACRU Variable	Jan	Feb	Mar	Apr	May	Jun	Jul	Aug	Sep	Oct	Nov	Dec
CAY	0.48	0.78	0.99	0.84	0.2	0.2	0.2	0.2	0.2	0.2	0.2	0.2
COIAM	0.25	0.2	0.2	0.2	0.2	0.2	0.2	0.2	0.2	0.2	0.2	0.3
COLON	50	50	50	50	50	50	50	50	50	50	50	50
CONST	0.4	0.4	0.4	0.4	0.4	0.4	0.4	0.4	0.4	0.4	0.4	0.4
PCSUCO	50	50	50	50	50	50	50	50	50	50	50	50
ROOTA	0.79	0.74	0.78	0.91	1.0	1.0	1.0	1.0	1.0	1.0	1.0	0.92
VEGINT	0.8	1.4	1.4	1.4	1.4	1.2	1.0	1.0	1.0	0.8	0.0	0.0

Wheat, Dryland, Winter, June Planting – Compoveg 3020204												
ACRU Variable	Jan	Feb	Mar	Apr	May	Jun	Jul	Aug	Sep	Oct	Nov	Dec
CAY	0.2	0.2	0.2	0.2	0.2	0.2	0.2	0.3	0.5	0.6	0.4	0.2
COIAM	0.2	0.2	0.2	0.2	0.3	0.3	0.5	0.2	0.2	0.2	0.2	0.2
COLON	50	50	50	50	50	50	50	50	50	50	50	50
CONST	0.4	0.4	0.4	0.4	0.4	0.4	0.4	0.4	0.4	0.4	0.4	0.4
PCSUCO	50	50	50	50	50	50	50	50	50	50	50	50
ROOTA	1.0	1.0	1.0	1.0	1.0	0.95	0.9	0.65	0.5	0.4	0.4	1
VEGINT	0.5	0.5	0.5	0.5	0.1	0.5	1.0	1.3	1.5	1.0	0.5	0.5

Subsistence Cropping General, Dryland, Summer Annual – Compoveg 5230101												
ACRU Variable	Jan	Feb	Mar	Apr	May	Jun	Jul	Aug	Sep	Oct	Nov	Dec
CAY	0.87	0.81	0.45	0.35	0.2	0.2	0.2	0.2	0.2	0.2	0.3	0.6
COIAM	0.2	0.2	0.25	0.3	0.3	0.3	0.2	0.2	0.2	0.35	0.3	0.25
COLON	50	50	50	50	50	50	50	50	50	50	50	50
CONST	0.4	0.4	0.4	0.4	0.4	0.4	0.4	0.4	0.4	0.4	0.4	0.4
PCSUCO	50	50	50	50	50	50	50	50	50	50	50	50
ROOTA	0.8	0.8	0.85	0.93	1.0	1.0	1.0	1.0	1.0	1.0	1.0	0.86
VEGINT	1.1	1.1	1.0	0.95	0.55	0.5	0.5	0.5	0.5	0	0.5	1.0

Table A.14. The parameter values used to represent sugarcane in HRU 6, based on recommendations in Schulze (2013) and Schulze and Davis (2018) which were based on Jewitt et al. (2009) and Schulze and Schütte (2014)

Sugarcane Dryland – Far North Coast of KwaZulu-Natal												
ACRU Variable	Jan	Feb	Mar	Apr	May	Jun	Jul	Aug	Sep	Oct	Nov	Dec
CAY	0.87	0.87	0.87	0.87	0.87	0.87	0.87	0.87	0.87	0.87	0.87	0.87
COIAM	0.35	0.35	0.35	0.35	0.35	0.35	0.35	0.35	0.35	0.35	0.35	0.35
COLON	60	60	60	60	60	60	60	60	60	60	60	60
CONST	0.5	0.5	0.5	0.5	0.5	0.5	0.5	0.5	0.5	0.5	0.5	0.5
PCSUCO	90	90	90	90	90	90	90	90	90	90	90	90
ROOTA	0.75	0.75	0.75	0.75	0.75	0.75	0.75	0.75	0.75	0.75	0.75	0.75
VEGINT	2	2	2	2	2	2	2	2	2	2	2	2

Sugarcane Dryland – North Coast of KwaZulu-Natal												
ACRU Variable	Jan	Feb	Mar	Apr	May	Jun	Jul	Aug	Sep	Oct	Nov	Dec
CAY	0.86	0.86	0.86	0.86	0.86	0.86	0.86	0.86	0.86	0.86	0.86	0.86
COIAM	0.35	0.35	0.35	0.35	0.35	0.35	0.35	0.35	0.35	0.35	0.35	0.35
COLON	60	60	60	60	60	60	60	60	60	60	60	60
CONST	0.5	0.5	0.5	0.5	0.5	0.5	0.5	0.5	0.5	0.5	0.5	0.5
PCSUCO	90	90	90	90	90	90	90	90	90	90	90	90
ROOTA	0.75	0.75	0.75	0.75	0.75	0.75	0.75	0.75	0.75	0.75	0.75	0.75
VEGINT	1.9	1.9	1.9	1.9	1.9	1.9	1.9	1.9	1.9	1.9	1.9	1.9

Sugarcane Dryland – South Coast of KwaZulu-Natal												
ACRU Variable	Jan	Feb	Mar	Apr	May	Jun	Jul	Aug	Sep	Oct	Nov	Dec
CAY	0.85	0.85	0.85	0.85	0.85	0.85	0.85	0.85	0.85	0.85	0.85	0.85
COIAM	0.35	0.35	0.35	0.35	0.35	0.35	0.35	0.35	0.35	0.35	0.35	0.35
COLON	60	60	60	60	60	60	60	60	60	60	60	60
CONST	0.5	0.5	0.5	0.5	0.5	0.5	0.5	0.5	0.5	0.5	0.5	0.5
PCSUCO	90	90	90	90	90	90	90	90	90	90	90	90
ROOTA	0.75	0.75	0.75	0.75	0.75	0.75	0.75	0.75	0.75	0.75	0.75	0.75
VEGINT	1.8	1.8	1.8	1.8	1.8	1.8	1.8	1.8	1.8	1.8	1.8	1.8

Sugarcane Dryland – KwaZulu-Natal Inland												
ACRU Variable	Jan	Feb	Mar	Apr	May	Jun	Jul	Aug	Sep	Oct	Nov	Dec
CAY	0.83	0.83	0.83	0.83	0.83	0.83	0.83	0.83	0.83	0.83	0.83	0.83
COIAM	0.35	0.35	0.35	0.35	0.35	0.35	0.35	0.35	0.35	0.35	0.35	0.35
COLON	60	60	60	60	60	60	60	60	60	60	60	60
CONST	0.5	0.5	0.5	0.5	0.5	0.5	0.5	0.5	0.5	0.5	0.5	0.5
PCSUCO	90	90	90	90	90	90	90	90	90	90	90	90
ROOTA	0.75	0.75	0.75	0.75	0.75	0.75	0.75	0.75	0.75	0.75	0.75	0.75
VEGINT	1.7	1.7	1.7	1.7	1.7	1.7	1.7	1.7	1.7	1.7	1.7	1.7

Table A.15.   The parameter values used to represent horticultural crops in HRU 6

Pineapples												
ACRU Variable	Jan	Feb	Mar	Apr	May	Jun	Jul	Aug	Sep	Oct	Nov	Dec
CAY	0.35	0.35	0.35	0.35	0.35	0.35	0.35	0.35	0.35	0.35	0.35	0.35
COIAM	0.3	0.3	0.3	0.3	0.3	0.3	0.3	0.3	0.3	0.3	0.3	0.3
COLON	50	50	50	50	50	50	50	50	50	50	50	50
CONST	0.35	0.35	0.35	0.35	0.35	0.35	0.35	0.35	0.35	0.35	0.35	0.35
PCSUCO	50	50	50	50	50	50	50	50	50	50	50	50
ROOTA	0.75	0.75	0.75	0.75	0.75	0.75	0.75	0.75	0.75	0.75	0.75	0.75
VEGINT	1.5	1.5	1.5	1.5	1.5	1.5	1.5	1.5	1.5	1.5	1.5	1.5

Citrus Orchards (based on Compoveg 3021101)												
ACRU Variable	Jan	Feb	Mar	Apr	May	Jun	Jul	Aug	Sep	Oct	Nov	Dec
CAY	0.67	0.67	0.67	0.67	0.67	0.67	0.67	0.67	0.67	0.67	0.67	0.67
COIAM	0.3	0.3	0.3	0.3	0.3	0.3	0.3	0.3	0.3	0.3	0.3	0.3
COLON	50	50	50	50	50	50	50	50	50	50	50	50
CONST	0.5	0.5	0.5	0.5	0.5	0.5	0.5	0.5	0.5	0.5	0.5	0.5
PCSUCO	90	90	90	90	90	90	90	90	90	90	90	90
ROOTA	0.4	0.4	0.4	0.4	0.4	0.4	0.4	0.4	0.4	0.4	0.4	0.4
VEGINT	1.7	1.7	1.7	1.7	1.7	1.7	1.7	1.7	1.7	1.7	1.7	1.7

Deciduous Fruit Orchards												
ACRU Variable	Jan	Feb	Mar	Apr	May	Jun	Jul	Aug	Sep	Oct	Nov	Dec
CAY	0.82	0.78	0.58	0.35	0.23	0.23	0.23	0.23	0.23	0.42	0.79	0.82
COIAM	0.3	0.3	0.3	0.3	0.3	0.3	0.3	0.3	0.3	0.3	0.3	0.3
COLON	50	50	50	50	50	50	50	50	50	50	50	50
CONST	0.5	0.5	0.5	0.5	0.5	0.5	0.5	0.5	0.5	0.5	0.5	0.5
PCSUCO	70	70	70	70	70	70	70	70	70	70	70	70
ROOTA	0.4	0.4	0.4	0.4	0.4	0.4	0.4	0.4	0.4	0.4	0.4	0.4
VEGINT	1.4	1.4	1.1	0.8	0.0	0.0	0.0	0.0	0.0	0.9	1.4	1.4

Wine Grapes (based on Compoveg 3021302)												
ACRU Variable	Jan	Feb	Mar	Apr	May	Jun	Jul	Aug	Sep	Oct	Nov	Dec
CAY	0.32	0.32	0.25	0.2	0.2	0.2	0.2	0.2	0.2	0.2	0.32	0.32
COIAM	0.3	0.3	0.3	0.3	0.3	0.3	0.3	0.3	0.3	0.3	0.3	0.3
COLON	50	50	50	50	50	50	50	50	50	50	50	50
CONST	0.55	0.55	0.55	0.55	0.55	0.55	0.55	0.55	0.55	0.55	0.55	0.55
PCSUCO	80	80	80	80	80	80	80	80	80	80	80	80
ROOTA	0.5	0.5	0.5	0.5	0.5	0.5	0.5	0.5	0.5	0.5	0.5	0.5
VEGINT	1.0	1.0	1.0	1.0	1.0	1.0	1.0	1.0	1.0	1.0	1.0	1.0

APPENDIX B – DEVELOPING A TRAINING PROGRAMME ON CLIMATE AND HYDROLOGICAL MODELS

R.E. Schulze, M.J.C. Horan, R.P. Kunz, T.G. Lumsden, S.I. Stuart-Hill, S. Schütte, D.J. Clark

B.1   Background

Aim 5 is to develop a training programme to capacitate the DWS climate change and other selected staff on climate and hydrological models. Here we report on developing this training programme.

The principle underlying the training will be to target both entry level and more senior staff and the training should include both theory and practical aspects. The training will encompass a total of approximately one month equivalent of contact time split into shorter sessions for each topic covered.

The following training packages will be delivered:
- Hydrological modelling concepts
- ACRU modelling course
- IWRM & climate change
- GCMs – What is climate change; understanding and interpreting GCM output and RCP scenarios; bias correction; preparing climate files for use in a hydrological model
- Developing and evaluating adaptation strategies (theory and workshop linked to Aim 4)
- Understanding the impacts of environmental change on hydrological responses (theory and then interpreting the results from this project)
- Using, analysing and interpreting data from the software utility developed in this project

The training packages are aimed at postgraduate level. The delivery site for the training will be either online, if possible or at DWS in Pretoria.

B.2 Training Modules

The training programme is outlined in Table B.1.

Table B.1   Envisaged training modules, themes, trainers, media and duration

	Module topic	Themes	Trainers	Media and length
1	Hydrological modelling concepts	Hydrological models and hydrological systems; Classification of Models; Model selection	Roland Schulze (CWRR)	Train via Zoom 1 -day
2	ACRU modelling course		Mark Horan (CWRR)	2-days at DWS national
3	IWRM & climate change		Roland Schulze (CWRR)	Train via Zoom 1 - day
4	GCMs	What is climate change; understanding and interpreting GCM output and RCP scenarios; bias correction; preparing climate files for use in a hydrological model	Trevor Lumsden (CSIR), Piotr Wolski (CSAG), Richard Kunz (CWRR)	Train via Zoom 1 -day
5	Adaptation	Developing and evaluating adaptation strategies	Roland Schulze, (CWRR)	Train via Zoom 1 -day
6	Impacts of environmental change on hydrological responses	Understanding the impacts of environmental change on hydrological responses. Theory and then interpreting the results from this project	Roland Schulze, Stefanie Schütte (CWRR)	Train via Zoom 1 -day
7	Using the software utility	Using, analyzing and interpreting data from the software utility developed in this project	Sean Thornton-Dibb, Richard Kunz, Stefanie Schütte (CWRR)	Train via Zoom 1 -day

APPENDIX C – SOFTWARE UTILITY VERSION 1.0
S.L.C. Thornton-Dibb, R.P Kunz, S. Schütte and D.C. Clark

Background

The Assessment Utility is a software tool that has been developed to facilitate the access and viewing of modelled output generated in the WRC project titled, In Connection with a National Assessment of Potential Climate Change Impacts on the Hydrological Yield of different Hydro-Climatic Zones in South Africa. The tool is loosely based on the Biofuels Assessment Utility developed in the WRC project by Kunz RP et. al. (2015). The Biofuels Assessment Utility was developed to read directly from daily output files from the ACRU model runs. This resulted in very large storage requirements for all the daily output files required by the utility. The project team decided that monthly output files were sufficient for this project which can be generated as part of the model run process and then read by the utility. The team also wanted the ability to visualise the Hydrological Yield, however it was calculated in a post process as was not part of the model output options thus requiring further customisations.

Software Utility Technology
The Assessment Utility is a desktop application written in .NET C# and makes use of the ESRI Map Objects libraries for the spatial map interface. There are limitations to the functionality of the map interface which are a result of these libraries that require .Net Framework 2/3. It is envisioned that that future improvements could be that the utility be made Web compatible along with an update to the map interface. The utility uses an XSD schema to link between the User Interface UI and the model data files.

References

KUNZ RP, DAVIS NS, THORNTON-DIBB SLC, STEYN JM, DU TOIT ES and JEWITT GPW (2015) *Assessment of biofuel feedstock production in South Africa: Atlas of water use and yield of biofuel crops in suitable growing areas*, Volume 3. WRC Report No. TT 652/15, Water Research Commission, Pretoria, South Africa.

Assessment Utility
User Manual
(Version 1.0.0.0)

on the project
WRC K5/2833

by

S.L.C. Thornton-Dibb, R.P Kunz, S. Schütte and D.C. Clark

Centre for Water Resources Research
School of Agricultural, Earth and Environmental Sciences
University of KwaZulu-Natal
Pietermaritzburg, South Africa

Installation

Minimum PC/laptop requirements:

1)   PC running Microsoft Windows 7/8/10 (32- or 64-bit).

2)   The Dot Net Framework 2/3 needs to be enabled in the Windows Add Remove Components.

3)   Please check the Microsoft Web site for updates/patches for the Dot Net Framework.

The Assessment Utility is made up of three parts:
a)   The software utility (Application).

b)   The spatial datasets (GIS coverages).

c)   The hydroclimatic datasets which contains time series data (i.e. ACRU monthly output files) per land use and climate run as well as the calculated hydrological yields per Quaternary Catchment.

To install the software utility and spatial datasets (i.e. part a and part b above):
1)   Run the setup.exe.

2)   This will install the utility and the spatial datasets.

To install the hydroclimatic datasets (i.e. part c above):
1)   Copy the <Land_Use>_db.exe file to the installation folder which is the following (by default):

Win 7/8/10 32/64-bit: C:\CWRR\Assessment Utility

2)   Run <Land_Use>_db.exe and make sure the destination folder is correct (as shown above). Then select Extract, followed by Yes for All. This will extract all the time series data files for the selected land use.

3)   Make sure there is sufficient hard disk space to extract the time series data for all required land uses.

4)   Once the entire database has been installed, delete the <Land_Use>_db.exe file which was manually copied to the application's installation folder.
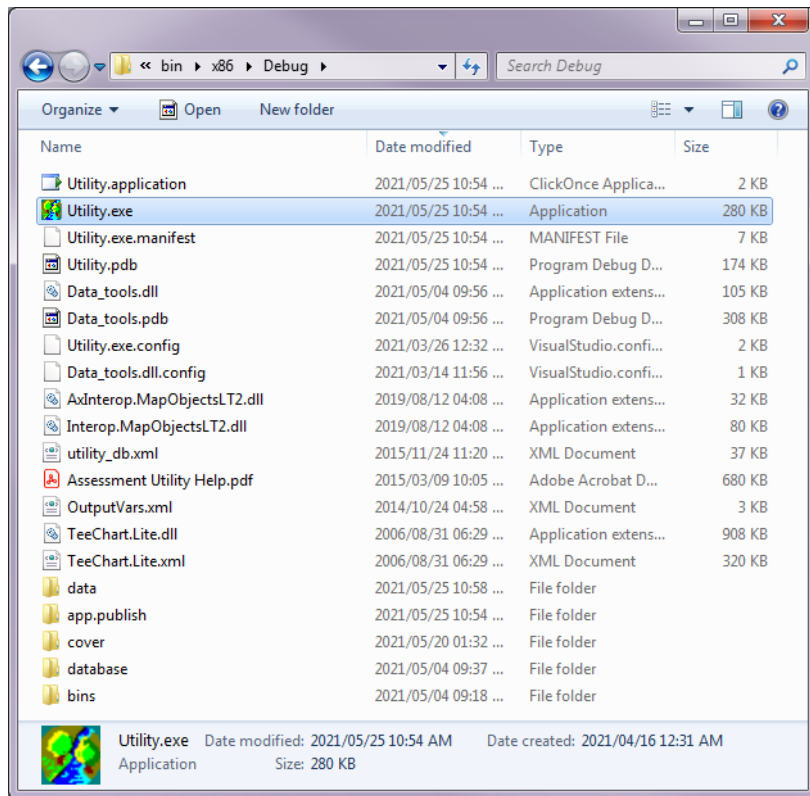
5)   Installation folder structure:

Figure 0.1   Installation folder structure

Using The Assessment Utility

The Assessment Utility.exe is run by selecting the shortcut from Start…Programs…CWRR, or by double-clicking the shortcut on the user's Desktop. The User Interface (UI) is shown in Figure 0.2.
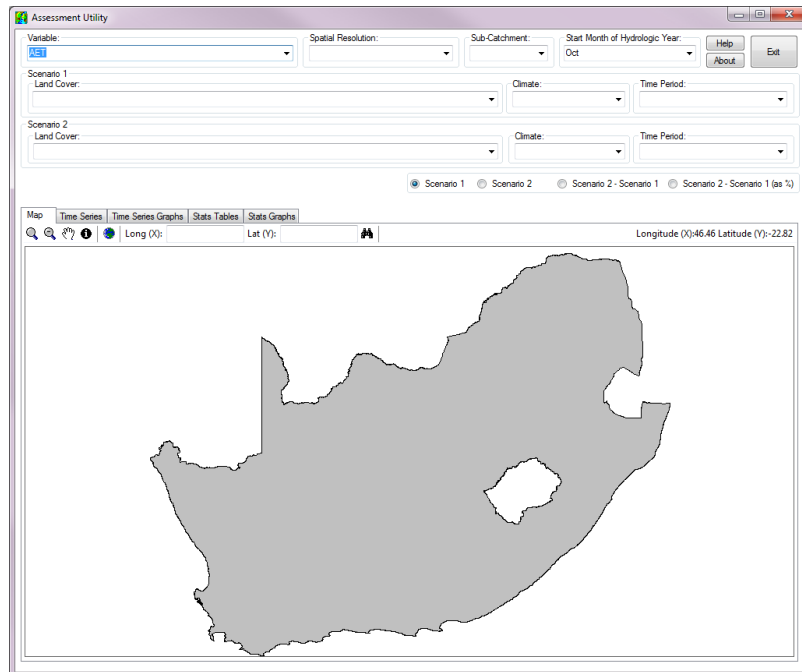

Figure 0.2   Assessment Utility's User Interface

Primary user selection options

The main user interface comprises of:
•   Combo Boxes and Option selection as displayed in Figure 0.3 and described in Table 0.1, and
•   Display Option Tabs as shown in Figure 0.8.
.
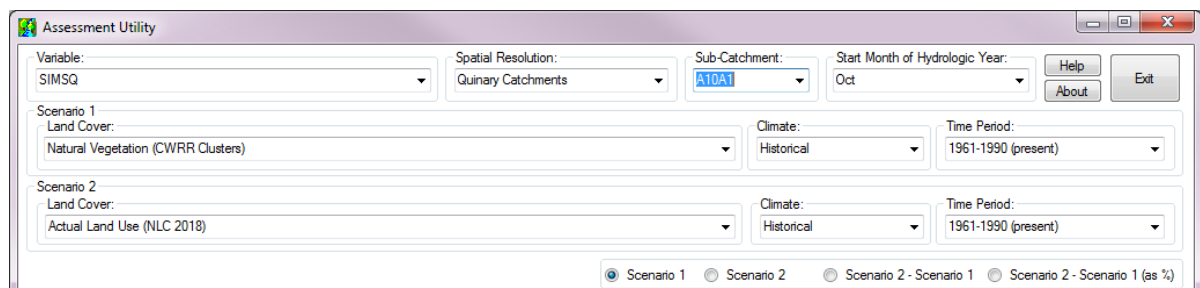
Figure 0.3   Assessment Utility's Combo Boxes and Option selection

Table 0.1   Description of each Combo Box and Options selection

Combo Boxes	Description
Variable	Output variable to be analysed (as listed in Error! Reference source not found.)
Spatial Resolution	Required spatial resolution of output variable
Sub-Catchment	The particular sub-catchment to be analysed
Start Month of Hydrologic Year	Select the start month for the annual statistics (January is the default)
Scenario 1 Land Cover	Either natural vegetation or actual land cover (for climate change analyses) Base land cover to be compared against (for land cover analyses))
Scenario 2 Land Cover	Land cover as for Scenario 1 (for climate change impact analyses) Proposed land cover to be analysed (for land cover analyses)
Scenario 1 Climate	Climate option for Scenario 1
Scenario 1 Time Period	Time period related to the climate option for Scenario 1
Scenario 2 Climate	Climate option for Scenario 2
Scenario 2 Time Period	Time period related to the climate option for Scenario 2
Option Selection	Description
Scenario 1	Display the output related to scenario 1 only
Scenario 2	Display the output related to scenario 2 only
Scenario 2 – Scenario 1	Display the absolute change between the scenarios
Scenario 2 – Scenario 1 (as %)	Display the relative change between the scenarios

Select the desired output variable (See Table 2) from the Variable Combo Box as shown in Figure 0.4. The default output variable selected is SIMSQ, i.e. simulated runoff (stormflow + baseflow) from the selected sub-catchment, which does not include contributions from upstream sub-catchments.
NOTE: Hydrological yield can only be viewed at Quaternary Resolution in the Map display tab. Not all variables are available in all configurations
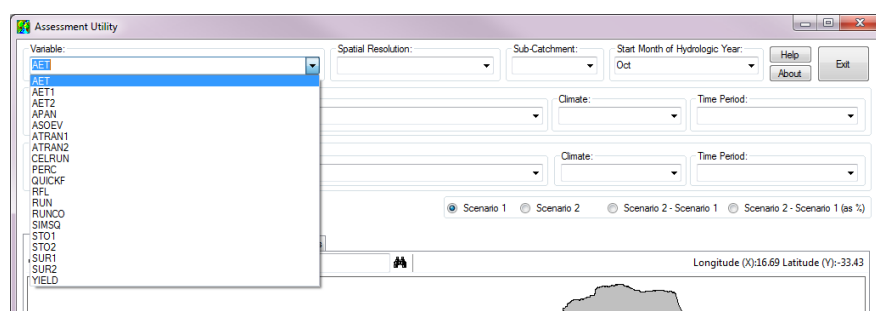

Figure 0.4   Assessment Utility's variable selection from a drop-down control

234

Table 0.2   Description (and units) of each output variable

Variable	Description	Aggregation	Units
AET	Total evaporation (i.e. actual evapotranspiration)	Sum	mm
APAN	A-pan equivalent reference evaporation	Sum	mm
ASOEV	Actual evaporation from the soil surface	Sum	mm
ATRAN1	Actual transpiration from the A-horizon	Sum	mm
ATRAN2	Actual transpiration from the B-horizon	Sum	mm
CAYD	Crop coefficient	Average	-
DPE	Maximum evaporation (potential evapotranspiration)	Sum	mm
EFRL	Effective rainfall (rainfall available for plant growth)	Sum	mm
QUICKF	Storm flow leaving catchment outlet on a given day	Sum	mm
RFL	Input rainfall, adjusted by monthly CORPPT values	Sum	mm
RUN	Base flow	Sum	mm
SIMSQ	Simulated runoff (storm flow + base flow) from the sub-catchment, excluding upstream contributions	Sum	mm
CELRUN	Simulated runoff (storm flow + base flow) from the sub-catchment, including all upstream contributions	Sum	mm
YIELD	Catchment Hydrological Yield (Mapped only) See **Catchment Hydrological Yield** (Section 0)		mm

Select the required **Spatial Resolution** at which the **Variable** should be displayed at in the *Map display tab*. This selection will determine the list of sub-catchments. Next, populate the **Scenario 1** and **Scenario 2** *Combo Boxes* with the desired options as shown in the example given.

Figure 0.5   Scenario options to be selected by the user

Select the **Climate** and **Time Period** for both **Scenario 1** and **Scenario 2**. The available **Time Period** options will vary depending on the **Climate** selected as shown in Figure 0.6.
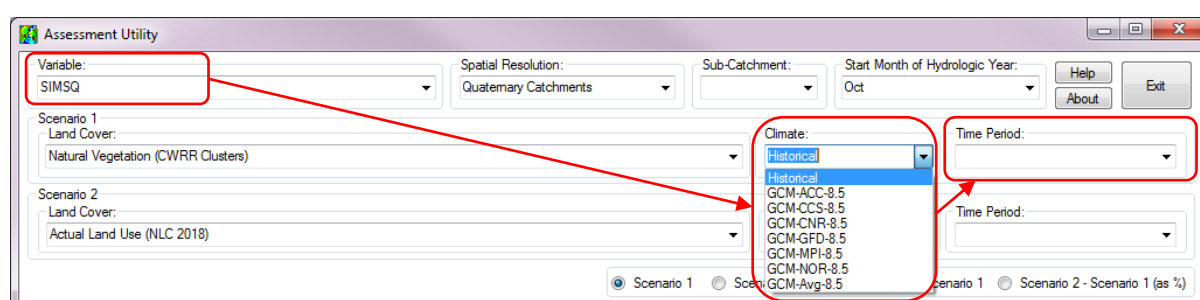

Figure 0.6   Time Period is determined by the Climate, which also depends on the selected Variable

Finally, select the specific **Sub-Catchment** to be analysed from the drop-down list as shown in Figure 0.7 below. Alternatively, the user can input a particular co-ordinate of interest in the **Long** and **Lat** input boxes and the utility will determine in which **Sub-Catchment** the point of interest resides when the search button is pressed.
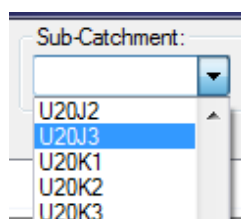

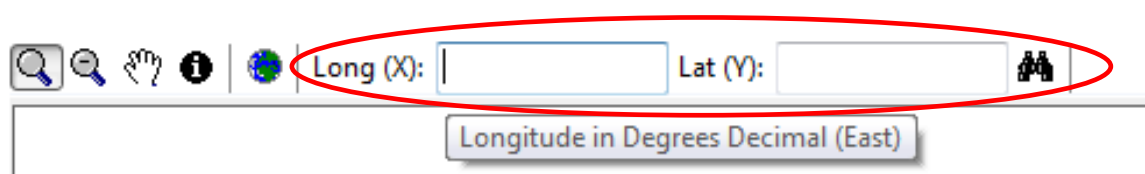Figure 0.7   **Sub-Catchment** drop-down *Combo Box*

Figure 0.8   Sub-Catchment selection via a geographic coordinate given by the user

The utility then loads the time series data for both selected scenarios (**Scenario 1** and **Scenario 2**). This enables the data comparison for the selected **Sub-catchment** and the statistical analysis to be performed. The utility also calculates the change (i.e. **Scenario 2** – **Scenario 1**), which is expressed as either an absolute difference or as a percentage change relative to **Scenario 1** (c.f. **Time Series** below for more information).

9.3.1   Display Option Tabs

The *display option tabs* enable simple navigation between the map view, simulated time series (data & graphs) and statistics (data & graphs).

Figure 0.9   Assessment Utility's Display Option Tabs

Table 0.3   Description for each of the Display Option Tabs

Tab	Description
Map	Map of spatial location of catchment output OR Yield results mapped
TimeSeries	Monthly output from the *ACRU* model in tabular format
TimeSeries Graphs	Monthly output from the *ACRU* model in graphed
Stats Tables	Stats of selected output in tabular format
Stats Graphs	Stats of selected output graphed

Map tab

The Map tab enables visualisation of the catchment boundaries as well as various tools to navigate to a particular **Sub-Catchment**, as given in Table 0.4.
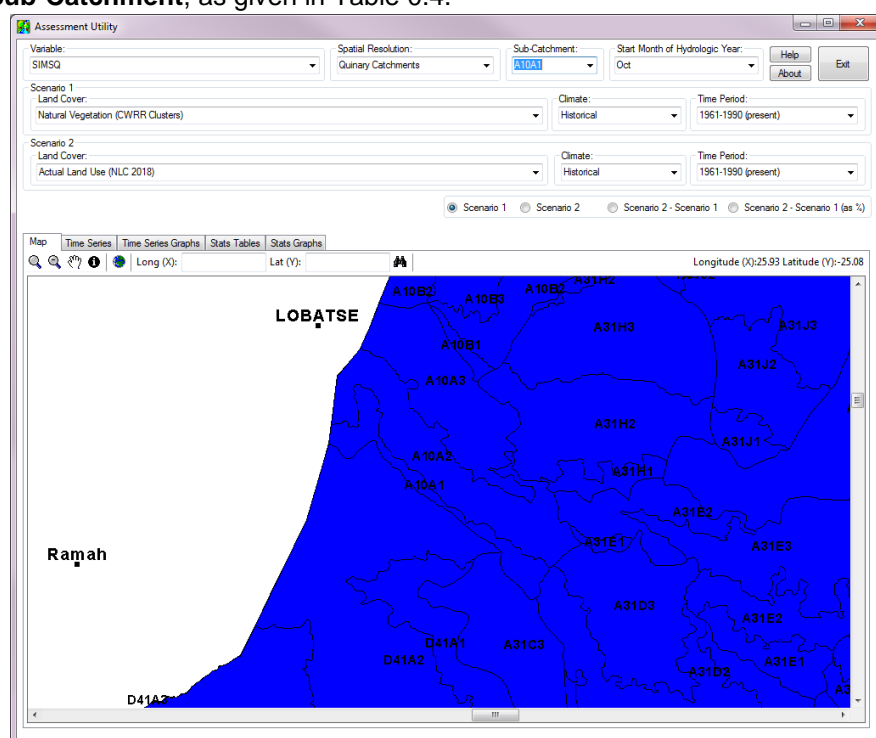

Figure 0.10 Assessment Utility's Map tab

Table 0.4   Map navigation tools

Icon	Name	Action
	Zoom	In the map window, left-click and hold, then drag the mouse to select an area of interest to zoom into
	Zoom Out	Left click on the map to zoom out
	Pan	On the map, left click and hold, then drag the mouse to pan around the map view
	Full	Zoom out to full extent of the map
	Identify	Left click on a polygon to identify the **Sub-Catchment**
	Find	Find a **Sub-Catchment** by inputting the Longitude (Long) and Latitude (Lat) in decimal degrees (use negative latitude values) Long (X): 28.36 Lat (Y): -25.95

Time series

The Time Series tab displays the monthly time series data for the selected sub-catchment's **Scenario 1** and **Scenario 2** in tabular format (

), as well as the calculated difference (i.e. **Scenario 2** – **Scenario 1**). These tables can be exported to comma delimited (CSV) files by selecting the corresponding **Save To Text File** button.
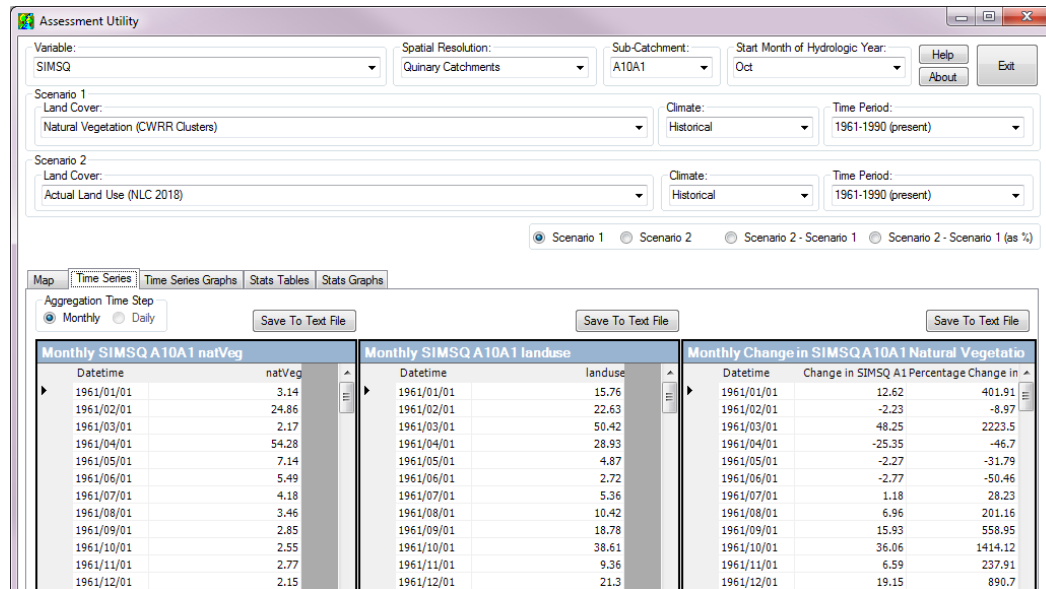

Figure 0.11 Assessment Utility's Time Series tab (data for illustration purposes only)

Time series graphs

The Time Series Graphs tab displays the time series for the selected sub-catchment's **Scenario 1** and **Scenario 2** in graphical format. The graphical view option has various buttons to enable closer inspection of the time series.

The time series graph can also be navigated by various left and right mouse clicks:

Reset graph	-	Double click
Pan graph	-	Right click, hold and drag mouse
Zoom graph	-	Left click, hold and drag mouse
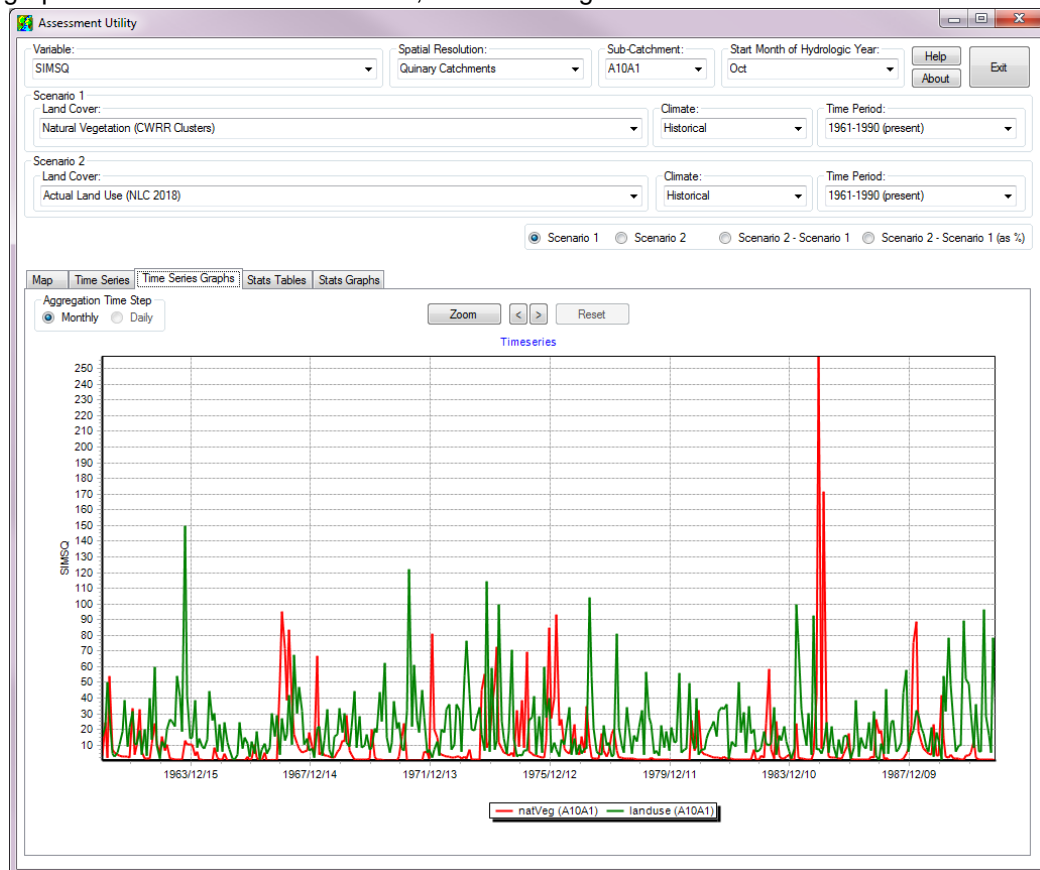
Figure 0.12 Assessment Utility's Time Series Graphs tab (data for illustration purposes only)

Stats tables

Statistics are only done on the monthly data. The start month for the calculation of annual statistics can be selected from the **Stats** drop-down option. These statistics can also be exported as comma separated (CSV) files.

The **Stats Tables** tab displays the calculated statistics in tabular format for the selected sub-catchment's **Scenario 1 (Fig. 0.13)**, or **Scenario 2** (Figure 0.14)**,** or the calculated difference in absolute terms (i.e. **Scenario 2 – Scenario 1** in Figure 0.13), or the calculated change in the Mean represented as a percentage (i.e. **Scenario 2 – Scenario 1** as %).

Scenario 2 – Scenario 1 (as %) is calculated by first determining the monthly and annual mean values for the respective land covers, and then subtracting the **Scenario 1** means from the corresponding **Scenario 2** means to determine their differences. The differences are then divided by the **Scenario 1** means and multiplied by 100 to obtain the monthly and annual changes as percentages. Subtracting the percentiles does not make mathematical sense and thus, these are not calculated (i.e. left empty in the table).
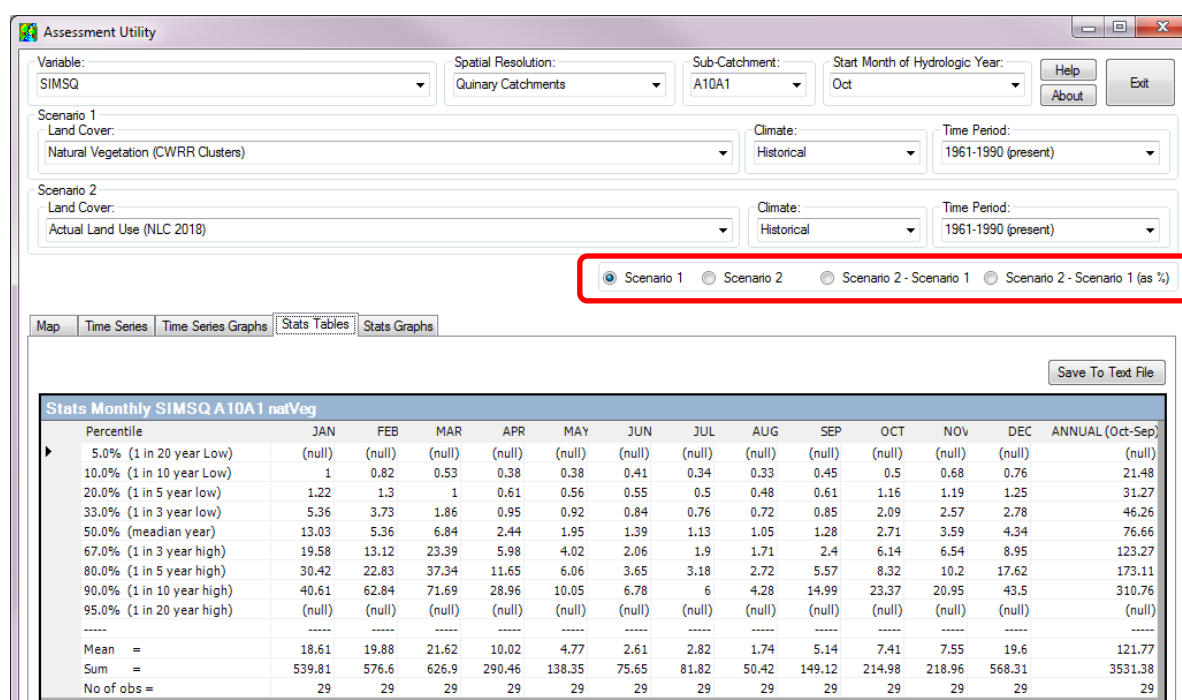

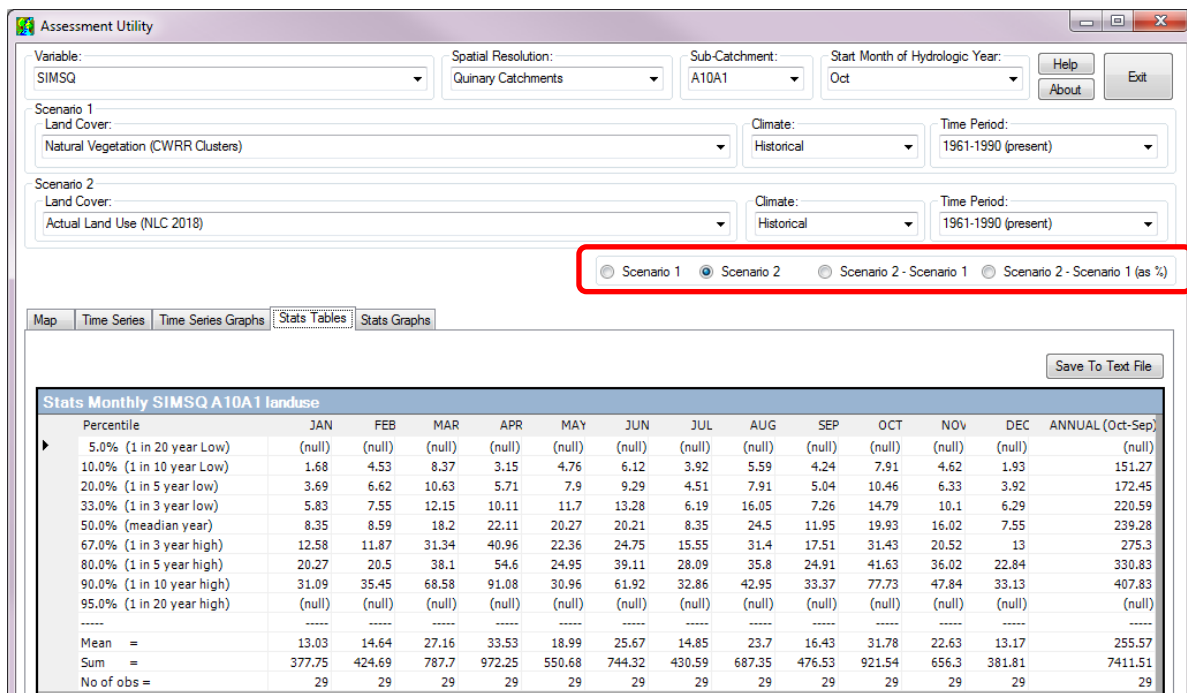Figure 0.13 Stats Tables tab (Scenario 1, data for illustration purposes only)

Figure 0.14 Stats Tables tab (Scenario 2, data for illustration purposes only)
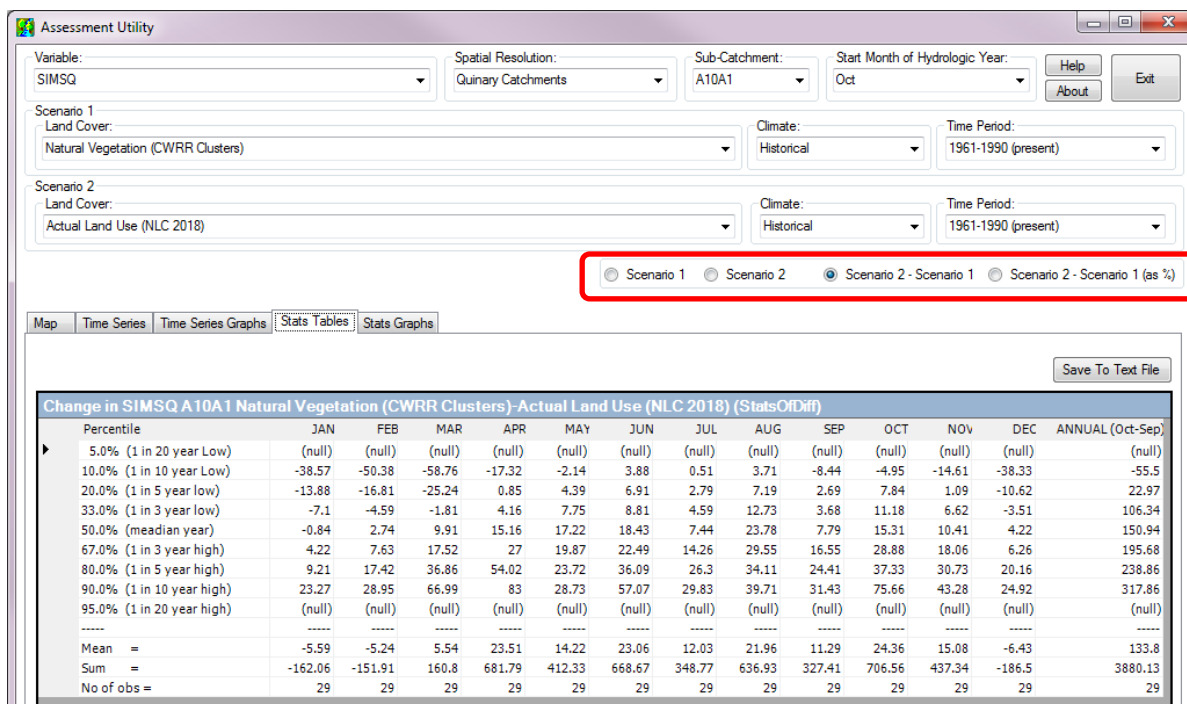

Figure 0.15 Stats Tables tab (Scenario 2 – Scenario 1, data for illustration purposes only)

Stats graphs

The Stats Graphs displays the probability of exceedance values in graphical format. The **Graph Options** enables annual or monthly curves to be switched on or off in the display. The graphs corresponding to the selection made on the **Stats Tables** tab will be plotted on this tab with the exception of **Scenario 2 – Scenario 1** (as %) as there are no percentiles calculated for this option. An Example of a **Scenario 1** graph in displayed in Figure 0.13.
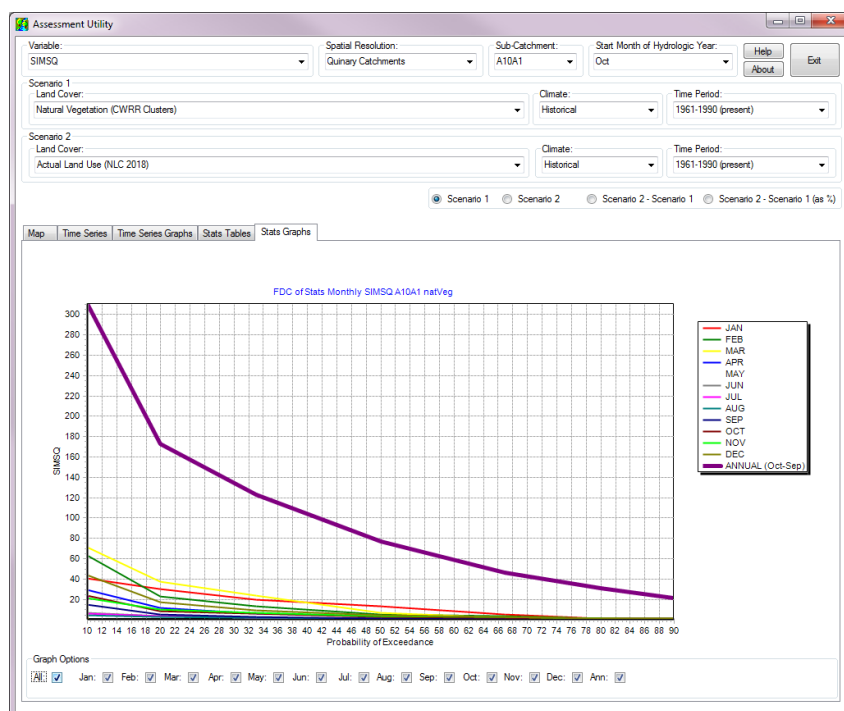

Figure 0.16 Time Statistics Graphs tab (Scenario 1, data for illustration purposes only)

Catchment Hydrological Yield

The Sub-Catchment's hydrological yield is displayed by selecting the Variable called YIELD. Next, the Spatial Resolution option is defaulted to Quaternary Catchment. The user then selects the desired options for **Scenario 1** and **Scenario 2**, i.e. Land Cover, Climate and Time Period. To view the different map outputs options, select from the Option Selection.
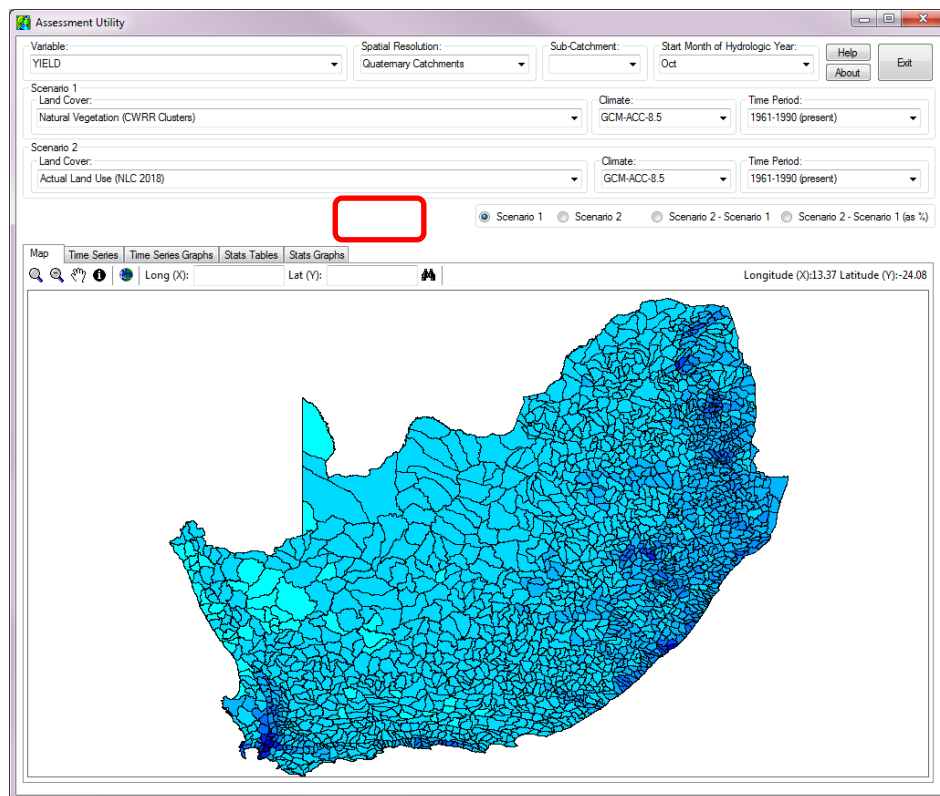
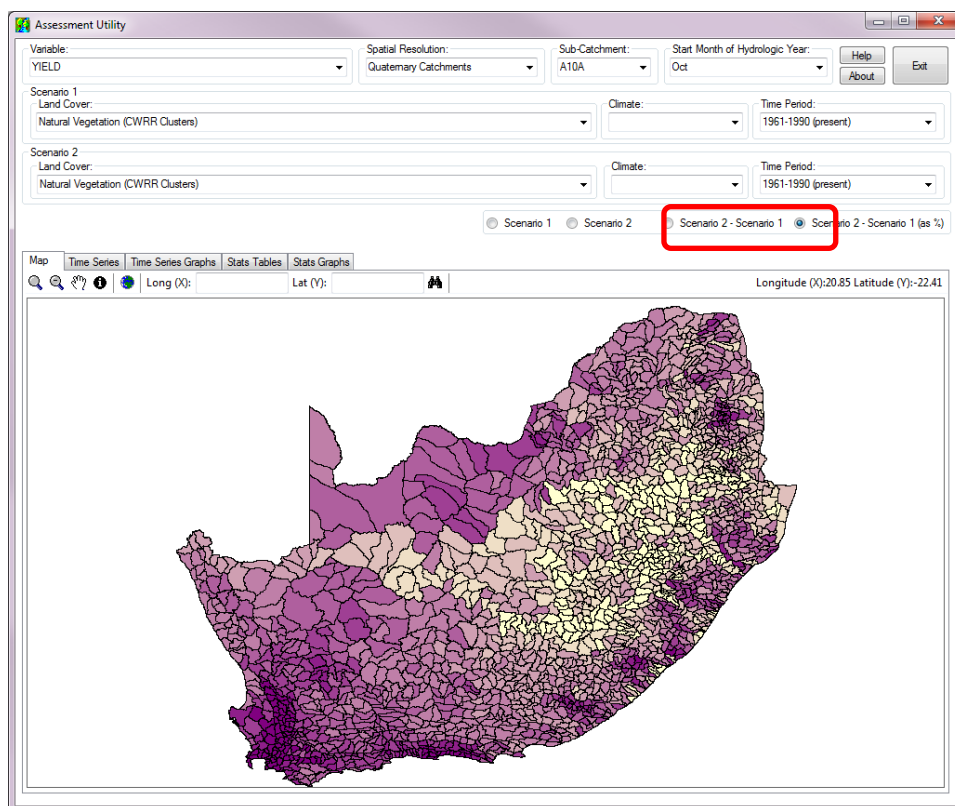Figure 0.17 Hydrological yield map for Scenario 1

Figure 0.18 Hydrological yield map for Scenario 2 – Scenario 1